A STUDY OF MIXED FORMULATIONS FOR THE FINITE ELEMENT ANALYSIS OF PLATES

by

CRISTOVAO MANUEL MOTA SOARES, M. Sc.

A thesis submitted for the degree of

Doctor of Philosophy

The University of Aston in Birmingham

December 1976

Faculty of Engineering
Department of Mechanical Engineering

Head of Department,
Professor K.Foster

Supervisor,
Mr.T.H.Richards

SUMMARY.

In this Thesis the mixed finite element analysis of laterally loaded arbitrary plan-form plates is examined. A computer program is described in which the properties of a mixed general quadrilateral plate element are included. Arbitrary elastic isotropic and orthotropic plate problems, where the orthotropic properties coincide with the coordinate axes, having variation of loading or changing flexural rigidity, may be solved. The effect of shear deformations is included in the derivation enabling the analysis of moderately thick plates.

Using the computer program, the behaviour of the element with respect to the convergence and accuracy of the results was tested under various loadings and its capability and effectiveness assessed by comparing the results with other analytical or numerical methods. The results of the mixed finite element program were also compared with those from an experimental technique, namely the Moire Method.

Supplementary to the main work, the properties of the mixed general quadrilateral element are derived for vibration and buckling analysis of thin plates and the predicted results are tested for convergence and effectiveness in the solution of free vibrations and elastic and plastic buckling of plates.

ACKNOWLEDGEMENTS.

The author would like to thank his Supervisor, Mr.T.H.Richards, for his encouragement and assistance throughout the course of this project.

The author is grateful to Mrs.M.Hasleton for the typing of this Thesis.

Finally, I dedicate this Thesis to my wife Marilu, and children Jose and Patricia.

CONTENTS

CONTENTS (contd)

CONTENTS (contd)

CONTENTS (contd)

CONTENTS (contd)

CONTENTS (contd)

CONTENTS (contd)

CONTENTS (contd)

NOTATION

A list of the more commonly used symbols and their meaning follows. All symbols are defined when introduced in the text. Rectangular matrices are indicated by [ ], and column vectors by braces { }. Rectangular matrices and column vectors transposes are indicated by $[\ ]^T$ and $\{\ \}^T$ respectively.

a,b	Linear dimensions of a plate in the x and y directions, respectively.
A	Area.
A_i	Element side.
C_1,C_2	Compliance coefficients.
D,D_x,D_y,D_1,D_{xy}	Bending and twisting rigdities.
Det	Determinant.
E	Young's modulus of elasticity.
E_s,E_t	Secant and tangent modulus.
F_x,F_y,F_z	Components of body forces per unit volume.
G	Shear modulus.
h,h_o	Plate thickness.
I	Second moment of area.
J_n	Jump term.
L	Beam length, constant.
ℓ	Length of a beam element.
M_x,M_y,M_n,M_s	Bending moments.
M_{xy},M_{ns}	Twisting moments.
n,s	Normal and tangential directions.
N_x,N_y,N_n	In-plane forces per unit length.
N_{xy},N_{ns}	In-plane shearing forces per unit length.
N_1,N_2,N_3,N_4	Interpolation functions.
p,p_o	Applied pressure.
P	Concentrated load.

q	Uniform load per unit length.
Q^*	Applied line load.
Q_x, Q_y, Q_n	Shearing forces.
s_u, s_σ	Portion of the edges where displacements and stresses are presented respectively.
s_n	Element boundary.
S, S_u, S_σ	General surface, and surfaces where displacements and stresses are prescribed respectively.
t	Time.
T	Kinetic energy.
ΔT	Change in temperature.
U, U^*	Strain energy and complementary strain energy.
V	Volume.
V_n	Effective shearing force.
w_i	Weight coefficients.
$W, \hat{W}$	Deflection, shape function.
W_{est}	External virtual work.
Work	Virtual work.
W_D	Work done.
X_b, Y_b, Z_b	Traction components per unit area.
α_i, β_i	Angles, parameters.
β_x, β_y	Rotations.
$\alpha_t, \alpha_x, \alpha_y$	Linear coefficients of thermal expansion.
δ	Variational operator.
$\varepsilon_x, \varepsilon_y, \varepsilon_z$	Direct strains.
$\gamma_{xy}, \gamma_{xz}, \gamma_{yz}$	Shear strains.
$\sigma_x, \sigma_y, \sigma_z$	Direct stresses.
$\tau_{xy} \tau_{yz} \tau_{zx}$	Shear stresses.
$\sigma_{x_o}, \sigma_{y_o}, \tau_{xy_o}$	Trial buckling stresses.
σ_{cr}, τ_{cr}	Critical elastic buckling stresses.
σ^*	Critical plastic buckling stress.

ζ, η	Natural coordinates.
μ	Poisson's ratio.
$\lambda, \lambda_b, \lambda_b^*$	Eigenvectors.
ρ	Mass per unit volume.
π_P	Potential energy functional.
π_G	Generalized energy functional.
$\pi_R, \pi_{R_D}, \pi_{R_B}$	Reissner functional for static, dynamic and buckling analyses, respectively.
ω	Natural frequency.
∇^2, ∇^4	Laplacian operators.
$[B]$	Operational matrix.
$[N], [N_W], [N_M]$	Matrices of interpolation functions.
$[C_e]$	Three dimensional compliance matrix.
$[C]$	Bending compliance matrix.
$[C_p]$	Plastic bending compliance matrix.
$[C_{TS}]$	Shear bending compliance matrix.
$[D]$	Bending elasticity matrix.
$\{f\}_e$	Element load vector.
$\{F\}$	Overall load vector.
$[\varepsilon], [\varepsilon_s], [h], [h_s]$	Mixed element partitioning matrices.
$[G], [H]$	Overall mixed element partitioning matrices.
$[I]$	Identity matrix.
$\{h\}_e$	Element nodal thicknesses vector.
$[J]$	Jacobian matrix.
$[J^*]$	Inverse of the Jacobian matrix.
$[k]_e$	Element mixed matrix.
$[K]$	Overall mixed matrix.
$[K^*]$	Overall stiffness matrix.
$[\ell_i], [L_K]$	Direction cosines transformation matrices.
$[L^*]$ $[L^*]^T$	Lower and upper triangular matrices respectively.
$[m]$	Element consistent mass matrix.

$[M]$	Overall consistent mass matrix.
$\{M\}$	Moments vector.
$[0], \{0\}$	Null matrix and vector.
$\{M\}_e$	Element nodal moments vector.
$\{p\}_e$	Element nodal pressures vector.
$\{r\}, \{r_s\}$	Element partitioning load vectors.
$[s]$	Element initial stiffness matrix.
$[S]$	Overall initial stiffness matrix.
$\{W\}_e$	Element nodal deflections vector.
$\{x\}_e \{y\}_e$	x,y cartesian coordinates vector.
$\{\delta\}_e$	Element mixed nodal deflections and moments vector.
$\{\delta\}$	Overall mixed deflections-moments vector.
$[\phi], [\psi]$	Matrices of position.
$\{\gamma\}, \{\alpha\}$	Generalized parameters.
$\{\varepsilon_e\}$	Three dimensional strain vector.
$\{\sigma_e\}$	Three dimensional stress vector.
$[\bar{\sigma}_o]$	Trial in-plane stress matrix.
$\{\lambda\}$	Curvatures matrix.

CHAPTER 1

INTRODUCTION

1) Introduction.

Plates are flat surface structures the thicknesses of which are relatively small compared with their in-plane dimensions. They are extensively used in modern technology, such as in aircrafts, ships, bridges, architectural structures and instruments because they offer enormous economical advantages as a consequence of their strength to weight ratio. The analytical methods of analysis of plates are restricted to simple cases of geometry, loading and boundary conditions. For complex plate problems various approximate numerical techniques must be used. In this connection the Rayleigh Ritz, Galerkin and Kantorovich methods can be used as long as one can derive displacement shape functions. For extremely difficult problems such as complex plane-form plates discretization methods such as finite difference and the finite element methods are currently used. The versatility and accuracy of the latter make it the most important development in Structural Analysis of recent years. In the finite element methods the continuum is replaced by a finite number of interconnected discrete elements, reducing the problem from one having an infinite number of degrees of freedom to one having a finite number.

The finite element method stems from the various methods of discretization amongst variational principles [1],[2], which provide rational bases for determining the mechanical characteristics of the substitute finite degree of freedom system. Of these - displacement, stress (equilibrium), hybrid and mixed formulations are available. In the present Thesis we are concerned with exploiting the last which has its base in the Reissner's Principle [3], which states that elastic equilibrium is distinguished by making a

certain functional denoted π_R a stationary, i.e. $\delta\pi_R = 0$, when the displacement and stress field are varied independently.

The mixed formulation for finite elements was firstly suggested by Herrmann [4], using a triangular element, for the analysis of laterally loaded plates, where shear deformations were for the first time rationally introduced for the analysis of moderately thick plates. Cook [5] introduced the mixed concept in the analysis of dynamics and buckling of thin plates. The attractions of the mixed formulation rely on the fact that inter-element compatibility conditions [2], which are difficult to meet in plate flexure, may be conveniently relaxed allowing the use of displacement and moments shape functions of lower order, which ease the computational effort. Since displacements and moments are assumed separately, the results for both fields are expected within the same order of accuracy, when the same order of interpolation functions are used for both fields. This peculiarity, unique to the mixed formulation, is of great importance because it offers the potential capability of predicting displacements with reasonable accuracy, but is also able to give a fairly accurate moment field (stress field). This is a potential advantage over the more widely used finite element displacement formulation, where some accuracy is lost through the process of differentiation of the displacement field to obtain the moment field, hence the stress field. These potential advantages, together with the ease with which shear deformations can be included in the formulation are attractions, which call for the further extension of the mixed formulation.

A literature survey of the mixed formulation showed that triangular elements are very sensitive to the element pattern division and that certain triangular mesh idealizations may lead to wrong sclutions [6]. The survey also showed that mixed rectangular elements are superior to triangular ones, except that they have

difficulties in representing plates of arbitrary plan-form. This difficulty can be overcome by the general mixed quadrilateral elements. As far as it is known, no formal investigation has been carried out using these types of elements together with the isoparametric concept, for the solution of static, dynamic and buckling problems of arbitrary plates.

This project is, therefore, aimed at extending the mixed finite element to utilizing general quadrilateral elements, with the isoparametric concept being used in the derivation of element properties.

A major part of this work was to develop a computer program based on a general quadrilateral element, where displacement and moments were assumed to change linearly within each element, for the analysis of thin and moderately thick elastic arbitrary plates. The plates may have orthotropic properties coinciding with the co-ordinate axes. Also any variation in the applied load and rigidity variations is to be accommodated. The computer program has been used to examine several plate bending situations. To assess the effectiveness of the element, the predictions were compared with those obtained by other analytical or numerical methods, and three cases, two of which no available numerical solution exists, were tackled by an experimental technique utilizing Moire fringes.

Supplementary to the main work was the further development of the mixed general quadrilateral element for dynamics (free vibrations) and buckling analysis of thin plates, and plastic buckling analysis of thin plates. A further aim was to test the general quadrilateral element and to carry out an assessment of its effectiveness in the solution of these problems. The predicted results are compared with exact and available numerical techniques.

The aims of this project were achieved. However, due to

lack of time, certain interesting aspects of the work had to be put aside and left as work to be continued in the future as discussed in Chapter 10.

CHAPTER 2

THEORY OF ELASTIC PLATES

2.1) Introduction

The elasticity theory and the variational approach are briefly presented. Also the Reissner's principle is introduced with reference to three dimensional solids.

The plate theory is derived by classical and variational techniques. The Reissner's principle is used to obtain the theory of moderately thick plates and in deriving the governing equations of thin plates for static, dynamic and buckling problems. Several methods for the solution of these equations are discussed.

2.1.1) Basic Relations in the Linear Theory of Elasticity and the Variational Approach.

The review of the fundamental relations of the mathematical theory of linear elasticity and the variational approach is based on the works of Timoshenko[7], Fung [8] and Washizu [1].

We shall consider an arbitrarily shaped continuum body in a system of rectangular coordinates x,y,z subject to external forces which are in equilibrium. The action of these forces deforms the body and each point undergoes a small displacement represented by the components u,v,w respectively parallel to the directions of the coordinate axes.

2.1.2) Equations of Equilibrium.

The three dimensions stress components associated with the chosen coordinate axes can be represented for any point of the body as a matrix

$$[\tau] = \begin{bmatrix} \sigma_x & \tau_{xy} & \tau_{xz} \\ \tau_{yx} & \sigma_y & \tau_{yz} \\ \tau_{zy} & \tau_{zy} & \sigma_z \end{bmatrix} \qquad (2.1.1)$$

where, for equilibrium of moments, see reference [8]

$$\tau_{xy} = \tau_{yx} \; ; \quad \tau_{xz} = \tau_{zx} \text{ and } \tau_{yz} = \tau_{zy} \qquad (2.1.2)$$

From equilibrium considerations throughout the continuum, elastic or not, the stress components have to satisfy the following equations:

$$\frac{\partial \sigma_x}{\partial x} + \frac{\partial \tau_{xy}}{\partial y} + \frac{\partial \tau_{xz}}{\partial z} + F_x = 0 \qquad \text{(a)}$$

$$\frac{\partial \sigma_y}{\partial y} + \frac{\partial \tau_{yx}}{\partial x} + \frac{\partial \tau_{zy}}{\partial z} + F_y = 0 \qquad \text{(b)} \qquad (2.1.3)$$

$$\frac{\partial \sigma_z}{\partial z} + \frac{\partial \tau_{zx}}{\partial x} + \frac{\partial \tau_{zy}}{\partial y} + F_z = 0 \qquad \text{(c)}$$

where $[\, F_x \;\; F_y \;\; F_z \,]$ are the components of the body forces per unit volume.

2.1.3) Strain-Displacement Relations

The strain-displacement relations are derived from geometrical considerations of infinitesimal displacements and they are represented by

$$\{\varepsilon_e\} = \begin{Bmatrix} \varepsilon_x \\ \varepsilon_y \\ \varepsilon_z \\ \gamma_{xy} \\ \gamma_{yz} \\ \gamma_{xz} \end{Bmatrix} = \begin{Bmatrix} \frac{\partial u}{\partial x} \\ \frac{\partial v}{\partial y} \\ \frac{\partial w}{\partial z} \\ \frac{\partial u}{\partial y} + \frac{\partial v}{\partial x} \\ \frac{\partial v}{\partial z} + \frac{\partial w}{\partial y} \\ \frac{\partial w}{\partial x} + \frac{\partial u}{\partial z} \end{Bmatrix} \qquad (2.1.4)$$

To ensure that a specified strain distribution leads to a displacement distribution which allows geometrical fit of

volume elements after distortion, the following relations, called compatibility equations, should be satisfied simultaneously:-

$$\frac{\partial^2 \varepsilon_x}{\partial y^2} + \frac{\partial^2 \varepsilon_y}{\partial x^2} = \frac{\partial^2 \gamma_{xy}}{\partial x \partial y} \; ; \quad 2\frac{\partial^2 \varepsilon_x}{\partial y \partial z} = \frac{\partial}{\partial x}\left(-\frac{\partial \gamma_{yz}}{\partial x} + \frac{\partial \gamma_{zx}}{\partial y} + \frac{\partial \gamma_{xy}}{\partial z}\right)$$

$$\frac{\partial^2 \varepsilon_y}{\partial z^2} + \frac{\partial^2 \varepsilon_z}{\partial y^2} = \frac{\partial^2 \gamma_{yz}}{\partial y \partial z} \; ; \quad 2\frac{\partial^2 \varepsilon_y}{\partial z \partial x} = \frac{\partial}{\partial y}\left(\frac{\partial \gamma_{yz}}{\partial x} - \frac{\partial \gamma_{zx}}{\partial y} + \frac{\partial \gamma_{xy}}{\partial z}\right) \qquad (2.1.5)$$

$$\frac{\partial^2 \varepsilon_z}{\partial x^2} + \frac{\partial^2 \varepsilon_x}{\partial z^2} = \frac{\partial^2 \gamma_{xz}}{\partial x \partial z} \; ; \quad 2\frac{\partial^2 \varepsilon_z}{\partial x \partial y} = \frac{\partial}{\partial z}\left(\frac{\partial \gamma_{yz}}{\partial x} + \frac{\partial \gamma_{zx}}{\partial y} - \frac{\partial \gamma_{xy}}{\partial z}\right)$$

2.1.4) Stress-Strain Relations.

The stress-strain relations given by Hooke's law can be represented in matrix notation as:

$$\{\varepsilon_e\} = [C_e]\,\{\sigma_e\} \qquad (2.1.6)$$

where

$$\{\sigma_e\} = [\sigma_x \;\; \sigma_y \;\; \sigma_z \;\; \tau_{xy} \;\; \tau_{yz} \;\; \tau_{xz}]^T \qquad (2.1.7)$$

and

$\{\varepsilon_e\}$ is the matrix equation (2.1.4).

For an homogenous isotropic material

$$[C_e] = \frac{1}{E}\begin{bmatrix} 1 & -\mu & -\mu & 0 & 0 & 0 \\ -\mu & 1 & -\mu & 0 & 0 & 0 \\ -\mu & -\mu & 1 & 0 & 0 & 0 \\ 0 & 0 & 0 & 2(1+\mu) & 0 & 0 \\ 0 & 0 & 0 & 0 & 2(1+\mu) & 0 \\ 0 & 0 & 0 & 0 & 0 & 2(1+\mu) \end{bmatrix} \qquad (2.1.8)$$

If the strains are required in terms of stresses then

$$\{\sigma_e\} = [C_e]^{-1}\,\{\varepsilon\}_e = [D_e]\;\{\varepsilon_e\} \qquad (2.1.9)$$

where the elasticity matrix is given by:

$$[D_e] = \frac{E}{(1+\mu)(1-\mu)} \begin{bmatrix} 1-\mu & \mu & \mu & 0 & 0 & 0 \\ \mu & 1-\mu & \mu & 0 & 0 & 0 \\ \mu & \mu & 1-\mu & 0 & 0 & 0 \\ 0 & 0 & 0 & \frac{1-2\mu}{2} & 0 & 0 \\ 0 & 0 & 0 & 0 & \frac{1-2\mu}{2} & 0 \\ 0 & 0 & 0 & 0 & 0 & \frac{1-2\mu}{2} \end{bmatrix} \qquad (2.1.10)$$

here, E is the Young's modulus for the material and μ is its Poisson's ratio.

2.1.5) Boundary Conditions

The boundary surface S of the body is assumed to consist of two parts, S_σ and S_u.

Over S_σ the surface tractions are prescribed

$$X_b = \bar{X}_b \; ; \quad Y_b = \bar{Y}_b \; ; \quad Z_b = \bar{Z}_b \qquad (2.1.11)$$

where $\bar{X}_b$, $\bar{Y}_b$, $\bar{Z}_b$ are the imposed surface traction components per unit area respectively in the directions of the coordinate axes, satisfying equilibrium at the surface by the equations:

$$\begin{aligned} X_b &= \sigma_x \ell + \tau_{xy} m + \tau_{xz} n \\ Y_b &= \tau_{yx} \ell + \sigma_y m + \tau_{yz} n \\ Z_b &= \tau_{zx} \ell + \tau_{yz} m + \sigma_z n \end{aligned} \qquad (2.1.12)$$

where ℓ,m,n are the direction cosines of the outward normal $\bar{n}$, see Fig.(2.1.1), of a point of the surface

i.e. $\ell = \cos(x,\bar{n})$; $m = \cos(y,\bar{n})$; $n = \cos(z,\bar{n})$ (2.1.13)

The geometric boundary conditions over S_u are expressed by

$$u = \bar{u} \qquad v = \bar{v} \qquad w = \bar{w} \qquad (2.1.14)$$

where $[\bar{u} \;\; \bar{v} \;\; \bar{w}]$ are the imposed displacements.

A general problem of elasticity in three dimensions, assuming small displacements require therefore the solution of:-

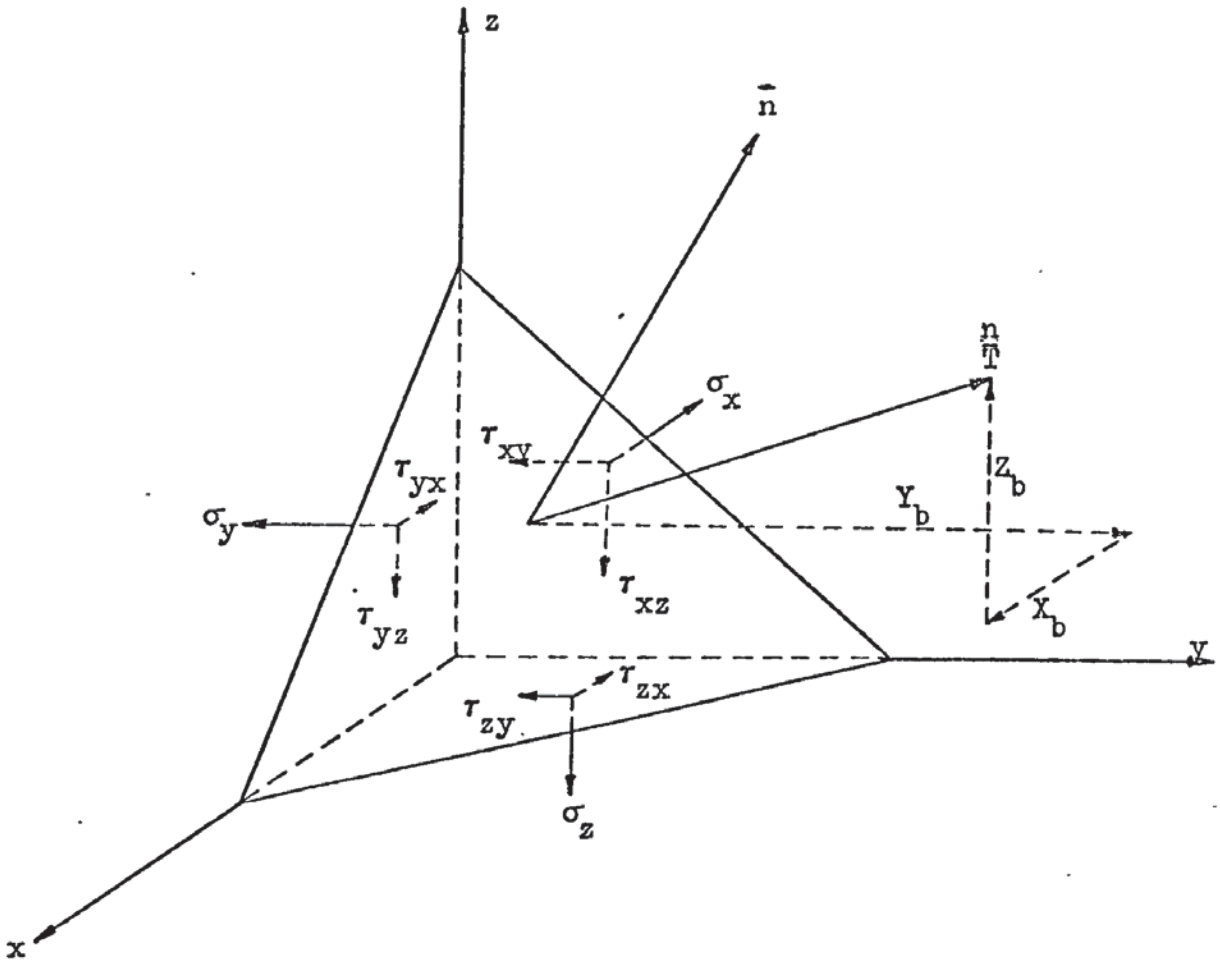

Fig.(2.1.1) Surface tractions on a tetrahedron.

- 3 equilibrium equations (2.1.3)
- 6 strain-displacement relations (2.1.4), satisfying equation (2.1.5)
- 6 stress-strain relations equations (2.1.6) and the boundary conditions (2.1.11) and (2.1.14) over the surface S of the body.

Although it is possible to establish enough equations to define the problem, the solution of these equations creates severe mathematical difficulties in general. Only in certain simple cases can they be overcome, yielding formulae for stresses and strains.

In general, treatment of practically significant situations requires an approximation of some kind. The above summary has implied the use of Newton's laws of motion. The problem may be alternatively formulated by means of a variational principle which has particular attractions for establishing approximate theories (as for beams or plates) and generating numerical methods.

2.1.6) Principle of Virtual Work.

There are several variational principles of mechanics, the principle of virtual work is perhaps the most basic from which others may be derived, references [1],[8].

Let us consider a body in equilibrium subject to a set of body forces [F_x F_y F_z], with mechanical boundary conditions specified over S_σ and geometrical boundary conditions specified over S_u, satisfying respectively equations (2.1.11) and (2.1.14).

Let the body undergo infinitesimal arbitrary displacements δu, δv, δw , and u,v,w are continuous and differentiable throughout the region. Such arbitrary displacements are called virtual displacements and the work of the forces acting through these dis-

displacements is called virtual work. Then the principle of virtual work asserts that the system is in equilibrium if the virtual work is zero.

That is

$$\delta(\text{Work}) = 0 \qquad (2.1.15)$$

Assuming that static equilibrium prevails, the external virtual work done by the body forces and the surfaces tractions is

$$\delta W_{est} = \int_V (F_x\,\delta v + F_y\,\delta v + F_z\,\delta w)dV + \int_{S_\sigma} (\bar{X}_b\,\delta u + \bar{Y}_b\delta v + \bar{Z}_b\,\delta w)dS \qquad (2.1.16)$$

where dV and dS are respectively infinitesimal elements of volume and surface of the body.

By substituting equations (2.1.12) into the second term of equation (2.1.16) we can write:

$$\int_{S_\sigma} (\bar{X}_b\delta u+\bar{Y}_b\delta v+\bar{Z}_b\delta w)dS = \int_{S_\sigma} \Big\{ (\sigma_x \ell + \sigma_{xy}\,m + \tau_{xz}\,n)\delta u + (\ldots.)\delta v + (\ldots.)\delta w \Big\} dS$$

Then, using Gauss's theorem, equation (2.1.16) becomes

$$\delta W_{est} = \int_V (F_x\delta u + F_y\,\delta v + F_z\,\delta w)dV + \int_V \Big\{ \frac{\partial}{\partial x}(\sigma_x\,\delta u) + \frac{\partial}{\partial y}(\tau_{xy}\,\delta u) + \frac{\partial}{\partial z}(\tau_{xz}\,\delta u) + \ldots + \frac{\partial}{\partial z}(\sigma_z\,\delta w) \Big\} dV$$

Differentiating the terms of the second integral and re-arranging yields :

$$\delta W_{est} = \int_V \left\{ \left(\frac{\partial}{\partial x}\sigma_x + \frac{\partial}{\partial y}\tau_{xy} + \frac{\partial}{\partial z}\tau_{xz} + F_x \right) \delta u + (\ldots)\delta v + (\ldots)\delta w \right\} dV$$

$$+ \int_V \left\{ \sigma_x \frac{\partial}{\partial x}\delta u + \sigma_y \frac{\partial}{\partial y}\delta v + \ldots + \tau_{xz}\left(\frac{\partial}{\partial z}\delta u + \frac{\partial}{\partial x}\delta w \right) \right\} dV$$

In according with the equilibrium equations (2.1.3) the above expression can be simplified to:

$$\delta W_{est} = \int_V \left\{ \sigma_x \frac{\partial}{\partial x}\delta u + \sigma_y \frac{\partial}{\partial y}\delta v + \ldots + \tau_{xz}\left(\frac{\partial}{\partial z}\delta u + \frac{\partial}{\partial x}\delta w \right) \right\} dV$$

For a statically applied virtual displacement:

$$\delta (\text{Work}) = \delta W_{est} + \delta W_{int} = 0$$

where δW_{int} is the internal virtual work.

Thus:

$$\delta W_{int} = - \int_V \{\delta e\}^T \{\sigma_e\} \, dv$$

where

$$\{\delta e\} = \begin{Bmatrix} \frac{\partial}{\partial x}\delta u \\ \frac{\partial}{\partial y}\delta v \\ \frac{\partial}{\partial z}\delta w \\ \frac{\partial}{\partial y}\delta u + \frac{\partial}{\partial x}\delta v \\ \frac{\partial}{\partial z}\delta v + \frac{\partial}{\partial y}\delta w \\ \frac{\partial}{\partial x}\delta w + \frac{\partial}{\partial z}\delta u \end{Bmatrix} \qquad (2.1.17)$$

and $\{\sigma_e\}$ is the matrix-relation (2.1. 7).

The principle of the virtual work can then be represented in matrix notation as:

$$\int_V \left(\{\delta e\}^T \{\sigma_e\} - \{\delta d\}^T \{\bar{F}\} \right) dV - \int_{S_\sigma} \{\delta d\}^T \{\bar{F}_b\} dS = 0 \qquad (2.1.18)$$

where

$$\{\bar{F}\} = [\, F_x \quad F_y \quad F_z \,]^T \qquad (2.1.19)$$

$$\{\bar{F}_b\} = [\, \bar{X}_b \quad \bar{Y}_b \quad \bar{Z}_b \,]^T \qquad (2.1.20)$$

$$\{d\} = [\, u \quad v \quad w \,]^T \qquad (2.1.21)$$

This principle is valid for any constitutive law. We shall now develop from it the very useful concept of total potential energy, which applies only to elastic bodies.

2.1.7) Principle of the Minimum Total Potential Energy.

If the system is conservative, and is an elastic one, a strain energy function U can be defined as:

$$U = \tfrac{1}{2} \{\varepsilon_e\}^T [D_e] \{\varepsilon_e\} \qquad (2.1.22)$$

with the property that

$$\{\sigma_e\} = \frac{\partial U}{\partial \{\varepsilon_e\}^T} \qquad (2.1.23)$$

where $\{\varepsilon_e\}$, $[D_e]$, $\{\sigma_e\}$ are respectively given by the relations (2.1.4), (2.1.10) and (2.1.7). Equations (2.1.17) can be represented as:

$$\{\delta e\} = \{\delta \varepsilon_e\} = [\, \delta\varepsilon_x \quad \delta\varepsilon_y \quad \delta\varepsilon_z \quad \delta\gamma_{xy} \quad \delta\gamma_{yz} \quad \delta\gamma_{xz} \,]^T \qquad (2.1.24)$$

Introducing equation (2.1.23) into equation (2.1.18), we obtain

$$\int_V \left(\delta U - \{\delta d\}^T \{\bar{F}\} \right) dV - \int_{S_\sigma} \{\delta d\}^T \{\bar{F}_b\} \, dS = 0 \qquad (2.1.25)$$

If the body forces and surface tractions are both conservative, then

$$\{\bar{F}\} = -\left[\frac{\partial G}{\partial u} \quad \frac{\partial G}{\partial v} \quad \frac{\partial G}{\partial w}\right]^T$$

and

$$\{\bar{F}_b\} = -\left[\frac{\partial g}{\partial u} \quad \frac{\partial g}{\partial v} \quad \frac{\partial g}{\partial w}\right]^T$$

where the functions $G(u,v,w)$ and $g(u,v,w)$ are called potentials of $\{\bar{F}\}$ and $\{\bar{F}_b\}$ respectively.

We can then represent equation (2.1.25) as:

$$\int_V \delta(U + G)dV + \int_{S_\sigma} \delta\, g\, ds = 0$$

which may then be written in a symbolic form as

$$\delta\pi_P = 0 \qquad (2.1.26)$$

where

$$\pi_P = \int_V (U + G)\, dV + \int_{S_\sigma} g\, dS$$

If $\{\bar{F}\}$ and $\{\bar{F}_b\}$ are constant i.e. independent of the displacements, the total potential energy functional can be represented by:

$$\pi_P = \int_V U\, dV - \int_V \{d\}^T \{\bar{F}\}\, dV - \int_{S_\sigma} \{d\}^T \{\bar{F}_b\} dS \qquad (2.1.27)$$

An interpretation of the statement (2.1.26) may be given as follows:

> Of all displacements satisfying the given boundary conditions, those which satisfy the equations of equilibrium are distinguished by a stationary (extreme) value of the potential energy.

The matrix $[D_e]$ is positive definite then the principle corresponds to an absolute minimum for stable equilibrium.

2.1.8) Generalized Energy Principle.

The principle of the minimum total potential energy can be generalized through the introduction of the Lagrangian multipliers, see references [1] [9]. Releasing restrictions on the conditions of compatibility and in the geometric boundary conditions over S_u, we can consider a functional π_G such that

$$\pi_G = \int_V U \, dv - \int_V \{d\}^T \{\bar{F}\} dv - \int_{S_\sigma} \{d\}^T \{\bar{F}_b\} \, dS$$

$$- \int_V \left[\left(\varepsilon_x - \frac{\partial u}{\partial x} \right) \lambda_1 + \dots + \left(\gamma_{xz} - \frac{\partial w}{\partial x} - \frac{\partial u}{\partial z} \right) \lambda_6 \right] dV$$

$$- \int_{S_u} \left[(u-\bar{u}) \, \gamma_1 + (v-\bar{v}) \, \gamma_2 + (w-\bar{w}) \, \gamma_3 \right] dS \qquad (2.1.28)$$

Regarding the three displacements, six strain components and nine Lagrange multipliers as independent, they may be given independent variations yielding

$$\delta \pi_G = 0$$

where

$$\delta\pi_G = \int_V \left\{ \left(\frac{\partial U}{\partial \varepsilon_x} \delta\varepsilon_x + \dots + \frac{\partial U}{\partial \gamma_{xz}} \delta\gamma_{xz} \right) - \{\delta d\}^T \{\bar{F}\} \right.$$

$$\left. - \left(\varepsilon_x - \frac{\partial u}{\partial x} \right) \delta\lambda_1 + \dots + \left(\delta\gamma_{xz} - \frac{\partial}{\partial x} \delta w - \frac{\partial}{\partial z} \delta u \right) \lambda_6 \right\} dV$$

$$- \int_{S_u} \left\{ (u-\bar{u}) \, \delta\gamma_1 + (v-\bar{v}) \, \delta\gamma_2 + (w-\bar{w}) \, \delta\gamma_3 \right\} dS - \int_{S_u} \left\{ \delta u \gamma_1 + \delta v \gamma_2 + \delta w \gamma_3 \right\} dS$$

$$- \int_{S_\sigma} \{\delta d\}^T \{\bar{F}_b\} \, dS$$

Integrating by parts, where appropriate using Green's

formula, and rearranging the terms yields:

$$\delta\pi_G = \int_V \left\{ \left(\frac{\partial U}{\partial \varepsilon_x} - \lambda_1 \right) \delta\varepsilon_x + \ldots + \left(\frac{\partial U}{\partial \gamma_{xz}} - \lambda_6 \right) \right.$$

$$- \left(\frac{\partial \lambda_1}{\partial x} + \frac{\partial \lambda_4}{\partial y} + \frac{\partial \lambda_6}{\partial z} + F_x \right) \delta u + (\ldots)\delta v + (\ldots)\delta w$$

$$\left. - \left(\varepsilon_x - \frac{\partial u}{\partial x} \right) \lambda_1 + \ldots + \left(\gamma_{xz} - \frac{\partial w}{\partial x} - \frac{\partial u}{\partial z} \right) \delta\lambda_6 \right\} dV$$

$$+ \int_{S_\sigma} \left\{ (X_b - \bar{X}_b)\delta u + (Y_b - \bar{Y}_b)\ \delta v + (Z_b - \bar{Z}_b)\delta w \right\} dS$$

$$+ \int_{S_u} \left\{ (X_b - \gamma_1)\delta u + (Y_b - \gamma_2)\ \delta v + (Z_b - \gamma_3)\ \delta w \right\} dS$$

$$- \int_{S_u} \left\{ (u - \bar{u})\ \delta\gamma_1 + (v - \bar{v})\ \delta\gamma_2 + (w - \bar{w})\ \delta\gamma_3 \right\} dS \qquad (2.1.29)$$

The conditions for π_G to be stationary are, then

$$\frac{\partial U}{\partial \varepsilon_x} = \lambda_1 \ \ldots\ ; \quad \frac{\partial U}{\partial \gamma_{xz}} = \lambda_6 \qquad \text{in } V \qquad (2.1.30)$$

$$X_b = \gamma_1;\ Y_b = \gamma_2\ ;\ Z_b = \gamma_3 \qquad \text{in } S_u \qquad (2.1.31)$$

$$\frac{\partial \lambda_1}{\partial x} + \frac{\partial \lambda_4}{\partial y} + \frac{\partial \lambda_6}{\partial z} + F_x = 0\ ; \qquad \text{in } V \qquad (2.1.32)$$

$$\varepsilon_x = \frac{\partial u}{\partial x}\ ; \quad \ldots\ \gamma_{xz} = \frac{\partial w}{\partial x} + \frac{\partial u}{\partial z} \quad \text{in } V \qquad (2.1.33)$$

$$X_b = \bar{X}_b\ ;\ Y_b = \bar{Y}_b\ ;\ Z_b = \bar{Z}_b \qquad \text{in } S_\sigma \qquad (2.1.34)$$

$$u = \bar{u}\ ;\ v = \bar{v}\ ;\ w = \bar{w} \qquad \text{in } S_u \qquad (2.1.35)$$

Thus we see that the Lagrangian multipliers have a physical meaning whose identification can easily be found by comparing relations (2.1.30) with (2.1.23), and from equation (2.1.31).

In fact, $(\lambda_1 \ \ldots\ \lambda_6)$ are the stress components $(\sigma_x \ \ldots\ \tau_{xz})$ and $(\gamma_1\ \ \gamma_2\ \ \gamma_3)$ the components of the surfaces tractions $(X_b\ \ Y_b\ \ Z_b)$.

It follows that :

- The equilibrium equations are equations (2.1.32)
- The strain-displacement relations are equations (2.1.33)
- The mechanical boundary conditions over S_σ are equations (2.1.34)
- The geometric boundary conditions over S_u are equations (2.1.35)

which are the so-called Euler equations and natural boundary conditions consequent upon requiring π_G to be stationary.

2.1.9) The Reissner Functional.

It has been shown through the generalization of the principle of the minimum total potential energy that the Lagrangian multipliers could be identified with the components of stress and with the imposed surface tractions. Assuming that such is true from the start, π_G could be written as:

$$\pi_G = \int_V \left\{ U - \{\varepsilon_e\}^T \{\sigma_e\} + \{\varepsilon_e\}^T \{\sigma_e\} \right\} dV$$

$$- \int_V \{d\}^T \{\bar{F}\} dV - \int_{S_\sigma} \{d\}^T \{\bar{F}_b\} dS$$

$$- \int_{S_u} (\{d\} - \{\bar{d}\})^T \{F_b\} \, dS \qquad (2.1.36)$$

where

$$\{\bar{d}\} = [\, \bar{u} \;\; \bar{v} \;\; \bar{w} \,]^T \qquad (2.1.37)$$

But we may define

$$U - \{\varepsilon_e\}^T \{\sigma_e\} = -U^*(\sigma) \qquad (2.1.38)$$

to be the complementary strain energy function given for a linear elastic solid by :

$$U^*(\sigma) = \tfrac{1}{2} \{\sigma_e\}^T [C_e] \{\sigma_e\} \qquad (2.1.39)$$

where $\{\sigma_e\}$ and $[C_e]$ are respectively given by relations (2.1.7) and (2.1.8).

Substituting equation (2.1.38) into (2.1.36), we obtain the so-called Reissner functional [3] as:

$$\pi_R = -\int_V U^*(\sigma)\, dV + \int_V \{\varepsilon_e\}^T \{\sigma_e\}\, dV - \int_V \{d\}^T \{\bar{F}\} dV$$

$$- \int_{S_\sigma} \{d\}^T \{\bar{F}_b\}\, dS - \int_{S_u} (\{d\} - \{\bar{d}\})^T \{F_b\}\, dS \qquad (2.1.40)$$

where $\{\varepsilon_e\}, \{\sigma_e\}, \{\bar{F}\}, \{\bar{F}_b\}, \{d\}, \{\bar{d}\}$ are respectively relations (2.1.4), (2.1.7), (2.1.19), (2.1.20), (2.1.21) and (2.1.37).

The variational principle may be interpreted as follows:

> Among all states of stress and displacement which satisfy the mechanical and displacement boundary conditions the actually occurring state of stress and displacement is determined by the variational equation:
>
> $$\delta \pi_R = 0 \qquad (2.1.41)$$

This stationary condition for π_R leads to:

a) The equations of equilibrium in V

b) The strain-displacement relations in V

c) The material properties through stress-strain relations

d) The requirements that $X_b = \bar{X}_b$, etc. on S_σ

e) The requirements that $u = \bar{u}$ etc. on S_u,

as the Euler equations and natural boundary conditions.

Before specializing the Reissner functional for the analysis of plates, we shall summarise the classical theory of thin plates relevant for our work.

2.2) Classical Theory of Thin Plates.

The "thickness" of the plate allows us to make certain assumptions about the nature of the stresses and displacements distribution which leads to a theory which is simpler than that for a general three dimensional solid. This feature enables the shape of the plate to be defined by describing the geometry of the middle surface [10].

The plate is referred to as a Cartesian coordinate system x,y,z, where the x,y coordinate plane corresponds to the middle plane or middle surface in the undeformed geometry, Fig.(2.2.1).

2.2.1) Assumptions.

If the thickness of the plate is small compared with the other in-plane dimensions and if the transverse deflections are small compared with the thickness h, then an approximate theory can be developed by making the following assumptions:-

1 - The middle surface remains neutral during bending. This implies that there is no deformation in the middle surface.

2 - The deformations normal and tangential to the middle surface are of negligible order of magnitude.

3 - Lines of the plate lying initially on a normal to the middle surface of the plate remain on the normal to the middle surface after bending.

The first assumption enables the displacement of any point of the plate parallel to the z axis to be represented by the deflection of the middle surface.

Thus :

$$w(x,y,z) = w(x,y,o) = W(x,y) = W \qquad (2.2.1)$$

From the second and third assumption

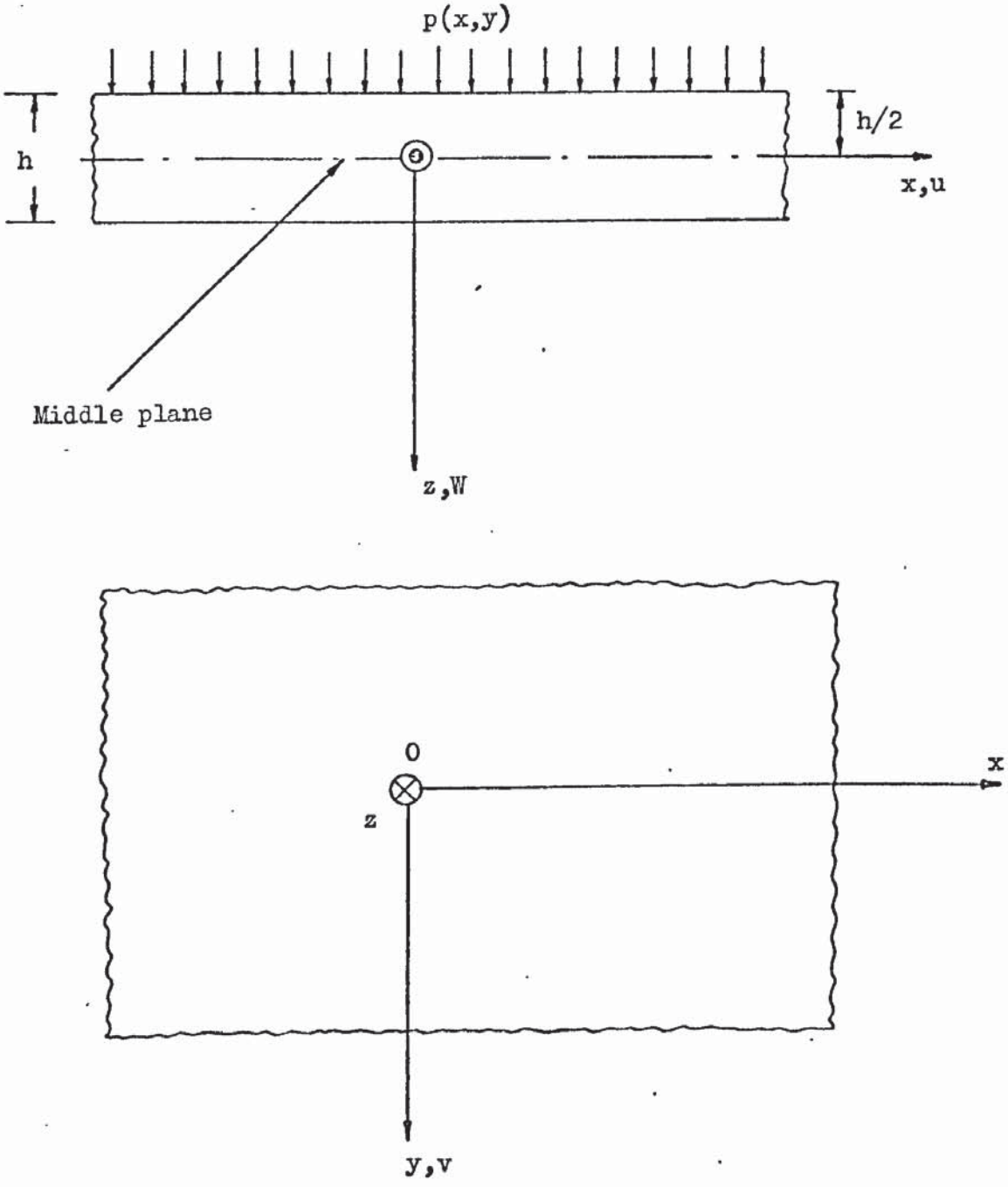

Fig.(2.2.1) Plate coordinate system.

$$\varepsilon_z = \gamma_{xz} = \gamma_{yz} \approx 0 \qquad (2.2.2)$$

and the stress normal to the middle surface is assumed negligible then

$$\sigma_z = 0 \qquad (2.2.3)$$

The validity of the second and third assumptions depend to a large extent to the ratio of the plate thickness to the in-plane dimensions of the plate.

Later we shall take into account γ_{xz}, γ_{yz} and to a certain extent σ_z, in the theory of "moderately" thick plates, due to Reissner [11].

Since the deformations are such that normal straight lines remain straight lines and normal to the middle surface (transverse shear deformations neglected), the displacements in the x,y direction due to the bending action can be represented as:

$$u = -z \frac{\partial W}{\partial x} \qquad \text{(a)}$$

$$v = -z \frac{\partial W}{\partial y} \qquad \text{(b)} \qquad (2.2.4)$$

In accordance with equations (2.1.4), (2.2.2), (2.2.4) the strain-deformation relations for a thin plate are:

$$\begin{Bmatrix} \varepsilon_x \\ \varepsilon_y \\ \gamma_{xy} \end{Bmatrix} = \begin{Bmatrix} \frac{\partial u}{\partial x} \\ \frac{\partial v}{\partial y} \\ \frac{\partial u}{\partial y} + \frac{\partial v}{\partial x} \end{Bmatrix} = z \begin{Bmatrix} -\frac{\partial^2 W}{\partial x^2} \\ -\frac{\partial^2 W}{\partial y^2} \\ -2\frac{\partial^2 W}{\partial x \partial y} \end{Bmatrix} \qquad (2.2.5)$$

Introducing the above simplifications the stress-strain relations (2.1.6) become:

$$\begin{Bmatrix} \varepsilon_x \\ \varepsilon_y \\ \gamma_{xy} \end{Bmatrix} = \frac{1}{E} \begin{bmatrix} 1 & -\mu & 0 \\ -\mu & 1 & 0 \\ 0 & 0 & 2(1+\mu) \end{bmatrix} \begin{Bmatrix} \sigma_x \\ \sigma_y \\ \tau_{xy} \end{Bmatrix} \tag{2.2.6}$$

Solving (2.2.6) for the stress components yields:

$$\begin{Bmatrix} \sigma_x \\ \sigma_y \\ \tau_{xy} \end{Bmatrix} = \frac{E}{1-\mu^2} \begin{bmatrix} 1 & \mu & 0 \\ \mu & 1 & 0 \\ 0 & 0 & \frac{1+\mu}{2} \end{bmatrix} \begin{Bmatrix} \varepsilon_x \\ \varepsilon_y \\ \gamma_{xy} \end{Bmatrix} \tag{2.2.7}$$

which are the basic relations of the classical theory of thin plates.

The stresses τ_{xz} and τ_{yz} can only be evaluated from the conditions of equilibrium (2.1.3 a,b).

2.2.2) Relations Between Internal Forces, Stresses and Deflections.

Considering an elemental parallelepiped cut out of the plate, as shown in Fig.(2.2.2) the shear forces intensities Q_x and Q_y are defined by:

$$Q_x = \int_{-h/2}^{h/2} \tau_{xz}\, dz. \tag{2.2.8}$$

$$Q_y = \int_{-h/2}^{h/2} \tau_{yz}\, dz \tag{2.2.9}$$

The stress components σ_x, σ_y, τ_{xy} can be reduced to

$M_x dy$, $M_y dx$, $M_{xy} dy$ and $M_{yx} dx$

where

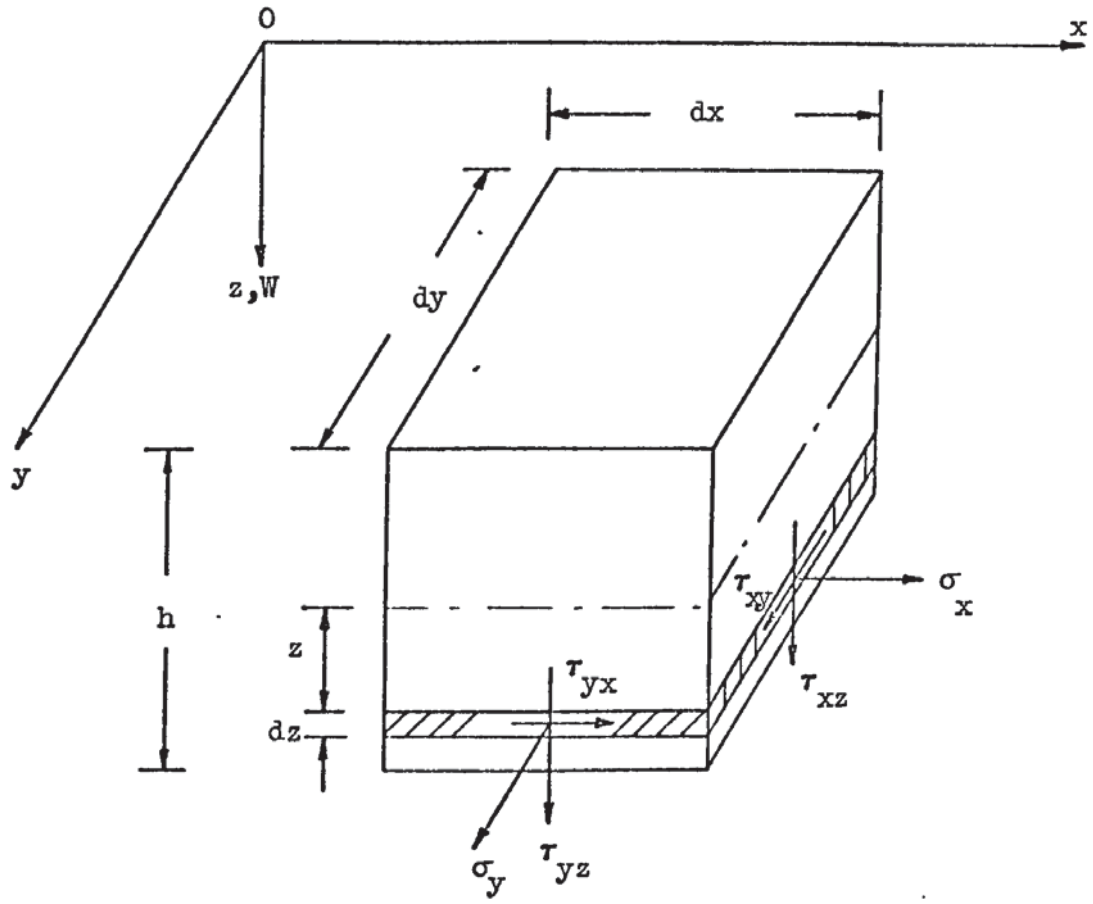

Fig.(2.2.2) Stress components on a plate element.

$$\begin{Bmatrix} M_x \\ M_y \\ M_{xy} \end{Bmatrix} = \int_{-h/2}^{h/2} \begin{Bmatrix} \dot{\sigma}_x \\ \sigma_y \\ \tau_{xy} \end{Bmatrix} z \, dz \tag{2.2.10}$$

and

$$M_{xy} = M_{yx} \tag{2.2.11}$$

M_x and M_y are bending moments per unit length and M_{xy} is the twisting moment per unit length. Normally they are called bending and twisting moments. The notation for these quantities, which will be used throughout this thesis, is shown in Fig.(2.2.3).

Integrating equation (2.2.10) using the matrix relations (2.2.7) and (2.2.5) yields

$$\begin{Bmatrix} M_x \\ M_y \\ M_{xy} \end{Bmatrix} = D \begin{bmatrix} 1 & \mu & 0 \\ \mu & 1 & 0 \\ 0 & 0 & \frac{1+\mu}{2} \end{bmatrix} \begin{Bmatrix} -\frac{\partial^2 W}{\partial x^2} \\ -\frac{\partial^2 W}{\partial y} \\ -\frac{2\partial^2 W}{\partial x \partial y} \end{Bmatrix} = [D] \{\lambda\} \tag{2.2.12}$$

where D, called the bending rigidity is given by

$$D = \frac{E h^3}{12(1 - \mu^2)} \tag{2.2.13}$$

and [D] is the bending elasticity matrix.

Inverting the matrix-relation (2.2.12) we get

$$\{\lambda\} = [C] \{M\} \tag{2.2.14}$$

where the curvature matrix is:

$$\{\lambda\} = \left[-\frac{\partial^2 W}{\partial x^2} - \frac{\partial^2 W}{\partial y^2} - \frac{2\partial^2 W}{\partial x \partial y} \right]^T \tag{2.2.15}$$

and

$$\{M\} = [M_x \quad M_y \quad M_{xy}]^T \tag{2.2.16}$$

The matrix [C], normally called the compliance matrix, is

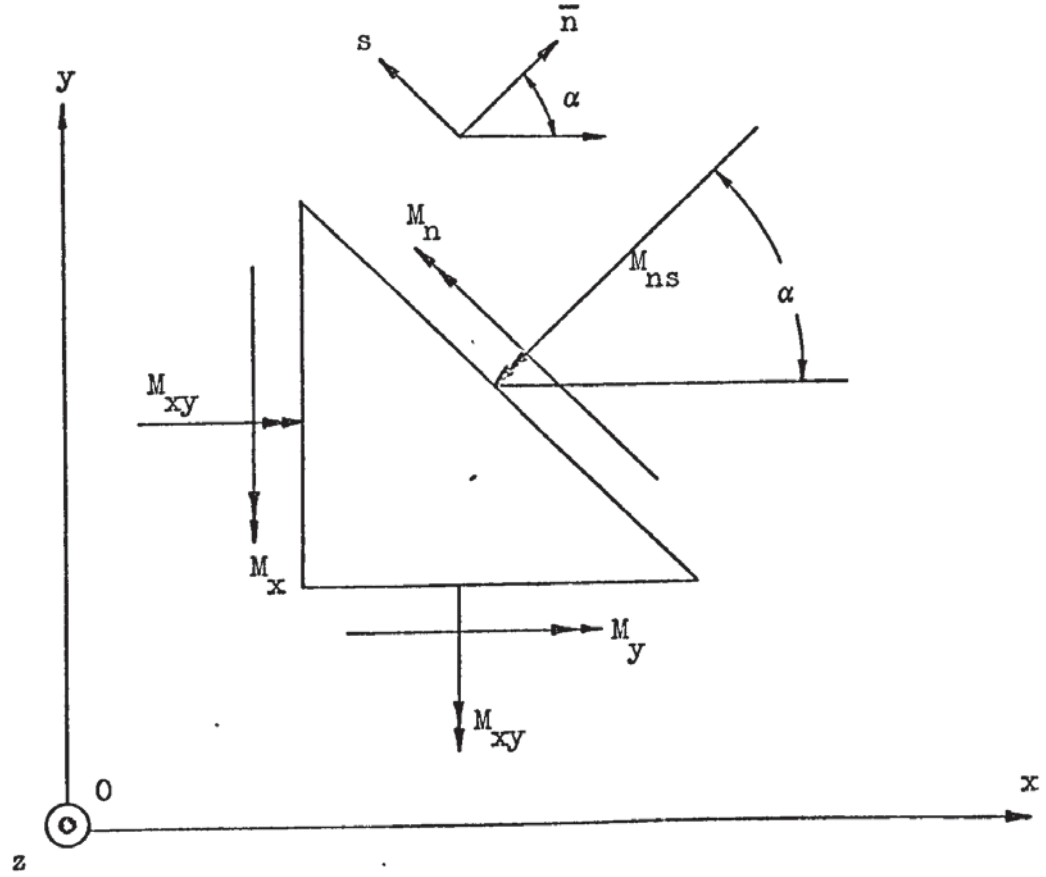

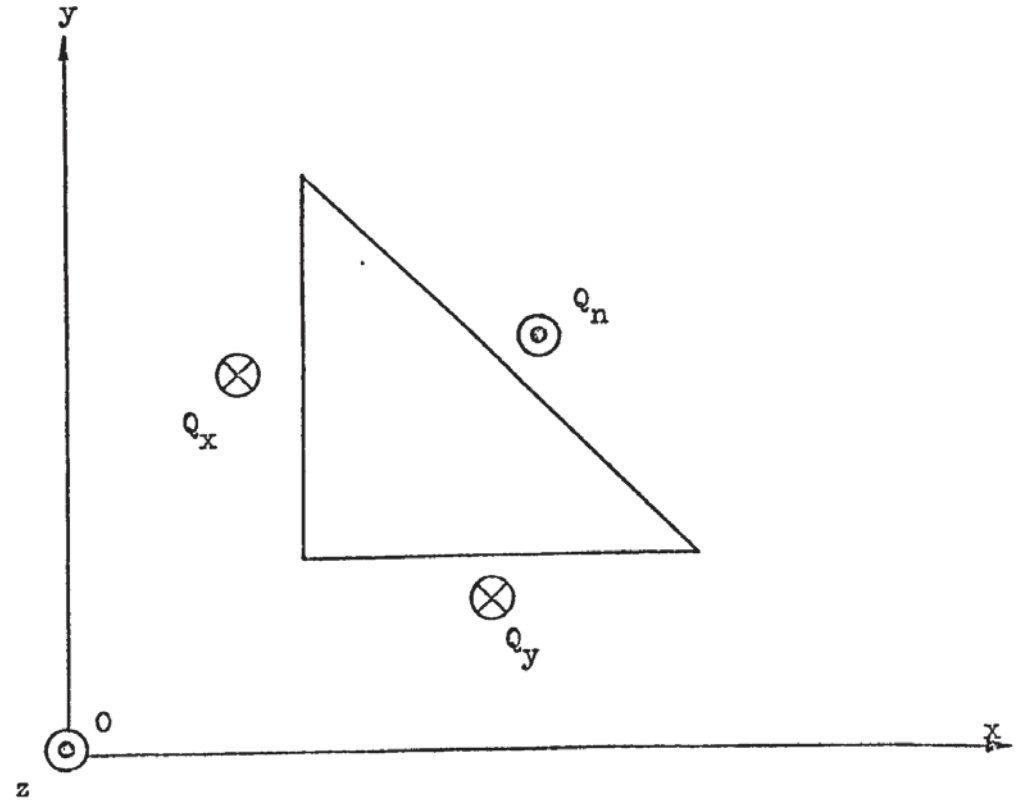

Fig.(2.2.3) Moments and shear notation.

$$[C] = \frac{12}{Eh^3}\begin{bmatrix} 1 & -\mu & 0 \\ -\mu & 1 & 0 \\ 0 & 0 & 2(1+\mu) \end{bmatrix} \qquad (2.2.17)$$

The stress-moments relations can be deduced from equation (2.2.7) and (2.2.12). Thus we have

$$\begin{Bmatrix} \sigma_x \\ \sigma_y \\ \tau_{xy} \end{Bmatrix} = \frac{12z}{h^3} \begin{Bmatrix} M_x \\ M_y \\ M_{xy} \end{Bmatrix} \qquad (2.2.18)$$

and the maximum stresses are at the plate surface, when $z = \pm \frac{h}{2}$. That is,

$$\begin{Bmatrix} \sigma_x \\ \sigma_y \\ \tau_{xy} \end{Bmatrix} = \pm \frac{6}{h^2} \begin{Bmatrix} M_x \\ M_y \\ M_{xy} \end{Bmatrix} \qquad (2.2.19)$$

If a transformation of coordinates (n,s,z) is required, simple equilibrium considerations, see Fig.(2.2.3), yield

$$\begin{Bmatrix} M_s \\ M_n \\ M_{ns} \end{Bmatrix} = \begin{bmatrix} \sin^2\alpha & \cos^2\alpha & -2\sin\alpha\cos\alpha \\ \cos^2\alpha & \sin^2\alpha & 2\sin\alpha\cos\alpha \\ -\sin\alpha\cos\alpha & \sin\alpha\cos\alpha & \cos^2\alpha-\sin^2\alpha \end{bmatrix} \begin{Bmatrix} M_x \\ M_y \\ M_{xy} \end{Bmatrix} \qquad (2.2.20)$$

and the normal shear force intensity is:

$$Q_n = [\cos\alpha \quad \sin\alpha] \begin{Bmatrix} Q_x \\ Q_y \end{Bmatrix} \qquad (2.2.21)$$

where α is the angle between the outward normal $\bar{n}$ and the x axis.

The principal bending moments, representing the extreme values and the angle at which they occur are given by:

$$(M_n)_{\substack{\max \\ \min}} = \frac{M_x + M_y}{2} \pm \frac{1}{2}\sqrt{(M_x-M_y)^2+4M_{xy}^2}$$

$$\alpha^* = \frac{1}{2}\tan^{-1}\left(\frac{2M_{xy}}{M_x-M_y}\right) \qquad (2.2.23)$$

and the maximum and minimum twisting moment is,

$$(M_{nt})_{\substack{max\\min}} = \pm \tfrac{1}{2} \sqrt{(M_x - M_y)^2 + 4M_{xy}^2} \qquad (2.2.24)$$

2.2.3) Derivation of the Governing Differential Equations.

Assuming that the load p(x,y) acting on a plate is normal to its surface and considering a small element cut of the plate as shown in Fig.(2.2.4), subject to small changes of moments and shearing forces intensitites, taking equilibrium of the transverse forces, we get

$$-Q_x\,dy - Q_y\,dx + \left(Q_x + \frac{\partial Q_x}{\partial x}\,dx\right)dy + \left(Q_y + \frac{\partial Q_y}{\partial y}\,dy\right)dx$$

$$+ p(x,y)dx\,dy = 0$$

after simplification it becomes

$$\frac{\partial Q_x}{\partial x} + \frac{\partial Q_y}{\partial y} + p(x,y) = 0 \qquad (2.2.25)$$

Taking equilibrium of the moments about an axis parallel to the y axis,

$$\left(M_x + \frac{\partial M_x}{\partial x}\,dx\right)dy - M_x\,dy + \left(M_{yx} + \frac{\partial M_{xy}}{\partial y}\,dy\right)dx - M_{yx}\,dx$$

$$- \left(Q_x + \frac{\partial Q_x}{\partial x}\,dx\right)dy\,\frac{dx}{2} - Q_x\,dy\,\frac{dx}{2} = 0$$

After simplification and neglecting 3rd order terms,

$$Q_x = \frac{\partial M_x}{\partial x} + \frac{\partial M_{yx}}{\partial y} \qquad (2.2.26)$$

Similarly taking moments about the x axis gives

$$Q_y = \frac{\partial M_y}{\partial y} + \frac{\partial M_{xy}}{\partial x} \qquad (2.2.27)$$

Since there are no forces in the x and y directions and no moments with respect to z the three derived equations define

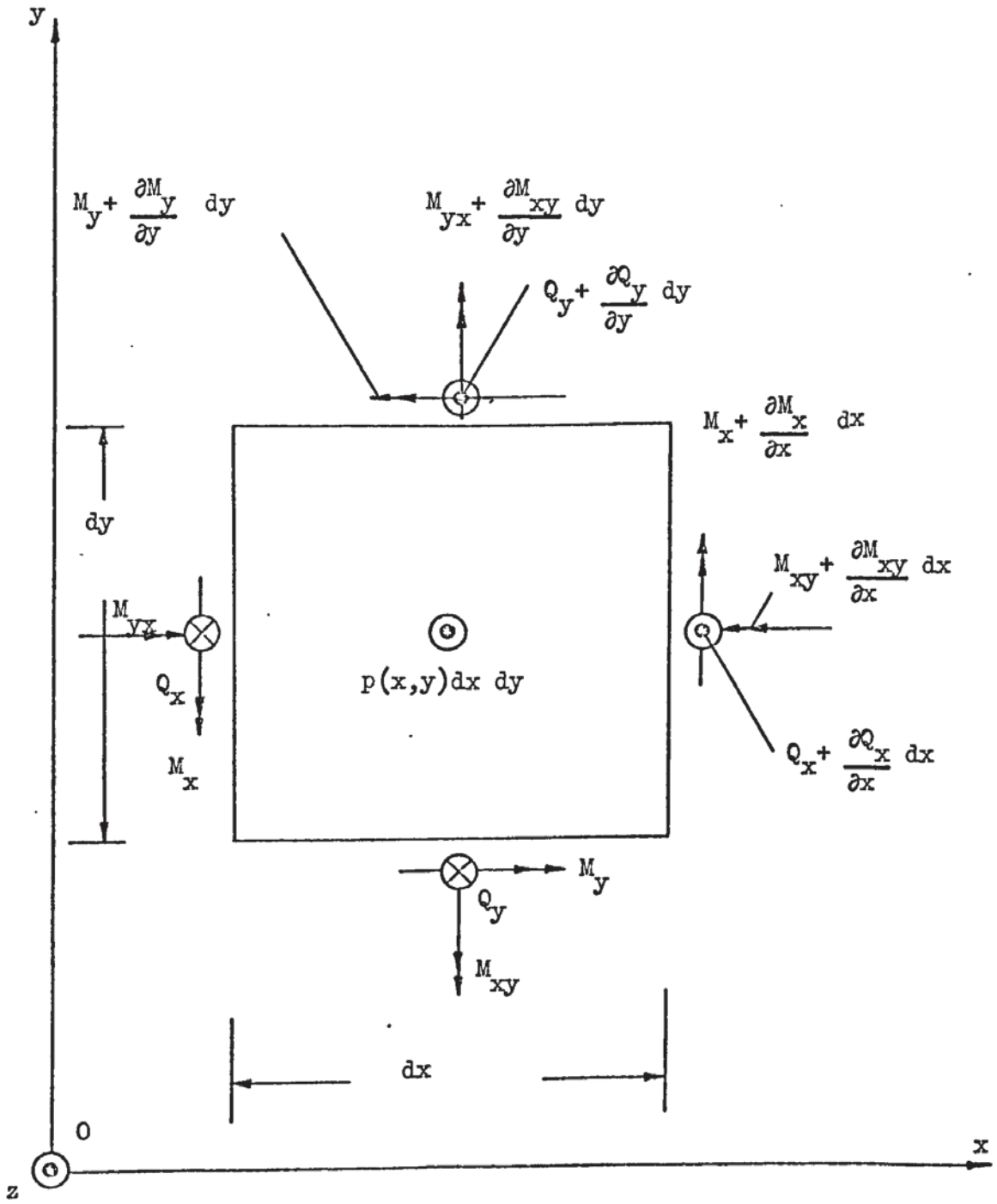

Fig.(2.2.4) Small element in equilibrium.

completely the equilibrium of the element. In fact, we could arrive at the same equations by multiplying the three dimensional differential equations (2.1.3) by z, neglecting the body forces, integrating over the thickness of the element and making use of relation (2.2.8) and (2.2.9).

Substituting equations (2.2.26) and (2.2.27) into (2.2.25) and noticing that $M_{xy} = M_{yx}$ the following single equilibrium equation is obtained:

$$\frac{\partial^2 M_x}{\partial x^2} + 2\frac{\partial^2 M_{xy}}{\partial x \partial y} + \frac{\partial^2 M_y}{\partial y^2} + p(x,y) = 0 \qquad (2.2.28)$$

Replacing the relations (2.2.12) into equation (2.2.28) to obtain some connection between $p(x,y)$ and the deflection of the middle surface W, yields the plate governing equation

$$\frac{\partial^4 W}{\partial x^4} + 2\frac{\partial^4 W}{\partial x^2 \partial y^2} + \frac{\partial^4 W}{\partial y^4} = \frac{p(x,y)}{D} \qquad (2.2.29)$$

or

$$\nabla^4 W = \frac{p(x,y)}{D} \qquad (2.2.30)$$

where

$$\nabla^4 = \left(\frac{\partial^2}{\partial x^2} + \frac{\partial^2}{\partial y^2}\right)^2 \qquad (2.2.31)$$

For any given plate problem, one seeks a solution to equation (2.2.30) which satisfies the known boundary conditions at the edges of the plate.

2.2.4) Boundary Conditions.

To solve the plate equation (2.2.30) one needs to satisfy the boundary conditions, for the given plate problem. Since equation (2.2.30) is a 4th order differential equation no more than two, either geometrical (transverse deflection W and normal

slope $\partial w/\partial n$) or mechanical boundary conditions can be imposed at a boundary. The mechanical prevailing variables at a boundary are the normal moment M_n, the twisting moment M_{ns} and the normal shear force intensity Q_n. Since 3 conditions are too many for the thin plate theory, the twisting moment M_{ns} and the normal shear force intensity Q_n must be reduced into one quantity, the so-called normal effective shear force intensity given by [10]

$$V_n = Q_n + \frac{\partial M_{ns}}{\partial s} \tag{2.2.32}$$

This force can be visualized by considering the edge of plate, divide into two sections of length Δs, see Figure (2.2.5a), the twisting moment M_{ns} can be expressed in one of the sections in terms of the twisting moment in the other adjacent section, by a Taylor's series, taking one term only. A third section of length Δs may be imagined between centre lines of the two mentioned sections. For this third section, the shear force is $Q_n \Delta s$. By Saint-Venant principle the twisting moment distribution in the original two sections can be represented by two moments having forces of intensity M_{ns} and $\left(M_{ns} + \frac{\partial M_{ns}}{\partial s} \Delta s\right)$ respectively with a separation of Δs between the forces, Figure (2.2.5b). Thus, for the centre panel, the shear force intensity V_n is seen as:

$$V_n = \frac{1}{\Delta s}\left[Q_n \Delta s + \left(M_{ns} + \frac{\partial M_{ns}}{\partial s} \Delta s\right) - M_{ns}\right]$$

$$= Q_n + \frac{\partial M_{ns}}{\partial s}$$

If there is a discontinuity in the boundary (i.e. if the boundary has corners), then from the preceding visualization regarding the representation of the twisting moment M_{ns} by a shear force intensity $+\frac{\partial M_{ns}}{\partial s}$, there will remain a concentrated force at such corners. For a rectangular plate simply supported at

two adjacent edges, Figure (2.2.5c) the corner force is [10]

$$R_o = 2 M_{xy}$$

which tends to lift the corner, if no anchorage is provided. For two clamped adjacent edges $R_o = 0$ since along these edges the twisting moment is zero. The case at the intersection of two free edges is similar.

The boundary conditions can thus be imposed as:

either $M_n = 0$ or $\frac{\partial W}{\partial n}$ is prescribed

either $V_n = 0$ or W is prescribed

Hence

for a simply supported boundary:

$$M_n = - D \left[\frac{\partial^2 W}{\partial n} + \mu \frac{\partial^2 W}{\partial s} \right] = 0$$

$$W = 0$$

for a built in boundary

$$\frac{\partial W}{\partial n} = 0$$

$$W = 0$$

and for a free boundary

$$M_n = 0$$

$$V_n = Q_n + \frac{\partial M_{ns}}{\partial s} = 0$$

2.3) The Reissner Variational Approach Applied to Plate Bending.

2.3.1) Introduction.

In this section the three dimensional Reissner functional equation (2.1.36) is specialized for the transverse bending of plates.

We shall begin with the general case of an elastic plate, where the effects of the transverse shear stresses

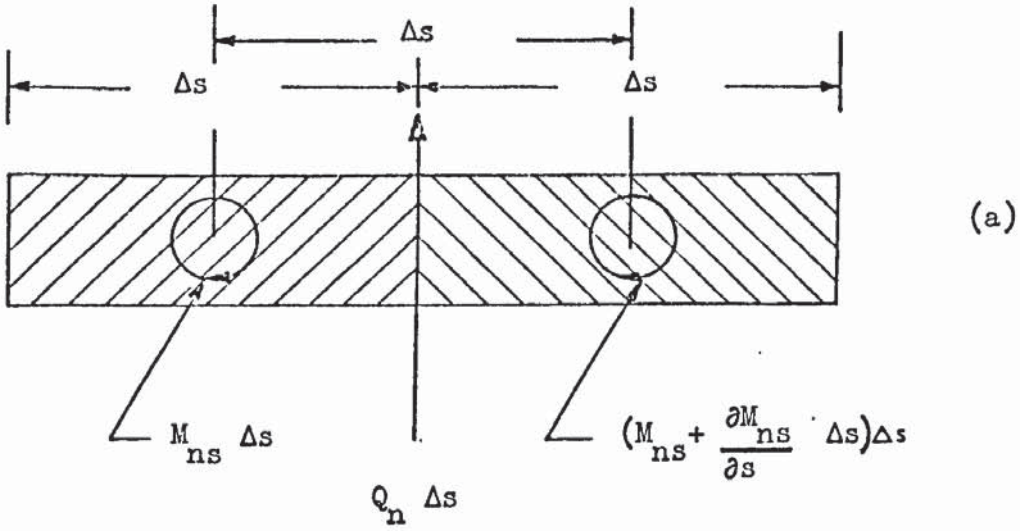
Δs
Δs
Δs
$M_{ns}\ \Delta s$
$(M_{ns} + \frac{\partial M_{ns}}{\partial s}\ \Delta s)\Delta s$
$Q_n\ \Delta s$

(a)

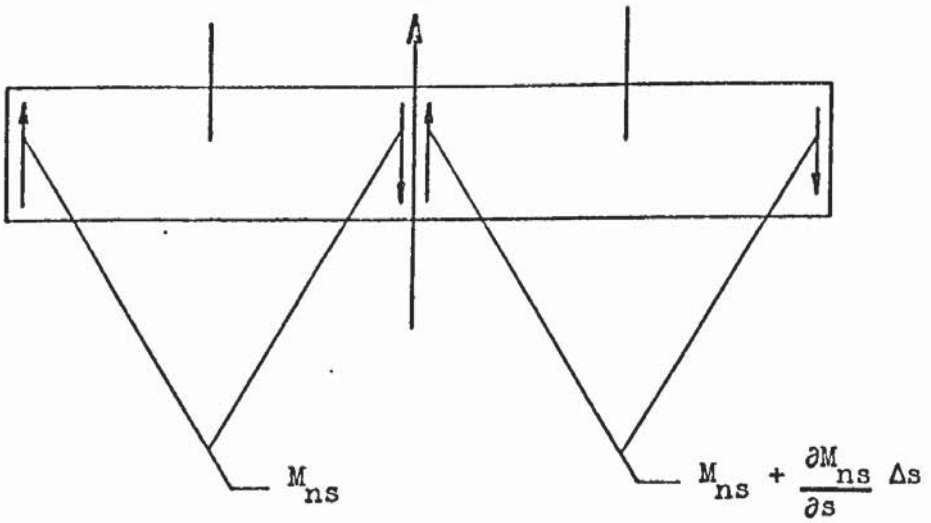
M_{ns}
$M_{ns} + \frac{\partial M_{ns}}{\partial s}\ \Delta s$

(b)

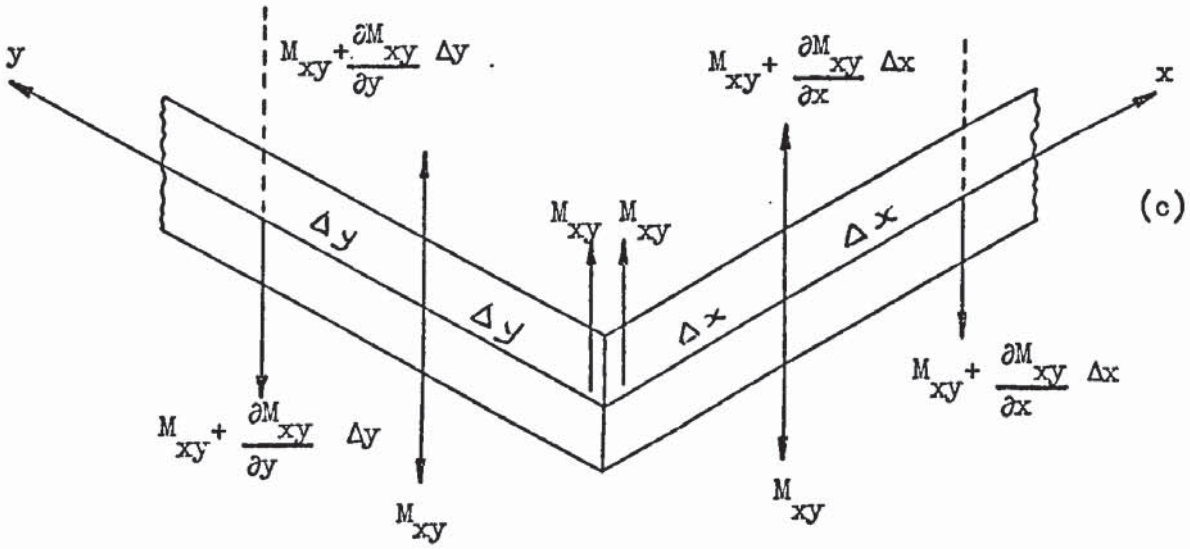
y
x
$M_{xy} + \frac{\partial M_{xy}}{\partial y}\ \Delta y$
$M_{xy} + \frac{\partial M_{xy}}{\partial x}\ \Delta x$
M_{xy}
M_{xy}
Δy
Δy
Δx
Δx
$M_{xy} + \frac{\partial M_{xy}}{\partial y}\ \Delta y$
M_{xy}
M_{xy}
$M_{xy} + \frac{\partial M_{xy}}{\partial x}\ \Delta x$

(c)

Fig.(2.2.5)

τ_{xz}, τ_{yz} are included and the effect of the normal stress, σ_z, is only partially taken into consideration. These will allow the satisfaction of three boundary conditions at each edge, as shown by Reissner [3],[11],[12]. The functional will then be simplified to correspond to the classical theory. The first derivation is referred to as "Moderately thick plate theory".

2.3.2) The Reissner Functional for Plate Bending.

In order to convertthe functional equation (2.1.36) into the form appropriate to the transverse bending of plates, we assume a distribution p(x,y) of normal stress and no tangential stress over the face $-z/2$ of the plate, and let the face $+z/2$ to be unloaded, as shown in Figure (2.2.1): for simplicity's sake, the body forces are disregarded. We assume further that the bending stresses are distributed linearly in accordance with the stress-moments relations equation (2.2.18) and that

$$\tau_{xz} = \frac{Q_x}{2h/3}\left[1 - \left(\frac{z}{h/2}\right)^2\right] \qquad (a)$$

$$\tau_{yz} = \frac{Q_y}{2h/3}\left[1 - \left(\frac{z}{h/2}\right)^2\right] \qquad (b) \qquad (2.3.1)$$

$$\sigma_z = \frac{3}{4}p\left[\frac{z}{h/2} - \frac{1}{3}\left(\frac{z}{h/2}\right)^3 + \frac{2}{3}\right] \qquad (c)$$

For the displacement field

$$w = w(x,y,z) = W(x,y,o) = W(x,y) \qquad (a)$$

$$u = z\,\beta_x \qquad (b) \qquad (2.3.2)$$

$$v = z\,\beta_y \qquad (c)$$

where β_x, β_y are "average rotations" of the normal to the middle plane of the plate, they are defined in a variational sense, such that they produce the same work done with the bending moments as the corresponding stress and displacement components, i.e.

$$\int_{-h/2}^{h/2} \sigma_x \, u \, dz = M_x \beta_x \quad ; \text{ etc.}$$

and W is a mean transverse deflection with respect to the plate thickness such that

$$\int_{-h/2}^{h/2} \tau_{xz} \, w(x,y,z)dz = Q_x W; \text{ etc.}$$

Introducing the above assumptions into the functional (2.1.40), integrating with respect to z, noticing for the boundary terms that Figure (2.2.3) applies so that

$$dS = dz \, ds$$

we obtain:

$$\pi_R = -\iint \frac{1}{2}\left[\frac{12}{Eh^3}\left(M_x^2 + M_y^2 - 2\mu M_x M_y + 2(1+\mu)M_{xy}^2\right) + \frac{12}{5hE}(1+\mu)(Q_x^2+Q_y^2) - \frac{12\mu}{5hE}(M_x + M_y)p\right]dx\,dy$$

$$+ \iint \left[M_x \frac{\partial \beta_x}{\partial x} + M_y \frac{\partial \beta_y}{\partial y} + M_{xy}\left(\frac{\partial \beta_x}{\partial y} + \frac{\partial \beta_y}{\partial x}\right) + Q_y\left(\beta_y + \frac{\partial W}{\partial y}\right) + Q_x\left(\beta_x + \frac{\partial W}{\partial x}\right)\right] dx\,dy$$

$$- \iint pW \, dx\,dy$$

$$- \int_{S_\sigma} \left[(\bar{M}_x \ell + \bar{M}_{xy} m)\beta_x + (\bar{M}_{xy}\ell + \bar{M}_y m)\beta_y\right]ds - \int_{S_\sigma} \bar{Q}_n W \, ds$$

$$- \int_{S_u} \left[(M_x \ell + M_{xy} m)(\beta_x - \bar{\beta}_x) + (M_{xy}\ell + M_y m)(\beta_y - \bar{\beta}_y)\right] ds$$

$$- \int_{S_u} Q_n (W - \bar{W}) ds \qquad (2.3.3)$$

Using relations (2.2.30) and

$$\beta_x = \ell\ \beta_n - m\ \beta_s \qquad \text{(a)}$$
$$\beta_y = m\ \beta_n + \ell\ \beta_s \qquad \text{(b)} \qquad (2.3.4)$$

to replace the boundary conditions for normal and tangential terms, yields

$$\pi_R = -\iint \frac{1}{2}\left[\frac{12}{Eh^3}\left(M_x^2+M_y^2-2\mu\, M_xM_y+2(1+\mu)M_{xy}^2\right)\right.$$
$$\left. + \frac{12}{5hE}(1+\mu)(Q_x^2+Q_y^2) - \frac{12\mu}{5hE}(M_x+M_y)p\right]dx\,dy$$
$$+\iint\left[M_x\frac{\partial\beta_x}{\partial x}+M_y\frac{\partial\beta_y}{\partial y}+M_{xy}\left(\frac{\partial\beta_x}{\partial y}+\frac{\partial\beta_y}{\partial x}\right)+Q_y\left(\beta_y+\frac{\partial W}{\partial y}\right)\right.$$
$$\left.+Q_x\left(\beta_x+\frac{\partial W}{\partial x}\right)\right]dx\,dy$$
$$-\iint p\,W\,dx\,dy$$
$$-\int_{s_\sigma}\left[\bar{M}_n\beta_n+\bar{M}_{ns}\beta_s+\bar{Q}_n W\right]ds$$
$$-\int_{s_u}\left[M_n(\beta_n-\bar{\beta}_n)+M_{ns}(\beta_s-\bar{\beta}_s)+Q_n(W-\bar{W})\right]ds \qquad (2.3.5)$$

where $\bar{M}_n$, $\bar{M}_{ns}$, $\bar{Q}_n$, $\bar{W}$, $\bar{\beta}_s$, $\bar{\beta}_n$ denote respectively prescribed quantities of normal moment, twisting moment, shear force intensity, deflection and normal and tangential rotations.

Assuming that the plate is divided into sub-domains, see Figure (2.3.1), and let two neighbouring sub-domains (a) and (b) be isolated; considering the common side it requires the the continuity of the transverse deflection W, normal rotation β_n, tangential rotation β_s, normal moment M_n, twisting moment M_{ns} and normal shear force Q_n. Anticipating that we will not be able to satisfy, at the sub-domains adjacent boundaries, all the above

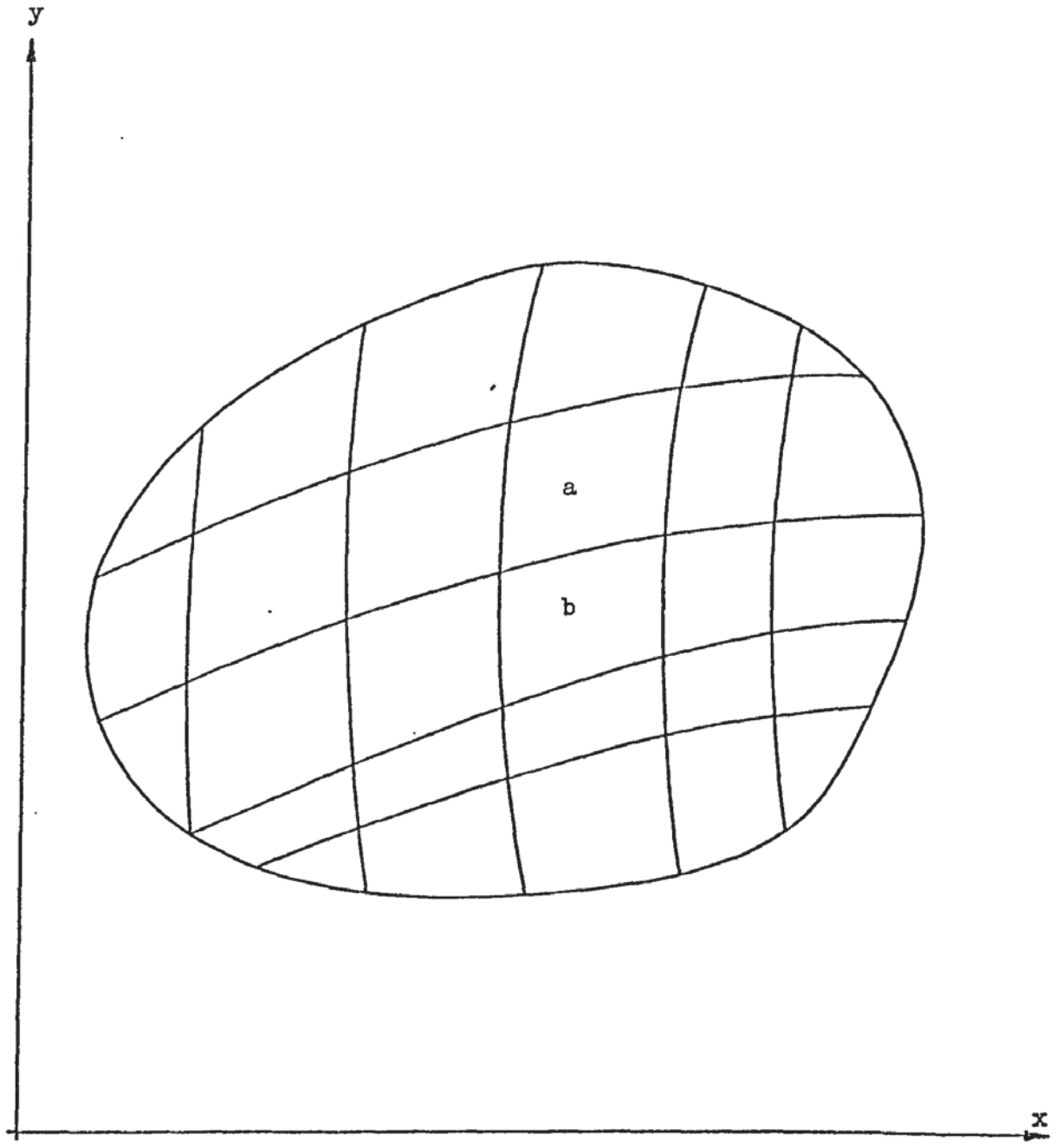

Fig.(2.3.1) Surface of a plate divided into sub-domains.

requirements, we need to convert π_R to a discretized form. The sub-domain continuity requirements follows from the requirements that the functional must be defined [2]. In converting the functional to a discretized form it is possible partially to integrate the terms in the second square bracket of equation (2.3.5).

Evaluating (2.3.5) over each sub-domain, integrating by parts and summing yields

$$\pi_R = \sum_n \Bigg\{ -\frac{1}{2} \iint_{A_n} \Bigg[\frac{12}{Eh^3}(M_x^2+M_y^2 -2\mu\, M_x M_y + 2(1+\mu)M_{xy}^2$$

$$+ \frac{12}{5hE}(1+\mu)(Q_x^2+Q_y^2) - \frac{12\mu}{5hE}(M_x+M_y)p \Bigg] dx\, dy$$

$$+ \iint_{A_n} \Bigg[-\frac{\partial M_x}{\partial x}\beta_x - \frac{\partial M_y}{\partial y}\beta_y - \frac{\partial M_{xy}}{\partial y}\beta_x - \frac{\partial M_{xy}}{\partial x}\beta_y$$

$$+ Q_y \beta_y + Q_x \beta_x - \frac{\partial Q_y}{\partial y} W - \frac{\partial Q_x}{\partial x} W \Bigg] dx\, dy$$

$$- \iint_{A_n} p\, W\, dx\, dy$$

$$+ \int_{s_{n,u}} \Big[M_n \bar{\beta}_n + M_{ns} \bar{\beta}_s - Q_n (W-\bar{W}) \Big] ds$$

$$- \int_{s_{n,\sigma}} \Big[(\bar{M}_n - M_n)\beta_n + (\bar{M}_{ns} - M_{ns})\beta_s + \bar{Q}_n W \Big] ds$$

$$+ \int_{s_n} Q_{n\_} W_{\_} ds + \int_{S_{n,I}} \Big[M_{n\_}\beta_{n\_} + M_{ns\_}\beta_{s\_} \Big] ds$$

$$+ J_n \Bigg\} \qquad (2.3.6)$$

In the above expressions A_n represents the area of a

sub-domain n, and s_n represents its total boundary. The jump term J_n, if it exists, involves only the interior portion of the boundary, $s_{n,I}$ and its form depends on what quantities at the inter sub- domain boundary are assumed to be continuous. The signal - below a variable denotes the variable at the interior side of a boundary.

Assuming an inter sub-domain continuity of M_n, M_{ns} and W, which we propose to accept in our later work, the jump term is given in reference [13], as:

$$J_n = -\int_{s_{n,I}} (M_n \beta_n + M_{ns} \beta_s) ds \qquad (2.3.7)$$

Assuming that the equilibrium equations (2.2.26) and (2.2.27) are satisfied and integrating the last two terms of the second square bracket again, and further assuming that the prescribed normal moment, twisting moment and transverse deflection are satisfied, i.e. $M_n = \bar{M}_n$, $M_{ns} = \bar{M}_{ns}$ on $s_{n,\sigma}$ and $W = \bar{W}$ on $s_{n,u}$. Then, we obtain the discretized form of the Reissner functional to be

$$\pi_R = \sum_n \left\{ -\frac{1}{2} \iint_{A_n} \left[\frac{12}{Eh^3} \left(M_x^2 + M_y^2 - 2\mu M_x M_y + 2(1+\mu) M_{xy}^2 \right) \right] dx\, dy \right.$$

$$- \iint_{A_n} \frac{6(1+\mu)}{5hE} \left[\left(\frac{\partial M_x}{\partial x} \right)^2 + 2 \frac{\partial M_{xy}}{\partial y} \frac{\partial M_x}{\partial x} + \left(\frac{\partial M_y}{\partial y} \right)^2 + \right.$$

$$\left. \left. + 2 \frac{\partial M_{xy}}{\partial x} \frac{\partial M_y}{\partial y} + \left(\frac{\partial M_{xy}}{\partial x} \right)^2 + \left(\frac{\partial M_{xy}}{\partial y} \right)^2 \right] dx\, dy \right.$$

$$+ \iint_{A_n} \frac{6\mu}{5hE} (M_x + M_y) p \; dx\, dy$$

$$\left. + \iint_{A_n} \left[\left(\frac{\partial M_y}{\partial y} + \frac{\partial M_{xy}}{\partial x} \right) \frac{\partial W}{\partial y} + \left(\frac{\partial M_x}{\partial x} + \frac{\partial M_{xy}}{\partial y} \right) \frac{\partial W}{\partial x} \right] dx\, dy \right.$$

$$- \iint_{A_n} p\, W\, dx\, dy - \int_{S_{n,\sigma}} \bar{Q}_n\, W\, ds$$

$$+ \int_{s_{n,u}} (M_n \bar{\beta}_n + M_{ns} \bar{\beta}_s)\, ds \Bigg\} \qquad (2.3.8)$$

Here, we assume continuity of M_n, M_{ns} and W at the inter sub-domain boundaries.

For thin plates, the complementary strain energy due to the stresses σ_z, τ_{xz} and τ_{yz} are assumed zero and the rotations are

$$\beta_x = - \frac{\partial W}{\partial x} \; ; \; \beta_y = - \frac{\partial W}{\partial y} \; : \; \beta_s = - \frac{\partial W}{\partial s} \; ; \; \beta_n = - \frac{\partial W}{\partial n} \qquad (2.3.9)$$

in accordance with the classical assumptions as represented by equations (2.2.4). Using equations (2.3.9) in the discretized form of the Reissner functional, equation (2.3.6), we obtain

$$\pi_R = \sum_n \Bigg\{ - \frac{1}{2} \iint_{A_n} \left[\frac{12}{Eh^3} \left(M_x^2 + M_y^2 - 2\mu\, M_x M_y + 2(1+\mu) M_{xy}^2 \right) \right] dx\, dy$$

$$+ \iint_{A_n} \left[\frac{\partial M_x}{\partial x} \frac{\partial W}{\partial x} + \frac{\partial M_y}{\partial y} \frac{\partial W}{\partial y} + \frac{\partial M_{xy}}{\partial y} \frac{\partial W}{\partial x} + \frac{\partial M_{xy}}{\partial x} \frac{\partial W}{\partial y} \right.$$

$$\left. - Q_y \frac{\partial W}{\partial y} - Q_x \frac{\partial W}{\partial x} - \frac{\partial Q_y}{\partial y} W - \frac{\partial Q_x}{\partial x} W \right] dx\, dy$$

$$- \iint_{A_n} pW\, dx\, dy$$

$$- \int_{s_{n,u}} \left[M_n \frac{\partial \bar{W}}{\partial n} + M_{ns} \frac{\partial \bar{W}}{\partial s} + Q_n (W - \bar{W}) \right] ds + \int_{s_{n,\sigma}} \left[(\tilde{M}_n - M_n) \frac{\partial W}{\partial n} + (\tilde{M}_{ns} - M_{ns}) \frac{\partial W}{\partial s} - \tilde{Q} W \right] ds$$

$$+ \int_{s_n} Q_{n-} W_- ds - \int_{s_{n,I}} \left[M_{n-} \frac{\partial W}{\partial n_-} + M_{ns} \frac{\partial W}{\partial s_-} \right] ds + J_n \Bigg\} \qquad (2.3.10)$$

We assume further that the prescribed normal moment and transverse deflection boundary conditions are satisfied and, for sake of generality, that the twisting moment M_{ns} is discontinuous at the inter sub-domain boundaries. The jump term associated with these conditions is given in reference [13] as:

$$J_n = + \int_{s_{n,I}} M_n \frac{\partial \bar{W}}{\partial n} \, ds \tag{2.3.11}$$

Substituting (2.3.11) into (2.3.10), integrating the last two terms of the second square bracket and assuming equilibrium within the sub-domains, yields

$$\pi_R = \sum_n \left\{ -\frac{1}{2} \iint_{A_n} \left[\frac{12}{Eh^3} \left(M_x^2 + M_y^2 - 2\mu \, M_x M_y + 2(1+\mu) M_{xy}^2 \right] dx \, dy \right.$$

$$+ \iint_{A_n} \left[\left(\frac{\partial M_y}{\partial y} + \frac{\partial M_{xy}}{\partial x} \right) \frac{\partial W}{\partial y} + \left(\frac{\partial M_x}{\partial x} + \frac{\partial M_{xy}}{\partial y} \right) \frac{\partial W}{\partial x} \right] dx \, dy$$

$$- \int_{s_n} M_{ns} \frac{\partial W}{\partial s} \, ds - \iint_{A_n} p \, W \, dx \, dy$$

$$\left. - \int_{s_{n,u}} M_n \frac{\partial \bar{W}}{\partial n} \, ds + \int_{s_{n,\sigma}} \left[\bar{M}_{ns} \frac{\partial W}{\partial s} - \bar{Q}_n \, W \right] ds \right\} \tag{2.3.12}$$

where

$$s_n = s_{n,I} + s_{n,u} + s_{n,\sigma} = \text{total boundary}$$

of the sub-domain n.

Using the integration formula:

$$\int_{s_{n,\sigma}} \bar{M}_{ns} \frac{\partial W}{\partial s} \, ds = \bar{M}_{ns} \, W \Big|_{s_{n,\sigma}} - \int_{s_{n,\sigma}} \frac{\partial \bar{M}_{ns}}{\partial s} \, W \, ds$$

Assuming $\bar{M}_{ns}$ continuous, and a close smooth curve for

the plate then:

$$\int_{s_{n,\sigma}} \bar{M}_{ns} \frac{\partial W}{\partial s} \, ds = - \int_{s_{n,\sigma}} \frac{\partial \bar{M}_{ns}}{\partial s} W \, ds \qquad (2.3.13)$$

which is true when the contribution of all domains are added, then equations (2.3.13) enables the introduction of the imposed effective shear intensity, related by expression (2.2.32) into equation (2.3.12).

The final form of the Reissner functional for thin plates is then:

$$\begin{aligned} \pi_R = \sum_n \Bigg\{ & - \frac{1}{2} \iint_{A_n} \left[\frac{12}{Eh^3} \left(M_x^2 + M_y^2 - 2\mu \, M_x M_y + 2(1+\mu) M_{xy}^2 \right) \right] dx \, dy \\ & + \iint_{A_n} \left[\left(\frac{\partial M_y}{\partial y} + \frac{\partial M_{xy}}{\partial x} \right) \frac{\partial W}{\partial y} + \left(\frac{\partial M_x}{\partial x} + \frac{\partial M_y}{\partial y} \right) \frac{\partial W}{\partial x} \right] dx \, dy \\ & - \int_{s_n} M_{ns} \frac{\partial W}{\partial s} \, ds - \iint_{A_n} p \, W \, dx \, dy \\ & - \int_{s_{n,u}} M_n \frac{\partial \bar{W}}{\partial n} \, ds - \int_{s_{n,\sigma}} \bar{V}_n \, W \, ds \Bigg\} \end{aligned} \qquad (2.3.14)$$

2.3.3) Reissner's Principle Applied to Plate Bending.

To determine the conditions for extremizing the Reissner functional, equation (2.3.8), we allow independent variations δW, δM_x, δM_y, δM_{xy}. After suitable manipulation and integration by parts, for full details see Appendix 1 , the variation of π_R becomes:

$$\delta \pi_R = \sum_n \Bigg\{ \iint_{A_n} \left[- \left(\frac{\partial^2 M_x}{\partial x^2} + 2 \frac{\partial^2 M_{xy}}{\partial x \partial y} + \frac{\partial^2 M_y}{\partial y^2} + p \right) \delta W \right.$$

$$+\left[-\frac{\partial^2 W}{\partial x^2}+2L\left(\frac{\partial^2 M_x}{\partial x^2}+\frac{\partial^2 M_{xy}}{\partial y\,\partial x}\right)+\frac{6\mu}{5hE}\,p-\frac{12}{Eh^3}\,(M_x-\mu M_y\right]\delta M_x$$

$$+\left[-\frac{\partial^2 W}{\partial y^2}+2L\left(\frac{\partial^2 M_y}{\partial y^2}+\frac{\partial^2 M_{xy}}{\partial y\,\partial x}\right)+\frac{6\mu}{5hE}\,p-\frac{12}{Eh^3}\,(M_y-\mu\,M_x)\right]\delta M_y$$

$$+\left[-2\,\frac{\partial^2 W}{\partial x\,\partial y}+2L\left(\frac{\partial^2 M_x}{\partial x\,\partial y}+\frac{\partial^2 M_y}{\partial y\,\partial x}+\frac{\partial^2 M_{xy}}{\partial x^2}+\frac{\partial^2 M_{xy}}{\partial y^2}\right)\right.$$

$$\left.-\frac{12}{Eh^3}\times 2(1+\mu)M_{xy}\right]\delta M_{xy}\Bigg]\,dx\,dy$$

$$+\int_{s_{n,\sigma}}(Q_n-\bar{Q}_n)\,\delta W\,ds-\int_{s_{n,u}}(\beta_n-\bar{\beta}_n)\,\delta M_n\,ds-\int_{s_{n,u}}(\beta_s-\bar{\beta}_s)\,\delta M_{ns}\,ds \qquad (2.3.15)$$

where

$$L=\frac{6(1+\mu)}{5hE} \qquad (2.3.16)$$

For π_R to be stationary, $\delta\pi_R = 0$. Then, since δW, δM_n, δM_{ns}, δM_x, δM_y, δM_{xy} are all arbitrary independent variations, this implies

$$-\frac{\partial^2 W}{\partial x^2}+2L\left(\frac{\partial^2 M_x}{\partial x^2}+\frac{\partial^2 M_{xy}}{\partial y\,\partial x}\right)+\frac{6\mu}{5hE}\,p-\frac{12}{Eh^3}\,(M_x-\mu M_y)=0 \qquad (a)$$

$$-\frac{\partial^2 W}{\partial y^2}+2L\left(\frac{\partial^2 M_y}{\partial y^2}+\frac{\partial^2 M_{xy}}{\partial y\,\partial x}\right)+\frac{6\mu}{5hE}\,p-\frac{12}{Eh^3}\,(M_y-\mu M_x)=0 \qquad (b) \qquad (2.3.17)$$

$$-\frac{\partial^2 W}{\partial x\,\partial y}+2L\left(\frac{\partial^2 M_x}{\partial x\,\partial y}+\frac{\partial^2 M_y}{\partial y\,\partial x}+\frac{\partial^2 M_{xy}}{\partial x^2}+\frac{\partial^2 M_{xy}}{\partial y^2}\right)-\frac{12}{Eh^3}\times 2(1+\mu)M_{xy}=0 \qquad (c)$$

$$\frac{\partial^2 M_x}{\partial x^2}+2\,\frac{\partial^2 M_{xy}}{\partial x\,\partial y}+\frac{\partial^2 M_y}{\partial y^2}+p=0 \qquad (d)$$

These are the Euler equations corresponding to $\delta\pi_R = 0$. Equations (2.3.17) are the fundamental relations which govern the behaviour of plates, including the effect of transverse shear deformation, see references [11] and [14]. The first three equations are strain-moment relations and the fourth is the plate equilibrium equation (2.2.28). The natural boundary conditions for the vanish of the boundary line integrals are

$$Q_n = \bar{Q}_n \quad ; \quad \beta_n = \bar{\beta}_n \; ; \quad \beta_s = \bar{\beta}_s \tag{2.3.18}$$

and the fundamental or "forced" boundary conditions

$$W = \bar{W} \; ; \quad M_n = \bar{M}_n \; ; \quad M_{ns} = \bar{M}_{ns} \tag{2.3.19}$$

From equations (2.3.18) it follows that

$$\begin{aligned} \beta_x &= -\frac{\partial N}{\partial x} + 2L\, Q_x \qquad \text{(a)} \\ \beta_y &= -\frac{\partial N}{\partial y} + 2L\, Q_y \qquad \text{(b)} \end{aligned} \tag{2.3.20}$$

where the shear force intensities Q_x and Q_y are given by equations (2.2.26) and (2.2.27).

The displacement components of equations (2.3.2b) and (2.3.2c) can finally be represented as:

$$\begin{aligned} u &= z\left[-\frac{\partial N}{\partial x} + 2L\, Q_x\right] \qquad \text{(a)} \\ v &= z\left[-\frac{\partial N}{\partial y} + 2L\, Q_y\right] \qquad \text{(b)} \end{aligned} \tag{2.3.21}$$

In a similar fashion, we could extremize the Reissner functionalequation (2.3.14) specialized for thin plates (that is, neglecting shear effects). Then, we would obtain, as the Euler-equations, three curvature-moment relations corresponding to equations (2.3.17 a,b,c) where the terms due to shear deformation are neglected. The fourth Euler equation would be the plate equilibrium equation (2.2.28). As natural boundary conditions we would obtain:

$$\begin{aligned} V_n &= \bar{V}_n \qquad \text{(a)} \\ \frac{\partial N}{\partial n} &= \frac{\partial \bar{N}}{\partial n} \qquad \text{(b)} \end{aligned} \tag{2.3.22}$$

The fundamental or "forced" boundary conditions would be :

$$M_n = \bar{M}_n \qquad \text{(a)}$$
$$W = \bar{W} \qquad (2.3.23)$$

2.4) Free Transverse Vibrations of Thin Plates.

Up to this stage we have considered only the case of structural bodies, and in particular elastic plates, in static equilibrium. However, plate problems often involve consideration of dynamic disturbances produced by time dependent external forces or displacements and, therefore, it is often required to know the effect of the vibrations on the performance of such structures. Although, we have limited ourselves to the study of natural frequencies and normal modes, they are a very important first step in the dynamic-response analysis of linear structures. In writing the governing differential equations of motion, for thin plates (i.e. shear deformation neglected) basically two approaches are possible, applying d'Alembert's dynamic equilibrium principle [15] or by a variational formulation [16]. We shall pursue, here, a formulation by forming the dynamic Reissner functional and then extremizing it, by analogy with Hamilton's principle, which is based in the Lagrangian functional, i.e.

$$\delta \int_{t_1}^{t_2} \mathcal{L}\, dt$$

where

$$\mathcal{L} = T - U$$

in which T is the kinetic energy of the system and U the total potential energy. Hamilton's variational principle may be interpreted as:

Among all possible time histories of displacement satisfying the given boundary conditions and which also satisfy conditions at times t_1 and t_2, the history which is the actual

solution makes the Lagrangian functional a stationary (minimum).

We say by analogy, because the dynamic functional that we pretend to form, being a mixed functional does not represent the Lagrangian as such, hence the stationary value cannot be shown to be a minimum. Nevertheless, it can be extremized .

2.4.1) Equation of Motion for Thin Plates.

Considering a vibrating plate the kinetic energy at the time t, due to the vertical movement of the particles of the plate, can be represented in terms of the deflection of the middle surface of the plate as:

$$T = \frac{1}{2} \iint_A \rho h \left(\frac{\partial W(x,y,t)}{\partial t} \right)^2 dx\, dy \qquad (2.4.1)$$

where ρ is the mass of the plate per unit volume and h its thickness.

The dynamic functional is formed as

$$\pi_{R_D} = \pi_R - T \qquad (2.4.2)$$

where π_R is the Reissner functional equation (2.3.14). Then

$$\delta \int_{t_1}^{t_2} (\pi_{R_D})\, dt = \sum_n \left\{ \delta \int_{t_1}^{t_2} \left\{ \iint_{A_n} \left[-\frac{1}{2} \left[\frac{12}{Eh^3} \left(M_x^2 + M_y - 2\mu M_x M_y + 2(1+\mu) M_{xy}^2 \right) \right] + \left(\frac{\partial M_y}{\partial y} + \frac{\partial M_{xy}}{\partial x} \right) \frac{\partial W}{\partial y} + \left(\frac{\partial M_x}{\partial x} + \frac{\partial M_{xy}}{\partial y} \right) \frac{\partial W}{\partial x} - pW \right] dx\, dy - \int_{s_n} M_{ns} \frac{\partial W}{\partial s}\, ds \right.$$

$$\left. - \int_{s_{n,u}} M_n \frac{\partial \overline{W}}{\partial n}\, ds - \int_{s_{n,\sigma}} \overline{V}_n W\, ds - \frac{1}{2} \iint_{A_n} \rho h \left(\frac{\partial W}{\partial t} \right)^2 dx\, dy \right\} dt \right\} = 0 \qquad (2.4.3)$$

which can be interpreted as follows: Among all possible time histories

of all states of stress and displacement which satisfy the mechanical and displacement boundary conditions and also the conditions at times t_1 and t_2, the history which is the actual solution makes π_{R_D} a stationary.

We extremize π_{R_D} by taking independent variations δW, δM_x, δM_y, δM_{xy}. Noticing that:

$$\delta \int_{t_1}^{t_2} \left\{ \iint_{A_n} \frac{1}{2} \rho h \left(\frac{\partial W}{\partial t}\right)^2 dx\, dy \right\} dt$$

$$= \int_{t_1}^{t_2} \left\{ \iint_{A_n} \rho h \frac{\partial W}{\partial t} \frac{\partial}{\partial t} \delta W \, dx\, dy \right\} dt$$

$$= \int_{t_1}^{t_2} \left\{ - \iint_{A_n} \rho h \frac{\partial^2 W}{\partial t^2} \delta W \, dx\, dy \right\} dt + \rho h \frac{\partial W}{\partial t} \delta W \Bigg|_{t_1}^{t_2} \qquad (2.4.4)$$

and that at times t_1 and t_2 the motion is prescribed, implying $\delta W = \delta M_x = \delta M_{xy} = 0$, hence the last term of relation (2.4.4) is zero i.e.

$$\delta \int_{t_1}^{t_1} \left\{ \iint_{A_n} \frac{1}{2} \rho h \left(\frac{\partial W}{\partial t}\right)^2 dx\, dy = \int_{t_1}^{t_2} \left\{ - \iint_{A_n} \rho h \frac{\partial^2 W}{\partial t^2} \delta W \, dx\, dy \right\} dt \qquad (2.4.5)$$

Noticing relation (2.4.5), and after suitable manipulation and integration by parts with respect to the spatial coordinates of all derivative terms yields:

$$\delta \int_{t_1}^{t_2} (\pi_{R_D})\, dt = \sum_n \left\{ \int_{t_1}^{t_2} \iint_{A_n} \left[- \left(\frac{\partial^2 M_x}{\partial x^2} + 2 \frac{\partial^2 M_{xy}}{\partial x \partial y} + \frac{\partial^2 M_y}{\partial y^2} + p - \rho h \frac{\partial^2 W}{\partial t^2} \right) \delta W \right.\right.$$

$$+ \left(- \frac{\partial^2 W}{\partial x^2} - \frac{12}{Eh^3} (M_x - \mu M_y) \right) \delta M_x + \left(- \frac{\partial^2 W}{\partial y^2} - \frac{12}{Eh^3} (M_y - \mu M_x) \right) \delta M_y$$

$$+\left(2\frac{\partial^2 W}{\partial x \partial y} - \frac{12}{Eh^3} \times 2(1+\mu)\, M_{xy}\right) \delta M_{xy} \Bigg] dx\, dy$$

$$+\int_{s_{n,\sigma}} (V_n - \bar{V}_n)\,\delta W\, ds + \int_{s_{n,u}} \left(\frac{\partial W}{\partial n} - \frac{\partial \bar{W}}{\partial n}\right) \delta M_n\, ds \Bigg\} dt = 0 \qquad (2.4.6)$$

Since δW, δM_x, δM_y, δM_{xy}, δM_n are all arbitrary independent variations this implies:

$$\frac{\partial^2 M_x}{\partial x^2} + 2\frac{\partial^2 M_{xy}}{\partial x \partial y} + \frac{\partial^2 M_y}{\partial y^2} + p - ph\frac{\partial^2 W}{\partial t^2} = 0 \qquad (2.4.7)$$

$$-\frac{\partial^2 W}{\partial x^2} - \frac{12}{Eh^3}(M_y - \mu M_x) = 0 \qquad (a)$$

$$-\frac{\partial^2 W}{\partial y^2} - \frac{12}{Eh^3}\left(M_y - \mu M_x\right) = 0 \qquad (b) \qquad (2.4.8)$$

$$-2\frac{\partial^2 W}{\partial x \partial y} - \frac{12}{Eh^3} \times 2(1+\mu)\, M_{xy} = 0 \qquad (c)$$

These are the Euler equations corresponding to

$$\delta \int_{t_1}^{t_2} (\pi_{R_D})\, dt = 0.$$

Equation (2.4.7) is the equation of motion which governs the behaviour of vibrating plates. Equations (2.4.8) are strain-moments relations. The natural boundary conditions for the vanish of the boundary line integrals are:

$$V_n = \bar{V}_n$$

$$\frac{\partial W}{\partial n} = \frac{\partial \bar{W}}{\partial n}$$

and the fundamental or "forced" boundary conditions

$$W = \bar{W}$$

$$M_n = \bar{M}_n$$

For free vibrations p = 0, and the equation of motion is

$$\frac{\partial^2 M_x}{\partial x^2} + 2\frac{\partial^2 M_{xy}}{\partial x \partial y} + \frac{\partial^2 M_y}{\partial y^2} - \rho h \frac{\partial^2 W}{\partial t^2} = 0 \qquad (2.4.9)$$

Combination of equation (2.4.9) with the matrix-relation (2.2.12) yields the familiar equation of motion for thin plates.

$$\frac{\partial^4 W}{\partial x^4} + 2\frac{\partial^4 W}{\partial x^2 \partial y^2} + \frac{\partial^4 W}{\partial x^4} + \rho \frac{h}{D} \frac{\partial^2 W}{\partial t^2} = 0 \qquad (2.4.10)$$

where D is the plate bending rigidity, given by equation (2.2.13).

Assuming a harmonic motion, we may write

$$W(x,y,t) = \hat{W}(x,y) \sin \omega t \qquad (2.4.11)$$

Here, $\hat{W}(x,y)$ is the shape function describing the modes of vibration of the middle surface of the plate and ω is the natural frequency of the vibrations. Substitution of equation (2. 4.11) into equation (2.4.10) gives:

$$\frac{\partial^4 \hat{W}}{\partial x^4} + 2\frac{\partial^4 \hat{W}}{\partial x^2 \partial y^2} + \frac{\partial^4 \hat{W}}{\partial y^4} - \rho \frac{h}{D} \omega^2 \hat{W} = 0 \qquad (2.4.12)$$

Normally, represented as an eigenvalue equation

$$\nabla^4 \hat{W} = \lambda^* \hat{W} \qquad (2.4.13)$$

where

$$\lambda^* = \rho \frac{h}{D} \omega^2 \qquad (2.4.14)$$

If an exact solution of equation (2.4.13) exists it will consist of infinite sets of frequencies and associated normal modes (eigenvalues and eigenvectors).

2.4.2) <u>The Dynamic Reissner Functional-Free Vibrations</u>.

For a plate vibrating freely and assuming homogeneous boundary conditions, i.e. (the specified, effective shear intensity

$\bar{V}_n$ and normal rotation $\partial\bar{W}/\partial n$ are assumed zero), the integral due to the load $p(x,y)$ and the last two line integrals of relation (2.4.3) are zero. The functional can then be simplified to:

$$\pi_{R_D} = \sum_n \left\{ \iint_{A_n} -\frac{1}{2}\left[\frac{12}{Eh^3}\left(M_x^2+M_y^2-2\mu\, M_xM_y+2(1+\mu)M_{xy}^2\right)\right] dx\,dy \right.$$

$$+\iint_{A_n}\left[\left(\frac{\partial M_y}{\partial y}+\frac{\partial M_{xy}}{\partial x}\right)\frac{\partial W}{\partial y}+\left(\frac{\partial M_x}{\partial x}+\frac{\partial M_{xy}}{\partial y}\right)\frac{\partial W}{\partial x}\right] dx\,dy$$

$$\left. -\int_{s_n} M_{ns}\,\frac{\partial W}{\partial s}\,ds-\frac{1}{2}\iint_{A_n}\rho h\left(\frac{\partial W}{\partial t}\right)^2 dx\,dy\right\} \qquad (2.4.15)$$

This functional will be the starting point for our dynamic work to be further developed in Chapter 6.

2.5) Buckling of Thin Plates.

2.5.1) Basic Concepts.

Thin plates are often subject to the action of a combination of compressive normal and shearing forces, $(\bar{N}_n,\bar{N}_{ns})$ assumed to act in the middle plane at the boundaries, as in Figure (2.5.1). If these in-plane edge forces are sufficiently small, the equilibrium of the plate is stable and the resulting deformations are characterized by the absence of transverse deformations (i.e. $w = 0$, $u \neq 0$, $v \neq 0$), hence only in-plane deformations appear in the plate.

As the loads $\bar{N}_n$, $\bar{N}_{ns}$ are increased gradually, at a certain combination of load intensity, a marked change in the behaviour of the deformation pattern takes place, the plate reaches a state of neutral equilibrium and the middle surface may be flat or curved. The states of the internal stresses associated with the

two forms of neutral equilibrium are fundamentally different. Under the flat form the plate undergoes pure membrane stresses while in the curved form bending stresses are also present. The edge load to accomplish this is called the elastic buckling critical load. Once this stage is reached the transverse deflection increases very rapidly and eventually the plate will collapse.

For a more complete discussion of the buckling theory of plates reference to the books of Timoshenko [17], Bulson [18] and Brush [19] is suggested.

2.5.2) The Reissner Functional for Buckling Problems.

Consider a differential element dx dy, and h, see Figure (2.5.1), without strains in the middle surface, beyond that caused initially by the edge loads. Suppose the element is displaced in the transverse direction, see Figure (2.5.2), a differential stretched length, say $\bar{dx}$, can be approximated as:

$$\bar{dx} = \left[1 + \left(\frac{\partial W}{\partial x}\right)^2\right]^{\frac{1}{2}} dx$$

By expansion of this expression in series by the use of the binomial theorem

$$\bar{dx} = \left[1 + \tfrac{1}{2}\left(\frac{\partial W}{\partial x}\right)^2 + \cdots\right] dx$$

hence, the increment for the differential element, in the x direction is

$$d\Delta x = \bar{dx} - dx = \tfrac{1}{2}\left(\frac{\partial W}{\partial x}\right)^2 dx$$

Similarly

$$d\Delta y = \tfrac{1}{2}\left(\frac{\partial W}{\partial y}\right)^2 dy$$

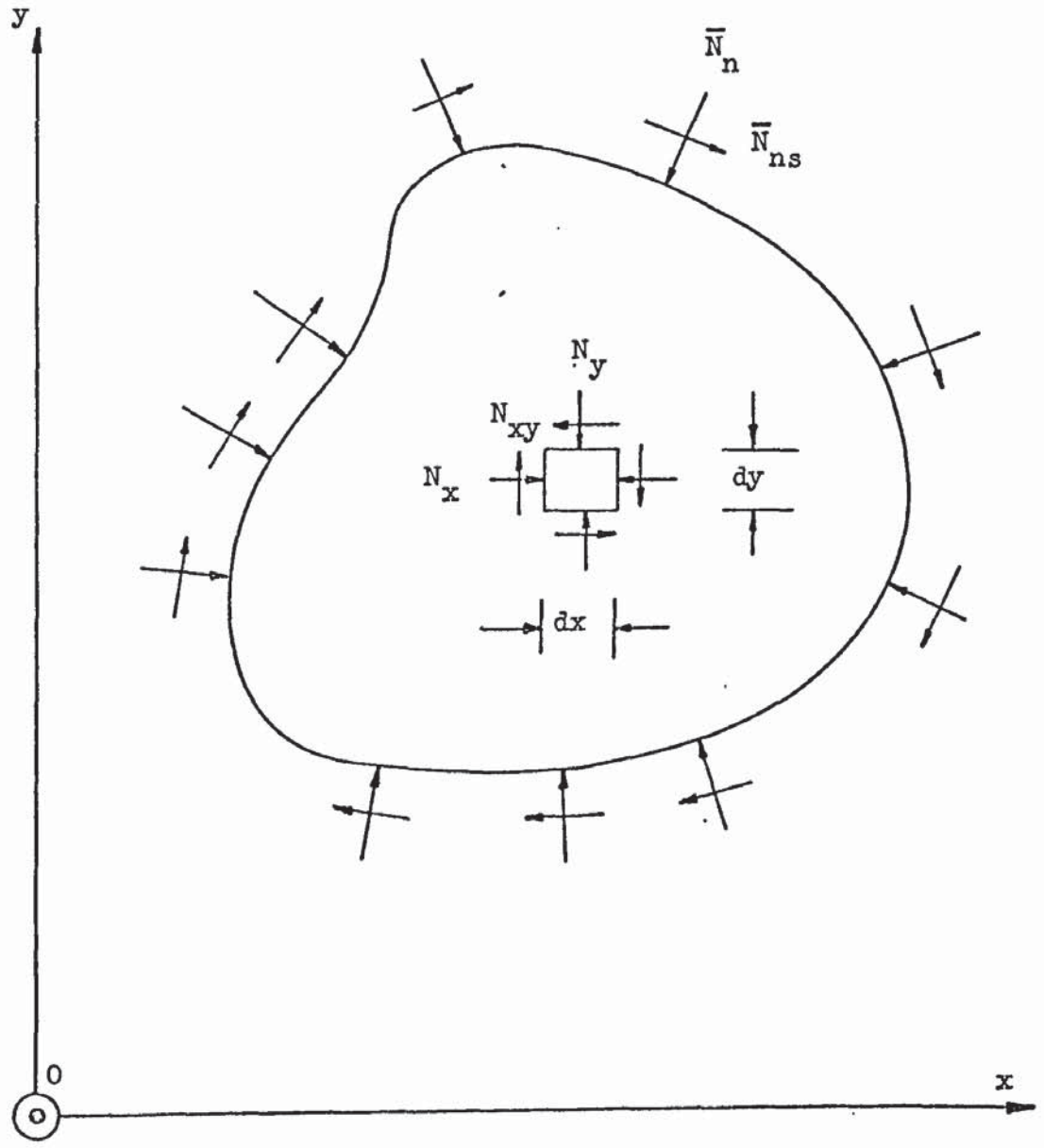

Fig.(2.5.1) Plate of general shape subject to in-plane edge loads $\bar{N}_n$, $\bar{N}_{ns}$ per unit length.

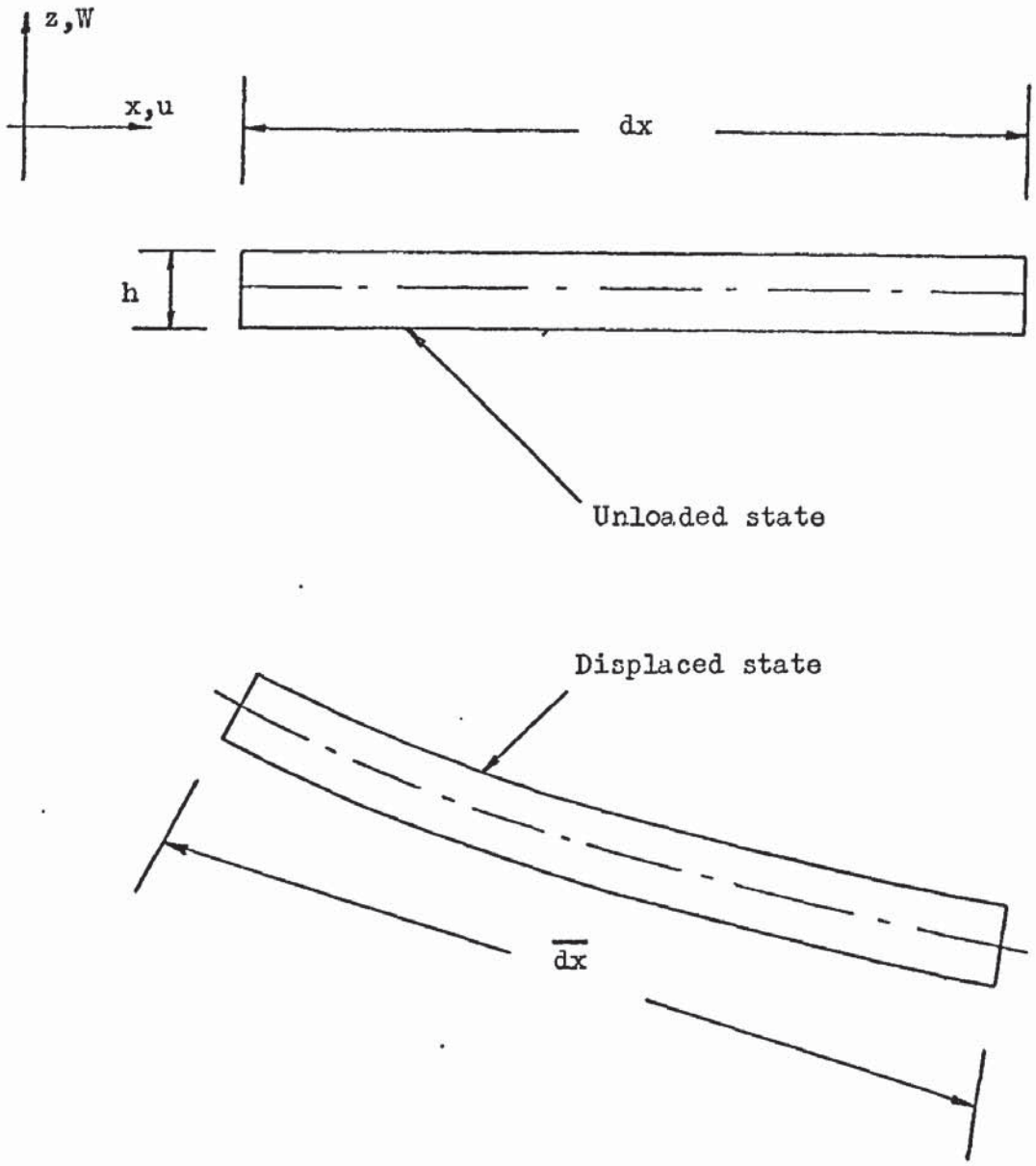

Fig.(2.5.2) Plate displacement geometry.

$$d\,\Delta xy = \frac{\partial W}{\partial x}\,\frac{\partial W}{\partial y}\,dy$$

The work of the forces $N_x dy, N_y dx, N_{xy} dx$ on the differential element is:

$$\tfrac{1}{2} N_x \left(\frac{\partial W}{\partial y}\right)^2 dy\,dx + \tfrac{1}{2} N_y \left(\frac{\partial W}{\partial y}\right)^2 dy\,dx +$$

$$+ N_{xy}\,\frac{\partial W}{\partial x}\,\frac{\partial W}{\partial y}\,dx\,dy$$

Thus, the total work done for the plate can be represented as:

$$W_D = \tfrac{1}{2} \iint_A \left[N_x \left(\frac{\partial W}{\partial x}\right)^2 + N_y \left(\frac{\partial W}{\partial y}\right)^2 + 2N_{xy}\,\frac{\partial W}{\partial x}\,\frac{\partial W}{\partial x} \right] dx\,dy \qquad (2.5.1)$$

where N_x, N_y, N_{xy} are internal in-plane forces per unit length, taken as positive in compression and acting in the middle plane of the plate.

We can now form the specialized Reissner functional by adding $-W_D$ to the Reissner functional equation (2.3.14), but letting the transverse load be $p = 0$.

The buckling Reissner functional is then

$$\pi_{R_B} = \sum_n \left\{ -\tfrac{1}{2} \iint_{A_n} \left[\frac{12}{Eh^3} \left(M_x^2 + M_y^2 - 2\mu M_x M_y + 2(1+\mu) M_{xy}^2 \right) \right] dx\,dy \right.$$

$$+ \iint_{A_n} \left[\left(\frac{\partial M_y}{\partial y} + \frac{\partial M_{xy}}{\partial x} \right) \frac{\partial W}{\partial y} + \left(\frac{\partial M_x}{\partial x} + \frac{\partial M_{xy}}{\partial y} \right) \frac{\partial W}{\partial x} \right] dx\,dy$$

$$\left. - \int_{s_n} M_{ns}\,\frac{\partial W}{\partial s}\,ds - \tfrac{1}{2} \iint_{A_n} \left[N_x \left(\frac{\partial W}{\partial x}\right)^2 + N_y \left(\frac{\partial W}{\partial y}\right)^2 + 2N_{xy}\,\frac{\partial W}{\partial x}\,\frac{\partial W}{\partial y} \right] dx\,dy \right\}$$

For neutral equilibrium in the buckled configuration:

$$\delta \pi_{R_B} = 0 \qquad (2.5.3)$$

Taking independent variations with respect to W, M_x, M_y, M_{xy}, integrating by parts and rearranging the terms yields:

$$\delta\pi_{R_B} = \sum_n \Bigg\{ \iint_{A_n} \Bigg[- \left(\frac{\partial^2 M_x}{\partial x^2} + 2\,\frac{\partial^2 M_{xy}}{\partial x \partial y} + \frac{\partial^2 M_y}{\partial y^2} \right.$$

$$\left. - N_x \frac{\partial^2 W}{\partial x^2} - N_y \frac{\partial^2 W}{\partial y^2} - 2N_{xy} \frac{\partial^2 W}{\partial x \partial y} \right) \delta W$$

$$+ \left(\frac{\partial N_x}{\partial x} + \frac{\partial N_{xy}}{\partial y} \right) \frac{\partial W}{\partial x}\ \delta W + \left(\frac{\partial N_y}{\partial y} + \frac{\partial N_{xy}}{\partial x} \right) \frac{\partial W}{\partial y}\ \delta W$$

$$+ \left(- \frac{\partial^2 W}{\partial x^2} - \frac{12}{Eh^3}\ (M_x - \mu\, M_y) \right) \delta M_x$$

$$+ \left(- \frac{\partial^2 W}{\partial y^2} - \frac{12}{Eh^3}\ (M_y - \mu M_x) \right) \delta M_y$$

$$+ \left(- 2\,\frac{\partial^2 W}{\partial x \partial y} - \frac{12}{Eh^3} \times 2(1+\mu) M_{xy} \right) \delta M_{xy} \Bigg] \, dx\, dy$$

$$+ \int_{s_{n,\sigma}} \left(V_n - N_n \frac{\partial W}{\partial n} - N_{ns} \frac{\partial W}{\partial s} - \bar{V}_n \right) \delta W \, ds$$

$$+ \int_{s_{n,u}} \left(\frac{\partial W}{\partial n} - \frac{\partial \bar{W}}{\partial n} \right) \delta M_n \, ds \Bigg\} = 0 \qquad (2.5.4)$$

Since δW, δM_x, δM_y, δM_{xy}, δM_n are all arbitrary independent variations we can deduce the Euler equations and natural boundary conditions from $\delta\pi_R = 0$. The second and third group of terms in the domain integral vanish because they involve the equilibrium equations, without body forces, which, for buckling problems, are assumed satisfied a priori [17]. In the first line integral the effective shear force V_n is now augmented by components of the in plane forces N_n and N_{ns} at the plate boundary.

The buckling governing equation is then:

$$\frac{\partial^2 M_x}{\partial x^2} + 2\frac{\partial^2 M_{xy}}{\partial x \partial y} + \frac{\partial^2 M_y}{\partial y^2} - N_x \frac{\partial^2 W}{\partial x^2} - N_y \frac{\partial^2 W}{\partial y^2} - 2N_{xy} \frac{\partial^2 W}{\partial x \partial y} = 0 \quad . \tag{2.5.5}$$

Introduction of the moment-curvature relations (2.2.12) into equation (2.5.5) yields the eigenvalue problem defined by the homogeneous differential equation:

$$D\nabla^4 W = -\left(N_x \frac{\partial^2 W}{\partial x^2} + N_y \frac{\partial^2 W}{\partial y} + 2N_{xy} \frac{\partial^2 W}{\partial x \partial y} \right) . \tag{2.5.6}$$

In a buckling analysis we presume that the resulting internal in-plane force distribution N_x, N_y, N_{xy} due to an arbitrary in-plane edge force $\bar{N}_n$, $\bar{N}_{ns}$ is known for some trial load level. Thus, we can assume that the resulting internal in-plane forces N_x, N_y, N_{xy} are represented by certain known expressions $N_{x_o}, N_{y_o}, N_{xy_o}$ with a common factor λ_b such that

$$[N_x \quad N_y \quad N_{xy}] = \lambda_b [N_{x_o} \quad N_{y_o} \quad N_{xy_o}] \tag{2.5.7}$$

Substituting relation (2.5.7) into equation (2.5.6), we get

$$D\nabla^4 W = -\lambda_b \left(N_{x_o} \frac{\partial^2 W}{\partial x^2} + N_{y_o} \frac{\partial^2 W}{\partial y^2} + N_{xy_o} \frac{\partial^2 W}{\partial x \partial y} \right) , \tag{2.5.8}$$

since

$$[N_{x_o} \quad N_{y_o} \quad N_{xy_o}] = h[\sigma_{x_o} \quad \sigma_{y_o} \quad \tau_{xy_o}]$$

where $[\sigma_{x_o} \quad \sigma_{y_o} \quad \sigma_{xy_o}]$ are the expressions for the state of stress due to a trial edge load and h is the plate thickness, we can represent equation (2.5.8) as:

$$D\nabla^4 W = -\lambda_b \left(h\,\sigma_{x_o} \frac{\partial^2 W}{\partial x^2} + h\,\sigma_{y_o} \frac{\partial^2 W}{\partial y^2} + h\,\tau_{xy_o} \frac{\partial^2 W}{\partial x \partial y} \right) \tag{2.5.9}$$

If an exact solution of equation (2.5.9) can be found it will consist of an infinite set of λ_b's and corresponding modes of buckling. The minimum value of λ_b is called the buckling factor and the critical load distribution will then be given by multiplying it by the trial load expressions.

2.6) Methods for the Solution of the Governing Differential Equations for Static, Dynamic and Buckling Plate Problems.

2.6.1) Exact Solutions.

To solve a static thin plate problem a linear partial differential equation of 4th order must be solved satisfying the characteristic boundary conditions of each individual problem. The exact solution requires therefore the satisfaction of the exact boundary conditions and the governing differential equation (2.2.30).

In general this is a very difficult problem to solve and consequently the exact solutions are very rare and are limited to a very small number of simple plate shapes, boundary conditions and loads. In the few cases which lend themselves to exact solutions the linearity of equation (2.2.30) was used, allowing the linear combination of solutions in accordance with the principle of superposition.

In general the exact solution is in the form

$$W(x,y) = W_H + W_p \qquad (2.6.1)$$

where W_H is the solution of the homogeneous equation

$$\nabla^4 W = 0 \qquad (2.6.2)$$

and W_p is the particular solution of equation (2.2.30).

The solution as given by equation (2.6.1) can be interpreted as the superposition of the homogeneous solution, W_H, when only edge forces are acting and the particular solution, W_p, due to the applied load.

We shall now briefly illustrate Navier and Levy's methods to a few situations of the type that we will subsequently treat by finite elements. A full account of the available analytical solutions for particular cases may be found in references [10],[17],[20]

a) Navier's Method

The simply supported rectangular plate was first solved

in 1820 by Navier [10]. The transverse load p(x,y), acting in a simply supported rectangular plate Figure (2.6.1), is first expanded as a double trignometric sine series:

$$p(x,y) = \sum_{m=1}^{\infty} \sum_{n=1}^{\infty} C_{mn} \sin \frac{m\pi x}{a} \sin \frac{n\pi y}{b} \tag{2.6.3}$$

The coefficients C_{mn} are determined by usual Fourier methods and are given by:

$$C_{mn} = \frac{4}{ab} \int_0^a \int_0^b p(x,y) \sin \frac{m\pi x}{a} \sin \frac{n\pi y}{b} \, dx \, dy \tag{2.6.4}$$

Assuming a deflection shape in the form of a double trigonometric sine series

$$W = \sum_{m=1}^{\infty} \sum_{n=1}^{\infty} b_{mn} \sin \frac{m\pi x}{a} \sin \frac{n\pi y}{b} \tag{2.6.5}$$

the boundary conditions are satisfied completely. Substituting relations (2.6.3) and (2.6.5) into the plate governing (2.2.30) yields:

$$b_{mn} \left(\frac{m^4\pi^4}{a^4} + \frac{2m^2n^2\pi^4}{a^2b^2} + \frac{n^4\pi^4}{b^4} \right) = \frac{1}{D} C_{mn} \tag{2.6.6}$$

hence, the unknown coefficients b_{mn} are given by

$$b_{mn} = \frac{C_{mn}}{D\pi^4 \left(\frac{m^2}{a^2} + \frac{n^2}{b^2} \right)^2} \tag{2.6.7}$$

Replacing equation (2.6.7) into (2.6.5) an analytical solution for the deflection of the plate is obtained as:

$$W = \frac{1}{\pi^4 D} \sum_{m=1}^{\infty} \sum_{n=1}^{\infty} \frac{C_{mn}}{\left(\frac{m^2}{a^2} + \frac{n^2}{b^2}\right)^2} \sin \frac{m\pi x}{a} \sin \frac{n\pi y}{b} \qquad (2.6.8)$$

The expressions for the moments can be obtained by replacing equation (2.6.8) into the moment-curvature relations equations (2.2.12).

(b) Levy's Method.

When a plate has a pair of opposite edges simply supported, solution may be affected by a special technique due to Levy [10]. The other two edges may be supported in an arbitrary manner. Furthermore the shape of the applied load should be the same on all sections perpendicular to the simply supported edges (i.e. $p = p(x)$). We will seek a solution in the form of equation (2.6.1). The assumption is then made that the component W_p of the deflection is independent of y, so that the plate governing equation (2.2.30) may be reduced to that of a strip:

$$\frac{d^4 W(x)}{dx^4} = \frac{p(x)}{D} \qquad (2.6.9)$$

This equation can be integrated directly and the constants of integration found from the boundary conditions at $x = 0$ and $x = a$. For convenience the origin of the coordinates system is taken at the middle of the edge $x = 0$, see Figure (2.6.2). To find the homogeneous solution, W_H, the deflection is expressed as a single sine series:

$$W_H(x,y) = \sum_{m=1}^{\infty} Y_m(y) \sin \frac{m\pi x}{a} \qquad (2.6.10)$$

where $Y_m(y)$ is a function of y only and yet to be determined. Equation (2.6.10) satisfies the boundary conditions at $x = 0, a$. Substituting equation (2.6.10) into the homogeneous differential

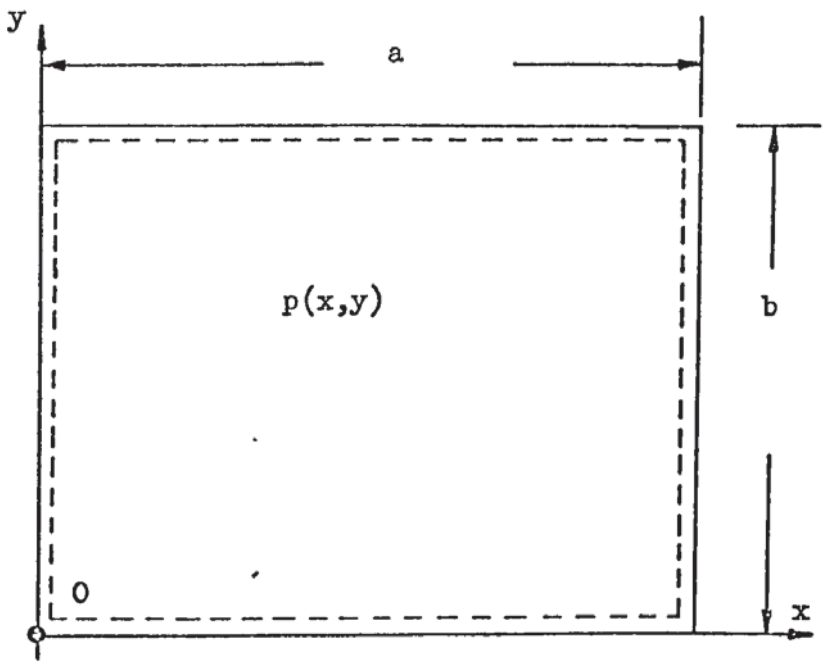

Fig.(2.6.1) Simply supported rectangular plate. Location of coordinate system for Navier's Method.

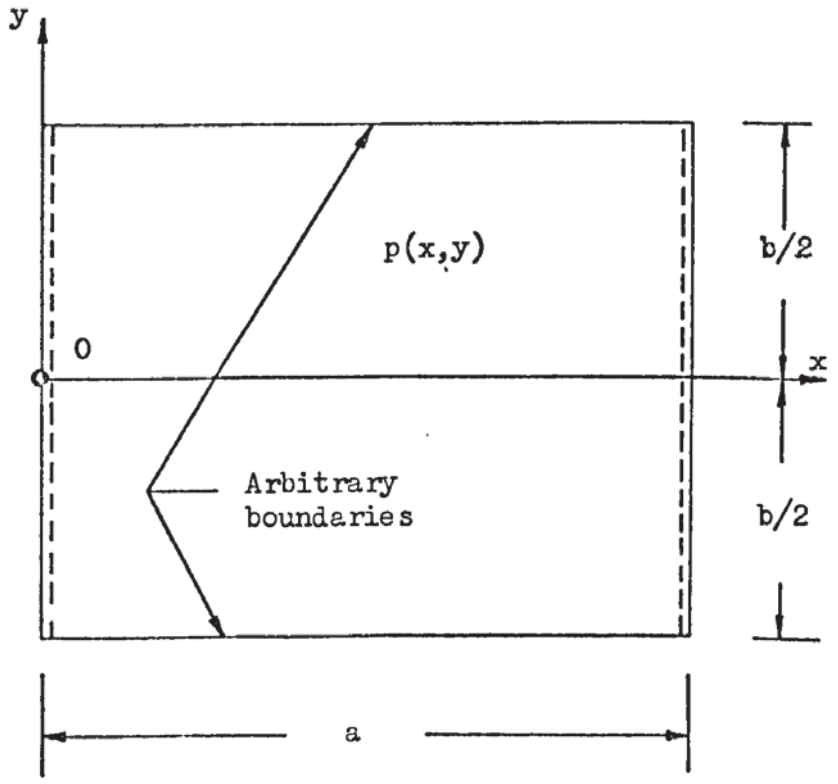

Fig.(2.6.2) Rectangular plate with two opposite edges simply supported, others arbitrary supported. Location of coordinate system for Levy's Method.

equation (2.6.2) yields

$$\sum_{m=1}^{\infty} \left(Y_m^{IV} - \frac{2m^2\pi^2}{a^2} Y_m'' + \frac{m^4\pi^4}{a^4} Y_m \right) \sin\frac{m\pi x}{a} = 0 \qquad (2.6.11)$$

Equation (2.6.11) can be satisfied for all values of x, only if $Y_m(y)$ satisfies the equation:

$$Y_m^{IV} - 2\frac{m^2\pi^2}{a^2} Y_m'' + \frac{m^4\pi^4}{a^4} Y_m = 0 \qquad (2.6.12)$$

A general solution of this equation may be taken in the form given in reference [10] as:

$$Y_m(y) = \frac{pa^4}{D}\left(A_m \cosh\frac{m\pi y}{a} + B_m \frac{m\pi y}{a}\sinh\frac{m\pi y}{a} + C_m \sinh\frac{m\pi y}{a} + D_m \frac{m\pi y}{a}\cosh\frac{m\pi y}{a} \right) \qquad (2.6.13)$$

The four integration constants are then determined from the boundary conditions at the edges $y = \pm b/2$.

The Levy's general solution is then:

$$W(x,y) = W_p + \sum_{m=1}^{\infty} Y_m(y) \sin\frac{m\pi x}{a} \qquad (2.6.14)$$

where W_p is found by direct integration of equation (2.6.9) and $Y_m(y)$ is found from equation (2.6.13).

(c) Rectangular Plates With One or More Edges Clamped.

The solution of rectangular plates with one or more edges clamped was introduced by Timoshenko [10]. The method involves solving the plate as a simply supported case, under any lateral load, then superposing the solution for a plate bent by edge bending moments at the clamped edges, with such a distribution as to render $\partial W/\partial n$ zero at the particular clamped edge.

(d) "Moderately" Thick Plates.

By solving equations (2.3.17 a,b,c) for the bending moments and substituting the appropriate derivatives of these expressions into equations(2.2.26) and (2.2.27) one gets:

$$Q_x - \frac{h^2}{10} \nabla^2 Q_x = - D \frac{\partial}{\partial x} \nabla^2 W - \frac{h^2}{10(1-\mu)} \frac{\partial p}{\partial x} \qquad (a)$$

$$Q_y - \frac{h^2}{10} \nabla^2 Q_y = - D \frac{\partial}{\partial y} \nabla^2 W - \frac{h^2}{10(1-\mu)} \frac{\partial p}{\partial y} \qquad (b) \qquad (2.6.15)$$

where

$$\nabla^2 = \frac{\partial^2}{\partial x^2} + \frac{\partial^2}{\partial y^2}$$

By noticing equations (2.2.26) and (2.2.27), the plate governing equation (2.3.17d) can be represented as:

$$\frac{\partial Q_x}{\partial x} + \frac{\partial Q_y}{\partial y} = - p \qquad (2.6.16)$$

Reissner, in references [11],[12], presented the plate governing equation in this form and showed that the system of equations (2.6.15) and (2.6.16) can be solved for p = 0, homogeneous solution, by introducing a stress function. To this homogeneous solution one has to add a particular integral to take into account the load p(x,y).

More recently Salerno & Goldberg [21] reported a particular integral for a general load p(x,y). They started by substituting equations (2.6.15 a,b) into equation (2.6.16) to obtain a more complete differential equation for the deflection of the plate as:

$$D\nabla^4 W = p - \frac{h^2}{10} \frac{2-\mu}{1-\mu} \nabla^2 p \qquad (2.6.17)$$

They assumed as a particular integral to the system (2.6.15), (2.6.16) the equations:

$$Q_{x_p} = -D \frac{\partial}{\partial x} \nabla^2 W - \frac{h^2}{10} \cdot \frac{2-\mu}{1-\mu} \frac{\partial p}{\partial x} \qquad (a)$$

$$Q_{y_p} = -D \frac{\partial}{\partial y} \nabla^2 W - \frac{h^2}{10} \cdot \frac{2-\mu}{1-\mu} \frac{\partial p}{\partial y} \qquad (b) \qquad (2.6.18)$$

Further, Q_{x_H} and Q_{y_H} are expressed in terms of a stress function ϕ by, [11],[12],

$$Q_{x_H} = \frac{\partial \phi}{\partial y} \qquad (a)$$

$$Q_{y_H} = -\frac{\partial \phi}{\partial x} \qquad (b) \qquad (2.6.19)$$

where ϕ is given by

$$\nabla^2 \phi - \frac{10}{h^2} \phi = 0 \qquad (2.6.20)$$

so that Q_{x_H} and Q_{y_H} are solutions of the homogeneous form of equations (2.6.15), (2.6.16). The complete solution for the shear force is then:

$$Q_x = Q_{x_p} + Q_{x_H} \qquad (a)$$

$$Q_y = Q_{y_p} + Q_{y_H} \qquad (b) \qquad (2.6.21)$$

hence, the problem is reduced to the difficult task of solving equations (2.6.17), and (2.6.20, (2.6.21) subject to either mechanical or displacement boundary conditions. They specialized the analysis inref. [21] using a Levy-type solution for

a) Uniformly loaded rectangular plate supported on all edges.

b) Uniformly loaded rectangular plate supported at two opposite edges and free at the other edges. No supporting results were shown in case (b).

e) Free Vibrations.

Basically either Navier or Levy's method of analysis are used to solve the homogeneous differential equation (2.4.12), in the very few cases where the shape and boundary conditions of

the plate are suitable.

For a simply supported rectangular plate, Figure (2.6.1), with p = 0, Navier's method is the classical method of analysis. The shape function $\hat{W}(x,y)$ can be given by double trigonometric series in the form of equation (2.6.5). Substituting equation (2.6.5) into equation (2.4.12) yields:

$$\frac{m^4\pi^4}{a^4} + 2\frac{m^2\pi^2}{a^2}\frac{n^2\pi^2}{b^2} + \frac{n^4\pi^4}{b^4} - \frac{\rho h\,\omega^2}{D} = 0 \qquad (2.6.22)$$

Associating ω, with the corresponding integers m and n equation (2.6.22) can be represented as:

$$\frac{\rho h}{D}\omega_{mn}^2 = \pi^4\left[\left(\left(\frac{m}{a}\right)^2 + \left(\frac{n}{b}\right)^2\right]^2\right. \qquad (2.6.23)$$

Solving for ω_{mn} gives:

$$\omega_{mn} = \pi^2\left[\left(\frac{m}{a}\right)^2 + \left(\frac{n}{b}\right)^2\right]\sqrt{\frac{D}{\rho h}} \qquad (2.6.24)$$

for m,n = 1,2,3, ...,

where ω_{mn} are the natural frequencies and the corresponding natural modes (or eigenvectors) are:

$$\hat{W}_{mn}(x,y) = b_{mn}\sin\frac{m\pi x}{a}\sin\frac{n\pi y}{b} \qquad (2.6.25)$$

for m,n = 1,2,3, ...,

Levy's type of solution can be applied to rectangular plates which are simply supported along a pair of opposite edges.

Thus, suppose a plate is simply supported at the edges x = 0 and x = a, and for convenient, we take a coordinate system as in Figure (2.6.1). The shape function $\hat{W}(x,y)$ can take the form of equation (2.6.10), as for the static case. Substituting it into equation (2.4.12), for a specific integer m yields:

$$Y_m^{IV} - 2\frac{m^2\pi^2}{a^2} Y_m'' + \left(\frac{m^4\pi^4}{a^4} - \frac{\rho h\omega^2}{D}\right) Y_m = 0 \qquad (2.6.26)$$

The general solution of equation (2.6.26) is given in reference [17] as:

$$Y_m(y) = c_1 e^{-\alpha y} + c_2 e^{\alpha y} + c_3 \cos \beta y + c_4 \sin \beta y \qquad (2.6.27)$$

where

$$\alpha = \sqrt{\omega\sqrt{\frac{\rho h}{D}} + \frac{m^2\pi^2}{a^2}} \qquad \text{(a)}$$

$$\beta = \sqrt{\omega\sqrt{\frac{\rho h}{D}} - \frac{m^2\pi^2}{a^2}} \qquad \text{(b)} \qquad (2.6.28)$$

The constants c_1, c_2, c_3, c_4 are determined from the boundary conditions at the edges $y = 0, b$. Utilizing the boundary conditions yields the frequency equation from which ω is determined. To illustrate, for the particular case where the edge $y = 0$ is simply supported and the edge $y = b$ is free, the boundary conditions in terms of shape functions are:

$$\hat{W} = 0 \; ; \; \frac{\partial^2 \hat{W}}{\partial y^2} + \mu \frac{\partial^2 \hat{W}}{\partial x^2} = 0, \text{ for } y = 0 \qquad \text{(a)}$$

$$\frac{\partial^2 \hat{W}}{\partial y^2} + \mu \frac{\partial^2 \hat{W}}{\partial x^2} = 0 \; ; \; \frac{\partial^3 \hat{W}}{\partial y^3} + (2-\mu) \frac{\partial^3 \hat{W}}{\partial x^2 \partial y} = 0, \text{ for } y = b \qquad \text{(b)} \qquad (2.6.29)$$

Equations (2.6.29a) are satisfied, if in the general solution equation (2.6.27), we take $c_1 = - c_2$ and $c_3 = 0$. Y_m can then be written as

$$Y_m(y) = A \sinh \alpha y + B \sin \beta y \qquad (2.6.30)$$

where A and B are constants. From equations (2.6.29b) we obtain two equations

$$\begin{bmatrix} \left(\alpha^2 - \mu\,\frac{m^2\pi^2}{a^2}\right)\sinh\alpha b & -\left(\beta^2+\mu\,\frac{m^2\pi^2}{a^2}\right)\sin\beta b \\ \alpha\left(\alpha^2 - (2-\mu)\,\frac{m^2\pi^2}{a^2}\right)\cosh\alpha b & -\beta\left(\beta^2+(2-\mu)\,\frac{m^2\pi^2}{a^2}\right)\cos\beta b \end{bmatrix} \begin{Bmatrix} A \\ B \end{Bmatrix} = \begin{Bmatrix} 0 \\ 0 \end{Bmatrix} \qquad (2.6.31)$$

For a non-trivial solution the determinant of the matrix should be zero, yielding:

$$\beta\left(\alpha^2-\mu\,\frac{m^2\pi^2}{a^2}\right)^2\tanh\alpha b = \alpha\left(\beta^2+\mu\,\frac{m^2\pi^2}{a^2}\right)^2\tan\beta b \qquad (2.6.32)$$

Since α and β contain ω, the natural frequencies can be found by solving equation (2.6.32). This equation has been solved for different plate ratios a/b and the results tabulated by Leissa [22]. Similarly we could specialize the method for other cases within the limits of the Levy's boundary conditions. For others that the above discussed Navier and Levy's solutions, the exact solution of free vibrations creates such severe mathematical complexities that analytical solutions cannot be obtained and it is necessary to resort to some approximate numerical process.

f) Buckling.

An analytical solution of the homogeneous differential equation (2.5.6) is only possible within the constraints of the Navier and Levy's method of analysis, for rectangular plates uniformly compressed in one direction, ($\bar{N}_x$ or $\bar{N}_y$ = constant). For a simply supported plate a x b, see Figure (2.6.3), one can use Navier's method exactly as for free vibrations. Substituting the double trignometric sine series equation (2.6.5) into equation (2.5.6) and taking within the plate $N_x = \bar{N}_x$ = constant (positive in compression) and $N_y = 0$, $N_{xy} = 0$, see Figure (2.6.3), yields:

$$\frac{m^4\pi^4}{a^4} + 2\,\frac{m^2\pi^2}{a^2}\cdot\frac{n^2\pi^2}{b^2} + \frac{n^4\pi^4}{b^4} = \bar{N}_x\left(\frac{m\pi}{a}\right)^2$$

or

$$\bar{N}_x\left(\frac{m\pi}{a}\right)^2 = D\,\pi^4\left[\left(\frac{m}{a}\right)^2 + \left(\frac{n}{b}\right)^2\right]^2 \qquad (2.6.32)$$

which is the equivalent of equation (2.6.23) in the analogous vibration case. Solving for $\bar{N}_x$ gives

$$\bar{N}_x = \left[m + \frac{1}{m}\,\frac{a^2}{b^2}\,n^2\right]^2 \frac{\pi^2 D}{a^2} = \lambda\,\frac{\pi^2 D}{a^2} \qquad (2.6.33)$$

The smallest $\bar{N}_x$ is given by taking n = 1, then

$$\lambda = \left[m + \frac{1}{m}\,\frac{a^2}{b^2}\right]^2 \qquad (2.6.34)$$

For a given aspect ratio a/b, the critical buckling factor is obtained by selecting m such that it renders λ a minimum. Thus

$$\lambda_{min} = \lambda_{cr} \qquad (2.6.35)$$

The buckling critical load is then obtained as:

$$\bar{N}_{x_{cr}} = \lambda_{cr}\,\frac{\pi^2 D}{a^2} \qquad (2.6.36)$$

Graphs plotting aspect ratio a/b versus λ_{cr} may be found in reference [17]. A sample of these graphs is shown in Figure (2.6.4).

Levy's method can be used for rectangular plates simply supported along two opposite edges perpendicular to the direction of compression and having various edge conditions. The procedure is very similar to the vibration case treated under (e). Equations (2.6.28) specialized for buckling problems are now

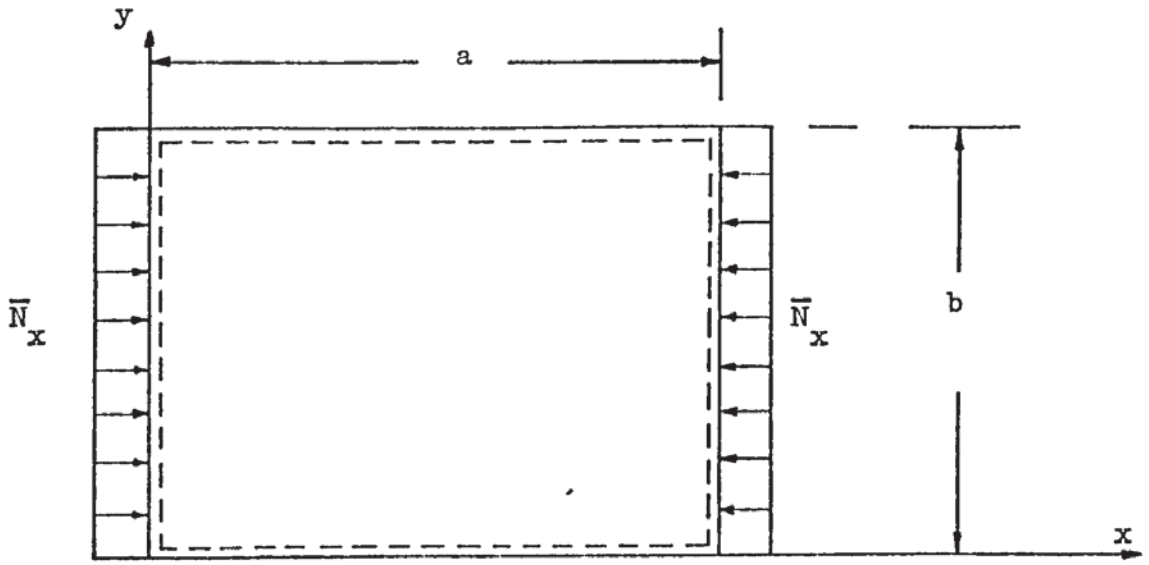

Fig.(2.6.3) Buckling of simply supported plate uniformly compressed in one direction.

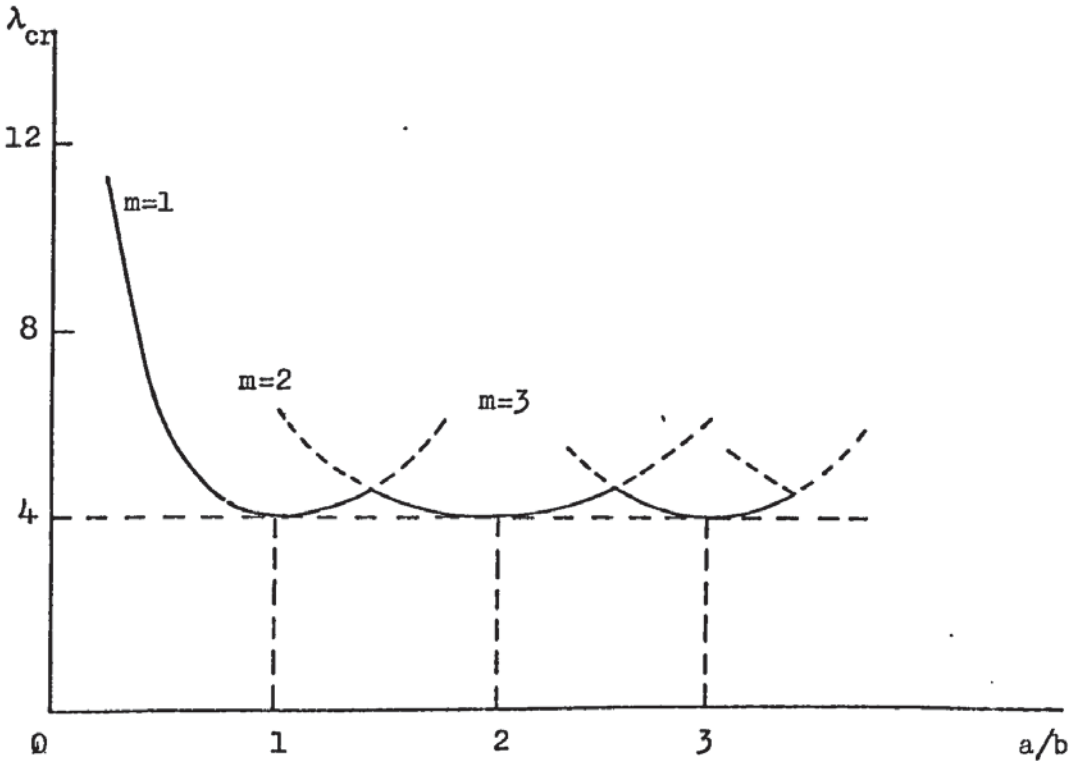

Fig.(2.6.4) Sample graph of λ_{cr} versus a/b.
Simply supported rectangular plate ($\bar{N}_x$ = constant).

$$\alpha = \sqrt{\sqrt{\frac{\bar{N}_x}{D}}\,\frac{m^2\pi^2}{a^2} + \frac{m^2\pi^2}{a^2}} \qquad \text{(a)}$$

$$\beta = \sqrt{\sqrt{\frac{\bar{N}_x}{D}}\,\frac{m^2\pi^2}{a^2} - \frac{m^2\pi^2}{a^2}} \qquad \text{(b)} \qquad (2.6.37)$$

which together with equations (2.6.10), (2.6.27) define the problem. Thus, if the edge $y = 0$ is simply supported and the edge $y = b$ is free say, we can use equation (2.6.32) together with equations (2.6.37) to evaluate the critical load, if the dimensions of the plate and the elastic constants are known.

2.6.2) Approximate Methods.

As we have illustrated above, rigorous solution of plate problems are only possible for simple cases of plate geometry, loading and boundary conditions: as the plate becomes more complex, the analysis becomes, at best, very cumbersome and usually impossible so that approximation methods become the only practical means of plate analysis. In this connection, finite difference and the variational methods of Ritz, Galerkin and Kantorovich have been used with the displacement finite element method becoming increasingly applied in recent years.

a) Finite Difference Method.

The finite difference method [20] is a numerical technique for obtaining approximate solutions of differential equations by replacing derivatives of the governing differential equation and the boundary conditions of the problem by difference quotients. These involve only values of the variables at some discrete points (nodes), located at the joints of the finite

difference mesh or network drawn over the region of interest. In general the continuum is divided into a square, hexagonal or other reference mesh.

The first derivative of a function f(x) at a point can be approximated using central differences by:

$$f'_m \simeq \Delta f_m = \frac{f_{m+1} - f_{m-1}}{2\ell}$$

where Δ is the difference operator corresponding to $D = \frac{d}{dx}$ in differentiation and f_{m+1}, f_{m-1} are the values of the function at the points m+1 and m-1 at distances ℓ apart from m, Figure (2.6.5).

Similarly approximations to higher derivates can be deduced. Partial difference operators are obtained as partial derivatives by operating on each variable in turn, keeping the others constant.

The finite difference representation of the governing plate equation (2.2.30) at the nodal points (m,n), for a square mesh of width ℓ, Figure (2.6.6) is [20]

$$\nabla^4 W \simeq \frac{1}{\ell^4}\Big[\, 20\, W_{m,n} - 8\left(W_{m+1,n} + W_{m-1,n} + W_{m,n+1} + W_{m,n-1}\right) + 2\left(W_{m+1,n+1} + W_{m-1,n+1} + W_{m+1,n-1} + W_{m-1,n-1}\right) + W_{m+2,n} + W_{m-2,n} + W_{m,n+2} + W_{m,n-2}\Big] = \frac{p_{m,n}}{D} \qquad (2.6.38)$$

where $p_{m,n}$ is the normal load at node m,n and ℓ is the mesh width between nodes in both directions.

The finite difference representation of equation (2.2.30) for other types of mesh may be found in ref. [23].

By representing the boundary conditions in finite difference form, introducing fictitious nodal points outside the plate, and applying equation (2.6.38) to all free nodes in turn we

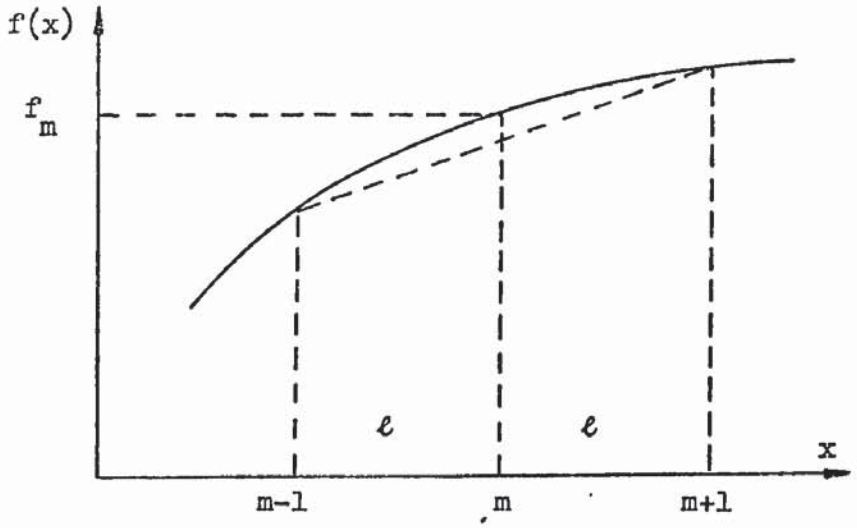

Fig.(2.6.5) Finite difference mesh in one direction.

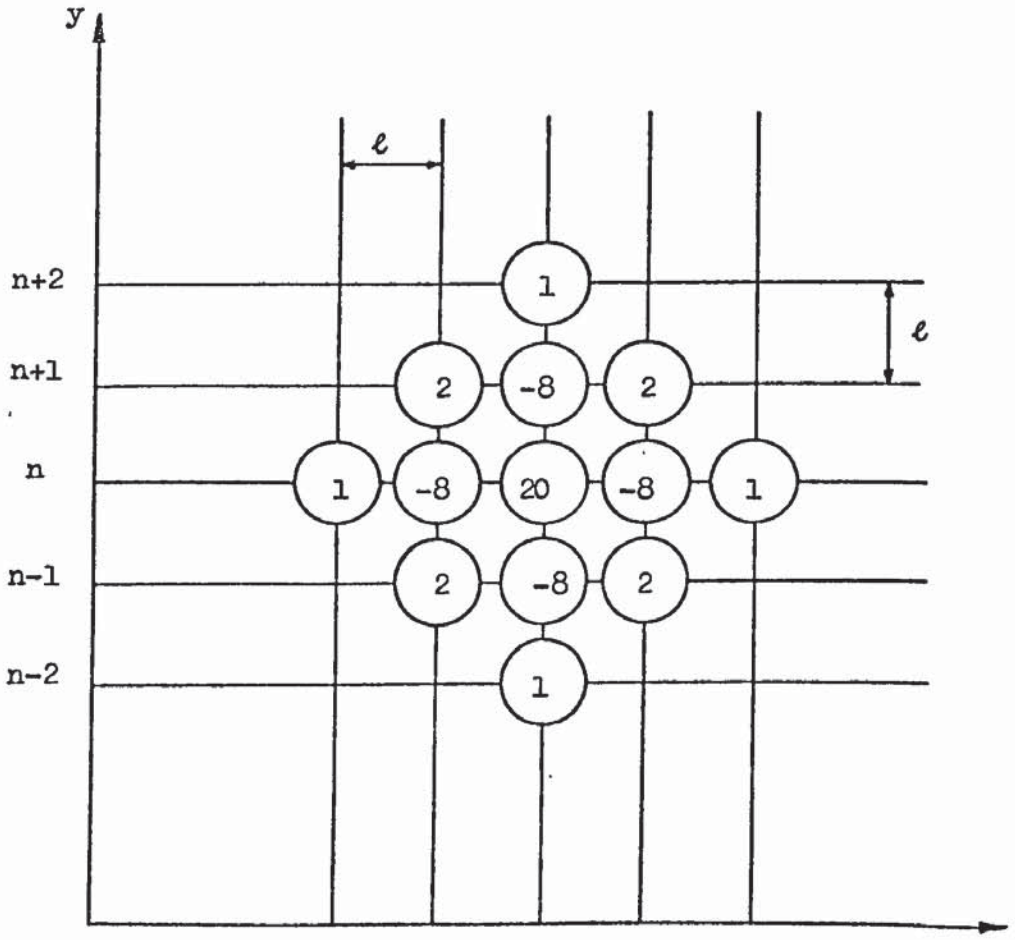

Fig.(2.6.6) Finite difference mesh in two dimensions.

obtain a system of simultaneous algebraic equations. The introduction of the fictitious nodes do not give additional deflection ordinates into the calculation due to the fact that the finite difference expressions of the boundary conditions allow their replacement by internal ones.

The system of equation can then be solved for the unknown nodal deflections.

The finite difference method is good for automatic-computation using a digital computer and some fairly difficult problems can be solved, but for irregular geometries the technique becomes very hard to use. Also the algebraic equations obtained are not very well conditioned and therefore the technique is less used today than it was before the appearance of the finite element method.

Similarly we could obtain a finite difference representation for free vibrations and buckling governing equation reducing the solution to that of an algebraic eigenvalue problem. A full description of the method and particular details about the introduction of boundary conditions for plate problems is well presented in references [20] [23].

b) Rayleigh-Ritz Method.

We have shown in this chapter through the application of the variational notation, the equivalence between the plate governing equation for small deflections and an energy formulation. Due to the difficulties of solving the plate equation one can use this equivalence to obtain approximate solutions by substituting into the system functional a system of shape functions for the wanted quantity with the coefficients to be determined by making the functional stationary.

The Rayleigh-Ritz method [1],[9],[16] involves replacing the deflection of the middle surface by a set of linear

independent functions such that:

$$W(x,y) = c_1 \phi_1(x,y) + c_2 \phi_2(x,y) + \ldots + c_n\phi_n(x,y) \qquad (2.6.39)$$

where $\phi_i(x,y)$, $i = 1,2,3 \ldots n$ are continuous shape functions that satisfy individually the geometric boundary conditions for any choice of the constants c_i, and are capable of representing the deflected plate surface.

Substituting equation (2.6.39) into the potential energy functionlequation (2.1.27), specialized for plate bending, and performance of the integrations results in

$$\pi_P = \pi_P(c_1, c_2, \ldots c_n)$$

Then, for a stationary π_P, $\delta\pi_P = 0$, which is equivalent to:

$$\frac{\partial \pi_P}{\partial c_i} = 0 \qquad (2.6.40)$$

$$i = 1,2,3 \ldots n$$

This process yields n simultaneous algebraic equations in the undetermined coefficients c_i.

Although the Rayleigh-Ritz method was originally developed for use with the potential energy functional, it can be applied with the Reissner functional, but now moments and deflections a re independently represented by shape functions satisfying the "forced" boundary conditions [16] and the constants are found as before by making the functional a stationary.

The Rayleigh-Ritz method can be used for plates of various shapes and thickness provided suitable shape functions can be found; but, if the geometry is irregular, generating suitable shape functions is difficult if not impossible. Various functions for a number of boundary conditions are suggested by Sziland [20].

c) Galerkin Method.

Galerkin's method [16] [20] can be applied to any type of boundary value problem provided that the governing differential equations have already been determined. It is aimed at giving a direct solution to the governing differential equation.

If the solution is imperfect, $\left(\nabla^4 W - \frac{p}{D}\right)$ is not zero, and may be viewed as some residual force. To reduce this to a minimum, we may calculate its virtual work and equate it to zero, hence:

$$\iint_A \left(\nabla^4 W - \frac{p}{D}\right) \delta W \, dx \, dy = 0 \qquad (2.6.41)$$

where δW is a virtual deflection consistent with the constraints of the problem.

By selecting a set of independent, continuous functions, capable of representing the lateral deflection in the form of equation (2.6.39), where each term must satisfy all boundary conditions of the problem, geometric and natural, and substituting equation (2.6.39) into equation (2.6.41) we get

$$\sum_{i=1}^{n} \delta c_i \iint_A \left(\nabla^4 W - \frac{p}{D}\right) \phi_i(x,y) \, dx \, dy = 0 \qquad (2.6.42)$$

Since equation (2.6.42) must be satisfied for all values of δc_i, it follows that:

$$\iint_A \left(\nabla^4 W - \frac{p}{D}\right) \phi_1(x,y)\, dx\, dy = 0$$

$$\iint_A \left(\nabla^4 W - \frac{p}{D}\right) \phi_2(x,y)\, dx\, dy = 0 \qquad (2.6.43)$$

$$\vdots$$

$$\iint_A \left(\nabla^4 W - \frac{p}{D}\right) \phi_n(x,y)\, dx\, dy = 0$$

Substituting equation (2.6.39) into equations (2.6.43) and evaluating the integrals over the entire plate surface yields a system of linear algebraic equations from which the c's can be found.

As a general method for the solution of boundary value problems Galerkin's method has the advantage over Rayleigh-Ritz in that it does not require the availability of an energy functional. Its applicability is dependent on the availability of suitable shape functions.

It can be extended to vibration and buckling problems: now the net result is the generation of an algebraic eigenvalue problem.

d) Kantorovich Method.

The Kantorovich method [16], [24] represents a form of solution which is intermediate between the Rayleigh-Ritz method and an exact solution. In both methods we seek to extremize the functional equation (2.1.27), specialized for plate bending. The shape functions ϕ_i are still chosen, but the constants c_i are replaced by unknown functions of, say, x ; then the quantities c_i are no longer constants but rather are unknown undetermined functions $c_i(x)$. In addition for greater generality,

we may add a term $\phi_o(x,y)$, so that:

$$W(x,y) = \phi_o(x,y) + \sum_{i=1}^{n} c_i(x)\, \phi_i(x,y) \qquad (2.6.44)$$

$\phi_o(x,y)$ satisfies the actual boundary conditions whilst the $\phi_i(x,y)$ satisfy the homogeneous boundary conditions (i.e. W, $\partial W/\partial n$).

Substituting equation (2.6.44) into the known functional π_P and carrying out the integration with respect to y yields an integral to be extremized which contains only one independent variable x.

Applying the Euler equation [9], the problem gives a set of n fourth-order ordinary differential equations in $c_i(x)$ to solve. Thus the exact forms of $c_i(x)$ to extremize π_P with respect to the chosen ϕ_i are determined by the problem itself.

The methods of solution reviewed under (b), (c), (d) above are based on choosing a set of functions which approximate part or the whole of the solution, reducing the problem to the solution of a system of simultaneous algebraic equations. Although these methods may be cumbersome and laborious they provide a useful tool for the solution of some plate problems when digital computers are not available.

e) The Finite Element Method.

The finite element method (f.e.m.) pioneered by Turner and Clough [25],[26] is the most significant development in structural analysis in recent years.

With the development of powerful digital computers the f.e.m. has gained considerable popularity and become a very important tool in the analysis of structural problems and in the broad field of continuum mechanics [27],[28].

The method, which will be described in more detail

in the following chapters, replaces the continuum by a finite number of discrete elements, such as triangles, rectangles, etc. interconnected at a finite number of nodal points.

By assuming a displacement and/or stress field within an element it is possible by the use of the appropriate energy functional and using a procedure similar to the Rayleigh-Ritz technique to derive an element matrix equation which may have generalized displacements, stresses or both, at the nodal points, as unknowns to be evaluated.

The Rayleigh-Ritz technique is applied to each element in turn and the overall problem is examined by assembling all the individual element properties in a suitable manner to be described.

The displacement method, based on the principle of minimum potential energy, is the most well known of all, for static, dynamic and buckling problems [13],[27] ,[28],[29],[30], but while this method is very effective when applied to such problems as plane stress or plane strain, for plate and shells problems, difficulties with interelement compatibility requirements render attractive alternative formulations based on mixed variational principle.

f) The Mixed Finite Element Method.

In the mixed finite element method stresses and displacements are assumed separately and by using the Reissner functional in one of the several possible alternatives, interelement continuity conditions [2],[13] may be conveniently relaxed allowing the use of stress/displacement shape functions of lower order which ease the computational effort. Since stresses and displacements are assumed separately they can be obtained with similar degrees of accuracy avoiding the decrease in accuracy

characteristic of the displacement method due to the process of numerical differentiation to obtain the stresses once the displacements are evaluated. The mixed method was pioneered by Herrmann [4],[31] in the static plate bending analysis.

2.6.3) Concluding Remarks.

In this chapter the theory of plates was reviewed, since the heart of our work is the Reissner functional applied to finite elements, we felt that it was illuminating to establish the governing equations in this way too.

Various analytical methods for the solution of plate problems were discussed. It was found that analytical solutions only exist for very simple cases of geometry, load and boundary conditions. For more complex problems approximate methods such as finite difference or the variational methods are necessary.

Under the variational methods, we outline the direct methods of Rayleigh-Ritz, Galerkin, and Kantorovich. All these methods depend, for accuracy of solution, on how closely the assumed deflection shape function approximates the actual deflection surface and the applicability depends on the availability of suitable shape functions.

The computer-programmable finite element method was mentioned as the most versatile and powerful of all the variational methods.

Finally, a mixed formulation of the finite element method was outlined which can be used as an alternative to the displacement f.e.m. in the solution of general plate problems. It is the main aim of the project described in this thesis to extend the application of the mixed method by using a general quadrilateral element for the solution of static problems for thin

and moderately thick plates, which may have rigidity variation, and orthotropic properties. Secondly we shall explore the behaviour of the element in the solution of dynamic and buckling problems.

CHAPTER 3

THE FINITE ELEMENT METHOD

3.1) Generalization of the Finite Element Approach.

The application of the finite element method to the solution of problems in the elastic continuum consists of the following procedure:

1) The continuum is divided into two-or three dimensional finite elements by ficticious lines or surfaces.

2) The elements are assumed to be interconnected at discrete points called "nodes" located on the element boundaries (however internal nodes are sometimes used). The finite elements, may, in general, be of triangular, rectangular or general quadrilateral form for the two dimensional continuum. The three dimensional solids may be divided into tetrahedral or prismatic elements. In some cases curved boundary elements may be used for good modelling and improved accuracy.

3) A suitable displacement and/or stress function is chosen, in terms of nodal-displacements and/or stress generalized parameters, to represent the displacement and/or stress field within the element.

4) By substituting the nodal coordinates of the element into the displacement and/or stress function and solving for the generalized coordinates in terms of nodal displacements and/or stresses then substituting back into the displacement and/or stress function, this function will then be in terms of generalized displacement and/or stress parameters and will be called a "shape function", In order to be able to obtain the shape functions in accordance with the above procedure the number of generalized parameters must be equal to the number of nodes times the number of nodal parameters. As will be shown later, it is possible to formulate the shape function

4) contd.

directly by using interpolation functions.

5) By substituting these shape function(s) into the appropriate energy functional, the latter is represented in terms of nodal parameters.

6) Extremization of the energy functional, i.e. taking variations with respect to the nodal parameters gives a matrix equation for each element, from which an element coefficient matrix and force and/or displacement vector is recognized.

7) The overall matrix-equation of the structure is then assembled by adding contributions of the element matrix-coefficients and loads and/or displacements to the appropriate locations in the overall coefficients matrix and overall load and/or displacement vector as discussed later.

8) The geometric and/or mechanical boundary conditions are imposed.

9) The equations are solved for the unknown displacements and/or stresses.

Mathematically the above procedure can be represented for the mixed approach as follows:

Let the displacement and stress field within the element be represented independently by

$$\{u\} = [\Phi]\{\gamma\} \qquad (a)$$
$$\{\sigma\} \quad [\psi]\{\alpha\} \qquad (b) \qquad (3.1.1)$$

where $\{u\}$ and $\{\sigma\}$ are vectors that contain all possible displacements and stress components, within the element, in the direction of the coordinate axes $[\Phi]$ and $[\psi]$ are matrices of position, which in general are of different order, and $\{\gamma\}$ and $\{\alpha\}$ are the generalized parameters.

Substituting in turn the nodal coordinates x,y into equations (3.1.1), the nodal values of the displacements and stresses will be:

$$\begin{aligned} \{u\}_e &= [A]\,\{y\} \qquad (a) \\ \{\sigma\}_e &= [P]\,\{\alpha\} \end{aligned} \tag{3.1.2}$$

In the case of the element of Figure (3.1.1) the nodal displacements and stresses are

$$\begin{aligned} \{u\}_e &= [u_1\ v_1\ u_2\ v_2\ u_3\ v_3\ u_4\ v_4\ ]^T \qquad (a) \\ \{\sigma\}_e &= [\sigma_{x_1}\ \ \sigma_{y_1}\ \tau_{xy_1} \cdots \sigma_{x_4}, \sigma_{y_4},\ \tau_{xy_4}]^T \qquad (b) \end{aligned} \tag{3.1.3}$$

and the matrices of position are of the same order, i.e. $[\Phi] = [\psi]$.

From equations (3.1.1) and (3.1.2), the element displacement and stresses will be:

$$\begin{aligned} \{u\} &= [\Phi]\,[A]^{-1}\,\{u\}_e = [N_u]\,\{u\}_e \qquad (a) \\ \{\sigma\} &= [\psi]\,[P]^{-1}\,\{\sigma\}_e = [N_\sigma]\,\{\sigma\}_e \qquad (b) \end{aligned} \tag{3.1.4}$$

where

$$\begin{aligned} [N_u] &= [\Phi]\,[A]^{-1} \qquad (a) \\ [N_\sigma] &= [\psi]\,[P]^{-1} = [\Phi]\,[P]^{-1} \qquad (b) \end{aligned} \tag{3.1.5}$$

It should be noted that the matrices [A] and [P] have to be square so that they can be inverted; this is only possible if the $\{y\}$ and $\{\alpha\}$ are of the same order as $\{u\}_e$ and $\{\sigma\}_e$ as stated in Section 3.1- item 4.

By appropropriate differentiation of the displacements, given by equation (3.1.4a), the strains $\{\varepsilon\}$ can be determined anywhere within the element as

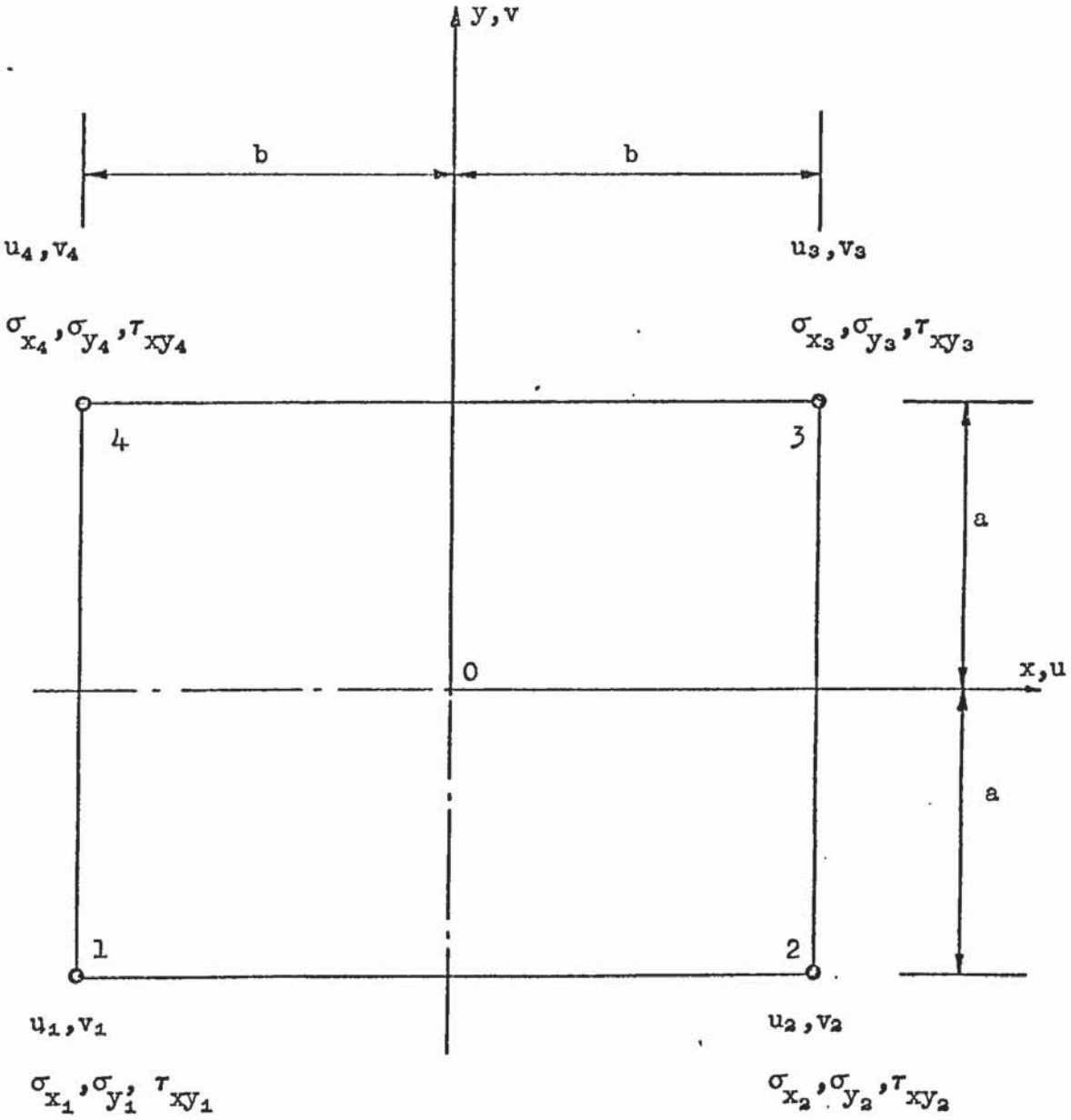

Fig.(3.1.1) A rectangular element in a plane stress or plain strain region.

$$\{\varepsilon\} = \begin{Bmatrix} \frac{\partial u}{\partial x} \\ \frac{\partial v}{\partial y} \\ \frac{\partial u}{\partial y} + \frac{\partial v}{\partial x} \end{Bmatrix} = [B_1\ B_2\ B_3\ B_4]\ \{u\}_e = [B]\ \{u\}_e \qquad (3.1.6)$$

If we choose to satisfy the displacement boundary conditions with our field variable models the Reissner functional equation (2.1.40), for the two dimensional continuum, in matrix notation, becomes

$$\pi_R = \iiint_V \left[-\tfrac{1}{2}\{\sigma\}^T [c] \{\sigma\}^T \{\varepsilon\} \{\sigma\} \right] dV - \iiint_V \{u\}^T \{\bar{F}\} dV - \iint_{S_\sigma} \{u\}^T \{\bar{F}_b\} dS \qquad (3.1.7)$$

where [c] is the plane stress/plane strain compliance matrix, $\{\bar{F}\}$ is the vector of components of body forces per unit volume and $\{\bar{F}_b\}$ is the vector of specified surface tractions over part of the surface in the x,y frame of reference.

If the interpolation functions giving our piecewise representation of $\{u\}$ and $\{\sigma\}$ obey certain continuity and compatibility conditions which we will discuss shortly, the functional π_R may be written as a sum of individual functionals defined for all the elements of the assemblage, that is:

$$\pi_R = \sum_{e=1}^{n} \left(\pi_R\right)_e \qquad (3.1.8)$$

where n is the total number of elements and the subscript (e) denotes an element.

By substituting the mixed variable model equations (3.1.4) into equation (3.1.7), we get for an element

$$\left(\pi_R\right)_e = \{\sigma\}_e^T [k_{\sigma\sigma}] \{\sigma\}_e^T + \{\sigma\}_e^T [k_{\sigma u}] \{u\}_e - \{u\}_e^T \{Q\}_e \qquad (3.1.9)$$

where

$$[k_{\sigma\sigma}] = -\,h \iint_A [N_\sigma]^T [c]\,[N_\sigma]\,dA \qquad (a)$$

$$[k_{\sigma u}] = h \iint_A [N_\sigma]^T [B]\,dA \qquad (b) \qquad (3.1.10)$$

$$\{Q\}_e = h \iint_A [N_u]^T \{\bar{F}\}dA + h \int_{s_\sigma} [N_u]^T \{\bar{F}_b\}d\ell_\sigma \qquad (c)$$

h is the thickness of the element and ℓ_σ is the length of the element where surface tractions are specified. For a stationary condition, taking variations with respect to the generalized parameters, yields for a typical element:

$$\frac{(\partial \pi_R)_e}{\partial \{\sigma\}_e^T} = [k_{\sigma\sigma}]\,\{\sigma\}_e + [k_{\sigma u}]\,\{u\}_e = 0 \qquad (a)$$

$$\frac{(\partial \pi_R)_e}{\partial \{u\}_e^T} = [k_{\sigma u}]^T\,\{\sigma\}_e - \{Q\}_e = 0 \qquad (b) \qquad (3.1.11)$$

which can be represented in matrix form as:

$$\begin{bmatrix} [k_{\sigma\sigma}] & \vdots & [k_{\sigma u}] \\ \cdots & \cdots & \cdots \\ [k_{\sigma u}]^T & \vdots & [0] \end{bmatrix} \begin{Bmatrix} \{\sigma\}_e \\ \{u\}_e \end{Bmatrix} = \begin{Bmatrix} \{0\} \\ \{Q\}_e \end{Bmatrix} \qquad (3.1.12)$$

When the "mixed" matrix and load vector is assembled for the overall structure, in accordance with the rules of assembly, which will be given later, a matrix-stress-displacement relation and a matrix-equilibrium equation for the overall problem will be obtained in the form:-

$$\begin{bmatrix} [K_{\sigma\sigma}] & \vdots & [K_{\sigma u}] \\ \cdots & \cdots & \cdots \\ [K_{\sigma u}]^T & \vdots & [0] \end{bmatrix} \begin{Bmatrix} \{\sigma\}_o \\ \{u\}_o \end{Bmatrix} = \begin{Bmatrix} \{0\} \\ \{Q\}_o \end{Bmatrix} \qquad (3.1.13)$$

where $\{\sigma\}_o$ and $\{u\}_o$ are the unknown stress and displacement vectors, which can be found, after introducing the boundary conditions, by solution of (3.1.13).

The resulting overall matrix is symmetric non-positive definite and the system can be solved using a Gaussian elimination technique.

3.2) Convergence Criteria.

The procedure for formulating the individual element properties from the variational principle and the possibility of adding these properties to obtain the overall matrix-equation rely on the assumption that the shape functions (interpolation functions) satisfy certain requirements. The requirements placed on the choice of the shape functions stem from the need to ensure that the functional still exists after the system has been discretized, and that an approximate solution converges to the correct one when an increased number of smaller elements is used, that is, when the mesh is refined. These requirements are:

1) The element shape functions [N] must be such that with a suitable choice of $\{u\}_e$ or/and $\{\sigma\}_e$ any constant value of $\{u\}$ or/and $\{\sigma\}$ or its derivatives present in the chosen energy functional should be able to be present in the limit as element size decreases to zero.

2) At the interelement interfaces (boundaries) the functional must be finite. This can be achieved either if the variables $\{u\}$ or/and $\{\sigma\}$ and any of its partial derivatives up to one order less than the higher order appearing in the functional are continuous or as described in Section 2.3.2 . This will preserve the validity of the summation implied into equation (3.1.8)

3.3) Plane Isoparametric Element. Direct Formulation of Shape Functions.

In Section 3.1 , the basis and classical process of obtaining the element properties of a finite element was briefly described. It is apparent that if we can directly construct a matrix [N] defined by any of equations (3.1.4), the necessity of computing and inverting the matrix [A] and/or [P] for each element can be avoided. In fact, in many cases it is possible to avoid the inversion by selecting shape functions in the form of interpolation functions as the basis for the chosen displacements and/or stress model. These interpolation functions must obey the convergence criteria of Section 3.2 .

In order to formulate shape functions for a general plane quadrilateral element we define a local coordinate system (natural system) ζ,η which permits the specification of a point within the element by a set of dimensionless numbers whose magnitude never exceed unity (Fig.3.3.1); the x,y coordinate system for the entire body or structure is called the global system. The relation between the global system (x,y) and the natural coordinates is, [32]

$$x = [N_1\ N_2\ N_3\ N_4] \begin{Bmatrix} x_1 \\ x_2 \\ x_3 \\ x_4 \end{Bmatrix} = [N]\ \{x\}_e \qquad (a)$$

$$y = [N_1\ N_2\ N_3\ N_4] \begin{Bmatrix} y_1 \\ y_2 \\ y_3 \\ y_4 \end{Bmatrix} = [N]\ \{y\}_e \qquad (b) \qquad (3.3.1)$$

in which $\{x\}_e$ and $\{y\}_e$ lists the nodal x,y Cartesian coordinates and

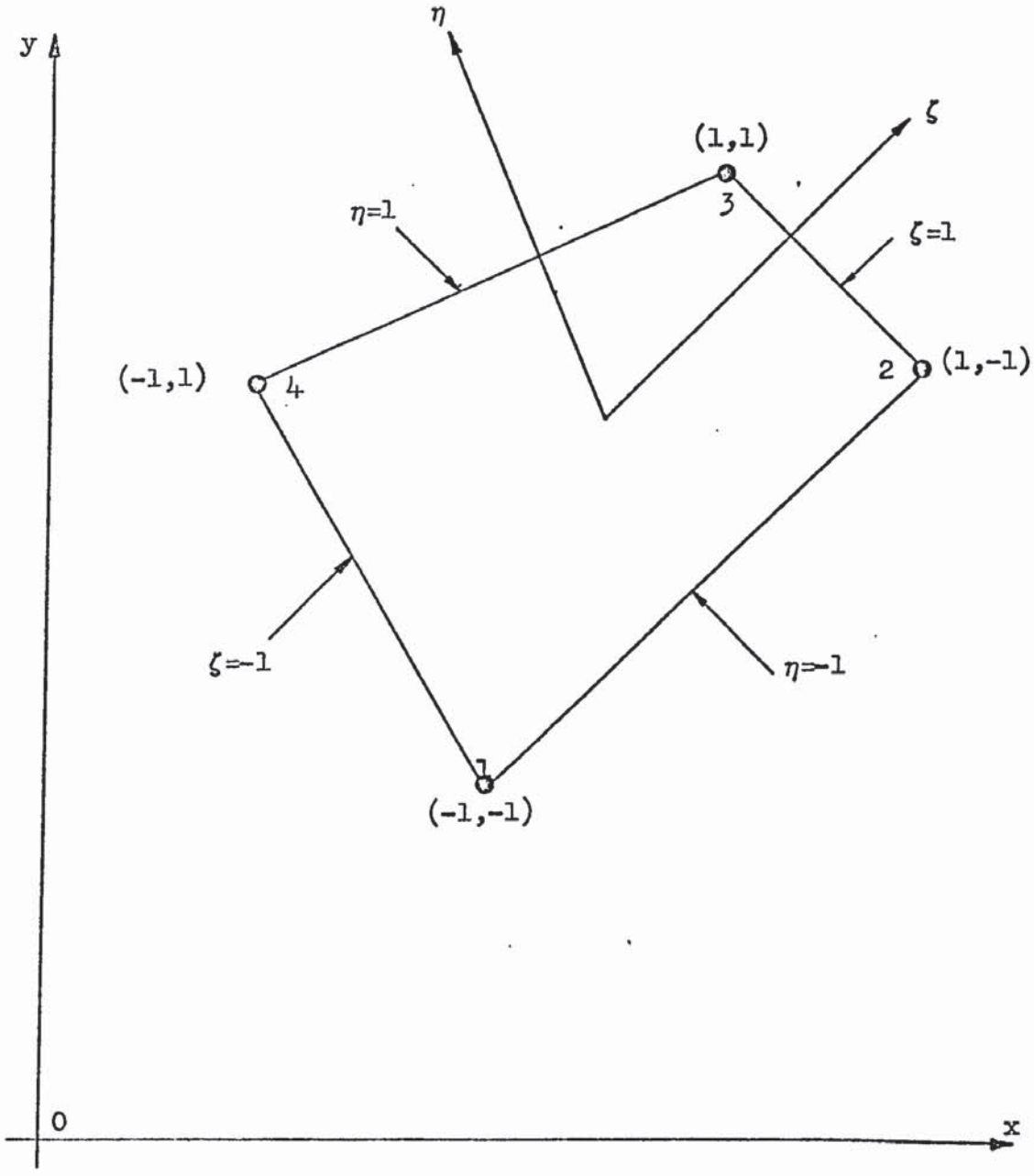

Fig.(3.3.1) General quadrilateral element.

$$N_1 = \tfrac{1}{4}(1-\zeta)(1-\eta) \quad (a)$$

$$N_2 = \tfrac{1}{4}(1+\zeta)(1-\eta) \quad (b)$$

$$N_3 = \tfrac{1}{4}(1+\zeta)(1+\eta) \quad (c)$$

$$N_4 = \tfrac{1}{4}(1-\zeta)(1+\eta) \quad (d) \qquad (3.3.2)$$

and the linear interpolation functions.

Using the isoparametric concept, that is, the displacements and/or stresses are defined by the same interpolation functions as used to define the element shape, we represent

$$u = \sum_{i}^{4} N_i u_i \quad ; \quad v = \sum_{i}^{4} N_i v_i$$

$$\sigma_x = \sum_{i}^{4} N_i \sigma_{x_i} \; ; \; \sigma_{y_i} = \sum_{i}^{4} N_i \sigma_y ; \; \tau_{xy} = \sum_{i}^{4} N_i \tau_{xy_i} \qquad (3.3.2)$$

The relations between any of the derivatives of the above variables in the two coordinate systems are established by the chain rule of differentiation

$$\begin{Bmatrix} \frac{\partial N_i}{\partial \zeta} \\ \frac{\partial N_i}{\partial \eta} \end{Bmatrix} = \begin{bmatrix} \frac{\partial x}{\partial \zeta} & \frac{\partial y}{\partial \zeta} \\ \frac{\partial x}{\partial \eta} & \frac{\partial y}{\partial \eta} \end{bmatrix} \begin{Bmatrix} \frac{\partial N_i}{\partial x} \\ \frac{\partial N_i}{\partial y} \end{Bmatrix} = [J] \begin{Bmatrix} \frac{\partial N_i}{\partial x} \\ \frac{\partial N_i}{\partial y} \end{Bmatrix} \qquad (3.3.2)$$

where [J] is the Jacobian matrix, which can be evaluated noting that

$$[J] = \begin{bmatrix} \frac{\partial N_1}{\partial \zeta} & \frac{\partial N_2}{\partial \zeta} & \frac{\partial N_3}{\partial \zeta} & \frac{\partial N_4}{\partial \zeta} \\ \frac{\partial N_1}{\partial \eta} & \frac{\partial N_2}{\partial \eta} & \frac{\partial N_3}{\partial \eta} & \frac{\partial N_4}{\partial \eta} \end{bmatrix} \begin{bmatrix} x_1 & y_1 \\ x_2 & y_2 \\ x_3 & y_3 \\ x_4 & y_4 \end{bmatrix} \qquad (3.3.3)$$

Solving equation (3.3.2) for $\partial N_i/\partial x$ and $\partial N_i/\partial y$ gives

$$\begin{Bmatrix} \frac{\partial N_i}{\partial x} \\ \frac{\partial N_i}{\partial y} \end{Bmatrix} = [J]^{-1} \begin{Bmatrix} \frac{\partial N_i}{\partial \zeta} \\ \frac{\partial N_i}{\partial \eta} \end{Bmatrix} \tag{3.3.4}$$

where $[J]^{-1}$ can be reprsented by

$$[J]^{-1} = [J^*] = \begin{bmatrix} J^*_{11} & J^*_{12} \\ J^*_{21} & J^*_{22} \end{bmatrix} \tag{3.3.5}$$

Thus, for example to evaluate $[B] = [B_1 \quad B_2 \quad B_3 \quad B_4]$ given by equation (3.1.6) yields

$$B_i = \begin{bmatrix} \frac{\partial N_i}{\partial x} & 0 \\ 0 & \frac{\partial N_i}{\partial y} \\ \frac{\partial N_i}{\partial y} & \frac{\partial N_i}{\partial x} \end{bmatrix} = \begin{bmatrix} J^*_{11} \frac{\partial N_i}{\partial \zeta} + J^*_{12} \frac{\partial N_i}{\partial \eta} & 0 \\ 0 & J^*_{21} \frac{\partial N_i}{\partial \zeta} + J^*_{22} \frac{\partial N_i}{\partial \eta} \\ J^*_{21} \frac{\partial N_i}{\partial \zeta} + J^*_{22} \frac{\partial N_i}{\partial \eta} & J^*_{11} \frac{\partial N_i}{\partial \zeta} + J^*_{12} \frac{\partial N_i}{\partial \eta} \end{bmatrix} \tag{3.3.6}$$

where the coefficients of the matrix $[J^*]$ are obtained by inverting the matrix relation (3.3.3).

For a typical integral, area integral, given by equations (3.1.10) the change of coordinates is

$$\iint_A (\ldots) \, dx \, dy = \int_{-1}^{1} \int_{-1}^{1} (\ldots) \det [J] \, d\zeta \, d\eta \tag{3.3.7}$$

where det [J] represents the determinant of [J].

Actual integration will in general have to be performed numerically using Gauss Quadrature. We will now outline the integration procedure that will be used in the formulation of the general quadrilateral plate element to be derived in Chapter 5.

3.4) Numerical Integration
Gauss Quadrature.

To evaluate a one-dimensional integral

$I = \int_{-1}^{1} f(\zeta)d\zeta$ in the simplest way, $f(\zeta)$ at the middle point is evaluated and multiplied by the length, then $I = 2\, f(\zeta_1)$, see Fig.(3.4.1), if $f(\zeta)$ happens to be a straight line the integration will be exact.

Generalization of this simple formula gives

$$I = \int_{-1}^{1} f(\zeta)d\zeta \simeq \sum_{i=1}^{n} w_i\, f(\zeta_i) \qquad (3.4.1)$$

where n is the number of points taken.

The Gauss quadrature method [29],[27] locates the sampling points and gives the appropriate "Weight" w_i, so that for a given number of them, the best accuracy is obtained.

For a two point quadrature, the coefficients are

ζ,η	w_i
$\pm$0.57735 02691 89626	1.00000 00000 00000

In two dimensions, Fig.(3.4.2) the quadrature formula is obtained by integrating first with respect to one coordinate and then with respect to the other.

$$I = \int_{-1}^{1}\int_{-1}^{1} f(\zeta,\eta)\, d\zeta\, d\eta = \int_{-1}^{1}\left[\sum_i w_i\, f(\zeta_i,\eta)\right] d\eta$$

$$= \sum_j w_j \left[\sum_i w_i\, f(\zeta_i,\eta_j)\right] = \sum_i \sum_j w_i w_j\, f(\zeta_i,\eta_j) \qquad (3.4.2)$$

For the 2 x 2 point Gauss quadrature used in this thesis yields:

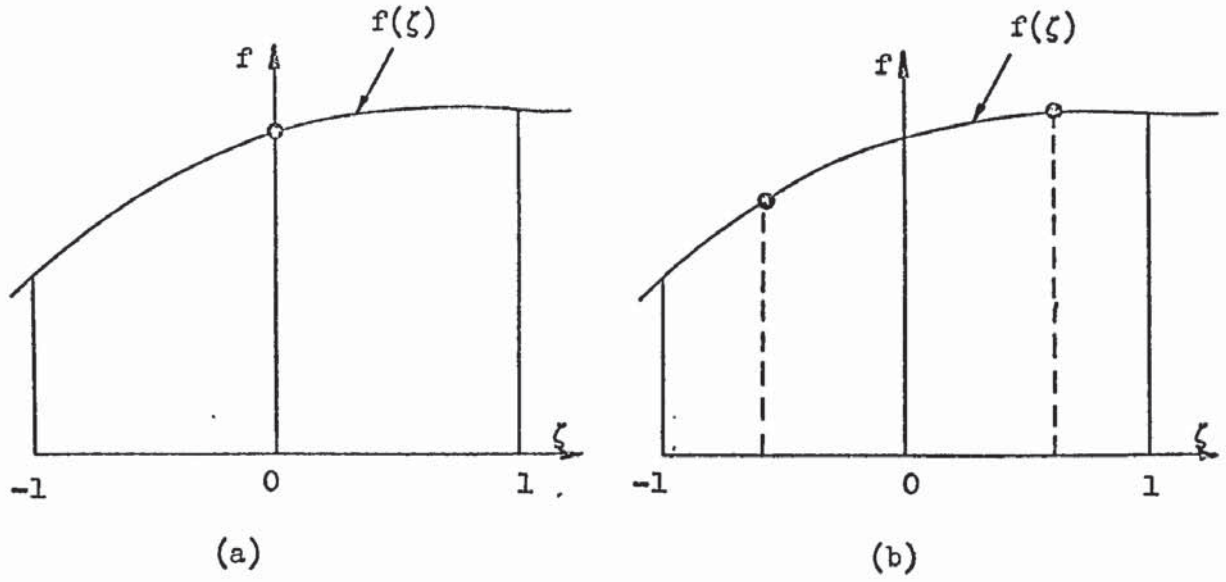

Fig.(3.4.1) One dimensional Gauss quadrature using (a) one (b) two points.

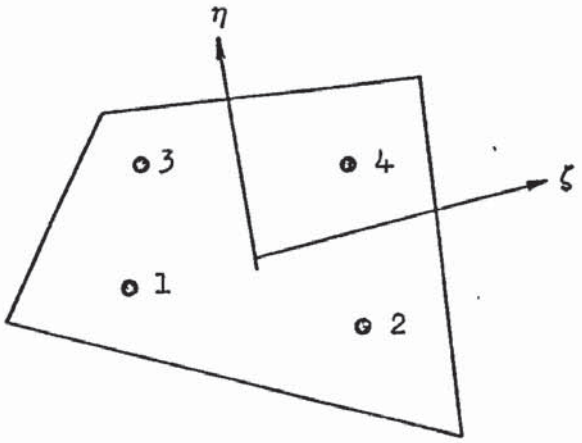

Fig.(3.4.2) 2 x 2 points Gauss quadrature.

$$I=(1.)(1.)\ f(\zeta_1,\eta_1) + (1.)(1.)\ f(\zeta_2,\eta_2)$$
$$+ (1.)(1.)\ f(\zeta_3,\eta_3) + (1.)(1.)\ f(\zeta_4,\eta_4) \qquad (3.4.3)$$

where the Gauss quadrature points are at $\zeta_i,\eta_i = \pm 0.57735\ldots$, see above table.

CHAPTER 4

LITERATURE SURVEY OR MIXED PLATE ELEMENTS.

4) Literature Survey of Mixed Plate Elements.

The finite element method is a numerical technique for obtaining approximate solutions to a wide variety of engineering and mathematical problems.

The first investigations were due to Turner, Clough, Martin and Topp[25] in 1956. They developed triangular elements, for plane stress, plane strain problems, whose properties were determined from the equations of elasticity. These investigators were the first to introduce what is known today as the direct stiffness method. Their research coincided with the advent of the digital computer, which opened the way to the solution of complex plane elasticity problems. After suitable investigations of the plane elasticity problem by Clough [26] in 1960, the finite element method gained its recognition. The concepts of the method applied to the bending of plates only appeared about 1960 with the publications of Melosh [33], Adini and Clough [34] and Papenfuss [35]. They all used rectangular elements, which still continue to be employed in practice today. Although these rectangular elements were found to violate the requirements of a valid minimum potential energy problem statement, they nevertheless gave good accuracy and represented a significant step forward in structural analysis. From 1963 to 1964, Besseling [36], Melosh [37], Fraeijs de Veubeke [38] and Jones [39] recognized that the finite element method was a form of the Ritz method and confirmed it as a general technique to solve elastic continuum problems. It then became clear that the developments in finite element plate bending were related with the need to study more intensively the variational principles with regard to the general problem of element formulation and to develop organized procedures for the definition functional representation of element behaviour. Thus, guidelines for the latter emerged, followed by extensive

publications in flat plate elements. A survey by Gallagher [40] shows how vast is the amount of literature on the subject.

There are other formulations based on the method of weighted residuals [41],[42] in which the Galerkin approach is a special case. The weighted residuals approach begins with the governing equations of the problem and proceeds without relying on formulating a functional or variational principle. These formulations are still at the beginning and they appear to be advantageous because it becomes possible to extend the finite element method to problems where no functional is avaiable, hence they have a great potential for the solution of all field problems by the finite element method.

The variational methods provide four basic types of finite element methods. The first and most used is derived from the principle of minimum total potential energy, presented briefly in Section 2.1.7. This is based on the assumption of a displacement field continuous over the entire body [27]. A second method, derived from the principle of minimum complementary energy [1], and based on an assumed equilibrium stress field, is known as the equilibrium or force method [43],[44],[45],[46]. A third method based on a modified complementary energy principle [46],[47],[48], for which compatible displacement functions are assumed along the inter-element boundaries in addition to the assumed equilibrating stress field in each element. This method is called the hybrid method. The fourth method, derived from the Reissner principle, presented in Section 2.1.9, is called the mixed method [4]. It is based on an assumed displacement field which is continuous over the entire solid and assumed stress fields for individual elements. A very comprehensive study of the methods briefly described above can be found in a paper by Pian and Tong [2]. They set, for the finite

element method, the so-called defined compatibility conditions at the interelement boundary which make a variational functional definable. The contribution, with regard to the Reissner functional, applied to thin plates, is enormous since the inter-element continuity of different combinations of stress and displacement were studied and the conditions for the functional to be definable were presented for the following cases:-

1) Continuity of W and $\frac{\partial W}{\partial n}$

2) Continuity of W and M_n

3) Continuity of M_{ns}, M_n and $\frac{\partial M}{\partial n}$

In the application to the finite element method, case (2) has special advantages over the most used displacement method. Here only the continuity of W and M_n are required over interelement boundaries, thus the shape functions can easily be constructed. A complement to the important information providedby this paper is the one regarding the discretized form of the Reissner functional for thin and moderately thick plates provided by Connor in reference [13], which studies the jump terms required for the different alternatives, enabling the integration of the derivative terms of the original Reissner functional, equation (2.3.5).

The first mixed finite element analysis was due to Herrmann [4] in 1965. He used the Reissner functional in the form of equation (2.3.8) to develop a triangular mixed element for moderately thick plates. This was the first time at which transverse shear effects were rationally included. The transverse displacement and moments were selected as the primary variables of the corresponding variational formulation; a linear variation was chosen for such variables.

Later, Herrmann [31] developed a six degrees of freedom triangular element, for thin plates only, with a linear variation ,

within each element, for the transverse displacement and constant bending moments. In this way, the mixed matrix equations involve only the nodal transverse displacement and three normal moments at the middle point of the respective sides. It should be noticed that the polynomial representation for the displacement is one order higher than that for the moments. The element is remarkable for its algebraic simplicity and low number of degrees of freedom. Cook [49] in 1968, applied the Herrmann element [31] to extend, for the first time, the mixed method to the solution of buckling problems. No supporting results were shown in his discussion. Later, Cook [50], developed a similar, triangular element, but using the Reissner functional in its original form, equation (2.3.5), specialized for thin plates. To allow for the discontinuity of $\partial W/\partial n$ at the interelement boundaries a jump term $\int_{s_n} \frac{\partial W}{\partial n} M_n \, ds$ was added to the functional. This element was tested in the solution of dynamic and buckling problems. The results, although converging to the correct answers, are disappointing due to the slow rate of convergence.

Visser [51], using a parabolically varying transverse displacement and linear moment distribution, within each element, developed a 12 degrees of freedom triangular element for thin plates. The assumed linear shape functions were first respectively expressed in terms of M_x, M_y, M_{xy} in the three corners of the triangle. Then these moments were transformed into normal moments along lines parallel to the three sides of the triangle. The internal normal moments which were in no way coupled to unknowns of the adjacent elements were removed for each element by a condensation process. In this way the final element formulation involved only the transverse displacements at the primary corner and secondary (middle side) nodes

and two normal moments at each primary node.

Tahiani [52] presented two mixed elements, by considering linear distribution for the transverse displacement and moments, and parabolic variations for the transverse displacement and moments respectively. The area-natural coordinate concept was used for the first time in a mixed formulation and the shape functions were formed in terms of these natural coordinates.

A mixed finite element triangular model with 24 degrees of freedom has been developed by Chatterjee and Setlur [53] for the solution of moderately thick plates in static bending. The Reissner functional was used in its original form, equation (2.3.5). In this model interelement compatability is entirely satisfied. Linear distribution is assumed independently for all variables present in the functional (transverse displacement, rotations, bending and twisting moments and shear intensities, i.e.

$$[\, W \quad \beta_x \quad \beta_y \quad M_x \quad M_y \quad M_{xy} \quad Q_x \quad Q_y \,]).$$

This formulation has the advantage that the quantities of interest are all obtained directly, but the total number of unknowns at a node is very high, hence, the computation effort increases considerably.

A rectangular mixed model for thin plate bending problems was proposed by Kikuchi and Ando [54] in 1972. The transverse displacement is assumed to vary linearly, and the twisting moment is directly calculated by the relation $M_{xy} = -D(1+\mu)\,\frac{\partial^2 W}{\partial x \partial y}$. M_x and M_y are assumed constant within the element and they are expressed in terms of normal moments along the sides of the rectangle. The element has eight degrees of freedom, four nodal transverse displacements located at the primary nodes and four normal bending moments at the secondary nodes. This element is compatible with the

Herrmann triangular element [31], hence they can be combined for the solution of arbitrary thin plates.

A comparison of results for the rectangular element of Kikuchi and Ando with the Herrmann triangular model [31] called attention to the fact that the Herrmann element is very sensitive to the element pattern division. For example for a 4 x 4 square mesh in a quarter plate, simply supported with a uniform load, where the square elements are made of 2 triangles, for the two possible alternatives, the variation between both Herrmann's results for the maximum bending moment and maximum deflection at the centre are 4.43 and 2.15% respectively. From this we can see the need for quadrilateral elements which are obtained directly.

More recently, Bron and Dhatt [6],[55] made a detailed study of the influence of various types of mesh subdivision on the convergence properties of the mixed triangular elements of references [4],[52]. Some of the interesting but undesirable results were reported which show that certain types of subdivision of the mixed triangular elements [4],[52] lead to wrong solutions. The wrong convergence is obtained with these elements whenever four or eight elements meet at a point. To overcome these anomalies they proposed two rectangular elements respectively with linear variation for transverse displacement and moments, and parabolic variations of transverse displacement and moments. The results obtained are very good for both elements.

This literature survey presents the development of mixed elements in the analysis of plates. The results of Kikuchi and Ando [54], and Bron and Dhatt [6] show the need for quadrilateral elements. As far as it is known, no formal investigation had been carried out in any general mixed quadrilateral elements based on the isoparametric concept. It is, therefore, believed that a considerable improvement in the mixed formulation may be achieved

in the study of this family of elements. The introduction of the isoparametric concept in the formulation will help the standardization of the generation of mixed element properties. The need for the study of the mixed formulation in the solution of dynamic and buckling problem is also apparent from the review.

In the following chapters, a general mixed quadrilateral element for the solution of arbitrary plate problems is developed. A study of the behaviour of the element in the analysis of static, dynamic and buckling problems will be presented.

CHAPTER 5

TREATMENT OF THE PLATE BENDING PROBLEM BY MIXED FINITE ELEMENT

5.1) Introduction.

The mixed finite element applicable to the bending analysis of structural plates of general geometric shape is presented here. The analysis is carried out both for thin plates, where shear deformations are neglected, and for "moderately" thick plates where shear defomrations are taken into consideration. The plates may have orthotropic properties in which the axes of orthotropy are parallel to the x,y,z axes.

In the finite element idealization, the plate is replaced by a net of finite elements interconnected at nodes or joints.

A typical general plate divided into general quadrilateral elements is shown in Fig.(5.1.1).

The element described in this work is a new general quadrilateral element, developed using the Reissner principle and the results it yields will subsequently be compared with known solutions obtained "exactly" or by means of other elements or different methods described in the literature.

A computer program based on the theory of a general quadrilateral element, where the coefficients of the element mixed matrix are obtained by numerical integration, using Gauss quadrature, is developed in Chapter 7.

5.2) General Formulation of the Mixed Finite Element-Static Case.

5.2.1) Thin Plates.

Consider a general thin plate divided into arbitrary finite elements and let the transverse deflection W and the moments $\{M\} = [M_x \quad M_y \quad M_{xy}]^T$ be independently assumed within each element by

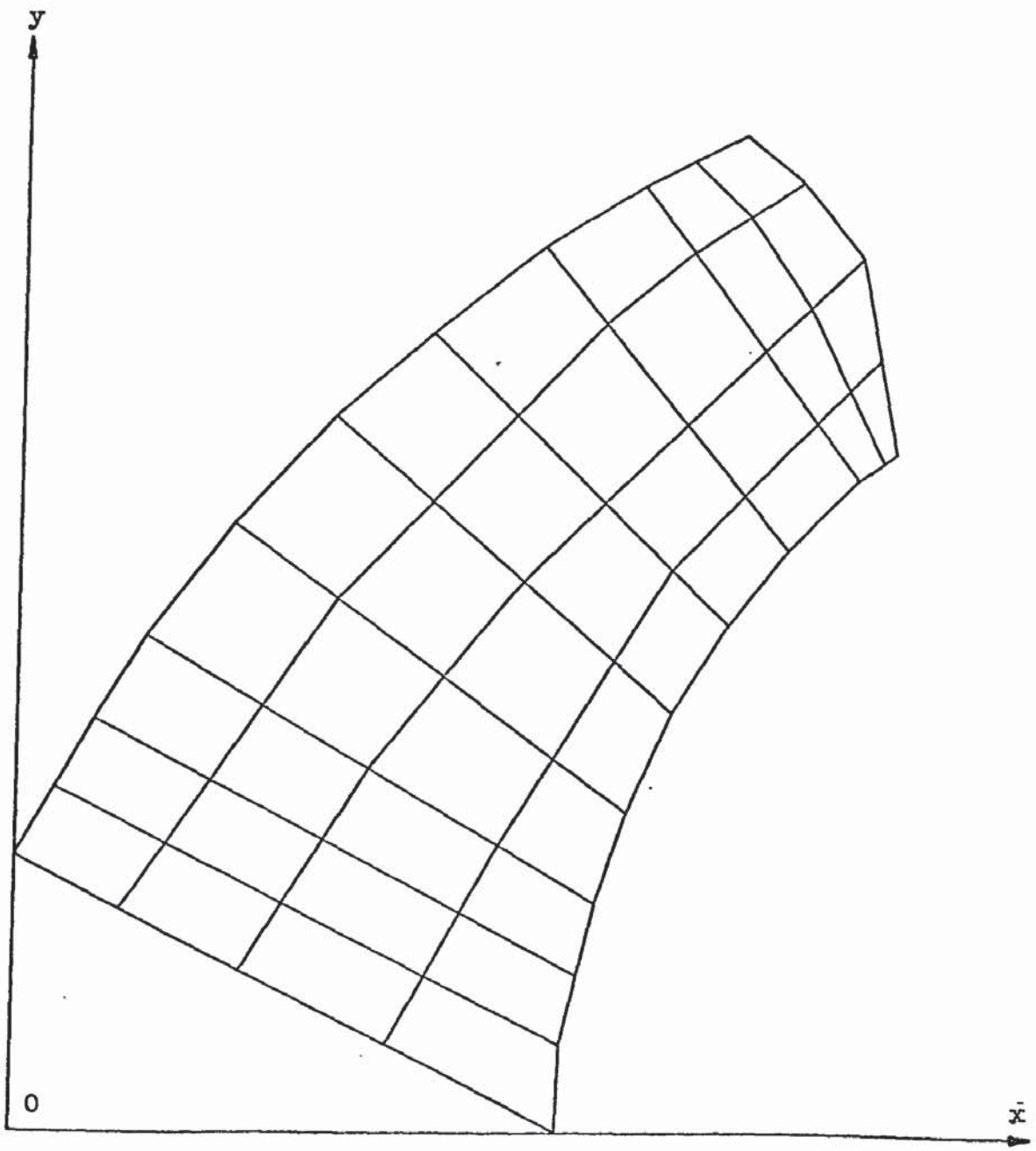

Fig.(5.1.1) Finite element representation of a plate.

$$W = [N_W]\ \{W\}_e \qquad (a)$$

$$\{M\} = \begin{bmatrix} N_{Mx} \\ N_{My} \\ N_{Mxy} \end{bmatrix} \{M\}_e = [N_M]\ \{M\}_e \qquad (b) \qquad (5.2.1)$$

in which $[N_W]$ and $[N_M]$ are interpolation functions (shape functions) dependent on natural coordinates, as seen in Chapter 3, and in the element nodal parameters (nodal deflections and moments)

$$\{W\}_e = [W_1 , W_2 , \ \dots\ , W_n] \qquad (a)$$

$$\{M\}_e = [M_{x_1} M_{y_1} M_{xy_1} , \ \dots\ , M_{x_m} M_{y_m} M_{xy_m}]^T \qquad (b) \qquad (5.2.2)$$

The interpolation functions for the transverse deflections and moments may be of different order and therefore the number of parameters which represent the deflections and moments might be different.

For the same order of deflection and moments interpolation functions, m = n, as shall be the case throughout this Thesis, the Reissner functional, equation (2.3.14), where inter-element compatibility of the transverse deflection W and normal moment M_n is maintained, can be represented in matrix notation, in its simplest form, for an element (e) as:

$$\left(\pi_R\right)_e = -\tfrac{1}{2}\iint_A \{M\}^T [C]\ \{M\} dA + \iint_A \{Q\}\{W'\} dA - \int_{s_n} M_{ns} \frac{\partial W}{\partial s}\, ds - \iint_A pW\, dA \qquad (5.2.3)$$

in which

$$\{M\} = [M_x \quad M_y \quad M_{xy}]^T$$

$$\{Q\} = [Q_x \quad Q_y]^T$$

$$\{W'\} = \left[\frac{\partial W}{\partial x} \quad \frac{\partial W}{\partial y}\right]^T$$

where the surface integrals are to be evaluated over the entire area of the element and the line integral is to be evaluated (in an

anti-clockwise direction) around each element boundary s_n.

By differentiating equation (5.2.1a) the slopes within the element are

$$\{W'\} = [N'_W]\ \{W\}_e \tag{5.2.4}$$

and, on the boundary s_n

$$\frac{\partial W}{\partial s} = [L_W]\ \{W'\} = [L_W]\ [N'_W]\ \{W\}_e = [Y]\ \{W\}_e \tag{5.2.5}$$

Differentiating equation (5.2.1b) in order to obtain the shear force intensities given by equations (2.2.26) and (2.2.27) within the element yields

$$\{Q\} = [N'_M]\ \{M\}_e \tag{5.2.6}$$

and, on the boundary, the twisting moment M_{ns} can be represented as:

$$M_{ns} = [L]\ [N_M]\ \{M\}_e = [L_{ns}]\ \{M\}_e \tag{5.2.7}$$

In both equations (5.2.5) and (5.2.7) $[L_W]$ and $[L]$ are direction cosines matrices.

After substituting the above derived equations into equation (5.2.3) we obtain:

$$\left(\pi_R\right)_e = -\tfrac{1}{2}\{M\}_e^T[g]\ \{M\}_e + \{M\}_e^T\ [h]\ \{W\}_e - \{W\}_e^T\ \{r\} \tag{5.2.8}$$

where

$$[g] = \iint_A [N_M]^T[C]\ [N_M]\ dA \qquad (a)$$

$$[h] = \iint_A [N'_M]^T[N'_W]\ dA - \oint_{s_n} [L_{ns}]^T[Y]ds \qquad (b) \tag{5.2.9}$$

$$\{r\} = \iint_A [N_W]^T p\ dA \qquad (c)$$

If we assume that the normal load $p(x,y)$ varies within the element, we might use the isoparametric concept by representing

$$p(x,y) = [N_p]\ \{p\}_e \tag{5.2.10}$$

in which $[N_p]$ contains interpolation functions.

The nodal pressure parameters are

$$\{p\}_e = [p_1 \quad p_2 \quad \ldots \quad p_n]^T \tag{5.2.11}$$

Then equation (5.2.9c) may be represented as:

$$\{r\} = \iint_A [N_W]^T [N_p] \{p\}_e \, dA \tag{5.2.12}$$

For the functional equation (5.2.8) to be stationary $\delta \pi_{R_e} = 0$, which implies taking variations with respect to the generalized parameters i.e.

$$\begin{Bmatrix} \dfrac{\partial \pi_{R_e}}{\partial \{M\}_e^T} \\ \dfrac{\partial \pi_{R_e}}{\partial \{W\}_e^T} \end{Bmatrix} = \begin{Bmatrix} 0 \\ 0 \end{Bmatrix}$$

yielding the mixed matrix equation

$$\begin{bmatrix} -[g] & [h] \\ [h]^T & [0] \end{bmatrix} \begin{Bmatrix} \{M\}_e \\ \{W\}_e \end{Bmatrix} = \begin{Bmatrix} \{0\} \\ \{r\} \end{Bmatrix} \tag{5.2.13}$$

Rather than list the nodal moments and nodal deflections separately we can rearrange the matrix equation (5.2.13) such that

$$[k] \{\delta\}_e = \{f\}_e \tag{5.2.14}$$

where the matrix containing all the nodal parameters for element e is

$$\{\delta\}_e = [W_1 \; M_{x_1} \; M_{y_1} \; M_{xy_1} \vdots \cdots \vdots \cdots \vdots W_n M_{x_n} M_{y_n} M_{xy_n}]^T \tag{5.2.15}$$

and the matrix containing the right hand side matrices $\{r\}$ and $\{0\}$ for an element is

$$\{f\}_e = [r_1\ 0\ 0\ 0 \vdots \cdots \vdots \cdots \vdots r_n\ 0\ 0\ 0]^T \qquad (5.2.16)$$

This new arrangement will facilitate the automatic assembly of the overall mixed matrix and the coding of the computer program.

5.2.2) "Moderately" Thick Plates.

The Reissner functional, suitable for orthotropic plates where the x,y,z axes are presumed parallel to the principal directions of an orthotropic material can be represented in matrix notation, in its simplest form, for an element (e), as

$$\left(\pi_R\right)_e = -\iint_A \tfrac{1}{2}\{M\}^T[C]\ \{M\}dA - \int \tfrac{1}{2}\{Q\}^T[C_{TS}]\ \{Q\}\ dA$$

$$+ \iint_A C_1\, p\, M_x\ dA + \iint_A C_2\ p\ M_y\ dA$$

$$+ \iint_A \{Q\}^T\{W\}\ dA - \iint_A p\ W\ dA \qquad (5.2.17)$$

in which [C] is a 3 x3 orthotropic bending compliance matrix, to be given later, and $[C_{TS}]$ is an orthotropic transverse bending shear compliance matrix given by

$$[C_{TS}] = \begin{bmatrix} C_{TS_{11}} & 0 \\ 0 & C_{TS_{22}} \end{bmatrix} = \frac{6}{5h}\begin{bmatrix} \frac{1}{G_{xz}} & 0 \\ 0 & \frac{1}{G_{yz}} \end{bmatrix} \qquad (5.2.18)$$

in which G_{yz} and G_{xz} are shear modulus which characterize changes of angles between the principal directions y and z, and x and z. C_1 and C_2 are elastic bending compliance constants given by

$$C_1 = \frac{12}{10h}\left(-\frac{\mu_{xz}}{E_z}\right)$$

$$C_2 = \frac{12}{10h}\left(-\frac{\mu_{yz}}{E_z}\right) \qquad (5.2.19)$$

where E_z is the Young's moduli for tension (compression) along the principal direction of elasticity z and μ_{xz}, μ_{yz} are the Poisson's ratios which characterize the decrease in the z direction during a tension applied into the x direction, etc.

In the case of isotropy, only two material constants E and μ are required. Then

$$\mu = \mu_{xy} = \mu_{xz} = \mu_{yz} \text{ etc., } ; \quad \frac{\mu_{xz}}{E_z} = \frac{\mu_{yz}}{E_z} = \frac{\mu}{E}$$
$$G = G_{xy} = G_{xz} = G_{yz} = \frac{E}{2(1+\mu)} \qquad (5.2.20)$$

The substitution of these two elastic constants into equation (5.2.17) gives the Reissner functional derived in Chapter 2 and given by equation (2.3.8), for general isotropic plates.

Substituting equations (5.2.1),(5.2.4) and (5.2.6) into equation (5.2.17) gives

$$\left(\pi_R\right)_e = -\tfrac{1}{2}\{M\}_e^T [g_s] \{M\}_e - \{M\}_e^T \{r_s\} + \{M\}_e^T [h_s] \{W\}_e - \{W\}_e^T \{r\} \qquad (5.2.21)$$

where

$$[g_s] = \iint_A [N_M]^T [C] [N_M] dA + \iint_A [N_M']^T [C_{TS}] [N_M'] dA \qquad (a)$$

$$\{r_s\} = \iint_A [N_{Mx}]^T C_1 \, p \, dA + \iint_A [N_{My}]^T C_2 \, p \, dA \qquad (b) \quad (5.2.22)$$

$$[h_s] = \iint_A [N_M']^T [N_W'] \, dA \qquad (c)$$

$$\{r\} = \iint_A [N_W]^T \, p \, dA \qquad (d)$$

The extremization of the functional equation (5.2.21) yields the element mixed matrix equation for "moderately" thick plates as:

$$\begin{bmatrix} -[\varepsilon_s] & \vdots & [h_s] \\ \cdots & \vdots & \cdots \\ [h_s]^T & \vdots & [0] \end{bmatrix} \begin{Bmatrix} \{M\}_e \\ \{W\}_e \end{Bmatrix} = \begin{Bmatrix} \{r_s\} \\ \{r\} \end{Bmatrix} \qquad (5.2.23)$$

Rearranging equation (5.2.23) in a similar way to that in paragraph (5.2.1) gives

$$[k_s]\ \{\delta\}_e = \{f_s\}_e \qquad (5.2.24)$$

where

$\{\delta\}_e$ is given by (5.2.15) and the load vector $\{f_s\}_e$ is a matrix containing the matrices $\{r_s\}$ and $\{r\}$ in the proper locations in accordance with equation (5.2.15).

5.3) Derivation of the General Linear Quadrilateral Element Characteristics-Plate Bending.

A typical arbitrary quadrilateral element is shown in Fig.(5.3.1), with nodes 1,2,3,4 numbered in anti-clockwise direction and sides 12; 23; 34; 41 respectively numbered 1,2,3,4. The Cartesian-coordinates x and y are related to the natural coordinates ζ,η within the element by the expressions (3.3.1),(3.3.2) given in Chapter 3.

The Cartesian coordinates of the nodes are denoted by (x_i,y_i). The lengths A_i of the element sides are given by

$$A_i = \sqrt{(x_i-x_j)^2 + (y_i-y_j)^2}$$

$$i = i,2,3,4 \qquad (5.3.1)$$

in which $j = i+1$ for $i = 1,2,3$

and $j = 1$ for $i = 4$

The sines and cosines of the element sides, angles "β_i" (angle between the side normal and the x axis) are given by the following, in which the notation defined by equation (5.3.1) is used:

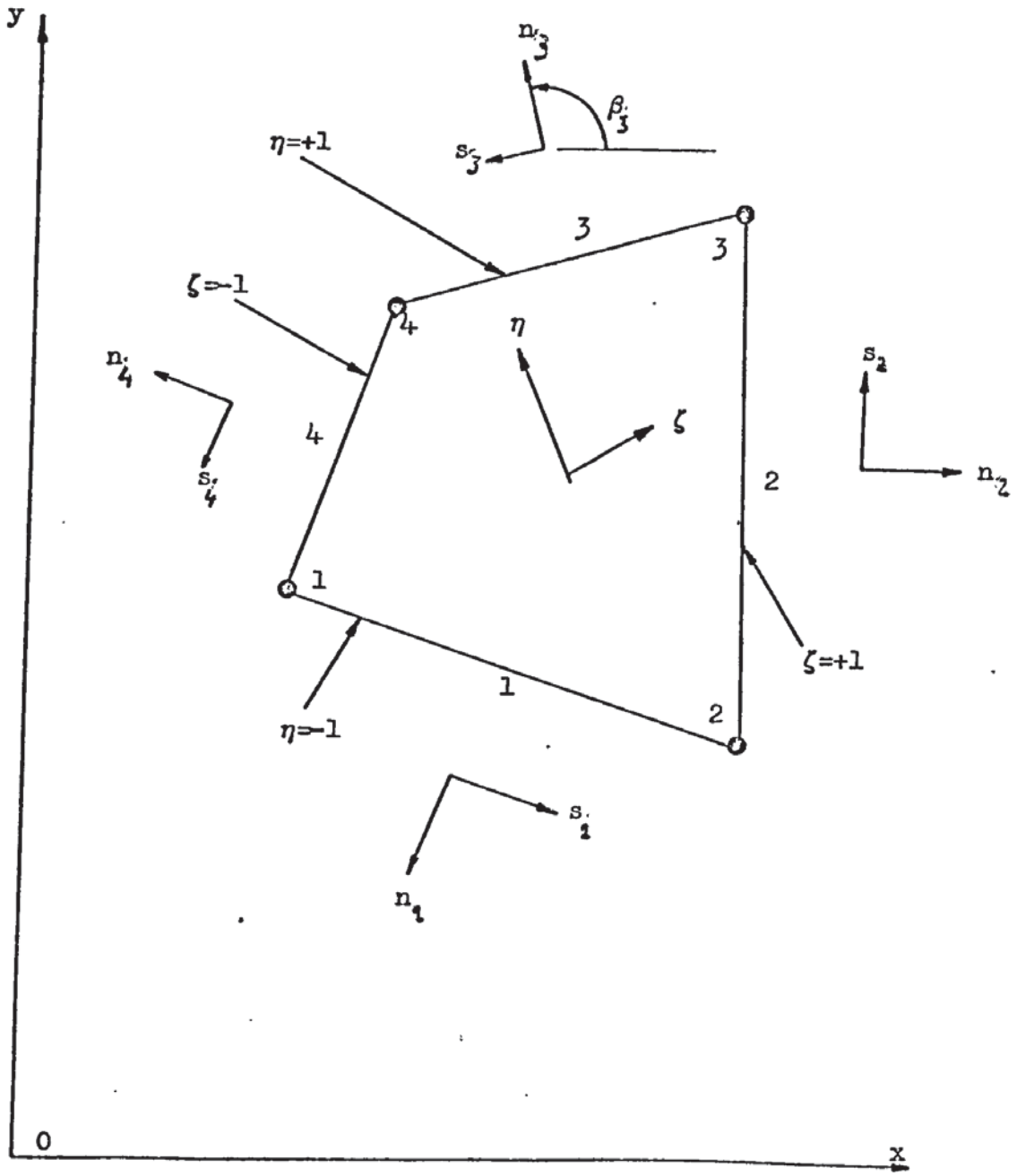

Fig.(5.3.1) Typical general quadrilateral plate element.Notation.

$$\sin \beta_i = \frac{x_i - x_j}{A_i} \qquad \text{(a)}$$

$$\cos \beta_i = \frac{y_j - y_i}{A_i} \qquad \text{(b)} \qquad (5.3.2)$$

5.3.1) Deflection and Moments-Interpolation Functions.

The transverse deflection and the moments are assumed independently within the element by

$$W = [N_1 \quad N_2 \quad N_3 \quad N_4] \begin{Bmatrix} W_1 \\ W_2 \\ W_3 \\ W_4 \end{Bmatrix} \quad \text{i.e. } W = [N_W]\{W\}_e \qquad (5.3.3)$$

$$\begin{Bmatrix} M_x \\ M_y \\ M_{xy} \end{Bmatrix} = \left[\begin{array}{ccc:ccc:ccc:ccc} N_1 & 0 & 0 & N_2 & 0 & 0 & N_3 & 0 & 0 & N_4 & 0 & 0 \\ 0 & N_1 & 0 & 0 & N_2 & 0 & 0 & N_3 & 0 & 0 & N_4 & 0 \\ 0 & 0 & N_1 & 0 & 0 & N_2 & 0 & 0 & N_3 & 0 & 0 & N_4 \end{array}\right] \begin{Bmatrix} M_{x_1} \\ M_{y_1} \\ M_{xy_1} \\ M_{x_2} \\ M_{y_2} \\ M_{xy_2} \\ M_{x_3} \\ M_{y_3} \\ M_{xy_3} \\ M_{x_4} \\ M_{y_4} \\ M_{xy_4} \end{Bmatrix} \qquad (5.3.4)$$

i.e. $\{M\} = [N_M]\{M\}_e$

in which the matrices $[N_W]$ and $[N_M]$ contain interpolation functions given by equations (3.3.2).

As the interpolation functions N_i are defined in terms of natural coordinates ζ and η it is necessary to change the derivatives to $\frac{\partial}{\partial x}$ and $\frac{\partial}{\partial y}$ whenever required. Noting that

$$\begin{Bmatrix} \frac{\partial N_i}{\partial \zeta} \\ \frac{\partial N_i}{\partial \eta} \end{Bmatrix} = \begin{bmatrix} \frac{\partial x}{\partial \zeta} & \frac{\partial y}{\partial \zeta} \\ \frac{\partial x}{\partial \eta} & \frac{\partial y}{\partial \eta} \end{bmatrix} \begin{Bmatrix} \frac{\partial N_i}{\partial x} \\ \frac{\partial N_i}{\partial y} \end{Bmatrix} = [J] \begin{Bmatrix} \frac{\partial N_i}{\partial x} \\ \frac{\partial N_i}{\partial y} \end{Bmatrix}$$

inverting gives

$$\begin{Bmatrix} \frac{\partial N_i}{\partial x} \\ \frac{\partial N_i}{\partial y} \end{Bmatrix} = [J]^{-1} \begin{Bmatrix} \frac{\partial N_i}{\partial \zeta} \\ \frac{\partial N_i}{\partial \eta} \end{Bmatrix} \qquad (5.3.5)$$

The Jacobian matrix can be evaluated by

$$[J] = \begin{bmatrix} \frac{\partial N_1}{\partial \zeta} & \frac{\partial N_2}{\partial \zeta} & \frac{\partial N_3}{\partial \zeta} & \frac{\partial N_4}{\partial \zeta} \\ \frac{\partial N_1}{\partial \eta} & \frac{\partial N_2}{\partial \eta} & \frac{\partial N_3}{\partial \eta} & \frac{\partial N_4}{\partial \eta} \end{bmatrix} \begin{bmatrix} x_1 & y_1 \\ x_2 & y_2 \\ x_3 & y_3 \\ x_4 & y_4 \end{bmatrix}$$

$$= \left[\begin{array}{c:c} -\frac{1}{4}(1-\eta)x_1+\frac{1}{4}(1-\eta)x_2 & -\frac{1}{4}(1-\eta)y_1+\frac{1}{4}(1-\eta)y_2 \\ +\frac{1}{4}(1+\eta)x_3-\frac{1}{4}(1+\eta)x_4 & +\frac{1}{4}(1+\eta)y_3-\frac{1}{4}(1+\eta)y_4 \\ \hdashline -\frac{1}{4}(1-\zeta)x_1-\frac{1}{4}(1+\zeta)x_2 & -\frac{1}{4}(1-\zeta)y_1-\frac{1}{4}(1+\zeta)y_2 \\ +\frac{1}{4}(1+\zeta)x_3+\frac{1}{4}(1-\zeta)x_4 & +\frac{1}{4}(1+\zeta)y_3+\frac{1}{4}(1-\zeta)y_4 \end{array}\right] \qquad (5.3.6)$$

i.e. $$[J] = \left[\begin{array}{c:c} J_{11} & J_{12} \\ \hdashline J_{21} & J_{22} \end{array}\right]$$

Inverting [J] yields

$$[J^*] = [J]^{-1} = \left[\begin{array}{c:c} \frac{J_{22}}{J_{11}J_{22}-J_{12}J_{21}} & -\frac{J_{12}}{J_{11}J_{22}-J_{12}J_{21}} \\ \hdashline -\frac{J_{21}}{J_{11}J_{22}-J_{12}J_{21}} & \frac{J_{11}}{J_{11}J_{22}-J_{12}J_{21}} \end{array}\right] \qquad (5.3.7)$$

i.e. $$[J^*] = \begin{bmatrix} J^*_{11} & J^*_{12} \\ J^*_{21} & J^*_{22} \end{bmatrix}$$

We can then represent an operating matrix [B], noticing equations (5.3.5) and (5.3.7), as

$$[B] = \begin{bmatrix} \frac{\partial N_1}{\partial x} & \frac{\partial N_2}{\partial x} & \frac{\partial N_3}{\partial x} & \frac{\partial N_4}{\partial x} \\ \frac{\partial N_1}{\partial y} & \frac{\partial N_2}{\partial y} & \frac{\partial N_3}{\partial y} & \frac{\partial N_4}{\partial y} \end{bmatrix} = \begin{bmatrix} B_{11} & B_{12} & B_{13} & B_{14} \\ B_{21} & B_{22} & B_{23} & B_{24} \end{bmatrix} \qquad (5.3.8)$$

in which

$$\begin{aligned}
B_{11} &= -\tfrac{1}{4}(1-\eta)\, J^*_{11} - \tfrac{1}{4}(1-\zeta)\, J^*_{21} && \text{(a)} \\
B_{12} &= +\tfrac{1}{4}(1-\eta)\, J^*_{11} - \tfrac{1}{4}(1+\zeta)\, J^*_{12} && \text{(b)} \\
B_{13} &= +\tfrac{1}{4}(1+\eta)\, J^*_{11} + \tfrac{1}{4}(1+\zeta)\, J^*_{12} && \text{(c)} \\
B_{14} &= -\tfrac{1}{4}(1+\eta)\, J^*_{11} + \tfrac{1}{4}(1-\zeta)\, J^*_{12} && \text{(d)} \qquad (5.3.9) \\
B_{21} &= -\tfrac{1}{4}(1-\eta)\, J^*_{21} - \tfrac{1}{4}(1-\xi)\, J^*_{22} && \text{(e)} \\
B_{22} &= +\tfrac{1}{4}(1-\eta)\, J^*_{21} - \tfrac{1}{4}(1-\zeta)\, J^*_{22} && \text{(f)} \\
B_{23} &= +\tfrac{1}{4}(1+\eta)\, J^*_{21} + \tfrac{1}{4}(1+\zeta)\, J^*_{22} && \text{(g)} \\
B_{24} &= -\tfrac{1}{4}(1+\eta)\, J^*_{21} + \tfrac{1}{4}(1-\zeta)\, J^*_{22} && \text{(h)}
\end{aligned}$$

5.3.2) Slope Matrices.

Differentiating equation (5.3.3) with respect to x and y at any point within the element gives

$$\begin{Bmatrix} \frac{\partial W}{\partial x} \\ \frac{\partial W}{\partial y} \end{Bmatrix} = \begin{bmatrix} \frac{\partial N_1}{\partial x} & \frac{\partial N_2}{\partial x} & \frac{\partial N_3}{\partial x} & \frac{\partial N_4}{\partial x} \\ \frac{\partial N_1}{\partial y} & \frac{\partial N_2}{\partial y} & \frac{\partial N_3}{\partial y} & \frac{\partial N_4}{\partial y} \end{bmatrix} \begin{Bmatrix} W_1 \\ W_2 \\ W_3 \\ W_4 \end{Bmatrix}$$

$$\text{i.e. } \{W'\} = [N'_W]\, \{W\}_e$$

The above relation can be evaluated by using the operating matrix [B] given by equations (5.3.8) and (5.3.9). It can be represented in terms of the nodal deflections as

$$\begin{Bmatrix} \frac{\partial W}{\partial x} \\ \frac{\partial W}{\partial y} \end{Bmatrix} = \begin{bmatrix} B_{11} & B_{12} & B_{13} & B_{14} \\ B_{21} & B_{22} & B_{23} & B_{24} \end{bmatrix} \begin{Bmatrix} W_1 \\ W_2 \\ W_3 \\ W_4 \end{Bmatrix} \qquad (5.3.10)$$

It is seen that for this case

$$[N_W'] = [B]$$

On the element boundary s_n equation (5.2.5) applies then

$$\frac{\partial W}{\partial s} = [L_W]_i \begin{Bmatrix} \frac{\partial W}{\partial x} \\ \frac{\partial W}{\partial y} \end{Bmatrix}_i$$

for i = 1,2,3,4

where (i) is the element side and the corresponding direction cosines matrix is evaluated by

$$[L_W]_i = [-\sin \beta_i \vdots \cos \beta_i]$$

for each element side using equations (5.3.1) and (5.3.2).

Substituting in the operating matrix [B] the natural coordinates value ± 1, corresponding to the coordinate ζ or η which happen to be constant along the side under study, gives

$$\frac{\partial W}{\partial s_i} = [-\sin \beta_i \vdots \cos \beta_i] \begin{bmatrix} B_{11} & B_{12} & B_{13} & B_{14} \\ B_{21} & B_{22} & B_{23} & B_{24} \end{bmatrix} \begin{Bmatrix} W_1 \\ W_2 \\ W_3 \\ W_4 \end{Bmatrix}$$

i.e $$\frac{\partial W}{\partial s_i} = [Y] \{W\}_e$$

where

$$[Y] = [Y_1 \quad Y_2 \quad Y_3 \quad Y_4] \qquad (a)$$

in which

$$\begin{aligned} Y_1 &= -B_{11} \sin\beta_i + B_{21} \cos\beta_i \quad (b) \\ Y_2 &= -B_{12} \sin\beta_i + B_{22} \cos\beta_i \quad (c) \\ Y_3 &= -B_{13} \sin\beta_i + B_{23} \cos\beta_i \quad (d) \\ Y_4 &= -B_{14} \sin\beta_i + B_{24} \cos\beta_i \quad (e) \end{aligned} \qquad (5.3.11)$$

5.3.3) Shear Force Intensity Matrix.

The shear force intensities Q_x and Q_y are expressed by equations (2.2.26) and (2.2.27) of Chapter 2.

Differentiating the matrix-relation (5.3.4) accordingly, within the element yields

$$\begin{Bmatrix} Q_x \\ Q_y \end{Bmatrix} = \left[\begin{array}{ccc:ccc:ccc:ccc} \frac{\partial N_1}{\partial x} & 0 & \frac{\partial N_1}{\partial y} & \frac{\partial N_2}{\partial x} & 0 & \frac{\partial N_2}{\partial y} & \frac{\partial N_3}{\partial x} & 0 & \frac{\partial N_3}{\partial y} & \frac{\partial N_4}{\partial x} & 0 & \frac{\partial N_4}{\partial y} \\ \hdashline 0 & \frac{\partial N_1}{\partial y} & \frac{\partial N_1}{\partial x} & 0 & \frac{\partial N_2}{\partial y} & \frac{\partial N_2}{\partial x} & 0 & \frac{\partial N_3}{\partial y} & \frac{\partial N_3}{\partial x} & 0 & \frac{\partial N_4}{\partial y} & \frac{\partial N_4}{\partial x} \end{array}\right] \begin{Bmatrix} M_{x_1} \\ M_{y_1} \\ M_{xy_1} \\ M_{x_2} \\ M_{y_2} \\ M_{xy_2} \\ M_{x_3} \\ M_{y_3} \\ M_{xy_3} \\ M_{x_4} \\ M_{y_4} \\ M_{xy_4} \end{Bmatrix} \qquad (5.3.12)$$

Substituting in the above matrix relation the components of the operating matrix [B] equations (5.3.9) gives the shear intensity forces in terms of the natural coordinates ζ and η and the nodal moments as:

$$\{Q\} = [N_W'] \{M\}_e \qquad (5.3.13)$$

where the new $[N_M']$ is

$$[N'_M] = \left[\begin{array}{c:c:c:c:c:c:c:c:c:c:c:c} B_{11} & 0 & B_{21} & B_{12} & 0 & B_{22} & B_{13} & 0 & B_{23} & B_{14} & 0 & B_{24} \\ \hdashline 0 & B_{21} & B_{11} & 0 & B_{22} & B_{12} & 0 & B_{23} & B_{13} & 0 & B_{24} & B_{14} \end{array}\right] \quad (5.3.14)$$

5.3.4) Normal Twisting Moment Along Each Element Side

The normal twisting moment M_{ns} in terms of the natural coordinates ζ and η and the nodal moments are given by equation (5.2.7) with ζ or $\eta = \pm 1$. The direction cosines matrix

$$[L] = [L_{11}L_{12}L_{13}] = [-\cos\beta_i \;\; \sin\beta_i \vdots \cos\beta_i \;\; \sin\beta_i \vdots \cos^2\beta_i \;\; -\sin^2\beta_i] \quad (5.3.15)$$

is taken from relation (2.2.20) and the components are evaluated using equations (5.3.1) and (5.3.2) for each element side in turn. The twisting moment M_{ns} can then be represented as

$$M_{ns} = [L_{11}N_1 \vdots L_{12}N_1 \vdots L_{13}N_1 \vdots L_{11}N_2 \vdots L_{12}N_2 \vdots L_{13}N_2 \vdots L_{11}N_3 \vdots L_{12}N_3 \vdots L_{13}N_3 \vdots L_{11}N_4 \vdots L_{12}N_4 \vdots L_{13}N_4] \begin{Bmatrix} M_{x_1} \\ M_{y_1} \\ M_{xy_1} \\ M_{x_2} \\ M_{y_2} \\ M_{xy_2} \\ M_{x_3} \\ M_{y_3} \\ M_{xy_3} \\ M_{x_4} \\ M_{y_4} \\ M_{xy_4} \end{Bmatrix} \quad (5.3.16)$$

i.e.

$$M_{ns} = [L_{ns}] \{M\}_e$$

with ζ or $\eta = \pm 1$

5.3.5) Mixed Element Matrix and Load Vector.

Having established the Jacobian transformation in the matrices $[N'_W]$ and $[N'_M]$ we can proceed to the integration of equations (5.2.9) and (5.2.22) by completing the change of co-ordinates to express the element component matrices in terms of the natural coordinates ζ and η. Then for

a) Thin Plates.

$$[g] = \int_{-1}^{1}\int_{-1}^{1} [N_M]^T [C] [N_M] \det [J] \, d\zeta \, d\eta \qquad (a)$$

$$[h] = \int_{-1}^{1}\int_{-1}^{1} [N_M']^T [N_W'] \det[J] d\zeta d\eta - \tfrac{1}{2}\int_{-1}^{1}[L_{ns}]^T[Y] \begin{matrix} d\zeta \\ \text{or} \\ d\eta \end{matrix} \qquad (b) \qquad (5.3.17)$$

$$\{r\} = \int_{-1}^{1}\int_{-1}^{1} [N_W]^T \, p \det [J] d\zeta d\eta \qquad (c)$$

and

b) "Moderately" Thick Plates.

$$[g_s] = \int_{-1}^{1}\int_{-1}^{1}[N_M]^T[C][N_M]\det[J]d\zeta d\eta + \int_{-1}^{1}\int_{-1}^{1}[N_M']^T[C_{TS}][N_M']\det[J]d\zeta d\eta \qquad (a)$$

$$\{r_s\} = \int_{-1}^{1}\int_{-1}^{1}[N_{M_x}]^T C_1 \, p \det[J]d\zeta d\eta + \int_{-1}^{1}\int_{-1}^{1}[N_{M_y}]^T C_2 \, p \det[J]d\zeta d\eta \qquad (b)$$

$$[h_s] = \int_{-1}^{1}\int_{-1}^{1}[N_M']^T [N_W'] \det[J]d\zeta d\eta \qquad (c) \quad (5.3.18)$$

$$\{r\} = \int_{-1}^{1}\int_{-1}^{1} [N_W]^T \, p \det [J]d\zeta d\eta \qquad (d)$$

In both cases, if the normal pressure $p(x,y)$ is not constant and is assumed to change linearly within the element, the load vector $\{f\}$ can be evaluated by substituting equation (5.2.10) into equations (5.3.18 b,d), after completing the change of coordinates yields:

$$\{r\} = \int_{-1}^{1}\int_{-1}^{1} [N_W]^T [N_p] \{p\}_e \det [J] d\zeta d\eta \qquad (a)$$

(5.3.19)

Similarly

$$\{r_s\} = \int_{-1}^{1}\int_{-1}^{1} [N_{M_x}]^T [N_p] C_1 \det[J] d\zeta d\eta + \int_{-1}^{1}\int_{-1}^{1} [N_{M_y}]^T [N_p] C_2 \det[J] d\zeta d\eta \qquad (b)$$

The matrices $[N_W]$, $[N_M]$, $[N_{M_x}]$, $[N_{M_y}]$, $[N_W']$, $[Y]$, $[N_M']$ and $[L_{ns}]$ were already defined respectively by equations (5.3.3), (5.3.4), (5.3.10), (5.3.11), (5.3.14) and (5.3.16). The compliance matrix [C] is given by equation (2.2.17) for isotropic plates. For orthotropic plates with principal directions of orthotropy coinciding with the x and y axes the matrix [C] in terms of the orthotropic elastic constants is given in reference [56] as

$$[C] = \begin{bmatrix} C_{11} & C_{12} & C_{13} \\ & C_{22} & C_{23} \\ \text{Symmetric} & & C_{33} \end{bmatrix} = \begin{bmatrix} \frac{12}{E_x h^3} & -\frac{12\mu_{yx}}{E_y h^3} & 0 \\ & \frac{12}{E_y h^3} & 0 \\ \text{Symmetric} & & \frac{12}{G_{xy} h^3} \end{bmatrix} \qquad (5.3.20)$$

h = thickness of the element

The shear compliance matrix $[C_{TS}]$ and the constants C_1 and C_2 were respectively defined by equations (5.2.18), (5.2.19) and (5.2.20) for isotropic and orthotropic materials.

The interpolation function $[N_p] = [N_W]$ and $\{p\}_e^T = [p_1 \quad p_2 \quad p_3 \quad p_4]$ is a vector with nodal pressures.

The components of the element mixed matrix can then be given as

a) Thin Plates

$$[g] = \begin{bmatrix} [g_{11}] & [g_{12}] & [g_{13}] & [g_{14}] \\ [g_{21}] & [g_{22}] & [g_{23}] & [g_{24}] \\ [g_{31}] & [g_{32}] & [g_{33}] & [g_{34}] \\ [g_{41}] & [g_{42}] & [g_{43}] & [g_{44}] \end{bmatrix}$$

where

$$[g_{ij}] = \int_{-1}^{1}\int_{-1}^{1} \begin{bmatrix} N_i\, C_{11} N_j & N_i\, C_{12} N_j & N_i C_{13} N_j \\ N_i\, C_{21} N_j & N_i\, C_{22} N_j & N_i C_{23} N_j \\ N_i\, C_{31} N_j & N_i\, C_{32} N_j & N_i C_{33} N_j \end{bmatrix} \det[J]\, d\zeta\, d\eta \qquad (5.3.21)$$

for i,j = 1,2,3,4

$$[h] = \begin{bmatrix} [h_{11}] & [h_{12}] & [h_{13}] & [h_{14}] \\ [h_{21}] & [h_{22}] & [h_{23}] & [h_{24}] \\ [h_{31}] & [h_{32}] & [h_{33}] & [h_{34}] \\ [h_{41}] & [h_{42}] & [h_{43}] & [h_{44}] \end{bmatrix}$$

where

$$[h_{ij}] = \int_{-1}^{1}\int_{-1}^{1} \begin{bmatrix} B_{1i} & B_{1j} \\ B_{2i} & B_{2j} \\ B_{2i}B_{1j}+B_{1i}B_{2j} \end{bmatrix} \det[J]\, d\zeta\, d\eta$$

$$-\tfrac{1}{2}\int_{-1}^{1} \begin{bmatrix} L_{11} N_i & Y_j \\ L_{12} N_i & Y_j \\ L_{13} N_i & Y_j \end{bmatrix} \begin{matrix} d\zeta \\ \text{or} \\ d\eta \end{matrix} \qquad (5.3.22)$$

for i,j = 1,2,3,4

in which the line integral is evaluated over the four sides of the element.

The load vector for p = constant is

a) contd.

$$\{r\} = \begin{Bmatrix} r_1 \\ r_2 \\ r_3 \\ r_4 \end{Bmatrix} = \int_{-1}^{1}\int_{-1}^{1} \begin{bmatrix} N_1 \\ N_2 \\ N_3 \\ N_4 \end{bmatrix} p \det[J] d\zeta d\eta \qquad (5.2.23)$$

or, assuming that $p(x,y)$ changes linearly within the element, the nodal forces of equation (5.2.23) become

$$r_i = \int_{-1}^{1}\int_{-1}^{1} \left(\sum N_i N_j p_j \right) \det[J] d\zeta d\eta \qquad (5.3.24)$$

for $i,j = 1,2,3,4$

b) "Moderately Thick Plates"

$$[g_s] = \left[\begin{array}{c:c:c:c} [g_{s_{11}}] & [g_{s_{12}}] & [g_{s_{13}}] & [g_{s_{14}}] \\ \hdashline [g_{s_{21}}] & [g_{s_{22}}] & [g_{s_{23}}] & [g_{s_{24}}] \\ \hdashline [g_{s_{31}}] & [g_{s_{32}}] & [g_{s_{33}}] & [g_{s_{34}}] \\ \hdashline [g_{s_{41}}] & [g_{s_{42}}] & [g_{s_{43}}] & [g_{s_{44}}] \end{array}\right]$$

where

$$[g_{s_{ij}}] = \int_{-1}^{1}\int_{-1}^{1} \left[\begin{array}{c:c:c} N_i C_{11} N_j & N_i C_{12} N_j & N_i C_{13} N_j \\ \hdashline N_i C_{21} N_j & N_i C_{22} N_j & N_i C_{23} N_j \\ \hdashline N_i C_{31} N_j & N_i C_{32} N_j & N_i C_{33} N_j \end{array}\right] \det[J] d\zeta d\eta$$

$$+ \int_{-1}^{1}\int_{-1}^{1} \begin{bmatrix} B_{1i} C_{TS_{11}} B_{ij} & 0 & B_{1i} C_{TS_{11}} B_{2j} \\ 0 & B_{2i} C_{TS_{22}} B_{2j} & B_{2i} C_{TS_{22}} B_{1j} \\ B_{2i} C_{TS_{11}} B_{ij} & B_{1i} C_{TS_{22}} B_{2j} & \begin{array}{l} B_{2i} C_{TS_{11}} B_{2j} + \\ B_{1i} C_{TS_{22}} B_{1j} \end{array} \end{bmatrix} \det[J] d\zeta d\eta \qquad (5.3.25)$$

for $i,j = 1,2,3,4$

b) contd.

$$[h_s] = \left[\begin{array}{c|c|c|c} [h_{s_{11}}] & [h_{s_{12}}] & [h_{s_{13}}] & [h_{s_{14}}] \\ \hline [h_{s_{21}}] & [h_{s_{22}}] & [h_{s_{23}}] & [h_{s_{24}}] \\ \hline [h_{s_{31}}] & [h_{s_{32}}] & [h_{s_{33}}] & [h_{s_{34}}] \\ \hline [h_{s_{41}}] & [h_{s_{42}}] & [h_{s_{43}}] & [h_{s_{44}}] \end{array}\right]$$

where

$$[h_{s_{ij}}] = \int_{-1}^{1}\int_{-1}^{1} \left[\begin{array}{c|c} B_{1i} & B_{1j} \\ \hline B_{2i} & B_{2j} \\ \hline B_{2i}\ B_{1j} + B_{1i}\ B_{2j} & \end{array}\right] \det[J]\,d\zeta\,d\eta \qquad (5.3.26)$$

for i,j = 1,2,3,4

The shear deformation contribution to the load vector is, for p = constant,

$$\{r_s\} = [\,[r_{s_1}]\ [r_{s_2}]\ [r_{s_3}]\ [r_{s_4}]\,]^T$$

where

$$\{r_{s_i}\} = \int_{-1}^{1}\int_{-1}^{1} \begin{bmatrix} N_i \\ 0 \\ 0 \end{bmatrix} C_1\ p\ \det[J]\,d\zeta\,d\eta + \int_{-1}^{1}\int_{-1}^{1} \begin{bmatrix} 0 \\ N_i \\ 0 \end{bmatrix} C_2 p\ \det[J]\,d\zeta\,d\eta \qquad (5.3.27)$$

for i = 1,2,3,4

If the load p(x,y) is assumed to change linearly within the element

$$\{r_{s_i}\} = \begin{Bmatrix} r_{s_1} \\ r_{s_2} \\ r_{s_3} \end{Bmatrix} = \int_{-1}^{1}\int_{-1}^{1} \begin{Bmatrix} \Sigma N_i N_j\ p_j\ C_1 \\ 0 \\ 0 \end{Bmatrix} \det[J]\,d\zeta\,d\eta$$

$$+ \int_{-1}^{1}\int_{-1}^{1} \begin{Bmatrix} 0 \\ \Sigma\ N_i\ N_j\ p_j\ C_2 \\ 0 \end{Bmatrix} \det[J]\,d\zeta\,d\eta \qquad (5.3.28)$$

for i,j = 1,2,3,4

The load vector $\{r\}$ is the same as for thin plates and therefore is given by equations (5.3.23) or (5.3.24).

Having expressed all matrices in terms of ζ and η they can be evaluated numerically using the Gauss quadrature formula at 4 and two integrating points respectively for the area and line integrals. The numerical integration procedure explained in Section 3.4 is used here.

5.3.6) Mixed-Element Matrix Equation.

Having established the matrices components $[g],[h],\{r\}$ for thin plates and $[g_s],[h_s],\{r_s\}$ $\{r\}$ for "moderately" thick plates we can rearrange the element-matrix equation such that

$$\left[\begin{array}{c:c:c:c} [k_{11}] & [k_{12}] & [k_{13}] & [k_{14}] \\ \hdashline [k_{21}] & [k_{22}] & [k_{23}] & [k_{24}] \\ \hdashline [k_{31}] & [k_{32}] & [k_{33}] & [k_{34}] \\ \hdashline [k_{41}] & [k_{42}] & [k_{43}] & [k_{44}] \end{array}\right] \left\{\begin{array}{c} \{\delta\}_1 \\ \{\delta\}_2 \\ \{\delta\}_3 \\ \{\delta\}_4 \end{array}\right\} = \left\{\begin{array}{c} \{f\}_1 \\ \{f\}_2 \\ \{f\}_3 \\ \{f\}_4 \end{array}\right\} \qquad (5.3.29)$$

$$\text{i.e. } [k]_e \{\delta\}_e = \{f\}_e$$

where for thin plates

$$[k_{ij}] = \left[\begin{array}{c:c} 0 & [h_{ij}]^T \\ \hdashline [h_{ij}] & -[g_{ij}] \end{array}\right] \qquad (5.3.30$$

$$\text{for } i,j = 1,2,3,4$$

in which $[g_{ij}]$ and $[h_{ij}]$ are respectively given by equations (5.3.21) and (5.3.22).

For "moderately" thick plates

$$[k_{ij}] = \begin{bmatrix} 0 & [h_{s_{ij}}]^T \\ [h_{s_{ij}}] & -[g_{s_{ij}}] \end{bmatrix} \qquad (5.3.31)$$

$$\text{for } i,j = 1,2,3,4$$

in which $[g_{s_{ij}}]$ and $[h_{s_{ij}}]$ are evaluated using equations (5.3.25) and (5.3.26).

The nodal parameters vector $\{\delta\}_e$ is the same in both cases and its vector components can be represented as:

$$\{\delta_i\}^T = [W \quad M_x \quad M_y \quad M_{xy}]_i^T \qquad (5.3.32)$$

$$\text{for } i = 1,2,3,4$$

The force vector components of $\{f\}_e$ are, for thin and "moderately" thick plates respectively, given by

$$\{f_i\} = [r_i \quad 0 \quad 0 \quad 0]_i^T \qquad \text{(a)}$$

$$\{f_i\} = [r_i [r_s]_i] = [r_i \; [r_{s_1} \quad r_{s_2} \quad 0]_i]_i^T \qquad \text{(b)} \qquad (5.3.33)$$

$$\text{for } i = 1,2,3,4$$

in which $\{r_i\}$ and $\{r_{s_i}\}$ are given by equations (5.3.23) or (5.3.24) and (5.3.27) or (5.3.28).

5.3.7) Representation of the Compliance Matrices.

In general the compliance coefficients may vary with the x and y due to the variation in thickness or the properties of the plate or both. In order to integrate to obtain the element matrix as developed in the last section, for cases of changing thickness, a linear variation of the thickness is assumed within the element.

By using the isoparametric concept the thickness within the element is represented as:

$$h = [N_h]\{h\}_e \qquad (5.3.34)$$

in which $[N_h]$ contains linear interpolation functions in terms of the natural coordinates ζ and η, and they are taken equal to $[N_W]$ i.e. $[N_h] = [N_W]$ where $[N_W]$ are the shape functions of equation (5.3.3). The vector

$$\{h\}_e = [h_1 \quad h_2 \quad h_3 \quad h_4]^T$$

lists the nodal thicknesses. The nodal thicknesses are previously evaluated at all nodes of the plate by replacing the nodal coordinates x and y in the general expression which defines the general thickness shape h(x,y) of the plate. These nodal thicknesses are then input in the computer program, as shall be explained later.

Since the element properties are evaluated numerically at the Gauss integrating points, the thickness is then automatically calculated at such points using equation (5.3.34) and the compliance coefficients evaluated.

Alternatively one may assume that the compliance coefficients are constants within each element and input the compliance at the centroid of each element. The various alternatives shall be fully explained in the description of the computer program.

5.4) Assembly of the Overall Mixed Matrix and Overall Load Vector.

Once the characteristics of the individual elements are known the overall problem can be studied by applying the Reissner Principle to the complete structure. The Reissner functional for an element in terms of the mixed element matrix and load vector may be represented as:

$$\pi_{R_e} = \tfrac{1}{2}\{\delta\}_e^T [k]_e \{\delta\}_e - \{\delta\}_e^T \{f\}_e$$

Hence, if the number of elements in the overall structure

is N then the Reissner functional for the overall structure will be

$$\pi_R = \tfrac{1}{2} \sum_{e=1}^{N} \{\delta\}_e^T [k]_e \{\delta\}_e - \sum_{e=1}^{N} \{\delta\}_e^T \{f\}_e \qquad (5.4.1)$$

The vector $\{\delta\}_e$ represents the nodal deflections and bending moments for element e.

Let us suppose, for the effect of simplification, an element with two nodes and two degrees of freedom per node.

For such an element, the vectors $\{\delta\}_e$ and $\{f\}_e$ may be represented as

$$\{\delta\}_e = \begin{Bmatrix} \begin{Bmatrix} W \\ M \end{Bmatrix}_1 \\ \begin{Bmatrix} W \\ M \end{Bmatrix}_2 \end{Bmatrix} = \begin{Bmatrix} \{\delta\}_1 \\ \{\delta\}_2 \end{Bmatrix}; \text{ and } \{f\}_e = \begin{Bmatrix} \begin{Bmatrix} f' \\ f^* \end{Bmatrix} \\ \begin{Bmatrix} f' \\ f^* \end{Bmatrix} \end{Bmatrix} = \begin{Bmatrix} \{f\}_1 \\ \{f\}_2 \end{Bmatrix}$$

If these two vectors are transformed to ones with global numbering containing the total number of degrees of freedom, then the element nodal parameters (nodal deflections and moments) and the element nodal force vector become

$$\{\delta_e\} = \begin{bmatrix} \text{- - - -} & \text{- - row 1 - - -} & \text{- -} \\ \{0\} & \text{- - row 2 - - -} & \{0\} \\ \{0\} & & \{0\} \\ \vdots & & \vdots \\ \text{- -,- -} & \text{- - row } 2\times(e_1-1) & \text{- -} \\ \{\delta_{e_1}\} & & \{f_{e_1}\} \\ \text{- - - -} & \text{- - row } 2\times e_1 & \text{- - -} \\ \text{- - - -} & \text{- - row } 2\times e_2-1 & \text{- - -} \\ \{\delta_{e_2}\} & & \{f_{e_2}\} \\ \text{- - - -} & \text{- - row } 2\times e_2 & \text{- - -} \\ \vdots & & \vdots \\ \{0\} & & \{0\} \end{bmatrix} = \{f_e\}$$

where e_1 and e_2 are the global node numbers which correspond to node number one and two of the element e. The vectors $\{\delta_e\}$ and $\{f_e\}$ are distinguished from $\{\delta\}_e$ and $\{f\}_e$ by taking the

suffix e inside the bracket to indicate that the only non-zero locations are the nodal vectors corresponding to element e.

The same notation will be used from the element mixed matrix.

To maintain the general nature of the element matrix-equation $[k]_e\{\delta\}_e = \{f\}_e$ the element matrix needs to be represented as:

$$[k_e] = \begin{bmatrix} 0 & 0 & \cdots & 0 & \cdots & 0 \\ \vdots & & & & & \\ & & [k_{e_1e_1}] & [k_{e_1e_2}] & & \leftarrow \text{row } 2\times(e_1-1)+1 \\ & & & & 0 & \leftarrow \text{row } 2\times e_1 \\ 0 & & & & & \leftarrow \text{row } 2\times(e_2-1)+1 \\ & & [k_{e_2e_1}] & [k_{e_2e_2}] & & \leftarrow \text{row } 2\times e_2 \\ & & \vdots & \vdots & 0 & \\ 0 & & \text{Col } 2\times(e_1-1)+1 & \text{Col } 2\times(e_2-1)+1 & & \\ \vdots & & & & & \\ 0 & & \text{Col } 2\times e_1 & \text{Col } 2\times e_2 & 0 & \end{bmatrix}$$

where

$$\begin{bmatrix} [k_{e_1e_1}] & [k_{e_1e_2}] \\ [k_{e_2e_1}] & [k_{e_2e_2}] \end{bmatrix} = \begin{bmatrix} [k]_{11} & [k]_{12} \\ [k]_{21} & [k]_{22} \end{bmatrix}_e = \begin{bmatrix} \begin{bmatrix} k_{11}k_{12} \\ k_{21}k_{22} \end{bmatrix} & \begin{bmatrix} k_{13}k_{14} \\ k_{23}k_{24} \end{bmatrix} \\ \begin{bmatrix} k_{31}k_{32} \\ k_{41}k_{42} \end{bmatrix} & \begin{bmatrix} k_{33}k_{34} \\ k_{43}k_{44} \end{bmatrix} \end{bmatrix}_e$$

All other locations in the matrix $[k_e]$ contain zeros.

The equation (5.4.1) can then be represented as

$$\pi_R = \tfrac{1}{2}\sum_{e=1}^{N} \{\delta_e\}^T[k_e]\{\delta_e\} - \sum_{e=1}^{N} \{\delta_e\}^T\{f_e\}$$

Expanding this summation yields

$$\pi_R = \tfrac{1}{2}\Big(\{\delta_1\}^T [k_1] \{\delta_1\} + \{\delta_2\}^T [k_2] \{\delta_2\} + \cdots + \{\delta_e\}^T [k_e] \{\delta_e\} + \cdots + \{\delta_N\}^T [k_N] \{\delta_N\} \Big) - \{\delta_1\}^T \{f_1\} + \{\delta_2\}^T \{f_2\} + \cdots + \{\delta_e\}^T \{f_e\} + \cdots + \{\delta_N\}^T \{f_N\} \qquad (5.4.2)$$

Replacing $\{\delta_e\}$ by the overall nodal parameters vector $\{\delta\}$, containing all the nodal deflection and bending moments of the structure, the equation (5.4.2) will not be affected because the zeros located in the element matrix and force vector will cancel the effect of the deflection and moments added to each of the vectors $\{\delta_e\}$.

After rearranging the terms, the equation (5.4.2) can be rewritten as

$$\pi_R = \tfrac{1}{2}\{\delta\}^T \Big([k_1] + [k_2] + \cdots + [k_e] + \cdots + [k_N] \Big) \{\delta\} - \{\delta\}^T \Big(\{f_1\} + \{f_2\} + \cdots + \{f_e\} + \cdots + \{f_N\} \Big)$$

or

$$\pi_R = \tfrac{1}{2}\{\delta\}^T \Big(\sum_{e=1}^{N} [k_e] \Big) \{\delta\} - \{\delta\}^T \Big(\sum_{e=1}^{N} \{f_e\} \Big)$$

Now extremizing the functional gives:

$$\frac{\partial \pi_R}{\partial \{\delta\}^T} = \Big(\sum_{e=1}^{N} [k_e] \Big) \{\delta\} - \sum_{e=1}^{N} \{f_e\} = 0$$

which may be abbreviated in the following form:

$$[K] \{\delta\} = \{F\} \qquad (5.4.3)$$

where $[K]$ and $\{F\}$ are the assembled overall mixed matrix and overall force vector.

From the above procedure the assembly rules for the overall mixed matrix and overall force vector can be stated as follows:

$$[K] = \sum_{e=1}^{N} [k_e] \qquad (a)$$

(5.4.4)

$$\{F\} = \sum_{e=1}^{N} \{f_e\} \qquad (b)$$

If the number of degrees of freedom per node is 4, and if the element has 4 nodes, as is the case with the general quadrilateral element, then the vectors $\{\delta_{e_1}\}$, $\{\delta_{e_2}\}$, $\{f_{e_1}\}$ and $\{f_{e_2}\}$ should be replaced by four values the first of which is given by 4 × (global node number -1) + 1; for the subsequent values 1 is added. Accordingly $[k_{e_1e_1}]$, $[k_{e_1e_2}]$, $[k_{e_2e_1}]$, $[k_{e_2e_2}]$ should be replaced by 4 × 4 matrices.

It has been shown that the overall matrix is the assemblage of the element mixed matrices. This overall matrix is banded because the (matrix) equation for a node will involve only those (partitioned) columns corresponding to the nodes connected to the particular node by elements. There is a distance from the diagonal beyond which no terms exist. This is called the banding of the matrix and the number of elements of the matrix from the diagonal term to the last in the band incluse is called the semi-bandwidth, see Fig.(5.4.2). Thus the semi-bandwidth depends upon the size of the mixed element matrix and upon the system of notation for the nodes. If the semi-bandwidth can be reduced then the solution time and storage requirements can be minimized. The reduction can be achieved by performing a systematic subdivision and adopting an appropriate sequence for the node numbers. Since the node numbers are used for numbering the nodal displacements and moments, the semi-bandwidth for the overall mixed matrix using the general quadrilateral element is given by:

$$BD = (DIF + 1) \times 4 \qquad (5.4.5)$$

where BD is the semi-bandwidth and DIF is the maximum largest difference occurring in the structure between two node numbers of a single element, accordingly the pattern for a plate divided into three rectangular elements, Fig.(5.4.1) is shown in Fig.(5.4.2).

5.5) Boundary Conditions.

The plate problem is not completely specified unless boundary conditions are incorporated, in fact the matrix equation (5.4.3) is singular and cannot be inverted to provide a solution for $\{\delta\}$. However if the boundary conditions for the problem are inserted, [K] is reduced to a non-singular symmetric non-positive definite matrix and the system of equation can then be solved. The prescribed quantities are deflections and moments. If the restrained moments are coincident with the x,y global ones the alteration to the equations is easily performed as will be shown in paragraph 5.7.3. In general this will not be the case, because when moments are prescribed, they will have to be in terms of the normal component M_n for thin plates and normal and tangential components M_n, M_{ns} when the effects of the shear deformation are taken into consideration. Thus the values of the normal and tangential moments $[M_s \quad M_n \quad M_{ns}]$ are utilized as unknowns at such points instead of the Cartesian global components $[M_x \quad M_y \quad M_{xy}]$.

It then follows that in such cases the first step is the modification of the matrix-equation (5.4.3) to account for the boundary conditions in terms of nodal normal and tangential moment components at localized nodes. That is only for those nodes where the imposed moments do not coincide with the

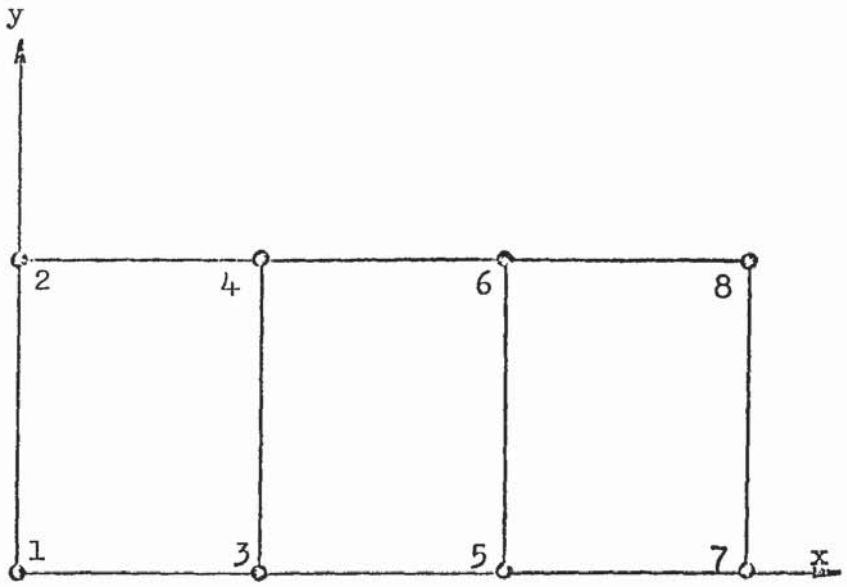

Fig.(5.4.1) Discretized plate.

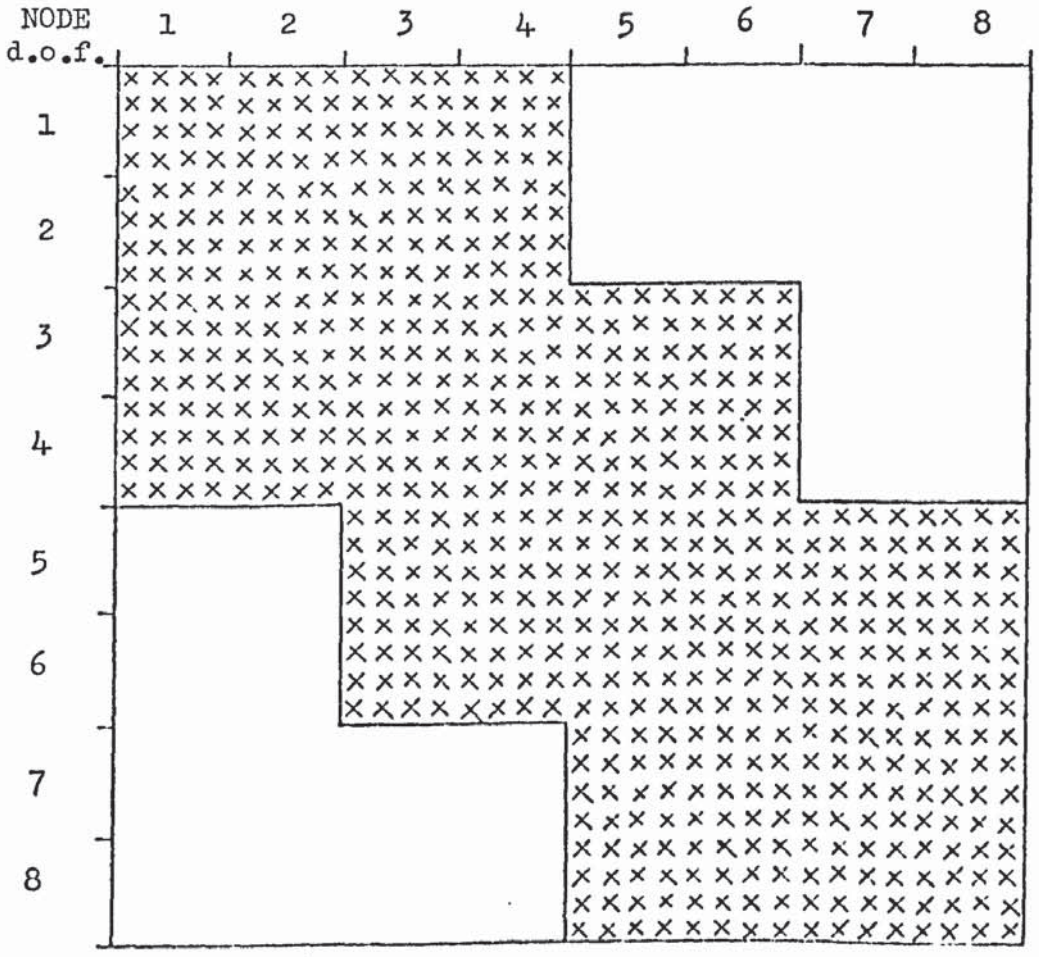

Fig.(5.4.2) Overall mixed matrix pattern.

Cartesian global nodal moments.

This alteration is done in the next paragraph.

5.5.1) Modification to the Governing Algebraic Equations.

The relations between the unknowns for a typical boundary node (i), Fig.(5.5.1) is given by:

$$\begin{Bmatrix} W \\ M_x \\ M_y \\ M_{xy} \end{Bmatrix} = \begin{bmatrix} 1 & 0 & 0 & 0 \\ 0 & \sin^2\beta & \cos^2\beta & -2\sin\beta\cos\beta \\ 0 & \cos^2\beta & \sin^2\beta & 2\sin\beta\cos\beta \\ 0 & -\cos\beta\sin\beta & \cos\beta\sin\beta & \cos^2\beta-\sin^2\beta \end{bmatrix} \begin{Bmatrix} W \\ M_s \\ M_n \\ M_{ns} \end{Bmatrix} \quad (5.5.1)$$

$$\text{i.e.} \quad \{\delta\}_i = [\ell_i]\,\{\delta'\}_i$$

where the primed vector $\{\delta'\}_i$ indicates the nodal components in the new normal axes. $[\ell_i]$ is a simple point transformation matrix and β is the angle between the normal of the true boundary at the i^{th} node and the x axis.

By using equation (5.5.1) the transformation for the entire nodal vector $\{\delta\}$ may be represented as

$$\{\delta\} = [L_K]\,\{\delta'\} \quad (5.5.2)$$

where the matrix $[L_K]$ has the following typical form:

$$[L_K] = \begin{bmatrix} [I] & \cdots & 0 & \cdots \\ \vdots & [I] & & \\ & \ddots & & \\ 0 & & [\ell_i] & \\ & & \ddots & \\ & & & [I] \end{bmatrix} \quad (5.5.3)$$

Here, [I] is an identity matrix of the same order as $[\ell_i]$, and the number of submatrices on the diagonal of $[L_K]$ is equal to the number of nodes in the overall assembly.

All other locations in the matrix $[L_K]$ are filled with

zeros.

The Reissner functional may be represented in matrix notation for the overall structure as:

$$\pi_R = \tfrac{1}{2} \{\delta\}^T [K] \{\delta\} - \{\delta\}^T \{F\}$$

in which [K] and {F} were already defined by equations (5.4.4).

Substituting equation (5.5.2) into the above relation gives:

$$\pi_R = \tfrac{1}{2}\{\delta'\}^T [L]^T [K] [L] \{\delta'\} - \{\delta'\}^T [L]^T \{F\}$$

Now extremizing the Reissner functional yields:

$$\frac{\partial \pi_R}{\partial \{\delta'\}^T} = [K'] \{\delta'\} - \{F'\} = 0$$

or

$$[K'] \{\delta'\} = \{F'\}$$

where

$$[K'] = [L]^T [K] [L] \qquad \text{(a)}$$
$$\{F'\} = [L]^T \{F\} \qquad \text{(b)} \qquad (5.5.4)$$

In fact the procedure to transform the mixed-matrix governing equation as outlined above is performed, in the developed computer program, at element level, before the coefficients are assembled in the overall mixed matrix for those nodes that require transformation only. Thus equation (5.5.4a) for the individual elements may be represented as

$$[k']_e = [L_K]^T [k]_e [L_K]$$

where $[L_K]$ is now a 16 × 16 matrix.

For example, if the i^{th} global node, corresponding to node number 2 (local numbering) of the e^{th} element, requires a transformation then the transformed matrix $[k']_e$ will have the following typical form:

$$[K]_e = \begin{bmatrix} [I]^T & [0] & [0] & [0] \\ [0] & [\ell_2]^T & [0] & [0] \\ [0] & [0] & [I]^T & [0] \\ [0] & [0] & [0] & [I]^T \end{bmatrix} \begin{bmatrix} [k_{11}] & [k_{12}] & [k_{13}] & [k_{14}] \\ [k_{21}] & [k_{22}] & [k_{23}] & [k_{24}] \\ [k_{31}] & [k_{32}] & [k_{33}] & [k_{34}] \\ [k_{41}] & [k_{42}] & [k_{43}] & [k_{44}] \end{bmatrix} \begin{bmatrix} [I] & [0] & [0] & [0] \\ [0] & [\ell_2] & [0] & [0] \\ [0] & [0] & [I] & [0] \\ [0] & [0] & [0] & [I]^T \end{bmatrix}$$

$$= \begin{bmatrix} [k_{11}] & [k_{12}][\ell_2] & [k_{13}] & [k_{14}] \\ [k_{21}] & [\ell_2]^T[k_{22}][\ell_2] & [\ell_2]^T[k_{23}] & [\ell_2]^T[k_{24}] \\ [k_{31}] & [k_{32}][\ell_2] & [k_{33}] & [k_{34}] \\ [k_{41}] & [k_{42}][\ell_2] & [k_{43}] & [k_{44}] \end{bmatrix}$$

Since the matrix $[k]_e$ is symmetric the only matrix multiplication required are performed in the upper part. For a typical local node (i) it corresponds to those partitioning matrices which belong to column (i) and row (i).

We will drop out the primed notation and assume either that all the boundary conditions are related to the x,y global axes or that they have been transformed to the normal system in which they may now be treated as global.

5.5.2) Contribution of the Natural Boundary Conditions to the Load Vector.

Contributions to the right end side of the mixed governing equation (5.4.3) will occur whenever boundary values of rotations and/or shears are specified, as can be seen by examining the Reissner functional of equations (2.3.8) or (2.3.14). The work done by a typical line integral when these quantities are specified can be represented as:

$$W_D = \int V^a I \, ds \qquad (5.5.5)$$

where V^a is the specified expression of the derived variable (shear or rotation) and I is the primary variable (deflection or moment).

Fig.(5.5.2) represents a portion of the plate boundary along which the presumed variable V^a is specified.

Since deflections and moments were assumed to vary linearly within the element, the assumed variable I is linear along a boundary s_i and was expressed by Herrmann [4] as

$$\begin{aligned} I &= I_K + (I_K - I_-)\ \frac{s}{A_i} && \text{for } 0 \geq s \geq -A_i \\ I &= I_K - (I_K - I_+)\ \frac{s}{A_j} && \text{for } A_j \geq s \geq 0 \end{aligned} \qquad (5.5.6)$$

with s measured from the point (x_K, y_K).

Substituting equations (5.5.6) into (5.5.5) yields

$$W_D = \int_{-A_i}^{o} V^a \left[I_K + (I_K - I_-)\ \frac{s}{A_i} \right] ds + \int_{o}^{A_j} V^a \left[I_K - (I_K - I_+)\ \frac{s}{A_j} \right] ds$$

Differentiating with respect to I_K gives:

$$\frac{\partial W_D}{\partial I_K} = \int_{-A_i}^{o} V^a \left[1 + \frac{s}{A_i} \right] ds + \int_{o}^{A_j} V^a \left[1 - \frac{s}{A_j} \right] ds \qquad (5.5.7)$$

The above expression must be evaluated and added to the force vector of the mixed governing equation to take into account the variation of I whenever shears or rotations are specified.

In most problems V^a is assumed constant along each boundary side ,hence for this particular case expression (5.5.7) can be represented as:

$$\frac{\partial W_D}{\partial I_K} = V^a_i\ \frac{A_i}{2} + V^a_j\ \frac{A_j}{2} \qquad (5.5.8($$

The above procedure can be clarified by considering the Fig.(5.4.1) as a thin plate in which a rotation β_n^* and an

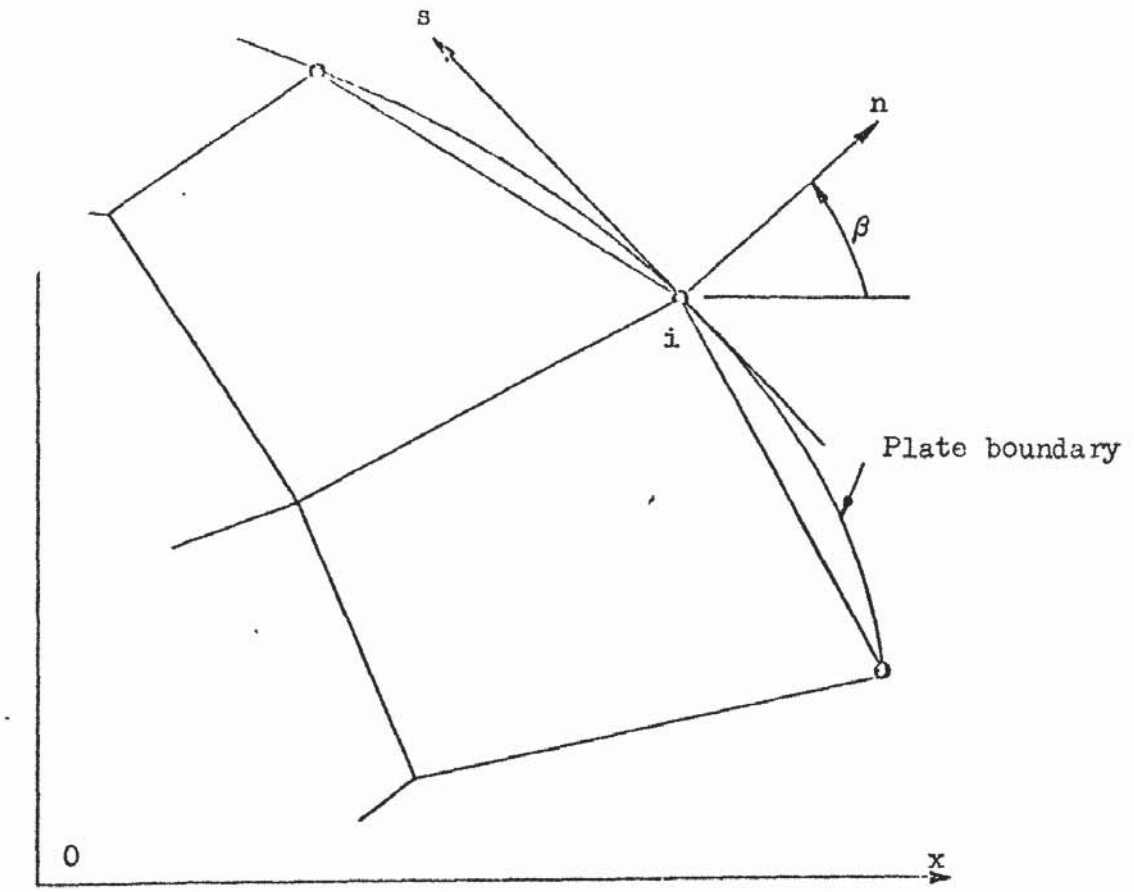

Fig.(5.5.1) Typical boundary node.

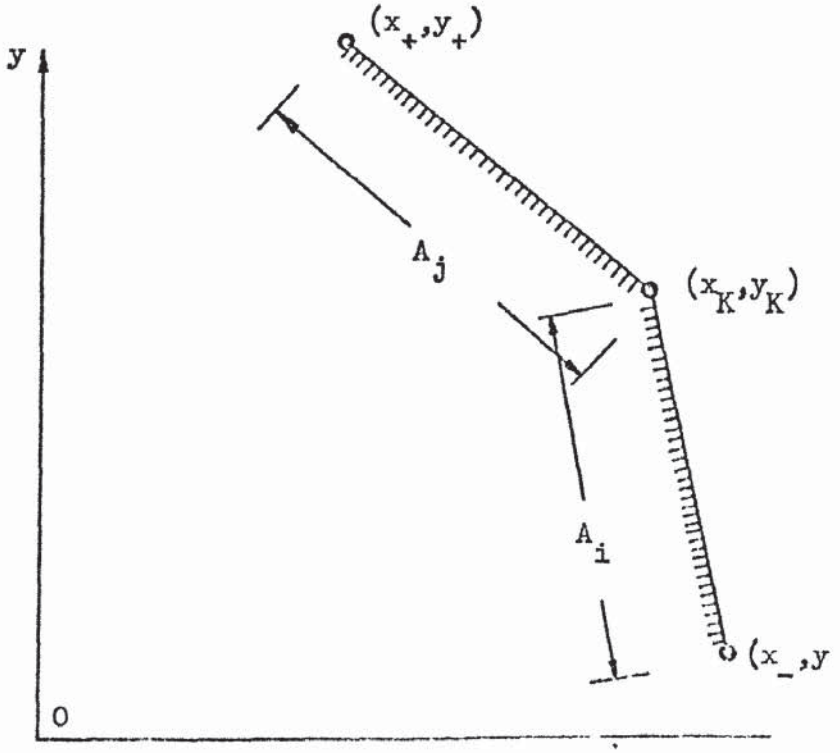

Fig.(5.5.2) Notation for boundary loads

effective shear V_n^* both constants are prescribed between node 1 and 5.

The sides of the elements in the y direction are all of length A. Then the load vector is given by :

$$\{F\} = \begin{Bmatrix} \begin{Bmatrix} F_w \\ F_{Mx} \\ F_{My} \\ F_{Mxy} \end{Bmatrix}_1 \\ \begin{Bmatrix} \vdots \end{Bmatrix}_2 \\ \begin{Bmatrix} F_w \\ F_{Mx} \\ F_{My} \\ F_{Mxy} \end{Bmatrix}_3 \\ \begin{Bmatrix} \vdots \end{Bmatrix}_4 \\ \begin{Bmatrix} \vdots \end{Bmatrix}_5 \\ \vdots \end{Bmatrix} = \begin{Bmatrix} 0 \\ 0 \\ \beta_n^* \times A/2 \\ 0 \\ \hline 0 \\ 0 \\ 0 \\ 0 \\ \hline 0 \\ 0 \\ \beta_n^* \times A/2 + \beta_n^* \times A/2 \\ 0 \\ \hline 0 \\ 0 \\ 0 \\ 0 \\ \hline 0 \\ 0 \\ \beta_n^* \times A/2 \\ 0 \\ \hline \vdots \end{Bmatrix} + \begin{Bmatrix} V_n^* \times A/2 \\ 0 \\ 0 \\ 0 \\ \hline 0 \\ 0 \\ 0 \\ 0 \\ \hline V_n^* \times A/2 + V_n^* \times A/2 \\ 0 \\ 0 \\ 0 \\ \hline 0 \\ 0 \\ 0 \\ 0 \\ \hline V_n^* \times A/2 \\ 0 \\ 0 \\ 0 \\ \hline \vdots \end{Bmatrix}$$

5.5.3) Prescribed Deflections and Moments.

If there is a prescribed value, zero or other than zero, on the i^{th} degree of freedom then

$$\delta_i = \delta_i^* \qquad (5.5.9)$$

Incorporating equation (5.5.9) into the governing mixed equation (5.4.3) yields:

$$\begin{bmatrix} K_{11} & K_{12} & \cdots & K_{1i} & \cdots & K_{1N} \\ K_{21} & K_{22} & \cdots & K_{2i} & \cdots & K_{2N} \\ \vdots & \vdots & & \vdots & & \vdots \\ 0 & 0 & & 1 & & 0 \\ \vdots & \vdots & & \vdots & & \vdots \\ K_{N1} & K_{N2} & \cdots & K_{Ni} & \cdots & K_{NN} \end{bmatrix} \begin{Bmatrix} \delta_1 \\ \delta_2 \\ \vdots \\ \delta_i \\ \vdots \\ \delta_N \end{Bmatrix} = \begin{Bmatrix} F_1 \\ F_2 \\ \vdots \\ \delta^* \\ \vdots \\ F_N \end{Bmatrix}$$

where N is the total number of degrees of freedom.

In order to preserve the symmetry of the above matrix-relation, it can be represented as:

$$\begin{bmatrix} K_{11} & K_{12} & \cdots & 0 & \cdots & K_{1N} \\ K_{21} & K_{22} & \cdots & 0 & \cdots & K_{2N} \\ \vdots & \vdots & & \vdots & & \vdots \\ 0 & 0 & \cdots & 1 & \cdots & 0 \\ \vdots & \vdots & & \vdots & & \vdots \\ K_{N1} & K_{N2} & \cdots & 0 & & K_{NN} \end{bmatrix} \begin{Bmatrix} \delta_1 \\ \delta_2 \\ \vdots \\ \delta_i \\ \vdots \\ \delta_N \end{Bmatrix} = \begin{Bmatrix} F_1 - K_{1i}\,\delta_i^* \\ F_2 - K_{2i}\,\delta_i^* \\ \vdots \\ \delta_i^* \\ \vdots \\ F_N - K_{Ni}\,\delta_i^* \end{Bmatrix} \qquad (5.5.10)$$

The above manipulation can then be summarized for a prescribed value on the i^{th} degree of freedom as follows:

$$\begin{aligned} F_j &= F_j - K_{ji}\,\delta_i^* && \text{for } j = 1,2,3 \ldots N \\ K_{im} &= K_{mi} = 0 && \text{for } m = 1,2,3 \ldots N \\ K_{ii} &= 1 \\ F_i &= \delta_i^* \end{aligned} \qquad (5.5.11)$$

An algorithm to perform automatically these manipulations, taking advantage of the banded nature of the matrix [K] is developed in Chapter 7.

For most cases the prescribed values are zero and they may be summarized in the following table:

BOUNDARY EDGE	THIN PLATES NODAL VARIABLES				MOD.THICK PLATES NODAL VARIABLES			
	W	M_s	M_n	M_{ns}	W	M_s	M_n	M_{ns}
Simply Supported	0		0		0		0	0
Clamped	0				0			0
Free			0				0	0
Symmetric				0				0

There is no problem in treating cases where the prescribed values are different from zero. If the plate is symmetric one can make use of symmetry by prescribing $M_{ns} = 0$ along the symmetric section.

5.6) The Load Vector.
Application for Certain Types of Loading.

The contributions to the load vector that were seen so far were due to an applied pressure, which could be taken as constant or changing linearly within the element. For moderately thick plates another contribution was due to the shear deformations taking into account τ_{xz}, τ_{yz} in the energy functional.

Further contributions occurred where rotations and/or shears were specified at the boundary, as was shown in paragraph 5.5..2..

The load vector will now be obtained for concentrated loads and line loads applied respectively at a node and at the nodal line of an element, lastly we will outline how loads due to an increase in the temperature of the plate may be implemented .

a) Concentrated Load.

Let a plate be divided into a finite element mesh with N nodes and assume a concentrated load P applied at the i^{th} node of the chosen mesh.

a) contd.

The work done by this force will be

$$W_D = P.(W)_i$$

where $(W)_i$ is the deflection at node i.

Differentiating the W_D with respect to $(W)_i$ gives

$$\frac{\partial W_D}{\partial (W)_i} = P$$

Then the contribution to the load vector is

$$\{F\} = \left[[0000]_1 \ \ldots \ [P000]_i \ [0000]_{i+1} \ \ldots \ [0000]_N \right]^T$$

b) Line Force.

Let us assume that a load Q* is applied along the sides connecting the global nodes (i-1) and (i+1) of the plate of Fig.(5.6.1).

The work done due to the load Q* is

$$W_D = \int_c^d Q^* . W \, ds$$

where W is the deflection along the line connecting the global node (i-1) and (i+1).

Following the procedure shown in paragraph 5.52 due to the linearlity of the deflection within the elements; the work done can be represented as:

$$W_D = \int_{-A_K}^{o} Q^* \left[W_i + (W_i - W_{i-1}) \ \frac{s}{A_K} \right] ds + \int_{o}^{A_{K+1}} Q^* \left[W_i - (W_i - W_{i+1}) \ \frac{s}{A_{K+1}} \right] ds$$

To get the load vector contribution at the i^{th} node the above expression is differentiated with respect

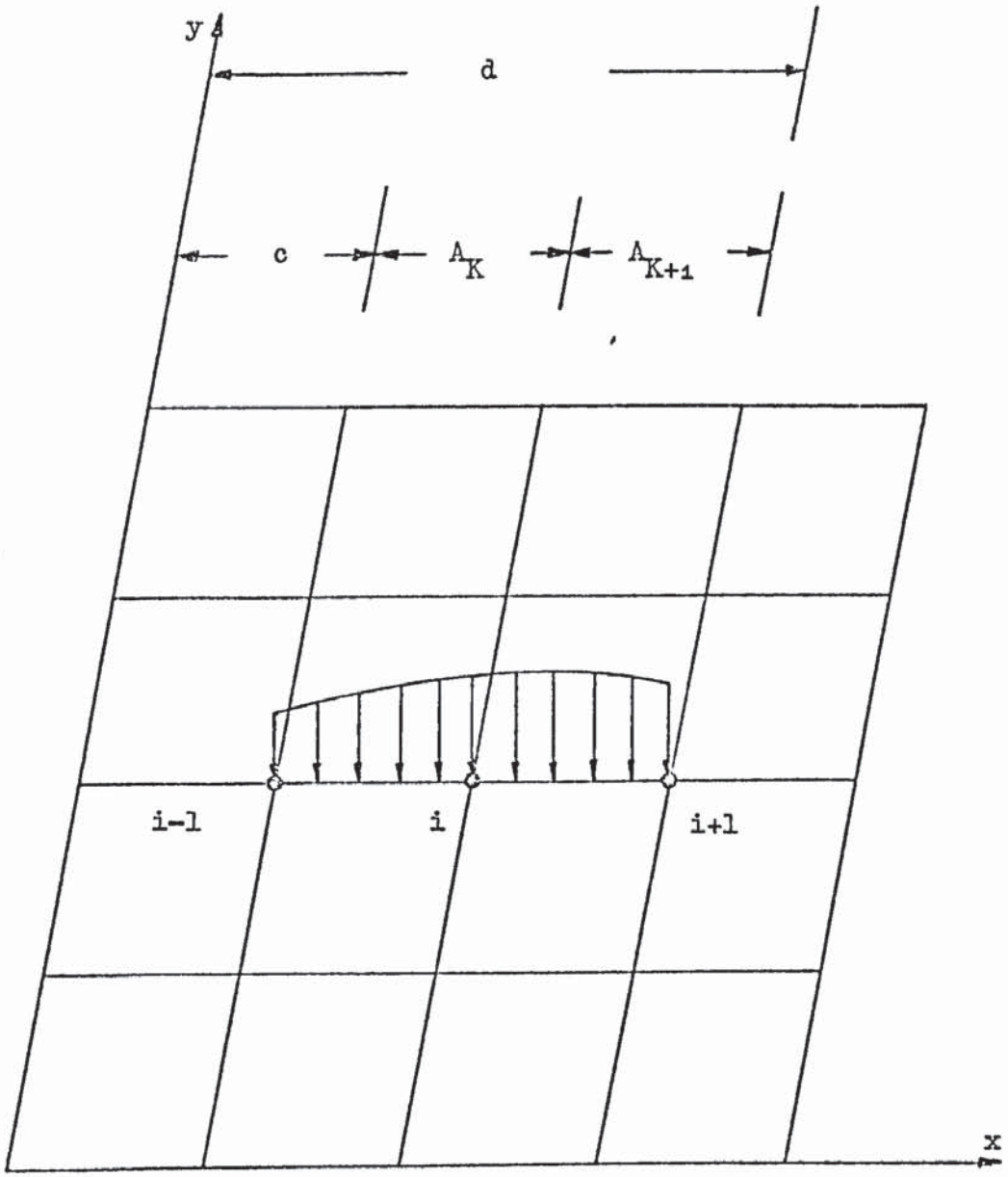

Fig.(5.6.1) Plate with a line force .

b) contd.

to the nodal parameter W_i yielding

$$\frac{\partial W_D}{\partial W_i} = \int_{-A_K}^{o} Q^* \left[1 + \frac{s}{A_K}\right] ds + \int_{o}^{A_{K+1}} Q^* \left[1 - \frac{s}{A_{K+1}}\right] ds$$

Integrating the above expression the fictitious concentrated force at node i can be obtained and added to the load vector. Similarly as in paragraph 5.5.2. if Q^* is constant the overall load vector will be contained in the following locations:

$$\{F\} = \left[\begin{bmatrix} 0000 \end{bmatrix}_1 \cdots \begin{bmatrix} \frac{QA_K}{2} & 000 \end{bmatrix}_{i-1} \begin{bmatrix} \frac{QA_K}{2} & 000 \\ + & \\ \frac{QA_{K+1}}{2} & \end{bmatrix}_i \begin{bmatrix} \frac{QA_{K+1}}{2} & 000 \end{bmatrix}_{i+1} \cdots [0]_N \right]^T$$

c) Load due to Temperature Change.

In general, when a two dimensional body experiences a change of temperature, see reference [57], a strain vector:

$$\{\varepsilon_o\} = \begin{Bmatrix} \alpha_x & \Delta T \\ \alpha_y & \Delta T \\ 0 \end{Bmatrix}$$

exists. Here, α_x and α_y are linear coefficients of thermal expansion for an orthotropic material in which the axes of orthotropy coincide with the x,y axes, ΔT is the temperature change. For isotropic materials the coefficient of thermal expansion is

$$\alpha_t = \alpha_x = \alpha_y$$

Considering plate bending , the work done due to a change of temperature ΔT across the plate thickness (i.e.

c) contd.

the difference of temperature at the lower and upper faces of the plate), using the plate nomenclature, can be re-presented for a finite element (e) as

$$(W_D)_e = \iint_A [M_x \quad M_y \quad M_{xy}] \begin{Bmatrix} \frac{12}{E_x h^3} & M_{t_x} \\ \frac{12}{E_y h^3} & M_{t_y} \\ 0 & \end{Bmatrix} dx\, dy \qquad (5.6.1)$$

where

$$M_{t_x} = E_x \int_{-h/2}^{h/2} \alpha_x \Delta T \; z \; dz \qquad M_{t_y} = E_y \int_{-h/2}^{h/2} \alpha_y \Delta T \; z \; ds$$

are the thermal moments due to a temperature change ΔT and E_x and E_y are the Young's modulus.

Substituting equation (5.3.4) into equation (5.6.1) and converting all the variables to the local ζ, η coordinate axis yields:

$$(W_D)_e = \{M\}_e^T \int_{-1}^{1}\int_{-1}^{1} \left[\begin{bmatrix} N_1 \\ 0 \\ 0 \\ N_2 \\ 0 \\ 0 \\ N_3 \\ 0 \\ 0 \\ N_4 \\ 0 \\ 0 \end{bmatrix} \times \frac{12}{E_x h^3} M_{t_x} + \begin{bmatrix} 0 \\ N_1 \\ 0 \\ 0 \\ N_2 \\ 0 \\ 0 \\ N_3 \\ 0 \\ 0 \\ N_4 \\ 0 \end{bmatrix} \times \frac{12}{E_y h^3} M_{t_y} \right] \det[J]\, d\zeta\, d\eta \qquad (5.6.2)$$

Differentiating equation (5.6.2) with respect to $\{M\}_e^T$ to get the contribution which should be added to the element load vector gives:

$$\frac{\partial(W_D)_e}{\partial\{M\}_e^T} = \begin{Bmatrix} \{r\}_1 \\ \{r\}_2 \\ \{r\}_3 \\ \{r\}_4 \end{Bmatrix}$$

where

$$\{r\}_i = \int_{-1}^{1}\int_{-1}^{1} \begin{Bmatrix} \frac{12}{E_x h^3} M_{t_x} N_i \\ \frac{12}{E_y h^3} M_{t_y} N_i \\ 0 \end{Bmatrix} \det[J]\,d\zeta\,d\eta \qquad \text{for } i = 1,2,3,4$$

Then the contributions to $\{f\}_e$ are:

$$\{f\}_e = \begin{Bmatrix} \{f\}_1 \\ \{f\}_2 \\ \{f\}_3 \\ \{v\}_4 \end{Bmatrix}$$

where

$$\{f\}_i = \int_{-1}^{1}\int_{-1}^{1} \begin{Bmatrix} 0 \\ \frac{12}{E_x h^3} M_{t_x} N_i \\ \frac{12}{E_x h^3} M_{t_y} N_i \\ 0 \end{Bmatrix}_i \det[J]\,d\zeta\,d\eta \qquad \text{for } i = 1,2,3,4$$

In order to avoid overloading the developed computer program the above derivation was not implemented, but if a problem appears where the change in temperature must be taken into consideration, the contributions to be added to the element load vector can be lumped, for each individual local node as follows:

$$\{f\}_i = \begin{Bmatrix} 0 \\ \frac{A^*}{4} \times \frac{12}{E_x h^3} M_{t_x} \\ \frac{A^*}{4} \times \frac{12}{E_y h^3} M_{t_y} \\ 0 \end{Bmatrix}_i \quad \text{for } i = 1,2,3,4$$

where A* is the area of the element and h is taken as the average thickness over the individual element. The global nodal contributions of all the elements are then added manually, and inputed as if they were concentrated forces in the proper locations of the overall load vector.

5.7) Solution of the Equations.

Having modified the system of mixed equations to include the prescribed deflections and moments, they are ready for solution. Although there are many methods [58] for the solution of very large systems of linear equations, in general they cannot be applied to the mixed overall-matrix equation. The mixed equations were obtained through the application of the Reissner principle which is only a stationary principle i.e. it does not identify either a minimum nor a maximum in the neighbourhood of the natural strained state; consequently the mixed matrix is non-positive definite. To avoid the zeros in the diagonal element, row interchange is required; the Gauss elimination method, reference [58], with row interchange is then used in the solution of the equations. The symmetry of the overall matrix is therefore lost throughout the numerical process. Consequently the complete band form of the matrix [K] needs to be stored as a two dimensional array.

5.8) Solution of the Plate Problem.

The solution of the system of linear equations yields the nodal deflections and moments directly; from these the information relating to the plate stressing problem can be obtained .

5.8.1) Moments, Shearing Forces and Stresses.

The principal bending moments M_p which give the maximum and minimum values of the principal bending stresses and the angle α^* at which they occur, and the maximum and minimum principal twisting moment M_{nt_p} can be evaluated by using at each nodal point equations (2.2.22) to (2.2.24) of Chapter 2.

The shearing force intensities are obtained by means of

$$\begin{Bmatrix} Q_x \\ Q_y \end{Bmatrix} = \left[\begin{array}{cccc:cccc:cccc} B_{11} & 0 & B_{21} & B_{12} & 0 & B_{22} & B_{13} & 0 & B_{23} & B_{14} & 0 & B_{24} \\ 0 & B_{21} & B_{11} & 0 & B_{22} & B_{12} & 0 & B_{23} & B_{13} & 0 & B_{24} & B_{14} \end{array}\right] \Big\{ M \Big\}_e \qquad (5.6.3)$$

where the B_{ij}'s are defined by equations (5.3.9).

The values of the normal shearing force intensity Q_n along a boundary whose angle between the outward normal and the x axis is β^* can be evaluated by:

$$Q_n = [\cos \beta^* \quad \sin \beta^*] \begin{Bmatrix} Q_x \\ Q_y \end{Bmatrix}$$

where $[Q_x \quad Q_y]^T$ is given by equation (5.6.3) for any point within each element.

The effective shearing forces can be evaluated from expression (2.2.32) and differentiating equation (5.3.16) as:

$$V_n = Q_n + \sum_{i=1}^{4} [-\sin\beta^* \vdots \cos\beta^*] \begin{bmatrix} L_{11}B_{1i} \vdots & L_{12}B_{1i} \vdots & L_{13}B_{1i} \\ L_{11}B_{2i} \vdots & L_{12}B_{2i} \vdots & L_{13}B_{2i} \end{bmatrix} \begin{Bmatrix} M_x \\ M_y \\ M_{xy} \end{Bmatrix}_i$$

where

$$[L] = [-\cos\beta^* \ \sin\beta^* \ \vdots \cos\beta^* \ \sin\beta^* \ \vdots \cos^2\beta^* - \sin^2\beta^*]$$

and the B_{ij}'s are given by relations (5.3.9)

The stress can then be evaluatdd by using equations (2.2.19). Similarly the principal stresses can be obtained.

5.8.2) Rotations.

For a thin plate, the rotations can be evaluated by equation (5.3.10) i.e.

$$\begin{Bmatrix} \beta_x \\ \beta_y \end{Bmatrix} = - \begin{bmatrix} B_{11} & B_{12} & B_{13} & B_{14} \\ B_{21} & B_{22} & B_{23} & B_{24} \end{bmatrix} \{W\}_e$$

where the B_{ij}'s are given by equation (5.3.9), and for "moderately" thick plates, equations (2.3.20) applies. Thus

$$\begin{Bmatrix} \beta_x \\ \beta_y \end{Bmatrix} = - \begin{bmatrix} B_{11} & B_{12} & B_{13} & B_{14} \\ B_{21} & B_{22} & B_{23} & B_{24} \end{bmatrix} \{W\}_e$$

$$+ \frac{12(1+\mu)}{5Eh} \begin{bmatrix} B_{11} & 0 & B_{21} \vdots & B_{12} & 0 & B_{22} \vdots & B_{13} & 0 & B_{23} \vdots & B_{14} & 0 & B_{24} \\ 0 & B_{21}B_{11} \vdots & 0 & B_{22}B_{12} \vdots & 0 & B_{23}B_{13} \vdots & 0 & B_{24}B_{14} \end{bmatrix} \{M\}_e$$

for isotropic materials, where E and μ are the material properties and h the plate thickness. For orthotropic materials the rotations are represented, see reference [14] as:

$$\begin{Bmatrix} \beta_x \\ \beta_y \end{Bmatrix} = - \begin{Bmatrix} \partial N/\partial x \\ \partial N/\partial y \end{Bmatrix} + \frac{6}{5h} \begin{bmatrix} 1/G_{xz} & 0 \\ 0 & 1/G_{yz} \end{bmatrix} \begin{Bmatrix} Q_x \\ Q_y \end{Bmatrix}$$

Thus:

$$\begin{Bmatrix}\beta_x\\ \beta_y\end{Bmatrix} = -\begin{bmatrix}B_{11} & B_{12} & B_{13} & B_{14}\\ B_{21} & B_{22} & B_{23} & B_{24}\end{bmatrix}\{W\}_e +$$

$$+\frac{6}{5h}\begin{bmatrix}1/G_{xz} & 0\\ 0 & 1/G_{yz}\end{bmatrix}\left[\begin{array}{cc:cc:cc:cc}B_{11} & 0 & B_{21} & B_{12} & 0 & B_{22} & B_{13} & 0 & B_{23} & B_{14} & 0 & B_{24}\\ 0 & B_{21} & B_{11} & 0 & B_{22} & B_{12} & 0 & B_{23} & B_{13} & 0 & B_{24} & B_{14}\end{array}\right]\{M\}_e$$

where G_{xz} and G_{yz} were already defined as shear moduli.

5.9) Concluding Remarks.

In the previous sections all the features which enable the solution of thin and moderately thick plates in static bending were developed and described for the mixed model, using a general quadrilateral element. A computer program whose details are given later, in Chapter 7, will be developed for the solution of arbitrary thin and moderately thick plates. The plates may have orthotropic properties in the directions of the coordinate axes, variable thickness and arbitrary load. The program will provide the following results:

a) Nodal Deflections

b) Nodal bending and twisting moments

c) Nodal principal bending moments and the pertinent angle

4) Shear force intensities at the centroid of each element.

CHAPTER 6

PLATE VIBRATION AND BUCKLING ANALYSIS BY THE MIXED FINITE ELEMENT METHOD

6.1) Introduction.

In this chapter we develop the characteristics of the mixed general quadrilateral element for the solution of free vibrations and elastic or plastic buckling of thin plates.

The mixed element properties and the overall eigenvalue problem are derived through the application of the Reissner's principle for dynamics and buckling problems.

6.2) Eigenvalue Problems with the Mixed Plate Element: Free Transverse Vibrations and Buckling.

6.2.1) Free Transverse Vibration.

The dynamic Reissner functional equation (2.4.15), for isotropic plates, where shear deformations are neglected, can be represented in matrix notation, for the e^{th} element as:

$$\left(\pi_{R_D}\right)_e = -\tfrac{1}{2}\{M\}_e^T[g]\{M\}_e+\{M\}_e^T[h]\{W\}_e - \tfrac{1}{2}\{\dot{W}\}_e\,[m]\,\{\dot{W}\}_e \qquad (6.2.1)$$

where the matrices [g] and [h] were already defined for the static case and are given by equations (5.3.17).

For orthotopic plates when generating the matrix [g], the coefficients of the compliance matrix [C] are given by equation (5.3.20). The vectors $\{M\}_e$ and $\{W\}_e$ are represented as before by relations (5.2.2). A dot denotes differentiation with respect to time t.

The matrix [m] is the so-called consistent mass matrix of the element e given by

$$[m] = \int_{-1}^{1}\int_{-1}^{1} \rho h\, [N_W]^T [N_W] \det[J]\, d\zeta\, d\eta$$

$$= \int_{-1}^{1}\int_{-1}^{1} \rho h \begin{bmatrix} N_1N_1 & N_1N_2 & N_1N_3 & N_1N_4 \\ & N_2N_2 & N_2N_3 & N_2N_4 \\ \text{Symmetric} & & N_3N_3 & N_3N_4 \\ & & & N_4N_4 \end{bmatrix} \det[J]\, d\zeta\, d\eta \qquad (6.2.2)$$

where the interpolation functions N_i, for i = 1,2,3,4 are given by equations (3.3.2). The determinant of the Jacobian is $\det[J] = J_{11}.J_{12} - J_{21}.J_{22}$ where the coefficients are defined by equation (5.3.6). The mass of the plate per unit volume is designated by ρ and the element thickness by h. If the thickness changes linearly within the element it is evaluated at the Gauss integrating points by $\{h\} = [N_h]\{h\}_e$, as in the static case where $[N_h] = [N_W]$ and $\{h\}_e = [h_1\ h_2\ h_3\ h_4]^T$, the thickness of the element at the nodes.

Applying the Reissner's principle for dynamics, relation (6.2.1), i.e. $\delta \int_{t_1}^{t_2} \left(\pi_{R_D}\right)_e dt = 0$, and noticing equation (2.4.5) we obtain

$$\int_{t_1}^{t_2} \{\delta M\}_e^T \left\{-[g]\{M\}_e + [h]\{W\}_e\right\} dt = 0$$

$$\int_{t_1}^{t_2} \{\delta W\}_e^T \left\{[h]^T\{M\}_e + [m]\{\ddot{W}\}\right\} dt = 0$$

Since the variations of the nodal bending moments and deflections are arbitrary, the expressions in parentheses must vanish. Therefore we obtain the mixed matrix governing equations of motion for the e^{th} element as:

$$-[g]\{M\}_e + [h]\{W\}_e = \{0\} \qquad (a)$$

$$[h]^T\{M\}_e + [m]\{\ddot{W}\}_e = \{0\} \qquad (b) \qquad (6.2.3)$$

Assuming harmonic motion

i.e. $W(x,y,t) = \hat{W}(x,y) \sin \omega t$

$M_x(x,y,t) = \hat{M}_x(x,y) \sin \omega t$, etc.

we obtain for the peak values of vectors $\{\hat{M}\}_e$ and $\{\hat{W}\}_e$

$$\left(\left[\begin{array}{c:c} -[g] & [h] \\ \hdashline [h]^T & [0] \end{array}\right] - \left[\begin{array}{c:c} [0] & [0] \\ \hdashline [0] & \omega^2[m] \end{array}\right] \right) \left\{\begin{array}{c} \{\hat{M}\}_e \\ \{\hat{W}\}_e \end{array}\right\} = \left\{\begin{array}{c} \{0\} \\ \{0\} \end{array}\right\}$$

or

$$\left[\begin{array}{cc} -[g] & [h] \\ [h]^T & [0] \end{array}\right] \left\{\begin{array}{c} \{\hat{M}\}_e \\ \{\hat{W}\}_e \end{array}\right\} = \left[\begin{array}{cc} 0 & 0 \\ 0 & \omega^2[m] \end{array}\right] \left\{\begin{array}{c} \{\hat{M}\}_e \\ \{\hat{W}\}_e \end{array}\right\} \qquad (6.2.4)$$

which is the eigenvalue matrix-relation for element e.

6.2.2) Buckling of Thin Plates.
Element Initial Stress Stiffness Matrix Derivation.

a) Elastic Buckling.

The Reissner functional applied for the buckling of thin plates, equation (2.5.2), can be represented for the e^{th} element as:

$$\left(U_{R_B}\right)_e = -\tfrac{1}{2}\{M\}_e^T[g]\{M\}_e + \{M\}_e^T[h]\{W\}_e - \tfrac{1}{2}\iint_{A_e} \{W'\}^T [\sigma_o] \{W'\} h \, dA \qquad (6.2.5)$$

where the matrices [g] and [h] were already defined by equations (5.3.17) and

a) contd.

$$\{W'\} = \left[\frac{\partial W}{\partial x} \quad \frac{\partial W}{\partial y}\right]^T$$

The matrix $[\sigma_o]$ contains the in-plane stresses. They are presumed known a priori, for an assumed trial edge load. For an arbitrary buckling problem they are obtained by solving it first as a plane stress case by either an appropriate analytical tool (if it exists) or numerical technique, including that of the finite element method. Thus, for some trial load level:

$$[\sigma_o] = \lambda_b [\bar{\sigma}_o] \tag{6.2.6}$$

where

$$[\bar{\sigma}_o] = \begin{bmatrix} \bar{\sigma}_{x_o} & \bar{\sigma}_{xy_o} \\ \bar{\sigma}_{xy_o} & \bar{\sigma}_{y_o} \end{bmatrix} \tag{6.2.7}$$

λ_b is a critical factor yet to be found and $\bar{\sigma}_{x_o}$ etc. are the in-plane stresses previously evaluated for a reference level of edge loads.

The stresses may be allowed to change linearly within the element by using the isoparametric concept. Thus:

$$[\bar{\sigma}_o] = \begin{bmatrix} \sum_{i=1}^{4} N_i \left(\bar{\sigma}_{x_o}\right)_i & \vdots & \sum_{i=1}^{4} N_i \left(\bar{\sigma}_{xy_o}\right)_i \\ \cdots\cdots & \vdots & \cdots\cdots \\ \sum_{i=1}^{4} N_i \left(\bar{\sigma}_{xy_o}\right)_i & \vdots & \sum_{i=1}^{4} N_i \left(\bar{\sigma}_{y_o}\right)_i \end{bmatrix} \tag{6.2.8}$$

where the linear interpolation functions N_i, for $i = 1,2,3,4$ are given by equations (3.3.2) and $\left[\bar{\sigma}_{x_o} \quad \bar{\sigma}_{y_o} \quad \bar{\sigma}_{xy_o}\right]_i$ are the nodal in-plane stresses. Similarly for the plate thickness, then :

a) contd.

$$h = [N_1 \quad N_2 \quad N_3 \quad N_4] \begin{Bmatrix} h_1 \\ h_2 \\ h_3 \\ h_4 \end{Bmatrix} \tag{6.2.9}$$

Substituting equation (5.3.10) and equation (6.2.6) into the last term of equation (6.2.5), and changing to the ζ,η coordinate system yields:

$$\left(\pi_{R_B}\right)_e = -\tfrac{1}{2}\{M\}_e^T [g] \{M\}_e + \{M\}_e^T [h] \{W\}_e - \tfrac{1}{2}\{W\}_e^T \lambda_b [s] \{W\}_e \tag{6.2.10}$$

where the initial stress stiffness matrix is generated by:

$$[s] = \int_{-1}^{1} \int_{-1}^{1} [B]^T [\bar{\sigma}_o] [B] h \det[J] d\zeta d\eta \tag{6.2.11}$$

in which $[B]$ is given by equations (5.3.8) and (5.3.9). The initial stress stiffness matrix can then be obtained by Gaussian quadrature. If $[\bar{\sigma}_o]$ and/or h change within the element they are evaluated using equations (6.2.8) and/or (6.2.9) at the four Gaussian integrating points.

Extremizing the functional equation (6.2.10) we obtain the homogeneous element mixed-matrix-equation given by:

$$\left(\begin{bmatrix} -[g] & [h] \\ [h]^T & [0] \end{bmatrix} - \begin{bmatrix} [0] & [0] \\ [0] & \lambda_b [s] \end{bmatrix} \right) \begin{Bmatrix} \{M\}_e \\ \{W\}_e \end{Bmatrix} = \begin{Bmatrix} \{0\} \\ \{0\} \end{Bmatrix}$$

or

$$\begin{bmatrix} -[g] & [h] \\ [h]^T & [0] \end{bmatrix} \begin{Bmatrix} \{M\}_e \\ \{W\}_e \end{Bmatrix} = \begin{bmatrix} [0] & [0] \\ [0] & \lambda_b [s] \end{bmatrix} \begin{Bmatrix} \{M\}_e \\ \{W\}_e \end{Bmatrix} \tag{6.2.12}$$

b) Plastic Buckling.

For plates, it is not unusual for the proportional limit of the material to be exceeded prior to reaching the critical buckling stress.

If this occurs, the elastic theory, presented in Section 2.5 and the application to the mixed finite element method of item (a) of this section, must be replaced by an analysis capable of dealing with the inelastic behaviour that exists between the proportional limit and the critical buckling stresses. Although the theory of plastic buckling of columns is well developed, there are several aspects in the theory of plstic buckling of plates which are still confused. The primary difficulty lies in the proper representation of the stress-strain relationship. That is, in the case of plastic buckling of columns the stresses are uniaxial, whereas in plate buckling, the state of stress is two-dimensional and it may assume a substantially different distribution among the stress components during buckling from that existing prior to buckling.

Furthermore plastic buckling can be analysed using either flow [59],[60] or deformation theories [61],[62] of plasticity, thus it makes an analytical solution, if it exists, very sensitive to the type of plasticity theory that is used. Pride [63], by comparing analytical published results obtained from both theories, has shown that a good correlation exists between the deformation theory and experimental results; consequently the deformation theory has been widely used in engineering applications [64]. Pifko [65] has applied successfuly, Stowell's theory of flat plates [62], in conjunction with the displacement method of the finite element analyses, using a rectangular

b) contd.

element.

We shall develop here a similar procedure for the mixed finite element analysis.

Stowell's theory makes use of the following fundamental assumptions, regarding the concept of effective stress, σ_{ef}, and effective strain, e_{ef}:

$$\sigma_{ef} = (\sigma_x^2 + \sigma_y^2 - \sigma_x \sigma_y + 3\tau_{xy}^2)^{\frac{1}{2}} \quad \text{(a)}$$

$$e_{ef} = \frac{2}{3^{\frac{1}{2}}} (e_x^2 + e_y^2 + e_x e_y + \frac{\gamma_{xy}^2}{4})^{\frac{1}{2}} \quad \text{(b)} \qquad (6.2.13)$$

where e_x, e_y, γ_{xy} are total strains.

These quantities are assumed to be uniquely related by :

$$e_{ef} = f(\sigma_{ef}) = \frac{\sigma_{ef}}{E_s} \qquad (6.2.14)$$

where E_s is the secant modulus.

The stress-strain relations consistent with (6.2.15) are

$$\begin{Bmatrix} e_x \\ e_y \\ \gamma_{xy} \end{Bmatrix} = \frac{1}{E_s} \begin{bmatrix} 1 & -\frac{1}{2} & 0 \\ -\frac{1}{2} & 1 & 0 \\ 0 & 0 & 3 \end{bmatrix} \begin{Bmatrix} \sigma_x \\ \sigma_y \\ \tau_{xy} \end{Bmatrix}$$

Expressions (6.2.14) have been conveniently related by Ramberg and Osgood [66], as shown graphically in Fig.(6.2.1).

The Ramberg and Osgood representation enables the secant modulus, E_s, and the tangential modulus, E_t, to be found using the following relations:

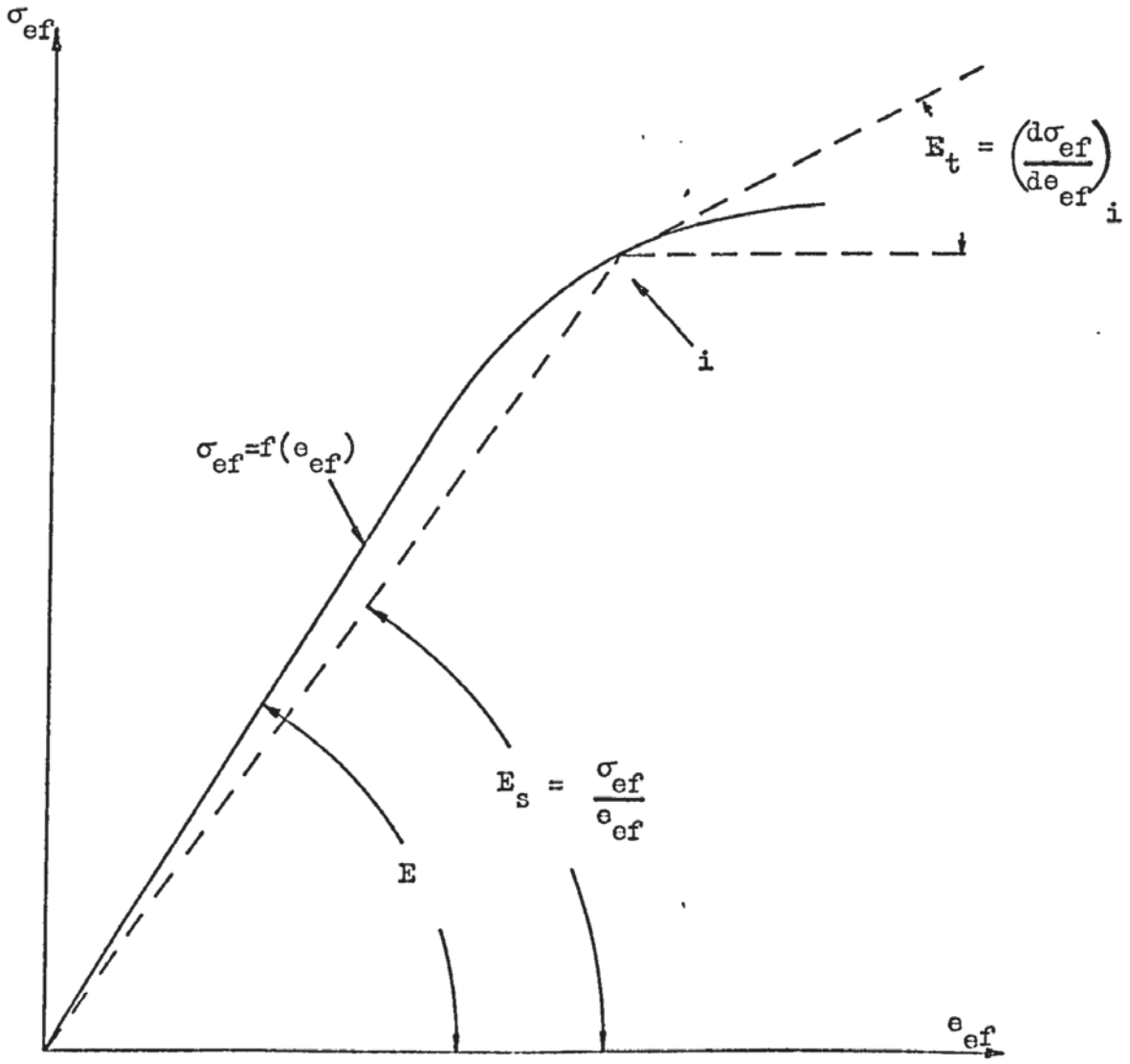

Fig.(6.2.1) Typical Ramberg-Osgood stress strain curve.

$$E_s = \frac{E}{1 + \left(\frac{3}{7}\right)\left(\frac{\sigma_{ef}}{\sigma_{0.7}}\right)^{(n-1)}} \qquad (a)$$

(6.2.15)

$$E_t = \frac{E}{1 + \left(\frac{3n}{7}\right)\left(\frac{\sigma_{ef}}{\sigma_{0.7}}\right)^{(n-1)}} \qquad (b)$$

$$n = 1 + \log_{10}\left(\frac{17}{7}\right) \Big/ \log_{10}\left(\sigma_{0.7}/\sigma_{0.85}\right) \qquad (c)$$

where $\sigma_{0.7}$ and $\sigma_{0.85}$ are the stresses at which the curve has a secant modulus of 0.7E and 0.85E respectively, σ_{ef} is evaluated using relation (6.2.13a) and n is a shape parameter evaluated by (6.2.15c).

Using these assumptions, from ref.[62] the moment curvature relations containing the effect of plastic yielding prior to buckling can be written as:

$$\begin{Bmatrix} M_x \\ M_y \\ M_{xy} \end{Bmatrix} = \frac{E_s h^3}{9} \begin{bmatrix} D_{11} & D_{12} & D_{13} \\ & D_{22} & D_{23} \\ \text{Symmetric} & & D_{33} \end{bmatrix} \begin{Bmatrix} -\frac{\partial^2 W}{\partial x} \\ -\frac{\partial^2 W}{\partial y} \\ -2\frac{\partial^2 W}{\partial x \partial y} \end{Bmatrix} \qquad (6.2.16)$$

$$\text{i.e. } \{M\} = [D_p]\,\{\lambda\}$$

where

$$D_{11} = 1 - \frac{3}{4} \frac{\sigma_x^2}{\sigma_{ef}^2} \left(1 - \frac{E_t}{E_s}\right)$$

$$D_{12} = \frac{1}{2} \left[1 - \frac{3}{2} \frac{\sigma_x \sigma_y}{\sigma_{ef}^2} \left(1 - \frac{E_t}{E_s}\right)\right]$$

$$D_{13} = -\frac{1}{4} \cdot \frac{3\, \sigma_x\, \tau_{xy}}{\sigma_{ef}^2} \left(1 - \frac{E_t}{E_s}\right) \qquad (6.2.17)$$

$$D_{22} = 1 - \frac{3}{4} \frac{\sigma_y^2}{\sigma_e^2} \left(1 - \frac{E_t}{E_s}\right)$$

$$D_{23} = -\frac{1}{4} \cdot \frac{3\, \sigma_y\, \tau_{xy}}{\sigma_{ef}^2} \left(1 - \frac{E_t}{E_s}\right)$$

$$D_{33} = \frac{1}{4} \left[1 - 3 \frac{\tau_{xy}^2}{\sigma_{ef}^2} \left(1 - \frac{E_t}{E_s}\right)\right]$$

Inverting the matrix relation (6.2.16) yields:

$$\{\lambda\} = [C_p]\, \{M\}$$

where $\{\lambda\}$ and $\{M\}$ are the vectors given by equations(2.2.15) and (2.2.16) and $[C_p]$, the compliance matrix containing the effects of plastic yielding prior to buckling, given by:

$$[C_p] = \frac{9}{E_s h^3} \begin{bmatrix} D_{11} & D_{12} & D_{13} \\ & D_{22} & D_{23} \\ \text{Symmetric} & & D_{33} \end{bmatrix}^{-1} \qquad (6.2.18)$$

where the coefficients D_{11}, etc., are evaluated with the help of equations (6.2.17).

Now reverting to the mixed-element eigenvalue relation (6.2.12), we can modify the partition matrix [g] i.e.

$$[g] = \int_{-1}^{1}\int_{-1}^{1} [N_M]^T [C] [N_M] \det[J] d\zeta d\eta$$

by replacing the elastic compliance [C] by $[C_p]$ given by relation (6.2.18).

Thus:

$$[g_p] = \int_{-1}^{1}\int_{-1}^{1} [N_W]^T [C_p] [N_W] \det[J] d\zeta d\eta \qquad (6.2.19)$$

Stowell [62] assumes a constant stress field in the prebuckling configuration, thus we always assume that the stresses are constant within each element.

The element eigenvalue relation can then be represented as:

$$\begin{bmatrix} -[g_p] & [h] \\ [h]^T & [0] \end{bmatrix} \begin{Bmatrix} \{M\}_e \\ \{W\}_e \end{Bmatrix} = \begin{bmatrix} [0] & [0] \\ [0] & \lambda_b[s] \end{bmatrix} \begin{Bmatrix} \{M\}_e \\ \{W\}_e \end{Bmatrix} \qquad (6.2.20)$$

where the generation of $[g_p]$ is obtained by evaluating equation (6.2.19).

As we shall see, the critical stresses will be found by a trial and error, iteration procedure, until the buckling criterion ($\lambda_b = 1$) for the overall structure is satisfied. The edge loads pertinent to this condition are the required plastic buckling edge loads.

6.2.3) Programmable Form of the Element Matrices-Eigenvalue Problem.

In order to be able to use the coding and procedure facilities of the "main" program, we had to revert the element mixed matrix, the consistent mass and initial stress stiffness matrix to a form consistent with Section 5.3.6

i.e. $[k]_e\{\delta\}_e = \omega^2[m^*]\{\delta\}_e$

and $[k]_e\{\delta\}_e = \lambda[s^*]\{\delta\}_e$

where $\{\delta\}_e$ is the vector defined by equation (5.3.32). The partitioned matrices of $[k]_e$ are given by the matrix relation (5.3.30) and the partitioned matrices of $[m^*]$ and $[s^*]$ are respectively evaluated by:

$$[m^*_{ij}] = \begin{bmatrix} 0 & 0 & 0 & 0 \\ 0 & 0 & 0 & 0 \\ 0 & 0 & 0 & 0 \\ 0 & 0 & 0 & m_{ij} \end{bmatrix} \quad \text{for } i,j = 1,2,3,4 \qquad (6.2.21)$$

and

$$[s^*_{ij}] = \begin{bmatrix} 0 & 0 & 0 & 0 \\ 0 & 0 & 0 & 0 \\ 0 & 0 & 0 & 0 \\ 0 & 0 & 0 & s_{ij} \end{bmatrix} \quad \text{for } i,j = 1,2,3,4 \qquad (6.2.22)$$

where the coefficients m_{ij} are given by equation (6.2.2), and s_{ij} by equation (6.2.11).

In the computer program the overall assembly is carried out in this form and then all the coefficients of the overall mixed matrix, consistent mass matrix or initial stress stiffness matrix are interchanged to the original form, where nodal deflections and moments are listed separately.

6.2.4) The Overall Assembly and The Eigenvalue Problem.

It remains to assemble the overall matrices and introduce the nodal boundary conditions; the form of the resulting matrices depend on how we list the nodal variables as referred to in Section 6.2.3.

For simplicity's sake, we assume in this section that the local and global nodal moments and deflections are listed

separately, and that for assembly purposes the element relations (6.2.4), (6.2.12), (6.2.20) apply.

Let the global deflections and moments be represented by:

$$\{W^*\} = [W_1^* \ , W_2^* \quad \ldots \quad W_n^*]^T$$

$$\{M^*\} = [\,[M^*]_1 [M^*]_2 \quad \ldots \quad [M^*]_n]^T$$

with $[M^*]_i = [M_x \ \ M_y \ \ M_{xy}]_{\text{node } i}$

and n representing the number of nodes.

The assembled form can be written, following a procedure similar to the one described in Section 5.4, as:

$$\begin{Bmatrix} \dfrac{\partial \pi_R}{\partial \{M^*\}_e^T} \\ \dfrac{\partial \pi_R}{\partial \{W^*\}_e^T} \end{Bmatrix} = \begin{bmatrix} -[G] & [H] \\ [H]^T & [0] \end{bmatrix} \begin{Bmatrix} \{M^*\} \\ \{W^*\} \end{Bmatrix} - \begin{bmatrix} [0] & [0] \\ [0] & \lambda[F] \end{bmatrix} \begin{Bmatrix} \{M^*\} \\ \{W^*\} \end{Bmatrix} = \begin{Bmatrix} \{0\} \\ \{0\} \end{Bmatrix}$$

or

$$\begin{bmatrix} -[G] & [H] \\ [H]^T & [0] \end{bmatrix} \begin{Bmatrix} \{M^*\} \\ \{W^*\} \end{Bmatrix} = \begin{bmatrix} [0] & [0] \\ [0] & \lambda[F] \end{bmatrix} \begin{Bmatrix} \{M^*\} \\ \{W^*\} \end{Bmatrix} \qquad (6.2.23)$$

where, for free vibrations [F] is a mass consistent matrix and $\lambda = \omega^2$; for buckling problems [F] is the initial stress stiffness matrix and $\lambda = \lambda_b$, the buckling factor.

The overall partitioned matrices ard then given by:

$$[G] = \sum_{e=1}^{N} [G_e] \qquad (a)$$

$$[H] = \sum_{e=1}^{N} [H_e] \qquad (b) \qquad (6.2.24)$$

$$[F] = \sum_{e=1}^{N} [F_e] \qquad (c)$$

N = Number of elements

where $[G_e]$, $[H_e]$, $[F_e]$ have the same dimensions as [G],[H],[F], but the only non-zero locations are those due to the coefficients of [g],[h],[f] for the e'th element, globally located. The matrix [f] represents respectively an element consistent mass matrix [m], or initial stress stiffness matrix [s], respectively for vibration and buckling problems.

The boundary conditions can now be prescribed in the form of zero nodal deflections and/or moments. This is done by deleting in both sides of relation (6.2.23) the rows and columns corresponding to the constrained degrees of freedom. The resulting matrix will be non-singular. For the remainder of this chapter we shall assume that the boundary conditions have been imposed and that the vectors $\{W^*\}_e$ and $\{M^*\}_e$ represent the free nodal deflections and moments.

Thus, the non-singular relation represented by (6.2.23) can be represented as:

$$\begin{aligned} -[G]\{M^*\} + [H]\{W^*\} &= [0]\{M^*\} \qquad (a) \\ [H]^T\{M^*\} &= \lambda[F]\{W^*\} \qquad (b) \end{aligned} \tag{6.2.25}$$

Solving relation (6.2.25a) for $\{M^*\}$ gives:

$$\{M^*\} = [G]^{-1}[H]\{W^*\} \tag{6.2.26}$$

Substituting the matrix relation (6.2.26) into (6.2.25b) yields:

$$[K^*]\{W^*\} = \lambda[F]\{W^*\} \tag{6.2.27}$$

where

$$[K^*] = [H]^T[G]^{-1}[H] \tag{6.2.28}$$

is a real symmetric positive definite matrix.

We are then left with the solution of the eigenvalue problem given by the matrix relation (6.2.27) i.e. For free vibrations:

$$[K^*]\{\hat{W}^*\} = \lambda[M]\{\hat{W}^*\} \tag{6.2.29}$$

where [M] is a real symmetric positive definite matrix, it is called

the overall consistent mass matrix. The λ's are the eigenvalues.

The natural frequencies are given by

$$\omega = \sqrt{\lambda}$$

The lowest ω is called the fundamental natural frequency. The vector $\{\hat{W}^*\}$ represents the eigenvector, i.e. the modd shape for the plate; that one corresponding to the smallest ω is the fundamental mode shape.

For buckling:

$$[K^*]\ \{W^*\} = \lambda_b\ [S]\ \{W^*\} \qquad (6.2.30)$$

Now, in general, the matrix [S] is only a real symmetric matrix, it is called the overall initial stress stiffness matrix, and therefore it is convenient, with a view to solution of the problem, to write equation (6.2.30) as:

$$[S]\ \{W^*\} = \lambda_b^*\ [K^*]\ \{W^*\} \qquad (6.2.31)$$

In view of the inverse relation between λ_b and λ_b^*, the first critical buckling factor λ_b is evaluated from the maximum value of λ_b^*. The vector $\{W\}_e$ represents the buckling mode: the one corresponding to the maximum λ_b^*, hence minimum λ_b, is the fundamental buckling mode.

For plastic-buckling, the sought critical stress state is obtained when the smallest $\lambda_b = 1$.

Thus, we convert the buckling criterion to the requirement that $\lambda_b^* = 1$ and the procedure to determine the plastic in-plane stresses (hence edge loads) is as follows:-

At some trial loading level, the stress state is calculated and the matrix [G] formed; the matrix [G] contains now coefficients which are generated using relation (6.2.19). The matrices $[K^*] = [H]^T[G]^{-1}[H]$ and [S] are computed based on these stresses. The eigenvalue is then solved and the highest value of λ_b^* is observed. If this value happens to be unity, the stated buckling criterion is satisfied and the trial in-plane stresses are

the critical ones, i.e. determinant ([K*] - [S]) = 0.

If λ_b^* is greater (less) than unity, the trial in-plane stresses are greater (less) than the desired critical state. Hence the in-plane stresses are decreased (increased) and the computation repeated.

Thus,a succession of eigenvalue problems must be solved for various in-plane stress levels in order to determine the critical in-plane stresses (hence critical buckling load).

The in-plane stresses pertinent to this condition are called plastic buckling stresses (hence plastic buckling loads).

The solution of the eigenvalue relations (6.2.28) and (6.2.29) is carried out using a standard subroutine available from the Computer Centre N.A.G. Library [67]. For a brief description, see Appendix 2.

CHAPTER 7

DEVELOPMENT OF THE MAIN PROGRAM FOR STATIC APPLICATIONS

7.1) Introduction.

The mathematical model of the mixed finite element method described in Chapter 5 has to be written in the form of a computer program. Before describing the computer coding, it will be helpful to recapitulate the essential steps of a mixed finite element formulation:

1) The plate is divided into suitable general quadrilateral elements and the nodes numbered in the most suitable form in order to obtain the minimum bandwidth.
2) Information regarding the geometry, compliance properties and applied load is made available for each element.
3) The element mixed matrix and force vector is evaluated in turn for each element.
4) The overall mixed matrix and force vector is assembled.
5) The overall mixed matrix and overall forced vector are modified in accordance with the prescribed nodal deflections and moments.
6) The system of algebraic linear equations is solved and the nodal deflections and moments found.
7) The stresses are calculated at a discrete number of points in the plate. Shear forces and rotations may then be evaluated for each element in turn.

Whenever possible and convenient the various processes are executed automatically using self-contained "Procedures" which, with little change, may be used in developing new elements.

7.2) Division of the Plate into Finite Elements.

The plate is divided into quadrilateral elements. Once the division is ready we can start recording the system topology, by numbering the elements consecutively, starting from

1. The numbering of the nodes is also done consecutively starting from 1, but one must have in mind the several possibilities and try to find the best one leading to the least semi-bandwidth. For example, considering Fig.(7.2.1) the recommended numbering is as in Fig.(7.2.1a) where the semi-bandwidth is 20, whereas in Fig.(7.2.1b) it is 28. Thus the storage requirements can be reduced and the overall solution time decreased by judicious nodal numbering. The node and element numbers should be put on the model for later reference, they will be part of the input data to be discussed in the next sections.

The relationship between a node number and the global degree of freedom, d_g, corresponding to a node n, will be:

$$d_g = 4 \times n - I \qquad (7.2.1)$$

$$\text{for } I = 3,2,1,0$$

which correspond respectively to

$$[W \quad M_x \quad M_y \quad M_{xy}]_n$$

That is, the nodal deflection and nodal bending and twisting moments of node n.

7.3) Algorithm to Evaluate the Jacobian, Derivatives and Product of Shape Functions at a Point.

The Jacobian J, equation (5.3.6), its determinant, the inverse of the Jacobian equation (5.3.7), the derivatives of the shape functions with respect to the x and y axes respectively, given by equations (5.3.8), (5.3.14) and the product of the shape functions:

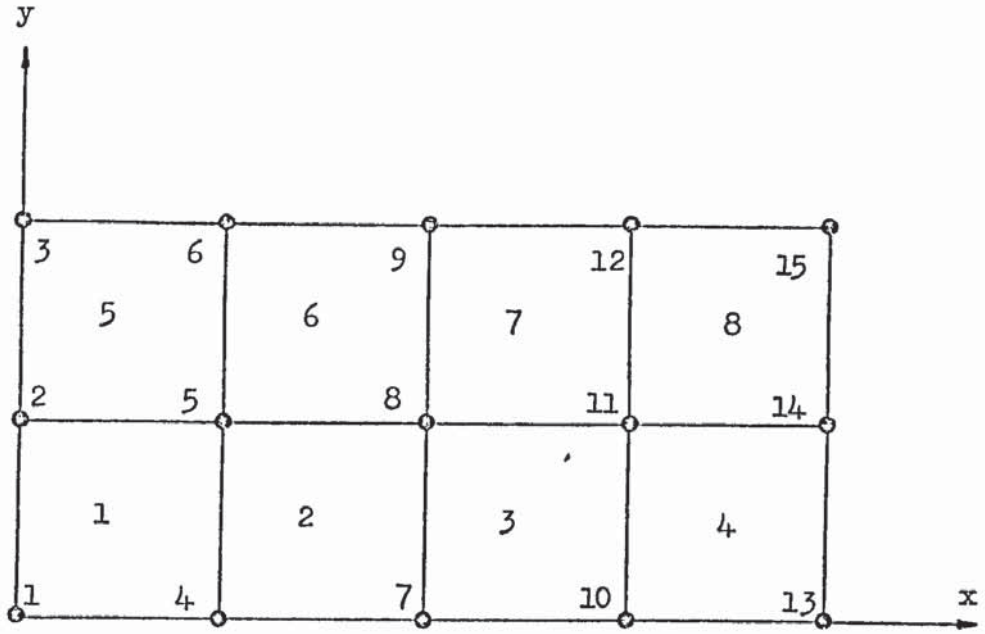

(a)

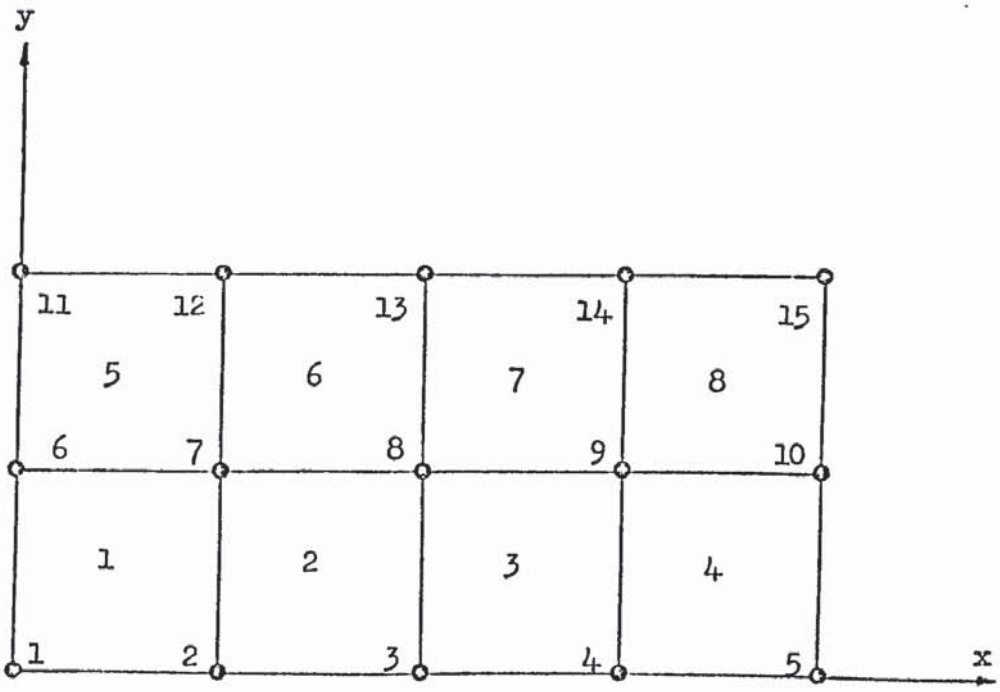

(b)

Fig.(7.2.1) Plate divided into finite elements.

$$SFM[I,J] = \begin{bmatrix} N_1N_1 & N_1N_2 & N_1N_3 & N_1N_4 \\ & N_2N_2 & N_2N_3 & N_2N_4 \\ & & N_3N_3 & N_3N_4 \\ & & & N_4N_4 \end{bmatrix} \qquad (7.3.1)$$

are evaluated at any required point within the general quadrilateral element, such as at the four Gaussian integrating points. A procedure AUX has been written to perform the required operations.

The variables involved in this procedure, where

I = Integer

R = Real variable

RA - Real array

IR - Integer array,

are:

L1 (R) Natural coordinate ζ

L2 (R) Natural coordinate η

B (RA) Derivative array representing [B] given by equation (5.3.8) or $[N_M']^T[B]$, where $[N_M']^T$ is equation (5.3.14)

SFM (RA) Product of shape functions array, see relation (7.3.1)

X (RA) x Cartesian coordinate array

Y (RA) y Cartesian coordinate array

U (R) Determinant

N (IR) Nodal connections array

CB (RA) Derivative array, representing $[N_M']^T$ given by relation (5.3.14)

JO (I) Integer denoting the work to be carried out

1 - For two dimensional numerical integration

2 - For one dimensional numerical integration

3 - To be used with procedure SHFORCE in evaluating Q_x and Q_y for each element.

The flow diagram for the procedure AUX(L1,L2,B,SFM,SF,X,Y,U,N,Z,CB,J0) is shown in Fig.(7.3.1).

Fig.(7.3.1) Flow diagram for the procedure AUX

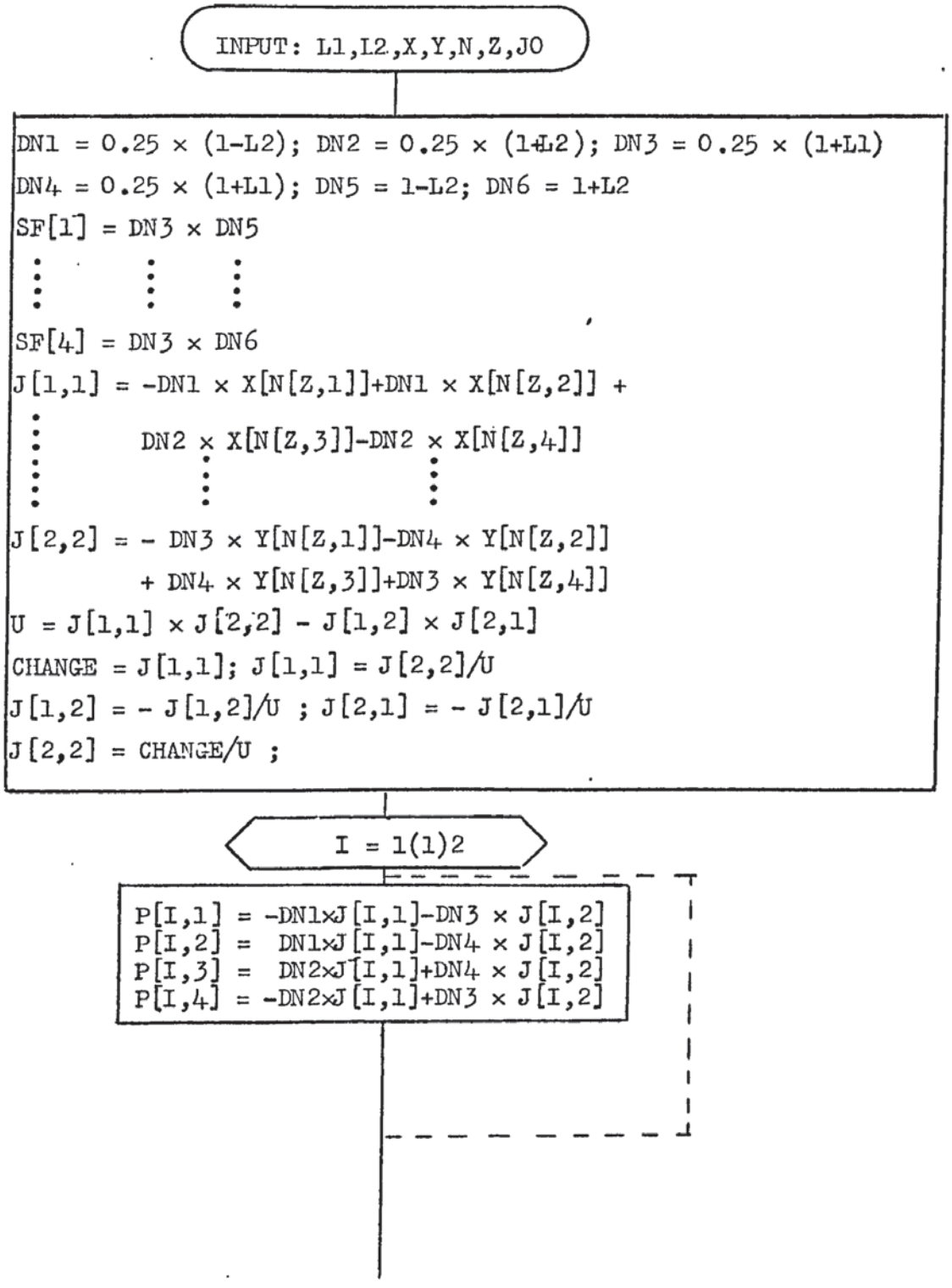

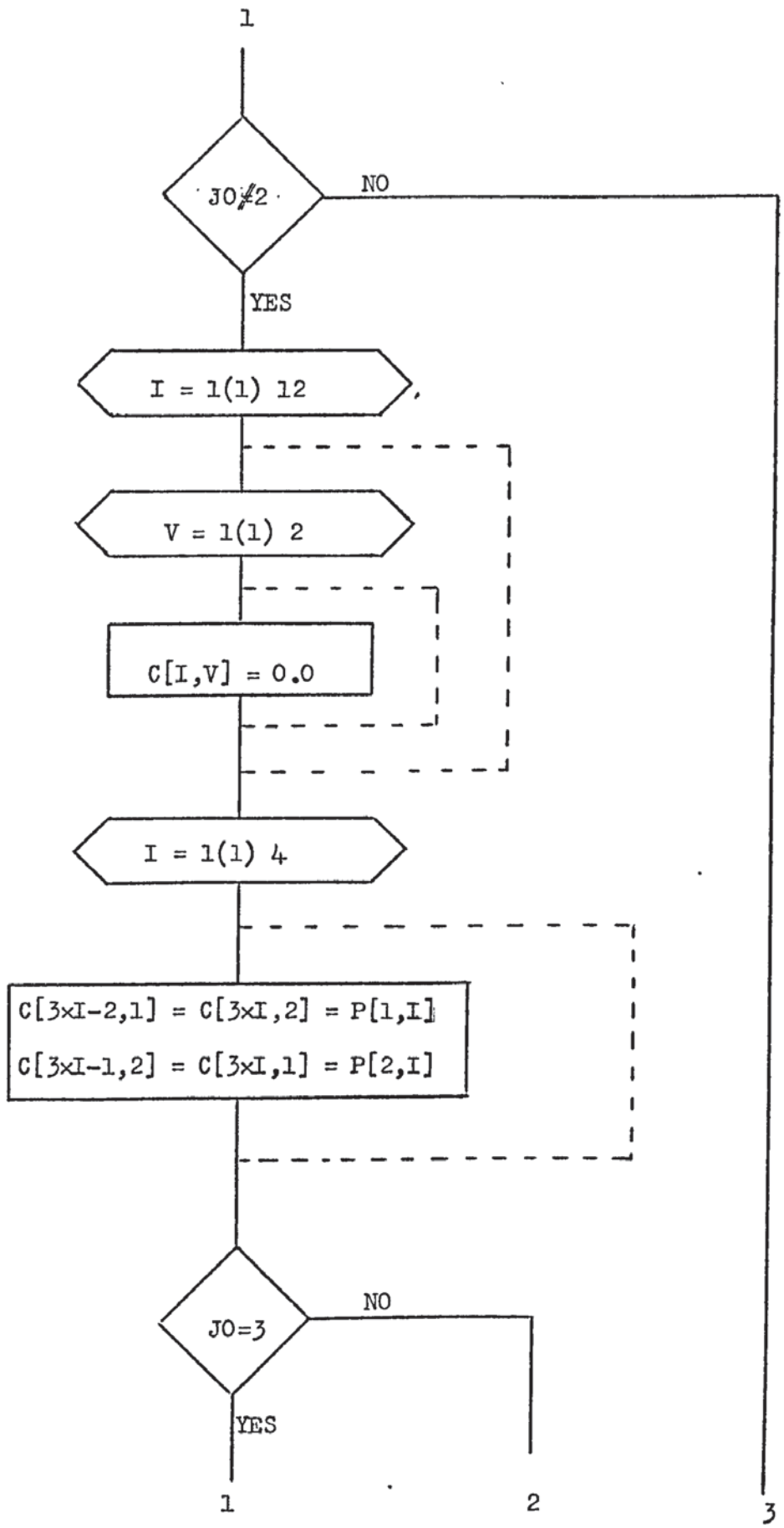
1
JO≠2
NO
YES
I = 1(1) 12
V = 1(1) 2
C[I,V] = 0.0
I = 1(1) 4
C[3×I-2,1] = C[3×I,2] = P[1,I]
C[3×I-1,2] = C[3×I,1] = P[2,I]
JO=3
NO
YES
1
2
3

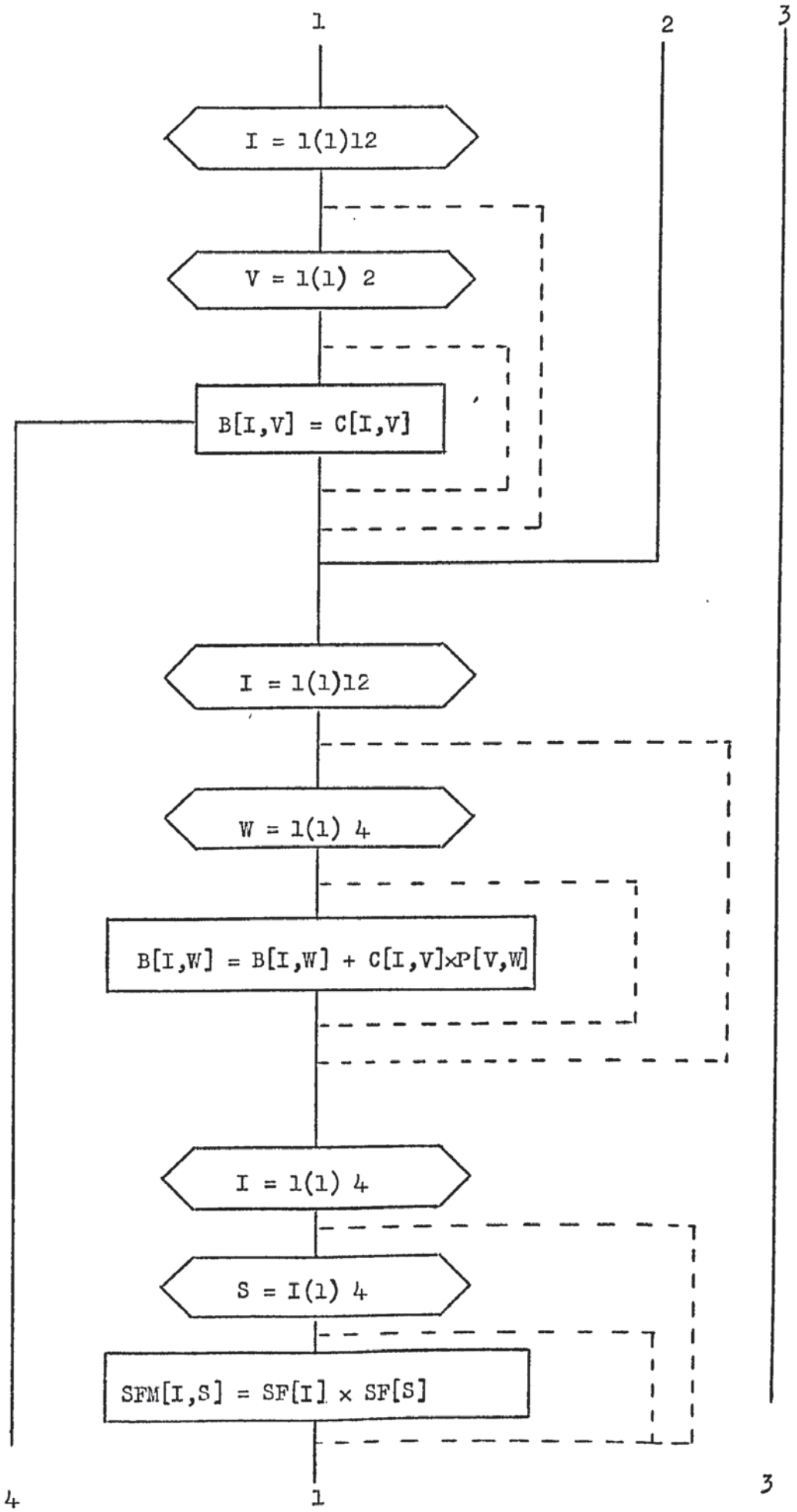
1
2
3
I = 1(1)12
V = 1(1) 2
B[I,V] = C[I,V]
I = 1(1)12
W = 1(1) 4
B[I,W] = B[I,W] + C[I,V]×P[V,W]
I = 1(1) 4
S = I(1) 4
SFM[I,S] = SF[I] × SF[S]
4
1
3

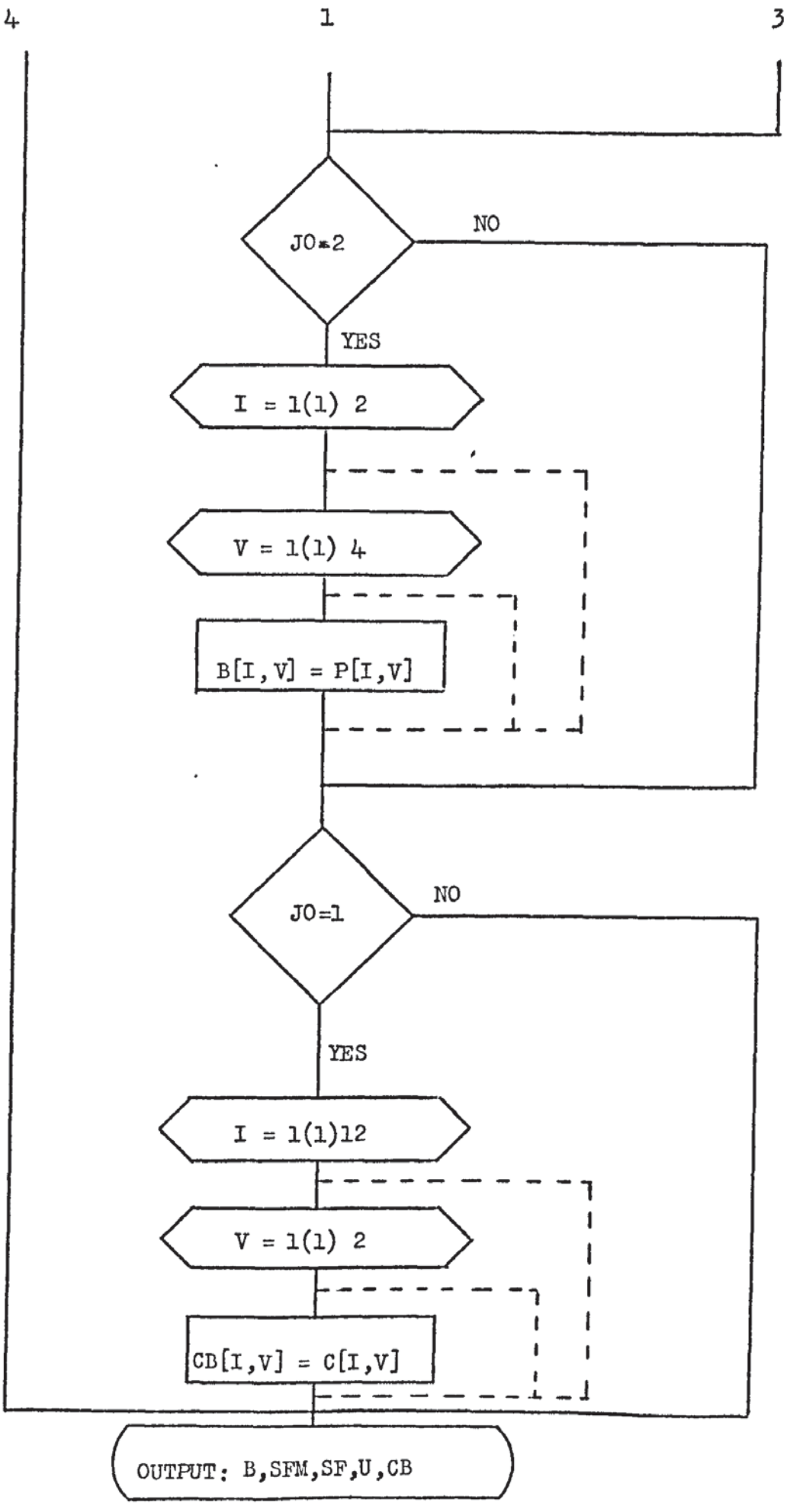
4
1
3
JO=2
NO
YES
I = 1(1) 2
V = 1(1) 4
B[I, V] = P[I, V]
JO=1
NO
YES
I = 1(1)12
V = 1(1) 2
CB[I, V] = C[I, V]
OUTPUT: B, SFM, SF, U, CB

7.4) Algorithm to Evaluate the Shear Deformation Contribution to the Mixed Matrix.

A procedure KESDEF, has been written to evaluate the contribution of the shear deformation to the element mixed matrix in the analysis of moderately thick plate. The coefficients due to the second term of the matrix $[g_{s_{ij}}]$, relation (5.3.25), are evaluated at each Gaussian integrating point, added and located in the element matrix in accordance with equation (5.3.31).

The variables involved in this algorithm are:

K	(RA)	Element mixed matrix array
CB	(RA)	Array with coefficients $[N'_M]^T$, relation (5.3.14) evaluated by procedure AUX
A	(R)	Determinant of the Jacobian x weight coefficient at the Gaussian integrating point. The determinant of the Jacobian is evaluated by AUX.
L	(R)	Compliance shear deformation coefficient (isotropic plates)
LX	(R)	Compliance shear deformation coefficient (orthotropic plates), xz plane
LY	(R)	Compliance shear deformation constant (orthotropic plates), yz plane
M	(I)	Material type 1 - Isotropic materials 2 - Orthotropic materials

The flow diagram for the procedure KESDEF (K,CB,A,L,LX,LY,M) is shown in Fig.(7.4.1).

Fig.7.4.1 - Flow diagram for the procedure KESDEF

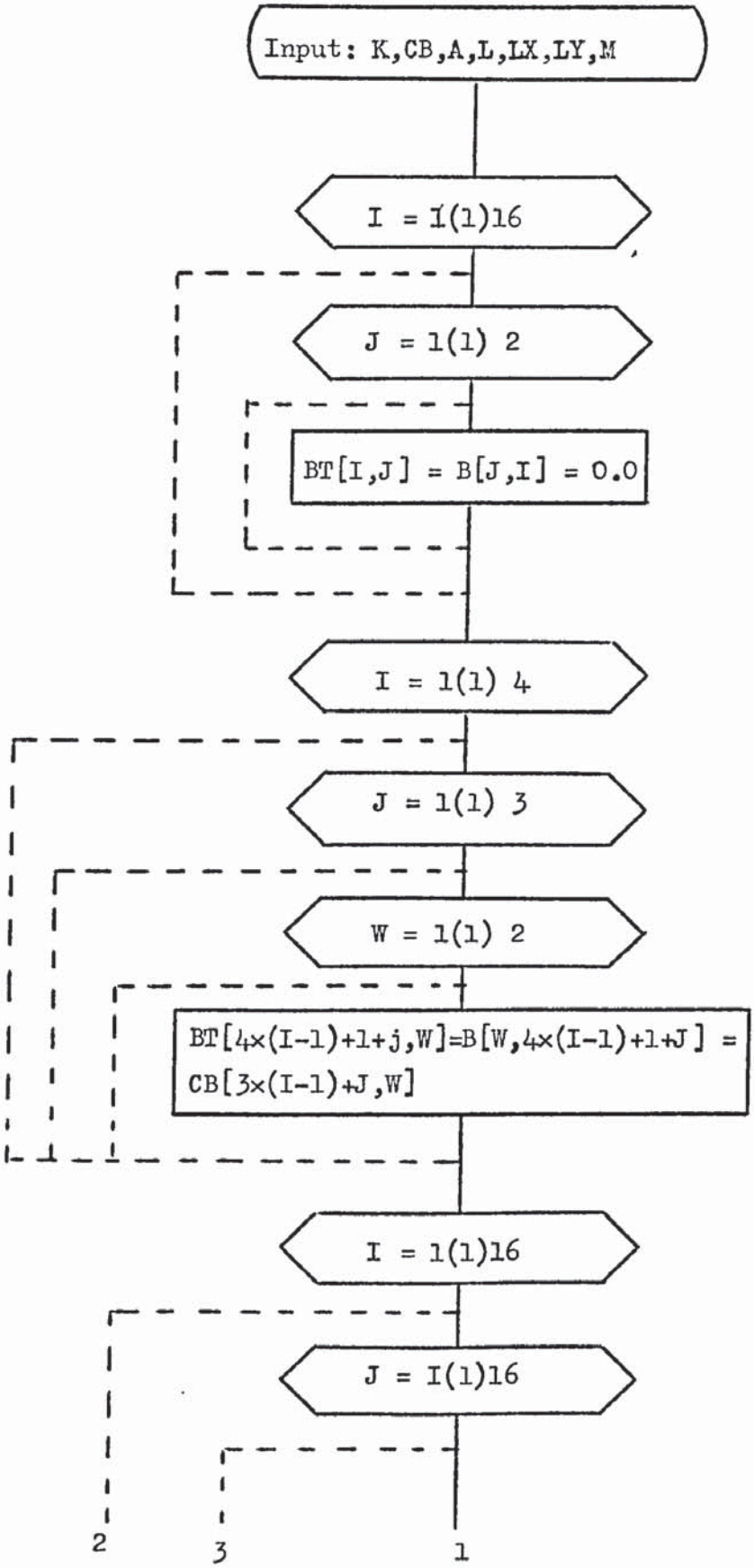

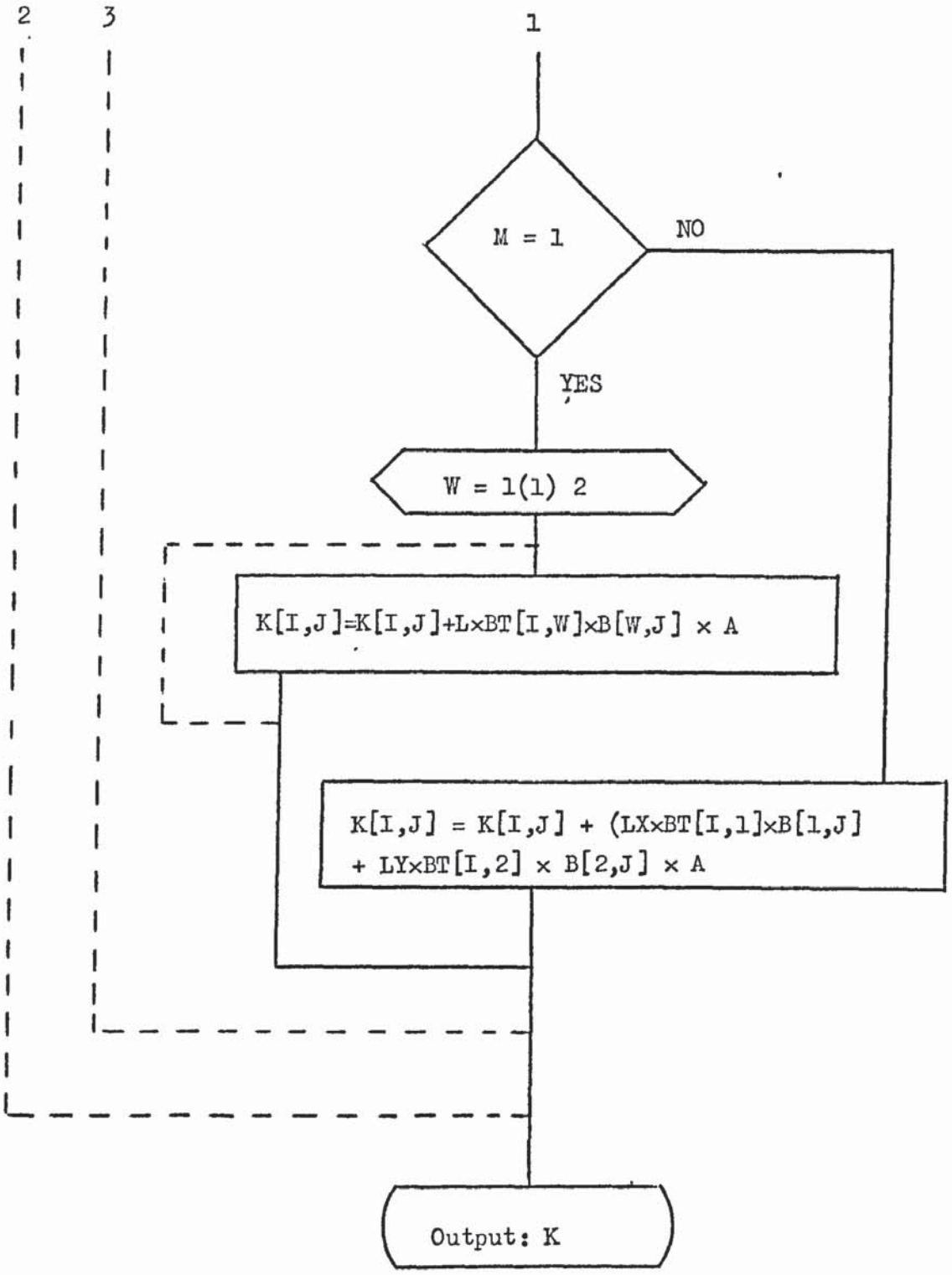
2
3
1
M = 1
NO
YES
W = 1(1) 2
K[I,J]=K[I,J]+L×BT[I,W]×B[W,J] × A
K[I,J] = K[I,J] + (LX×BT[I,1]×B[1,J]
+ LY×BT[I,2] × B[2,J] × A
Output: K

7.5) Algorithm to Evaluate the Coefficients of the Mixed Matrix Due to the Line Integral.

The integral $\int_{s_n} M_{ns} \frac{\partial N}{\partial s} ds$, which contributes to the 2nd term of equation (5.3.22), for thin plates, is evaluated numerically around each element. A procedure MNSWSDS has been written to generate these coefficients. The variables involved in this procedure are:

WW	(RA)	Weight coefficient array
A	(RA)	Gaussian points natural coordinates array
KE	(RA)	Element mixed matrix array
D	(RA)	Direction cosines array
X	(RA)	x coordinate array
Y	(RA)	y coordinate array
N	(IA)	Nodal connections array
Z	(I)	Element counter
C	(RA)	Cosine of angles of sides array
SI	(RA)	Sine of angles of sides array
L	(RA)	Length/2 of element sides array

The arrays C,SI,L,D are evaluated by calling up the procedure SIDES.

Fig.(7.5.1) shows the flow diagram for the procedure

MNSWSDS (WW, A, KE, D, X, Y, N, Z, C, SI, L)

Fig.(7.5.1) Flow diagram for procedure MNSWSDS

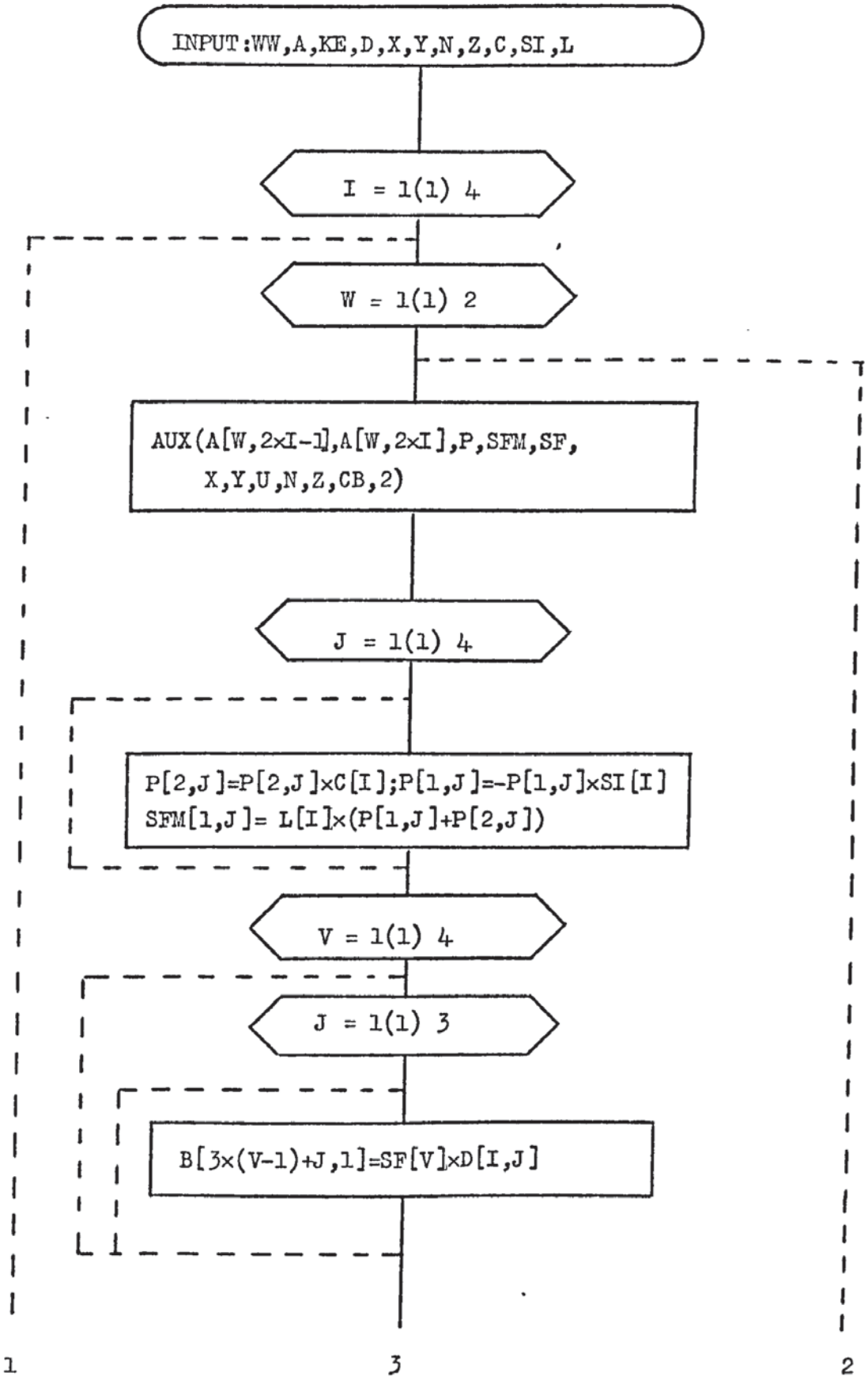

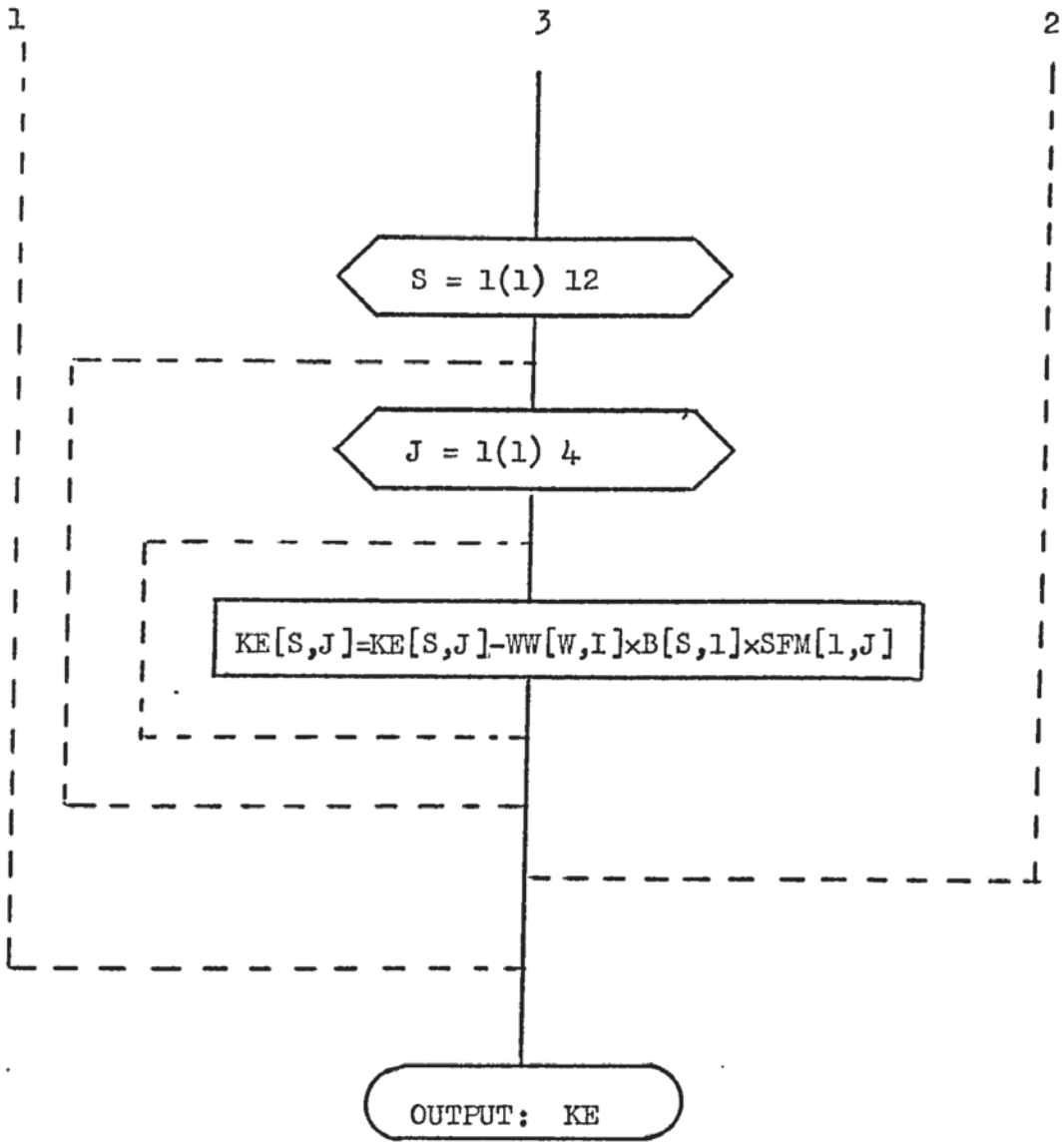
1
3
2
S = 1(1) 12
J = 1(1) 4
KE[S,J]=KE[S,J]-WW[W,I]×B[S,1]×SFM[1,J]
OUTPUT: KE

7.6) Algorithm for the Complete Generation of the Element Mixed Matrix and Element Load Vector.

The numerical integration, to obtain the coefficients of the element mixed matrix, array KE, and element load vector array FE, is carried out using Gaussian quadrature, see Section 3.4, at 4 and 2 integrating points, respectively for the area integrals of KE and FE, and for the line integral of KE, in the analysis of thin plates.

The procedure AUX, described by the flow diagram of Fig.(7.3.1) is called up in the element loop of the program to evaluate the variables which will enable the execution of the numerical integral. The coefficients which will later form KE and FE, common to both thin and moderately thick plates, are then evaluated, taking in consideration the input control data with regard to the thickness and variation of the distributed load. For the integration of the partitioning matrix [g] equation (5.3.17a), which is also the first term of equation (5.3.18a), we only need to integrate 8 different coefficients, related by the array A, see Fig.(7.6.1). The coefficients are later multiplied by the constant values of the compliance matrix, array C, and located in KE, in accordance with equations (5.3.30) or (5.3.31) by the procedure KEFORM.

The array B2 evaluates the contribution of the first term of [h], given by equation (5.3.22).

For "moderately" thick plates, the second term of equation (5.3.18a) is evaluated using procedure KESDEF, described by the flow diagram of Fig.(7.4.1).

For "thin plates" the line integral needs to be evaluated around each element in turn, hence the procedure SIDES is called up to evaluate the length/2 of the sides and the required

direction cosines, which are accepted by the procedure MNSWSDS, to integrate numerically the second term of the matrix $[h_{ij}]$, equation (5.3.22).

The procedure KEFORM is then called up to complete and add the mixed element coefficients, in accordance with the matrix-relations (5.3.30), or (5.3.31).

The load vector due to a distributed load, matrix relation (5.3.23) or (5.3.24) and (5.3.27 or (5.3.28) respectively for thin and moderately thick plates is also evaluated in this loop and located in the array FE in accordance with equation (5.3.33).

Fig.(7.6.1) Flow diagram for the generation of the element mixed matrix and element load vector.

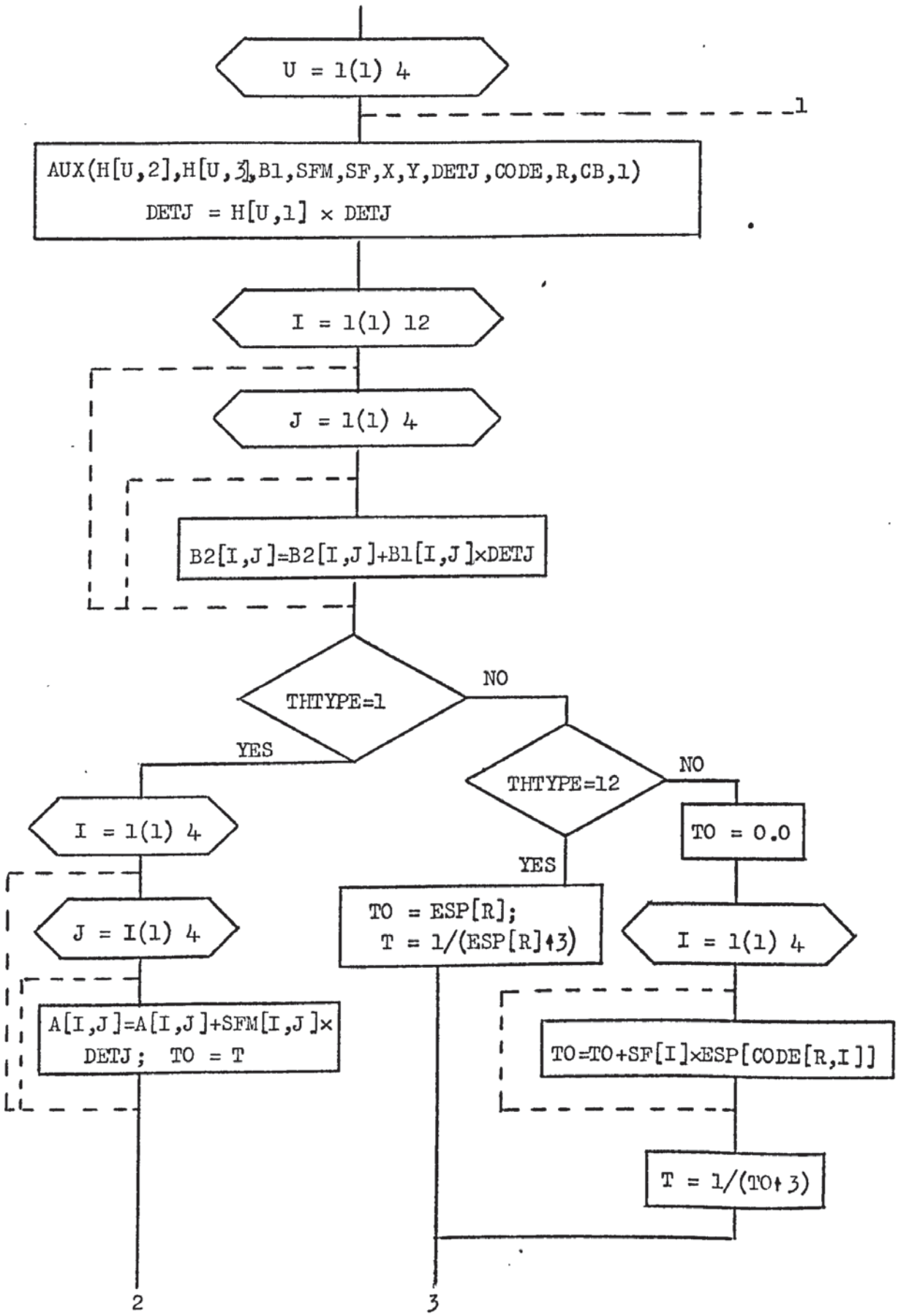

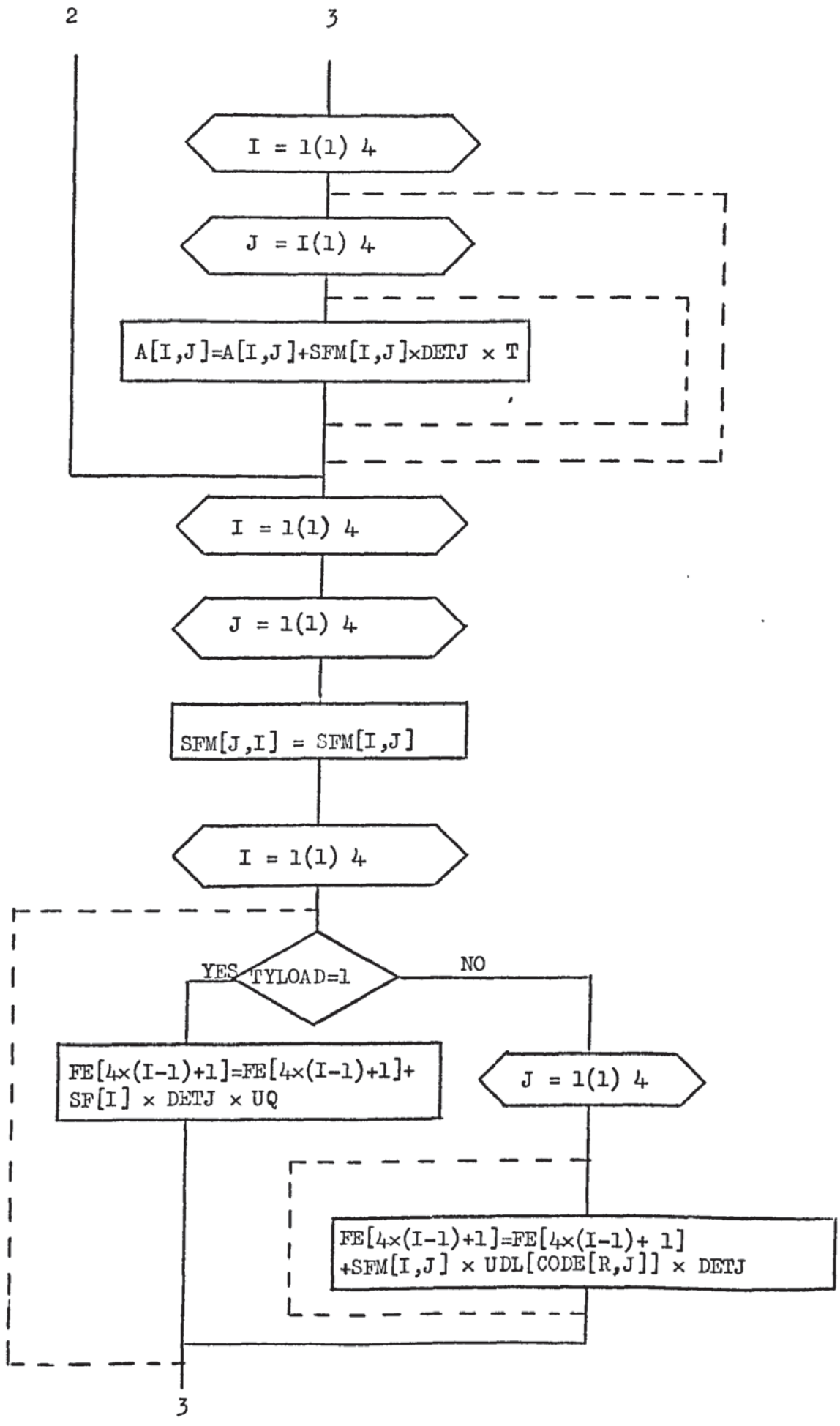
2
3
I = 1(1) 4
J = I(1) 4
A[I,J]=A[I,J]+SFM[I,J]×DETJ × T
I = 1(1) 4
J = 1(1) 4
SFM[J,I] = SFM[I,J]
I = 1(1) 4
YES
TYLOAD=1
NO
FE[4×(I-1)+1]=FE[4×(I-1)+1]+
SF[I] × DETJ × UQ
J = 1(1) 4
FE[4×(I-1)+1]=FE[4×(I-1)+ 1]
+SFM[I,J] × UDL[CODE[R,J]] × DETJ
3

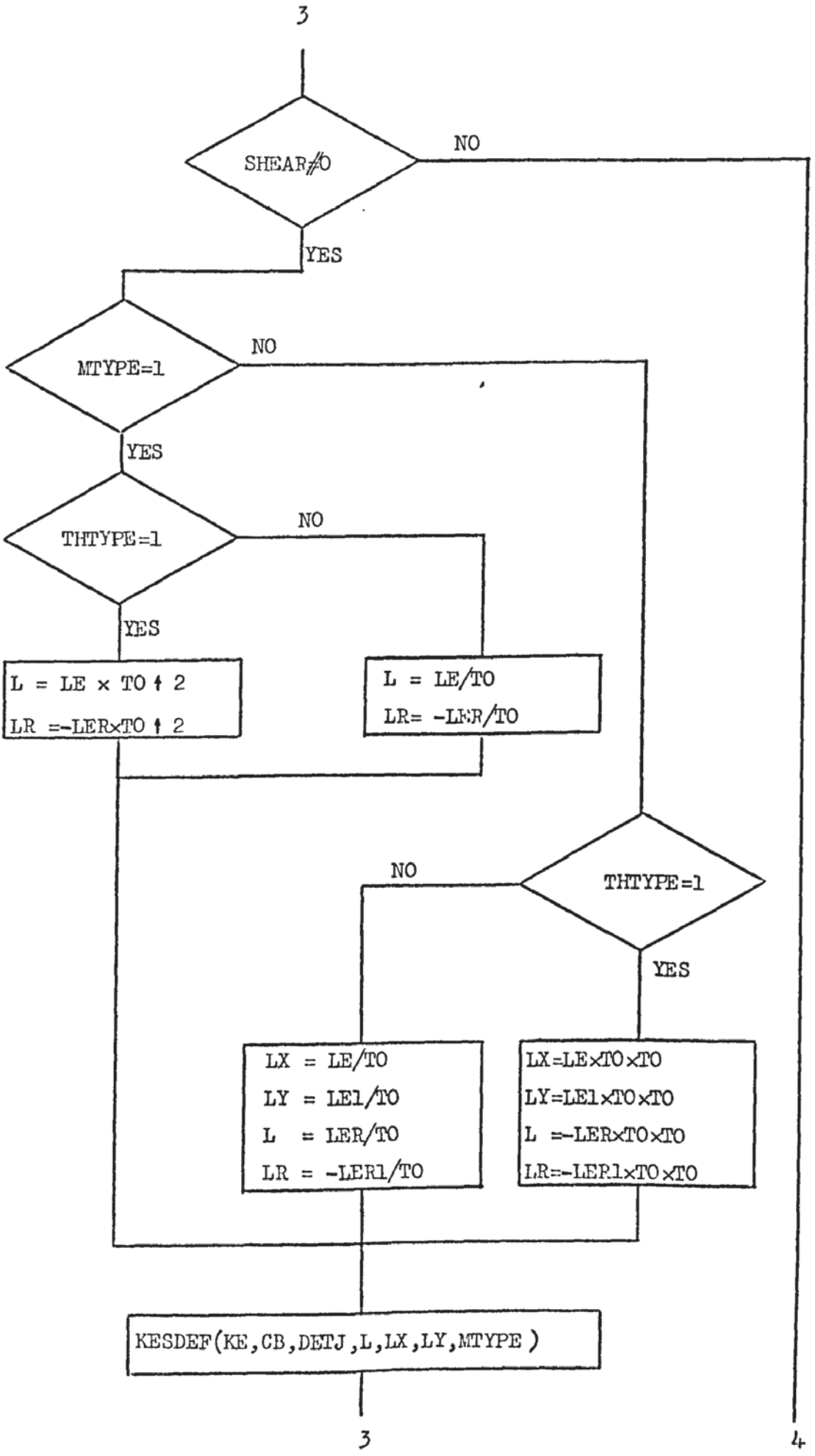
3
SHEAR≠0
NO
YES
MTYPE=1
NO
YES
THTYPE=1
NO
YES
L = LE × TO ↑ 2
LR =-LER×TO ↑ 2
L = LE/TO
LR= -LER/TO
THTYPE=1
NO
YES
LX = LE/TO
LY = LE1/TO
L = LER/TO
LR = -LER1/TO
LX=LE×TO×TO
LY=LE1×TO×TO
L =-LER×TO×TO
LR=-LER1×TO×TO
KESDEF(KE,CB,DETJ,L,LX,LY,MTYPE)
3
4

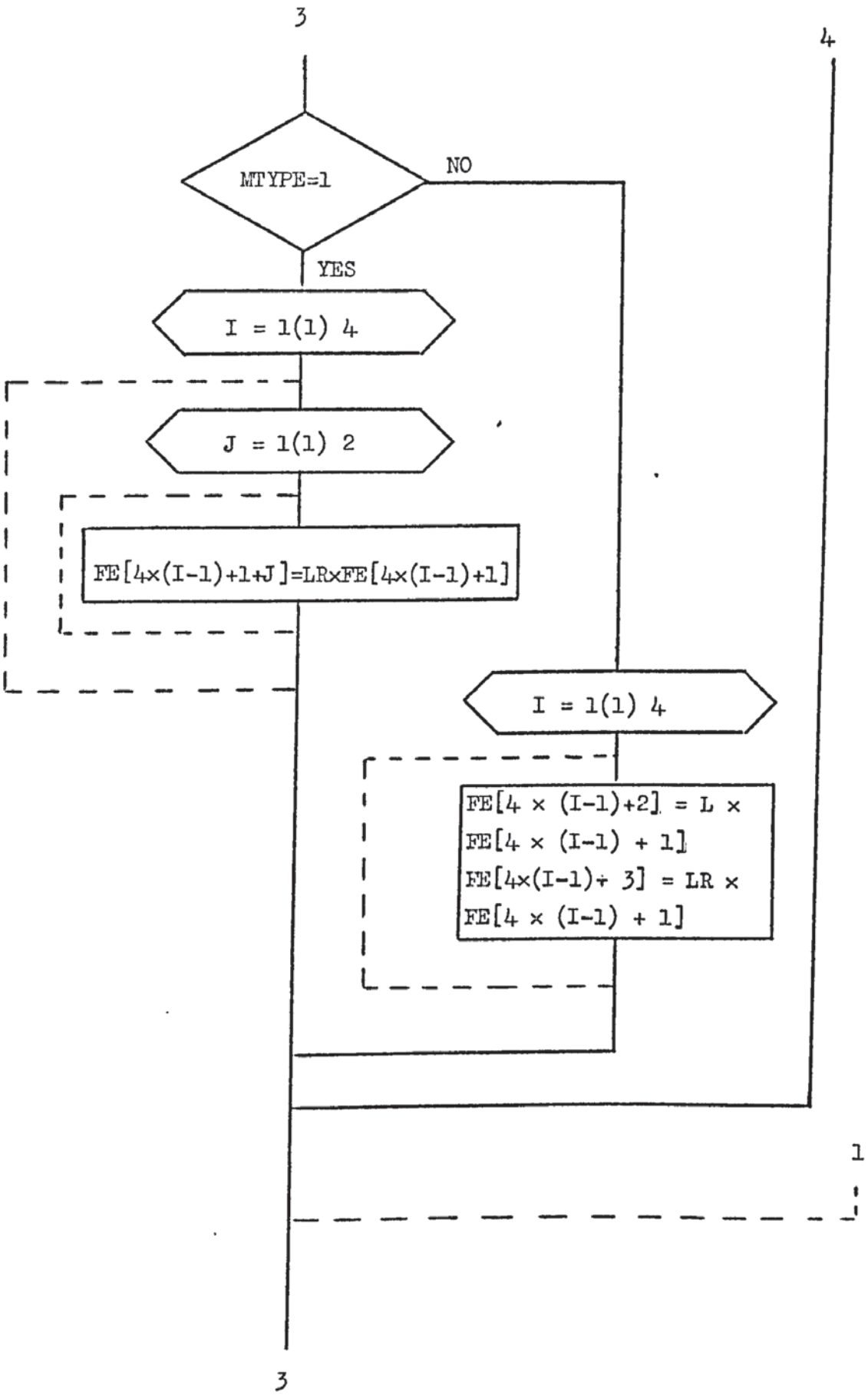
3
4
MTYPE=1
NO
YES
I = 1(1) 4
J = 1(1) 2
FE[4×(I-1)+1+J]=LR×FE[4×(I-1)+1]
I = 1(1) 4
FE[4 × (I-1)+2] = L ×
FE[4 × (I-1) + 1]
FE[4×(I-1)+ 3] = LR ×
FE[4 × (I-1) + 1]
1
3

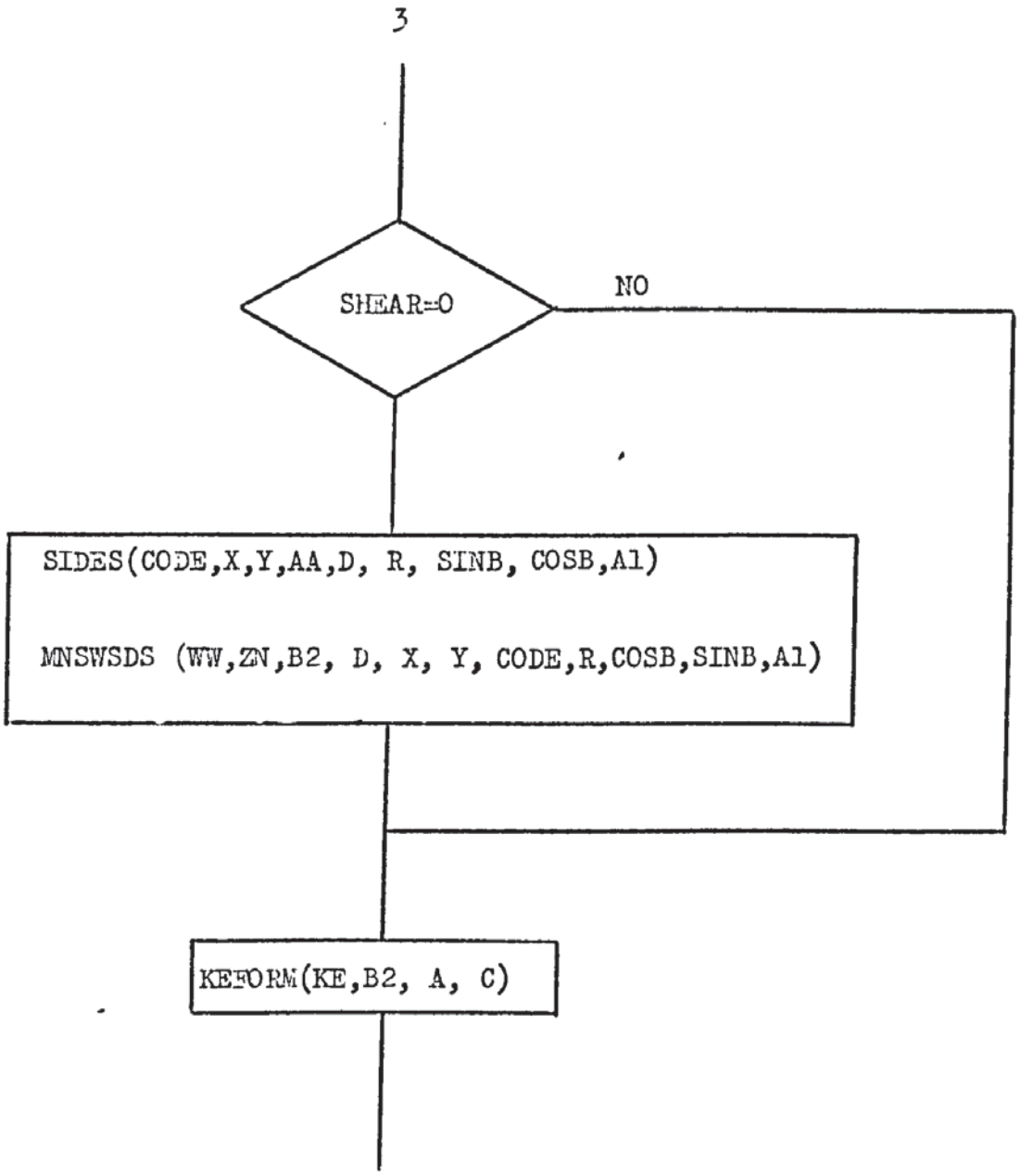
3
SHEAR=0
NO
SIDES(CODE,X,Y,AA,D, R, SINB, COSB,A1)
MNSWSDS (WW,ZN,B2, D, X, Y, CODE,R,COSB,SINB,A1)
KEFORM(KE,B2, A, C)

7.7) Algorithm for the Modification of the Overall Mixed Matrix and Overall Load Vector.

In order to be able to introduce general boundary conditions for the bending and twisting moments, in terms of normal and tangential components, a local change of axes from the global x,y to a local n,s axes is required, as explained in Section 5.5.1. The overall matrix [K] and load vector {F} must then be changed accordingly. The modification in [K] is executed at element level, i.e. by modifying the element mixed matrix [k], for those elements with boundary nodes requiring transformation of axes only.

It can easily be shown by following the approach developed in Section 5.5.1, that the modifications required at element level are respectively:

NODE 1:

$$\begin{bmatrix} [e]^T[k_{11}][e] & [e]^T[k_{12}] & [e]^T[k_{13}] & [e]^T[k_{14}] \\ [k_{21}][e] & [k_{22}] & [k_{23}] & [k_{24}] \\ [k_{31}][e] & [k_{32}] & [k_{33}] & [k_{34}] \\ [k_{41}][e] & [k_{42}] & [k_{43}] & [k_{44}] \end{bmatrix}$$

NODE 2:

$$\begin{bmatrix} [k_{11}] & [k_{12}][e] & [k_{13}] & [k_{14}] \\ [e]^T[k_{21}] & [e]^T[k_{22}][e] & [e]^T[k_{23}] & [e]^T[k_{24}] \\ [k_{31}] & [k_{32}][e] & [k_{33}] & [k_{34}] \\ [k_{41}] & [k_{42}][e] & [k_{43}] & [k_{44}] \end{bmatrix}$$

NODE 3:

$$\begin{bmatrix} [k_{11}] & [k_{12}] & [k_{13}][e] & [k_{14}] \\ [k_{21}] & [k_{22}] & [k_{23}][e] & [k_{24}] \\ [e]^T[k_{31}] & [e]^T[k_{32}] & [e]^T[k_{33}][e] & [L]^T[k_{34}] \\ [k_{41}] & [k_{42}] & [k_{43}][e] & [k_{44}] \end{bmatrix}$$

NODE 4:

$$\begin{bmatrix} [k_{11}] & [k_{12}] & [k_{13}] & [k_{14}][e] \\ [k_{21}] & [k_{22}] & [k_{23}] & [k_{24}][e] \\ [k_{31}] & [k_{32}] & [k_{33}] & [k_{34}][e] \\ [e]^T[k_{41}] & [e]^T[k_{42}] & [e]^T[k_{43}] & [e]^T[k_{44}]\ [e] \end{bmatrix}$$

where the matrix $[e]$ is a direction cosine matrix given by equation (5.5.1), evaluated from the value of the angle which the normal n makes with the x axis; the angles are inputed in degrees as we shall see in the description of the input data. The matrices $[k_{ij}]$ are the partitioning matrices of the element mixed matrix. A procedure TRANSF has been written to transform the element mixed matrix array KE, when a local modification at a boundary node is required. This procedure calls up another three procedures, MATMULT, MATMULT1, MATMULT2, which respectively evaluate products $[e]^T[k_{ij}][e]$; $[e]^T[k_{ij}]$; $[e][k_{ij}]$ where $[e]$ is a 4×4 direction cosine matrix and $[k_{ij}]$ are the 4×4 partitioning matrices shown above.

The procedure is called up in the element generation loop of the program, as can be seen by the general flow diagram of Fig.(7.13.1).

The load vector modification, equation (5.5.4b), is carried out directly after the complete assembly, only for those nodes that require transformation by calling up the procedure LOADTR.

The variables involved in the procedure TRANSF, flow diagram of Fig.(7.7.1) are:

W	(I)	Local node number
K	(RA)	Mixed element array
B	(R.A)	Direction cosines array

The variables for the procedure LOADTR, flow diagram of Fig.(7.7.2) are:

B	(R.A)	Direction cosines array
F	(R.A)	Overall load vector array
S	(I)	Counter for the direction cosines array
Q	(I)	Global node number

Fig.(7.7.1) Flow diagram for proceduro TRANSF

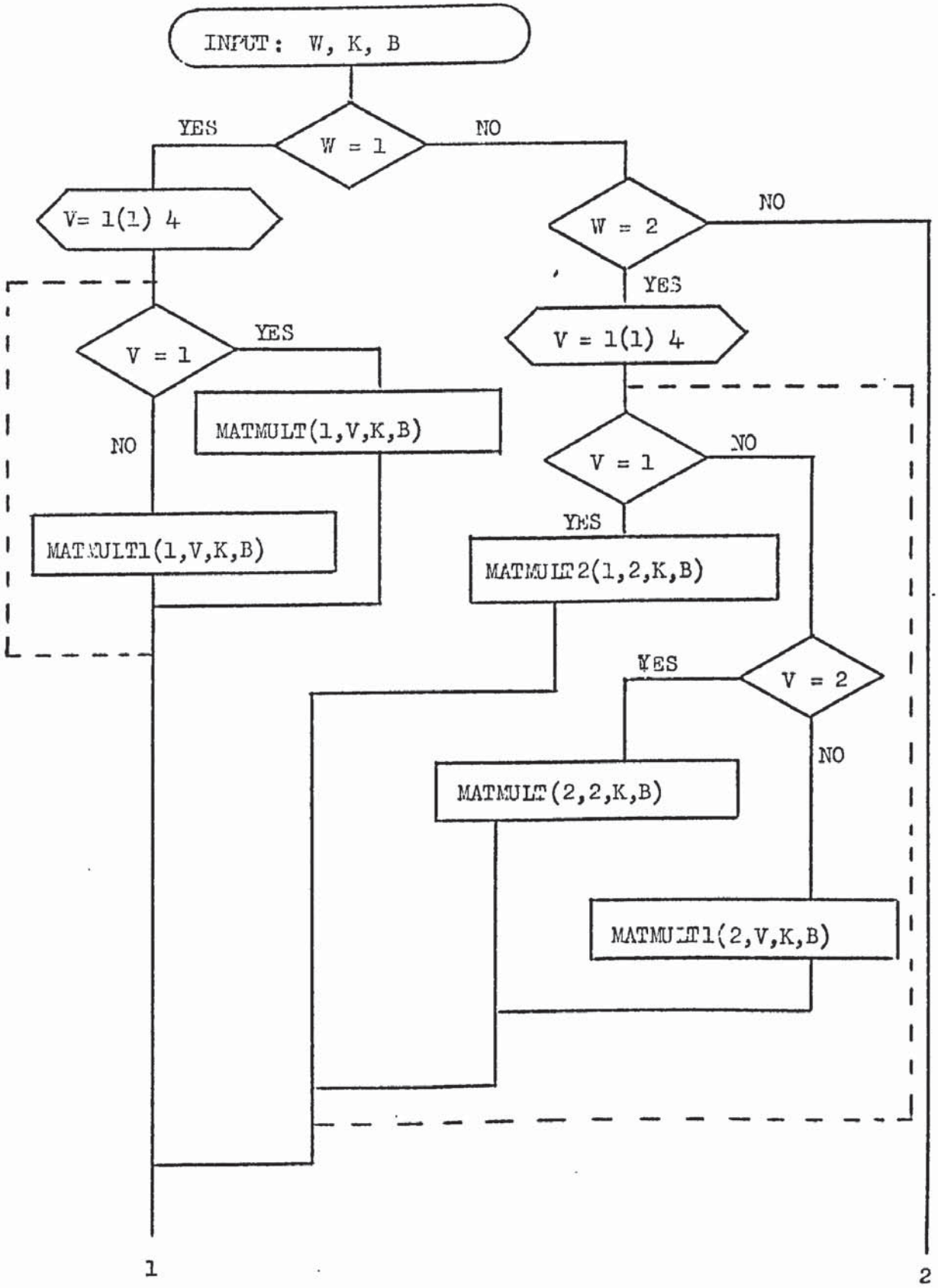

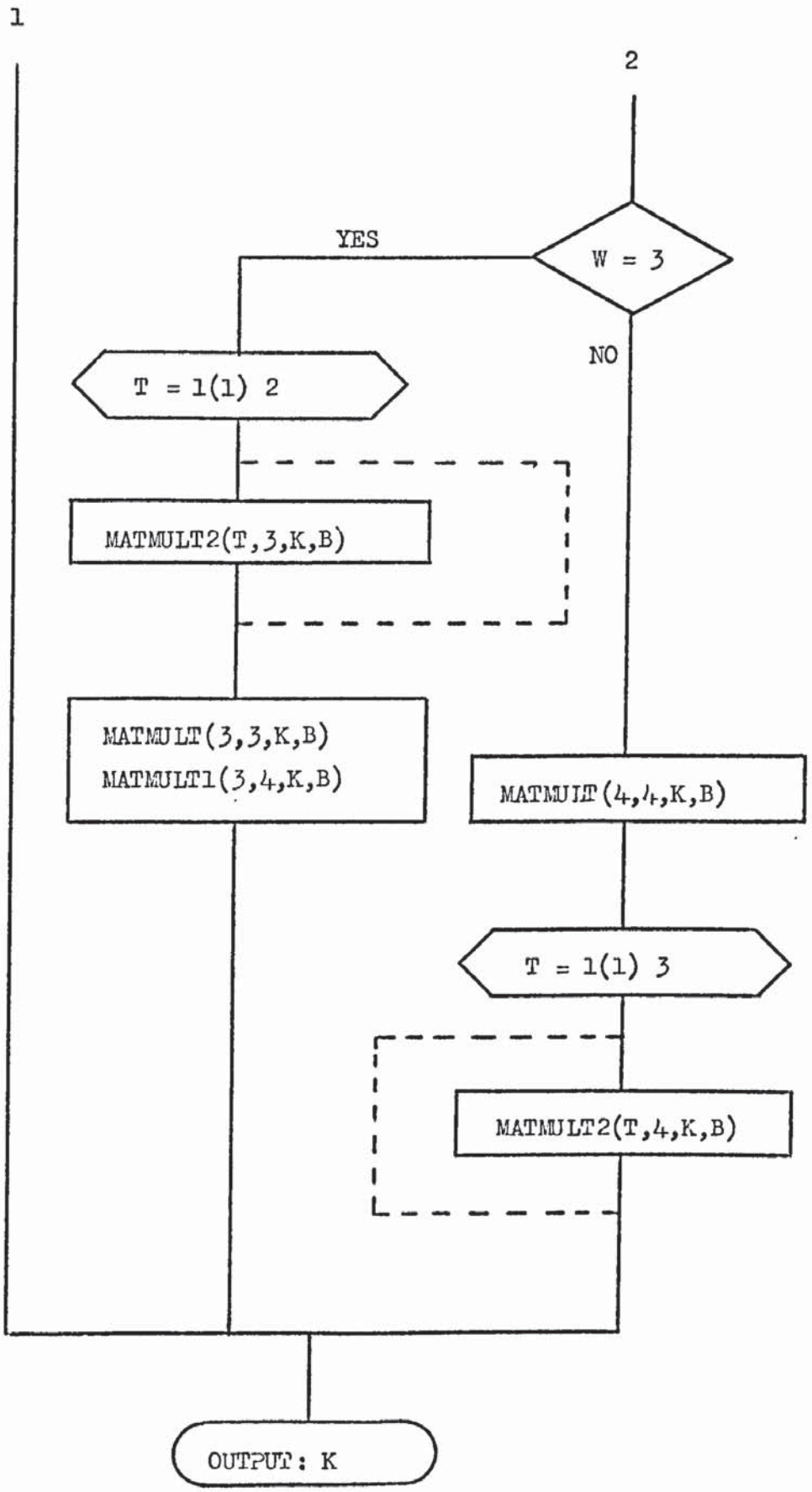
1
2
W = 3
YES
NO
T = 1(1) 2
MATMULT2(T,3,K,B)
MATMULT(3,3,K,B)
MATMULT1(3,4,K,B)
MATMULT(4,4,K,B)
T = 1(1) 3
MATMULT2(T,4,K,B)
OUTPUT: K

Fig.(7.7.2) Flow diagram for procedure LOADTR

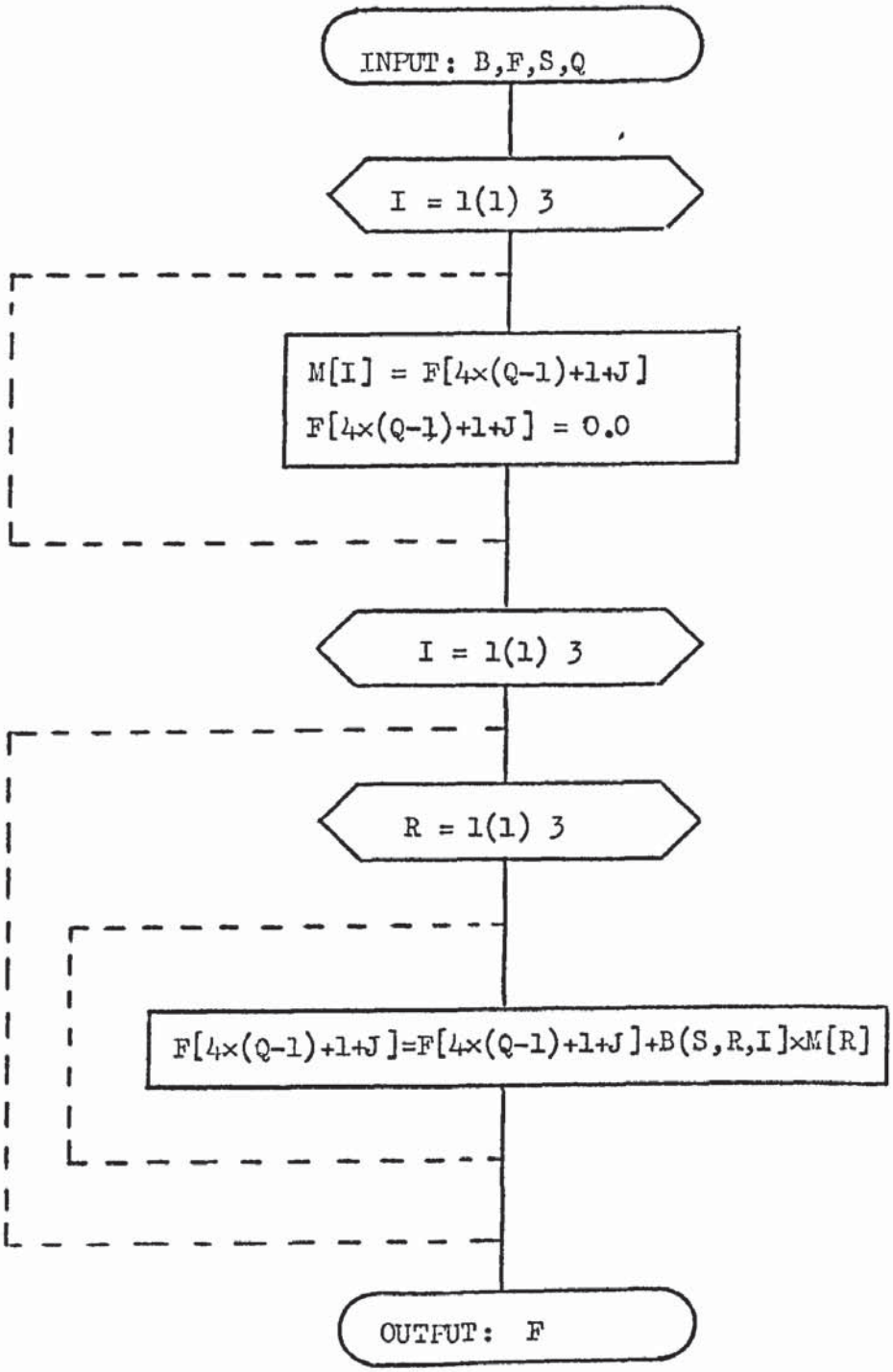

7.8) Storage Scheme for the Overall Mixed Matrix and Overall Assembly.

Due to the fact that only a limited number of nodal points are connected directly by adjacent elements in a structural idealization, the mixed matrix equation (5.4.3) is found to be sparsely populated. If the nodal points are numbered systematically as shown in Section 7.2 , the non-zero elements are located near the leading diagonal in a band form.

Due to the non-availability of a convenient standard procedure for the solution of linear equations, where the mixed matrix of the linear structure is banded, symmetric but non-positive definite, we could not take full advantage of the symmetric properties. The complete band form had to be stored as a two dimensional array, since the symmetry will be lost during the interchange process for the solution of the equations by Gauss elimination, with row interchange, to avoid zeros in the diagonal, due to the non-positiveness of the mixed matrix.

A procedure BAND was developed to evaluate the semi-bandwidth, hence bandwidth which are related by:

Bandwidth = 2 × Semi-bandwidth-1

where the semi-bandwidth is given by equation (5.4.5).

The variables of the procedure BAND(CODE,BD,N.M),flow diagram of Fig.(7.8.1), include:

CODE	(IA)	Nodal connections array
BD	(I)	Semi-bandwidth of overall mixed matrix
N	(I)	Total number of elements
M	(I)	Bandwidth of overall mixed matrix

Fig.(7.8.1) Flow diagram for procedure BAND

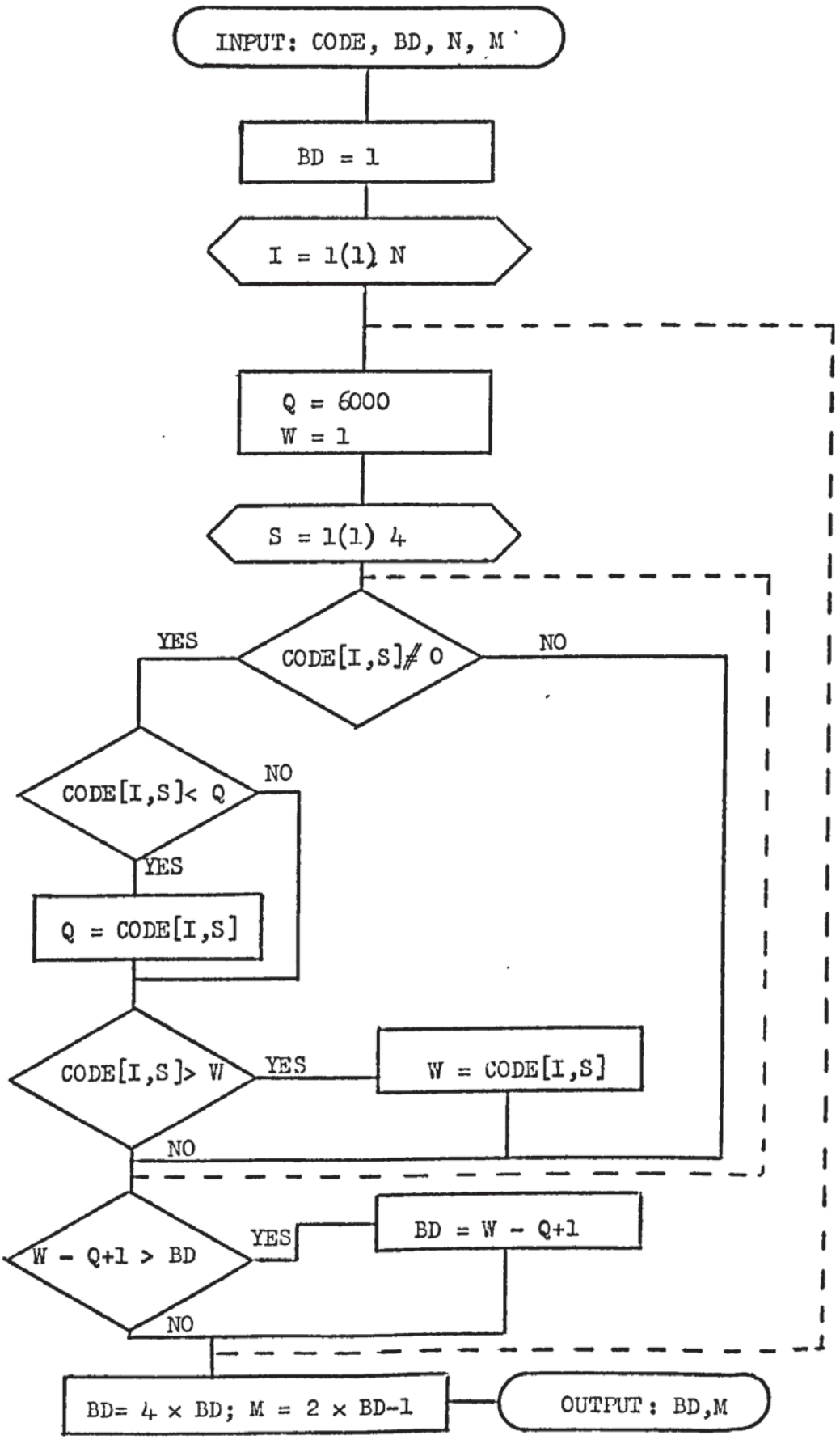

The overall mixed matrix of equation (5.4.3) will then be stored as a two dimensional array, which can be well illustrated by a typical case, see Fig.(7.8.2), say,

bandwidth = 3, rows = 7

$$\begin{bmatrix} k_{11} & k_{12} & 0 & 0 & 0 & 0 & 0 \\ k_{21} & k_{22} & k_{23} & 0 & 0 & 0 & 0 \\ 0 & k_{32} & k_{33} & k_{34} & 0 & 0 & 0 \\ 0 & 0 & k_{43} & k_{44} & k_{45} & 0 & 0 \\ 0 & 0 & 0 & k_{54} & k_{55} & k_{56} & 0 \\ 0 & 0 & 0 & 0 & k_{65} & k_{66} & k_{67} \\ 0 & 0 & 0 & 0 & 0 & k_{76} & k_{77} \end{bmatrix} \Rightarrow \begin{bmatrix} 0 & k_{11} & k_{12} \\ k_{21} & k_{22} & k_{23} \\ k_{32} & k_{33} & k_{34} \\ k_{43} & k_{44} & k_{45} \\ k_{54} & k_{55} & k_{56} \\ k_{65} & k_{66} & k_{67} \\ k_{76} & k_{77} & 0 \end{bmatrix}$$

Fig.(7.8.2)

Following the procedure outlined in Section 5.4 the process of "Assembly" of the overall mixed matrix is one of transferring the individual element mixed coefficients into appropriate positions in the overall matrix. The "address" or location of a coefficient in an element mixed matrix is defined by its row and column number and similarly for the overall matrix, thus, the overall mixed matfix is generated from the element mixed matrix by relating the addresses in the element with those in the overall structure.

A procedure ASSEMBLY, has been written to "assemble" the lower triangular part of the band mixed matrix, as illustrated in Fig.(7.8.2). When the "assembly" is complete the two dimensional array K is modified by the statements of prescribed deflections and moments by calling up the procedure BOUNDARY. Then the coefficients of the lower part of the overall mixed matrix are transposed to complete the two dimensional

array K.

The variables involved in the Procedure ASSEMBLY, flow diagonal of Fig.(7.8.3) are:

Q	(IA)	Nodal connections array
K	(RA)	Overall mixed array
A	(RA)	Mixed element array
R	(I)	Counter for element number
B	(I)	Semi-bandwidth
DF	(I)	Identification value
		16 - for plate elements
		8 - when called by procedure BEAM

Fig.(7.8.3) Flow diagram for procedure ASSEMBLY

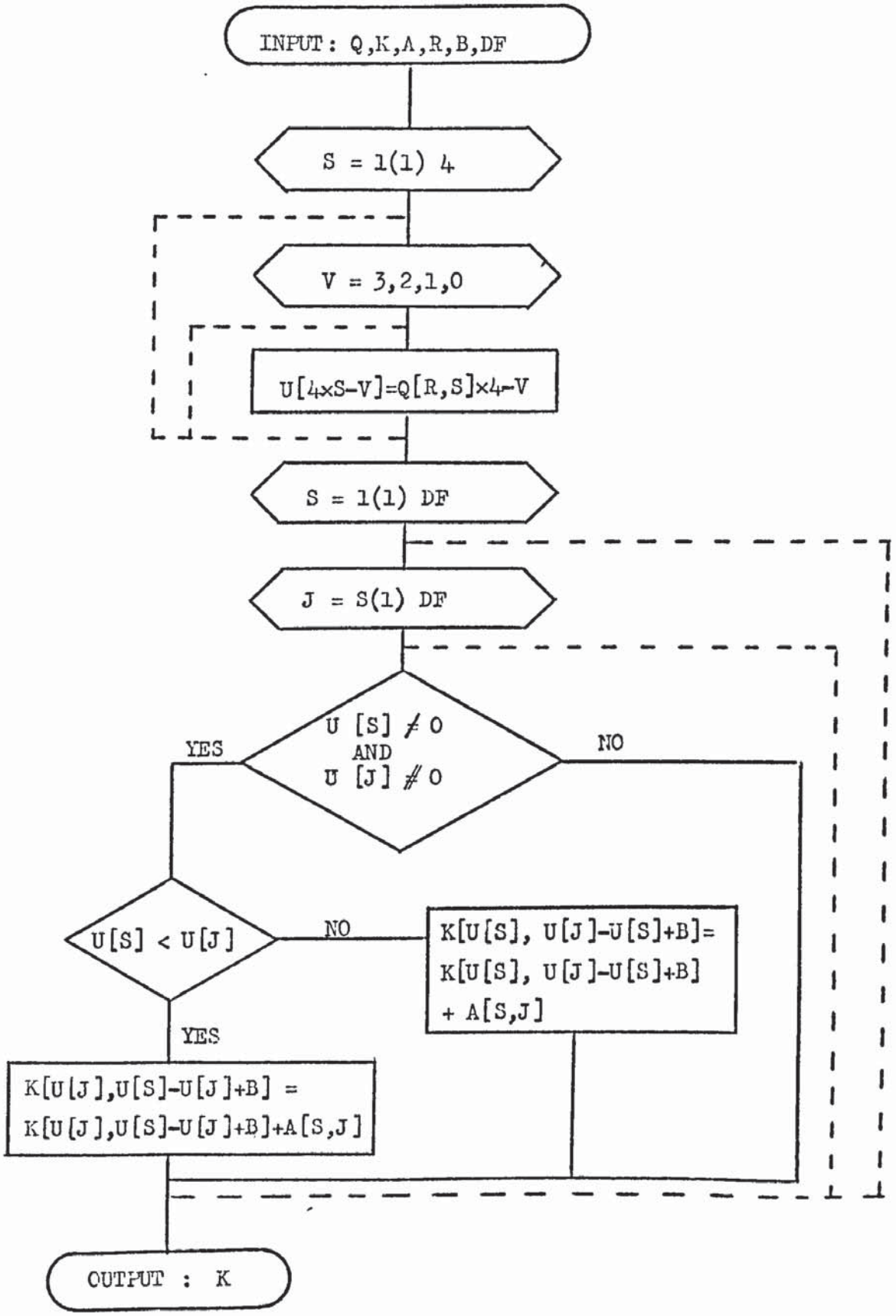

7.9) Algorithm for the Statement of Prescribed Deflections and Moments.

A procedure BOUNDARY has been written to modify the overall load array F and overall mixed array K to include the statements of prescribed deflections and moments. The procedure is based on the theory given in Section 5.5.3.

The variables of this procedure are

VV	(I)	Identification of prescribed quantity 3 Deflection 2 Moment M_x or M_s 1 Moment M_y or M_n 0 Moment M_{xy} or M_{ns}
W	(I)	Global node number of prescribed quantity
TO	(R)	Numerical value of prescribed quantity
BD	(I)	Semi-bandwidth -1
F	(RA)	Overall load array
K	(RA)	Overall mixed array
G	(I)	Total number of degrees of freedom

The flow diagram for the procedure BOUNDARY is given by Fig.(7.9.1).

Fig.(7.9.1) Flow diagram for procedure BOUNDARY

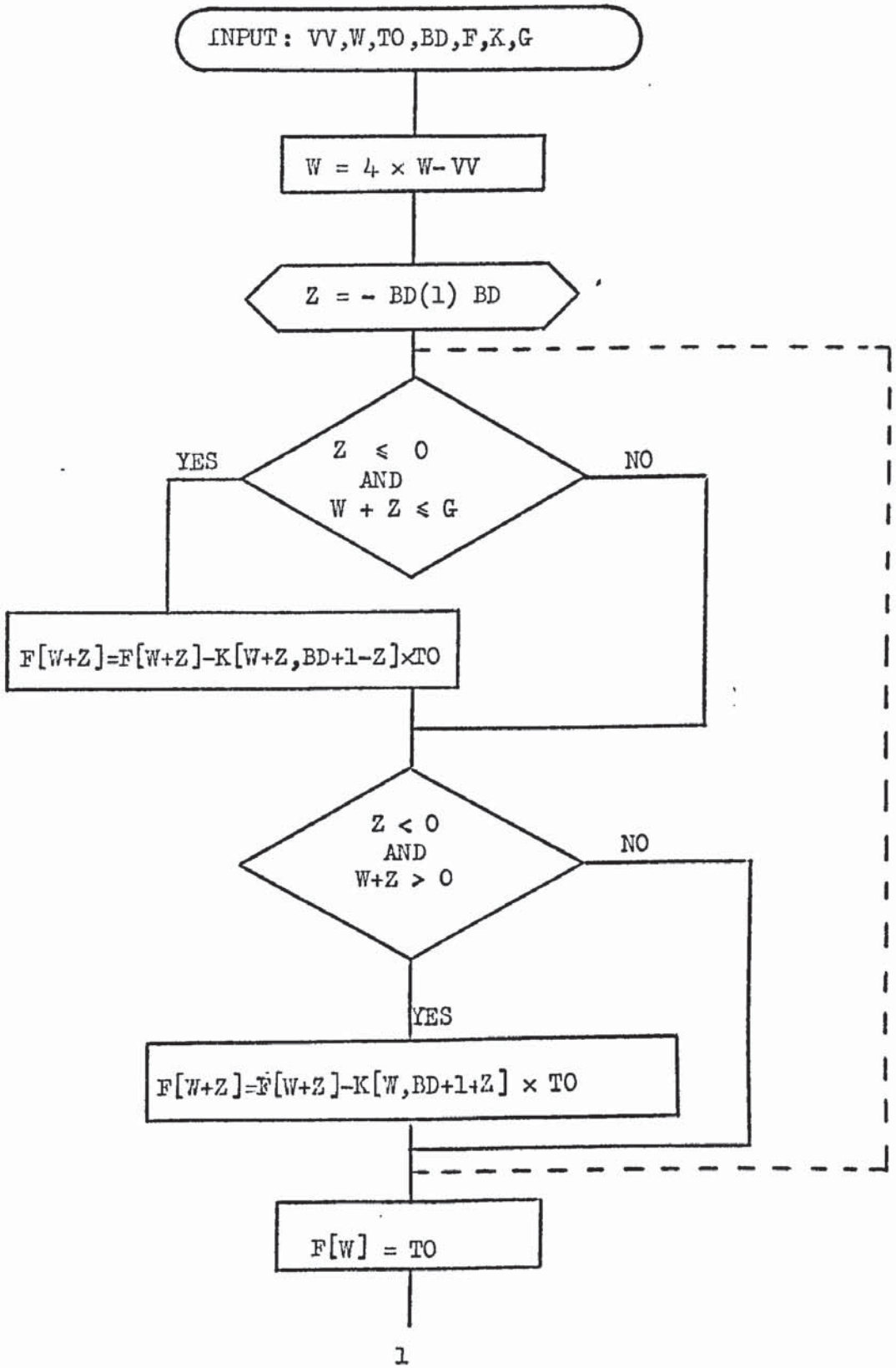

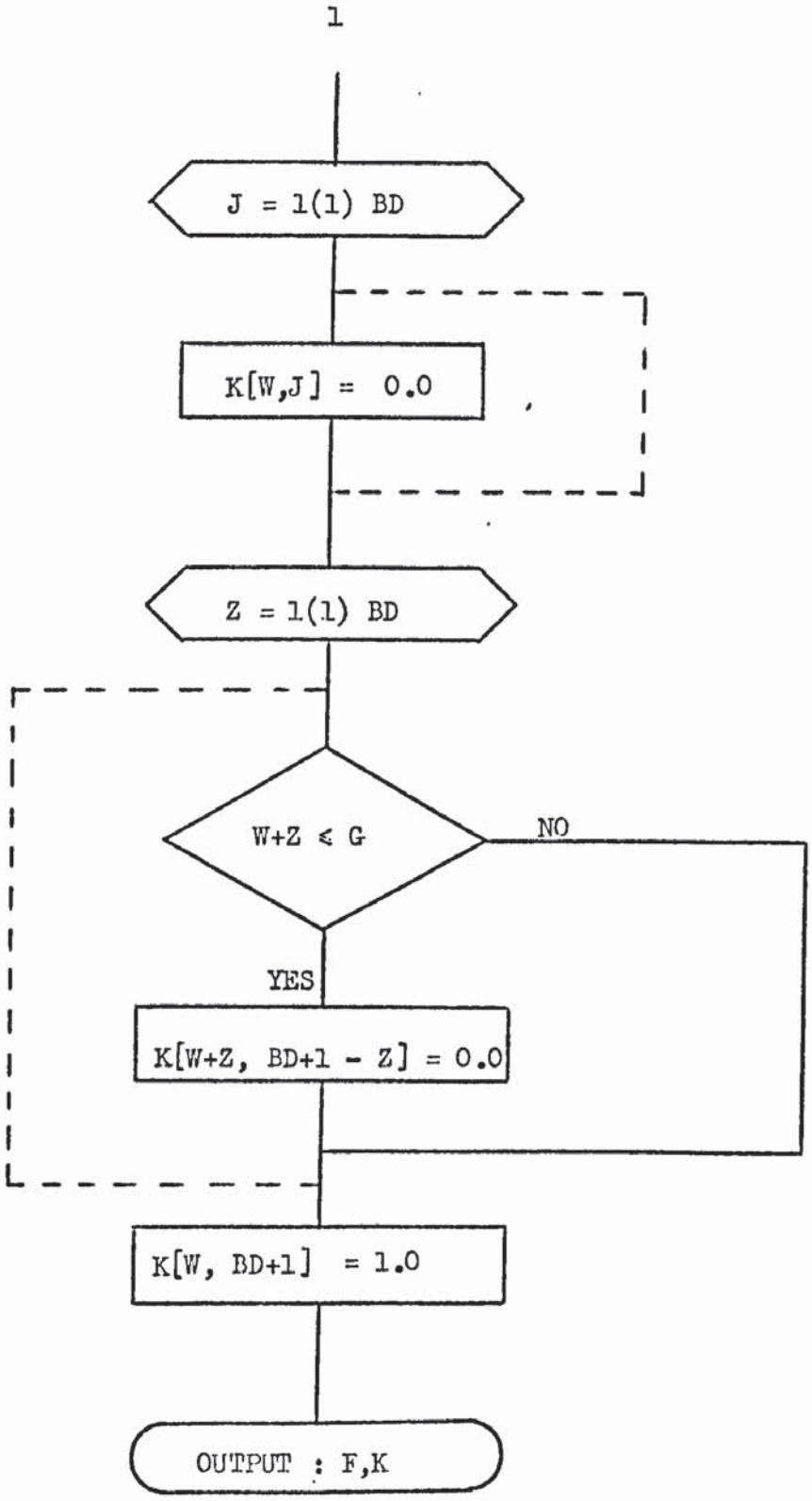
1
J = 1(1) BD
K[W,J] = 0.0
Z = 1(1) BD
W+Z ≤ G
NO
YES
K[W+Z, BD+1 - Z] = 0.0
K[W, BD+1] = 1.0
OUTPUT : F,K

7.10) Inclusion of the Beam Element Mixed Matrix in the Computer Program.

A procedure BEAM has been developed to include in the program the element mixed matrix of a beam element developed in Appendix 3. At the present stage the beam element can safely be used only for the solution of beam problems. For reinforced plates, with few ribs, where the ribs are parallel to the global axes some further tests are required to confirm the suitability of the combination, unfortunately, due to the limited time available it was not possible to pursue the problem further. Also due to the characteristics of the chosen Reissner principle the twisting of the beam could not be considered so that its range of application is limited to symmetric situations where twisting of the beam does not arise.

The flow diagram for the procedure BEAM is given in Fig.(7.10.1).

The variables involved in this procedure are described below:

R	(I)	Element counter
U	(I)	Element nodal connections
X	(R.A)	x nodal coordinate array
Y	(R.A)	y nodal coordinate array
E	(R.A)	Material properties array
EM	(I.A)	Group of identification of material properties array
IJ	(R.A)	2nd Moment of area and length array for the different groups
T	(I.R)	Group of identification of array IJ
K	(R.A)	Overall mixed array
B	(R.A)	Mixed element array
BD	(I)	Semi-bandwidth

Fig.(7.10.1) Flow diagram for procedure BEAM

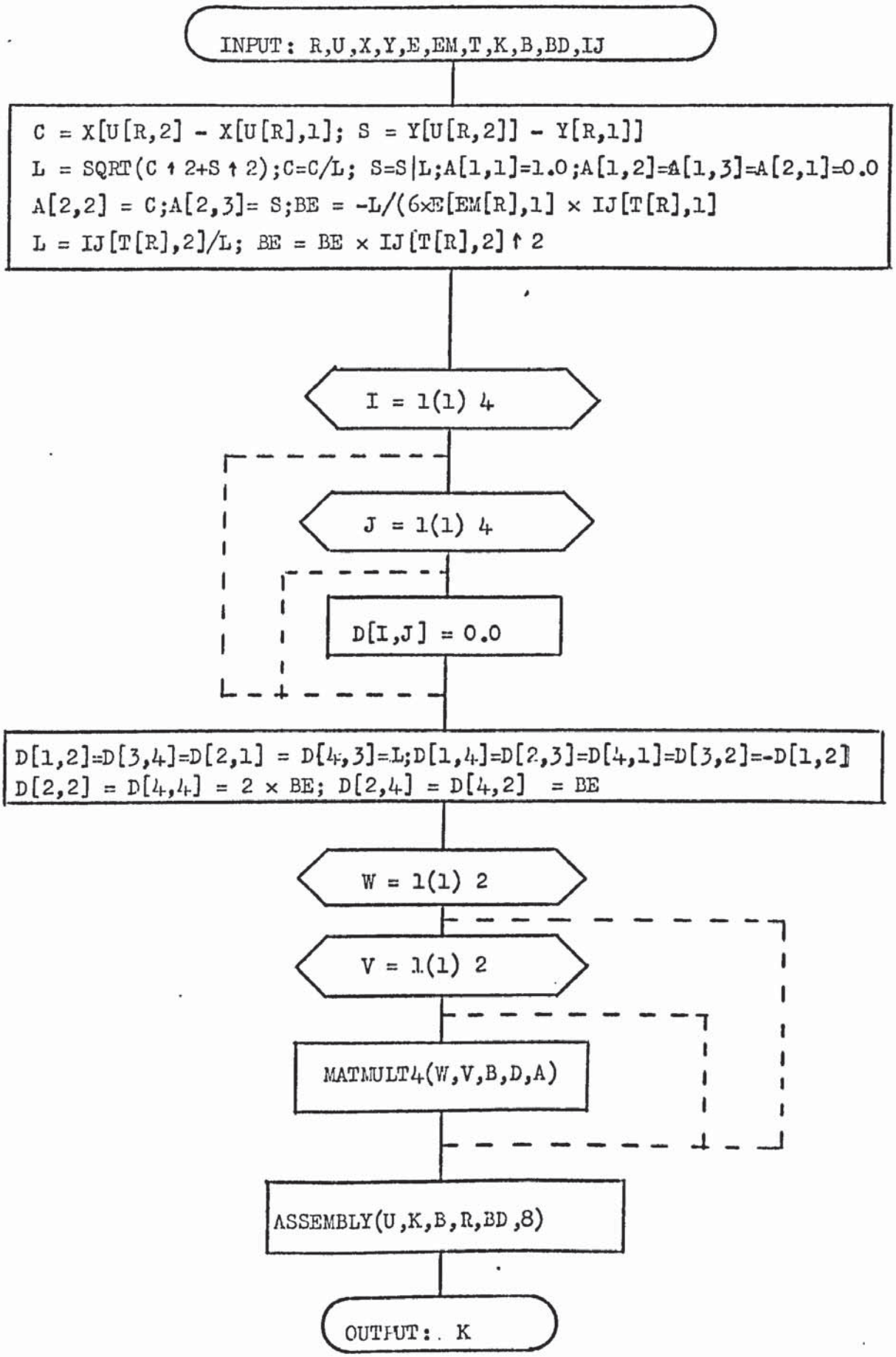

7.11) Solution of the Equations.

The algorithm used for this purpose was BANDSOLVE which was developed by Thurnau [68] for the solution of the matrix equation $[A]\{X\} = \{B\}$ when [A] is of large order and sparse with a band centred in the main diagonal including all the non-zero elements.

The procedure call is BANDSOLVE(C,N,M,V), where parameter N is the order of A, and M is the bandwidth. BANDSOLVE operates only on the band portion of A, given in the N x M array C. The band elements of a given row of A appear in the same row of C but shifted such that element A[I,J] becomes C[I,J-I+(M+1)/2]. All band elements whether zero or not must be given. The values of undefined elements of C such as C[1,1] or C[N,M], are irrelevant because they are not used. The array V initially contains the vector $\{B\}$. After the solution the array V contains the solution vector $\{X\}$. The contents of array C are destroyed during solution which is done by Gauss elimination with row interchanges, followed by back substitution.

7.12) Solution of the Problem.

BANDSOLVE gives the nodal deflections and nodal moments. From the nodal moments the principal bending moments and shear forces are evaluated by calling up procedures PRINBM and SHFORCE. A procedure for the evaluation of the rotations was not included in the program, but if the need arises it can easily be implemented.

7.13) The Overall Picture.

A brief description of the computer program as a whole is given in the form of the simplified flow diagram of Fig.(7.13.1). The main procedures which may be called for the relevant computations are indicated.

The definitions of the relevant variables are as follows:

R	(I)	Counter for the element number
N	(I)	Total number of elements
CODE	(IA)	Nodal connections
U	(I)	Counter for the integrating points
SHEAR	(I)	Type of problem to be solved
		0 - Thin plate
		1 - Moderately thick plate
ET	(I)	Number of nodes requiring n,s transformation
GC	(I)	Total number of specified boundary conditions

Fig.(7.13.1) A general simplified flow diagram for the complete program

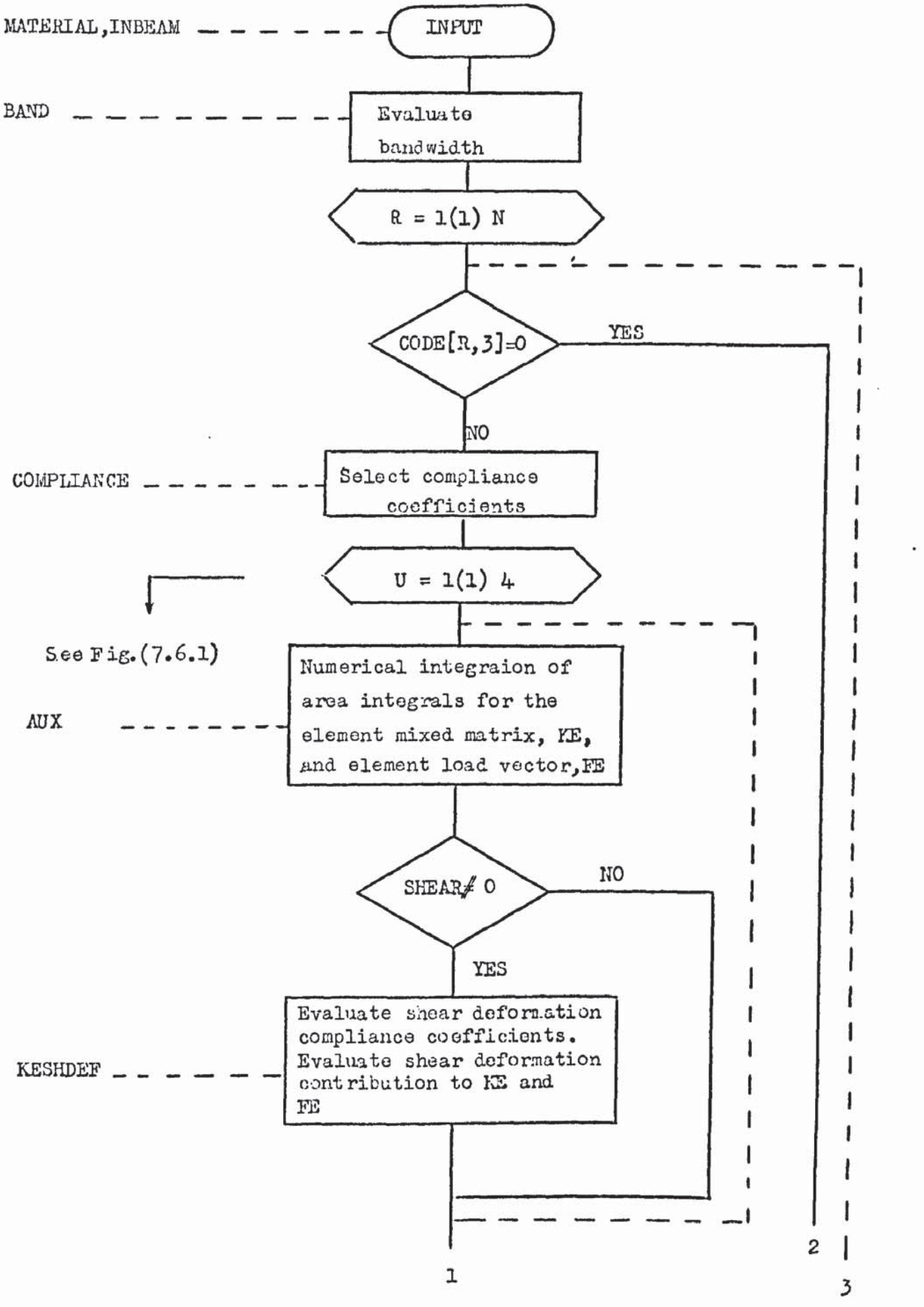

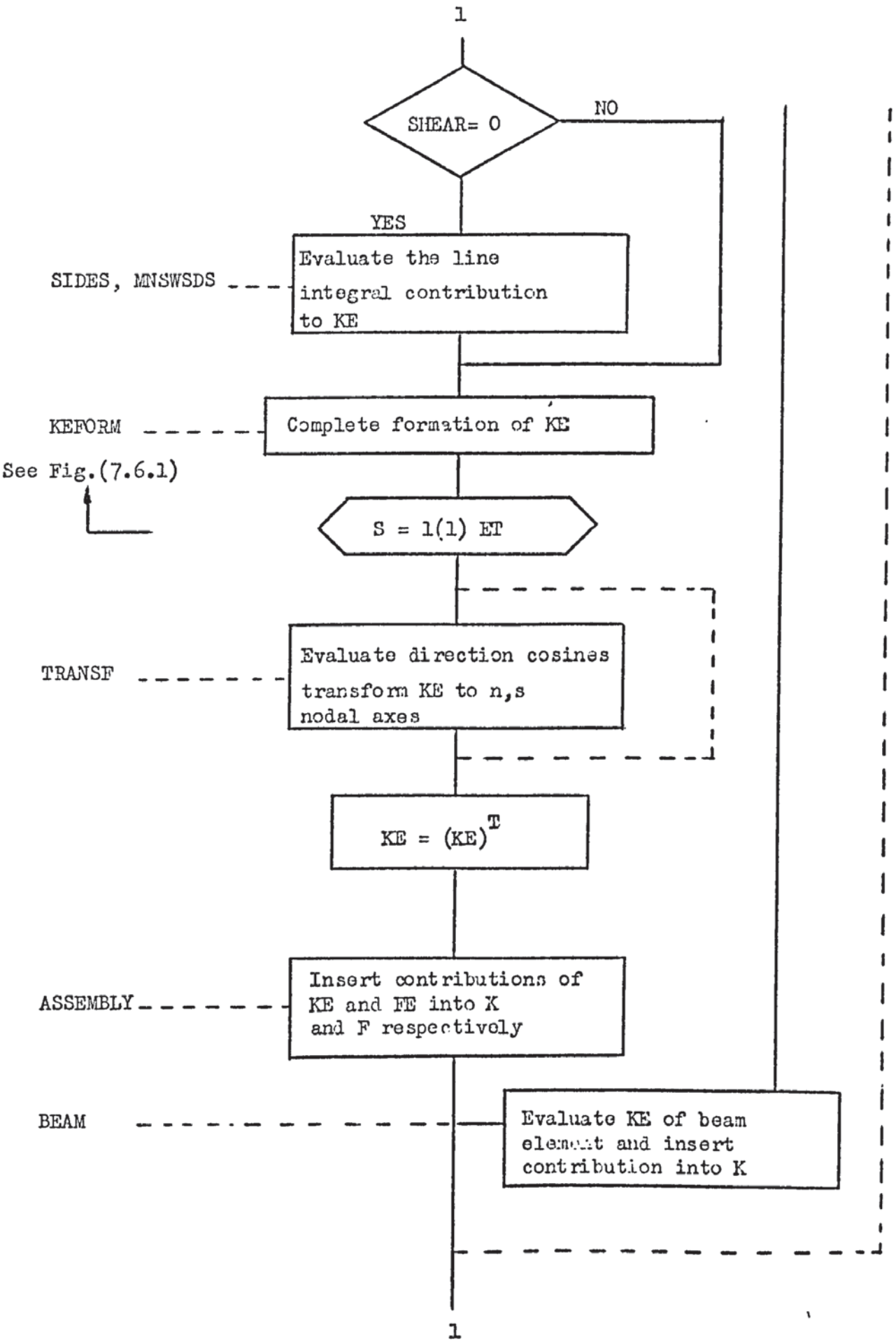
1
SHEAR= 0
NO
YES
SIDES, MNSWSDS
Evaluate the line integral contribution to KE
KEFORM
Complete formation of KE
See Fig.(7.6.1)
S = 1(1) ET
TRANSF
Evaluate direction cosines transform KE to n,s nodal axes
KE = (KE)^T
ASSEMBLY
Insert contributions of KE and FE into K and F respectively
BEAM
Evaluate KE of beam element and insert contribution into K
1

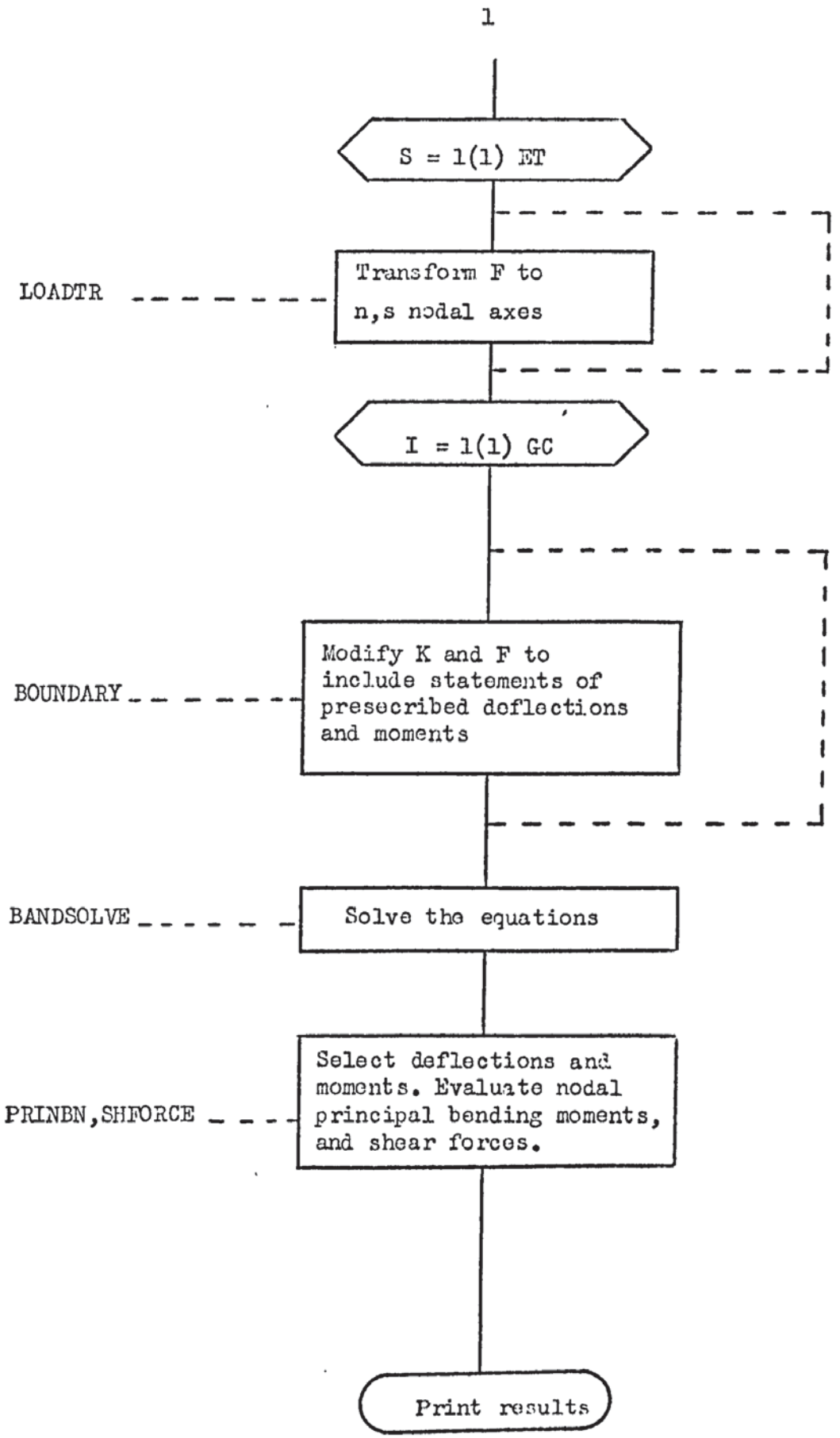
1
S = 1(1) ET
LOADTR
Transform F to n,s nodal axes
I = 1(1) GC
BOUNDARY
Modify K and F to include statements of presecribed deflections and moments
BANDSOLVE
Solve the equations
PRINBN,SHFORCE
Select deflections and moments. Evaluate nodal principal bending moments, and shear forces.
Print results

7.14) The Input Data.

In this section the input data is described. A simplified flow chart Fig.(7.14.1) will be given as a guide to input data, and the detailed flow charts for the procedure. Material and INBEAM, Fig.(7.14.2), (7.14.3), which contain data to be input are also explained. At the end of the section two specific examples will be given to act as a guide to data preparation should this guide be required.

7.14.1) Description of the Input Data.

a) Control Data.

The variables which need to be read in, in the correct order of the flow diagram of Fig.(7.14.1), can be defined as:

Variable	Type	Description
NSETS	(I)	The number of plates to be analysed in a run
SHEAR	(I)	Defines if a set of data is going to be analysed as a "thin" or "moderately" thick plate 0 for "thin plates" 1 for "moderately" thick plate
MTYPE	(I)	Defines if the plate is isotropic or orthotropic 1 for isotropic plates 2 for orthotropic plates
THTYPE	(I)	This variable is related to the type of thickness of the plate 1 thickness constant all over 12 thickness constant within each element 2 thickness varying all over the plate

a) contd.

TYLOAD	(I)	The type of loading 1 for uniform load or/and concentrated loads 2 varying load all over the plate, with or without concentrated loads
NMAT	(I)	Number of different materials of which the plate is formed. To each different material should correspond at least one element.
NB	(I)	Defines if the program is being used for the solution of a beam problem. 0 for plates 1 for beams alone or for testing reinforced plates
NII	(I)	Total number of beam elements involved in the analysi, if any.
N	(I)	Total number of elements
GG	(I)	Total number of nodes
ET	(I)	Total number of nodes whose d.o.f. require transformation for the imposition of the boundary conditions in terms of normal components 0 when no transformation is required
GC	(I)	Total number of specified boundary conditions (i.e. deflections plus bending and twisting momonts)

b) Applied Distributed Load.

Following the inputed control data, we require to read in the values of the applied distributed load. If the control variable TYLOAD=1, then the unique value of the real variable UQ, representing the constant pressure distribution all

Fig.(7.14.1) Flow chart for the input data

a) Control data

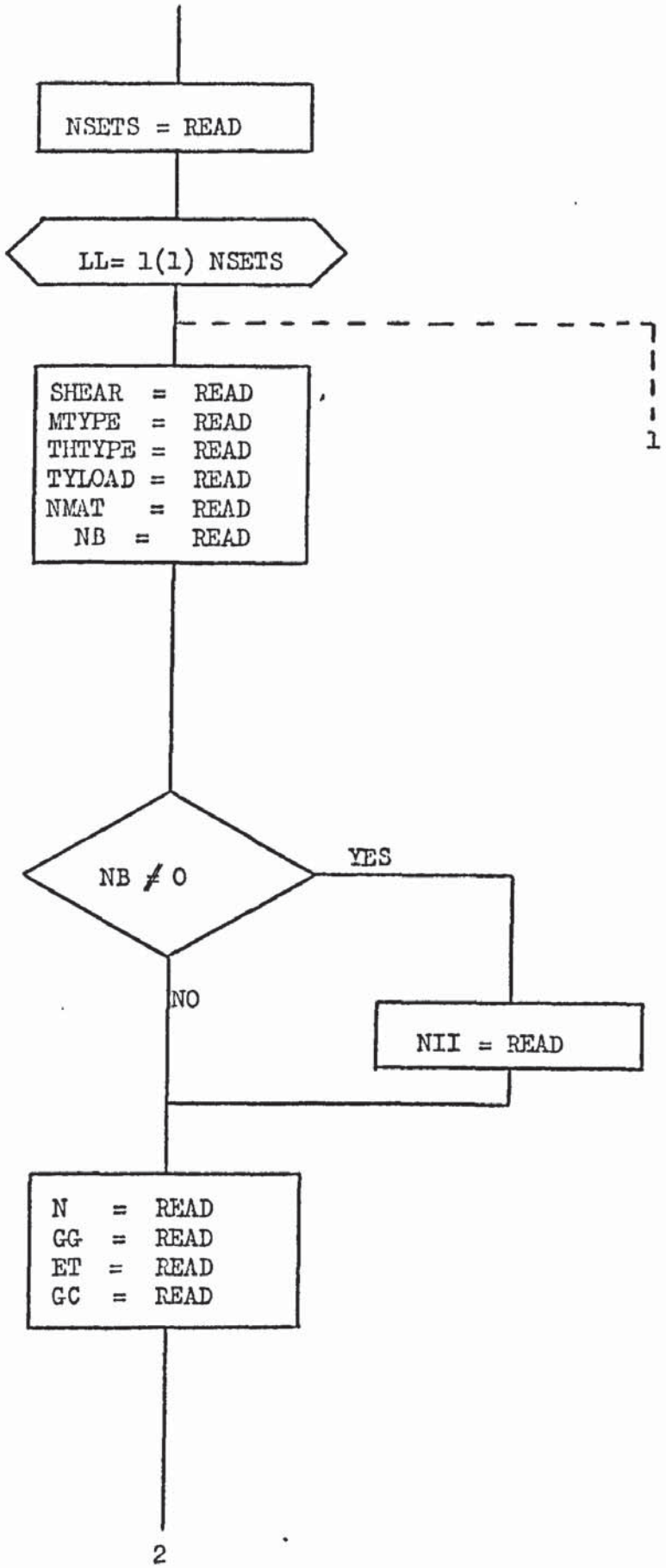

2

b) Applied distributed load

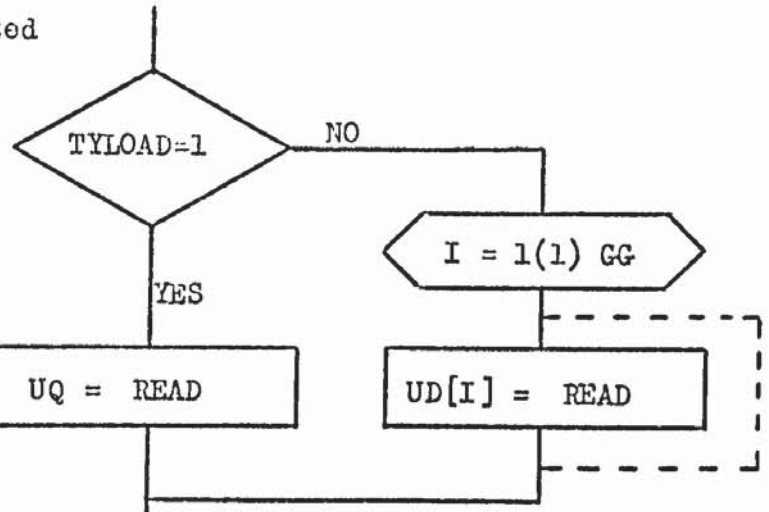

c) Thickness variation

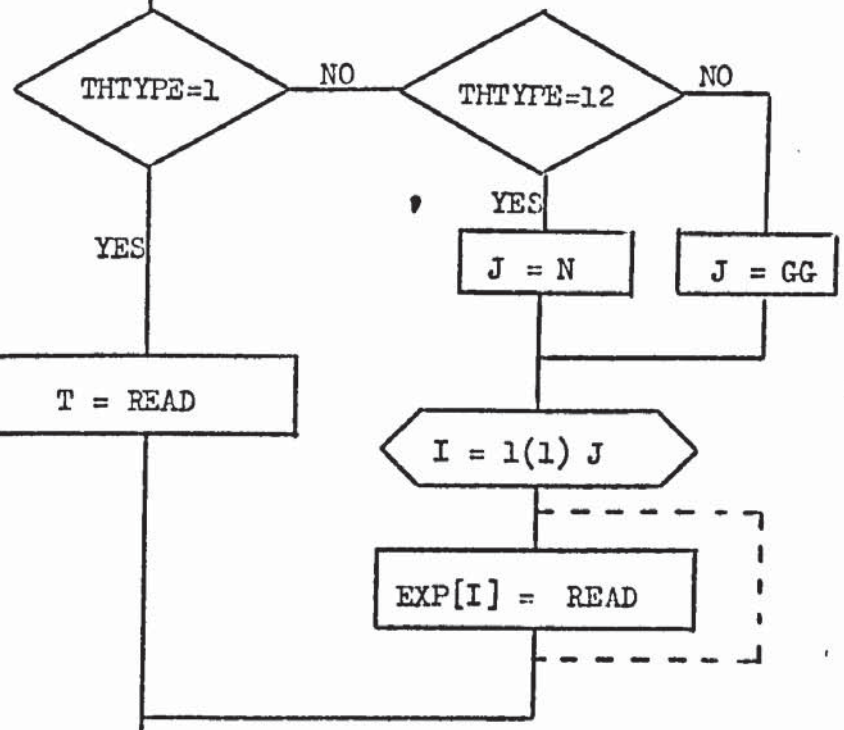

d) Material properties Group identification

MATERIAL(N,MTYPE,NMAT,E,EMAT,CC, THTYPE, SHEAR)
See flow diagram of Fig.(7.14.2).

e) Beam element geometry Group identification

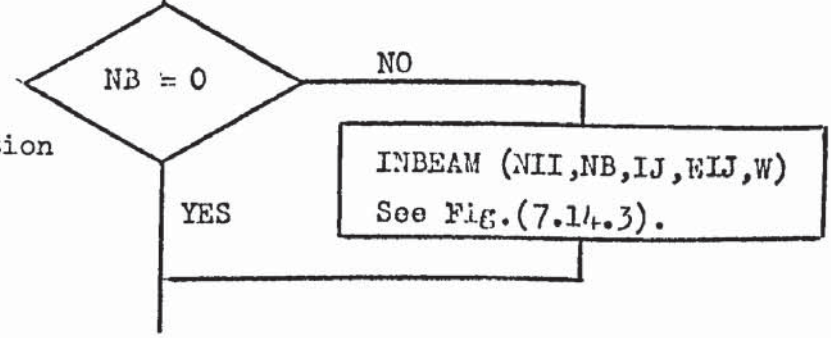

2

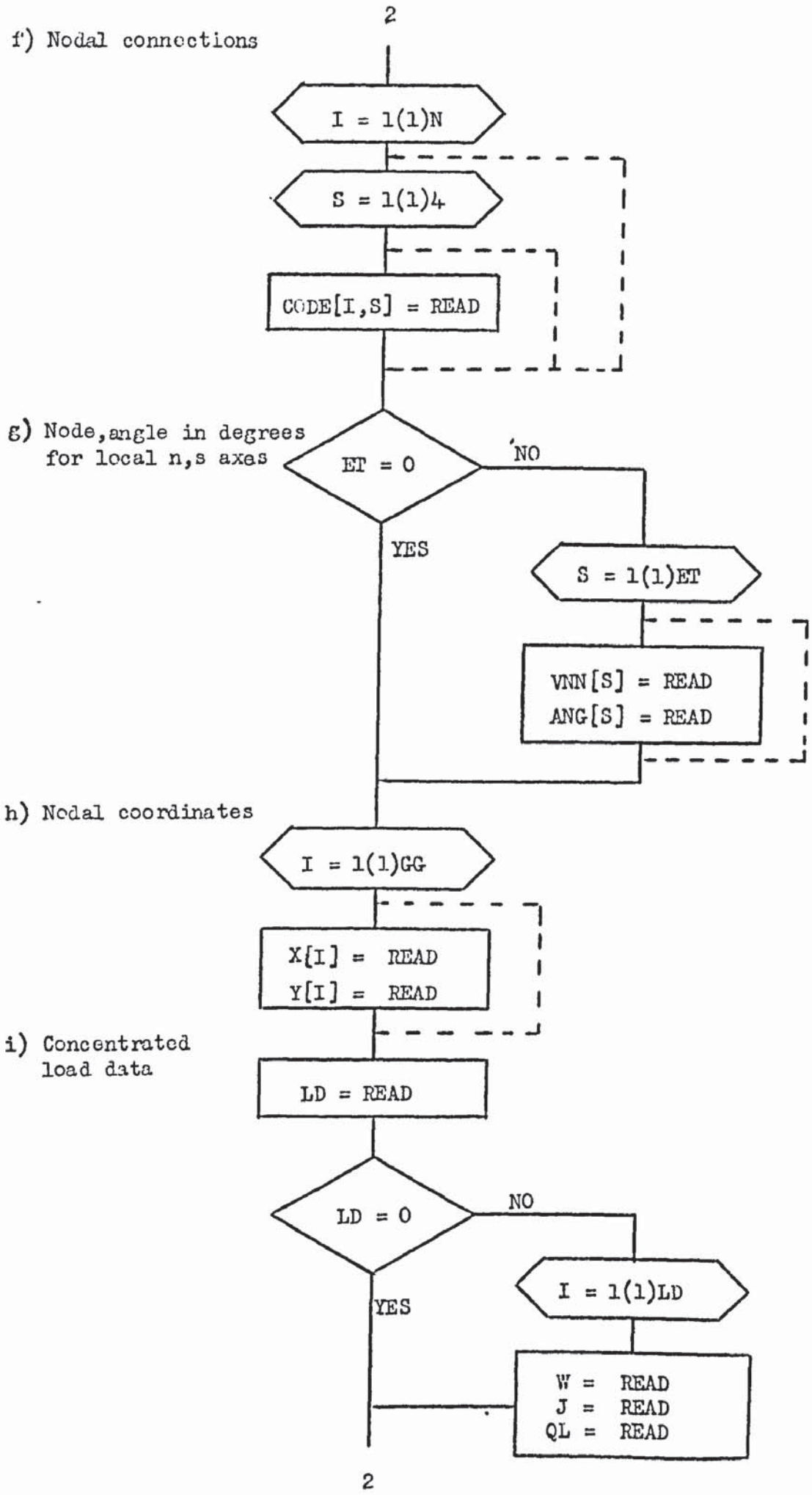
2
f) Nodal connections
I = 1(1)N
S = 1(1)4
CODE[I,S] = READ
g) Node,angle in degrees for local n,s axes
ET = 0
NO
YES
S = 1(1)ET
VNN[S] = READ
ANG[S] = READ
h) Nodal coordinates
I = 1(1)GG
X[I] = READ
Y[I] = READ
i) Concentrated load data
LD = READ
LD = 0
NO
YES
I = 1(1)LD
W = READ
J = READ
QL = READ
2

j) Specified boundary conditions

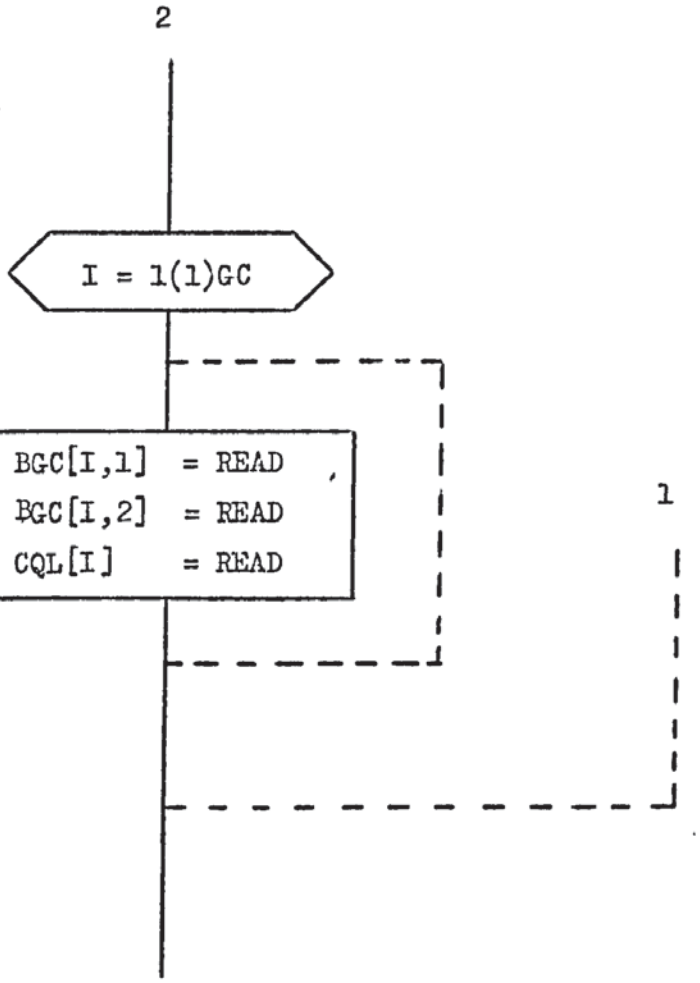

b) contd.

over the plate is inputed.

For a varying pressure, all over the plate, the real array UDL [I], for I:=1,2,... GG, where GG is the control variable which represents the total number of nodes, reads in the nodal values of the varying pressure.

c) Thickness Variation.

For plates with uniform thickness, THYTYPE = 1, the only value required to be inputed is the one corresponding to the real variable T, which represents the constant thickness of the plate.

If THTYPE = 12, the values of the element thicknesses are inputed through the real array ESP [I], for element, I = 1,2, ...N, where N is the total number of elements. It corresponds to a plate having each element with a constant thickness.

Finally, if THTYPE=2, the thickness is assumed to change all over the plate, thus the array ESP [I] now reads in the nodal thicknesses, for node I:=1,2,3 ... GG, where GG is the control variable, representing the total number of nodes.

d) Material Properties and Group Identification.

In order to reduce input data, the material properties are inputed only for each set of elements of different material.

For thin isotropic plates, SHEAR=0, MTYPE=1, we need to read in for each set, the numerical values of the material constants

$$E \ , \ \mu$$

For thin orthotropic plates, SHEAR=0, MTYPE=2, we require

d) contd.

respectively

$$E_x \ , \ E_y \ , \ \frac{E_y}{\mu_{yx}} \ , \ G_{xy}$$

For moderately thick isotropic plates, SHEAR=1, MTYPE=1 and the input is:

$$E \ , \ \mu$$

For moderately thick orthotropic plates, SHEAR=1, MTYPE 2, we require

$$E_x, \ E_y, \ \frac{E_y}{\mu_{yx}}, \ G_{xy}, \ \frac{E_z}{\mu_{zx}} \ , \ \frac{E_z}{\mu_{zy}} \ , \ G_{xz}, \ G_{yz}$$

It may well happen that we need to read in directly the compliance coefficients, as in the case of the study of rectangular plates reinforced with many equidistant stiffness in one or two mutually perpendicular directions, by the equivalent orthotropic plate method [10],[20]. Then, for thin plates, SHEAR=0, THTYPE=1, MTYPE=2, and the required data is:

$$C_{11}, \ C_{22}, C_{12}, \ C_{33},$$

for the moderately thick case, SHEAR=1, THTYPE=1 and MTYPE=2 the input data required is:

$$C_{11}, C_{22}, C_{12}, C_{33}, \ \frac{12\mu_{zx}}{E_z h^3} \ , \ \frac{12\mu_{zy}}{E_z h^3} \ , \ \frac{12}{G_{xz} h^3}, \ \frac{12}{G_{yz} h^3}$$

where $C_{11}, C_{22}, C_{12}, C_{33}$ are the equivalent compliance coefficients.

The procedure MATERIAL, flow diagram of Fig.(7.14.2), where the involved variables are:

(d) contd.

N	(I)	Total number of elements
M	(I)	Material type, already described
NM	(I)	Total number of different materials
E	(RA)	Material properties array
EM	(IA)	Array with identification of groups of different material
C	(RA)	Array with coefficients of material properties ready to be accepted by procedure COMPLIANCE
TT	(I)	Type of thickness, already described
SHEAR	(I)	Already defined,

reads in the material constants and the sets of identification numbers, for the different types of material.

The real array E [I,S] reads in the values of the material parameters, in the form just described for I = 1,2,...NM, the dummy variable S depends on the control variables SHEAR and M. The integer array EM [I], for I = 1,2 ... N, where N = total number of elements reads in the group identification number of the elements. As an example regarding the input procedure MATERIAL, consider Fig.(7.2.1a) as a thin orthotropic plate, made of two different materials, where the elements 1,2,7,8 and 3,4,5,6 have different properties. The read-in should then proceed with the numerical values of the material constants and identification code as follows:

E_x, E_y, $\frac{E_y}{\mu_{yx}}$, G_{xy} (1st set)

E_x', E_y', $\frac{E_y'}{\mu_{yx}}$, G_{xy}' (2nd set)

} Array E

1,1,2,2,2,2,1,1 - Array EM

If beam elements are also involved in the structure,

Fig.(7.14.2) Flow diagram for procedure MATERIAL

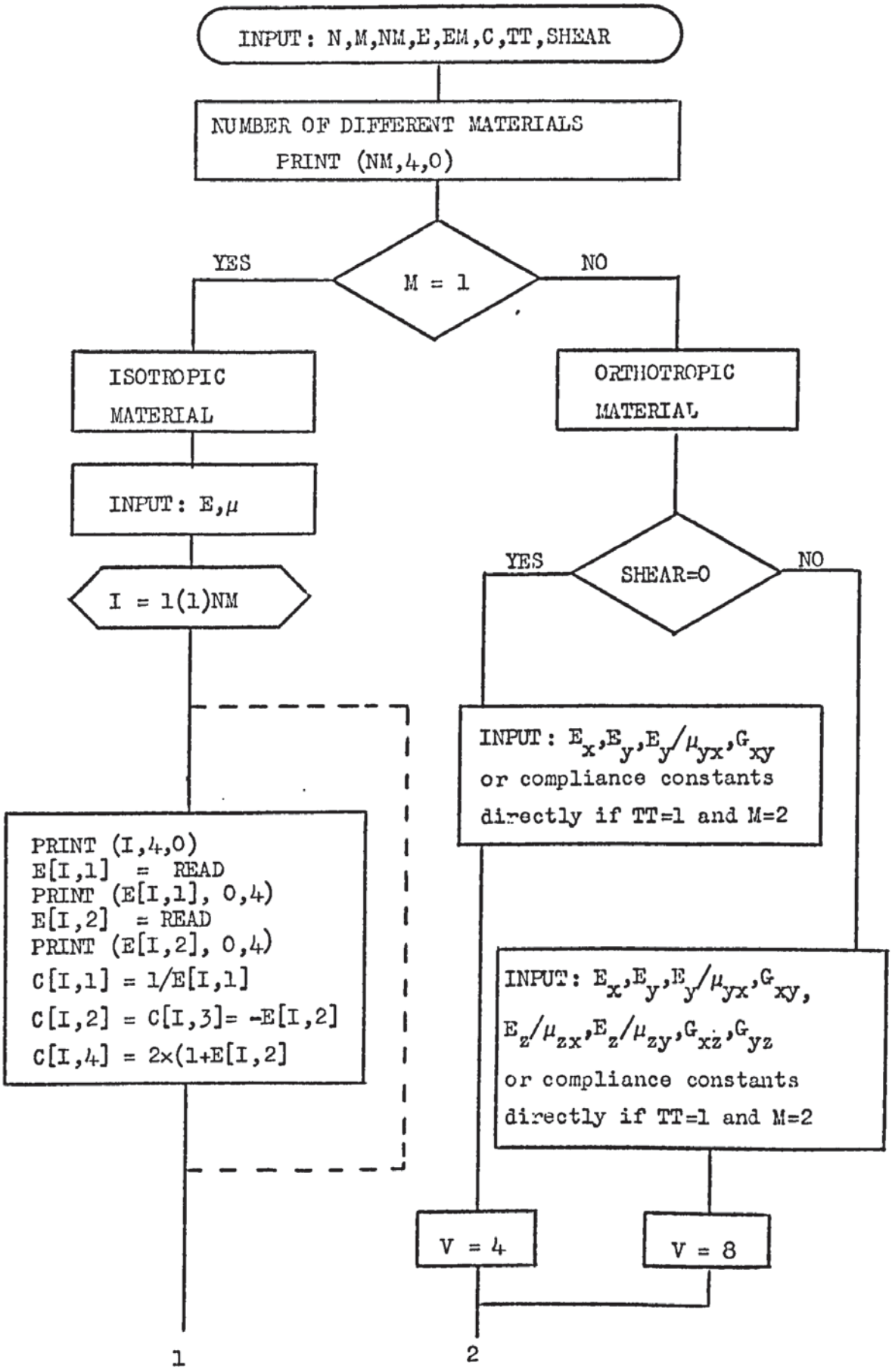

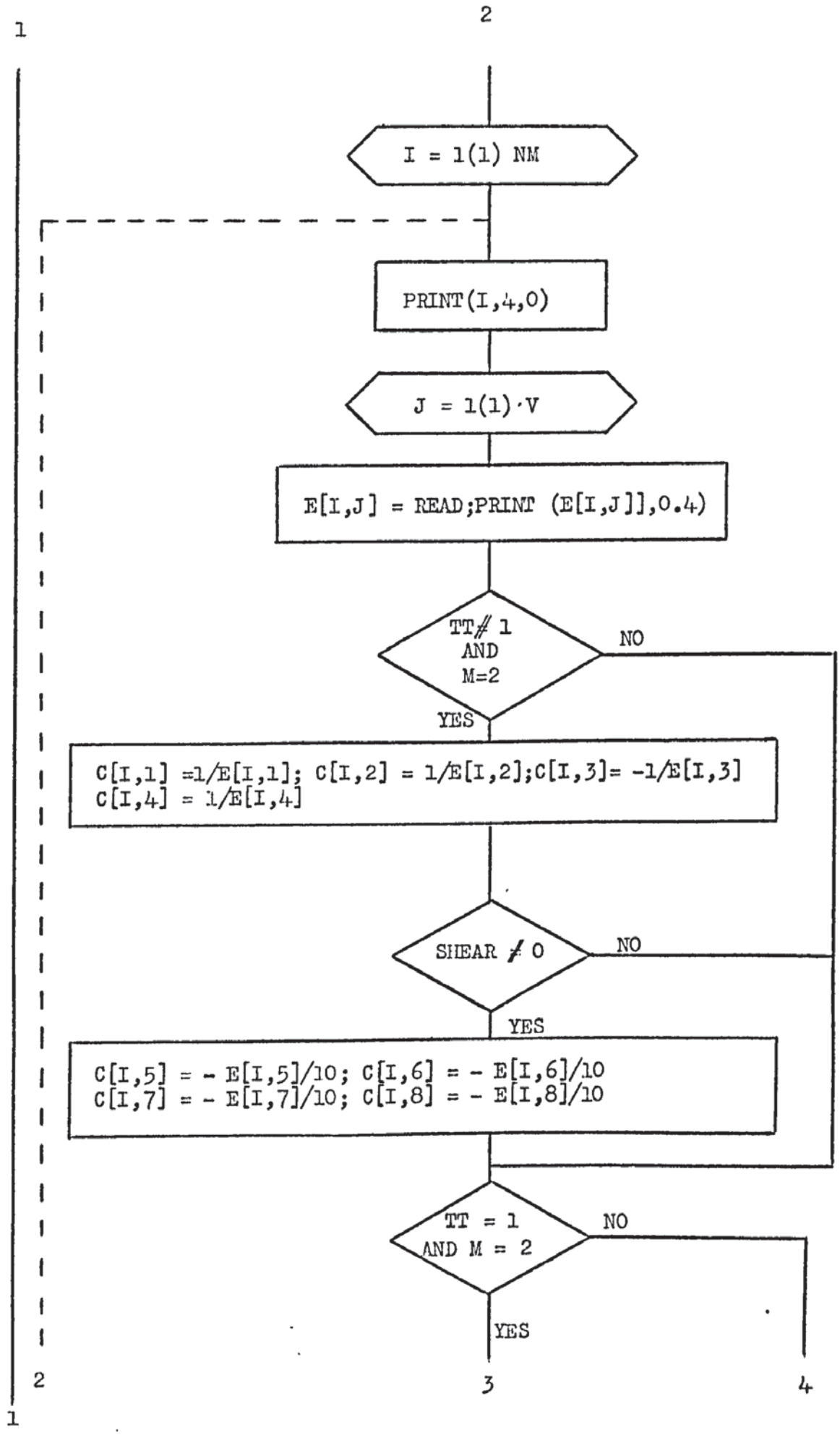
1
2
I = 1(1) NM
PRINT(I,4,0)
J = 1(1)·V
E[I,J] = READ;PRINT (E[I,J]],0.4)
TT≠ 1
AND
M=2
NO
YES
C[I,1] =1/E[I,1]; C[I,2] = 1/E[I,2];C[I,3]= -1/E[I,3]
C[I,4] = 1/E[I,4]
SHEAR ≠ 0
NO
YES
C[I,5] = - E[I,5]/10; C[I,6] = - E[I,6]/10
C[I,7] = - E[I,7]/10; C[I,8] = - E[I,8]/10
TT = 1
AND M = 2
NO
YES
2
3
4
1

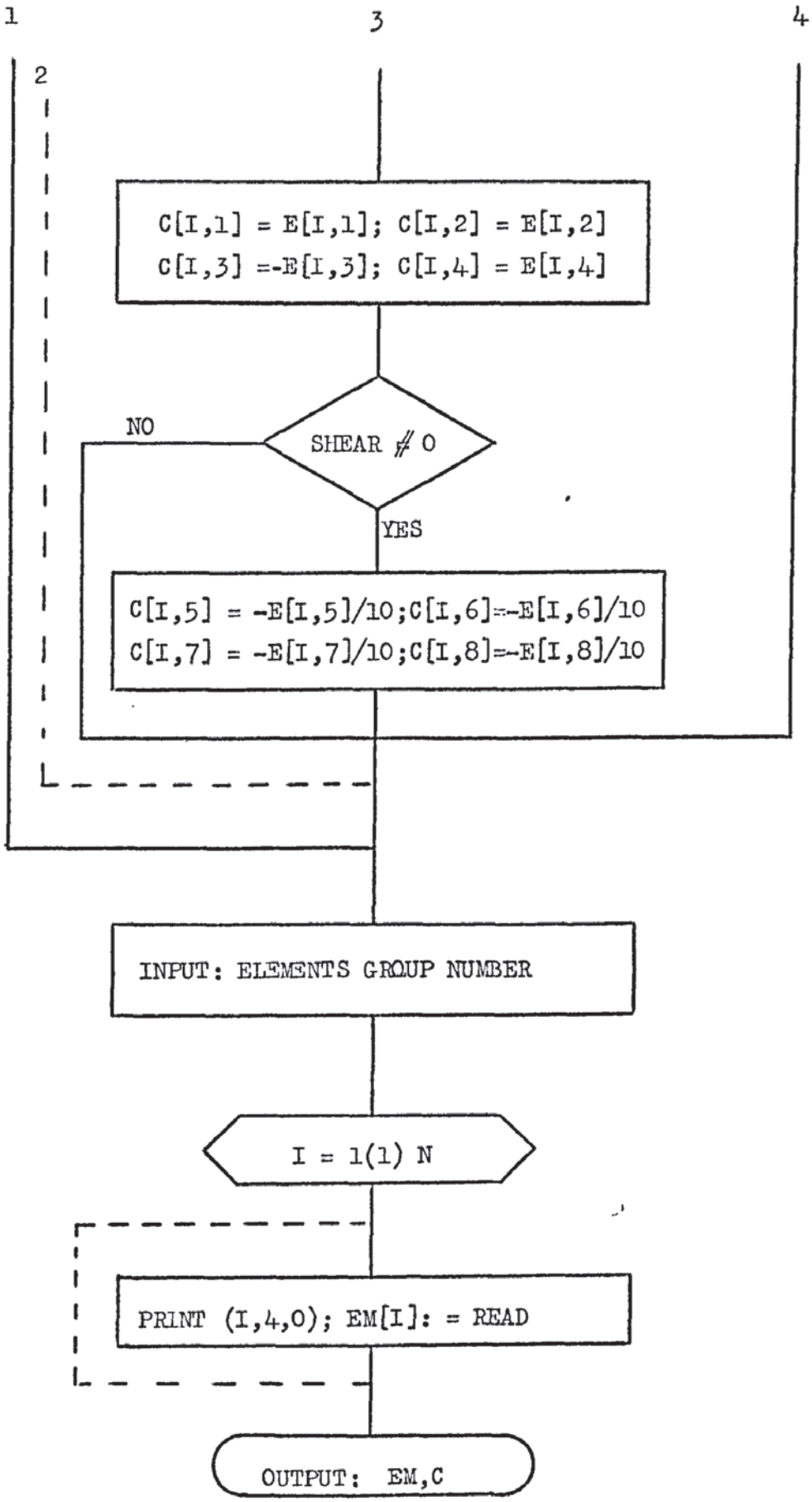
1
3
4
2
C[I,1] = E[I,1]; C[I,2] = E[I,2]
C[I,3] =-E[I,3]; C[I,4] = E[I,4]
NO
SHEAR ≠ 0
YES
C[I,5] = -E[I,5]/10;C[I,6]=-E[I,6]/10
C[I,7] = -E[I,7]/10;C[I,8]=-E[I,8]/10
INPUT: ELEMENTS GROUP NUMBER
I = 1(1) N
PRINT (I,4,0); EM[I]: = READ
OUTPUT: EM,C

d) contd.

the value of the Young's modulus for the sets of beam elements having different material properties are inputed using the procedure MATERIAL, as they were plate material parameters. That is, to the first coefficient of the array E is assigned the value of the Young's modulus and the remaining coefficients are set to any values, because they are not required.

e) Beam Element Geometry and Group Identification.

A procedure INBEAM, described by the flow diagram of Fig.(7.14.3),was developed to provide the input of the geometric beam data. The variables involved in this procedure are:

Z	(I)	Total number of different geometric properties
G	(I)	Total number of beam elements
IJ	(RA)	2nd moment of area, and overall length of the beam (for the testing of reinforced plates or 1.0 (for the solution of beam problems).
T	(IA)	Group type array
W	(I)	Beam element global number

The input for this procedure can be illustrated by considering the example of Fig.(7.14.4).

If Fig.(7.14.4) is part of a reinforced plate being tested, the input required is:

0.5 , 200 (1st group)

1.0 , 200 (2nd group)

1,1 , 2,2 3,1

3,1: 3 = element global number; 1 = group number

For the solution of a beam problem alone, the

Fig.(7.14.3) Flow diagram for procedure INBEAM

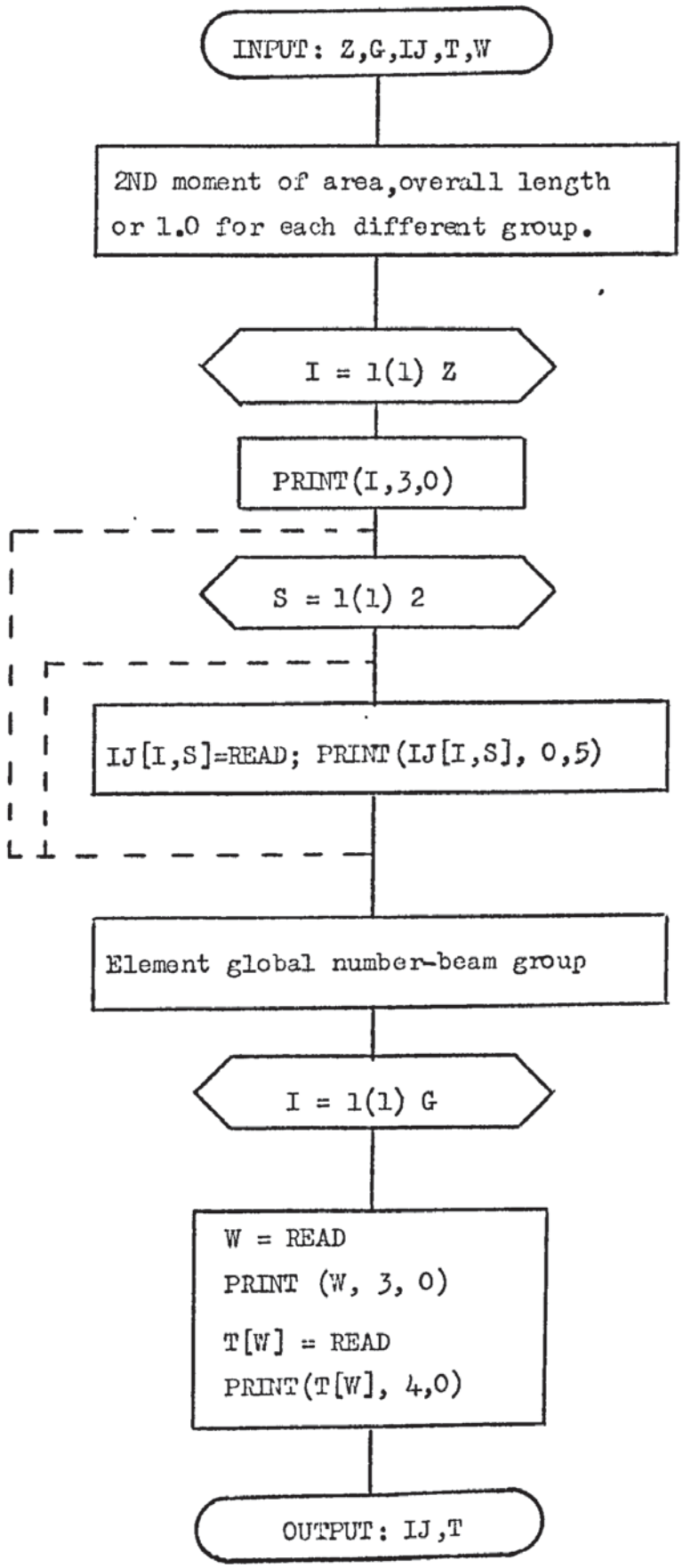

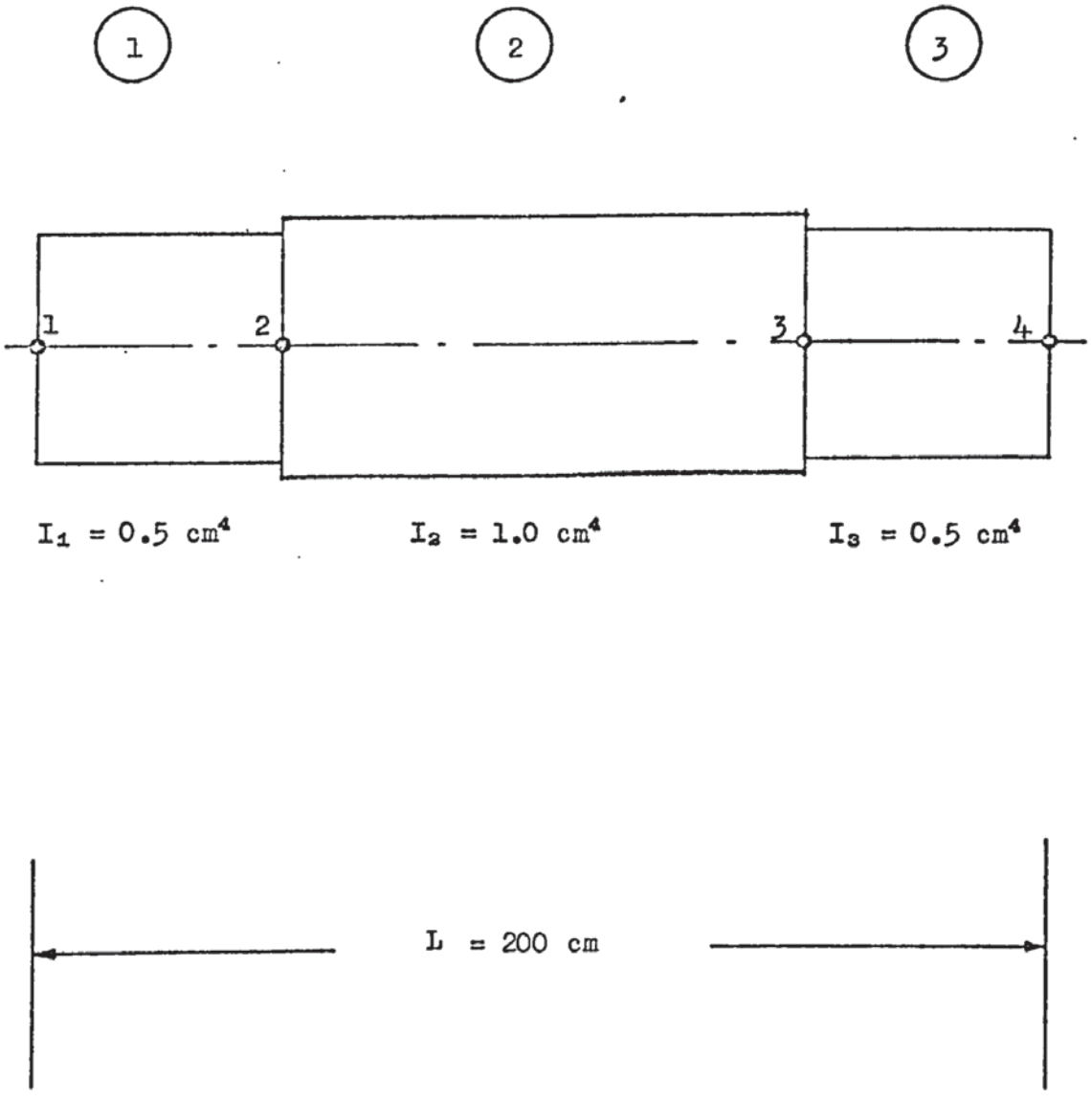

Fig.(7.14.4) Finite element coarse representation of a beam.

g) contd.

input required is:

0.5 , 1.0

1.0 , 1.0

1,1 2,2 3,1

f) Nodal Connections.

The nodal connections are represented by the integer array CODE [I,S], for I = 1,2, ...N and S = 1,2,3,4 where N is the control variable representing the total number of elements, including beam elements, and S represents the local node number of the element concerned. Forexample for Fig.(7.2.1a) the nodal connections should be read in as follows:

1,4,5,2 4,7,8,5 7,10,11,8 10,13,14,11

2,5,6,3 5,8,9,6 8,11,12,9 11,14,15,12

If there are beam elements, the nodal connections corresponding to S = 3,4 are read in as zeros.

g) Node and Angle for Local n,s Axes Transformation.

If the control variable ET $\neq$ 0, then, it is required to input the node number and the angle corresponding to the local normal axis. The angle is the one defined by the chosen normal n and the x axis, measured in degrees for the node concerned. The integer array representing the nodes requiring transformation is VNN[S], and the angle is represented by the real array ANG[S], for S = 1,2, ... ET.

h) Nodal Coordinates.

The nodal Cartesian coordinates are represented by the real arrays X,Y [I] for nodes I = 1,2, ... GG, in which GG is the control variable representing the total number of nodes.

i) Concentrated Load Data.

The value assigned to the integer LD, represents the number of concentrated quantities, which required to be added to the load vector. It needs to be read in always, whether there are concentrated loads or not; if there are not concentrated quantities LD is inputed as zero, else LD is the number of concentrated loads to be read in. The variables involved in the inputing are the identification integer W,J, and the real variable QL, representing the loaded quantity. The integer W is equivalent to I, in relation (7.2.1) and I represents the global node number. Thus, the sequence for inputing is: d.o.F. identification integer, node, value of the concentrated quantity for I = 1,2, ... LD. For example, taking the plate of Fig.(7.2.1a) with a concentrated load, say, P = 1.0 KN at node 8, the read-in should be:

LD	W , J , QL
1	3 , 8 , 1.0

j) Specified Boundary Conditions.

The number of imposed boundary conditions is controlled by the integer GC. The input is done through the integer array BGC [I,1], BGC [I,2] for I = 1,2, ... GC, and the real array C Q L [I] for I = 1,2, ... GC.

The array BGC [I,1] stores the degrees of freddom identification, in accordance with equation (7.2.1). This is:

3 for deflection W

2 for bending moment M_x or M_s

1 for bending moment M_y or M_n

0 for bending moment M_{xy} or M_{ns}

The column BGC [I,2] stores the global node number.

j) contd.

The array CQL [I], stores the value of the imposed deflections or moments. The correct order to input is then:

d.o.f. identification, global node number, value of the imposed boundary condition.

A listing of the complete program is given in Appendix 4.

7.14.2 Samples of Input Data.

a) 1st Sample
The problem.

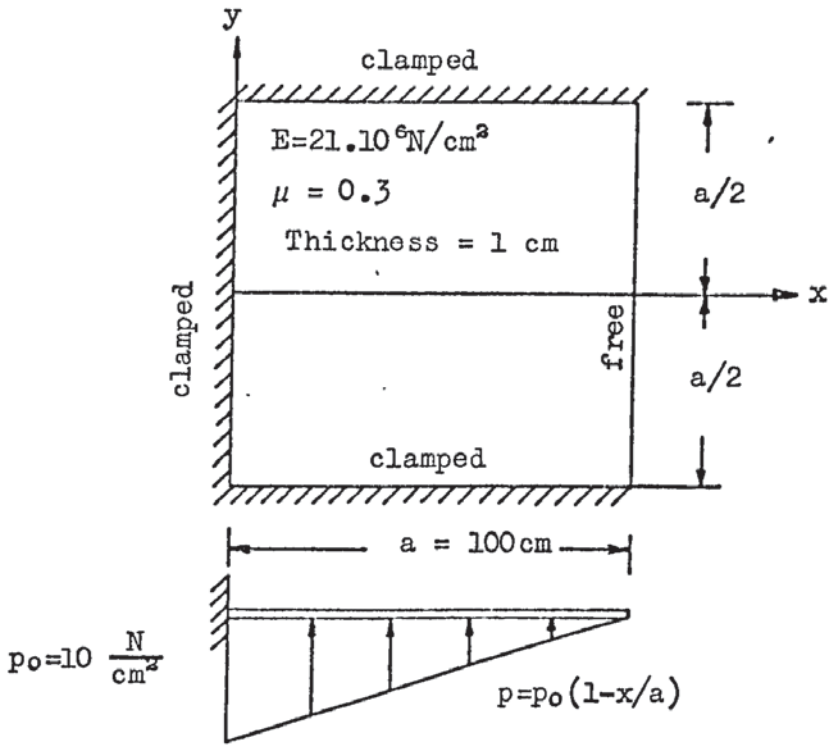

The discretized plate.

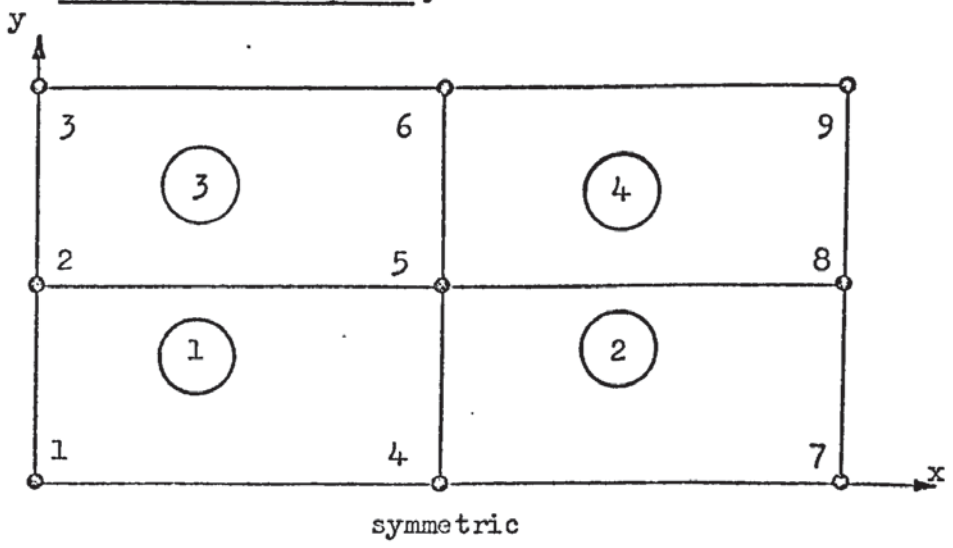

Due to symmetry only half of the plate is required.

The Input data

```
    1
    0    1    1    1    1    0+   4    9    0    11
 10.0  10.0  10.0  5.0  5.0  5.0  0.0  0.0  0.0
  1.0
  21 000 000      0.3
    1    1    1    1
  1   4    5    2      4    7    8    5      2    5    6    3
  5   8    9    6
  0.0   0.0      0.0     25.0     0.0      50.0
  50.0  0.0      50.0    25.0     50.0     50.0
 100.0  0.0     100.0    25.0    100.0     50.0
  0
  0    1   0.0        0    4   0.0        0    7   0.0
  2    7   0.0        2    8   0.0        2    9   0.0
  3    1   0.0        3    2   0.0        3    3   0.0
  3    6   0.0        3    9   0.0                   .
```

+Note: This zero refers to absence of any reinforcing beam

b) 2nd Sample

The problem.

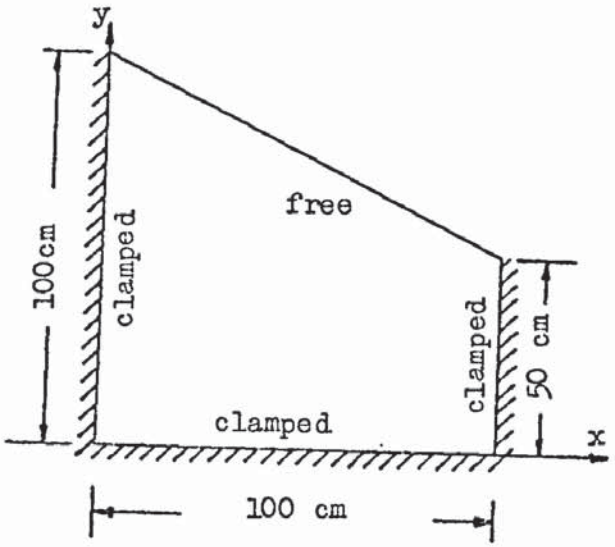

$E_x = 21.10^6$ N/cm²
$E_y = 4.10^6$ N/cm²
$\frac{E_y}{\mu_{yx}} = 70.10^6$ N/cm²
$G_{xy} = 7.10^6$ N/cm²
p = constant = 10 N/cm²
P = 500 N at { x = 50 cm, y = 30 cm
h = constant = 1 cm

The discretized plate.

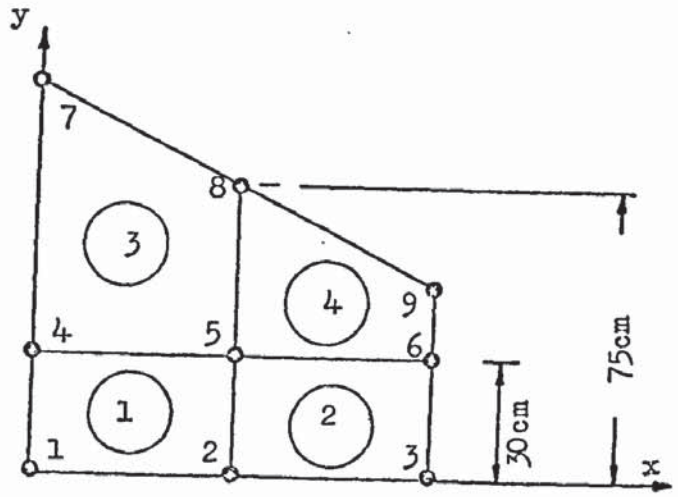

The input data.

```
1
0    2    1    1    1    0+    4    9    3    10
10.0
 1.0
```

```
21000 000.0          4000 000.0          70000 000.0
 7000 000.0
   1     1     1     1
   1  2  5  4          2  3  6  5          4  5  8  7
   5  6  9  8
   7   45.0             8   45.0             9   45.0
 0.0    0.0           50.0    0.0          100.0    0.0
 0.0   30.0           50.0   30.0          100.0   30.0
 0.0  100.0           50.0   75.0          100.0   50.0
   1       3        5       500.0

   1     7   0.0          1     8     0.0          1     9     0.0
 3   1   0.0          3   2   0.0                3   3   0.0
 3   4   0.0          3   6   0.0                3   7   0.0
 3   9   0.0
```

+Note: This zero refers to absence of any reinforcing beam

CHAPTER 8

DEVELOPMENT OF THE COMPUTER PROGRAM FOR VIBRATION AND BUCKLING PROBLEMS

8.1) Introduction.

The mathematical model of the mixed finite element method described in Chapter 6, for the analysis of free vibrations and buckling was written in the form of a test program based on the "Static" main program developed in Chapter 7. The treatment of the eigenvalue problems in this Thesis is therefore a by-product of the main static work. If we had wished to reach this stage at the outset, the program, for dynamic and buckling problems, could have been designed more efficiently with regard to computer storage. Since the overall mixed matrix K, and overall consistent mass or initial stress stiffness array MA are assembled in full (square matrices), the treatment of plate problems, using this test program, is limited to systems having no more than (30-40) non-constrained nodes (i.e. nodal points free to move in the z direction) on the available ICL 1904S Computer.

8.2) Rearrangement of the Assembled Overall Arrays K and MA.

The element mixed matrix and element consistent mass matrix or initial stress stiffness matrix were formed as shown in Section (6.2.3), in order to use the coding and assembly facilities developed for the main program. For the solution of the eigenvalue problem, we therefore need to interchange the coefficients of the array K and MA to the partitioning form given by equation (6.2.23). The procedure INTERCHANGE (K,M.IN,N), flow diagram of Fig.(8.2.1), was written to carry out the required manipulation. The variables related with this procedure are:

K	(RA)	Overall mixed array
M	(RA)	Overall consistent mass or initial stiffness array
IN	(IA)	Degree of freedom address array
N	(I)	Total number of nodes times four minus the total number of boundary conditions

Fig.(8.2.1) Flow diagram of procedure INTERCHANGE

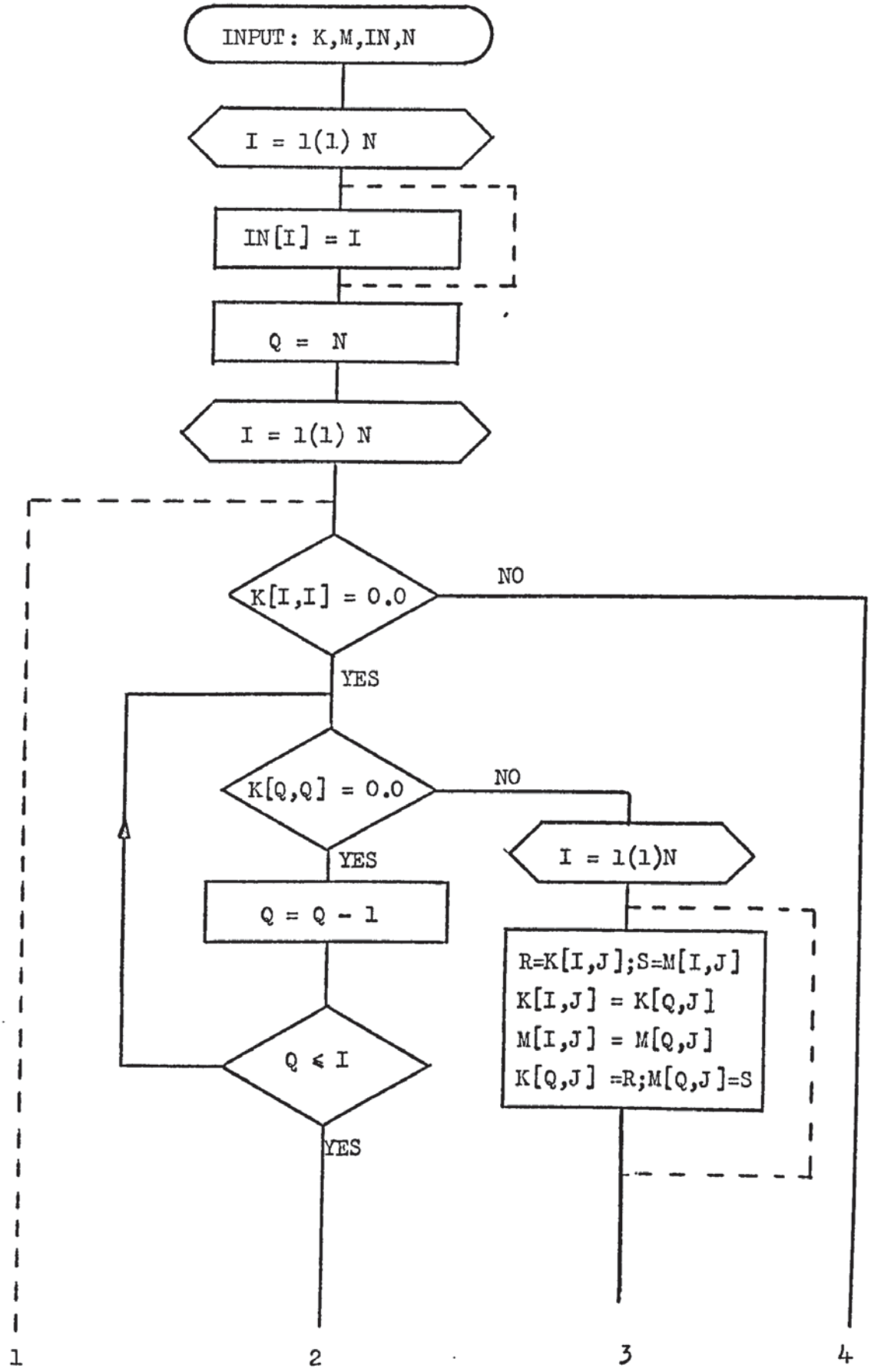

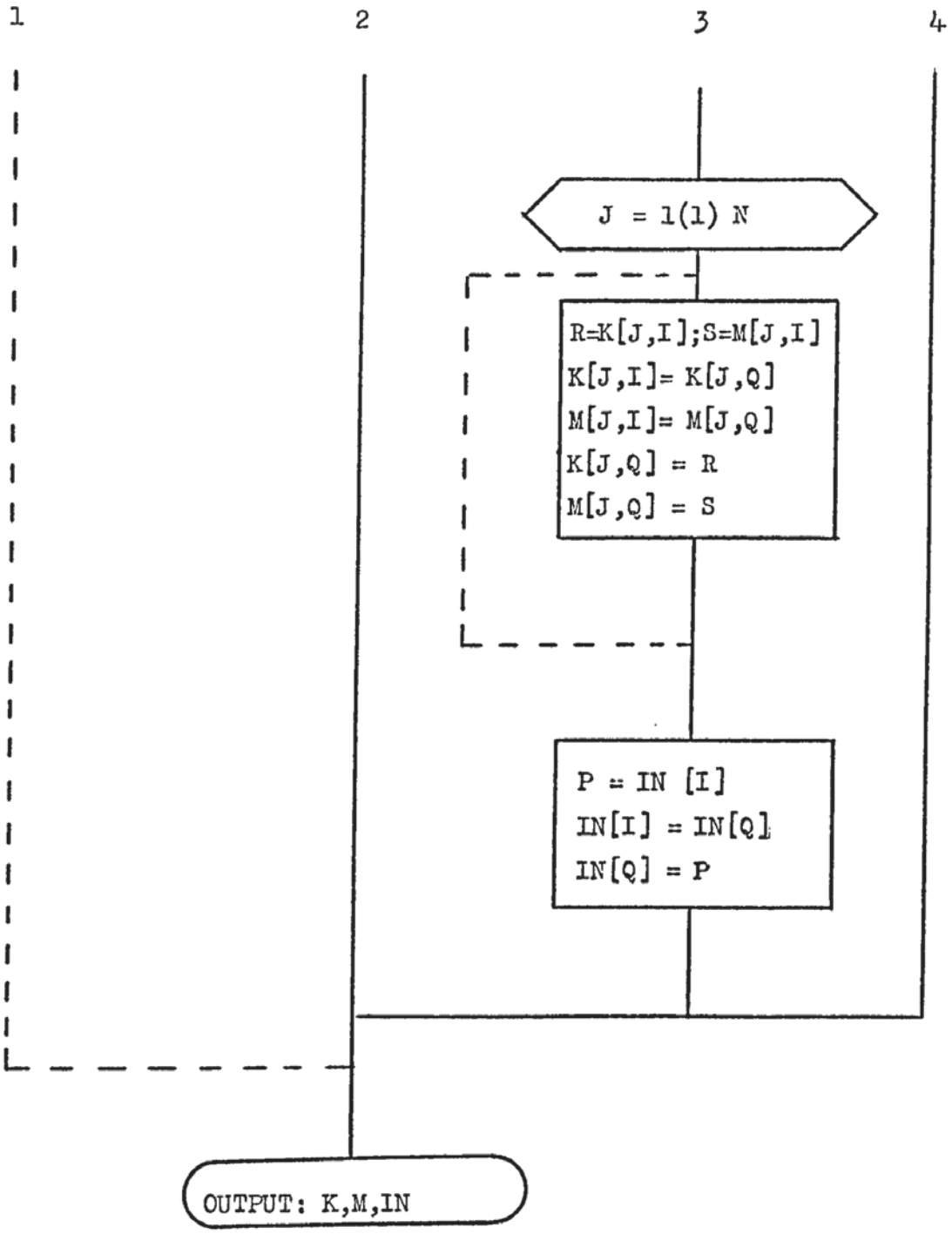
1
2
3
4
J = 1(1) N
R=K[J,I];S=M[J,I]
K[J,I]= K[J,Q]
M[J,I]= M[J,Q]
K[J,Q] = R
M[J,Q] = S
P = IN [I]
IN[I] = IN[Q]
IN[Q] = P
OUTPUT: K,M,IN

8.3) The Elimination of the Nodal Moments Degrees of Freedom.

The procedure INTERCHANGE carried out the rearrangement of the coefficients of the arrays K and MA so as to group nodal moments and nodal translations separately, as shown in equation (6.2.23). Upon elimination of $\{M^*\}$ we get the eigenvalue problem in the form of equation (6.2.27), where

$$[K^*] = [H]^T [G]^{-1} [H]$$

The inversion of [G] is obtained indirectly by the solution of the system:

$$[G] [X] = [H]$$

hence

$$[X] = [G]^{-1} [H]$$

This is carried out by the algorithm EQSOLV developed by Wilkinson [69] for the solution of symmetric positive definite equations by the Cholesky factorization method. The algorithm solves the system of equations [A] [X] = [B] where [A] is a symmetric positive definite matrix of order N × N, and [B] is a N × R matrix of R right end sides. The solution [X] overwrites [B].

The fully populated condensed symmetric positive definite stiffness matrix [K*] is then obtained by executing the product $[H]^T[X]$, i.e.

$$[K^*] = [H]^T[X]$$

8.4) Solution of the Problem.

The standard procedure F02AEA, reference [67], yields the eigenvalues and eigenvectors.

Depending upon the type of problem being solved the relevant information, as developed in Section 6.2.4, for free vibrations and buckling, is selected and outputed.

8.5) The Overall Picture.

A brief description of the "test eigenvalue program" as a whole is given in the form of a flow diagram. The procedures which may be called for some of the operations are mentioned.

The new control variables are:

ZZ	(I)	Counter for the number of iterations in the solution of plastic buckling problems.
BUCK	(I)	Defines the problem: 100 Free vibrations 101 Buckling
PL	(I)	Defines if iterations are required: 0 - Free vibrations and elastic-buckling 1 - Plastic-buckling
AREA	(R)	To this variable is assigned the value of buckling factor, to control the iterations in plastic buckling (see Section 6.2.4).

Fig.(8.5.1) Eigenvalue test program. Simplified flow diagram.

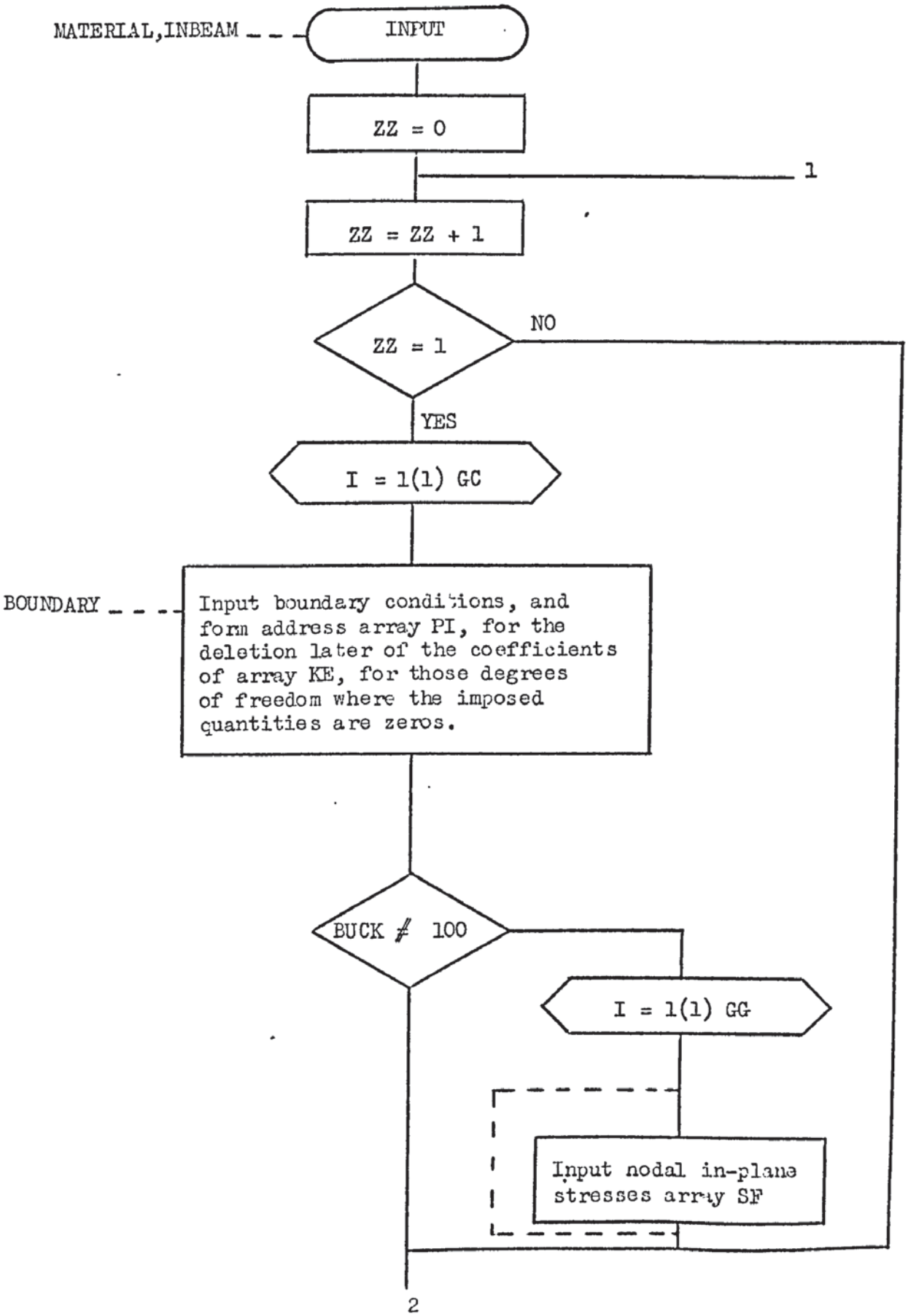

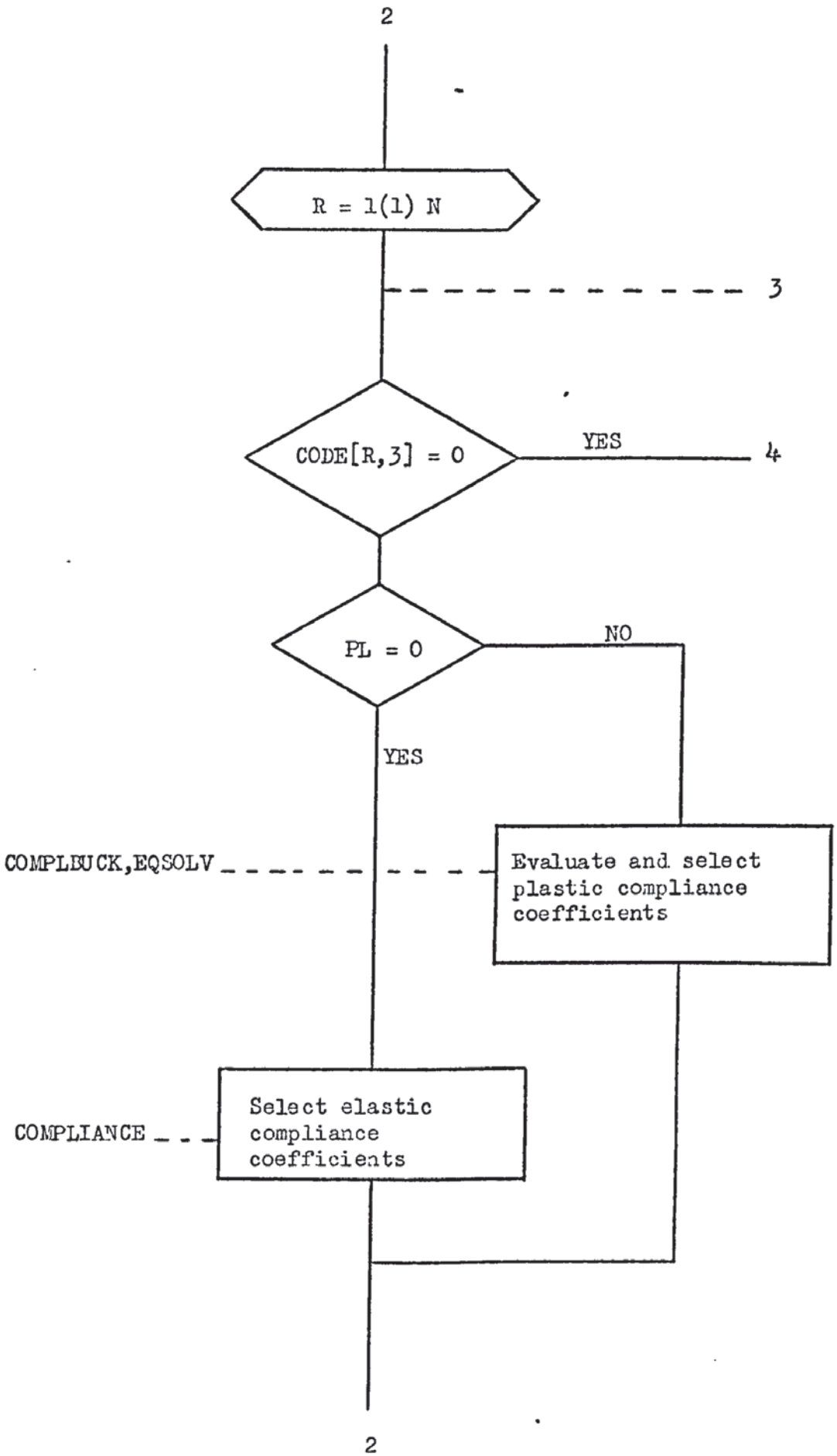
2
R = 1(1) N
3
CODE[R,3] = 0
YES
4
PL = 0
NO
YES
COMPLBUCK,EQSOLV
Evaluate and select plastic compliance coefficients
COMPLIANCE
Select elastic compliance coefficients
2

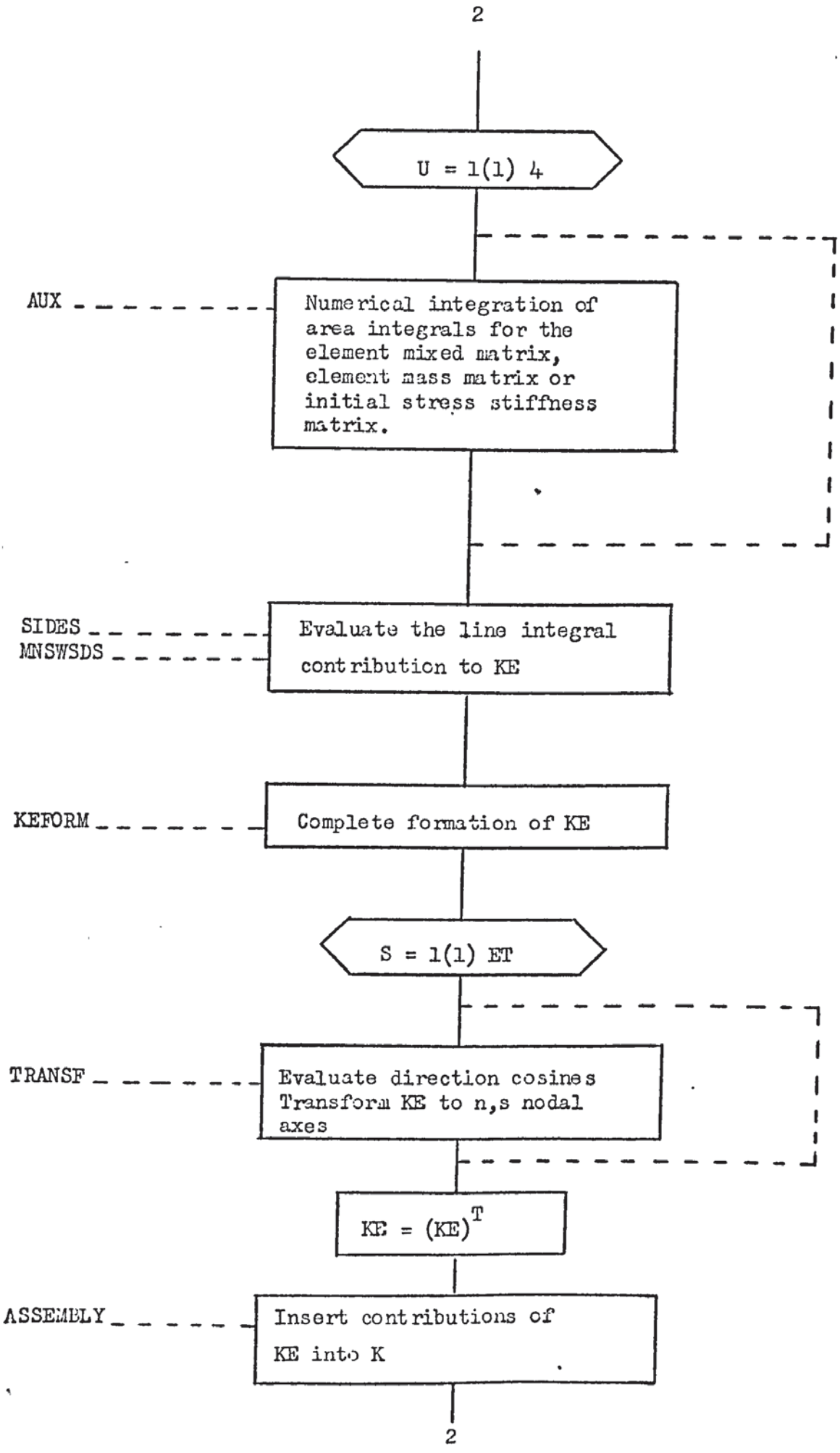
2
U = 1(1) 4
AUX
Numerical integration of area integrals for the element mixed matrix, element mass matrix or initial stress stiffness matrix.
SIDES
MNSWSDS
Evaluate the line integral contribution to KE
KEFORM
Complete formation of KE
S = 1(1) ET
TRANSF
Evaluate direction cosines Transform KE to n,s nodal axes
KE = (KE)^T
ASSEMBLY
Insert contributions of KE into K
2

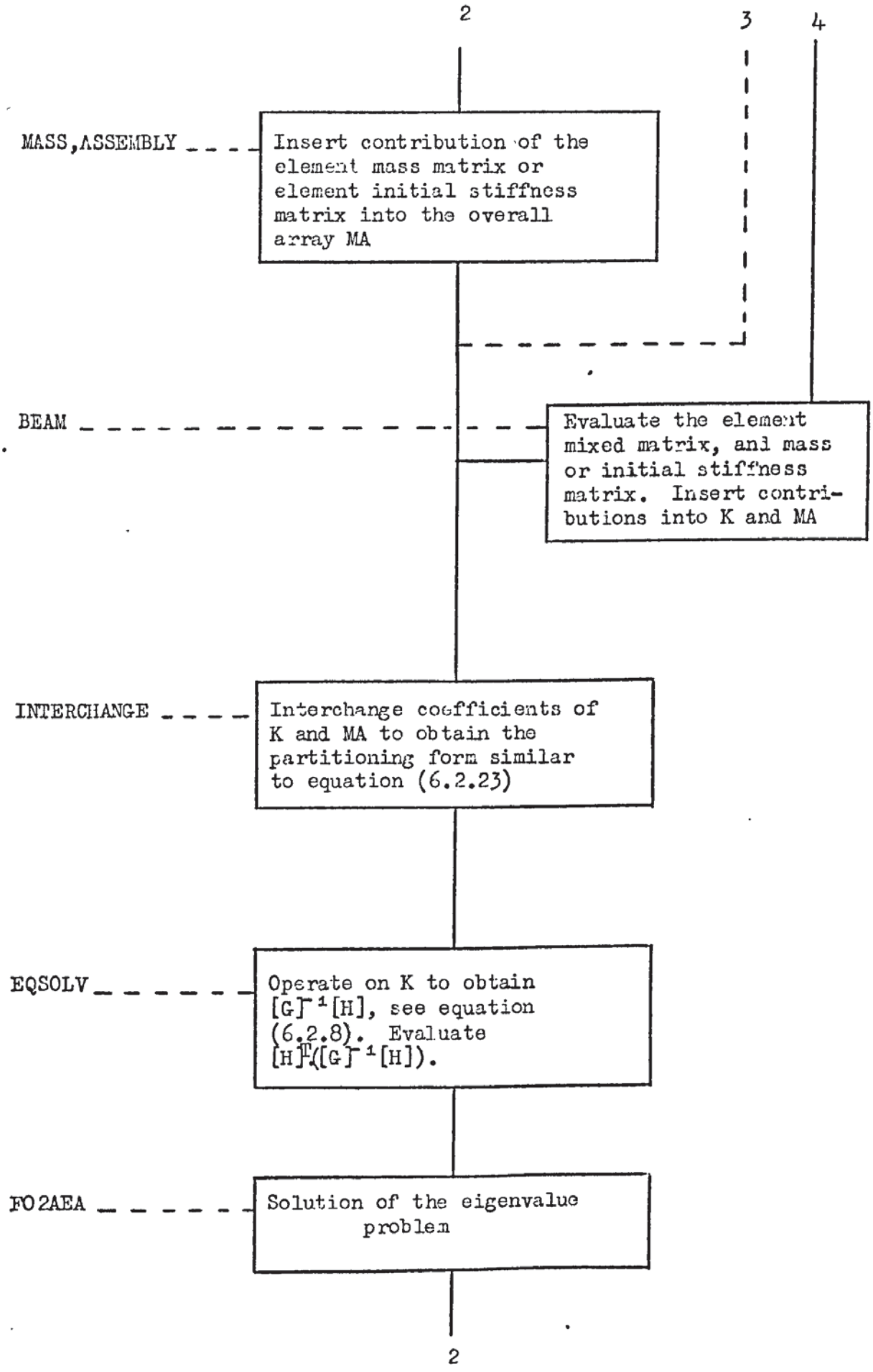
2
3
4
MASS,ASSEMBLY
Insert contribution of the element mass matrix or element initial stiffness matrix into the overall array MA
BEAM
Evaluate the element mixed matrix, and mass or initial stiffness matrix. Insert contributions into K and MA
INTERCHANGE
Interchange coefficients of K and MA to obtain the partitioning form similar to equation (6.2.23)
EQSOLV
Operate on K to obtain $[G]^{-1}[H]$, see equation (6.2.8). Evaluate $[H]^T([G]^{-1}[H])$.
F02AEA
Solution of the eigenvalue problem
2

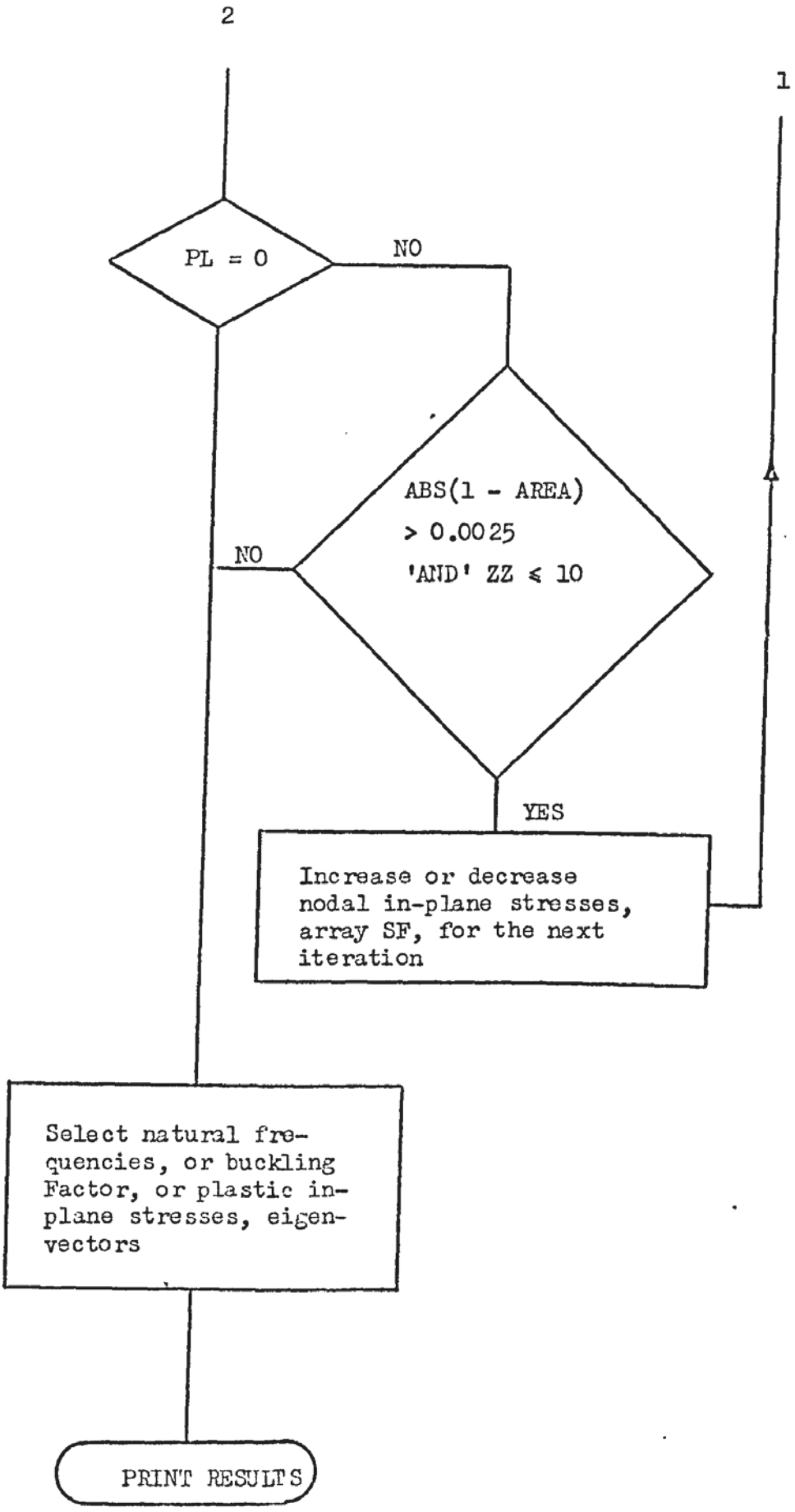
2
1
PL = 0
NO
ABS(1 - AREA)
> 0.0025
'AND' ZZ ≤ 10
NO
YES
Increase or decrease nodal in-plane stresses, array SF, for the next iteration
Select natural frequencies, or buckling Factor, or plastic in-plane stresses, eigenvectors
PRINT RESULTS

8.6) Description of the Input Data.

The input data for this test program is very similar to that described in Section (7.14.1) for the "static main program". The extra new variables not yet defined are:

NW	(I)	Total number of nodal points free to move in the z direction.
MD	(R)	Mass of the plate per unit volume.
UQ	(R)	Shape parameter of the Ramberg-Osgood stress strain curve, for plastic buckling. 0.0 for vibrations and elastic buckling.
VV	(I)	Local nodal degree of freedom identification number 3 - Deflection 2 - Bending Moment M_x or M_s 1 - Bending Moment M_y or M_n 0 - Twisting Moment M_{xy} or M_{ns}
W	(I)	Number of boundary node
TA	(R)	Imposed quantity, assigned always the value 0.0.
ST	(RA)	Nodal in-plane stress array, for each node $\bar{\sigma}_{x_o}$, $\bar{\sigma}_{y_o}$, $\bar{\tau}_{xy_o}$, calculated separately as a plane stress problem.

For the analysis of plastic-buckling problems, the procedure MATERIAL, reads in the Young's modulus, E, of the material and the value of the stress $\sigma_{0.7}$ (i.e. the stress at which the Ramberg-Osgood stress strain curve, see Section 6.2.2b, has a secant modulus of 0.7E). The value of $\sigma_{0.7}$ is read in instead of the Poisson's ratio, μ. The material group identification number is inputed exactly as before. For free vibrations and elastic buckling problems the input, through the procedure MATERIAL, is as shown in Section 7.14 - item d.

If beam elements are involved, but only for free vibrations and elastic buckling problems, the input through the procedure INBEAM

consists of:

2nd moment of area, area of the cross section of the beam element, mass per unit volume or trial buckling force, overall length of the beam (reinforced plates) or 1.0 (beam alone). By assigning the value 1.0 to the overall length of the beam, the beam element relation (A.3.16) is transformed into relation (A.3.15) for the solution of beam problems alone. The element number-group identification is inputed exactly as before, see Section 7.14 item e.

A flow diagram for the input data is shown in Fig.(8.6.1) and the listing of the program is in Appendix 5.

Fig.(8.6.1) Flow chart for the input data "Test eigenvalue program"

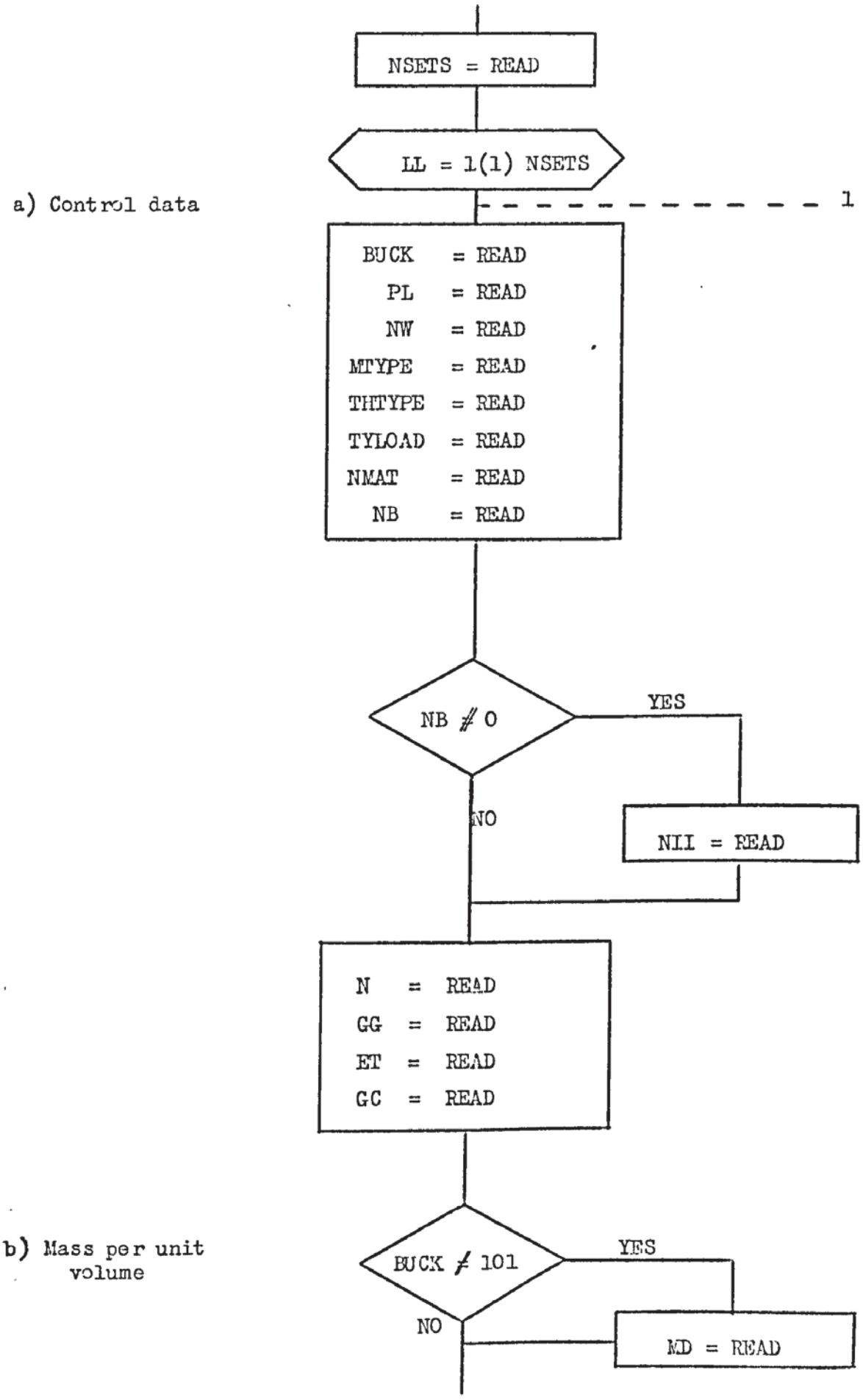

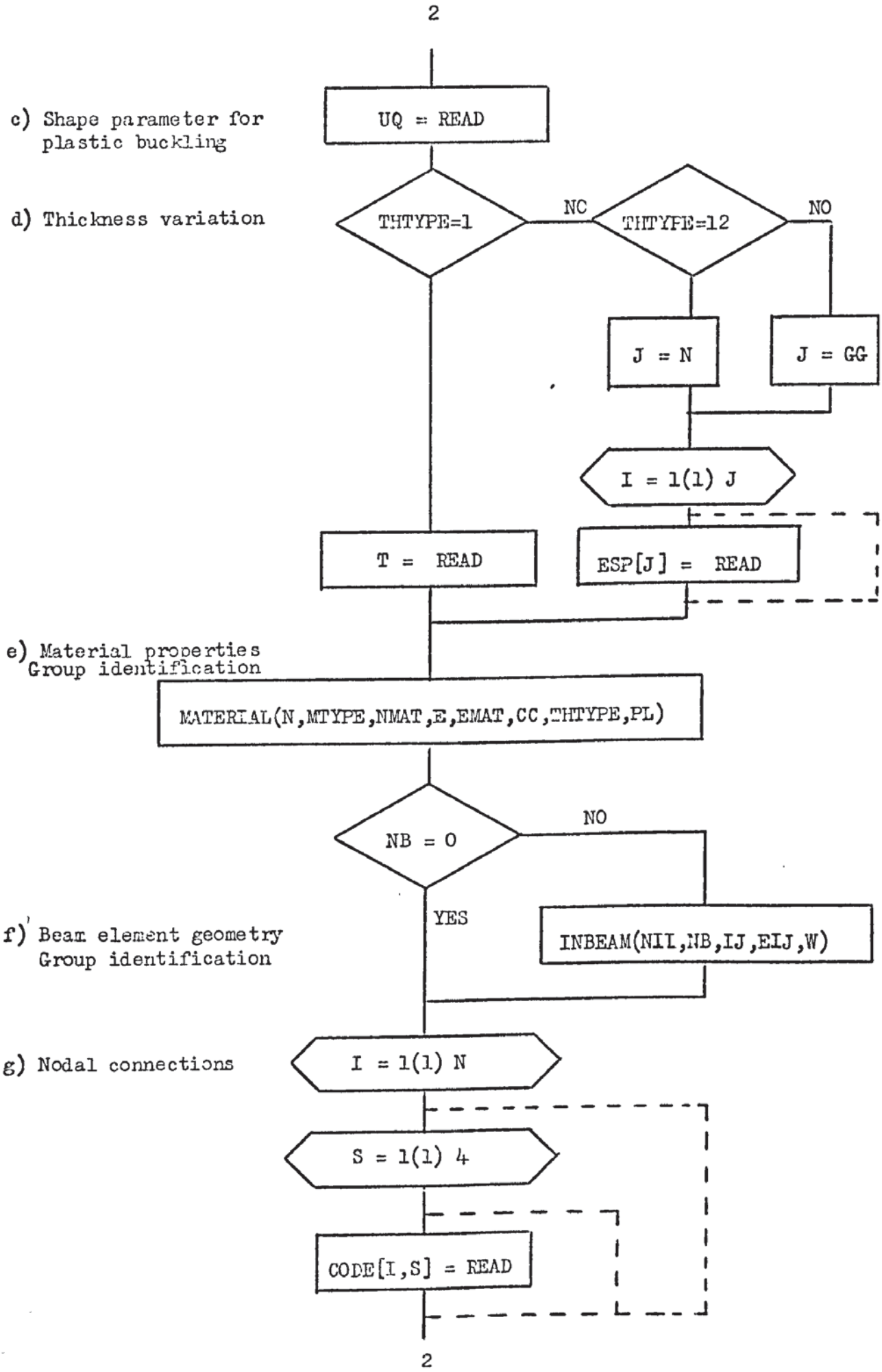
2
c) Shape parameter for plastic buckling
UQ = READ
d) Thickness variation
THTYPE=1
NC
THTYPE=12
NO
J = N
J = GG
I = 1(1) J
T = READ
ESP[J] = READ
e) Material properties Group identification
MATERIAL(N,MTYPE,NMAT,E,EMAT,CC,THTYPE,PL)
NB = 0
NO
YES
f) Beam element geometry Group identification
INBEAM(NII,NB,IJ,EIJ,W)
g) Nodal connections
I = 1(1) N
S = 1(1) 4
CODE[I,S] = READ
2

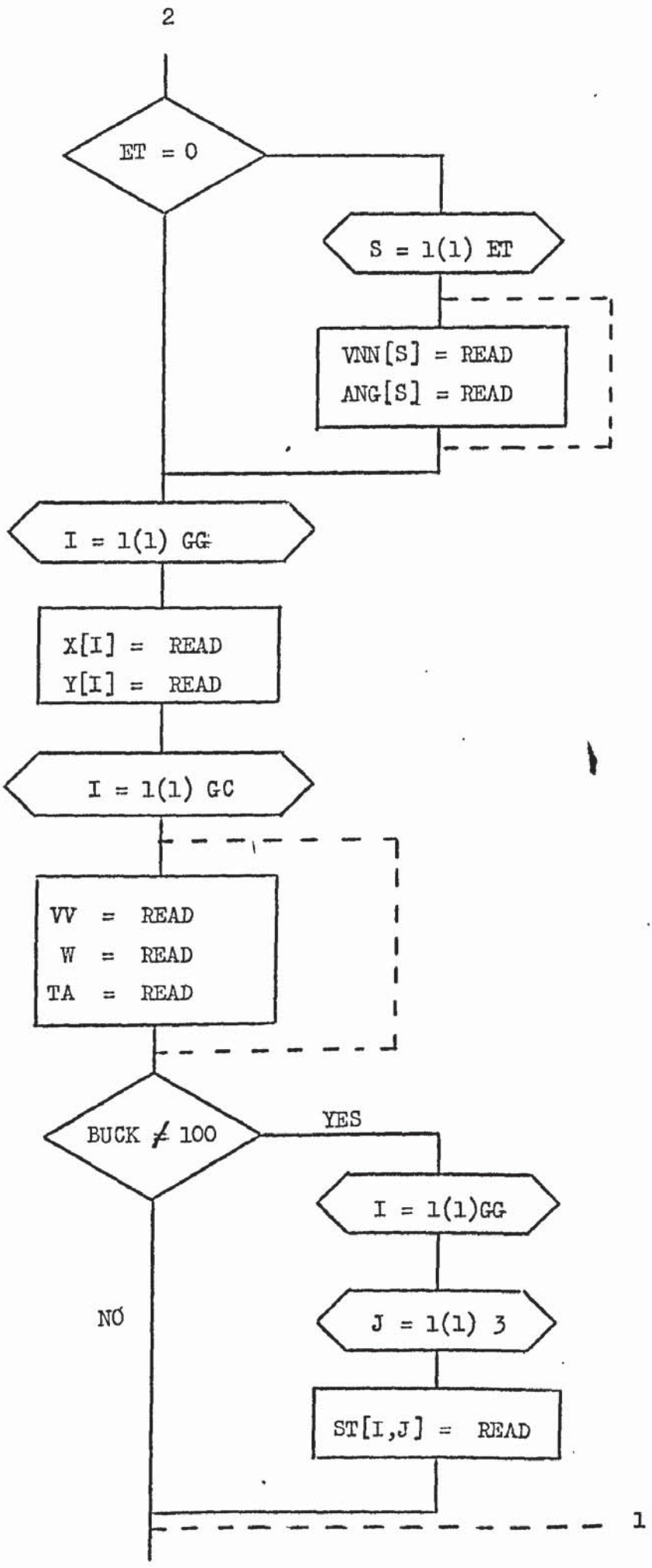
2
h) Node, angle in degrees for local n,s axes
ET = 0
S = 1(1) ET
VNN[S] = READ
ANG[S] = READ
i) Nodal coordinates
I = 1(1) GG
X[I] = READ
Y[I] = READ
I = 1(1) GC
j) Specified boundary conditions
VV = READ
W = READ
TA = READ
k) Nodal in-plane stresses
BUCK ≠ 100
YES
NO
I = 1(1)GG
J = 1(1) 3
ST[I,J] = READ
1

8.6.1 Samples of Input Data.

a) Free Vibrations.

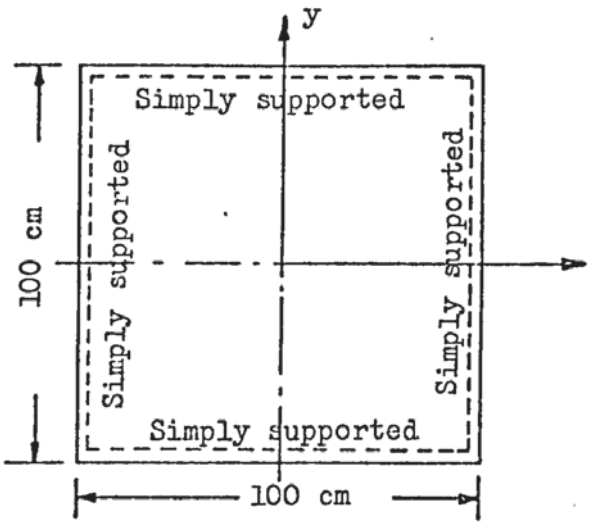

$E = 21.10^6\ N/cm^2$

$\mu = 0.3$

$\rho = 0.008\ Kg/cm^3$

$h = 1\ cm$

The discretized plate.

Due to symmetry only $\frac{1}{4}$ of the plate is required.

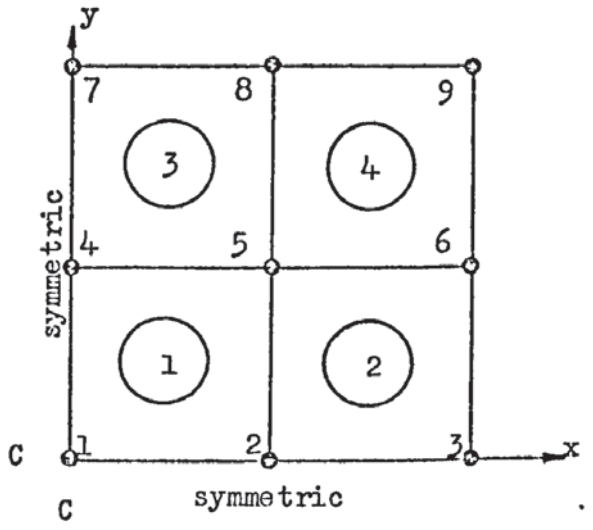

The input data

```
1
100    0    4    1  1  1  1    0+     4     9     0     16
0.008
0.0
1.0
21000 000.0      0.3
1      1    1    1
1      2    5    4      2  3    6    5      4  5  8  7
5      6    9    8
0.0    0.0      25.0    0.0    50.0    0.0
0.0    25.0     25.0    25.0   50.0    25.0
0.0    50.0     25.0    50.0   50.0    50.0
3    3    0.0        3    6    0.0        3    9    0.0
3    7    0.0        3    8    0.0        2    3    0.0
2    6    0.0        2    9    0.0        1    7    0.0
1    8    0.0        1    9    0.0        0    1    0.0
0    2    0.0        0    3    0.0        0    4    0.0
0    7    0.0
```

+Note: Plate problem without reinforcing beams

b) Elastic Buckling.

The problem.

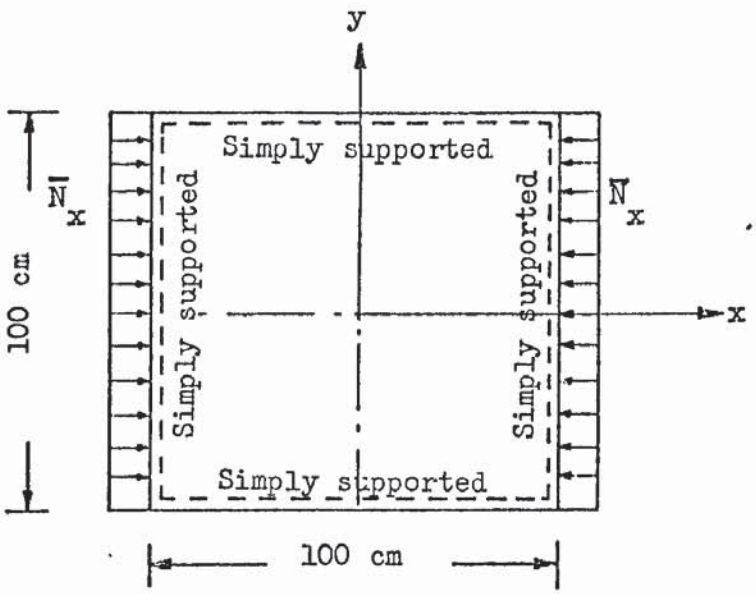

$E = 21.10^6$ N/cm²

$\mu = 0.3$

h = 1 cm

$\bar{N}$ = 1 N/cm (trial load)

The discretized plate.

As shown in item (a)

Values of the nodal in-plane stresses.

Since $\bar{N}_x$ = 1 N/cm and h = 1 cm the in-plane stresses σ_{x_o}, σ_{y_o}, τ_{xy_o} are constant for each node, i.e.

$\bar{\sigma}_{x_o} = 1$ N/cm² $\bar{\sigma}_{y_o} = 0.0$ $\bar{\tau}_{xy_o} = 0.0$.

For arbitrary shapes the stresses are calculated previously for the assumed trial load as a plane stress problem.

The input data.

```
1
101     0     4     1 1 1 1     0+     4     9     0     16

0.0
1.0
21 000 000.0          0.3
1   1   1   1
1   2   5   4         2   3   6   5         4 5   8   7       5 6 9 8

0.0     0.0     25.0     0.0     50.0     0.0
0.0     25.0    25.0     25.0    50.0     25.0
0.0     50.0    25.0     50.0    50.0     50.0

3     3     0.0       3     6     0.0       3     9     0.0
3     7     0.0       3     8     0.0       2     3     0.0
2     6     0.0       2     9     0.0       1     7     0.0
1     8     0.0       1     9     0.0       0     1     0.0
0     2     0.0       0     3     0.0       0     4     0.0
0     7     0.0

1.0     0.0     0.0       1.0     0.0     0.0       1.0     0.0     0.0
1.0     0.0     0.0       1.0     0.0     0.0       1.0     0.0     0.0
1.0     0.0     0.0       1.0     0.0     0.0       1.0     0.0     0.0
```

c) Plastic buckling.

The problem.

As in item (b), but assuming a Ramberg-Osgood shape parameter n = 10.0 and $\sigma_{0.7} = 3.4 \cdot 10^5$ N/cm^2.

The only alterations in the input data of item (b) are:

Line 2

101 1* 4 1 1 1 1 0+ 4 9 0 16 10.0**

Line 5

21000 000.0 340000.0***

* Plastic buckling
** Ramberg-Osgood shape parameter
*** Ramberg-Osgood stress $\sigma_{0.7}$
\+ Plate problem without reinforcing beams

CHAPTER 9

STATIC, DYNAMIC AND BUCKLING APPLICATIONS OF MIXED PLATE ELEMENT

9.1) Introduction.

Before the mixed general quadrilateral element developed in the previous chapters can be applied with confidence, it is necessary to obtain some information regarding the convergence of the results. This is achieved by comparing the mixed finite element results of some problems for which exact, numerical or experimental solutions exist. The method of mesh idealization, the boundary conditions and loads are shown in the applications.

In this chapter the convergence properties of the general mixed quadrilateral element are presented with reference to the following problems:

1) Static problems of thin and moderately thick plates.
2) Free flexural vibrations of thin plates.
3) Elastic and Plastic Buckling of thin plates.

9.2) Static Plate Bending Problems-Convergence Tests.

In this section several examples of plate bending problems are solved using the "Main" computer program. The tests are aimed at illustrating the convergence of the results as the element sub-division of the plate is refined.

9.2.1) "Convergence"Tests-Uniform Square Plate Under Uniform Load.

The first set of tests relate to a square plate under uniform pressure. In all cases, due to the symmetric properties about the centre lines of the square, only one quarter of the plate is analysed and subdivided into a square mesh 2 x 2, 4 x 4, 6 x 6, respectively, as presented in Fig.(9.2.1), the appropriate boundary conditions at the lines of symmetry being zero normal twisting moment, i.e. $M_{ns} = 0$.

The boundary conditions are either all simply supported,

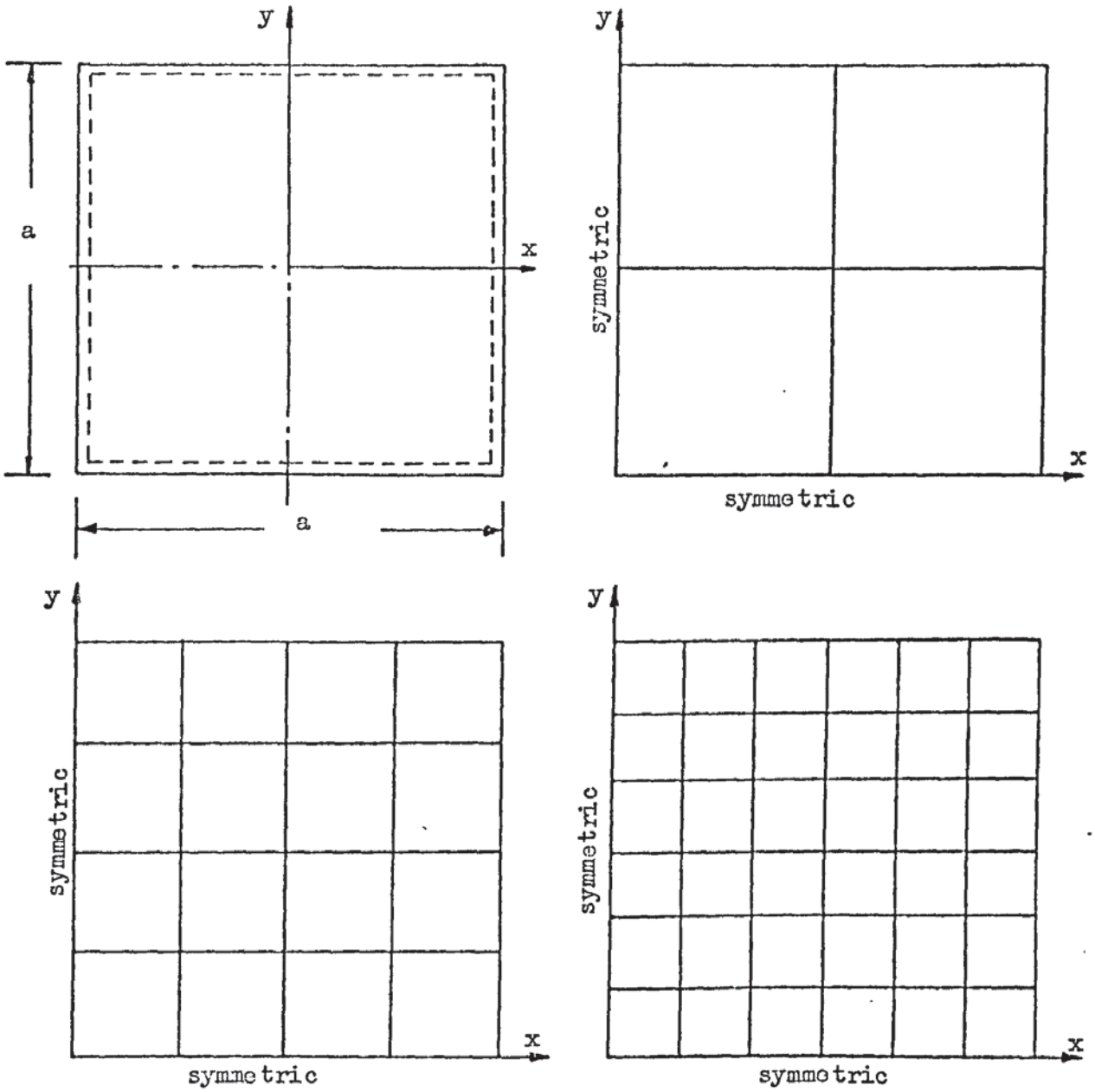

Case (1a) $D = D_o$; $\mu = 0.3$; $p = p_o$

Case (1b) $D_x; D_y = 6.025\ D_x$; $D_1 = 0.375\ D_x; D_{xy} = 0.937\ D_x$; $p = p_o$

Case (1c) $E = E_o$; $h_o/a = 0.05; 0.10; 0.15; 0.20; 0.25$

Fig.(9.2.1) Simply Supported Square Plate

Cases (1a,b,c) Square meshes 2×2, 4×4, 6×6 in a quarter plate.

for case (1a), (1b), (1c) or all clamped for case (1d).

a) Thin Isotropic Simply Supported Plate-Case (1a).

The discrete results of the program which are plotted against the analytical solution of ref.[10] for the deflection and bending moment parameters along the centre lines of the plate are shown in Fig.(9.2.2 a,b,c). Table (9.2.1) presents the values obtained for the parameters of the maximum deflection, W, and maximum bending moment, M_x, at the centre of the plate, from which the errors for the maximum deflection and bending moment are:

4.3% , 9.6%,

1.0% , 2.1%,

0.47% , 0.83%,

respectively for the meshes 2 × 2, 4 × 4, 6 × 6, which show very good convergence properties as the mesh is refined.

b) Thin Orthotropic Plate-Simply Supported-Case (1b).

The special case of orthotropy in a square plate may be the result of construction using an isotropic material, i.e, evenly spaced ribs in orthogonal directions or it may be the result of a special anisotropy of the material in two orthogonal directions. The orthotropic properties of the plate coincided with the x and y axes.

Fig.(9.2.3 a,b) and Table (9.2.2) present the results for this orthotropic case.

From Table (9.2.2) the error for the maximum deflection, W, and maximum bending moments M_x and M_y at the centre of the plate are respectively:

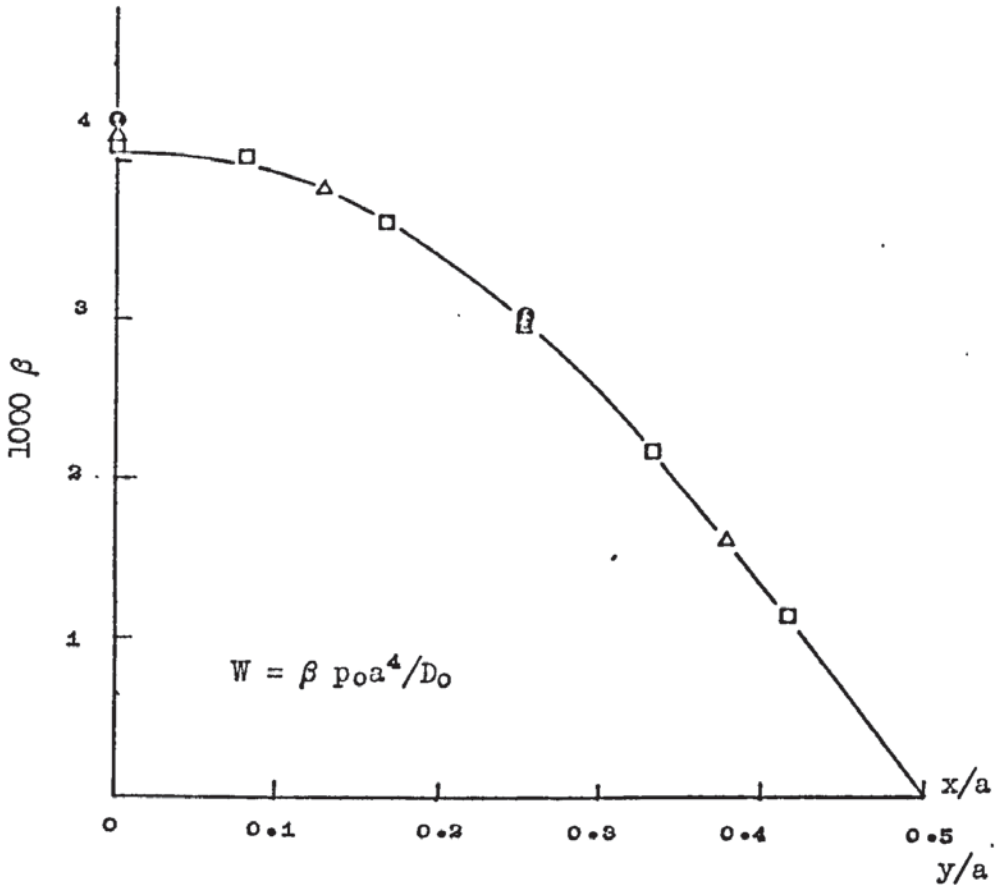

Fig.(9.2.2a)

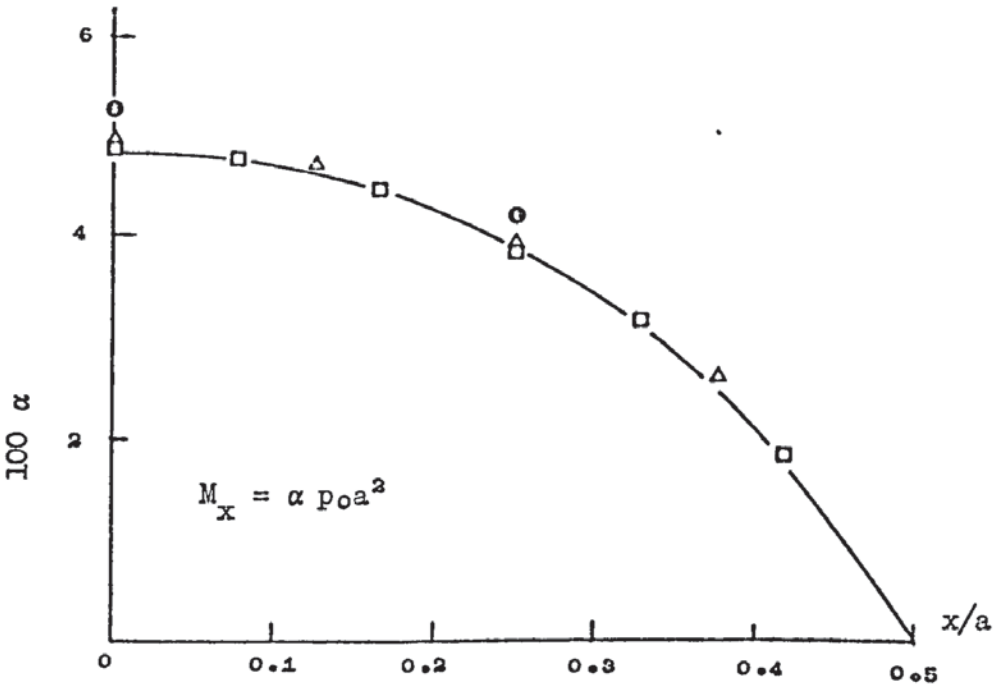

Fig. (9.2.2b)

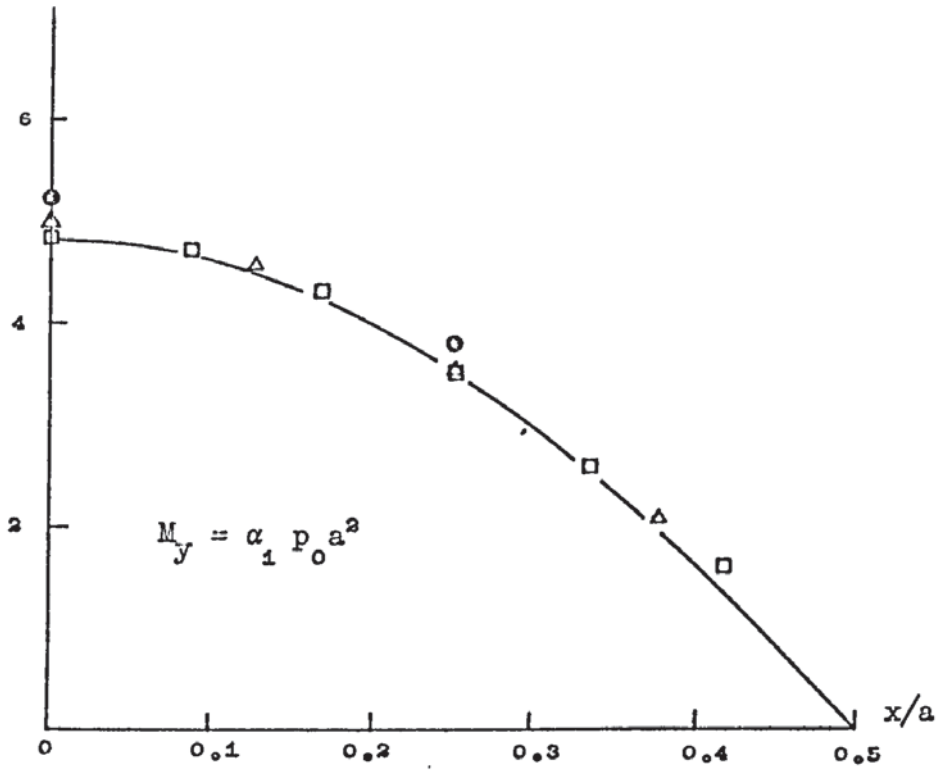

Fig.(9.2.2c)

Fig.(9.2.2) Solution to case (1a)

—— Series Solution (ref.[10])

along the centre lines

(⊙), (△), (□) Mixed Finite

Element meshes 2 × 2, 4 × 4, 6 × 6.

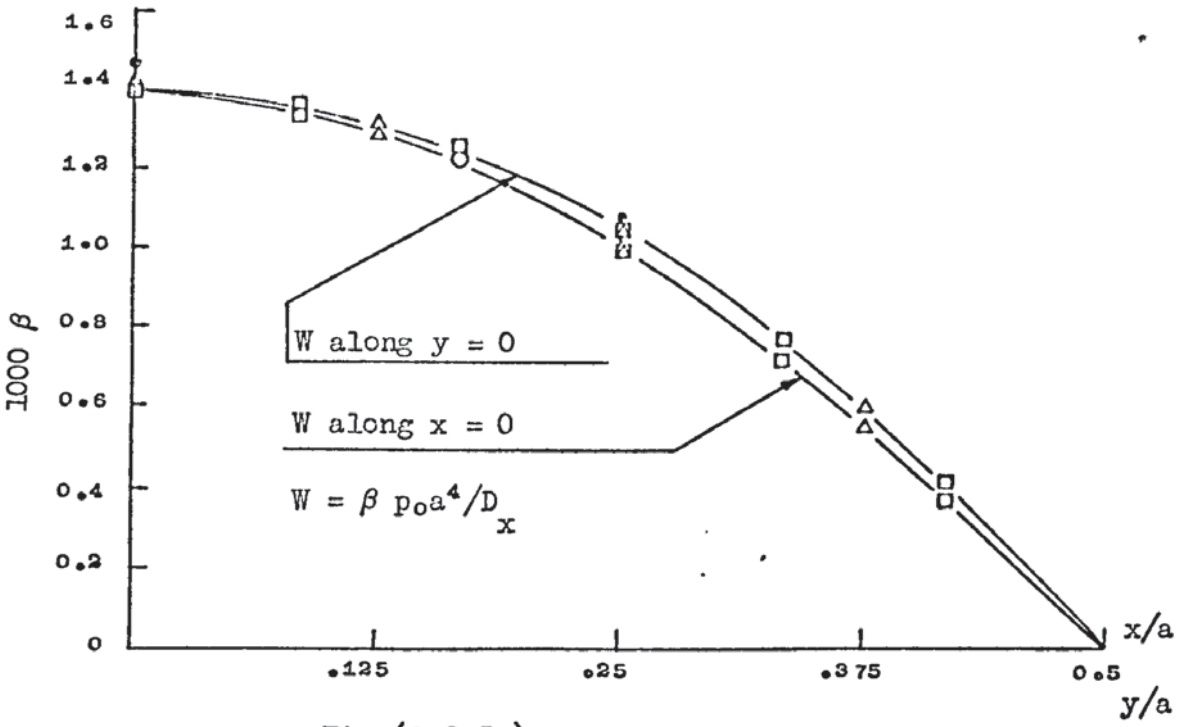

Fig.(9.2.3a)

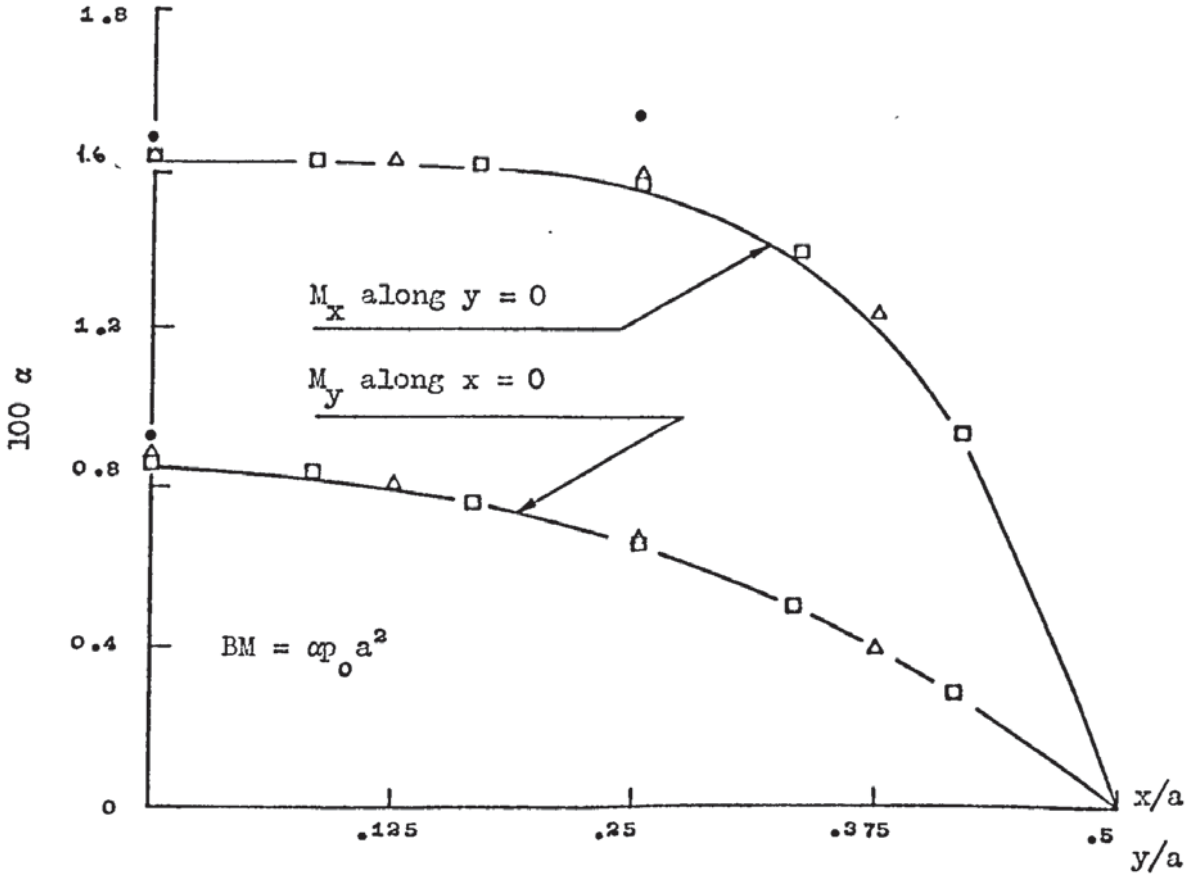

Fig.(9.2.3b)

Fig.(9.2.3) Solution to case (1b)
_____ Series Solution (ref.[10])
(•),(△),(□) Mixed Finite element meshes 2 × 2, 4 × 4, 6 × 6.

TABLE (9.2.1) Deflection and Bending Moment for Case (1a)

Mesh	$(W)_{max}$ $\div \frac{p_o}{D_o} a^4$	$(M_x)_{max}$ $\div p_o a^2$
2 × 2	0.004237	0.0525
4 × 4	0.004106	0.0489
6 × 6	0.004081	0.0483
Exact [10]	0.004062	0.0479

TABLE (9.2.2) Deflection and Bending Moments-Orthotropic plate - Case (1b)

x = 0 ; y = 0			
Mesh	$(W)_{max}$ $\div p_o a^4/D_x$	$(M_x)_{max}$ $\div p_o a^2$	$(M_y)_{max}$ $\div p_o a^2$
2 × 2	0.001452	0.01686	0.09186
4 × 4	0.001409	0.01629	0.08557
6 × 6	0.001402	0.01620	0.08452
Exact [10]	0.001396	0.01614	0.08371

4.0% , 4.5% , 9.7%,

0.93% , 0.93% , 2.2%,

0.43% , 0.37% , 0.97%,

for the square grids. The results show a very good rate of convergence towards the "exact" values given by the analytical solution of reference [10], taking the first 25 terms of the infinite series.

c) "Moderately" Thick Plate-Simply Supported - Case (1c).

Table (9.2.3) shows the values of the parameters for the maximum deflection, W, and the maximum bending moment, M_x, at the centre of the plate for the plate thickness ratio of 0.25 and the values are compared with the analytical solution of ref.[21]. The edge boundary conditions prescribed in the above reference are the vanishing of the deflection, W, normal bending moment, M_n, and rotation of the edge in the direction of the edge, β_s. These boundary conditions result in the same distribution of shear intensity resultant Q_x, Q_y and twisting moment M_{xy}, as given by the classical thin plate theory. Hence, for comparison only $W = 0$ and $M_n = 0$ are imposed at the edge boundaries.

The results show that they converge rapidly towards the correct solution as the mesh is refined. The problem has also been solved for several plate thickness ratios ranging from 0.05 to 0.25 using a 6×6 mesh only. The results are given in tabular form, Table (9.2.4), and in graphical form, Fig.(9.2.4). The increase in the predicted maximum deflection parameter due to the shear deformation is 4.8% for a thickness ratio of 0.1. For a thickness ratio of 0.25 the increase in the predicted maximum deflection parameter is about 28.1%. The increases for the analytical solutions are respectively 4.4

TABLE (9.2.3) Central Deflection and Bending Moment for Case (1c)

$h/a = 0.25$ $\mu = 0.3$ Mesh	$(W)_{max} \div P_o a^4/E_o h_o^3$ At $x = 0; y = 0$	$(M_x)_{max} \div P_o a^2$ At $x = 0; y = 0$
2×2	0.05923	0.05318
4×4	0.05723	0.04987
6×6	0.05686	0.04928
Thick plate theory [21]	0.05656	0.04880
Thin plate theory [10]	0.04437	0.04790

TABLE (9.2.4) Deflection and Bending Moment-Case (1c)

Thickness ratio $\frac{h_o}{a}$	$(W)_{max} \div p_o a^4/E_o h_o^3$		$(M_x)_{max} \div p_o a^2$	
	at x = 0 ; y = 0		at x = 0 ; y = 0	
	Reissner theory ref[21]	Mixed F.E. 6 x 6 mesh	Reissner theory ref [21]	Mixed F.E. 6 x 6 mesh
.05	0.04486	0.04506	0.04790	0.04837
.10	0.04632	0.04654	0.04810	0.04849
.15	0.04876	0.04899	0.04820	0.04868
.20	0.05217	0.05244	0.04850	0.04894
.25	0.05656	0.05686	0.04880	0.04928

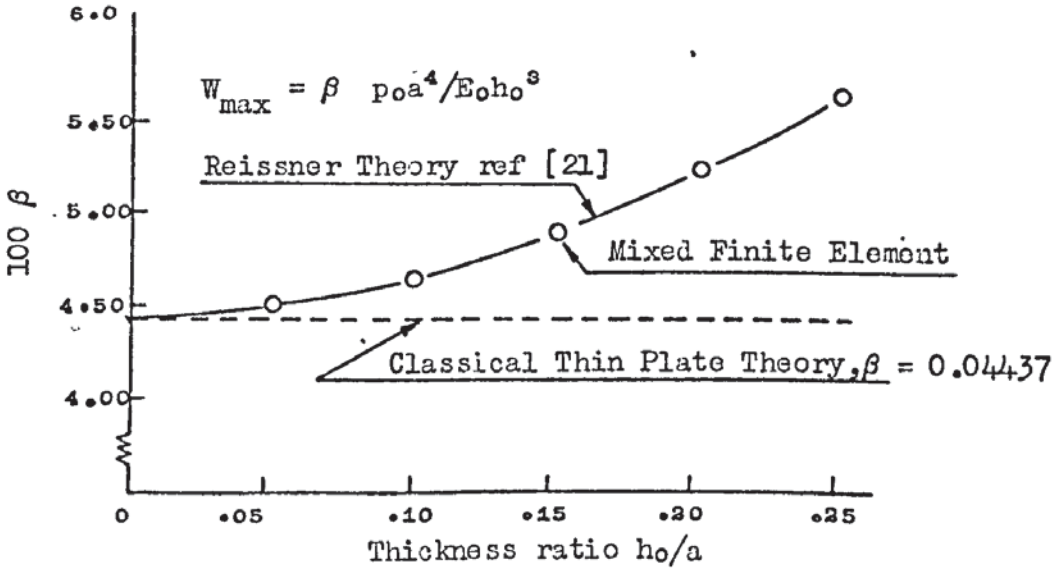

Fig.(9.2.4) Influence of Transverse Shear for case (1c).

c) contd.

and 27.5%. Fig.(9.2.4) shows clearly the importance of the inclusion of the shear deformation on the maximum deflection for different aspect ratios, hence the importance of its inclusion if more realistic results are required.

The increase in the predicted parameter of the maximum bending moment, M_x, for the aspect ratios 0.1 and 0.25 are respectively 1.23 and 2.88%, which correspond to an analytical variation of 0.42 and 1.88%.

d) Thin Isotropic Clamped Plate-Case (1d).

The dimensions and divisions of the plate are as given in Fig.(9.2.1). The distribution of the parameters for W and M_x along the centre line are shown in Fig.(9.2.5 a,b). Table (9.2.5) gives the values of the parameters for the maximum deflection W, maximum bending moment, M_x, at the clamped edge, and the bending moment, M_x, at the centre of the plate. The errors involved are respectively:

20.79% , 4.45% , 37.03%,
5.84% , 1.24% , 7.28%,
2.68% , 0.55% , 2.75%,

for the mesh 2 × 2, 4 × 4 and 6 × 6.

The results at the centre of the plate show that the value of the parameters for the central deflection and bending moment, M_x, are very poor for the grid 2 × 2, but they converge rapidly as the mesh is refined. A further test was carried out using an 8 × 8 square mesh and the parameters for the central deflection, W, and bending moment, M_x, were found to have an error of 1.5%.

9.2.2) "Convergence" Tests - Uniform Plate Under Concentrated Load.

In this section the effect of the concentrated load in a square isotropic plate is investigated. The dimensions and mesh used in the analysis are as given in Fig.(9.2.1), but now the uniform pressure is replaced by a concentrated load P, applied at the centre. The plate is either simply supported or clamped at the four edges.

a) Square Plate-Simply Supported-Case (2a).

The parameters for the deflection and bending moment, M_x, along the centre line $y = 0$ are represented graphically in Fig.(9.2.6). Table (9.2.6) gives the value of the deflection parameter at the point of application of the concentrated load. From these results it can be seen that the predicted deflection curve is accurate. The bending moment is also predicted accurately except for the values of the central portion of the plate. At the centre of the plate the theoretical bending moment is infinite and with a steep gradient. Consequently, a fine mesh is required to enable the model to represent the bending moment near the central part of the plate. This phenomenon is peculiar to this particular problem and not to the mixed element model.

At the centre of the plate the predicted bending moment parameter, α, is 0.3440, 0.416 and 0.4534 for the 2 x 2, 4 x4, 6 x 6 meshes, respectively. The corresponding errors for the maximum deflection parameter are 16.1, 4.8 and 2.3%.

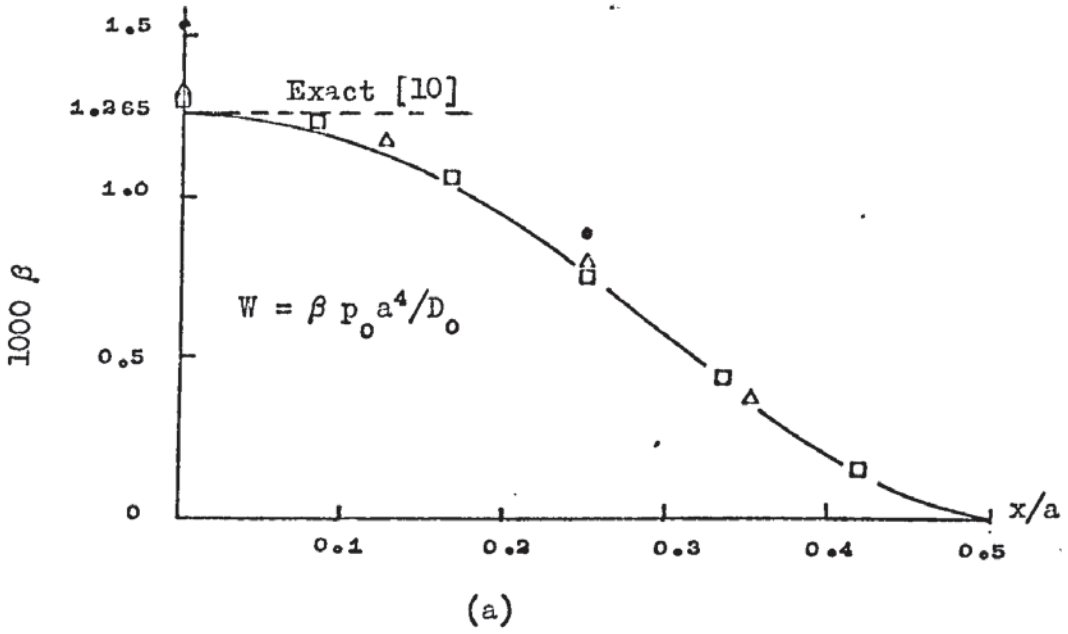

(a)

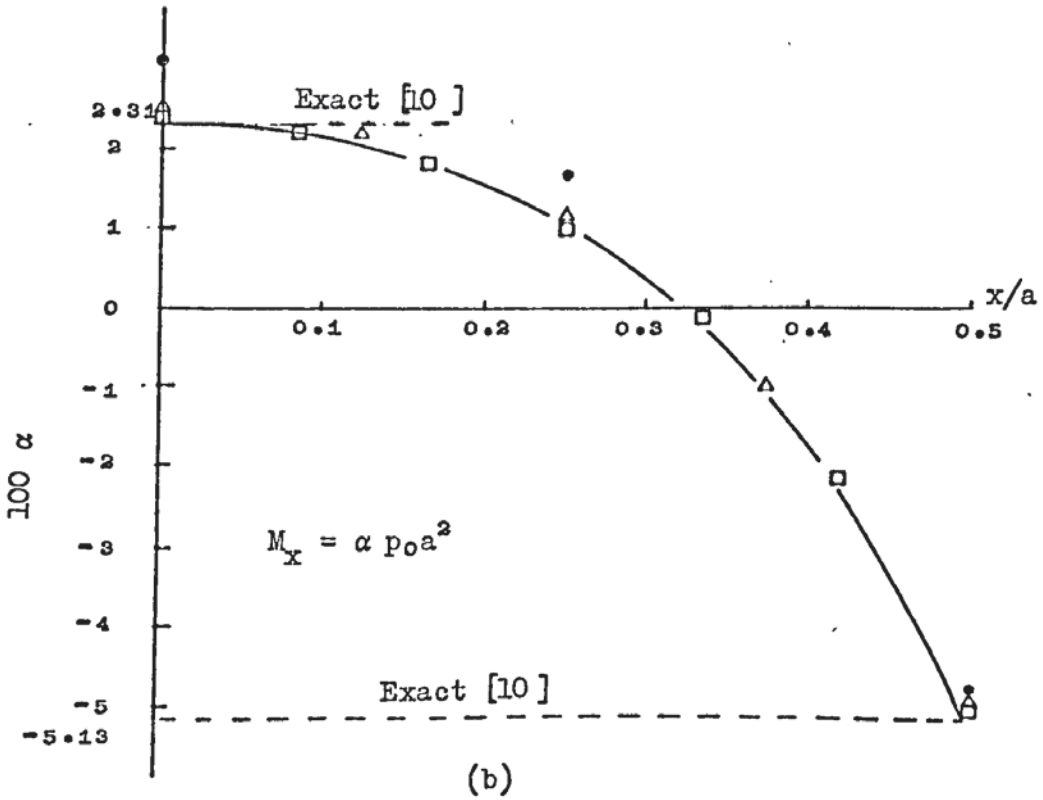

(b)

Fig.(9.2.5) Solution to case (1d)

____ Series Solution (ref [10]) along the centre lines (•), (△), (□) Mixed Finite Element meshes 2 × 2, 4 × 4, 6 × 6.

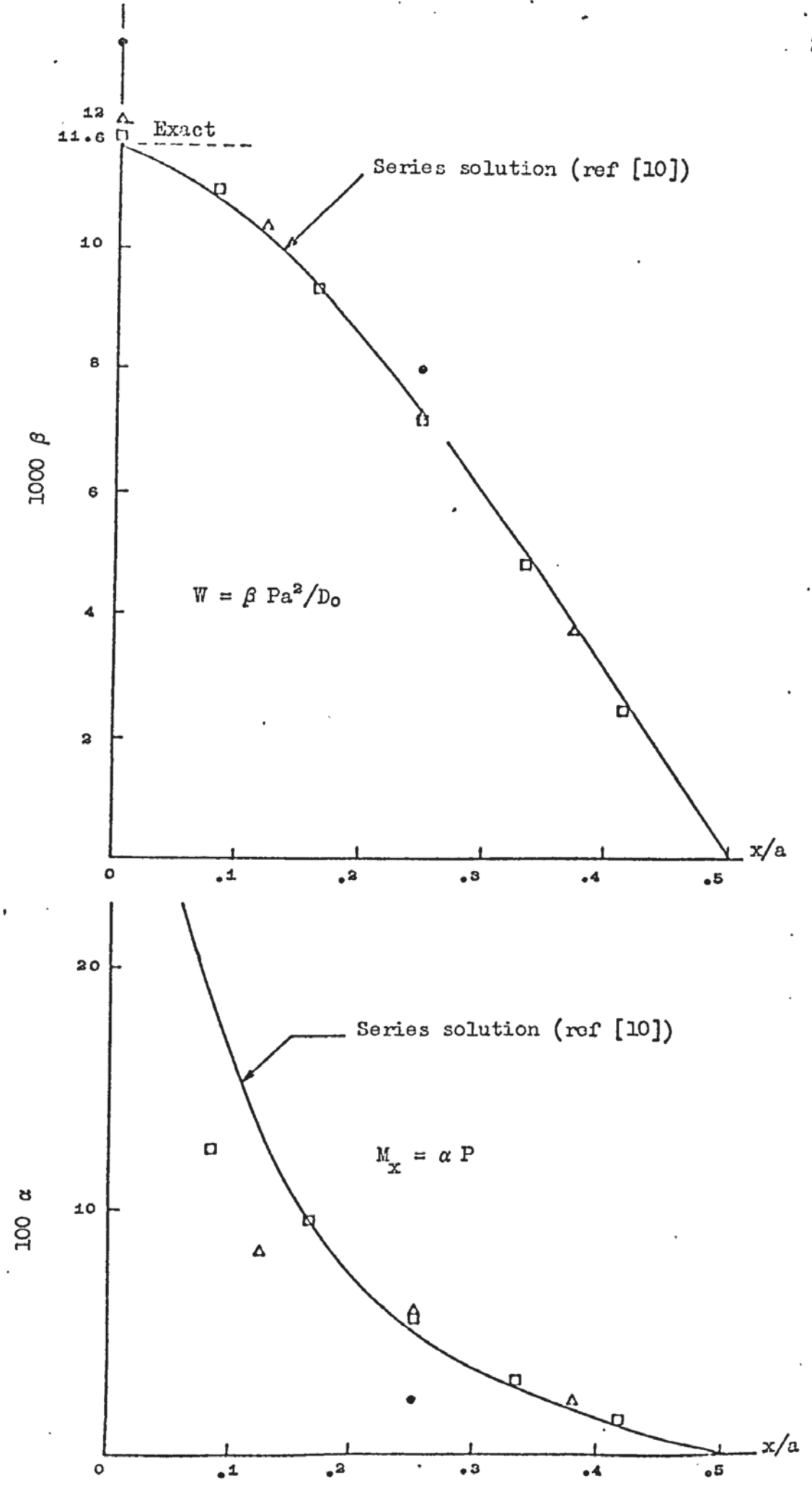

Fig.(9.2.6) Solution to case (2a), along centre line
(•),(△),(□) Meshes 2 × 2, 4 × 4, 6 × 6.

TABLE (9.2.5) Deflections and Bending Moments for Case (1d)

Mesh	$(W)_{max} \div p_o a^4/D_o$	$(M_x)_{max} \div p_o a^2$	$(M_x)_{centre} \div p_o a^2$
2 × 2	0.001528	-0.049018	0.031655
4 × 4	0.001339	-0.050666	0.024783
6 × 6	0.001299	-0.051016	0.023735
Exact [10]	0.001265	-0.0513	0.0231

TABLE (9.2.6) Deflections for Case (2a)

$(W)_{max} \div \frac{P a^2}{D_o}$			
Mesh			Exact [10]
2 × 2	4 × 4	6 × 6	
0.01347	0.01216	0.01187	0.01160

b) Square Plate-Clamped Edges Concentrated Load-Case (2b).

Fig.(9.2.7) shows the distribution of the parameters for the deflection and bending moment along the centre line y = 0. Table (9.2.7) presents the value of these parameters for the deflection at the centre and for the maximum bending moment, M_x, at the clamped edge, x = 0.5.

As can be seen the results converge quite rapidly to the exact solution as the mesh is refined. At the centre of the plate the errors for the maximum deflection are respectively

23.75 , 8.39 and 4.3%

and for the maximum bending moment at the clamped edge are

14.48 , 2.39 and 1.27%

for the meshes tested.

This clamp problem, with the concentrated load at the centre, causes a very steep variation of moments, and therefore, a fine mesh is required in order to predict accurately the values near the point load. Again, this is a pecularity of the problem and not of the mixed elemont.

9.2.3) "Convergence Tests"-Uniform Rectangular Plate-Combination of Boundary Conditions- Case (3).

The problem tested is a uniformly loaded thin rectangular plate that is simply supported along two opposing edges, fixed along a third and free along the remaining side. The configuration and mesh used in the tests are shown in Fig.(9.2.8). The symmetric properties along the line x = a were exploited, hence only half the plate was subdivided into a 4 x 4 and 8 x 8 square mesh.

Fig.(9.2.9) gives comparisons of the approximated mixed finite element solution with that of the infinite series solution plotted in reference [55]. The agreement between the mixed finite

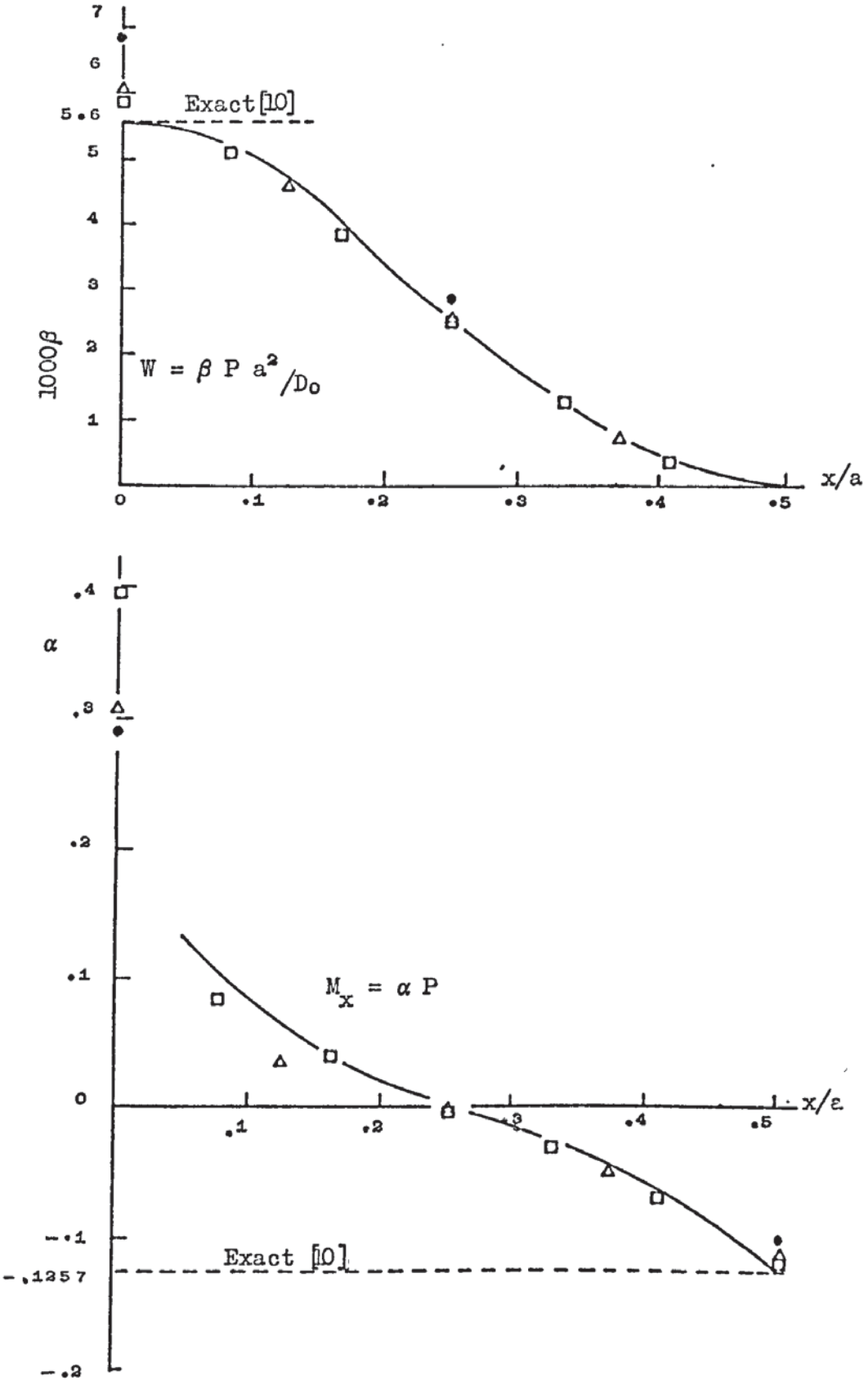

Fig.(9.2.7) Solution to Case (2b)
—— Series Solution (ref [10])
(•), (△), (□) Mixed Finite Element meshes 2 × 2, 4 × 4, 6 × 6.

CASE (3)

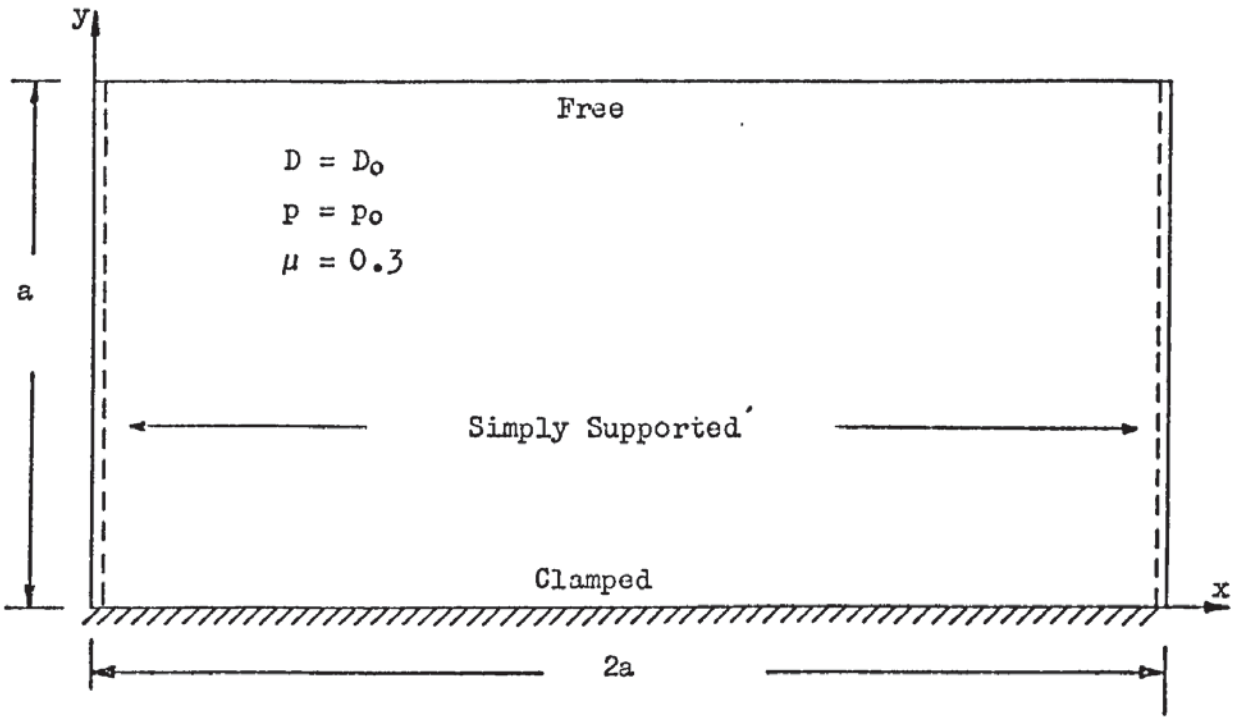

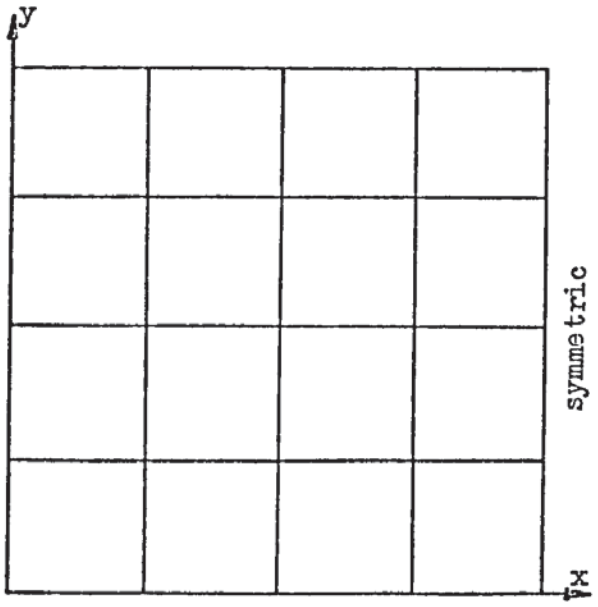

Mesh 4 × 4

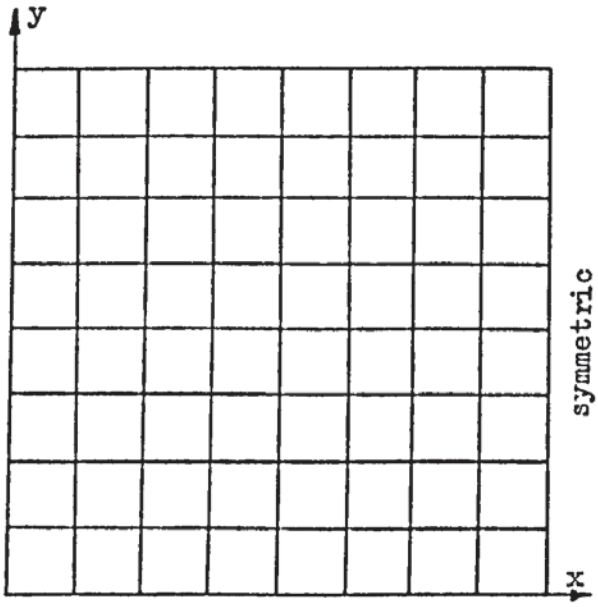

Mesh 8 × 8

Fig.(9.2.8)

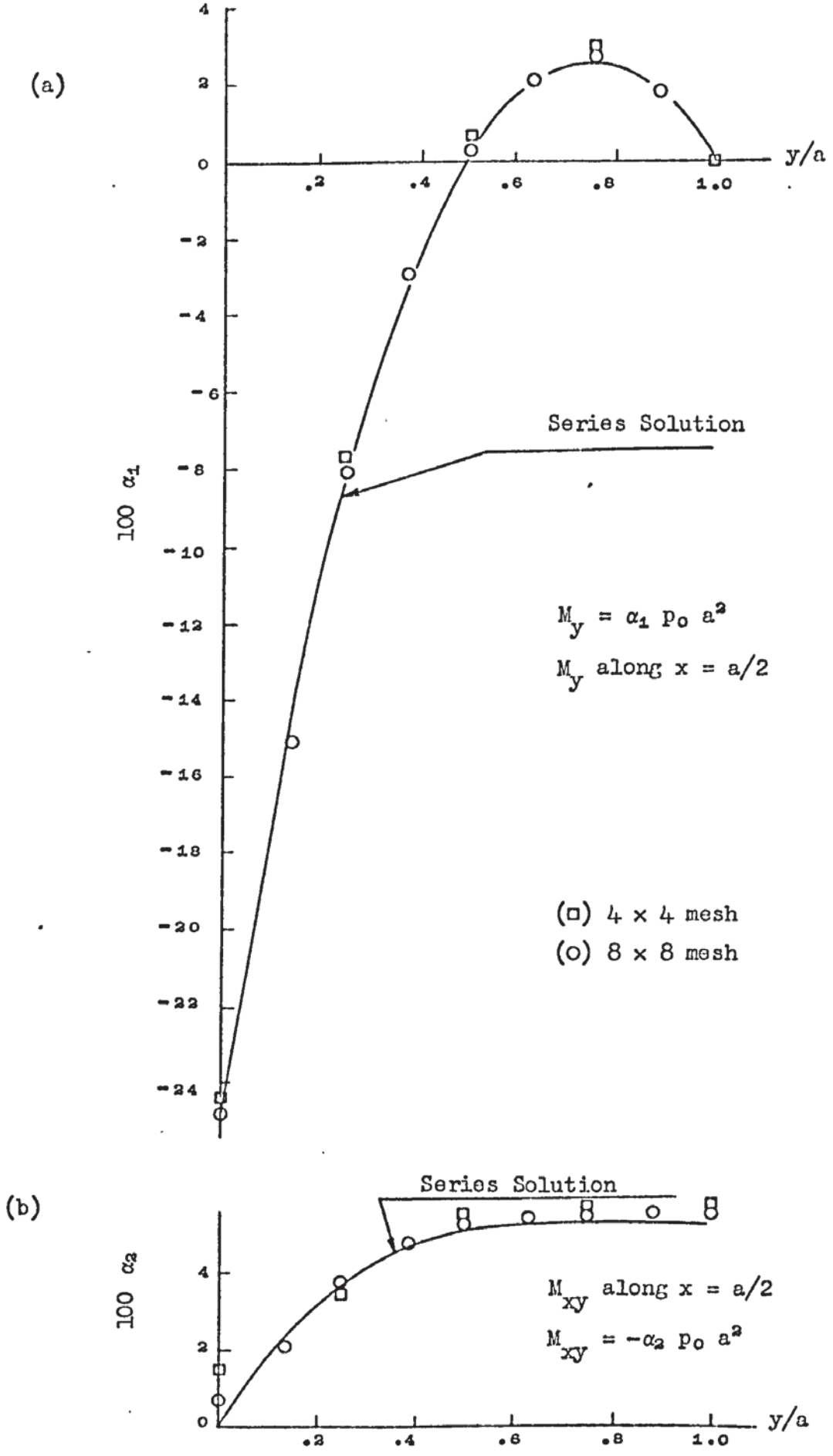

Fig.(9.2.9) Solutions to case (3).

(c)

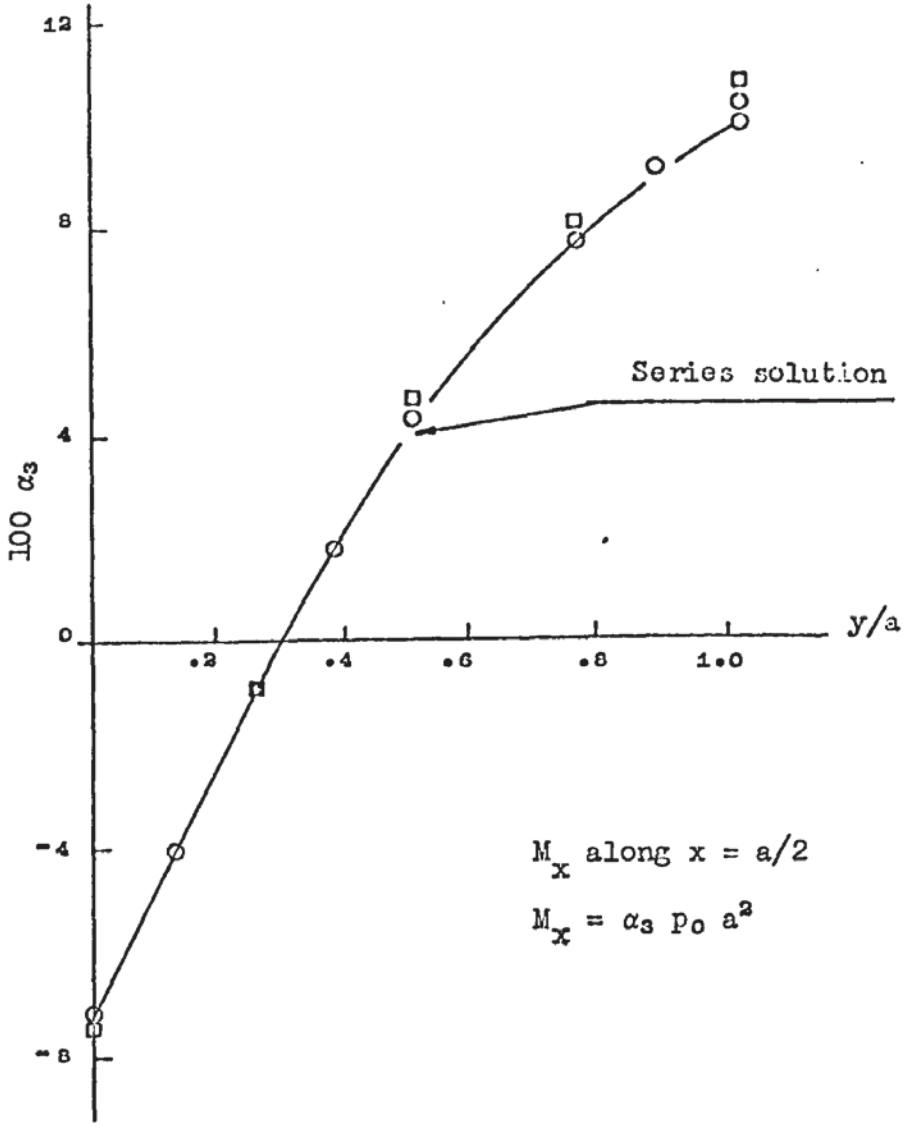
12
8
4
0
-4
-8
100 α_3
.2
.4
.6
.8
1.0
y/a
Series solution
M_x along x = a/2
$M_x = \alpha_3 p_o a^2$

(d)

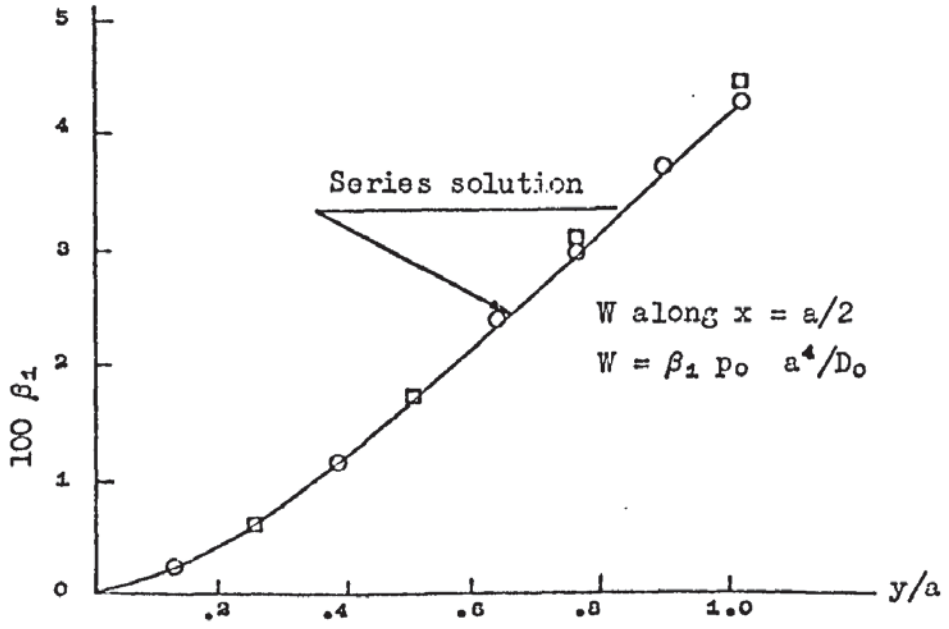
5
4
3
2
1
0
100 β_1
.2
.4
.6
.8
1.0
y/a
Series solution
W along x = a/2
$W = \beta_1 p_o a^4/D_o$

(e)

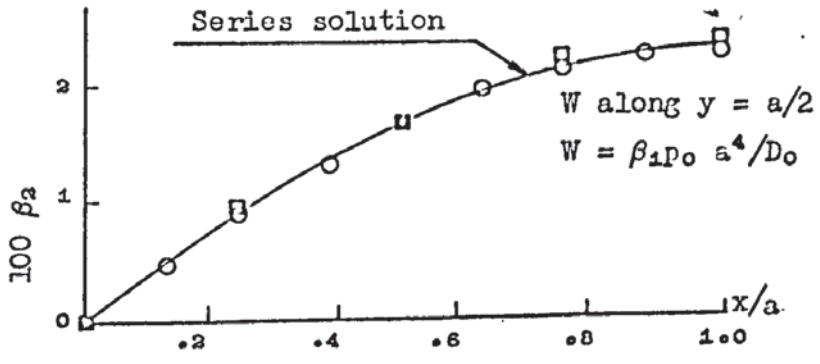
Series solution
W along y = a/2
W = β1p0 a4/D0
100 β2
0
1
2
x/a
.2
.4
.6
.8
1.0

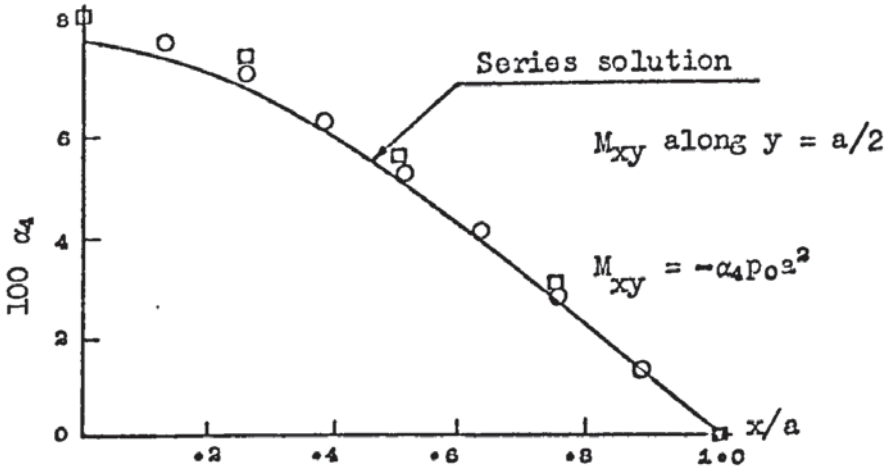
Series solution
Mxy along y = a/2
Mxy = -α4p0a2
100 α4
0
2
4
6
8
x/a
.2
.4
.6
.8
1.0

(f)

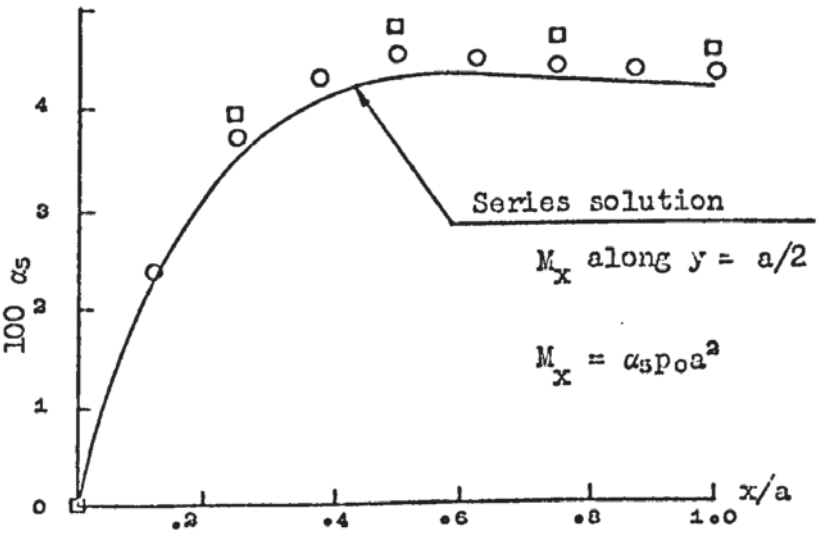
Series solution
Mx along y = a/2
Mx = α5p0a2
100 α5
0
1
2
3
4
x/a
.2
.4
.6
.8
1.0

(g)

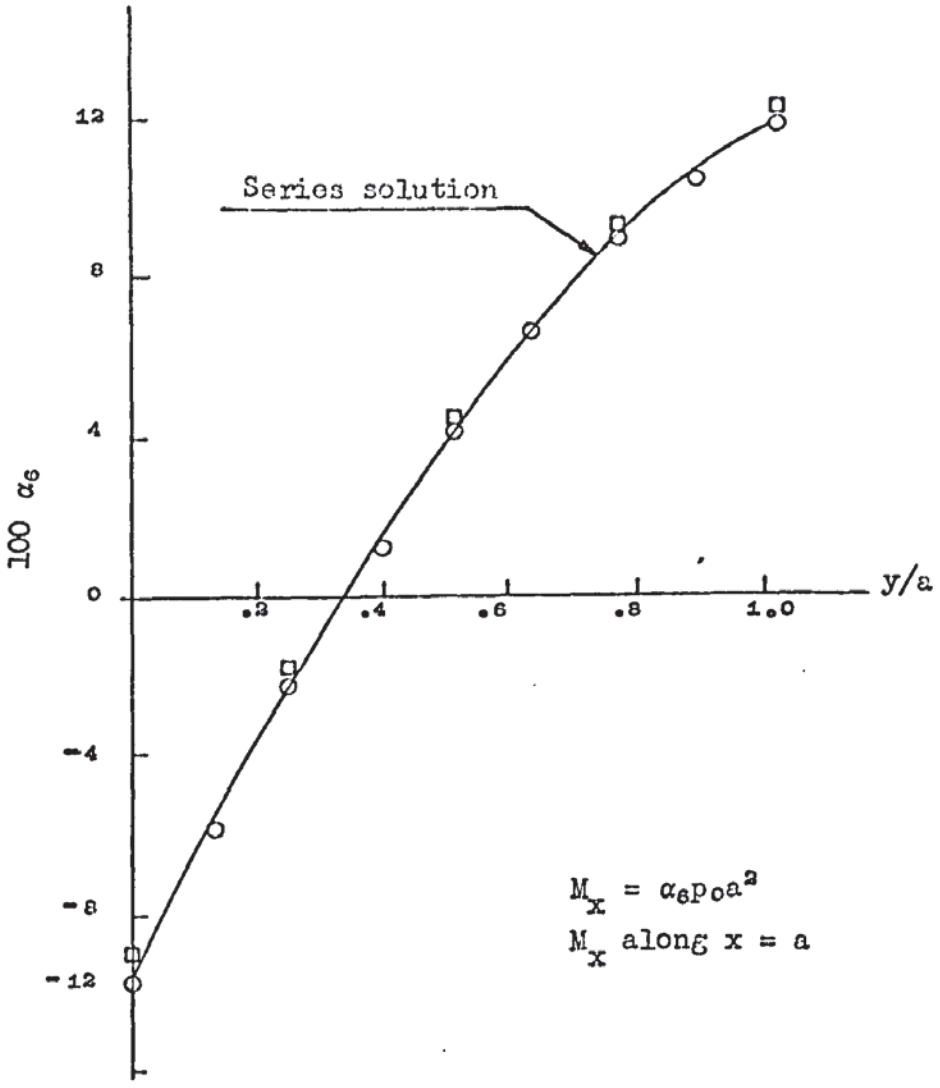
12
8
4
0
-4
-8
-12
100 α_6
Series solution
.2
.4
.6
.8
1.0
y/a
$M_x = \alpha_6 p_o a^2$
M_x along x = a

(h)

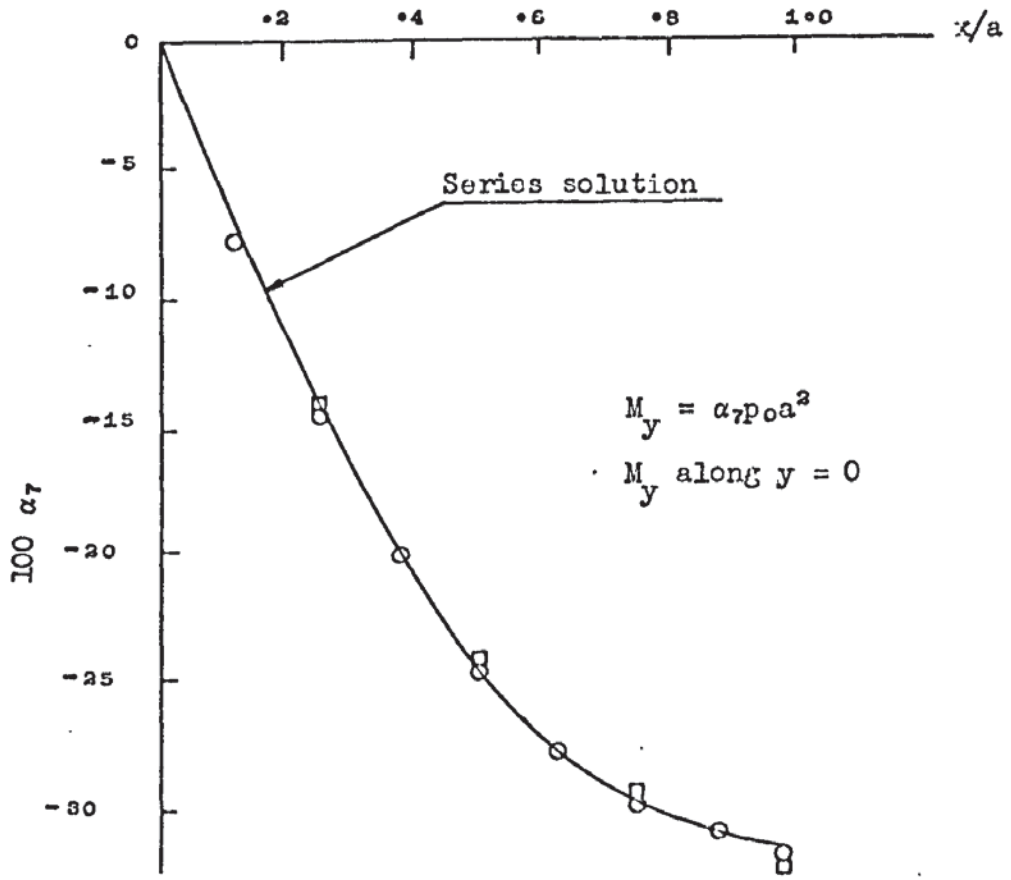
0
-5
-10
-15
-20
-25
-30
100 α_7
.2
.4
.6
.8
1.0
x/a
Series solution
$M_y = \alpha_7 p_o a^2$
M_y along y = 0

element solution and the series solution is very good and they show that the solution improves as the mesh is refined.

Table (9.2.8) shows the values for the maximum predicted parameters for the deflection and bending moment, M_x, at $x = a$, $y = a$ and for the maximum bending moment, M_y, at $x = a$, $y = 0$. The comparisons with the analytical values of ref.[10] give the following errors:

4.43% , 5.46% , 1.13%

1.15% , 1.27% , 0.28%

respectively for the two grids tested.

9.2.4) Comparison of the Convergence of the Mixed Element with other Elements.

Desai and Abel [30] investigated the rate of convergence of the central deflection of a clamped square plate, with a central concentrated load, for a certain number of elements derived using different plate bending element formulations. The basis for comparison was a function $N(BD)^2$. N is the number of equations used in the discretization and BD is the semi-bandwidth of the equations. $N(BD)^2$ is a useful measure of the computer time required to solve the equations.

Against the elements investigated in reference [30], the general mixed quadrilateral element is compared here.

A brief description of the elements taken for comparison is also included as part of Fig.(9.2.10). The graph of Fig. (9.2.10) shows that the mixed element converges well and shows competitive qualities. It should be emphasized that the results presented do not necessarily define the proper parameter comparison of accuracy and efficiency. The ideal measure should account for such factors as programming effort, time of solution, versatility and interpretability of results and should also take into account

TABLE (9.2.7) Deflection and Bending Moment for Case (2b)

		At x = a/2; y = 0
Mesh	$(W)_{max} \div \frac{P a^2}{D_o}$	$(M_x)_{max} \div P$
2 × 2	0.00693	-0.1075
4 × 4	0.00607	-0.1227
6 × 6	0.00584	-0.1214
Exact [10]	0.00560	-0.1257

TABLE (9.2.8) Deflection and Bending Moments for Case (3)

	x = a ; y = a		x = a ; y = 0
Mesh	$(W)_{max} \div \frac{P_o a^4}{D_o}$	$(M_x)_{max} \div p_o a^2$	$(M_y)_{max} \div p_o a^2$
4 × 4	0.06078	0.1236	-0.3154
8 × 8	0.05887	0.1187	-0.3181
Exact [10]	0.0582	0.1172	-0.319

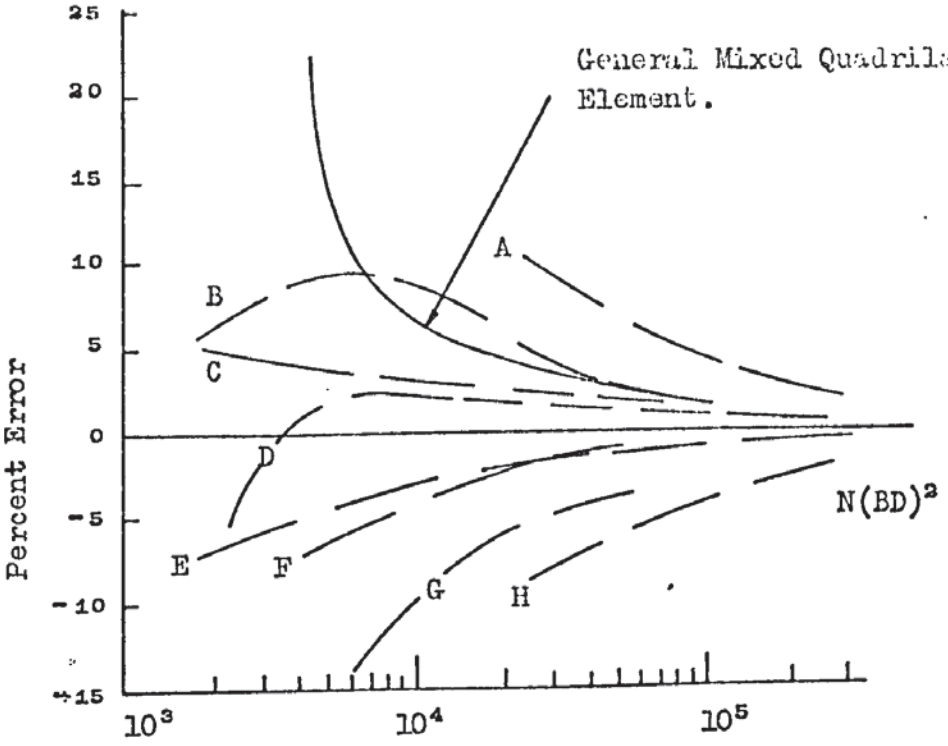

Symbol	Method	Description of Element
A	Force	2 triangles; linear moments.
B	Displacement	Nonconforming but complete; rectangle.
C	Force	2 triangles; linear stress function.
D	Displacement	Nonconforming but complete rectangle; cubic beam function plus uniform twist.
E	Displacement	4 triangles; cubic model.
F	Mixed (Lagrange Multiplier)	4 triangles; cubic disk-cements, quadratic stress parameter.
G	Hybrid (Equilibrium)	2 triangles; quadratic stresses, cubic interface displacements.
H	Displacement	2 triangles; cubic model.

Fig.(9.2.10) Comparison of the rate of convergence of the central deflection, for a simply supported square plate with a concentrated load.

the final results, that is the accuracy of the moments. The ability to solve plate problems taking shear deformations into consideration, without any extra computer effort is an important factor which adds to the attraction of the mixed element.

9.2.5) Concluding Remarks.

In the last three sub-sections the general mixed quadrilateral finite element is tested for convergence under the favourable conditions of uniformity of load and under the adverse conditions of concentrated loads.

The analysis shows that convergence to the correct solution is good except for the bending moments in the neighbourhood of the point load where we would not have expected good agreement because of the singular nature of the solution. The results of these numerical tests give a guide to the number of elements required to obtain a certain degree of accuracy. This experience is used in the next section in the solution of several problems for various shapes, loads, rigidity and combination of boundary conditions which show the "accuracy" of the element and its applicability.

The convergence properties of the element as represented by Fig.(9.2.10) are good and competitive with other finite elements. The mixed element has the important advantage that the effect of shear deformation, which is significant for moderately thick plates, can be taken into account with a minimum of effort and without increasing the number of degrees of freedom of the element, as happens in displacement models.

9.3) Static Plate Problems - General Applications.

In Section 9.2 the general mixed finite element was tested for convergence for several cases of load and boundary conditions. In this section the results from the mixed finite element program are compared for a number of problems with analytical and other numerical solutions. The loading conditions include uniform pressure, linearly varying pressure, a uniform line moment

and a uniform shear load. The problem of a plate, the thickness of which varies according to some known expression and that of a plate with a hole, are also analysed. The geometric shapes involved are respectively a skew, a square and a circular plate with a central hole. The symmetric properties of the plates are taken into account whenever it is possible and convenient.

The comparisons are shown graphically whenever there are available solutions, otherwise deflections and beding moments are compared at specified points. In each individual case the information regarding the boundary conditions, applied load, rigidity and the grid used are shown in the relevant figure. The letters designating the boundary conditions are respectively

F - Free

C - Clamped

S - Simply Supported.

In some cases, the identifier BM is used to mean either M_y or M_x as appropriate.

9.3.1) Discussion of Results.

In the preceding section, several problems were solved to test the accuracy of the general mixed finite element and to demonstrate its versatility in the solution of flexural plate problems.

It can be seen that the agreement of the predicted solutions from the mixed finite element with those from other methods is in general excellent. The only exception is the bending moment, M_x, along $x = 0$, (Fig.9.3.6), in the solution of the problem of Case (3). The value of this moment, at the edge where the uniform line moment M_o is applied, is found to be very large as compared with the finite difference method [70]. Elsewhere in the plate, the agreement from both solutions is very good.

The accuracy of the results has proved to be, generally, good. However, there are a few points which deserve particular attention.

The solution of Case (1) was intended to show the expected "accuracy" of the element and its applicability to a very important and difficult class of problems of frequent occurrence in engineering. The solution of these skew plates have only been reported for "thin" skew plates under a uniformly distributed load or a concentrated load at the centre and they were only solved for a very limited range of angles of skew. The graphical results of Fig.(9.3.2) show clearly the good behaviour of the normal bending moment given by the mixed finite element when compared with the solution given by Morley [71] along the edge AA'. It is known, ref.[71], that the normal edge bending moment M_n should have zero values at the corners of a clamped skew plate. Regarding this particularity the mixed finite element gives a better result since the value at the acute corner given by Morley [71] fails to obtain zero, where the value by the present approach was practically zero. The values at the centre of the plate (Table 9.3.1) show a discrepancy of about 4.6% for the maximum deflection, and 11 and 5% for the maximum and minimum principal bending moments respectively. An increase in the number of elements will improve the accuracy.

The problem of the circular plate with a hole again shows the applicability of the element in the solution of general plate problems, where the moments at the edges require a transformation of axes, as seen in Section 5.5, prior to the imposition of the proper boundary conditions. This case was solved in accordance with the classical and moderately thick plate solution and the results are shown on Table (9.3.2) and Fig.(9.3.10). The errors in the maximum deflection and bending moment were respectively 2.12

CASE (i) C-C-C-C

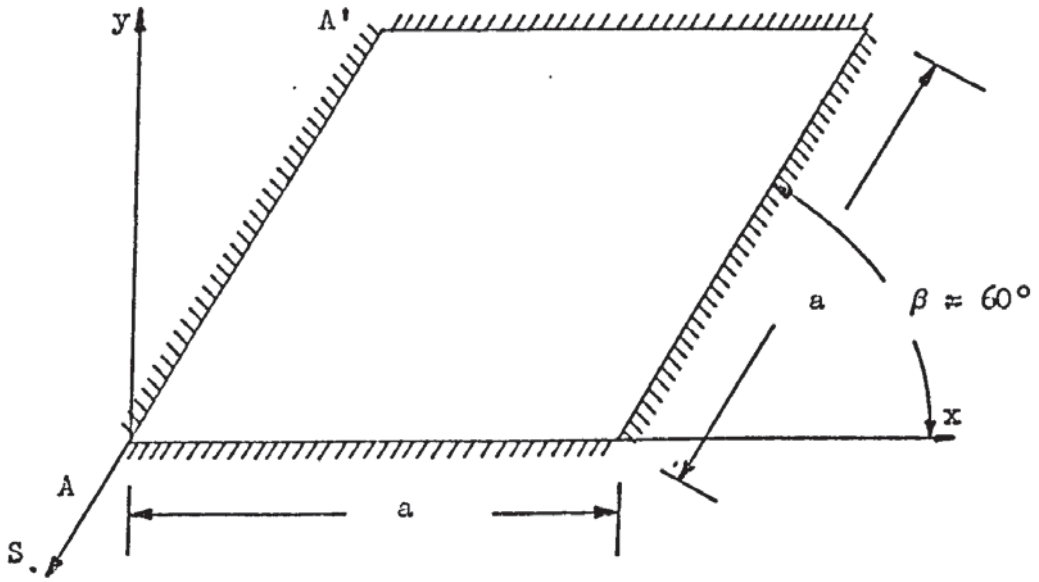

$D = D_o$; $p = p_o$; $\mu = 0.3$

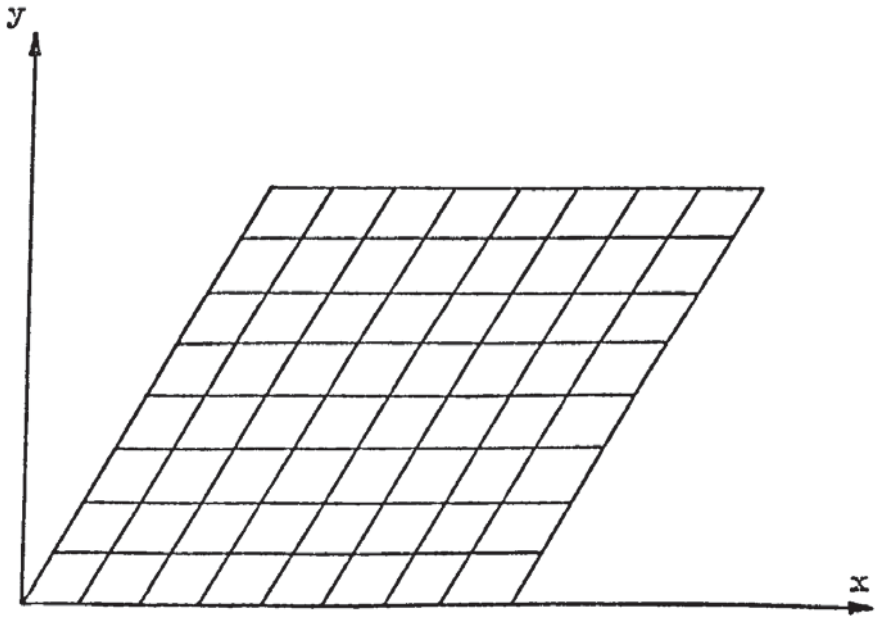

Fig.(9.3.1)

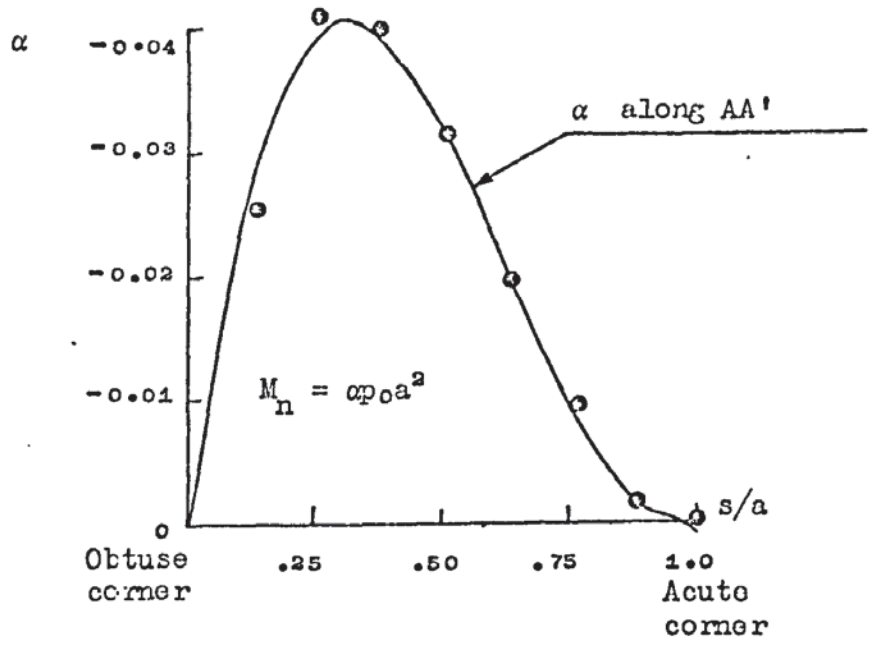

Fig.(9.3.2) Solution to case (i)
—— Variational Solution of two successive boundary value problems (ref.[71])
(o) Mixed Finite element.

TABLE (9.31) Deflection and Principal Bending Moments for case (i)

	Values at the Centre		
	$(W)_{max} \div p_o a^4/D_o$	$(M_p)_{max} \div p_o a^2$	$(M_p)_{min} \div p_o a^2$
Mixed F.E.	0.000804	0.02196	0.01621
Morley [71]	0.000769	0.01979	0.01544

CASE (ii) S-C-C-C

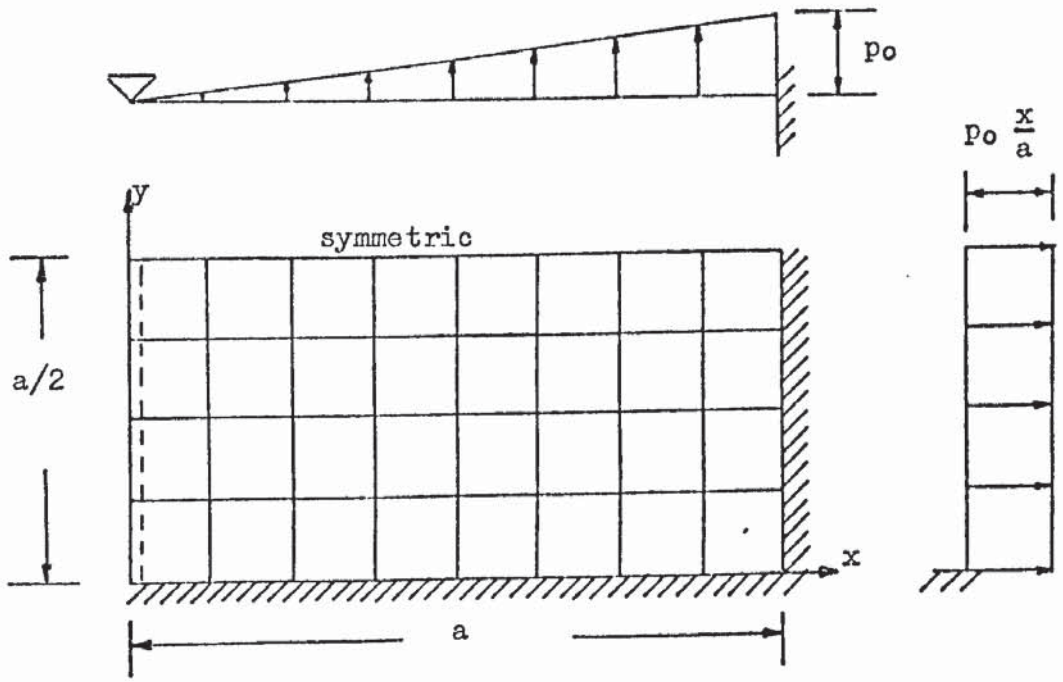

$D = D_o$, $\mu = 0.2$

Fig.(9.3.3)

CASE (iii) C-C-C-F

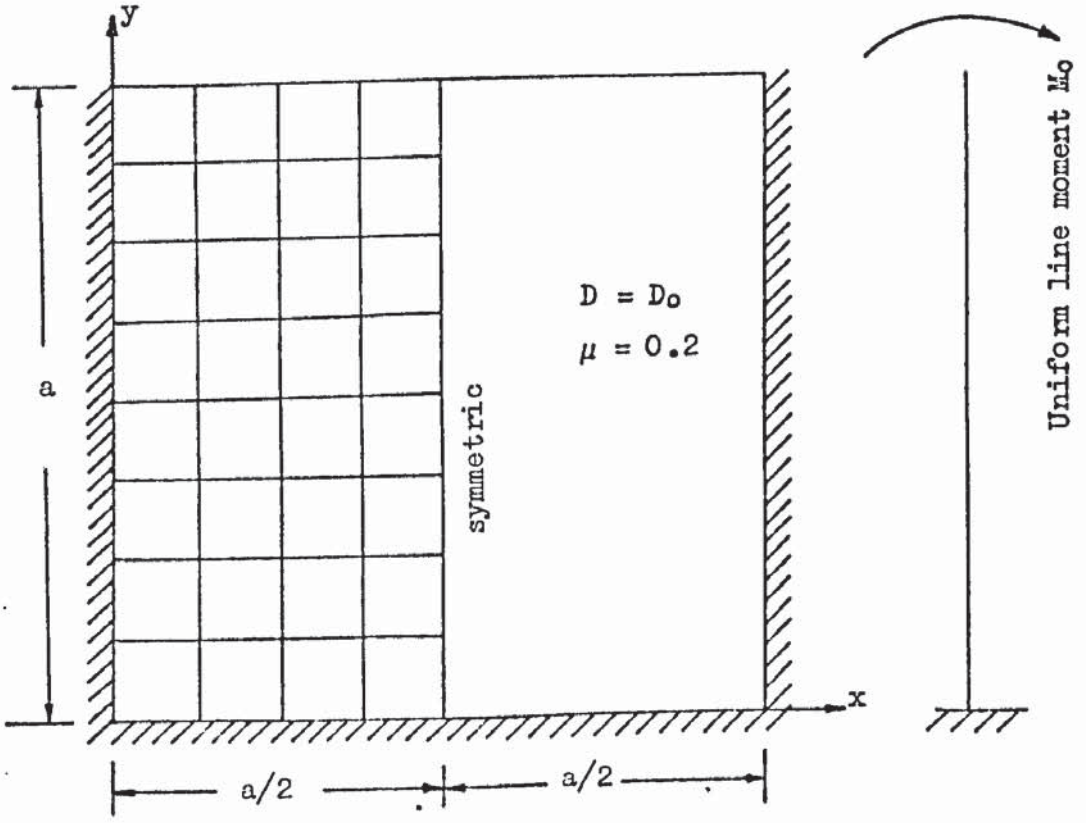

Fig.(9.3.4)

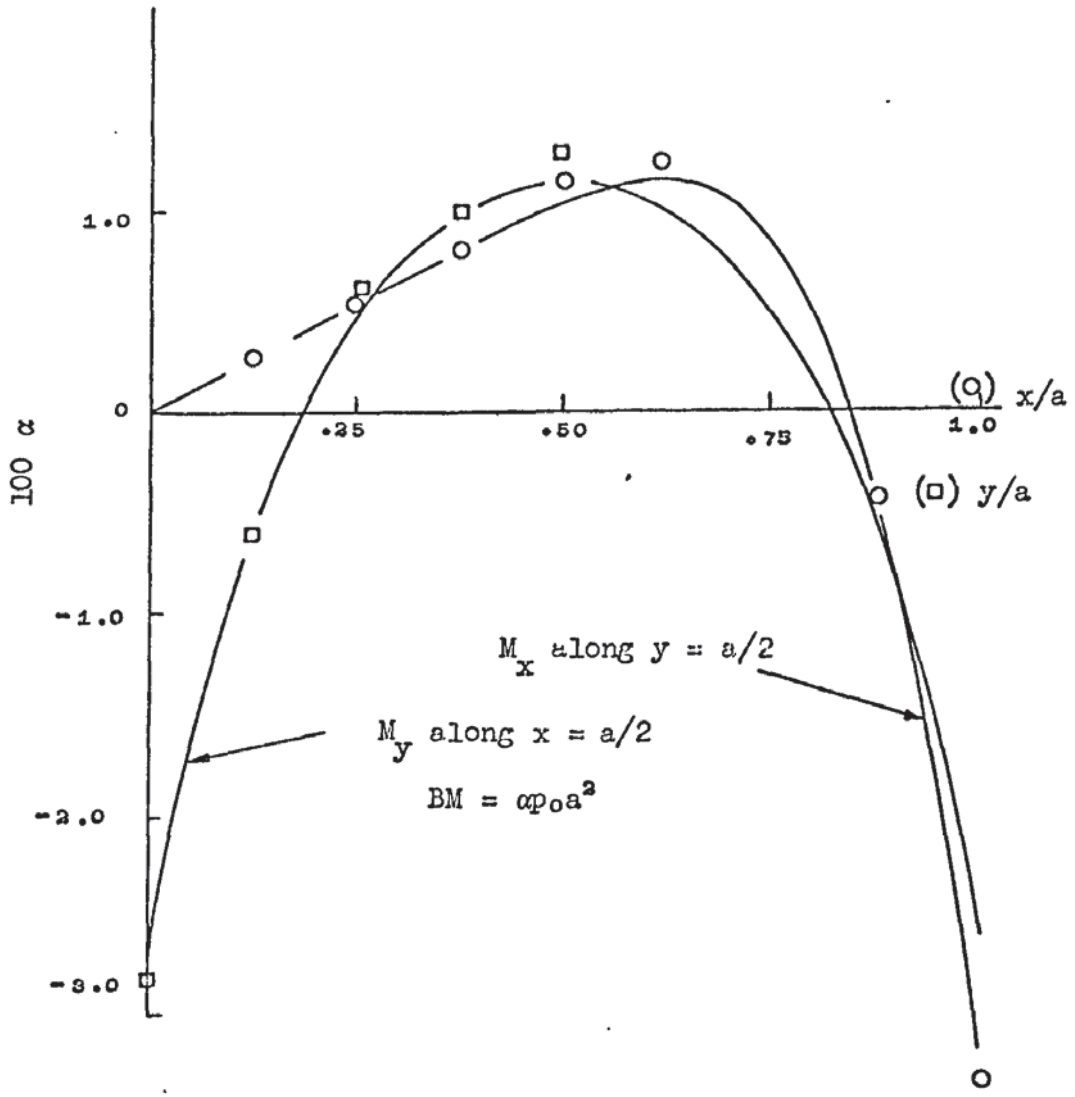

Fig.(9.3.5) Solutions to case (ii)

(□),(○) Mixed Finite Element Method
____ Finite Difference Method (ref.[70]).

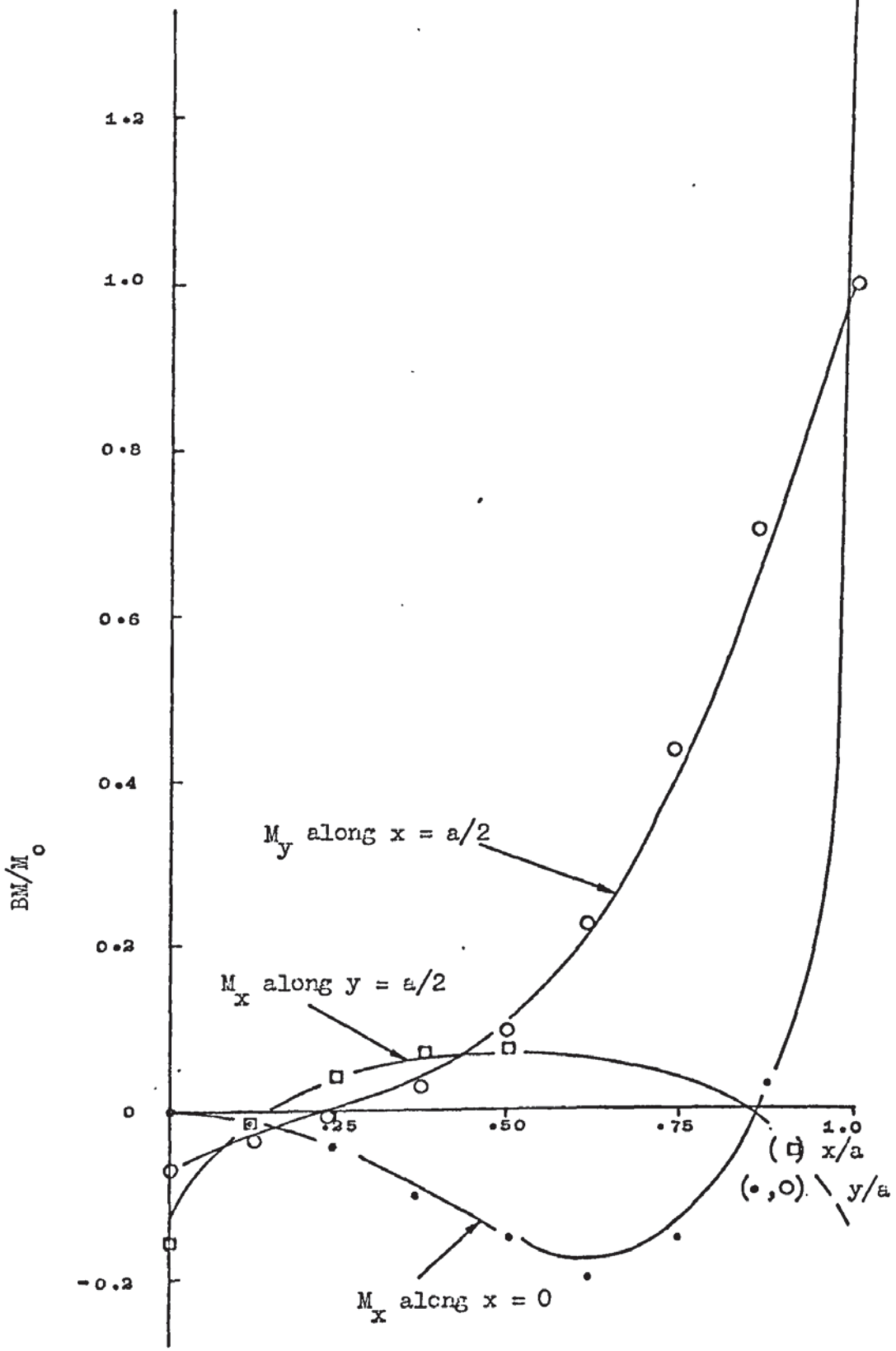

Fig.(9.3.6) Solutions to case (iii)

(•),(○),(□) Mixed Finite Element Method

——— Finite Difference Method (ref.[70]).

CASE (iv) Variable Thickness C-S-S-S

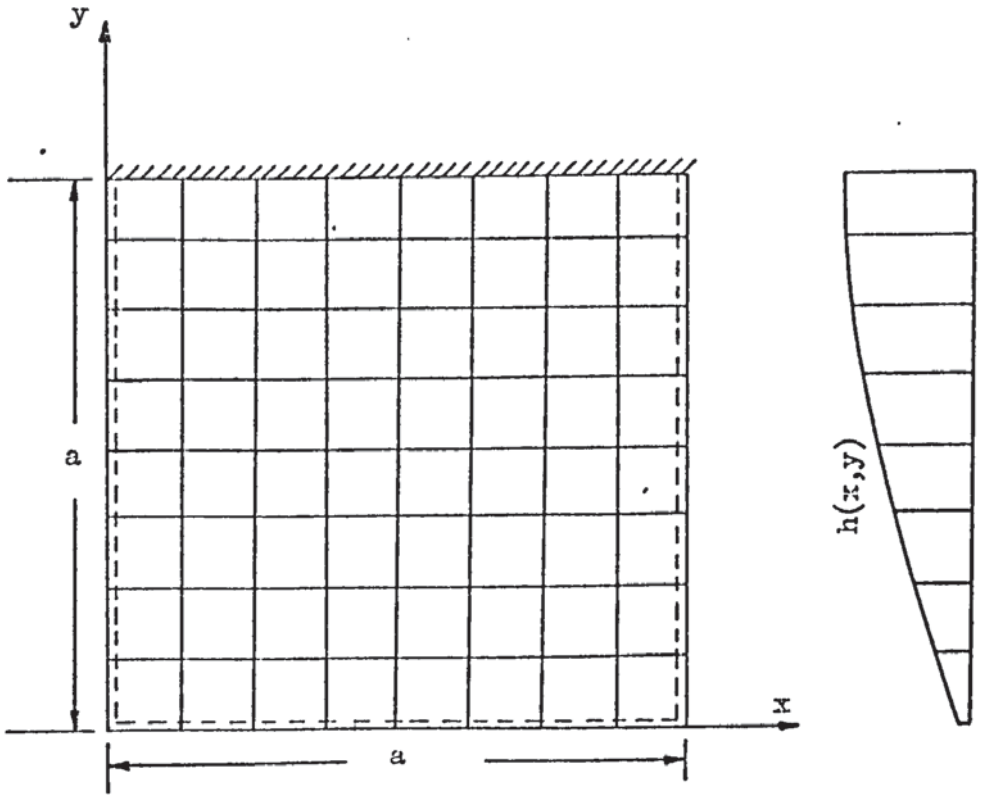

$p=p_o, \mu=0.25$

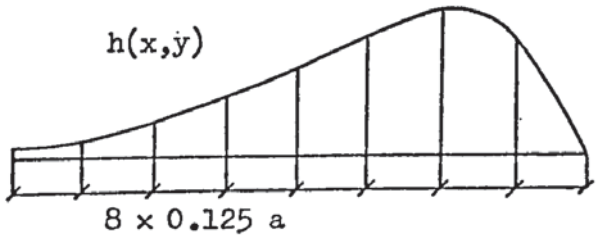

The thickness of the plate, h, is given by:

$$h = 2\sin\left(\frac{\pi}{6} + \frac{\pi y}{3a}\right)\left[0.1674+2.175\left(1-\frac{x}{a}\right)^{\frac{1}{2}}\left(\frac{x}{a}\right)\right].$$

The rigidity, $D(x,y)$ is expressed in terms of the rigidity D_o, at $x = \frac{5}{8}a$, $y=0$ at which point $h = 1$.
The plate is divided into an 8×8 square mesh.

Fig.(9.3.7)

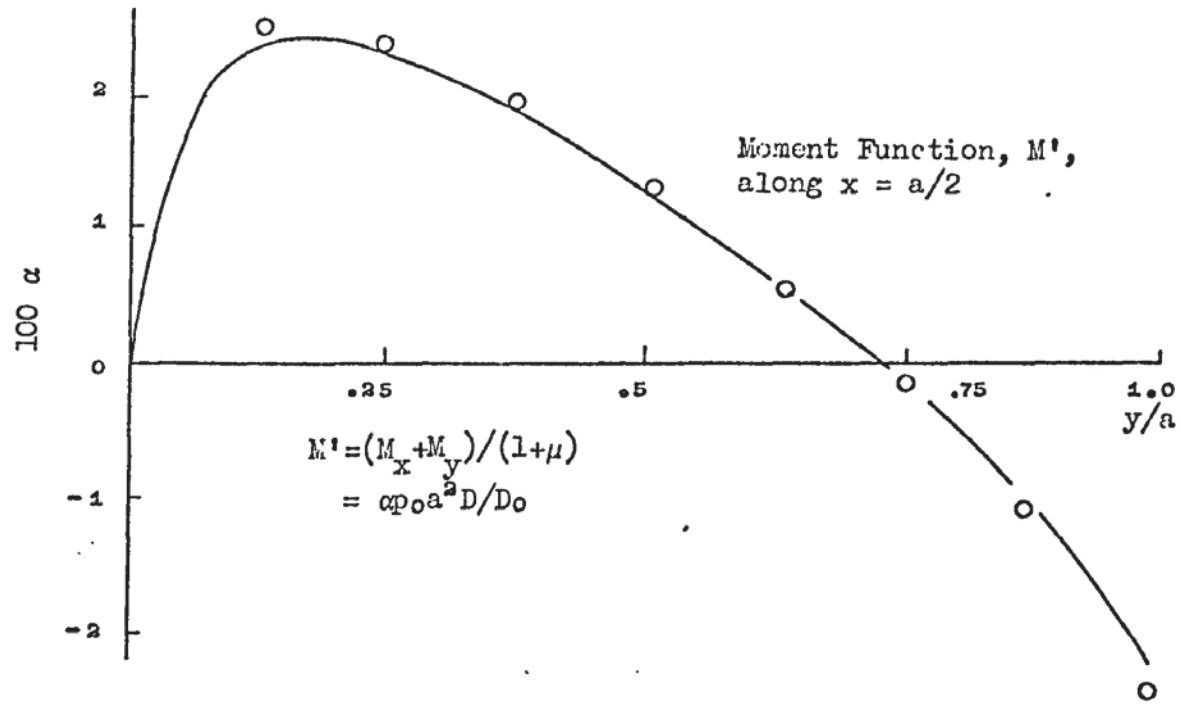

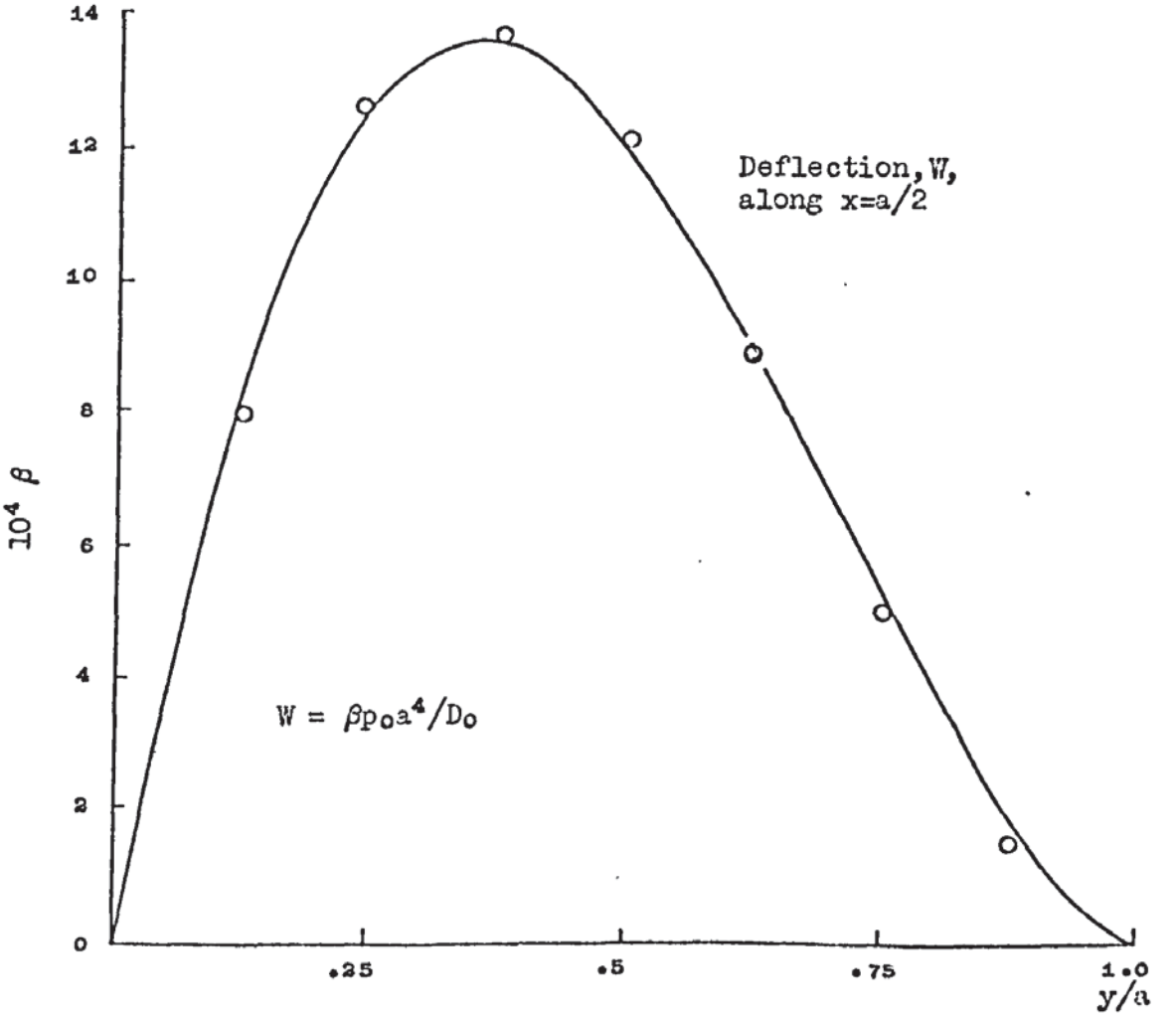

Fig.(9.3.8) Solutions to case (iv)
(o) Mixed Finite Element
—— Finite Difference Method with pure resistance electrical analogue computer (ref [72]).

CASE (v) Circular Plate S-F

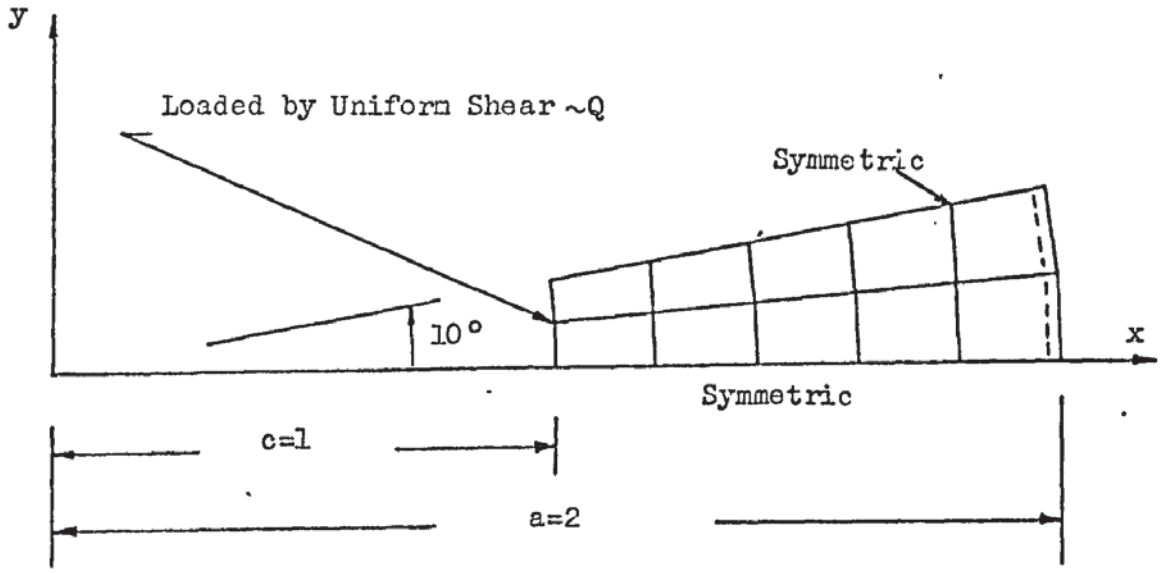

(a) Thin Plate $D = D_o$; $\mu = 0.3$

(b) Thick Plate

$$\alpha = \left(\frac{h}{2a}\right)^2 \quad ; \quad \beta = \frac{3(1-\mu^2)a^2 \, c \, Q}{E_o h^3}$$

$$\mu = 0.3$$

For $\alpha = 0.06$; 0.14 ; 0.25

Fig.(9.3.9)

TABLE (9.3.2) Deflection and Bending Moment for Case (va) "Thin Plate"

$\frac{a}{c} = 2$	At x = c , y = o	
	$(W)_{max} \div Q\ a^2/D_o$	$(BM)_{max} \div Q$
Mixed Finite Element	0.3784	1.543
Exact[10]	0.3866	1.5550

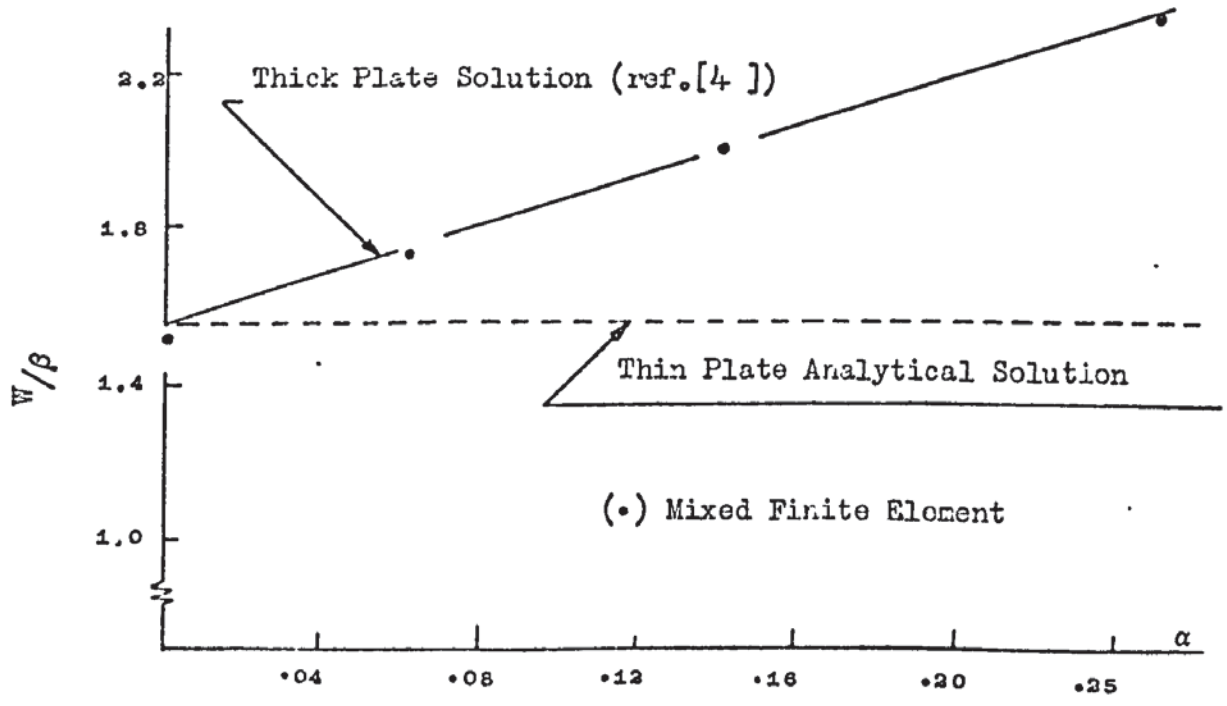

Fig.(9.3.10) Solutions for case (v,a,b).

and 0.45% for the classical thin plate solution. The "exact" thick plate solution was obtained by the perturbation approach and shown graphically in reference [4]. The agreement between the approximate solution and the thick plate analysis is excellent.

9.4) Experimental Tests - Static Problems.

In Sections 9.2 to 9.3, results from the main computer program for various cases of static loading, geometry and boundary conditions were compared with known published results in order to test the accuracy of the general quadrilateral mixed finite element. It was felt that experience in an experimental method for the analysis of plates would be a desirable complement. At the same time a further test on the applicability of the general quadrilateral mixed finite element when applied to the solution of thin plates of varying rigidity, under static loading, may be obtained through the experimental procedure. The Moire Technique, which was developed by Ligtenberg [73] in 1955 for the experimental analysis of transversely loaded plates, was used for these purposes.

The fundamentals of the Moire Technique and the technical and experimental details may be found in Appendix 6.

9.4.1) Details of the Test Cases.

The experimental technique was used to find the slopes in three different plate problems, namely:

Case (1) - A square clamped plate with uniform thickness under uniform pressure (Fig.9.4.1a).

Case (2) - A square clamped plate with a central portion whose thickness was twice that of the remainder of the plate, also under uniform pressure (Fig.9.4.1b).

Case (3) - A square clamped plate with central square hole, under two concentrated loads (Fig.9.4.1c).

9.4.2) Comparison of Results from the Computer Program with Those from the Experiment.

To analyse the three cases shown in Fig.(9.4.1) it was necessary to find the flexural rigidity D of a 5 mm thick black perspex sheet having the same material specification as the plate models. A square piece of black perspex loaded at its four corners was used in the manner described by Lightenberg [73] and the experimental value was found to be 3648.34 N.cm, for $\mu = 0.335$.

The photographs of the fringe patterns representing $\frac{\partial N}{\partial x}$ are respectively shown for cases (1), (2), (3) by Figs.(9.4.2), (9.4.3), (9.4.4a). Fig.(9.4.4b) gives the fringe pattern of $\frac{\partial N}{\partial y}$ for test case (3). The fringe patterns of $\frac{\partial W}{\partial y}$ for case (1) and (2) are not represented. However, due to symmetry about two perpendicular axes, they can be obtained by turning the Figs.(9.4.2, 9.4.3) through 90°. The fringe patterns were analysed as described in the Appendix 6, sub-section A.6.7, and the variation of the slopes across the plate were plotted (Fig.9.4.5a, 9.4.6a,9.4.7a,b). Because of the symmetry of the problems the slopes are only given for half a model. By graphically integrating these slope curves, as explained in Appendix 7, we obtained the experimental deflection variations along the same section of the plate, which are respectively shown in (Figs.9.4.5b, 9.4.6b, 9.4.8 a,b). The corresponding deflections from the mixed finite element model were also plotted.

It can be seen that in test cases (1) and (2) the agreement between the experimental and the mixed finite element on the values of the deflection along the section y = 17.8 cm,

is excellent. The agreement for the deflection along sections x = 7.8 cm and y = 15.2 cm shows a relatively large difference in the values of the two methods for case (3).

Tables (9.4.1), (9.4.2), (9.4.3) show the comparison of experimental bending moments and the mixed finite element results for cases (1), (2), (3) at certain points. The agreement is excellent for case (1). For case (2) the difference in the value of the maximum bending moment at the clamped boundary, x = 0, y = 17.8 cm is very large. The discrepancy may be attributed to errors due to the last interference fringe at the built-in edge being at some little distance from that edge. Also the fringe photographs were only enlarged to half the size of the model, hence errors due to the graphical differentiation (Appendix 7) are more pronounced. The moments for case (3), obtained from half scale fringe photographs, have shown a relatively large difference especially at the point x = 7.8 cm, y = 15.2 cm. The apparent analytical reason for the discrepancy might be the presence of a hole and a concentrated load near by. However, since the deflections were also not very good, it is believed the discrepancy is due to experimental errors. As a proof that the discrepancy is due to experimental errors, the slopes $\frac{\partial w}{\partial y}$ along x = 6.0 cm were plotted (Fig.9.4.9), and compared with the values obtained directly from the semi-analytical finite element method of reference [74], and they also show a very large discrepancy.

9.4.3) Concluding Remarks.

The objective of the experiment was to gain practical knowledge of the Moire Technique for the experimental analysis of thin plates in bending, and to check the results from the computer program with a source other than analytical or numerical solution.

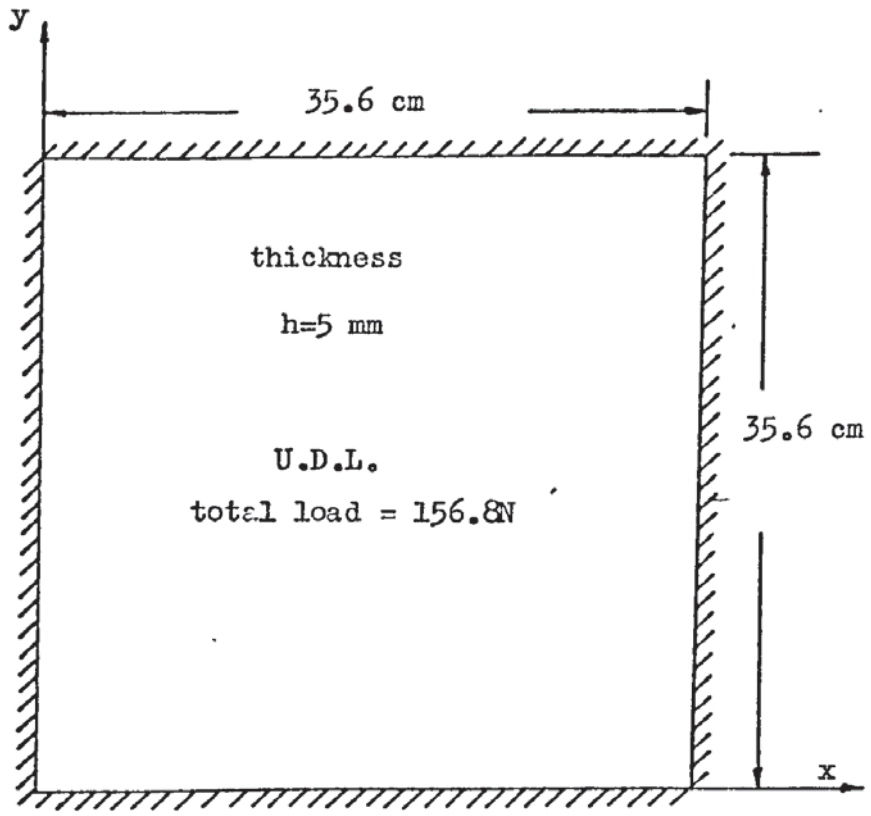

(a) case (1)

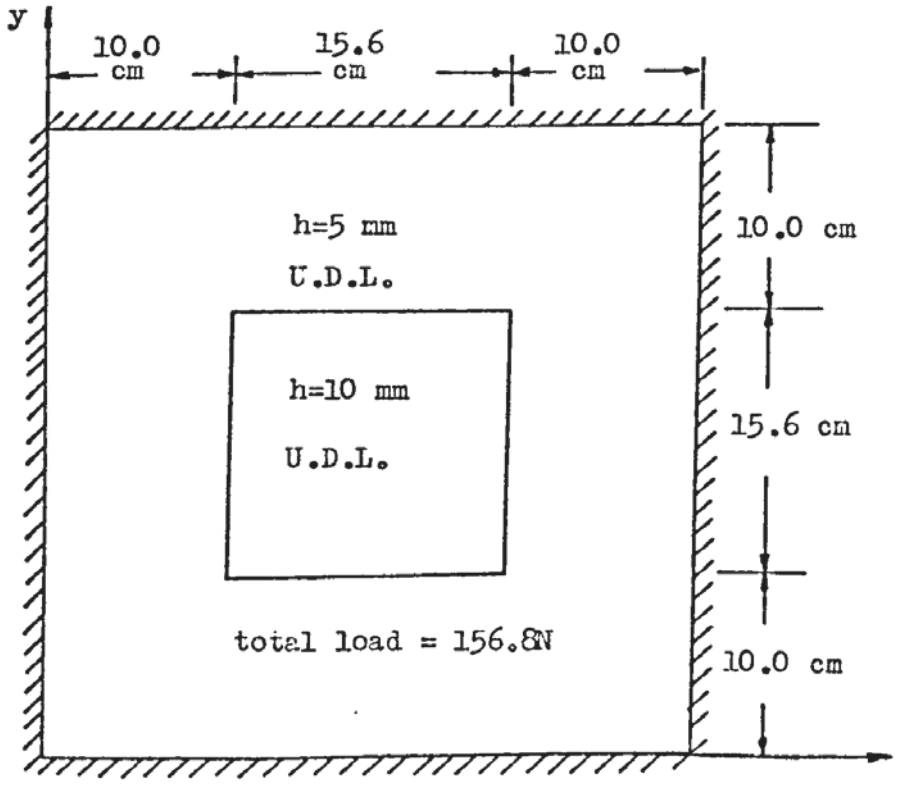

(b) case (2)

Fig.(9.4.1) Details of experimental test cases.

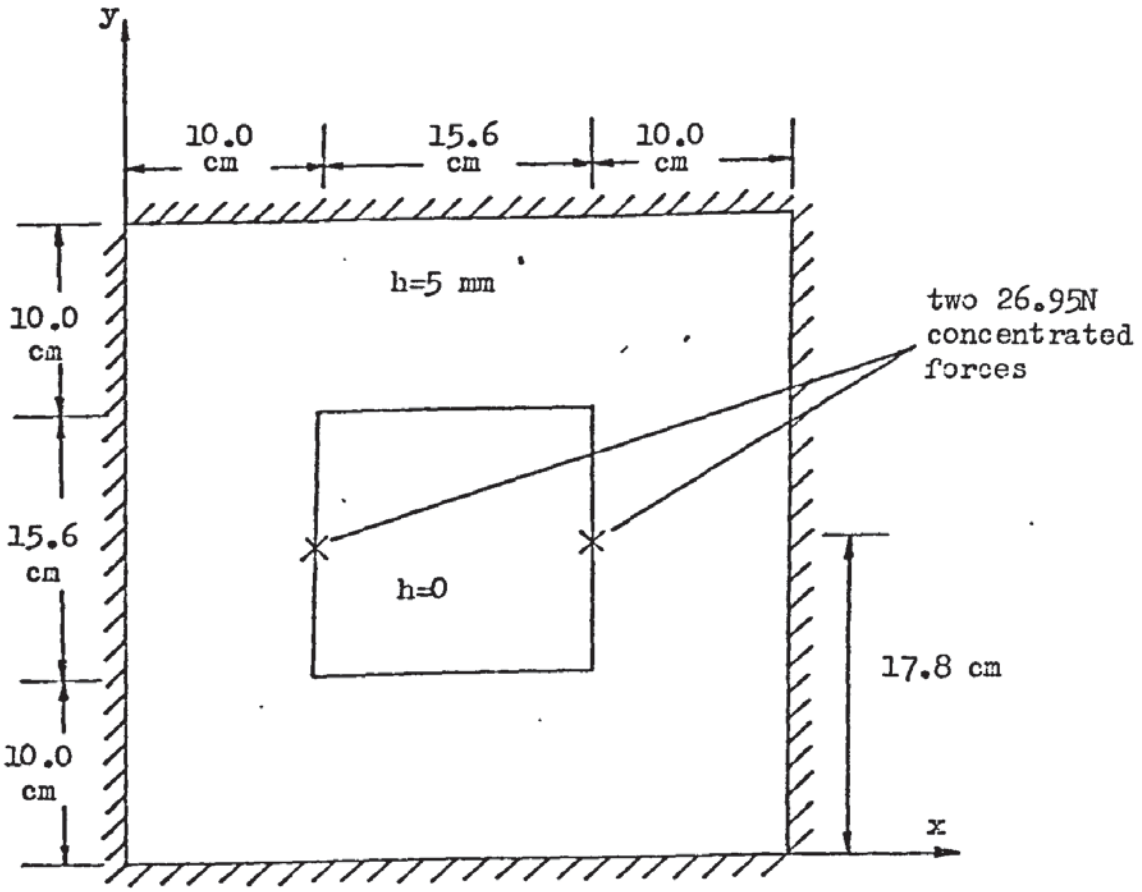

Fig.(9.4.1c) case (3).

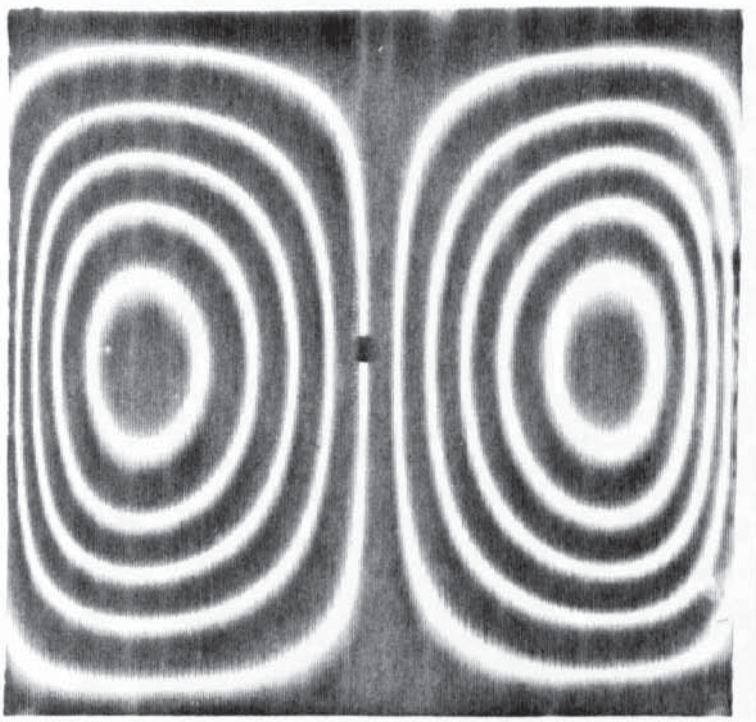

Fig.(9.4.2) Fringe photograph of the slope $\frac{\partial W}{\partial x}$ for the problem in test case (1)

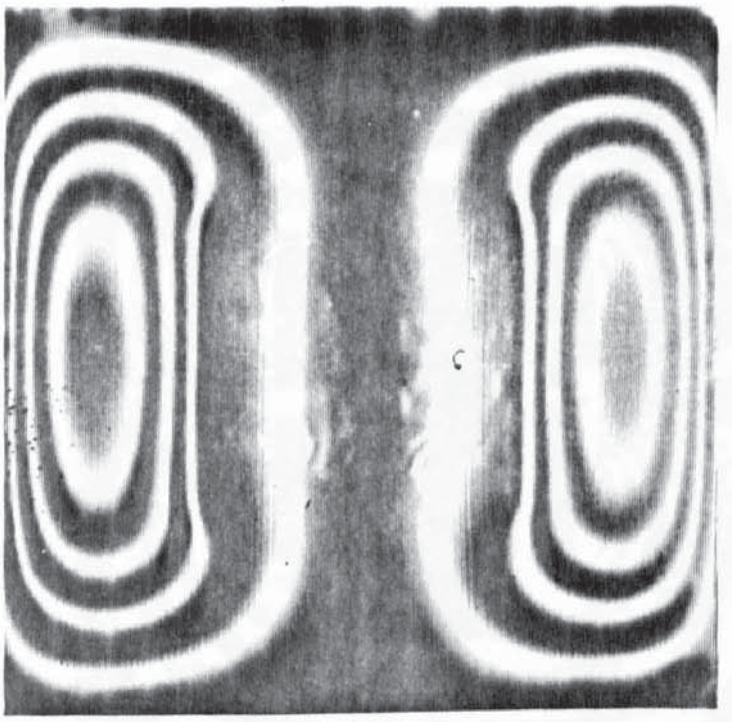

Fig.(9.4.3) Fringe photograph of the slope $\frac{\partial W}{\partial x}$ for the problem in test case (2).

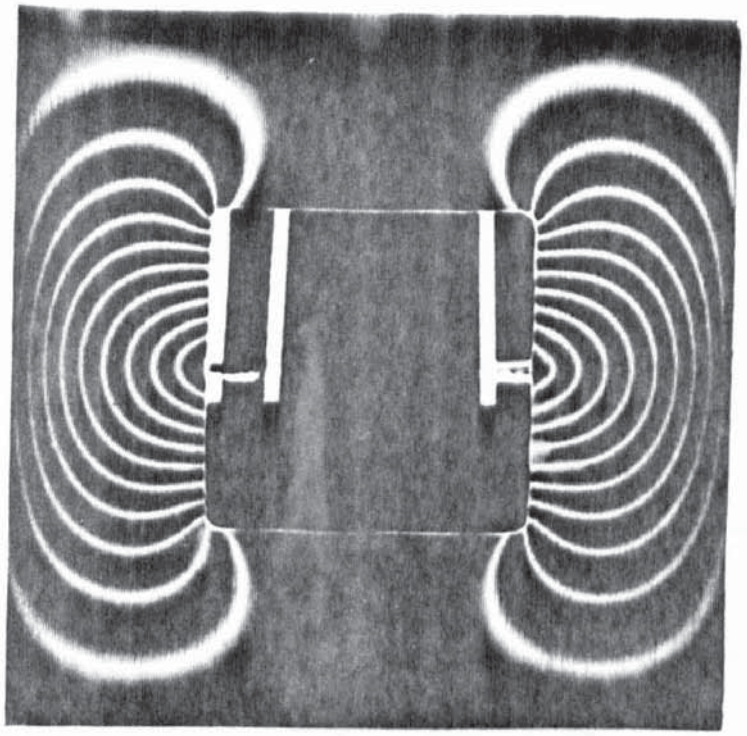

Fig.(9.4.4a) Fringe photograph of the slope $\frac{\partial W}{\partial x}$ for the problem in test case (3)

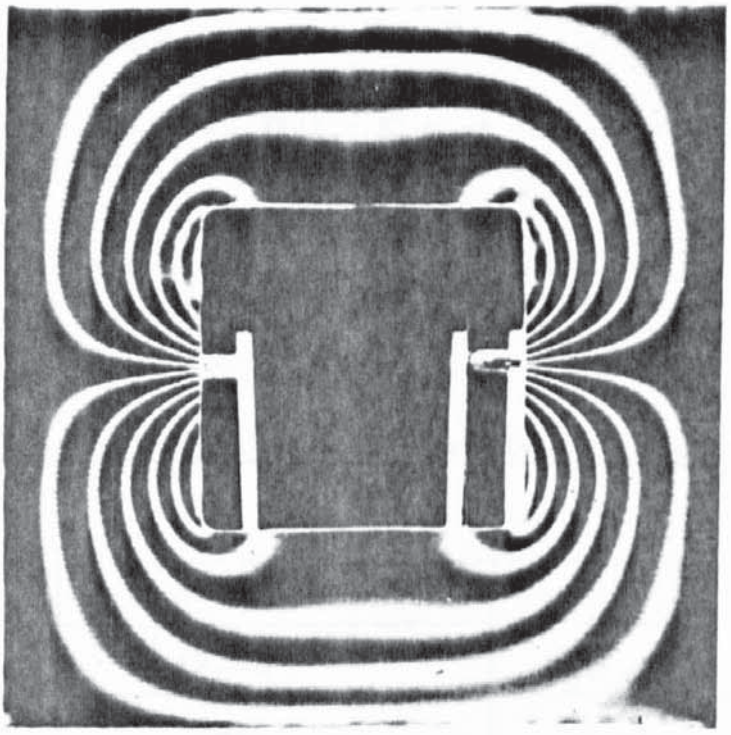

Fig.(9.4.4b) Fringe photograph of the slope $\frac{\partial W}{\partial y}$ for the problem in test case (3)

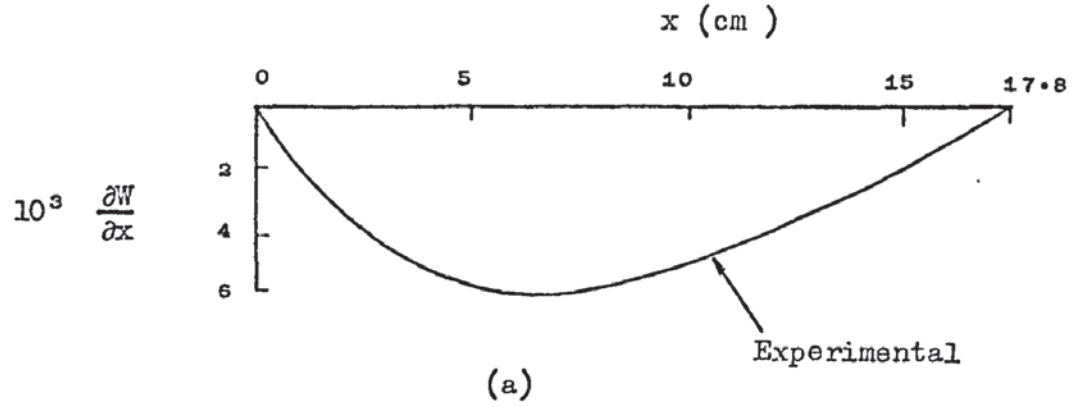

(a)

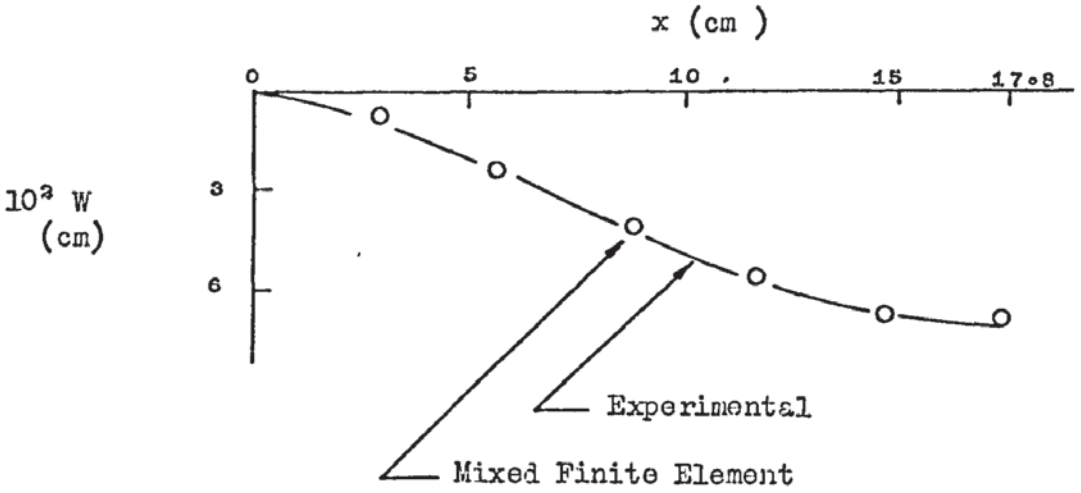

(b)

(a) - Experimental values of the slope $\frac{\partial W}{\partial x}$ along y=17.8 cm, for case (1).

(b) - Experimental and Mixed Finite Element values of the deflection along y=17.8 cm, for case (1).

Fig.(9.4.5)

TABLE (9.4.1) Deflection and Bending Moments for Case (1)

	Centre of Plate	Edge x=0; y=17.8 cm
	M_x(N.cm)	M_x(N.cm)
Experimental	3.82	-7.63
Mixed (6x6)	3.72	-8.00
Exact [10]	3.62	-8.04

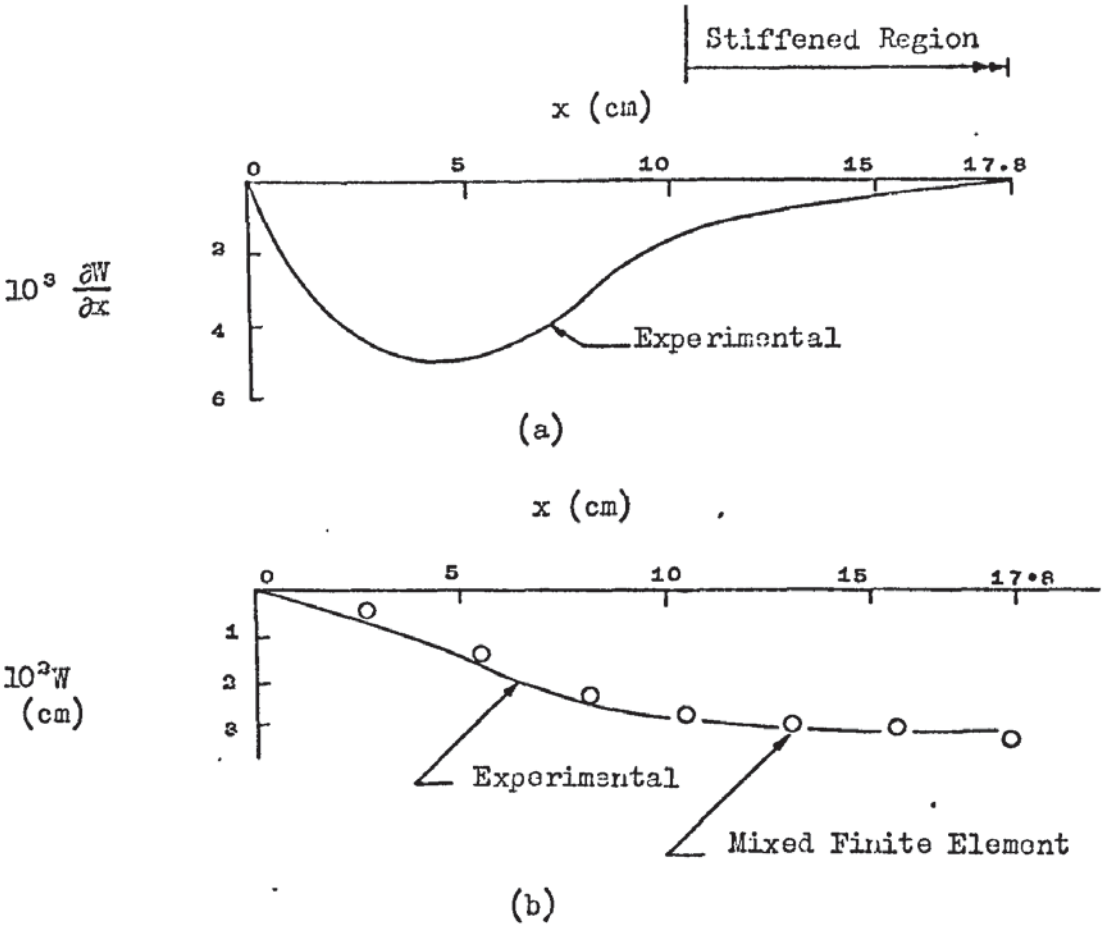

(a) - Experimental values of the slope $\frac{\partial W}{\partial x}$ along y=17.8 cm, for case (2).

(b) - Experimental and Mixed Finite Element values of the deflection along y=17.8 cm, for case (2).

Fig.(9.4.6)

TABLE (9.4.2) Bending Moments for Case (2).

	Centre of Plate	Edge x=0; y=17.8 cm
	M_x (N.cm)	M_x (N.cm)
Experimental	0.639	-1.34
Mixed (7x7)	0.641	-0.659

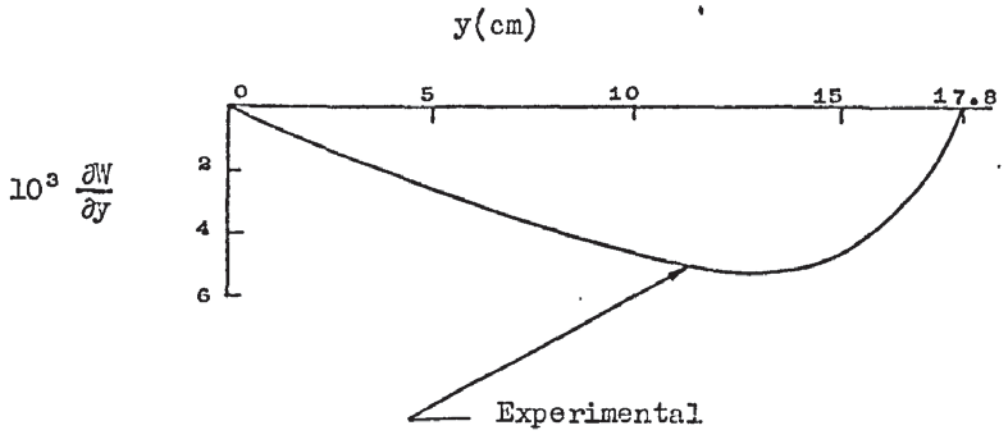

Fig.(9.4.7a) Experimental values of $\frac{\partial W}{\partial y}$ along x=7.8 cm, for case (3).

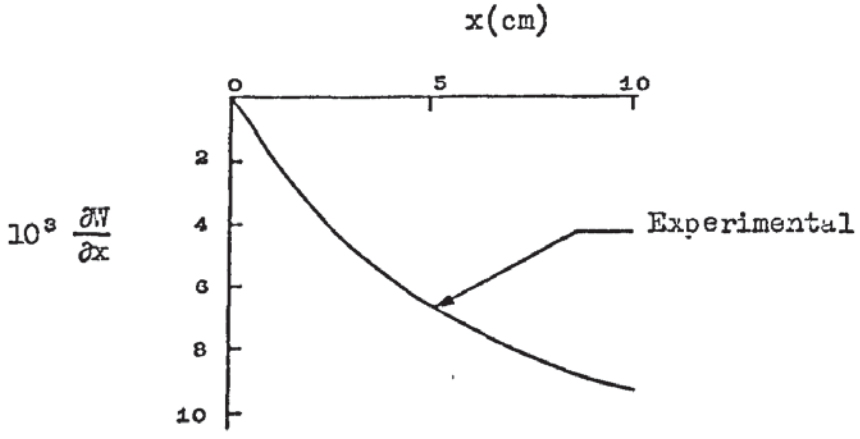

Fig.(9.4.7b) Experimental values of $\frac{\partial W}{\partial x}$ along y=15.2 cm, for case (3).

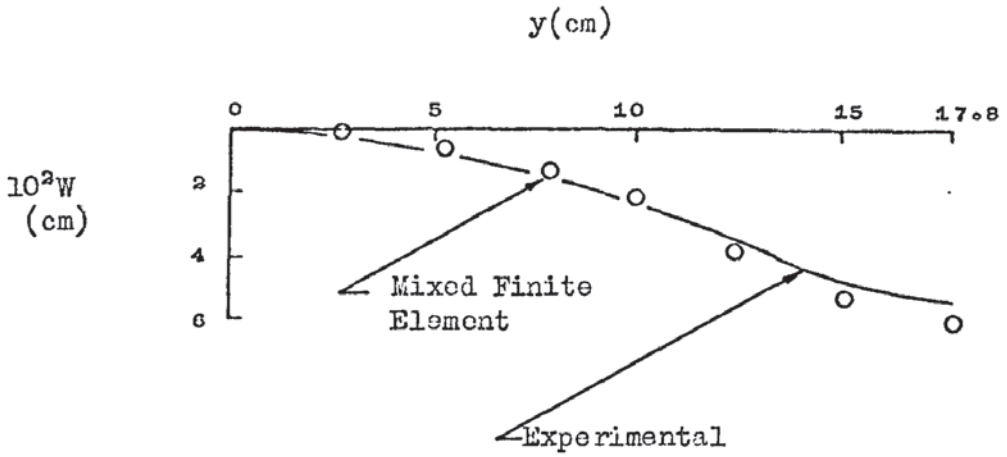

Fig.(9.4.8a) Experimental and Mixed Finite Element values of the deflection along x=7.8 cm, for case (3).

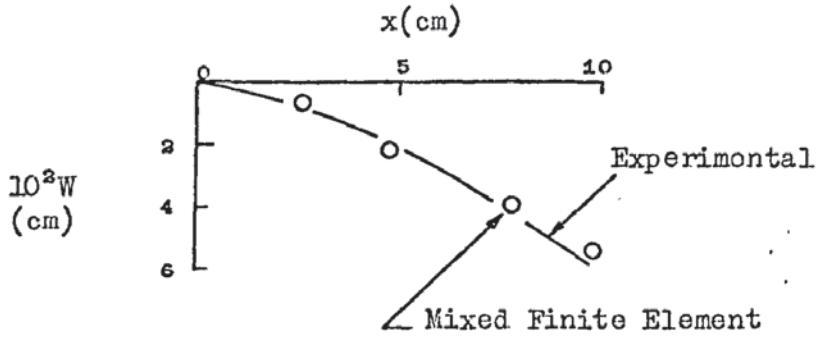

Fig.(9.4.8b) Experimental and Mixed Finite element values of the deflection along y=15.2 cm, for case (3).

TABLE (9.4.3) Bending Moments for Case (3)

	At x = 0; y = 15.2cm	At x = 7.8 cm; y = 15.2 cm	
	M_x(N.cm)	M_x(N.cm)	M_y (N.cm)
Experimental	8.0	0.75	2.4
Mixed	9.6	0.24	5.6

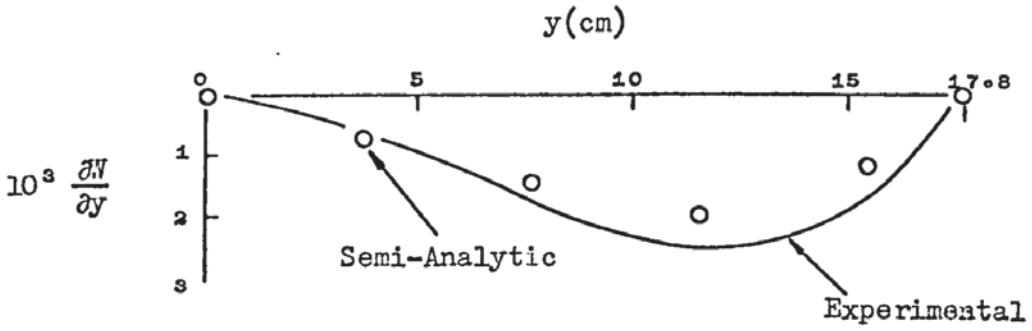

Fig.(9.4.9) Experimental and Semi-Analytic values of the slope $\frac{\partial W}{\partial y}$ along x=6.0 cm, from computer program of reference [74], for case (3).

It was noticed that there are too many sources of error in the technique to be as simple as it is theoretically. Difficulties were experienced in the application of the load to simulate uniform pressure. The number of levers with concentrated loads which could be applied at the same time were limited to two due to the structure arrangement of the apparatus and levers. It is very difficult to keep the load pins horizontal and without buckling.

The use of the black perspex, which is very good for the production of more fringes, makes it difficult to determine an appropriate value of the bending rigidity, D, and to be sure of the exact value of the applied load. This is due to a great increase in the creep rate due to the variations in temperature of the model experienced during the experiment.

9.5) Free Vibrations.

In this section, the general mixed quadrilateral element is tested for convergence and accuracy in the solution of free vibration of thin plate problems. Three plate problems are solved. Since analytical solutions are seldom known, the predicted results are also compared with experimental and other finite element solutions.

9.5.1) Simply Supported Plate.

The natural frequencies of the simply supported square plate, Case (1), shown in Fig.(9.5.1), were predicted by the mixed general quadrilateral element using 2×2, 4×4, 6×6 and 8×8 finite element meshes to represent the plate. These results are compared with the analytical solutions. The results for the 8×8 mesh are obtained by solving a 4×4 mesh representation of one quarter of the plate by taking consideration of the symmetry

conditions.

The results of Table (9.5.1) show that the fundamental frequency of the plate can be predicted within 1% with relatively little computing effort. The accuracy of this frequency predicted by 2 × 2, 3 × 3, 4 × 4, 6 × 6 and 8 × 8 meshes were 12 , 6 , 3 , 1.5, 1% respectively.

The accuracy of the frequency of the second mode predicted by a 3 × 3, 4 × 4 and 6 × 6 meshes are within 24 , 15 , 7% of the theoretical value.

Also the 6 × 6 mesh is capable of predicting the first 8 natural frequencies with an error of 1 , 7 , 18 , 10 , 16 , 12, 11 and 5% respectively.

It should be noticed that for the 2 × 2, 3 × 3 , 4 × 4 and 6 × 6 meshes the final eigenvalue problem has only 1 , 4 , 9 and 25 degrees of freedom. Fig.(9.5.2) compares the efficiency of the mixed element with other displacement models when predicting the fundamental natural frequency of plates. It is seen from the curve corresponding to the final number of degrees of freedom of the eigenvalue problem, that the mixed element is very efficient and compares favourably with displacement elements. However, from the curve of the total number of degrees of freedom of the system, the mixed element is not as efficient as the displacement elements.

It can be concluded that the natural frequencies predicted by the mixed element model are converging to the exact values, but this convergence is not necessarily monotonical. Also an advantage of the mixed element is that the total number of degrees of freedom are reduced to a much smaller number and, therefore, the final eigenvalue problem is very small and can be solved without much computer effort. The element compares favourably with displacement elements.

Case (1) S-S-S-S

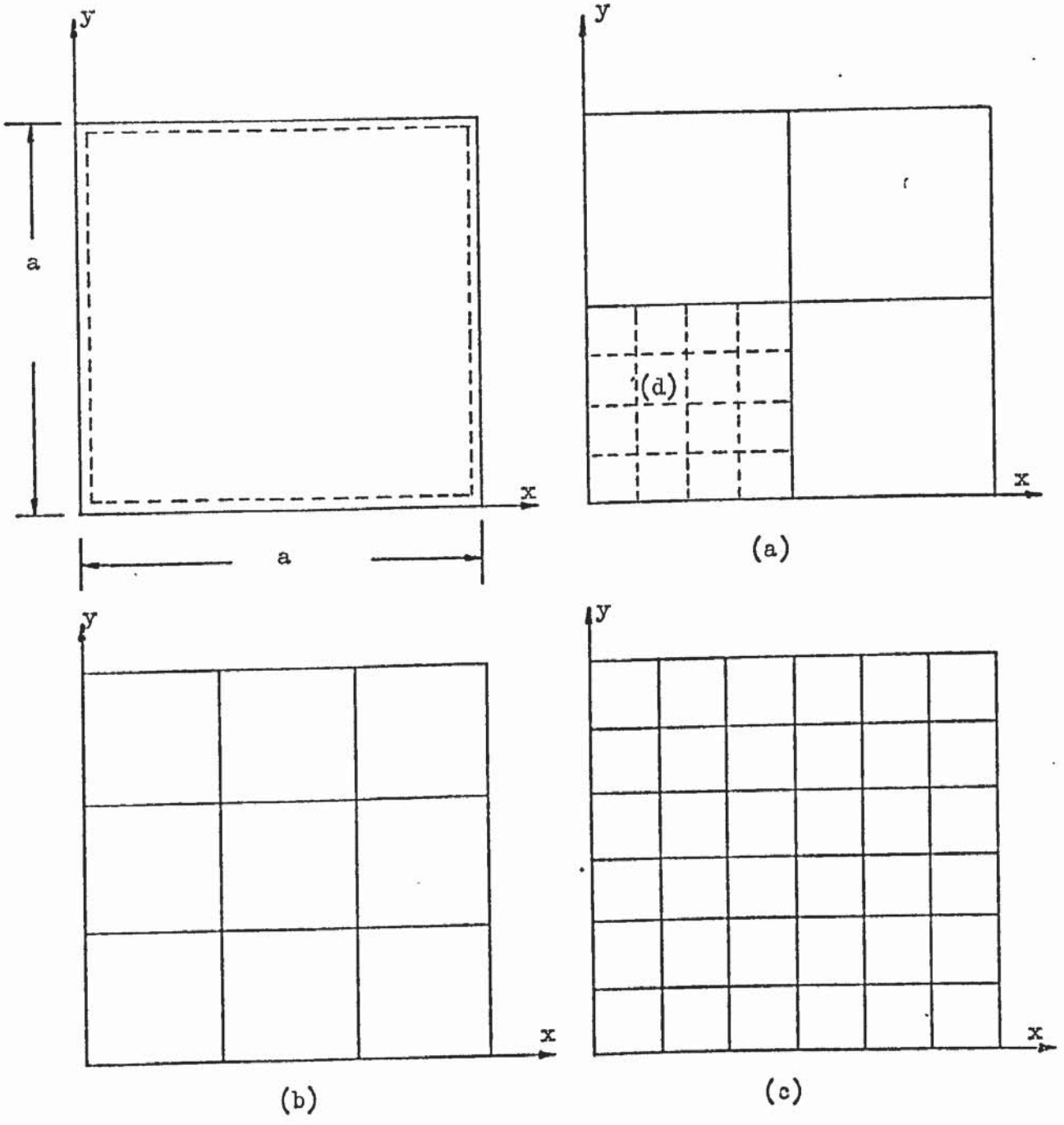

$D = D_o$; $\mu = 0.3$; $\rho = \rho_o$; $h = h_o$

Fig.(9.5.1)

Table (9.5.1) Natural Frequencies for the Simply Supported Square Plate Case (1).

Frequency ω_{mn}	$\omega_{mn} \div \left(\frac{\pi^2}{a^2}\sqrt{\frac{D_o}{\rho_o h_o}}\right)$					
	Exact Ref.[15] m^2+n^2	MESH				
		2 × 2	3 × 3	4 × 4	6 × 6	8 × 8*
ω_{11}	2.000	2.2378	2.1140	2.0656	2.0295	2.0166
ω_{12}	5.000		6.2150	5.7371	5.3294	
ω_{13}	10.000		9.4132	8.9520	8.4580	11.0021
ω_{23}	13.000			13.4255	11.7892	
ω_{14}	17.000			15.7597	14.5916	
ω_{33}	18.000			21.3430	20.1402	19.2860
ω_{34}	25.000				22.5556	

*Note: Obtained from a 4 × 4 mesh, using one quarter of the plate and symmetry conditions

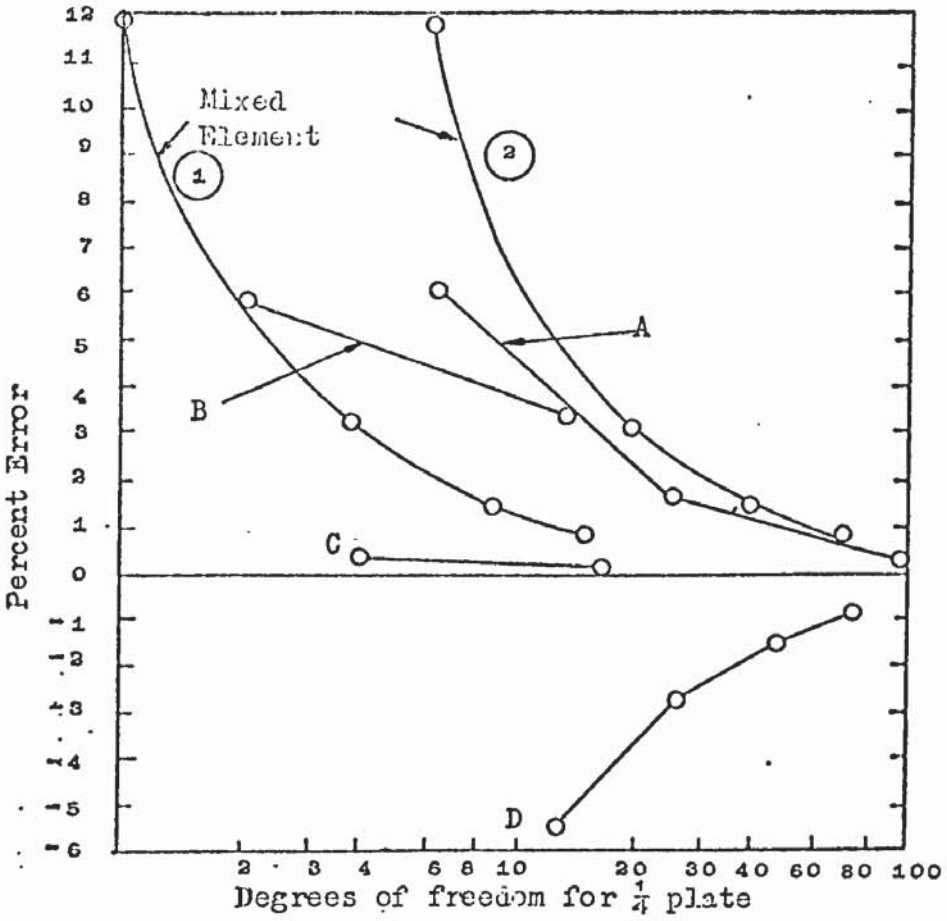

(1) - Convergence curve corresponding to degrees of freedom of final eigenvalue problem.

(2) - Convergence curve corresponding to the total number of degrees of freedom of model.

Symbol	Method	Description of Element
A	Displacement	2 triangles; cubic model.
B	Displacement	Conforming but incomplete rectangle; polynomial terms up to 6th order.
C	Displacement	Complete and conforming rectangle; cubic Hermitian polynomial model.
D	Displacement	Nonconforming but complete rectangle; cubic model.

Fig.(9.5.2) Prediction of lowest frequency of simply supported square plate by several elements (ref [30]).

9.5.2) Clamped Plate.

The natural frequencies of the clamped square plate, Case (2), shown in Fig.(9.5.3) are predicted by the same finite element grid as the previous section, with the exception of the 2 x 2 mesh. These results are compared with the energy solution by Barton [75].

The results of Table (9.5.2) show that an 8 x 8 mesh of the element is capable of predicting the frequency of the fundamental mode within 0.2%. The 4 x 4 mesh, which is the coarsest grid used in this example already predicts the frequency within 0.5%.

The element is also capable of predicting the frequency of the fourth mode within acceptable accuracy and the convergence is monotonical. The 8 x 8 mesh calculates the natural frequency of this mode with an error of 9%.

9.5.3) Cantilever Plate.

The natural frequencies of the cantilever square plate, Case (3), are analysed by 1 x 1, 2 x 2, 3 x 3 meshes of mixed elements, as presented in Fig.(9.5.4) and Table (9.5.4). The results show that the element is capable of predicting accurately the lower and higher modes of the cantilever plate. Also, in this particular application, the convergence properties of the element are good. The solution is converging to the solution of the Reissner's approach [76].

From Table (9.5.3) it is seen that the element developed here is much more accurate than the mixed element of Cook [50]. For a 2 x 2 mesh, Cook's element predicts the first five natural frequencies with a discrepancy of 5 , 8 , 15 , 9 , and 15% respectively, from the energy solution of Barton [75]. The corresponding discrepancies of the present solution are 2 , 4 , 5.6, 3 and 0.3% respectively. The present and Cook [50] results are predicted

Case (2) C-C-C-C

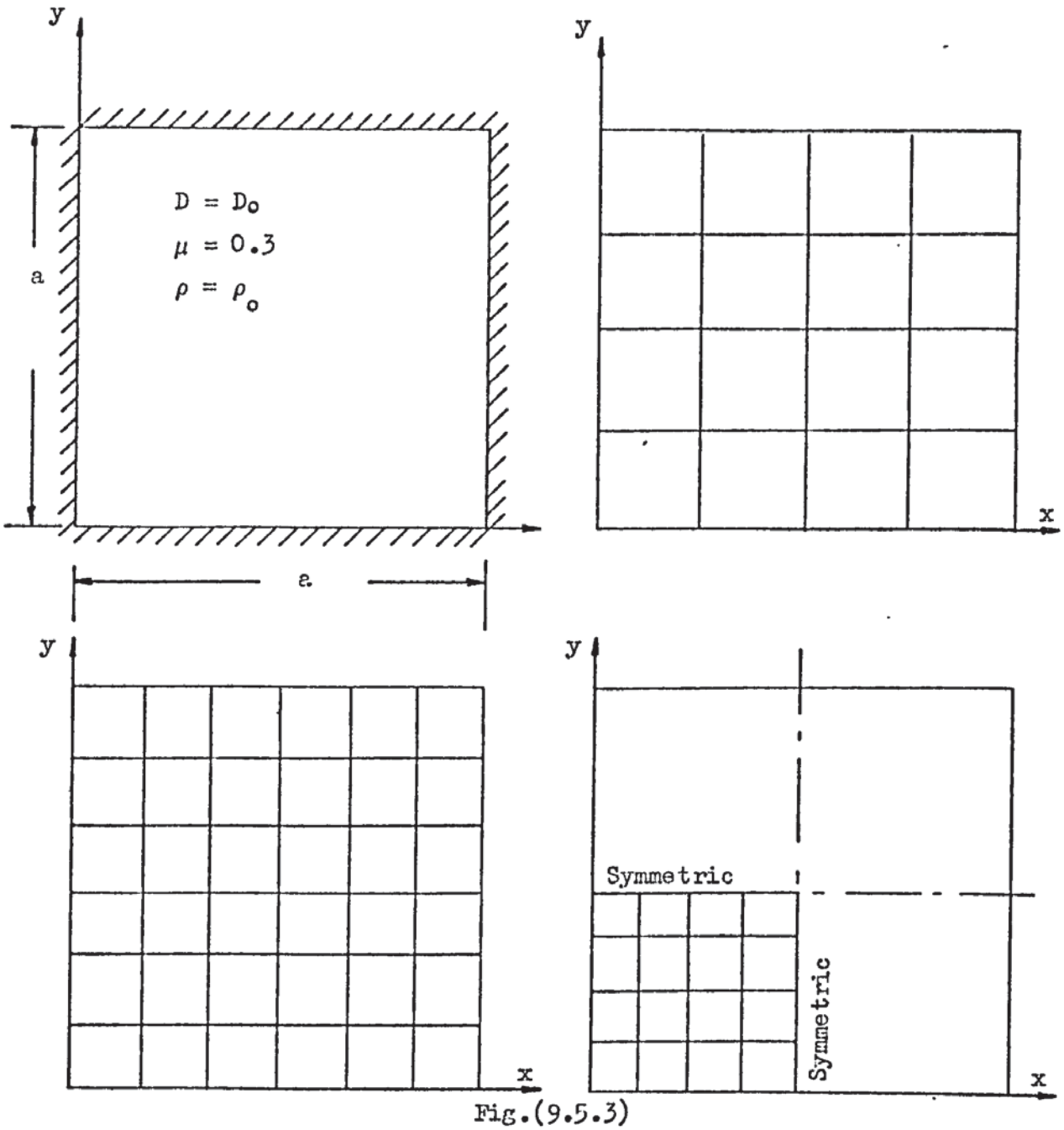

Fig.(9.5.3)

TABLE (9.5.2) Solution to Case (2)

Mode	$\omega \div \left(\frac{\pi^2}{a^2}\sqrt{\frac{D_o}{\rho_o h_o}}\right)$			
	Finite Element mesh			Energy sol., ref[75]
	4 × 4	6 × 6	8 × 8*	
1	3.6284	3.6378	3.6399	3.6465
4	15.4235	15.3097	14.5620	13.3845

*Note: From a 4 × 4 mesh, using symmetry.

using models with 3 × 3 meshes. In both cases the final eigenvalue problem has 12 degrees of freedom.

Also from Table (9.5.3) it can be seen that the mixed element is as accurate as the displacement element of Dawe [77]. However, the mixed element is more efficient since the final eigenvalue problem is smaller. For a 2 × 2 mesh of Dawe element which leads to a 21 degrees of freedom eigenvalue problem, the discrepancies of the values of the first five natural frequencies with reference to the Barton solution [75] are 1.0 , 0.0 , 1.6 , 4.3 and 3.1%. The equivalent discrepancies of a 2 × 2 mesh of mixed elements, which leads to a final eigenvalue of 6 degrees of freedom are 2.3 , 2.3 , 6.1 , 3.5 and 2.2%. Although these discrepancies are larger than the element of ref.[77] they are obtained by a much smaller eigenvalue problem.

It should be noticed for eigenvalue problems with the same degrees of freedom, the mixed element is more efficient than the Dawe model. For instance, the discrepancies of 1 × 1 mesh of Dawe's elements, which lead to an eigenvalue with 8 degrees of freedom, are: 5 , 5 , 41 , 31 and 49%.

Also the Dawe model is converging to the energy solution of Barton [75], while the present model is converging to the Reissner's solution of reference [76]. For the first three modes, the percentage differences of the natural frequencies predicted by these solutions are 1.6 , 3.3 and 6.4%, which is of the same order of magnitude as the discrepancies between the two elements.

Table (9.5.4) shows the frequency parameters predicted by a 3 × 3 mesh of mixed elements and these values are compared with the lower and upper bounds presented by Leissa [22]. All the computed 12 frequency parameters are within acceptable accuracy. It should be noticed that the 12 computed frequency parameters are

Case (3) C-F-F-F

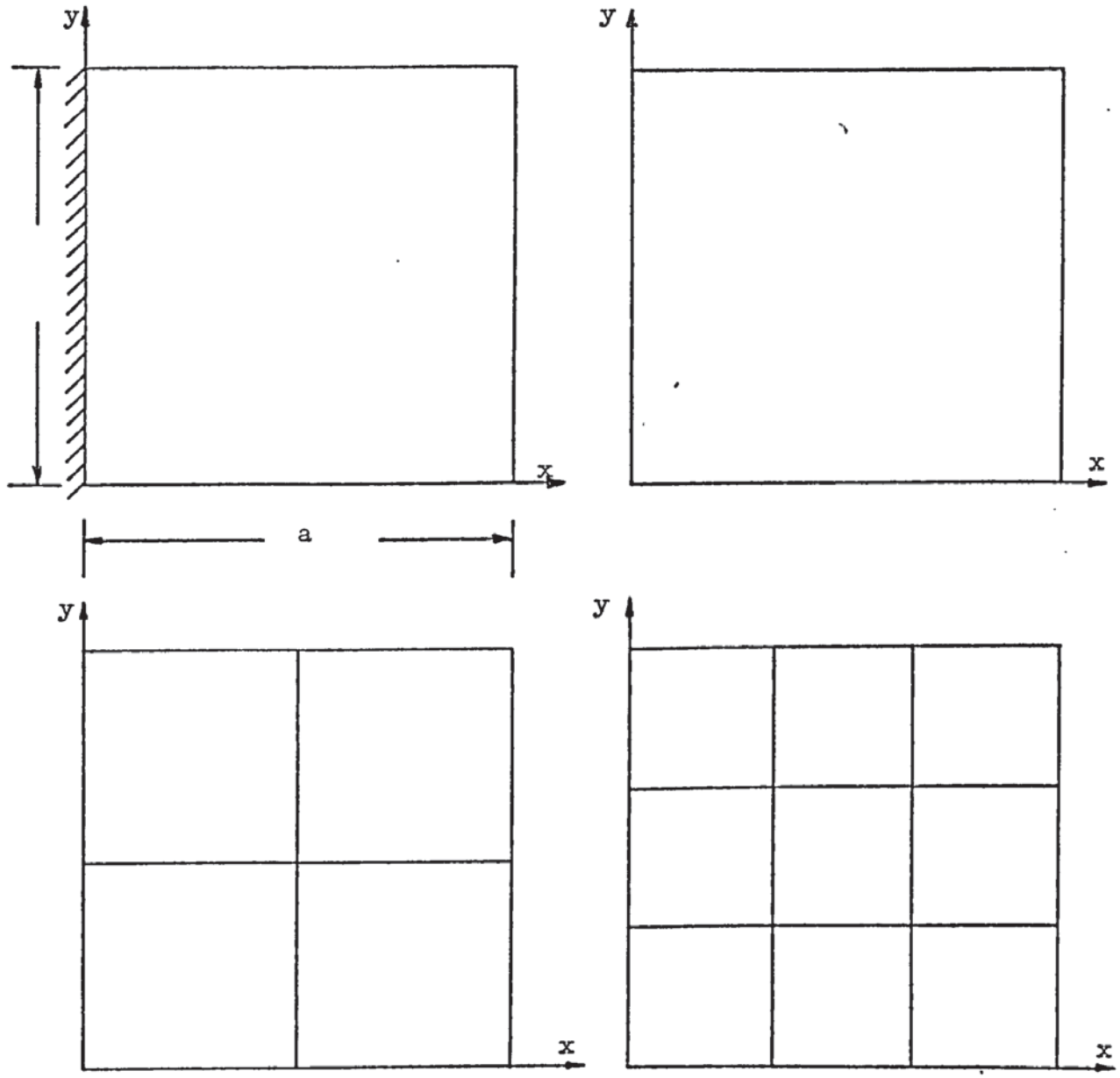

$D = D_o$; $\mu = 0.29$; $\rho = \rho_o$; $h = h_o$

Fig.(9.5.4)

TABLE (9.5.3) Natural Frequencies for Square Cantilever Plate, Case (3)

		$\omega_n \div \left(\frac{1}{a^2}\sqrt{\frac{D_o}{\rho_o h_o}}\right)$				
		VIBRATION MODE				
Mesh	Source	1	2	3	4	5
1 x 1	Present Results	3.000	9.12			
2 x 2		3.415	8.353	22.750	28.403	30.482
3 x 3		3.424	8.210	22.646	28.394	31.267
1 x 1	Ref.[50]	2.55	6.69	13.26		
2 x 2		3.16	7.51	16.43	23.14	24.83
3 x 3		3.32	7.91	18.68	25.22	27.08
1 x 1	Ref.[77]	3.32	8.93	30.32	35.86	46.39
2 x 2		3.46	8.55	21.77	26.33	30.23
3 x 3		3.47	8.53	21.67	26.85	30.80
Experi-mental	Ref.[78]	3.37	8.26	20.55	27.15	29.75
Energy Solution	Ref.[75]	3.494	8.547	21.44	27.46	31.17
Reissner's Approach	Ref.[76]	3.44	8.27	20.14		

TABLE (9.5.4) Natural Frequencies of a Cantilever Square Plate, Case (3)

Mode	LEISSA [22]		Mixed Element 3 x 3
	Lower Bound	Upper Bound	
1	3.4305	3.4823	3.424
2	-	8.55	8.210
3	20.874	21.367	22.646
4	26.501	27.278	28.394
5	-	31.10	31.267
6	51.502	54.301	52.776
7	60.249	61.450	70.619
8	-	64.20	71.715
9	-	71.10	76.002
10	92.143	97.321	90.615
11	-	-	91.272
12	115.68	119.51	121.787
	$\omega_n \div \left(\frac{1}{a^2}\sqrt{\frac{D_o}{\rho_o h_o}}\right)$		

calculated from a final eigenvalue of 12 degrees of freedom. Thus, in the mixed model, all the eigenvalues of the final eigen problem can be accurate. This is a consequence of the reduction of degrees of freedom being exact, and the eigenvalues of the final eigen problem being the eigenvalues of the original eigen problem . This fact is an advantage over displacement models. In displacement models any reduction of degrees of freedom by the Eigenvalue Economizer [27] is approximate, and only a few of the lower eigenvalues of the reduced eigen problem are close to the eigenvalue of the original eigen problem.

9.5.4) Concluding Remarks.

From these applications it is concluded that, in general, the element developed for dynamic analysis of plates is capable of predicting the natural frequencies and mode shapes. Also the element is superior to the mixed element of Cook [50]. The mixed element developed here compares favourably with displacement elements.

The major advantage of the mixed elements is that the natural frequencies of structures can be predicted accurately by the solution of small eigenvalue problems. In general the final eigenvalue problem of mixed models is much smaller than the eigenvalue problem of displacement models. Since the solution of the eigenvalue problem requires large computing time, this reduction of the number of degrees of freedom increases the efficiency of mixed elements in the dynamic analysis of structures. This fact can be of major importance in the dynamic analysis of large structures.

The mixed formulation of the dynamic problem reduces considerably the size of the final eigenvalue problem, given by equation (6.2.29). In this equation the degrees of freedom corresponding to the bending and twisting moments are already eliminated.

This elimination is carried out by equation (6.2.28) without approximation.

The exact reduction of degrees of freedom in mixed models is equivalent to the approximate reduction, known as the Eigenvalue Economizer [27],[29], of degrees of freedom in displacement models. It should be noticed that after elimination of degrees of freedom of displacement models by the Eigenvalue Economizer, the reduced stiffness matrix has the same form as equation (6.2.28).

Since this reduction of degrees of freedom is exact for mixed models, all the eigenvalues predicted by the final eigen problem are the eigenvalues of the original eigen problem. However, in displacement models this reduction is approximate and only the lower-eigenvalues of the reduced eigen problem are close to the eigenvalues of the original eigen problem.

9.6) Buckling.

In this section the general mixed quadrilateral element is applied to the elastic and plastic buckling alaysis of plates. The accuracy and convergence of the element are compared with exact and other finite element solutions. With one exception, the symmetry of the plate model is taken into consideration.

9.6.1) Simply Supported Elastic Plate-Uniform Axial Compression.

The buckling factor of a simply supported square plate, subjected to a uniform axial compression, is calculated by mixed general quadrilateral models. The plate, Case (1), and the meshes used are presented in Figs.(9.6.1 a) and (9.6.2).

It is clear, from Table (9.6.1), that for this application the mixed element is extremely efficient and accurate. The predicted

buckling factor is within 0.4% of the exact value. A 2 x 2 mesh of mixed elements with only 20 degrees of freedom and a final eigenvalue problem of 4 degrees of freedom predicts the buckling factor within 1.5% of the exact value.

9.6.2) Simply Supported Elastic Plate-Uniform-Bi-Axial Compression.

The buckling factor of a simply supported square plate subject to uniform-bi-axial compression, Case (2), Fig.(9.6.1b) is predicted by mixed element models, whose meshes are presented in Fig.(9.6.2).

Again, the element behaviour is excellent, as presented in Table (9.6.1). The predicted buckling factor is within 0.4% of the exact value. Also, a coarse mesh of 2 x 2 elements predicts the buckling factor with an error of 1.4%.

9.6.3) Clamped Elastic Plate-Uniform-Bi-Axial Compression.

The buckling factor of a square plate subjected to uniform bi-axial compression is represented by mixed elements. The plate, Case (3), is shown in Fig.(9.6.1c) and the meshes in Fig.(9.6.2).

It can be concluded from Table (9.6.1) that in this application the mixed model is accurate and converges quickly, but its behaviour is not as good as in previous buckling applications. The predicted buckling factor is within 1.4% of the exact values. However a 2 x 2 representation predicts the buckling factor with 10% error.

9.6.4) Simply Supported Elastic Plate-Uniform Shear.

The buckling factor of a simply supported rectangular plate, subject to uniform shear, Case (4), Fig.(9.6.3), is pre-

dicted by mixed models.

Table (9.6.2) shows the limitations of the element when applied to shear buckling. The buckling factor predicted by 5×5 model is 23% in error. The predicted buckling factor for the three meshes tested is converging quite quickly, but a finer mesh is required to obtain an accuracy of the same order of magnitude as in the previous cases. The element is superior to the mixed element of Cook [50]. It should be noticed that in this application the Kapur [79] displacement model requires 123 degrees of freedom to predict the buckling mode within 6%.

It can be concluded that the mixed element requires a fine mesh to represent plates where the shear buckling mode is predominant.

9.6.5) Simply Supported Orthotropic Elastic Plate - Uniform-Axial Compression.

The critical buckling stress of an orthotropic elastic plate, Case (5), Fig.(9.6.4) is predicted by a 3×4 mesh of mixed elements and listed in Table (9.6.3). The predicted critical buckling stress is within 1.2% of the analytical solution of reference [80].

9.6.6) Simply Supported Plastic Plate-Bi-Axial Compression.

The critical plastic buckling stress of a simply supported square plate, subject to uniform bi-axial compression, Case (6), shown in Fig.(9.6.5), is predicted by the mixed model. The model is applied to plates with several thicknesses and the corresponding exact values of the elastic and plastic buckling stress, and the plastic buckling stress computed from the program are shown in Table (9.6.4). These results contain widely varying degree of plastic deformation at the critical stress. The thickness range corresponds to a range of buckling stresses from a value close to

the elastic limit up to a value well into the plastic range. As the state of stress penetrates further into the plastic range, the material stiffness decreases, so that the plastic buckling stress decreases relative to the corresponding elastic buckling stress. The decrease varies from 6 to 60% for the range of thicknesses examined, which shows clearly the importance of the plastic analysis in the solution of buckling problems.

From Table (9.6.4) it is concluded that the mixed element is very accurate when analysing these particular plates. A 2 x 2 grid of elements is capable of predicting the critical plastic buckling stresses with an average absolute discrepancy of 0.5%. It should be noticed that the eigenvalue iteration tolerance in these applications is 0.25%.

9.6.7) Clamped Plastic Plate - Uniform Axial Compression.

A mixed element model is applied to the plastic buckling analysis of a clamped square plate, Case (7), shown in Fig.(9.6.6). The predicted critical buckling stress, for the thicknesses 0.6, 0.7, 0.8 inches, is compared with a plastic displacement finite element solution of Pifko and Isakson [65], and with the corresponding exact elastic buckling stress, in Table (9.6.5). The average absolute discrepancy between the present and ref.[65] solutions is about 2.3%, with an eigenvalue iteration tolerance of 0.5%. It should be noticed that the number of degrees of freedom of the present model is 26 and in ref.[65] is 145. The final eigenvalue problem of the present solution has only 4 degrees of freedom.

The results show a widely varying degree of plastic deformation corresponding to a decrease of the predicted plastic buckling stress relative to the corresponding exact elastic buckling stress for the range of thicknesses examined, ranging from 15 to 44.8%.

CASE (1) S-S-S-S

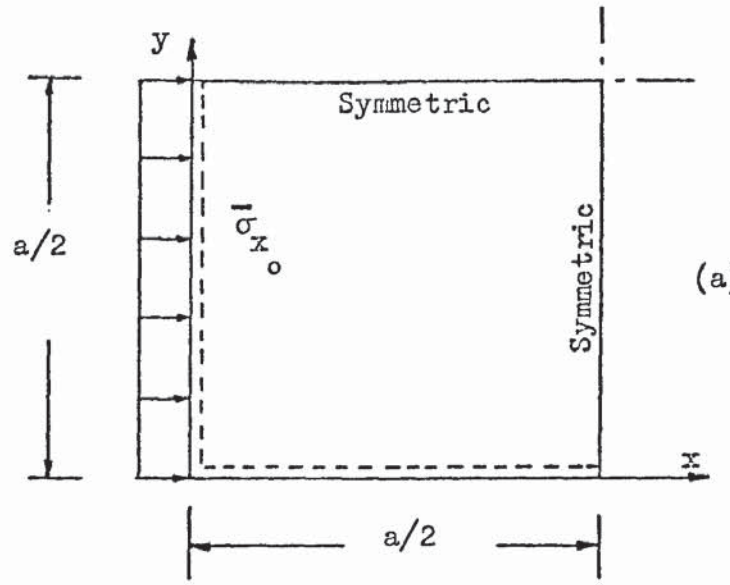

(a)

$D = D_o$
$\mu = 0.3$
$h = h_o$
$\bar{\sigma}_{x_o}$ = Constant
$\bar{\sigma}_{y_o} = 0.0$
$\tau_{xy_o} = 0.0$

CASE (2) S-S-S-S

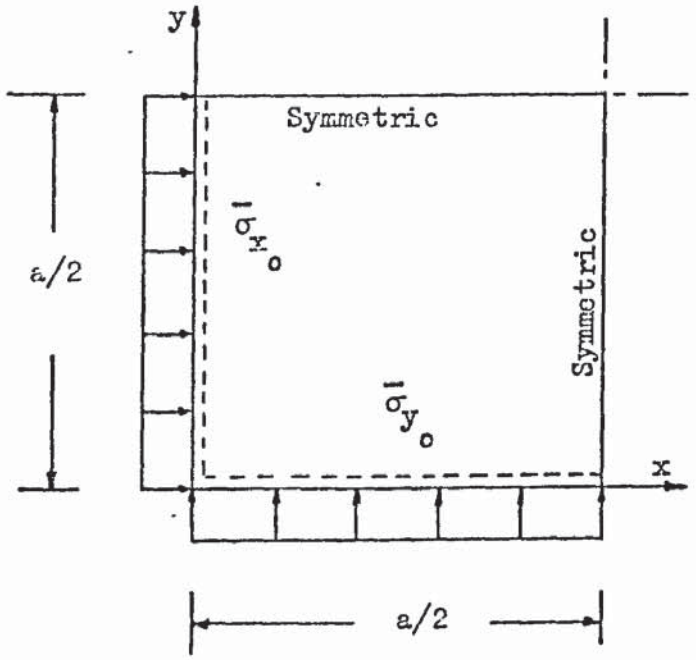

(b)

$D = D_o$
$\mu = 0.3$
$h = h_o$
$\bar{\sigma}_{x_o} = \bar{\sigma}_{y_o}$ = Constant
$\tau_{xy_o} = 0.0$

CASE (3) C-C-C-C

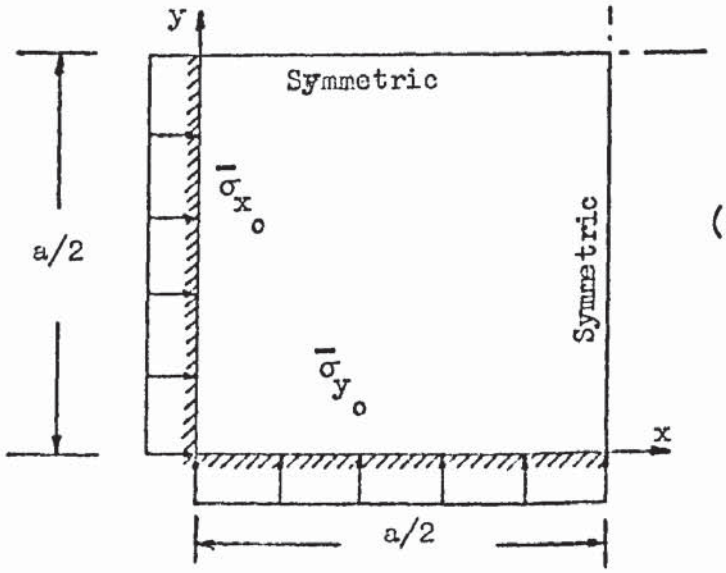

(c)

$D = D_o$
$\mu = 0.3$
$h = h_o$
$\bar{\sigma}_{x_o} = \bar{\sigma}_{y_o}$ = Constant
$\bar{\tau}_{xy_o} = 0.0$

Fig.(9.6.1)

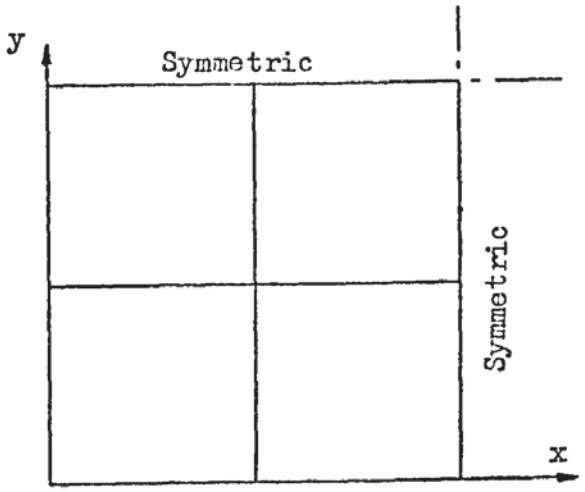

2 × 2

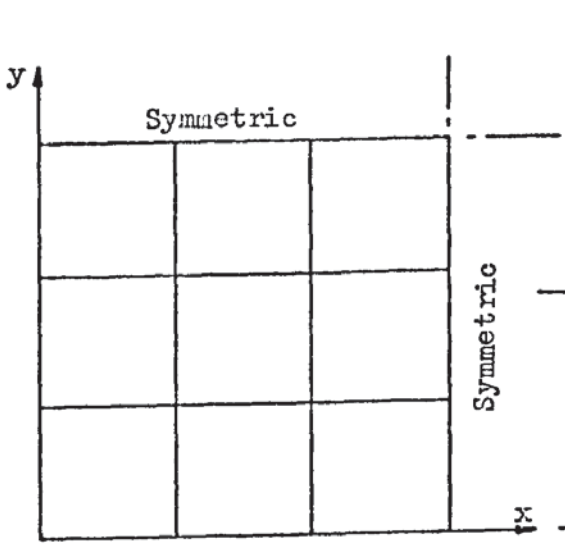

3 × 3

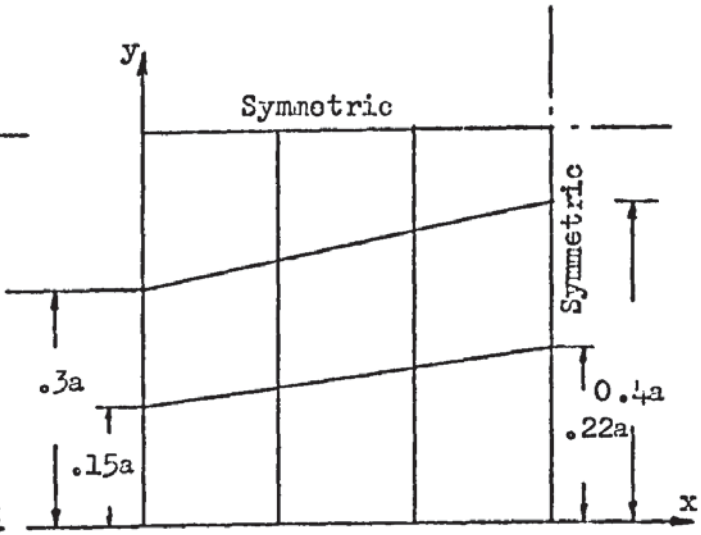

3 × 3*
(Only for case (1))

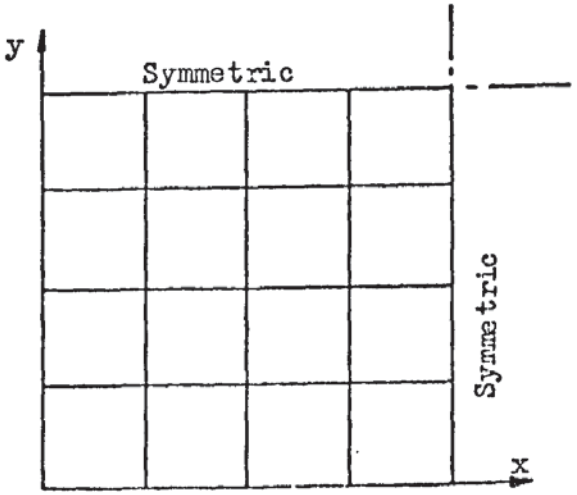

4 × 4

Fig.(9.6.2) Finite Element meshes for cases (1-2-3).

TABLE (9.6.1) Critical Stresses of Square Plates Under Uniform Plane Stresses - Cases (1),(2),(3)

Loading Type	Mesh			Exact ref.[17]
	2 x 2	3 x 3	4 x 4	
Case (1) S-S-S-S Uniform axial compression	4.0544	4.0262 4.0328*	4.0150	4.0
Case (2) S-S-S-S Uniform-bi-axial compression	2.0272	2.0131	2.0075	2.0
Case (3) C-C-C-C Uniform-bi-axial compression	5.8536	5.4677	5.3920	5.315
	$\sigma_{cr} \div \left(\pi^2 D_o / a^2 h_o\right)$			

*Noto: Irregular mesh

CASE (4) S-S-S-S

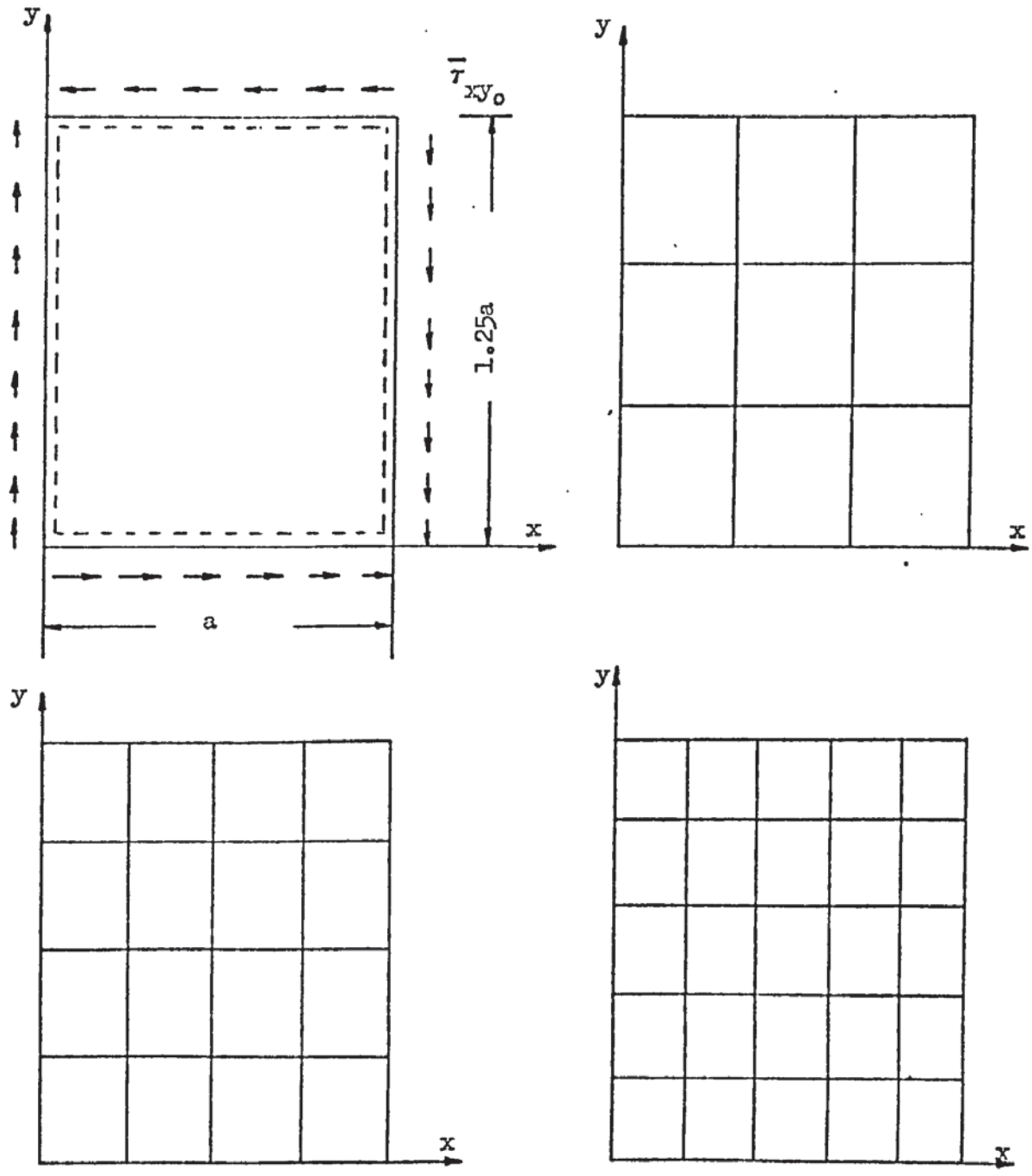

$D = D_o$; $\mu = 0.3$; $h = h_o$

$\bar{\sigma}_{x_o} = \bar{\sigma}_{y_o} = 0$; τ_{xy_o} = Constant

Fig.(9.6.3)

TABLE (9.6.2) Critical Shear Buckling Stress for Case (4).

Mesh	Source	$\tau_{cr} \div \left(\pi^2 D_o / a^2 h_o\right)$
3 × 3	Present Element	15.415
4 × 4	"	10.850
5 × 5	"	9.471
4 × 4	ref.[50]	4.589
6 × 6	"	6.094
4 × 4	ref.[79]	6.945
6 × 6	"	7.247
Exact	ref.[17]	7.71

CASE (5) Orthotropic Plate S-S-S-S

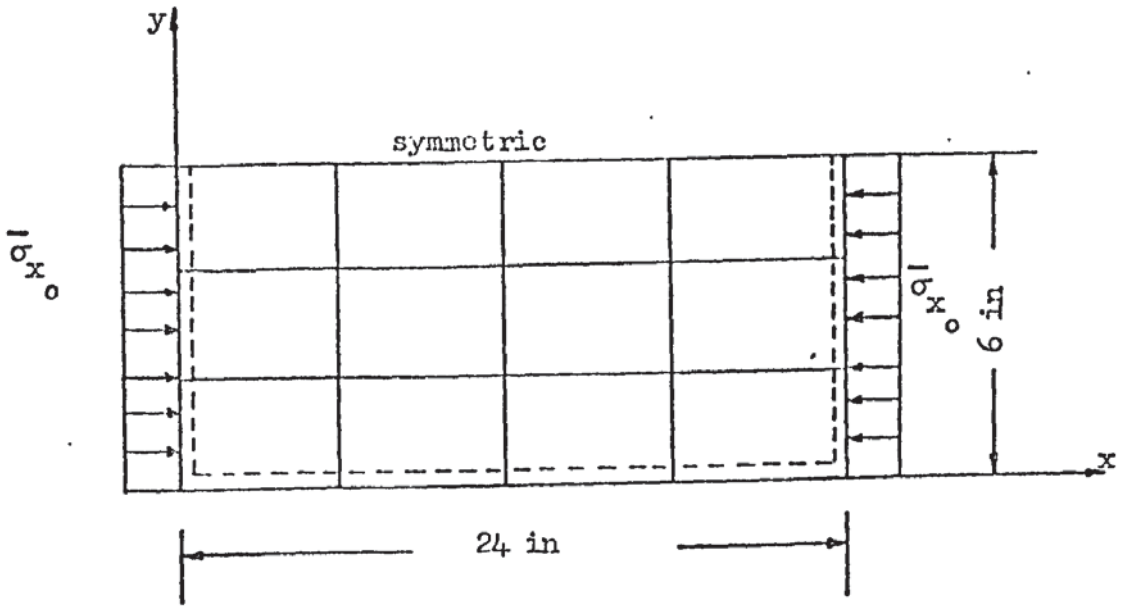

$E_x = 30 \cdot 10^6$ p.s.i. ; $E_y = 5 \cdot 10^6$ p.s.i.

$E_y/\mu_{yx} = 10 \cdot 10^7$ p.s.i. ; $G_{xy} = 10 \cdot 10^6$ p.s.i.

h = 0.1 in

$\bar{\sigma}_{x_o} = 1.0$ p.s.i. ; $\bar{\sigma}_{y_o} = 0.0$; $\bar{\tau}_{xy_o} = 0.0$

Fig.(9.6.4)

TABLE (9.6.3) Critical Buckling Stress for Case (5)

Mesh	Critical Stress p.s.i.
3 × 4	4101.55
Exact ref[80]	4053.2

CASE (6) Plastic Buckling S-S-S-S

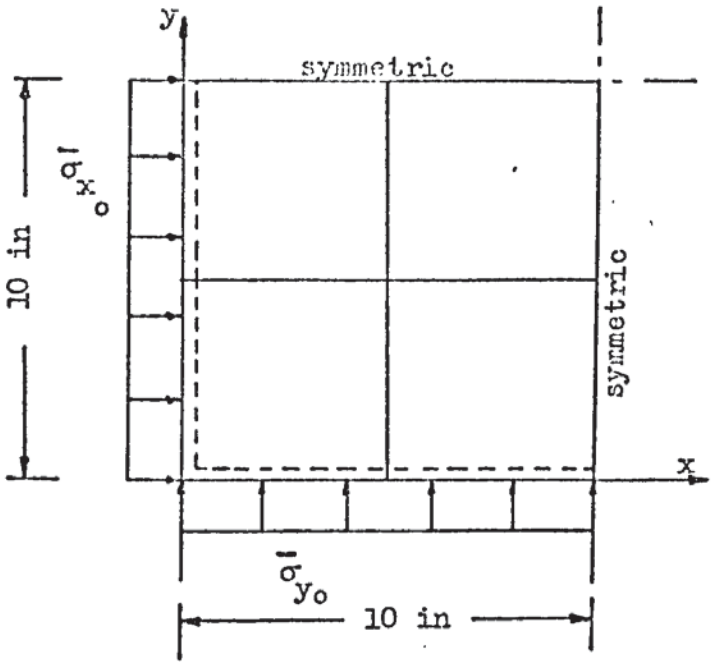

Thickness h_o (in)
1.12500
1.29980
1.60231
2.08258

σ^* = Critical Plastic buckling stress

$$\alpha = \frac{\bar{\sigma}_{x_o}}{\sigma^*} = 1.0,\ \beta = \frac{\bar{\sigma}_{y_o}}{\sigma^*} = 1.0\ ;\ \gamma = \frac{\bar{\tau}_{xy_o}}{\sigma^*} = 0.0$$

$E = 10^7$ p.s.i. ; $\sigma_{0.7} = 10^5$ p.s.i. ; n = 10; $\mu = 1/2$

Fig.(9.6.5)

CASE (7) Plastic Buckling C-C-C-C

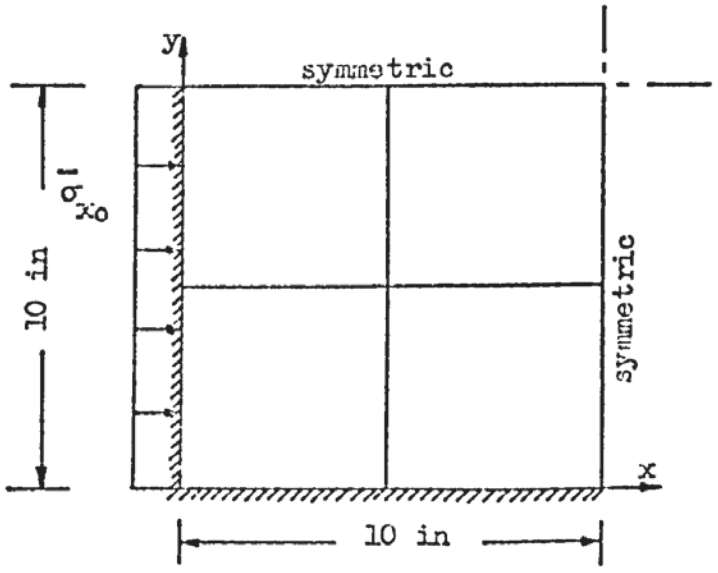

Thickness h_o (in)
0.6
0.7
0.8

$$\alpha = \frac{\bar{\sigma}_{x_o}}{\sigma^*} = 1.0;\ \beta = \frac{\bar{\sigma}_{y_o}}{\sigma^*} = 0.0\ ;\ \gamma = \frac{\bar{\tau}_{xy_o}}{\sigma^*} = 0.0$$

$E = 10^7$ p.s.i. ; $\sigma_{0.7} = 10^5$ p.s.i. ; n = 10; $\mu = 1/2$

Fig.(9.6.6)

TABLE (9.6.4) Plastic Buckling Stress for Case (6)

Thickness h_o (in)	σ^*(p.s.i.) Exact [62], [65]	σ^*(p.s.i.) Present Analysis	Elastic critical stress, (p.s.i.) Exact [17]
1.12500	65000	65831	69394
1.29980	75000	75500	92631
1.60231	85000	85200	140773
2.08258	95000	95000	237810

TABLE (9.6.5) Plastic Buckling Stress for Case (7)

Thickness h_o (in)	σ^*(ps.i.) Finite element analysis ref.[65],6x6 mesh	σ^*(p.s.i.) Present analysis	Elastic critical stress,(p.s.i.) Exact [17]
0.6	81712	84339	99385
0.7	91234	93530	135277
0.8	97549	98720	176687

9.6.8) Concluding Remarks.

The applications have demonstrated that the mixed element is in general very efficient and accurate in the analysis of elastic and plastic buckling of plates. In general the mixed element is probably more efficient than the displacement models, since it requires the solution of smaller eigenvalue problems.

In the elastic and plastic buckling analysis of plates, where the shear buckling mode is predominant, a fine finite element mesh should be used in order to predict accurately the buckling mode.

CHAPTER 10

DISCUSSION AND CONCLUSIONS

10) Discussion and Conclusions.

The main objective of the work described in this Thesis was the development of a mixed general quadrilateral element and corresponding computer program for the static analysis of arbitrary thin and moderately thick elastic isotropic and orthotropic plates and an assessment of its effectiveness.

It was first necessary to examine the Reissner principle in its application to static, dynamic and buckling problems by means of the finite element procedure. Also the literature survey of mixed elements showed that, in general, rectangular elements are superior to triangular elements, except that the rectangular elements have difficulty in representing aribtrary plates. This difficulty can be overcome by quadrilateral elements. Since no quadrilateral mixed element has been presented in the literature, it was decided to develop this element based on the isoparametric concept.

Supplementary to the main work was the further development of the general quadrilateral element for free vibrations and buckling analysis of thin elastic isotropic and orthotropic plates, and plastic buckling analysis of thin plates.

A further objective of this Thesis is to estimate the efficiency and accuracy of the general mixed quadrilateral element, its applicability, limitations, advantages and disadvantages in the static, vibrations and buckling analysis of plates.

These objectives have been achieved as described in the Thesis.

10.1) Mixed Element-Statics.

The applications show the efficiency and applicability of the mixed element to the static analysis of general plates.

The convergency tests demonstrate that for static analysis of plates, the predicted deflections and the bending and twisting moments converge monotonically and rapidly to exact solutions. Also, as illustrated in Section 9.2.4, the element compares favourably with other elements with respect to:

i) Accuracy.

ii) Computer time required to solve the algebraic equations arising from the analysis of a plate problem.

The general quadrilateral mixed element developed in the present work has a particular advantage over the other mixed plate rectangular elements in its ability to represent general boundary conditions.

Another advantage of the element is the facility for incorporating the effects of shear deformation in the analysis of plates, which are not easily incorporated by the displacement models. Further, the element yields the bending and twisting moments directly, thus avoiding the differentiation of the displacement field as in the displacement models. Unfortunately in the literature, the majority of the finite element displacement calculations are for displacement analysis and the values of the moments are not presented. Consequently it was not always possible to compare the moments of the mixed element with values from displacement elements. However, since the mixed formulation predicts the moments as accurately as the displacements, it is believed that the mixed element developed is superior to displacement elements for the calculation of moments.

The behaviour of the element in the static analysis of plate structures with skew boundaries and arbitrary thickness and load is extensively illustrated in this Thesis. In all these applications relatively coarse meshes of mixed elements were capable of predicting displacement and moments accurately, these values

were compared with known analytical, numerical or experimental solutions.

The major disadvantage of mixed elements is that the governing system of algebraic equations is non-positive definite. Since just a few procedures to solve these type of equations are presented in the literature, this is a major practical disadvantage which hopefully will be overcome by further research in the solution of non-positive definite equations.

10.2) Mixed Element-Vibrations.

The element yields the lower natural frequencies of plates accurately and with relatively little computer effort. In all applications only a coarse mesh was required to predict accurately these natural frequencies and the element is as accurate as good displacement elements. Also the element is an improvement over the previously developed mixed element.

The major advantage of the mixed elements is that the natural frequencies of structures can be predicted accurately by the solution of small eigenvalue problems. In general, these eigen problems are of much smaller order than the eigen problems derived from displacement models, and require much less computing time for the solution.

Another advantage of the mixed element is that the total number of degrees of freedom of the model (deflections and moments) can be reduced exactly. In the calculations of the eigenvalues and eigenvectors, we may reduce the computational effort significantly by eliminating either the deflections or moments in the formulation. In the present work we eliminated the moments, as shown in Section 6.2.4. This has a similar effect to the condensation technique, the so-called eigenvalue economizer, used with displacement models, but in the present work there is no approximation involved. Thus, the

eigenvalues predicted by the final eigen problem of a mixed model are the eigenvalues of the original eigen problem, while the eigenvalues of the reduced eigen problem of a displacement model, using the eigenvalue economizer technique, are reasonably accurate only for the lower eigenvalues of the original eigen problem. The same feature is noticed in buckling analysis.

In vibration analysis the mixed formulation leads to a positive definite eigenvalue problem, as represented in Section 6.2.4, thus avoiding one of the difficulties of the mixed formulation for static analysis.

10.3) Mixed Element-Buckling.

The element yields accurately and efficiently the buckling factors or the critical plastic buckling stresses of plates. However, in the particular case of buckling analysis of plates, where the shear mode is predominant, the mixed model should be represented by a fine mesh of elements.

Mixed elements have a significant advantage in buckling analysis, since the degrees of freedom corresponding to the nodal bending and twisting moments can be eliminated by an exact transformation, as shown in Section 6.2.4, while in the displacement models the reduction of the total number of degrees of freedom is only approximated. The same fact occurs in vibration analysis as described above.

Since the reduced overall stiffness matrix $[K^*]$, relation (6.2.28), is symmetric and positive definite no difficulties are experienced in the solution of the final buckling eigenvalue problem.

10.4) Experimental Tests.

The experimental tests were carried out mainly to gain some experience in the Moire Technique, which claims to be fast,

easy and accurate. Supplementary to that was the comparison of the predicted values of the mixed quadrilateral element, with the experimental results. Both objectives were partially achieved successfully.

Three plate problems were compared in Section 9.4.2. For two of them, with rigidity variations, there are no analytical solutions available.

The agreement between experiment and mixed finite element predictions for the transverse deflection distribution were found to be excellent for all cases but one.

The agreement for the bending moments, was excellent for Case (1), but the predicted results of the mixed element showed a better accuracy than the experimental ones, when compared with the analytical solution. The agreement for the bending moment at the centre of the plate, Case (2), is excellent, but at the clamped edge it is not good. The discrepancies in Case (3), for both deflections and moments, are mainly due to experimental errors, a conclusion which is supported by the discrepancies which were found in the comparison of an experimental slope curve distribution, with corresponding results predicted by a well proved semi-analytical finite element technique [74].

10.5) Further Development.

The development of a mixed parabolic plate element can be an objective of a further extension of the work of this Thesis. However, there is an increase in computational effort to calculate the element matrices but less elements have to be used to obtain the same accuracy. It should be noticed that the parabolic isoparametric plane stress element is much more accurate than the corresponding quadrilateral element. Therefore, it is believed that the mixed parabolic element can be very successful in static dynamic

and buckling analysis of plates.

The development of a quadrilateral mixed element with W, β_x, β_y, M_x, M_y, M_{xy} as degrees of freedom per node is important. This element will be applicable to reinforced plates, since it will be possible to connect it with a mixed beam element, taking into consideration the twist of the beam.

A semi-analytical mixed plate element may be contemplated for the static, dynamic and buckling analysis of plates. This semi-analytical model will have some limitations in its applicability, but where applicable it will reduce considerably the number of degrees of freedom of the system.

The further application of the mixed element to predict the dynamic stresses of structures due to arbitrary dynamic forces is another possible extension of the work of this Thesis. The mixed model calculates the eigenvectors in terms of displacements. These eigenvectors can be transformed into eigenvectors of moments by a simple matrix transformation. Alternatively the moment eigenvectors can be calculated directly .The displacements and moments eigenvectors are the eigenvectors of the original system. The dyanmic stresses and the transient response can then be calculated by the Modal Analysis Method, using eigenvalues,and the eigenvectors of the original system. By the use of the mixed element we can avoid the differentiation of the dynamic response to calculate the dynamic stresses which is a major disadvantage and source of inaccuracy of the displacement models.

The mixed general quadrilateral model has thus been shown to be versatile, and accurate in the solution of static, dynamic and buckling analysis of plate problems. These merits, together with the ease in computational effort, make it a powerful alternative in the solution of those problems.

EXTREMIZATION OF THE REISSNER FUNCTIONAL FOR "MODERATELY THICK PLATES"

To determine the conditions for extremizing the Reissner functional, equation (2.3.8), we allow independent variations δW, δM_x, δM_y, δM_{xy}. Then

$$\delta\pi_R = \sum_n \Bigg\{ \iint_{A_n} \Bigg[-C\, M_x\, \delta M_x - C\, M_y\, \delta M_y + C\, \mu M_x\, \delta M_y + C\, \mu M_y\, \delta M_x$$

$$- 2\, C(1+\mu)\, M_{xy}\, \delta M_{xy} - 2L\, \frac{\partial M_x}{\partial x}\, \frac{\partial \delta M_x}{\partial x} - 2L\, \frac{\partial M_{xy}}{\partial y}\, \frac{\partial \delta M_x}{\partial x}$$

$$- 2L\, \frac{\partial M_x}{\partial x}\, \frac{\partial \delta M_{xy}}{\partial y} - 2L\, \frac{\partial M_y}{\partial y}\, \frac{\partial \delta M_y}{\partial y} - 2L\, \frac{\partial M_{xy}}{\partial x}\, \frac{\partial \delta M_y}{\partial y}$$

$$- 2L\, \frac{\partial M_y}{\partial y}\, \frac{\partial \delta M_{xy}}{\partial x} - 2L\, \frac{\partial M_{xy}}{\partial x}\, \frac{\partial \delta M_{xy}}{\partial x}$$

$$+ \frac{6\mu}{5Eh}\, p\, \delta M_x + \frac{6\mu}{5Eh}\, p\, \delta M_y$$

$$+ \frac{\partial M_y}{\partial y}\, \frac{\partial \delta W}{\partial y} + \frac{\partial W}{\partial y}\, \frac{\partial \delta M_y}{\partial y} + \frac{\partial M_{xy}}{\partial x}\, \frac{\partial \delta W}{\partial y} + \frac{\partial W}{\partial y}\, \frac{\partial \delta M_{xy}}{\partial x}$$

$$+ \frac{\partial M_x}{\partial x}\, \frac{\partial \delta W}{\partial x} + \frac{\partial W}{\partial x}\, \frac{\partial \delta M_x}{\partial x} + \frac{\partial M_{xy}}{\partial y}\, \frac{\partial \delta W}{\partial x} + \frac{\partial W}{\partial x}\, \frac{\partial \delta M_{xy}}{\partial y}$$

$$- p\, \delta W \Bigg] dx\, dy - \int_{s_{n,\sigma}} \bar{Q}_n\, \delta W\, ds$$

$$+ \int_{s_{n,u}} \bar{\beta}_n\, \delta M_n\, ds + \int_{s_{n,u}} \bar{\beta}_s\, \delta M_{ns}\, ds \Bigg\}$$

where the constants C and L are respectively given by

$$C = \frac{12}{Eh^3}$$

$$L = \frac{6(1+\mu)}{5hE}$$

Integrating by parts, all terms with derivatives and regrouping yields

$$\delta\pi_R = \sum_n \Bigg\{ \iint_{A_n} \Bigg[\Bigg[\frac{\partial^2 M_x}{\partial x^2} + 2\frac{\partial^2 M_{xy}}{\partial x \partial y} + \frac{\partial^2 M_y}{\partial y^2} + p \Bigg] \delta W$$

$$+ \Bigg[-\frac{\partial^2 W}{\partial x^2} + 2L\left(\frac{\partial^2 M_{xy}}{\partial y \partial x} + \frac{\partial^2 M_x}{\partial x^2}\right) + \frac{6\mu}{5hE} p - C(M_x - \mu M_y) \Bigg] \delta M_x$$

$$+ \Bigg[-\frac{\partial^2 W}{\partial y^2} + 2L\left(\frac{\partial^3 M_{xy}}{\partial x \partial y} + \frac{\partial^2 M_y}{\partial y^2}\right) + \frac{6\mu}{5hE} p - C(M_y - \mu M_x) \Bigg] \delta M_y$$

$$+ \Bigg[-2\frac{\partial^2 W}{\partial x \partial y} + 2L\left(\frac{\partial^2 M_x}{\partial x \partial y} + \frac{\partial^2 M_y}{\partial y \partial x} + \frac{\partial^2 M_{xy}}{\partial x^2} + \frac{\partial^2 M_{xy}}{\partial y^2}\right)$$

$$- 2(1+\mu) C. M_{xy} \Bigg] \delta M_{xy} \Bigg] dx\, dy$$

$$+ \int_{s_{n,\sigma}} \left[\ell\left(\frac{\partial M_{xy}}{\partial y} + \frac{\partial M_x}{\partial x}\right) + m\left(\frac{\partial M_y}{\partial y} + \frac{\partial M_{xy}}{\partial x}\right) - \bar{Q}_n \right] \delta W$$

$$- \int_{s_{n,u}} \Bigg[\ell\left[-\frac{\partial W}{\partial x} + 2L\left(\frac{\partial M_x}{\partial x} + \frac{\partial M_{xy}}{\partial y}\right) \right] \delta M_x + m\left[-\frac{\partial W}{\partial y} + 2L\left(\frac{\partial M_y}{\partial y} + \frac{\partial M_{xy}}{\partial x}\right) \right] \delta M_y$$

$$+ \ell\left[-\frac{\partial W}{\partial y} + 2L\left(\frac{\partial M_y}{\partial y} + \frac{\partial M_{xy}}{\partial x}\right) \right] \delta M_{xy} + m\left[-\frac{\partial W}{\partial x} + 2L\left(\frac{\partial M_x}{\partial x} + \frac{\partial M_{xy}}{\partial y}\right) \right] \delta M_{xy}$$

$$- \bar{\beta}_n \delta M_n - \bar{\beta}_s \delta M_{ns} \Bigg] ds \Bigg\}$$

Let the "average" rotations be

$$\beta_x = -\frac{\partial W}{\partial x} + 2L\left(\frac{\partial M_x}{\partial x} + \frac{\partial M_{xy}}{\partial y}\right) \qquad \text{(A.1.1)}$$

$$\beta_y = -\frac{\partial W}{\partial y} + 2L\left(\frac{\partial M_y}{\partial y} + \frac{\partial M_{xy}}{\partial x}\right) \qquad \text{(A.1.2)}$$

Using the transformation relations (2.220) for the moments and

$$\beta_x = \ell \beta_n - m \beta_s$$

$$\beta_y = m \beta_n - \ell \beta_s$$

for the rotations permits the simplification of the last line integral to

$$\int_{s_{n,u}} - \left[+ \beta_n \left[\ell^2 \delta M_x + m^2 \delta M_y + 2\ell m \delta M_{xy} \right] - \bar{\beta}_n \delta M_n \right.$$

$$\left. + \beta_s \left[-\ell m \delta M_x + m \ell \delta M_y + (\ell^2 - m^2) \delta M_{xy} \right] - \bar{\beta}_s \delta M_{ns} \right] ds$$

Then the simplified form of the variational equation is

$$\delta \pi_R = \sum_n \left\{ \iint_{A_n} \left[-\left[\frac{\partial^2 M_x}{\partial x^2} + 2 \frac{\partial^2 M_{xy}}{\partial x \partial y} + \frac{\partial^2 M_y}{\partial y^2} + p \right] \delta W \right.\right.$$

$$+ \left[- \frac{\partial^2 W}{\partial x^2} + 2L \left(\frac{\partial^2 M_{xy}}{\partial y \partial x} + \frac{\partial^2 M_x}{\partial x^2} \right) + \frac{6\mu}{5hE} p - C (M_x - \mu M_y) \right] \delta M_x$$

$$+ \left[- \frac{\partial^2 W}{\partial y^2} + 2L \left(\frac{\partial^2 M_{xy}}{\partial x \partial y} + \frac{\partial^2 M_y}{\partial y^2} \right) + \frac{6\mu}{5hE} p - C (M_y - \mu M_x) \right] \delta M_y$$

$$+ \left[- 2 \frac{\partial^2 W}{\partial x \partial y} + 2L \left(\frac{\partial^2 M_x}{\partial x \partial y} + \frac{\partial^2 M_y}{\partial y \partial x} + \frac{\partial^2 M_{xy}}{\partial x^2} + \frac{\partial^2 M_{xy}}{\partial y^2} \right) \right.$$

$$\left.\left. - 2(1+\mu) C M_{xy} \right] \delta M_{xy} \right] dx\, dy$$

$$+ \int_{s_{n,\sigma}} (Q_n - \bar{Q}_n) \delta W \, ds - \int_{s_{n,u}} (\beta_n - \bar{\beta}_n) \delta M_n \, ds$$

$$- \int (\beta_s - \bar{\beta}_s) \delta M_{ns} \, ds = 0 \qquad (A.1.3)$$

APPENDIX 2

SOLUTION OF THE EIGENVALUE PROBLEM

To solve the eigenvalue relation say

$$[S]\ [W^*] = \lambda_b^*\ [K^*]\ \{W^*\}$$

where [S] and [K*] are symmetric and [K*] is positive definite, the problem is reduced to the standard symmetric eigen-problem by making use of the Cholesky factorization [69],[81] of [K*].

For if [L*] is defined by

$$[K^*] = [L^*]\ [L^*]^T$$

where [L*] is a lower bound triangular matrix, then

$$[S]\ \{W^*\} = \lambda_b^*\ [K^*]\ \{W^*\} \text{ implies}$$

$$([L^*]^{-1}\ [S]\ [L^*]^{-T})([L^*]^T\{W^*\}) = \lambda_b^*\ ([L^*]^T\ \{W^*\})$$

where $[L^*]^{-T} = ([L^*]^{-1})^T$.

hence the eigenvalue is reduced to:

$$[P]\{y\} = \lambda_b^*\ \{y\}$$

where [P] is symmetric and given by

$$[P] = [L^*]^{-1}\ [S]\ [L^*]^{-T}$$

and

$$\{y\} = [L^*]^T\ \{W^*\}.$$

Householder's method [82] is used to reduce the symmetric matrix [P] to a symmetric tridiagonal matrix by orthogonal transformations and the eigenvalues are found using the QL algorithm [83].

An eigenvector $\{z\}$ of the derived problem is related to an eigenvector $\{W^*\}$ of the original problem by:

$$\{z\} = [L^*]^T\{W^*\}.$$

The eigenvectors $\{z\}$ are determined using the QL algorithm and are normalized so that $\{z\}^T\{z\} = 1$; the eigenvectors of the original problem are then determined by solving $\{W\} = [L^*]^T\{z\}$ and are normalized so that:

$$\{W\}^T[K^*]\ \{W\} = 1.$$

A standard procedure F02AEA, to implement the above

description, is available from the Computer Centre N.A.G.Library [67].

APPENDIX 3

DERIVATION OF THE BEAM ELEMENT PROPERTIES

To assist understanding of the Reissner's Principle and the mixed finite element, we develop here the mixed properties of a beam element.

A.3.1) Reissner Functional.

To discuss the Reissner functional for the one dimensional technical beam theory, consider a beam of length L, subject to a uniform transverse load q per unit length, in-plane force P, see Fig.(A.3.1), and with zero body force distribution.

Then:

$$I_R = -\frac{1}{2}\int_0^L \frac{M_x^2}{EI}\,dx - \int_0^L M_x \frac{d^2W}{dx^2}\,dx - \frac{1}{2}\int_0^L P\left(\frac{dW}{dx}\right)^2 dx - \int_0^L q\,W\,dx \qquad (A.3.1)$$

where EI is the flexural rigidity, and M_x, W are respectively continuous differentiable functions representing the bending moments and transverse deflections.

Integrating by parts, the second integral of equation (A.3.1) yields:

$$I_R = -\frac{1}{2}\int_0^L \frac{M_x^2}{EI}\,dx + \int_0^L \frac{dM_x}{dx}\frac{dW}{dx}\,dx - \frac{1}{2}\int_0^L P\left(\frac{dW}{dx}\right)^2 dx - \int_0^L q\,W\,dx \qquad (A.3.2)$$

Eqution (A.3.2) is the starting point for the derivation of the beam element properties.

A.3.2) Mixed Finite Element Properties.

Let us divide the beam into finite elements; for the e th element:

$$(I_R)_e = -\frac{1}{2}\int_0^\ell \frac{M_x^2}{EI}\,dx + \int_0^\ell \frac{dM_x}{dx}\frac{dW}{dx}dx - \frac{1}{2}\int_0^\ell P\left(\frac{dW}{dx}\right)^2 dx - \int_0^\ell q\,W\,dx \qquad (A.3.3)$$

Assuming within the element a natural coordinate ζ, see Fig.(A.3.2),

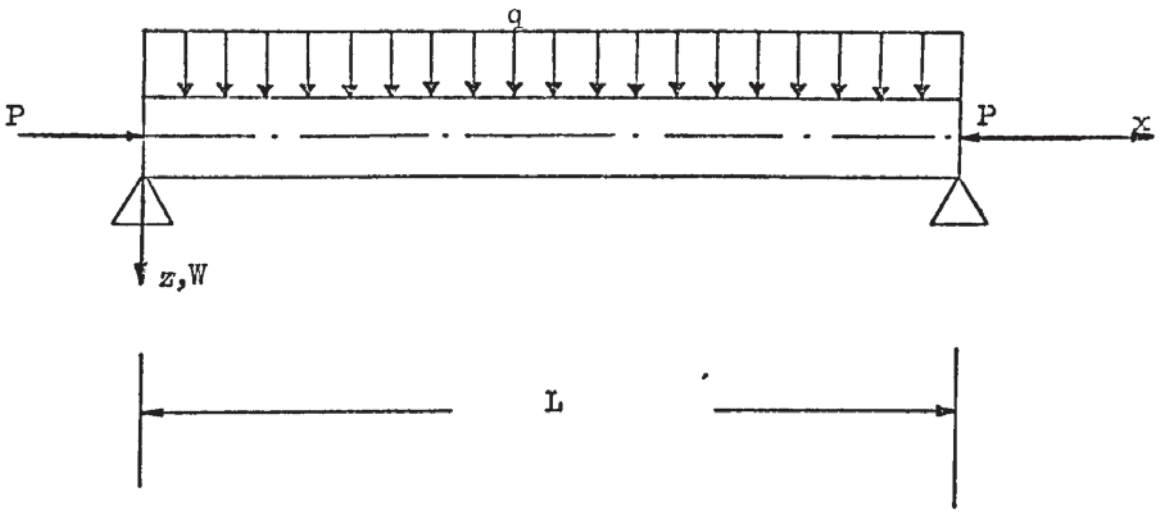

Fig.(A.3.1) Simply supported beam.

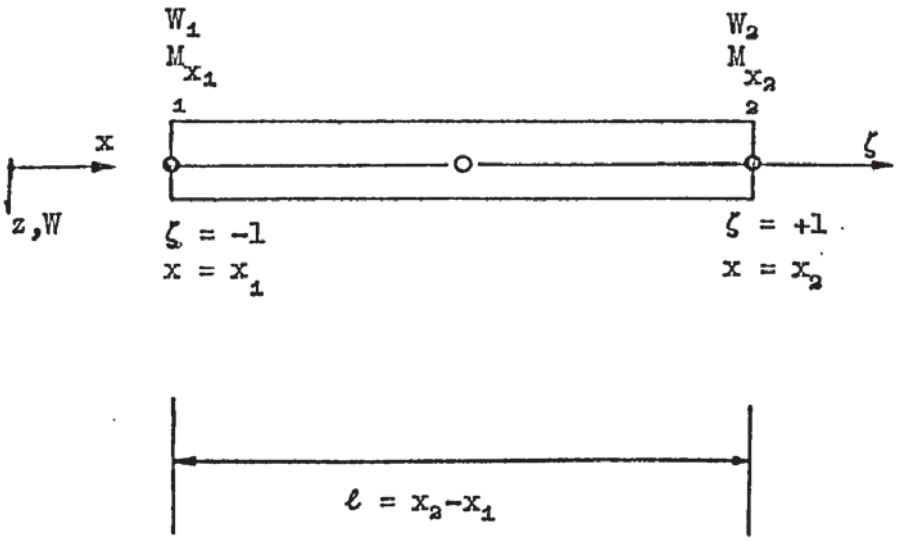

Fig.(A.3.2) Beam element.

such that:

$$x = \begin{bmatrix} \frac{1}{2}(1-\zeta) & \frac{1}{2}(1+\zeta) \end{bmatrix} \begin{Bmatrix} x_1 \\ x_2 \end{Bmatrix} \qquad (A.3.4)$$

$$\text{i.e. } x = [N]\ \{x\}_e$$

where x_1, x_2 are the nodal coordinates at node 1 and 2, and $\zeta = -1$, $\zeta = +1$ respectively at node 1 and node 2.

Solving equation (A.3.4) for ζ gives:

$$\zeta = \frac{x-(x_1+x_2)/2}{(x_2-x_1)/2} = \frac{x-(x_1+x_2)/2}{\ell/2} \qquad (A.3.5)$$

Differentiating (A.3.5) with respect to x yields:

$$\frac{d}{dx} = \frac{d\zeta}{dx}\frac{d}{d\zeta} = \frac{2}{\ell}\frac{d}{d\zeta} \qquad (A.3.6)$$

hence

$$dx = \frac{\ell}{2}\, d\zeta \qquad (A.3.7)$$

Assuming linear variations for M_x and W within the element,

$$M_x = \begin{bmatrix} \frac{1}{2}(1-\zeta) & \frac{1}{2}(1+\zeta) \end{bmatrix} \begin{Bmatrix} M_{x_1} \\ M_{x_2} \end{Bmatrix}$$

$$\text{or } M_x = [N]\ \{M\}_e, \qquad (A.3.8)$$

and

$$W = \begin{bmatrix} \frac{1}{2}(1-\zeta) & \frac{1}{2}(1+\zeta) \end{bmatrix} \begin{Bmatrix} W_1 \\ W_2 \end{Bmatrix}$$

$$\text{or } W = [N]\ \{W\}_e. \qquad (A.3.9)$$

Hence, using equation (A.3.6)

$$\frac{dM_x}{dx} = \frac{2}{\ell}\frac{dM_x}{d\zeta} = \begin{bmatrix} -1/\ell & 1/\ell \end{bmatrix} \begin{Bmatrix} M_{x_1} \\ M_{x_2} \end{Bmatrix}$$

$$\text{i.e. } \frac{dM_x}{dx} = [B]\ \{M\}_e \qquad (A.3.10)$$

$$\frac{dW}{dx} = \frac{2}{\ell}\frac{dW}{d\zeta} = \begin{bmatrix} -1/\ell & 1/\ell \end{bmatrix} \begin{Bmatrix} W_1 \\ W_2 \end{Bmatrix}$$

$$\text{i.e. } \frac{dW}{dx} = [B]\ \{W\}_e \qquad (A.3.11)$$

Substituting relations (A.3.7) to (A.3.11) into the Reissner functional equation (A.3.3) and changing the limits of integration yields:

$$(I_R)_e = -\tfrac{1}{2}\{M\}_e^T[g]\{M\}_e + \{M\}_e^T[h]\{W\}_e - \tfrac{1}{2}\lambda\{W\}_e^T[s]\{W\}_e - \{W\}_e^T\{r\} \qquad \text{(A.3.12)}$$

with $P = \lambda \bar{P}$

where $\bar{P}$ is a trial load, and λ the buckling factor.

The partitioned matrices are evaluated by:

$$[g] = \int_{-1}^{1} [N]^T \left[\frac{1}{EI}\right] [N] \frac{\ell}{2}\, d\zeta \qquad \text{(a)}$$

$$[h] = \int_{-1}^{1} [B]^T[B] \frac{\ell}{2}\, d\zeta \qquad \text{(b)} \qquad \text{(A.3.13)}$$

$$[s] = \int_{-1}^{1} \bar{P}[B]^T[B] \frac{\ell}{2}\, d\zeta \qquad \text{(c)}$$

$$\{r\} = \int_{-1}^{1} [N]^T q \frac{\ell}{2}\, d\zeta \qquad \text{(d)}$$

Extremizing the functional equation (A.3.12) yields:

$$\begin{Bmatrix} \dfrac{\partial I_R}{\partial \{M\}_e^T} \\ \dfrac{\partial I_R}{\partial \{W\}_e^T} \end{Bmatrix} = \left(\left[\begin{array}{c:c} -[g] & [h] \\ \hdashline [h]^T & [0] \end{array}\right] - \left[\begin{array}{c:c} [0] & [0] \\ \hdashline [0] & \lambda[s] \end{array}\right] \right) \begin{Bmatrix} \{M\}_e \\ \{W\}_e \end{Bmatrix} = \begin{Bmatrix} \{0\} \\ \{r\} \end{Bmatrix} \qquad \text{(A.3.14)}$$

In the beam boding problem, the in-plane $\bar{P}$ is assumed zero, hence $[s] = [0]$.

For the buckling problem the right end side of (A.3.14) is zero.

After integrating the expressions (A.3.13), the relation (A.3.14) can be represented in full as:

$$\left(\begin{bmatrix} -\frac{2\ell}{6EI} & -\frac{\ell}{6EI} & \frac{1}{\ell} & -\frac{1}{\ell} \\ -\frac{\ell}{6EI} & -\frac{2\ell}{6EI} & -\frac{1}{\ell} & \frac{1}{\ell} \\ \frac{1}{\ell} & -\frac{1}{\ell} & 0 & 0 \\ -\frac{1}{\ell} & \frac{1}{\ell} & 0 & 0 \end{bmatrix} - \lambda \begin{bmatrix} 0 & 0 & 0 & 0 \\ 0 & 0 & 0 & 0 \\ 0 & 0 & \frac{\bar{P}}{\ell} & -\frac{\bar{P}}{\ell} \\ 0 & 0 & -\frac{\bar{P}}{\ell} & \frac{\bar{P}}{\ell} \end{bmatrix} \right) \begin{Bmatrix} M_{x_1} \\ M_{x_2} \\ W_1 \\ W_2 \end{Bmatrix} = \begin{Bmatrix} 0 \\ 0 \\ q\ell/2 \\ q\ell/2 \end{Bmatrix} \quad \text{(A.3.15)}$$

Substituting M_x by a function

$$M_x' = \frac{M_x}{L} ,$$

the so-called scaled bending moment, the relation (A.3.15) can be represented by:

$$\left(\begin{bmatrix} -\frac{2\ell L^2}{6EI} & -\frac{\ell L^2}{6EI} & \frac{L}{\ell} & -\frac{L}{\ell} \\ -\frac{\ell L^2}{6EI} & -\frac{2\ell L^2}{6EI} & -\frac{L}{\ell} & \frac{L}{\ell} \\ \frac{L}{\ell} & -\frac{L}{\ell} & 0 & 0 \\ -\frac{L}{\ell} & \frac{L}{\ell} & 0 & 0 \end{bmatrix} - \lambda \begin{bmatrix} 0 & 0 & 0 & 0 \\ 0 & 0 & 0 & 0 \\ 0 & 0 & \frac{\bar{P}}{\ell} & -\frac{\bar{P}}{\ell} \\ 0 & 0 & -\frac{\bar{P}}{\ell} & \frac{\bar{P}}{\ell} \end{bmatrix} \right) \begin{Bmatrix} M_{x_1}' \\ M_{x_2}' \\ W_1 \\ W_2 \end{Bmatrix} = \begin{Bmatrix} 0 \\ 0 \\ q\ell/2 \\ q\ell/2 \end{Bmatrix} \quad \text{(A.3.16)}$$

The element consistent mass matrix [m] may be found by replacing the transverse load q (which would contribute the term $-\int_0^{\ell} q\, W\, dx$ to the functional I_R) by the d'Alembert load $\rho \frac{d^2W}{dt^2}$,

where ρ is the mass per unit volume. To find the natural frequencies, one replaces $\lambda[s]$ by $\omega^2[m]$ in relation (A.3.14), with the right end side as a $\{0\}$ vector. The element consistent mass matrix is evaluated by:

$$[m] = \int_{-1}^{1} \rho\, A\, [N]^T [N] \, \frac{\ell}{2} \, d\zeta$$

$$= \rho A \ell \begin{bmatrix} \frac{1}{3} & \frac{1}{6} \\ \frac{1}{6} & \frac{1}{3} \end{bmatrix},$$

where A is the section area of the element (e).

APPENDIX 4

LISTING OF THE MAIN PROGRAM

```
'BEGIN' 'COMMENT'  MOTA SOARES ;
'PROCEDURE' BOUNDARY(VV,W,TO,BD,F,K,G);
'INTEGER' VV,W,G,BD;
'REAL' TO;
'ARRAY' F,K;
'BEGIN' 'INTEGER' Z,J;  W:=4*W-VV;
NEWLINE(1);
          'FOR' Z:=-BD 'STEP' 1 'UNTIL' BD  'DO'
            'BEGIN'
           'IF' Z 'GE' 0 'AND' W+Z 'LE' G 'THEN'
          F[W+Z]:=F[W+Z]-K[W+Z,BD+1-Z]*TO;
          'IF' Z<0 'AND' W+Z>0 'THEN'
          F[W+Z]:=F[W+Z]-K[W,BD+1+Z]*TO;
            'END';
          F[W]:=TO;
          'FOR' J:=1 'STEP' 1 'UNTIL' BD 'DO'
          K[W,J]:=0;
          'FOR' Z:=1 'STEP' 1 'UNTIL' BD 'DO'
          'IF' W+Z 'LE' G 'THEN'
          K[W+Z,BD+1-Z]:=0;
          K[W,BD+1]:=1;
'END' PROC BOUNDARY;
'PROCEDURE'  INBEAM(Z,G,IJ,T,W );
'ARRAY' IJ;  'INTEGER' 'ARRAY' T; 'INTEGER' Z,G,W;
'BEGIN' 'INTEGER' I,S;
WRITETEXT('(' '('1C')'ELE%TYPE%%%%BEAM%PROPERTIES
'('1C')' ')');
'FOR' I:=1 'STEP' 1 'UNTIL' Z  'DO'
'BEGIN' PRINT(I,3,0) ;SPACE(5);
'FOR' S:=1,2  'DO'
'BEGIN'  IJ[I,S]:=READ; PRINT( IJ[I,S],0,5);
'END'; NEWLINE(1);
'END';
WRITETEXT('('('('2C')'BEAM%ELEMENT '('5S')' GEOMETRY% TYPE '('1C')''')');
'FOR' I:=1 'STEP' 1 'UNTIL' G 'DO'
'BEGIN'
          SPACE (5);
W:=READ; PRINT(W,3,0);
SPACE(10);
T[W]:=READ; PRINT(T[W],4,0); NEWLINE(1);
'END';
'END' PROC INBEAM ;
'PROCEDURE' MATMULT4(T,V,K,C,B);
'ARRAY' K,C,B; 'INTEGER' T,V;
'BEGIN' 'COMMENT'  [B]T*[C]*[B]  4*4 MATRIX;
'INTEGER' I,J,R,S,N,G;
N:=(T-1)*4;  G:=(V-1)*4;
'FOR'R:=1 'STEP' 1 'UNTIL' 4 'DO' 'FOR' S:=1'STEP' 1 'UNTIL' 4 'DO'
'FOR'I:=1 'STEP' 1 'UNTIL' 2 'DO' 'FOR' J:=1'STEP' 1 'UNTIL' 2 'DO'
K[N+R,G+S]:=K[N+R,G+S]+B[I,R]*C[(T-1)*2+I,(V-1)*2+J]*B[J,S] ;
'END' PROC MATMULT4;
'PROCEDURE' BEAM(R,U,X,Y,E,EM,T,K,B,BD,IJ);

'VALUE' BD;
'ARRAY' X,Y,K,B,E,IJ;
'INTEGER' 'ARRAY' EM,U,T;
'INTEGER' BD,R;
'BEGIN' 'ARRAY' A[1:2,1:3],D[1:4,1:4];'INTEGER' I,J,W,V;
```

```
        'REAL' S,C,L,BE ;
C:=X[U[R,2]]-X[U[R,1]]; S:=Y[U[R,2]]-Y[U[R,1]]; L:=SQRT(C↑2+S↑2);
        C:=C/L ; S:=S/L;  A[1,1]:=1.0; A[1,2]:=A[1,3]:=A[2,1]:=0.0;
        A[2,2]:=C ;  A[2,3]:=S ;
BE:=-L/(6*E[EM[R],1]*IJ[T[R],1]);
L:=IJ[T[R],2]/L;
BE:=BE*IJ[T[R],2]↑2;
'FOR' I:=1,2,3,4 'DO' 'FOR' J:=1,2,3,4 'DO' D[I,J]:=0.0;
D[1,2]:=D[3,4]:=D[2,1]:=D[4,3]:=L;
D[1,4]:=D[2,3]:=D[4,1]:=D[3,2]:=-D[1,2];


D[2,2]:=D[4,4]:=2*BE;  D[2,4]:=D[4,2]:= BE ;
'FOR' W:=1,2 'DO' 'FOR'V:=1 'STEP' 1 'UNTIL' 2 'DO'
MATMULT4(W,V,B,D,A);
ASSEMBLY(U,K,B,R,BD    ,8);
'END' PROC BEAM;
'PROCEDURE' ASSEMBLY(Q,K,A,R,B,    DF);
'INTEGER' R,B,DF;
'INTEGER' 'ARRAY' Q  ;
'ARRAY' K,A;
'BEGIN' 'INTEGER' 'ARRAY' U[1:16];
'INTEGER' S,V,J;
'FOR' S:=1,2,3,4  'DO' 'FOR' V:=3,2,1,0 'DO'
U[4*S-V]:=  Q[R,S]*4-V ;
'FOR' S:=1 'STEP' 1 'UNTIL' DF 'DO'
'FOR' J:=S 'STEP' 1 'UNTIL' DF 'DO'
'IF' U[S] 'NE' 0 'AND' U[J] 'NE' 0 'THEN'
'BEGIN' 'IF' U[S] 'LE' U[J] 'THEN'
K[U[J],U[S]-U[J]*B ]:=K[U[J],U[S]-U[J]*B]+A[S,J]
'ELSE'
K[U[S],U[J]-U[S]*B]:=K[U[S],U[J]-U[S]*B]+A[S,J];
'END';
'END' PROC ASSEMBLY;
'PROCEDURE' MATERIAL(N,M,NM,E,EM,C,TT,SHEAR);
'ARRAY' E,C ;
'INTEGER' 'ARRAY' EM;
'INTEGER' M,NM,TT,N,SHEAR;
'BEGIN'
'INTEGER' I,J,V;
WRITETEXT('('NUMBER%OF%DIFF.%MATERIALS')');
PRINT(NM,4,0);NEWLINE(1);
'IF' M=1 'THEN'
WRITETEXT('('ISOTROPIC%MATERIAL '('1C')''')') 'ELSE'
WRITETEXT('('ORTHOTROPIC % MATERIAL  '('1C')' ')');
'IF' M=1 'THEN' 'GOTO ' LG1 'ELSE' 'GOTO' LG2;
LG1: WRITETEXT('('MAT.TYPE '('10S')' YOUNGS% MOD.'('13S')'
     POISONS % RATIO '('1C')''')');
'FOR' I:=1  'STEP' 1 'UNTIL' NM 'DO'
'BEGIN'
PRINT(I,4,0);SPACE(10);
E[I,1]:=READ; PRINT(E[I,1],0,4);SPACE(10);
E[I,2]:=READ; PRINT(E[I,2],0,4);NEWLINE(1);
C[I,1]:=1/E[I,1];
              C[I,2]:=C[I,3]:=-E[I,2]; C[I,4]:=2*(1+E[I,2]);
'END'; 'GOTO' LG3;
LG2:

'IF' SHEAR=0 'THEN'
WRITETEXT('('MAT. TYPE'('2S')'EX'('13S')'EY'('11S')'E1'('11S')'
GXY'('1C')'  ')')
'ELSE'
```

```
WRITETEXT('('MAT. TYPE'('2S')'EX'('13S')'EY'('11S')'E1'('11S')'
GXY'('13S')'E2'('11S')'E3'('11S')'GXZ'('11S')'GYZ'('1C')' ')');
'IF' SHEAR=0 'THEN' V:=4 'ELSE' V:=8;
'FOR' I:=1 'STEP' 1 'UNTIL' NM 'DO'
'BEGIN' PRINT(I,4,0);
'FOR' J:=1 'STEP' 1 'UNTIL' V 'DO'
'BEGIN' E[I,J]:=READ ; PRINT(E[I,J],0,4);
SPACE(1);
'END'; NEWLINE(1);
'IF' TT 'NE' 1 'AND' M =2 'THEN'
'BEGIN'
C[I,1]:=1/E[I,1] ; C[I,2]:=1/E[I,2]; C[I,3]:=-1/E[I,3];

C[I,4]:=1/E[I,4];
'IF' SHEAR 'NE' 0 'THEN'
'BEGIN' C[I,5]:=-1.2/E[I,5];C[I,6]:=-1.2/E[I,6];
C[I,7]:=-1.2/E[I,7];  C[I,8]:=-1.2/E[I,8];
'END';
'END';
'IF' TT=1 'AND' M=2 'THEN'
'BEGIN' C[I,1]:=E[I,1];C[I,2]:=E[I,2];C[I,3]:=-E[I,3];
C[I,4]:=E[I,4];
'IF' SHEAR 'NE' 0 'THEN'
'BEGIN' C[I,5]:=-E[I,5]/10; C[I,6]:=-E[I,6]/10;
C[I,7]:=-E[I,7]/10;  C[I,8]:=-E[I,8]/10;
'END';
'END';
'END';
LG3: WRITETEXT('('ELEMENT'('10S')'MAT.TYPE '('1C')'')');
'FOR' I:=1  'STEP' 1  'UNTIL'  N 'DO'
'BEGIN' PRINT(I,4,0); SPACE(10);
EM[I]:=READ; PRINT(EM[I],4,0); NEWLINE(1);
'END' ;
'END' PROC  MATERIAL ;
'PROCEDURE' COMPLIANCE(R,TT,MT,EM,CC,C,T);
'VALUE' TT,MT,R;
'INTEGER''ARRAY' EM;
'ARRAY'  CC,C;
'INTEGER' R,TT,MT;
'REAL' T;
'BEGIN' 'REAL' S   ; 'INTEGER' I,J;
'IF' MT=1 'THEN'
  'BEGIN' C[1,1]:=C[2,2]:=1; C[1,2]:=C[2,1]:=CC[EM[R],2];
          C[3,3]:=CC[EM[R],4];
  'END' 'ELSE'
  'BEGIN' C[1,1]:=CC[EM[R],1]; C[1,2]:=C[2,1]:=CC[EM[R],3];
      C[2,2]:=CC[EM[R],2]; C[3,3]:=CC[EM[R],4];
  'END';
 C[1,3]:=C[2,3]:=C[3,1]:=C[3,2]:=0.0;
  'IF' TT=1  'AND'  MT=1  'THEN'
 'BEGIN'  S:=-12*CC[EM[R],1]/(T↑3);
  'FOR' I:=1,2,3 'DO' 'FOR' J:=1,2,3 'DO' C[I,J]:=S*C[I,J]:'GOTO' FIM;
 'END';
  'IF' TT'NE' 1 'AND' MT=1  'THEN'
  'BEGIN'  S:=-12*CC[EM[R],1];
      'FOR' I:=1,2,3 'DO' 'FOR' J:=1,2,3'DO' C[I,J]:=S*C[I,J];'GOTO'FIM;
   'END';

   'IF' TT 'NE' 1  'AND'  MT 'NE' 1 'THEN'
   'BEGIN' 'FOR' I:=1,2,3 'DO' 'FOR' J:=1,2,3 'DO' C[I,J]:=-12*C[I,J] ;
        'GOTO'  FIM;
```

```
    'END';

'IF' TT=1 'AND' MT=2 'THEN'
  'FOR' I:=1,2,3 'DO' 'FOR' J:=1,2,3 'DO' C[I,J]:=-C[I,J] ;
FIN;
'END' PROC COMPLIANCE ;
'PROCEDURE' PRINBM(I,F,M);
'ARRAY' F; 'INTEGER'I; 'REAL' M;
'BEGIN' 'REAL' A,B,C;
PRINT(I,4,0); SPACE(5);
A:=(F[4*I-2]+F[4*I-1])/2;
B:=F[4*I-2]-F[4*I-1];
C:=SQRT(0.25*B↑2+F[4*I]↑2);
M:=A+C; PRINT(M,0,4); SPACE(10);

M:=A-C; PRINT(M,0,4); SPACE(10);
'IF' ABS(2*F[4*I])<ABS(5000*B) 'THEN'
'BEGIN'
M:=28.64782*ARCTAN(2*F[4*I]/B); PRINT(M,2,2);
'END'
'ELSE' 'IF' F[4*I]=0 'THEN'
'BEGIN' M:=0.0;PRINT(M,1,1);
'END' 'ELSE'
'BEGIN' M:=45; PRINT(M,2,2);
'END';
NEWLINE(1);
'END' PROC PRINBM;
'PROCEDURE' MATMULT3(W,S,F,B);
'ARRAY' F,B;
'INTEGER'W,S;
'BEGIN''ARRAY' M[1:3]; 'INTEGER' I,J;
    'FOR' I:=2,1,0 'DO'
  'BEGIN'
    M[3-I]:=F[4*W-I]; F[4*W-I]:=0.0;
  'END';
  'FOR' I:=2,1,0 'DO' 'FOR' J:=1,2,3 'DO'
   F[4*W-I]:=F[4*W-I]+B[S,3-I,J]*M[J];
'END' PROC MATMULT3;
'PROCEDURE' MATMULT(T,V,K,B);
'VALUE' T,V;
'ARRAY' K,B;
'INTEGER' T,V;
'BEGIN' 'COMMENT' [B]T*[C]*[B];
'INTEGER' I,J,R,S,N,G;
N:=(T-1)*4; G:=(V-1)*4;
'BEGIN' 'ARRAY' C[N+1:N+4,G+1:G+4];
'FOR' I:=N+1 'STEP' 1 'UNTIL' N+4 'DO'
'FOR' J:=G+1 'STEP'1 'UNTIL' G+4 'DO'
'BEGIN' C[I,J]:=K[I,J]; K[I,J]:=0.0;
'END';
'FOR' R:=1 'STEP' 1 'UNTIL' 4 'DO'
'FOR' S:=1 'STEP' 1 'UNTIL' 4 'DO'
'FOR' I:=1 'STEP' 1 'UNTIL' 4 'DO'
'FOR' J:=1 'STEP' 1 'UNTIL' 4 'DO'
K[N+R,G+S]:=K[N+R,G+S]+B[I,R]*C[N+I,G+J]*B[J,S];
'END';
'END' PROC MATMULT;
'PROCEDURE' MATMULT1(T,V,K,B);

   'VALUE' T,V;
```

```
'ARRAY' K,B;
'INTEGER' T,V;
'BEGIN'
'COMMENT'  [B]T*[C];
'INTEGER' N,G,I,J,R;
N:=(T-1)*4;  G:=(V-1)*4;
'BEGIN' 'ARRAY' C[N+1:N+4,G+1:G+4];
'FOR' I:=N+1 'STEP' 1 'UNTIL' N+4 'DO'
'FOR' J:=G+1 'STEP'1 'UNTIL' G+4 'DO'
'BEGIN'  C[I,J]:=K[I,J];  K[I,J]:=0.0;
'END';
'FOR' I:=1 'STEP' 1 'UNTIL' 4 'DO'
'FOR' J:=1 'STEP' 1 'UNTIL' 4 'DO'
'FOR' R:=1,2,3,4 'DO'
K[N+I,G+J]:=K[N+I,G+J]+B[R,I]*C[R+N,J+G];
'END';
'END' PROC MATMULT1;

'PROCEDURE' MATMULT2(T,V,K,B);
'VALUE' T,V;
'ARRAY' K,B;
'INTEGER' T,V;
'BEGIN'
'COMMENT' [C]*[B];
'INTEGER' N,G,I,J,R;
N:=(T-1)*4;  G:=(V-1)*4;
'BEGIN' 'ARRAY' C[N+1:N+4,G+1:G+4];
'FOR' I:=N+1 'STEP' 1 'UNTIL' N+4 'DO'
'FOR' J:=G+1 'STEP'1 'UNTIL' G+4 'DO'
'BEGIN'  C[I,J]:=K[I,J];  K[I,J]:=0.0;
'END';
'FOR' I:=1 'STEP' 1 'UNTIL' 4 'DO'
'FOR' J:=1 'STEP' 1 'UNTIL' 4 'DO'
'FOR' R:=1,2,3,4 'DO'
K[N+I,G+J]:=K[N+I,G+J]+C[N+I,G+R]*B[R,J];
'END';
'END' PROC MATMULT2;
'PROCEDURE' TRANSF(W,K,B);
'INTEGER' W;
'REAL' 'ARRAY' K,B;
'BEGIN' 'INTEGER' T,V;
'IF' W=1 'THEN'
'BEGIN' 'FOR' V:=1,2,3,4 'DO''IF' V=1 'THEN' MATMULT(1,V,K,B)
'ELSE' MATMULT1(1,V,K,B);
'GOTO' PAT;
'END';
'IF' W=2 'THEN'
'BEGIN' 'FOR' V:=1,2,3,4 'DO' 'IF'V=1 'THEN'MATMULT2(1,2,K,B)
'ELSE' 'IF'V=2 'THEN'MATMULT(2,2,K,B) 'ELSE'MATMULT1(2,V,K,B);
'GOTO' PAT;
'END';
'IF' W=3 'THEN'
'BEGIN' 'FOR' T:=1,2 'DO' MATMULT2(T,3,K,B);MATMULT(3,3,K,B);
MATMULT1(3,4,K,B);
'GOTO' PAT;
'END';
'BEGIN' MATMULT(4,4,K,B);
'FOR' T:=1,2,3 'DO' MATMULT2(T,4,K,B);
'END';
PAT:
```

```
'END' PRO TRANSF;
'PROCEDURE' LOADTR(B,F,S,Q);
'INTEGER' S,Q;'ARRAY'B,F;
'BEGIN' 'INTEGER' I,R;'ARRAY' M[1:3];
'FOR' I:=1,2,3 'DO'
'BEGIN' M[I]:=F[4*(Q-1)+1+I];F[4*(Q-1)+1+I]:=0.0;
'END';
'FOR' I:=1,2,3 'DO' 'FOR' R:=1,2,3 'DO'
F[4*(Q-1)+1+I]:=F[4*(Q-1)+1+I] +B[S,R,I]*M[R];
'END' LOADTR;
          'PROCEDURE' BANDSOLVE(C,N,M,V);
'VALUE' N,M;
'INTEGER' N,M;
'REAL' 'ARRAY' C,V;
'BEGIN'
'INTEGER' JM,LR,I,PIV,R,J;
'REAL' T;
LR:=(M+1)'/'2;
'FOR' R:=1 'STEP' 1 'UNTIL' LR-1 'DO'

'FOR' I:=1 'STEP' 1 'UNTIL' LR-R 'DO'
'BEGIN'
'FOR' J:=2 'STEP' 1 'UNTIL' M 'DO'
C[R,J-1]:=C[R,J];
C[R,M]:=C[N+1-R,M+1-I];=0
'END' OF ROW SHIFTING AND ZERO PLACEMENT;
'FOR' I:=1 'STEP' 1 'UNTIL' N-1 'DO'
'BEGIN'
PIV:=I;
'FOR' R:=I+1 'STEP' 1 'UNTIL' LR 'DO'
'IF'  ABS(C[R,1])>ABS(C[PIV,1]) 'THEN'
PIV:=R;
'IF' PIV 'NE' I 'THEN'
'BEGIN' T:=V[I];
V[I]:=V[PIV];
V[PIV]:=T;
'FOR' J:=1 'STEP' 1 'UNTIL' M 'DO'
'BEGIN' T:=C[I,J];
C[I,J]:=C[PIV,J];
C[PIV,J]:=T
'END' J
'END' OF ROW INTERCHANGE;
V[I]:=V[I]/C[I,1];
'FOR' J:=2 'STEP' 1 'UNTIL' M 'DO'
C[I,J]:=C[I,J]/C[I,1];
'FOR' R:=I+1 'STEP' 1 'UNTIL' LR 'DO'
'BEGIN' T:=C[R,1];
V[R]:=V[R]-T*V[I];
'FOR' J:=2 'STEP' 1 'UNTIL' M 'DO'
C[R,J-1]:=C[R,J]-T*C[I,J];
C[R,M]:=0;
'END' R;
'IF' LR 'NE' N 'THEN' LR:=LR+1
'END' OF TRIANGULARIZATION;
V[N]:=V[N]/C[N,1];
JM:=2;
'FOR' R:=N-1 'STEP' -1 'UNTIL' 1 'DO'
'BEGIN' 'FOR' J:=2 'STEP' 1 'UNTIL' JM 'DO'
V[R]:=V[R]-C[R,J]*V[R-1+J];
'IF' JM 'NE' M 'THEN' JM:=JM+1
```

```
'END' OF BACK SOLUTION;

'END' BANDSOLVE;
'PROCEDURE' AUX(L1,L2,B,SFM,SF,X,Y,U,N,Z,CB,JO);
'VALUE' L1,L2,Z,JO;
'INTEGER' Z,JO;
'REAL' L1,L2,U;
'INTEGER' 'ARRAY' N;
'ARRAY' X,Y,B,SF,SFM,CB;
'BEGIN'
'ARRAY' P[1:2,1:4],J[1:2,1:2],C[1:12,1:2];
'INTEGER' I,V,W,S;
'REAL' CHANGE,DN1,DN2,DN3,DN4,DN5,DN6;
'COMMENT' EVALUATES THE JACOBIAN J ITS DETERMINNANT U,
THE ARRAY B AND SHAPE  FUNCTIONS AT THE INTEGRATING POINT;
DN1:=0.25*(1-L2);
DN2:=0.25*(1+L2);
DN3:=0.25*(1-L1);
DN4:=0.25*(1+L1);
DN5:=1-L2;  DN6:=1+L2;
SF[1]:=DN3*DN5;SF[2]:=DN4*DN5;SF[3]:=DN4*DN6;SF[4]:=DN3*DN6;
J[1,1]:=-DN1*X[N[Z,1]]+DN1*X[N[Z,2]]+DN2*X[N[Z,3]]-DN2*X[N[Z,4]];

J[1,2]:=-DN1*Y[N[Z,1]]+DN1*Y[N[Z,2]]+DN2*Y[N[Z, 3]]-DN2*Y[N[Z,4]];
J[2,1]:=-DN3*X[N[Z,1]]-DN4*X[N[Z,2]]+DN4*X[N[Z,3]]+DN3*X[N[Z,4]];
J[2,2]:=-DN3*Y[N[Z,1]]-DN4*Y[N[Z,2]]+DN4*Y[N[Z,3]]+DN3*Y[N[Z,4]];
'COMMENT' U REPLACES DET J;
U:=J[1,1]*J[2,2]-J[1,2]*J[2,1];
CHANGE:=J[1,1];
J[1,1]:=J[2,2]/U;
J[1,2]:=-J[1,2]/U;
J[2,1]:=-J[2,1]/U;  J[2,2]:=CHANGE/U;
'FOR' I:=1,2 'DO'
'BEGIN'
P[I,1]:=-DN1*J[I,1]-DN3*J[I,2];
P[I,2]:=DN1*J[I,1]-DN4*J[I,2];
P[I,3]:=DN2*J[I,1]+DN4*J[I,2];
P[I,4]:=-DN2*J[I,1]+DN3*J[I,2];
'END';
'IF' JO 'NE' 2 'THEN'
'BEGIN'
'FOR' I:=1 'STEP' 1 'UNTIL' 12 'DO'
'FOR' V:=1,2 'DO' C[I,V]:=0.0;
'FOR' I:=1 'STEP' 1 'UNTIL' 4 'DO'
'BEGIN'
C[3*I-2,1]:=C[3*I,2]:=P[1,I];
C[3*I-1,2]:=C[3*I,1]:=P[2,I];
'END';
'IF' JO=3 'THEN'
'BEGIN'  'FOR' I:=1 'STEP' 1 'UNTIL' 12 'DO'
'FOR' V:=1,2 'DO' B[I,V]:=C[I,V];
        'GOTO' TAG;
          'END';
'COMMENT' [C]*[P] TO ORTAIN CONTRIBUTION KEMW;
'FOR' I:=1 'STEP' 1 'UNTIL' 12 'DO'
'FOR' W:=1 'STEP' 1 'UNTIL' 4 'DO'
'BEGIN'
B[I,W]:=0.0;
'FOR' V:=1,2 'DO'
B[I,W]:=B[I,W]+C[I,V]*P[V,W];
```

```
'END';
'COMMENT' COEF OF THE MULT OF SHAPE FUNCTIONS TO EVA. KEM CONT.;
'FOR' I:=1,2,3,4 'DO'

'FOR' S:=I 'STEP' 1 'UNTIL' 4 'DO'
          SFM[I,S]:=SF[I]*SF[S];
'END';
'IF' JO=2 'THEN'
'BEGIN'
'FOR' I:=1,2 'DO' 'FOR' V:=1,2,3,4 'DO'  B[I,V]:=P[I,V];
'END';
'IF' JO=1 'THEN'
'FOR' I:=1 'STEP' 1 'UNTIL' 12 'DO'
'FOR' V:=1,2 'DO' CB[I,V]:=C[I,V];
TAG:'END' OF AUX;
'PROCEDURE' KEFORM(K,B,S,C);
'ARRAY' K,B,S,C;
'BEGIN'
'INTEGER' I,J,V;
'FOR' I:=1,2,3  'DO' 'FOR' J:=1,2,3 'DO'
'BEGIN'

K[1+I,J+1 ]:=K[1+I,J+1 ]+S[1,1]*C[I,J];
K[1+I,J+5 ]:=K[1+I,J+5 ]+S[1,2]*C[I,J];
K[1+I,J+9 ]:=K[1+I,J+9 ]+S[1,3]*C[I,J];

K[1+I,J+13]:=K[1+I,J+13]+S[1,4]*C[I,J];
K[5+I,J+5]:=K[5+I,J+5]+S[2,2]*C[I,J];
K[5+I,J+9]:=K[5+I,J+9]+S[2,3]*C[I,J];
K[5+I,J+13]:=K[5+I,J+13]+S[2,4]*C[I,J];
K[9+I,J+9 ]:=K[9+I,J+9 ]+S[3,3]*C[I,J];
K[9+I,J+13]:=K[9+I,J+13]+S[3,4]*C[I,J];
K[13+I,J+13]:=K[13+I,J+13]+S[4,4]*C[I,J];
'END';
'FOR' I:=1,2,3,4 'DO' 'FOR' V:=1,2,3,4 'DO'
'FOR' J:=1,2,3 'DO'
'BEGIN'
K[4*(I-1)+1+J,4*(V-1)+1]:=K[4*(I-1)+1+J,4*(V-1)+1]+
B[3*(I-1)+J,V];
K[4*(V-1)+1,4*(I-1)+1+J]:=K[4*(V-1)+1,4*(I-1)+1+J]+
B[3*(I-1)+J,V];
'END';
'FOR' I:=1 'STEP' 1 'UNTIL' 16 'DO'
'FOR' J:=I 'STEP' 1 'UNTIL' 16 'DO' K[J,I]:=K[I,J];
'END' PROC KEFORM;
'PROCEDURE' KESHDEF(K,CB,A,L,LX,LY,M);
'ARRAY' K,CB;
'REAL' A,L,LX,LY;
'INTEGER' M;
'BEGIN' 'ARRAY' BT[1:16,1:2],B[1:2,1:16];
'INTEGER' I,J,W;
'FOR' I:=1 'STEP' 1 'UNTIL' 16 'DO'
 'FOR' J:=1,2 'DO' BT[I,J]:=B[J,I]:=0.0;
'FOR' I:=1 'STEP' 1'UNTIL' 4 'DO'
'FOR' J:=1,2,3 'DO' 'FOR' W:=1,2 'DO'
BT[4*(I-1)+1+J,W]:=B[W,4*(I-1)+1+J]:=CB[3*(I-1)+J,W];
'FOR' I:=1 'STEP' 1 'UNTIL' 16 'DO'
'FOR' J:=I 'STEP' 1 'UNTIL' 16 'DO'
'BEGIN' 'IF' M=1 'THEN'
'BEGIN'
```

```
  'FOR' W:=1,2 'DO'
  K[I,J]:=K[I,J]+L*BT[I,W]*B[W,J]*A
  'END' 'ELSE'
  K[I,J]:=K[I,J]+(LX*BT[I,1]*B[1,J]+LY*BT[I,2]*B[2,J])*A;
  'END';

  'END' PROC KESHDEF;
  'PROCEDURE'  BAND(CODE,BD,N,M);
               'INTEGER'N,BD,M;'INTEGER''ARRAY' CODE ;
  'BEGIN' 'INTEGER' S,I,Q,W ;
               BD:=1 ;
               'FOR' I:=1   'STEP' 1  'UNTIL'  N 'DO'
        'BEGIN'
               Q:=6000  ;  W:=1 ;
      'FOR' S:=1 'STEP' 1 'UNTIL' 4 'DO'
               'IF'  CODE[I,S]  'NE' 0  'THEN'
         'BEGIN'
               'IF'  CODE[I,S] < Q  'THEN'  Q:=CODE[I,S] ;
               'IF'  CODE[I,S] > W  'THEN'  W:=CODE[I,S] ;
          'END';
           'IF' W-Q+1>BD 'THEN'BD:=W-Q+1;
          'END';
              WRITETEXT('('('2C')'HALFBANDWIDTH'('5S')')');
           BD:=4*BD;
              PRINT(BD,4,0) ;
           M:=2*BD-1;
           NEWLINE(2);
 'END' PROC BAND;

'PROCEDURE' SIDES(CODE,X,Y,AA,D,R,SINB,COSB,A1);
'INTEGER' 'ARRAY' CODE;
'ARRAY' X,Y,AA,D,SINB,COSB,A1;
'INTEGER' R;
'BEGIN' 'ARRAY' XX,YY[1:4];
'INTEGER' I;
          XX[1]:=X[CODE[R,1]]-X[CODE[R,2]];
          XX[2]:=X[CODE[R,2]]-X[CODE[R,3]];
XX[3]:=X[CODE[R,3]]-X[CODE[R,4]];
XX[4]:=X[CODE[R,4]]-X[CODE[R,1]];
          YY[1]:=Y[CODE[R,1]]-Y[CODE[R,2]];
          YY[2]:=Y[CODE[R,2]]-Y[CODE[R,3]];
YY[3]:=Y[CODE[R,3]]-Y[CODE[R,4]];
YY[4]:=Y[CODE[R,4]]-Y[CODE[R,1]];
      'FOR' I:=1 'STEP' 1 'UNTIL' 4 'DO'
       'BEGIN'
            A1[I]:=SQRT(XX[I]↑2+YY[I]↑2);
             SINB[I]:=XX[I]/A1[I];
             COSB[I]:=-YY[I]/A1[I];
A1[I]:=0.5*A1[I];
             AA[I,1]:=COSB[I]↑2 ;
             AA[I,2]:=SINB[I]↑2 ;
             AA[I,3]:=2*SINB[I]*COSB[I] ;
             D[I,1]:=-0.5*AA[I,3] ;
             D[I,2]:=-D[I,1] ;
             D[I,3]:=AA[I,1]-AA[I,2] ;
'END';
'END' PROC SIDES;

'PROCEDURE' MNSWSDS(WW,A,KE,D,X,Y,N,Z,C,SI,L);
'INTEGER' Z;
```

```
'ARRAY' WW,A,KE,D,X,Y,C,SI,L;
'INTEGER' 'ARRAY' N;
'BEGIN' 'ARRAY' B[1:12,1:1],P[1:2,1:4],SF[1:4],
SFM[1:4,1:4],CB[1:1,1:1];
'INTEGER' I,J,S,V,W;
'REAL' U;
'FOR' I:=1,2,3,4 'DO' 'FOR' W:=1,2    'DO'

'BEGIN'
AUX(A[W,2*I-1],A[W,2*I],P,SFM,SF,X,Y,U,N,Z,CB,2);
'FOR'J:=1,2,3,4 'DO'
'BEGIN' P[2,J]:=P[2,J]*C[I];    P[1,J]:=-P[1,J]*SI[I];
SFM[1,J]:=L[I]*(P[1,J]+P[2,J]);
'END';
'FOR' V:=1,2,3,4 'DO' 'FOR' J:=1,2,3 'DO'
B[3*(V-1)+J,1]:=SF[V]*D[I,J];
'FOR' S:=1 'STEP' 1 'UNTIL' 12 'DO'
'FOR' J:=1,2,3,4 'DO'
KE[S,J]:=KE[S,J]-WW[W,I]*B[S,1]*SFM[1,J];
'END';
'END' PROC MNSWSDS;
'PROCEDURE' SHFORCE(QXY,X,Y,N,Z,F);
'ARRAY' QXY,X,Y,F;
'INTEGER' 'ARRAY' N;
'INTEGER' Z;
'BEGIN'  'ARRAY' B[1:12,1:2],SFM[1:1,1:1],SF[1:4],CB[1:1,1:1];
'REAL' U;
'INTEGER' J,V,S;
'FOR' J:=1,2 'DO' QXY[1,J]:=0.0;
AUX(0,0,B,SFM,SF,X,Y,U,N,Z,CB,3);
'COMMENT' SHEAR FORCE  QX AND QY;

'FOR' J:=1,2 'DO' 'FOR' S:=1,2,3,4 'DO'
'FOR'V:=2,1,0 'DO'
QXY[1,J]:=QXY[1,J]+F[4*S-V]*B[3*S-V,J];
PRINT(Z,4,0);SPACE(5);      PRINT(QXY[1,1],0,4);SPACE(10);
PRINT(QXY[1,2],0,4); NEWLINE(1);
'END' PROC SHFORCE;
'BEGIN'
'ARRAY'          WW[1:2,1:4],ZN[1:2,1:8],SF[1:4],SFM[1:4,1:4],
      H[1:9,1:3],CB[1:12,1:2];
            'INTEGER' N,M,V,S,Q,R,J,I,W,G,BD,GC,DF,LL,NSETS,U,Z,ET,
MTYPE,THTYPE,TYLOAD,NE,NB    ,NUQ,NII ,
ET1,NUDL,GA,GG,NMAT,LD,VV, SHEAR;
'REAL' W1,W2,W3,T,UQ,E1,QL,TO,L,LR,LE,LER,LX,LY,LE1,LER1;
NSETS:=READ;
'FOR' I:=1,2 'DO'
'BEGIN'
'FOR' J:=2,7 'DO'
ZN[I,J]:=-1;
'FOR' J:=3,6 'DO' ZN[1,J]:=1;
'END';
'FOR' I:=1,2,3,4 'DO' H[I,1]:=1.0;
W1:=0.57735026919;
H[1,2]:=H[1,3]:=H[2,3]:=H[3,2]:=W1;
H[2,2]:=H[3,3]:=H[4,2]:=H[4,3]:=-W1;
ZN[1,1]:=ZN[1,4]:=ZN[1,5]:=ZN[1,8]:=-W1;
ZN[2,1]:=ZN[2,4]:=ZN[2,5]:=ZN[2,8]:=W1;
'FOR' I:=1,2 'DO' 'FOR' J:=1,2,3,4 'DO' WW[I,J]:=1.0;
        'FOR'  LL:=1 'STEP' 1 'UNTIL' NSETS 'DO'
```

```
     'BEGIN'
 SHEAR:=READ;
  'IF' SHEAR=0 'THEN'
 WRITETEXT('(' '('1C')'THIN%PLATE%THEORY '('3C')' ')')
 'ELSE'
 WRITETEXT('(' '('1C')' PLATE%THEORY%INCLUDING%SHEAR%
 DEFORMATION '('3C')' ')');
 MTYPE:=READ; THTYPE:=READ; TYLOAD:=READ;
 NMAT:=READ;

 NB:=READ;'IF' NB 'NE' 0  'THEN'
 NII:=READ;
              N:=READ ;
             GG:=READ ;
 ET:=READ;
 GC:=READ;
              WRITETEXT('('NO.% OF % ELEMENTS')') ;
              PRINT(N,3,0) ;
              NEWLINE(2) ;
              WRITETEXT('('NO.% OF% DEGREES % OF% FREEDOM')') ;
     G:=4*GG;
                PRINT( G,3,0);
 'IF' NB=0 'THEN' NII:=1;
              NEWLINE(2) ;
 'IF' ET=0 'THEN' ET1:=1 'ELSE' ET1:=ET;
 'IF' SHEAR=0 'THEN' NE:=4 'ELSE' NE:=8;
 'IF'  TYLOAD=1 'THEN' NUDL:=1 'ELSE' NUDL:=GG;
       'BEGIN'
 'ARRAY' B[1:ET1,1:3,1:3],F[1:G],E[1:NMAT,1:NE],ESP[1:GG ],UDI[1:NUDL],
       CC[1:NMAT,1:NE],IJ[1:NII,1:3] ,SINB,COSB[1:4],ANG[1:ET1];
 'INTEGER' 'ARRAY' CODE[1:N,1:4],VNS,VNN,VNT[1:ET1],EMAT[1:N],
 EIJ[1:N],BGC[1:GC,1:2];
 'COMMENT' TYLOAD=1 FOR UN.PRES.W/OR/WITHOUT CONC.
 LOADS, TYLOAD=2 NODAL PRES. SPEC. W/OR/WITHOUT

 CONC. LOADS;
 'IF' TYLOAD=1 'THEN'
 'BEGIN'  WRITETEXT('('UNIFORM%PRESSURE')');
 UQ:=READ; PRINT(UQ,0,5);NEWLINE(1);
 'END' 'ELSE'
 'BEGIN' WRITETEXT('('NODE%%%PRESSURE'('1C')' ')');
 'FOR' I:=1 'STEP' 1 'UNTIL' GG 'DO'
 'BEGIN' UDL[I]:=READ;PRINT(I,3,0);
 PRINT(UDL[I],0,5);
 NEWLINE(1);
 'END';
 'END';

 WRITETEXT('(' '('1C')'NODE/ELEM%%%%THICKNESS '('1C')' ')');
 'IF' THTYPE=1  'THEN'
 'BEGIN' T:=READ;SPACE(12);PRINT(T,0,3);
 NEWLINE(4);
 'END' 'ELSE'
 'BEGIN' 'IF' THTYPE=12 'THEN' J:=N 'ELSE' J:=GG;
 'FOR' I:=1 'STEP' 1 'UNTIL' J 'DO'
 'BEGIN'
 ESP[I]:=READ;
 PRINT(I,4,0); SPACE(5)  ; PRINT(ESP[I],0,5); NEWLINE(1);
 'END';
```

```
'END';
MATERIAL(N,MTYPE,NMAT,E,EMAT,CC,THTYPE,SHEAR);
'COMMENT' INPUT BEAM PROPERTIES 2NDMOMENT OF AREA ,LENGTH
AND RESPECTIVE ELEMENT IJ TYPE ;
'IF' NB 'NE' 0 'THEN'
INBEAM(NII,NB,IJ,EIJ,W );
              WRITETEXT ('('ELEMENT '('10S')' CODE ')') ;
              'FOR' I:=1 'STEP' 1 'UNTIL' N 'DO'
       'BEGIN'
              NEWLINE(2);
              PRINT(I,4,0) ;

              'FOR' S:=1 'STEP' 1 'UNTIL' 4 'DO'
       'BEGIN'
              CODE[I,S]:=READ ;
              PRINT(CODE[I,S],4,0) ;
         'END';
         'END';
WRITETEXT('(' '('1C')'NODE%TRANSF%%ANGLE%DEG.
'('1C')' ')');
'FOR' S:=1 'STEP' 1 'UNTIL' E1 'DO'
'BEGIN'
VNN[S]:=READ;PRINT(VNN[S],4,0);
SPACE(4);
ANG[S]:=READ;PRINT(ANG[S],3,3);
NEWLINE(1);
ANG[S]:=3.141592654*ANG[S]/180;
'END';
              'COMMENT' TO CALCULATE HALFBANDWIDTH ;
       'BEGIN'
'ARRAY' D,AA[1:4,1:3],A1[1:4],CQL[1:GC],
B2[1:12,1:4],
KE[1:16,1:16],B1[1:12,1:4],A[1:4,1:4],
QXY[1:1,1:2],
     FF[1:16],X,Y[1:GG],                C[1:3,1:3];
'REAL' AREA,S1,DETJ;
WRITETEXT('('NODE '('6S')' X%COO'('11S')'Y%COO '('1C')' ')');

'FOR'I:=1 'STEP' 1 'UNTIL' GG 'DO'
'BEGIN'
NEWLINE(1);
PRINT(I,4,0);
SPACE(2);
X[I]:=READ;
PRINT(X[I],0,4);
Y[I]:=READ;
SPACE(2);
PRINT(Y[I],0,4);
NEWLINE(2);
'END';
               'FOR' I:=1 'STEP' 1 'UNTIL' G 'DO'
              F[I ]:=0;
 LD:=READ;
'COMMENT' READ IN CONC. LOAD VECTOR;
NEWLINE(1);
'FOR' I:=1 'STEP' 1 'UNTIL' LD 'DO'
'BEGIN'
WRITETEXT('('NODE%%%POSITION%%LOAD '('1C')'   ')');
W:=READ; PRINT(W,3,0);
```

```
J:=READ; PRINT(J,3,0);
QL:=READ; PRINT(QL,0,6);
NEWLINE(1);
W:=4*W-J;  F[U]:=F[W]+QL;
'END';
NEWLINE(4);
'COMMENT' READ IN BOUNDARY CONDITIONS;
WRITETEXT('(' POSITION%%%NODE%%%PRESC. VALUE '('1C')' ')');
'FOR' I:=1 'STEP' 1 'UNTIL' GC 'DO'
'BEGIN' BGC[I,1]:=READ;PRINT(BGC[I,1],3,0);
SPACE(2);
BGC[I,2]:=READ; PRINT(BGC[I,2],3,0);
CQL[I]:=READ;PRINT(CQL[I],0,5);
NEWLINE(1);

'END';
     NEWLINE(1);
BAND(CODE,BD,N,M);
NEWLINE(1);
'BEGIN' 'ARRAY' K[1:G,1:M];
'FOR' I:=1 'STEP' 1 'UNTIL' G 'DO'
'FOR' J:=1 'STEP' 1 'UNTIL' M 'DO' K[I,J]:=0.0;
     'FOR' R:=1  'STEP' 1 'UNTIL' N 'DO'
     'BEGIN'
'FOR' I:=1 'STEP' 1 'UNTIL' 16 'DO'
'FOR' J:=1 'STEP' 1 'UNTIL' 16 'DO'  KE[I,J]:=0.0;
'FOR'I:=1 'STEP' 1 'UNTIL' 16 'DO' FE[I]:=0.0;
'FOR'I:=1 'STEP' 1 'UNTIL' 12 'DO'
'FOR' J:=1,2,3,4 'DO' B2[I,J]:=0.0;
'FOR'I:=1,2,3,4 'DO' 'FOR' J:=I 'STEP' 1  'UNTIL' 4 'DO'
A[I,J]:=0.0;
'IF' CODE[R,3] 'NE' 0  'THEN'
'BEGIN'
COMPLIANCE(R,THTYPE,MTYPE,EMAT,CC,C,T) ;
'IF' SHEAR 'NE' 0 'THEN'
'BEGIN' 'IF' MTYPE=1 'THEN'
'BEGIN' LE:=C[3,3]/10;LER:=C[1,2]/10;
'END''ELSE'
'BEGIN' LE:=CC[EMAT[R],7]; LE1:=CC[EMAT[R],8];
LER:=CC[EMAT[R],5]; LER1:=CC[EMAT[R],6];
'END';

'END';
'FOR' U:=1 'STEP' 1 'UNTIL' 4 'DO'
'BEGIN'
AUX(H[U,2],H[U,3],B1,SFM,SF,X,Y,DETJ,CODE,R,CB,1);
DETJ:=H[U,1]*DETJ;
'FOR' I:=1 'STEP' 1 'UNTIL' 12 'DO' 'FOR' J:=1,2,3,4 'DO'
B2[I,J]:=B2[I,J]+B1[I,J]*DETJ;
'IF' THTYPE=1 'THEN'
'BEGIN'
'FOR' I:=1,2,3,4 'DO' 'FOR' J:=I 'STEP' 1 'UNTIL' 4 'DO'
A[I,J]:=A[I,J]+SFM[I,J]*DETJ;  TO:=T;
'END' 'ELSE'
'BEGIN'
'IF' THTYPE=12 'THEN'
'BEGIN' TO:=ESP[R];
T:=1/(ESP[R]↑3);
'END'  'ELSE'
'BEGIN'
```

```
  'BEGIN' TO:=0.0;
'FOR' I:=1,2,3,4 'DO' TO:=TO*SF[I]*ESP[CODE[R,I]];
'END';
T:=1/(TO↑3);
'END';
   'FOR' I:=1,2,3,4  'DO' 'FOR' J:=I  'STEP' 1 'UNTIL' 4 'DO'
    A[I,J]:=A[I,J]+SFM[I,J]*DETJ*T ;
'END';
'FOR' I:=1,2,3,4 'DO' 'FOR' J:=1,2,3,4 'DO'
SFM[J,I]:=SFM[I,J];
'FOR'I:=1,2,3,4 'DO'
'BEGIN' 'IF' TYLOAD=1 'THEN'
FE[4*(I-1)+1]:=FE[4*(I-1)+1]+SF[I]*DETJ*UQ 'ELSE'
 'FOR' J:=1,2,3,4 'DO'
FE[4*(I-1)+1]:=FE[4*(I-1)+1]+
SFM[I,J]*UDL[CODE[R,J]]*DETJ;

'END';
 'IF'  SHEAR 'NE' 0 'THEN'
'BEGIN' 'IF' MTYPE=1 'THEN'
'BEGIN' 'IF' THTYPE=1 'THEN'
'BEGIN' L:=LE*TO↑2;LR:=-LER*TO↑2;
'END' 'ELSE'
'BEGIN' L:=LE/TO;  LR:=-LER/TO;
'END' ;
'END' 'ELSE'
'BEGIN' 'IF' THTYPE=1 'THEN'
'BEGIN' LX:=LE*TO*TO;LY:=LE1*TO*TO;
L:=-LER*TO*TO;LR:=-LER1*TO*TO;
'END' 'ELSE'
'BEGIN' LX:=LE/TO;LY:=LE1/TO;L:=-LER/TO; LR:=-LER1/TO;
'END';
'END';
KESHDEF(KE,CB,DETJ,L,LX,LY,MTYPE);
'IF' MTYPE=1 'THEN'
'BEGIN'
'FOR' I:=1,2,3,4 'DO' 'FOR' J:=1,2 'DO'
FE[4*(I-1)+1+J]:=+LR*FE[4*(I-1)+1];
'END' 'ELSE'
'BEGIN' 'FOR' I:=1,2,3,4 'DO'
'BEGIN' FE[4*(I-1)+2]:=L*FE[4*(I-1)+1];
FE[4*(I-1)+3]:=LR*FE[4*(I-1)+1];
'END';
'END';

'END';
'END';
     NEWLINE(1);
'IF' SHEAR=0 'THEN'
'BEGIN'
SIDES(CODE,X,Y,AA,D,R,SINB,COSB,A1);
MNSWSDS(WW,ZN,B2,D,X,Y,CODE,R,COSB,SINB,A1);
'END';
KEFORM(KE,B2,A,C);
'FOR'S:=1 'STEP' 1 'UNTIL' ET 'DO'
'BEGIN' 'FOR' W:=1,2,3,4 'DO'
 'BEGIN' 'IF' CODE[R,W]=VNN[S] 'THEN'
'GOTO' L8 'ELSE' 'GOTO' L9;
L8:
'BEGIN' A[2,2]:=A[3,3]:=SIN(ANG[S])↑2;
```

```
A[2,3]:=A[3,2]:=COS(ANG[S])↑2;
A[4,3]:=COS(ANG[S])*SIN(ANG[S]);
A[4,2]:=-A[4,3];A[2,4]:=-2*A[4,3];
A[3,4]:=2*A[4,3];A[4,4]:=A[2,3]-A[2,2];
A[1,1]:=1.0;
'FOR' I:=2,3,4 'DO' A[1,I]:=A[I,1]:=0.0;
TRANSF(W,KE,A);
'FOR' I:=1,2,3 'DO' 'FOR' J:=1,2,3 'DO'
B[S,I,J]:=A[1+I,1+J];
'GOTO' L10;
'END';
L9:
'END';
L10:
'END';
'FOR' I:=1 'STEP' 1 'UNTIL'16 'DO'
'FOR' J:=I 'STEP' 1 'UNTIL' 16 'DO' KE[J,I]:=KE[I,J];
ASSEMBLY(CODE,K,KE,R,BD   ,16);

'FOR' S:=1,2,3,4 'DO'
 'FOR' J:=3,2,1 'DO'
F[CODE[R,S]*4-J]:=F[CODE[R,S]*4-J]+FE[4*S-J];
'END' 'ELSE'
BEAM(R,CODE,X,Y,E,EM AT,EIJ,K,KE,BD,IJ);
'END' LOOP EL. MATRIX;
'FOR' S:=1 'STEP' 1 'UNTIL' ET 'DO'
'BEGIN' Q:=VNN[S];LOADTR(B,F,S,Q);
'END';
    WRITETEXT('('('2C')'OVERALL%STIFFNESS%MATRIX')');
WRITETEXT('('('2C')'OVERALL%NODAL%FORCING%VECTOR')');
BD:=BD-1;
'FOR' I:=1 'STEP' 1 'UNTIL' GC 'DO'
'BEGIN'  VV:=BGC[I,1]; W:=BGC[I,2];
TO:=CQL[I];
BOUNDARY(VV,W,TO,BD,F,K,G);
'END';
          'FOR' R:=1 'STEP' 1 'UNTIL' BD 'DO'
          'FOR' S:=1 'STEP' 1 'UNTIL' G 'DO'
          'IF' S>BD+1-R 'THEN'
          K[S-BD-1+R,M+1-R]:=K[S,R];
        BANDSOLVE(K,G,M,F);
NEWLINE(2);
WRITETEXT('('NODE'('9S')'DEFLECTION%W '(' 2S')'MOM%MX'(' 7S')'MOM%MY
      '(' 7S')'MOM%MXY '('1C')' ')');
'FOR' I:=1 'STEP' 1 'UNTIL' GG 'DO'
'BEGIN'  PRINT(I,4,0); SPACE(5);
'FOR' S:=3,2,1,0 'DO'

'BEGIN' PRINT(F[I*4-S],0,4);
'END';
NEWLINE(1);
'END';
NEWLINE(2);
WRITETEXT('('PRINCIPAL%BENDING%MOMENTS'('1C')'NODE'('9S')'BM%MAX
        '('19S')'BM%MIN '('15S')' ANGLE  '('1C')' ')');
'FOR' I:=1 'STEP' 1 'UNTIL' GG 'DO'
PRINBM(I,F,UQ);
NEWLINE(2);
WRITETEXT('('SHEARING % FORCE% PER %ELEMENT'('1C')'ELEMENT '(' 9S')'
        QX '('20S')'QY  '('1C')' ')');
```

```
'FOR' S:=1 'STEP' 1 'UNTIL' ET 'DO'
'BEGIN' W:=VNN[S];
MATMULT3(W,S,F,B);
'END';
'FOR' Z:=1 'STEP' 1 'UNTIL' N 'DO'
'IF' CODE[Z,3] 'NE' 0 'THEN'
'BEGIN'
'FOR' S:=1,2,3,4  'DO' 'FOR' V:=2,1,0 'DO'
FE[4*S-V]:=F[CODE[Z,S]*4-V];
SHFORCE(QXY,X,Y,CODE,Z,FE);
'END';
'END';
'END';
      'END';
NEWLINE(20);
   'END';
      'END';
         'END' OF PROGRAM;
```

APPENDIX 5

LISTING OF THE TEST EIGENVALUE PROGRAM

```
'BEGIN' 'COMMENT' MOTA SOARES ;
'PROCEDURE' POZAEA(A,B,N,P,V,IFAIL);
'VALUE' N; 'INTEGER'N,IFAIL; 'ARRAY' A,B,R,V;
'ALGOL';
'PROCEDURE' COMPLBUCK(II,S,SO,E,M,EM,U,K,FAIL);
'ARRAY' II,S,E,SO;
'INTEGER' 'ARRAY' U,EM;
'REAL' M;
'INTEGER' R;
'LABEL' FAIL;
'BEGIN' 'ARRAY' K[1:3,1:6];
'REAL' A,B,C,D,F,SI1,SI,ET,ES;
'INTEGER' I,W,J;
'FOR' I:=1,2 'DO' 'FOR' J:=1,2 'DO' SO[I,J]:=0,0;
 'FOR' I:=1,2,3,4 'DO'
'BEGIN'
SO[1,1]:=SO[1,1] +S[U[R,I],1]/4;
SO[1,2]:=SO[1,2]+S[U[R,I],3]/4;
SO[2,2]:=SO[2,2]+S[U[R,I],2]/4;
'END';SO[2,1]:=SO[1,2];
A:=SO[1,1]↑2; B:=SO[2,2]↑2; C:=SO[1,1]*SO[2,2];D:=3*(SO[1,2]↑2);
SI1:=A+B-C+D; SI:=SQRT(SI1);
F:=(SI/E[EM[R],2])↑(M-1); ET:=E[EM[R],1]/(1+(3*M//)*F);
ES:=E[EM[R],1]/(1+3//*F);ET:=1-ET/ES;
ES:=9/ES;
K[1,1]:=(1-0,75*A*ET/SI1);K[1,2]:=K[2,1]:=0,5*(1-1,5*C*ET/SI1);
K[1,3]:=K[3,1]:=0,75*SO[1,1]*SO[1,2]*ET/SI1;
K[2,2]:=(1-0,75*B*ET/SI1);
K[2,3]:=K[3,2]:=0,75*SO[2,2]*SO[1,2]*ET/SI1;
K[3,3]:=0,25*(1-D*ET/SI1);
'FOR' W:=1,2,3 'DO' 'FOR' J:=1,2,3 'DO' K[W,3+J]:=0,0;
K[1,4]:=K[2,5]:=K[3,6]:=1,0;
'COMMENT' INVERSION TO GET PLASTIC COMP MATRIX;
EOSOLV(3,3,K,K,FAIL);
'FOR' I:=1,2,3 'DO' 'FOR' J:=1,2,3 'DO' III[I,J]:=ES*K[I,3+J];
'END' PROC COMPLBUCK;

'PROCEDURE' MASS(M,P,K,MA,CODE,R,MD,Z);
'ARRAY' M,K,MA;
'INTEGER' 'ARRAY' CODE,P;
'REAL' MD;
'INTEGER' R,Z;
'BEGIN' 'INTEGER' I,J,B;
'FOR' I:=1,2,3,4 'DO' 'FOR' J:=1 'DO'
'IF' Z=100 'OR' Z=201 'THEN'
M[I,J]:=M[I,J]*MD;
'FOR' I:=1 'STEP' 1 'UNTIL' 16 'DO'
'FOR' J:=1 'STEP' 1 'UNTIL' 16 'DO' K[I,J]:=0,0;
K[1,1]:=M[1,1];K[1,5]:=K[5,1]:=M[1,2];K[1,9]:=K[9,1]:=M[1,3];
K[1,13]:=K[13,1]:=M[1,4]; K[5,5]:=M[2,2];
K[5,9]:=K[9,5]:=M[2,3];K[5,13]:=K[13,5]:=M[2,4];

K[9,9]:=M[3,3]; K[9,13]:=K[13,9]:=M[3,4];
K[13,13]:=M[4,4];
ASSEMBLY(CODE,MA,K,R,B,P,16);
'END' PROC MASS;
'PROCEDURE' BOUNDARY(VV,W,TA,P);
'INTEGER' VV,W;'REAL' TA; 'INTEGER' 'ARRAY' P;
'BEGIN' 'INTEGER' I,J;
VV:=READ;PRINT(VV,3,0);SPACE(2);
```

```
W:=READ;PRINT(W,3,0);SPACE(2);
W:=4*W-VV;SPACE(3);
TA:=READ;PRINT(TA,0,3);NEWLINE(1);
P[W]:=0;
'END' PROC BOUNDARY;

'PROCEDURE' EOSOLV (N,R,A,B  ,FAIL);
  'VALUE' N,R;
  'INTEGER' N,R;
  'ARRAY' A,B  ;
  'LABEL' FAIL;
'BEGIN'
'COMMENT'  THIS PROCEDURE SOLVES THE EQUATION LA][X]=[B];
'PROCEDURE' CHOLDET1 (N,A,P,D1,D2,FAIL);
  'VALUE' N;
  'INTEGER' D2,N;
  'REAL' D1;
  'ARRAY' A,P;
  'LABEL' FAIL;
'COMMENT'  REF.: HANDBOOK FOR AUTOMATIC COMPUTATION,
                 J. H. WILKINSON AND C. REINSCH;
'BEGIN'
  'INTEGER' I,J,K;
  'REAL' X;
  D1:=1;  D2:=0 ;
  'FOR' I:=1 'STEP' 1 'UNTIL' N 'DO'
  'FOR' J:=1 'STEP' 1 'UNTIL' N 'DO'
'BEGIN'
  X:=A[I,J];
  'FOR' K:=I-1 'STEP' -1 'UNTIL' 1 'DO'
  X:=X-A[J,K]*A[I,K];
  'IF' J=I 'THEN'
'BEGIN'
  D1:=D1*X;
  'IF' X=0 'THEN'
'BEGIN'
  D2:=0; 'GOTO' FAIL;
'END';
L1 : 'IF' ABS(D1) 'GE' 1 'THEN'
'BEGIN'
  D1:=D1*0,0625;  D2:=D2+4;  'GOTO' L1;
'END';
L2 : 'IF' ABS(D1) < 0,0625 'THEN'
'BEGIN'
  D1:=D1*16;  D2:=D2-4;  'GOTO' L2;
'END';
  'IF' X < 0 'THEN' 'GOTO' FAIL;
  P[I]:=1/SQRT(X);
'END'  'ELSE' A[J,I]:=X*P[I];
'END';
'END' OF PROCEDURE CHOLDET1;
'PROCEDURE' CHOLSOL1 (N,R,A,P,B  );

  'VALUE' R,N;
  'INTEGER' R,N;
  'ARRAY' A,B,P  ;
'BEGIN'
  'INTEGER' I,J,K;
  'REAL' Z;
  'FOR' J:=N+1 'STEP' 1 'UNTIL' N+R 'DO'
```

```
'BEGIN'
'COMMENT' SOLUTION OF LY=B ;
  'FOR' I:=1 'STEP' 1 'UNTIL' N 'DO'
'BEGIN'
  Z:=B[I,J];
  'FOR' K:=I-1 'STEP' -1 'UNTIL' 1 'DO'

  Z:=Z-A[I,K]*B[K,J];
  B[I,J]:=Z*P[I];
'END';
'COMMENT' SOLUTION OF UX=Y ;
  'FOR' I:=N 'STEP' -1 'UNTIL' 1 'DO'
'BEGIN'
  Z:=B[I,J];
  'FOR' K:=I+1 'STEP' 1 'UNTIL' N 'DO'
  Z:=Z-A[K,I]*B[K,J];
  B[I,J]:=Z*P[I];
'END';
'END';
'END' OF PROCEDURE CHOLSOL1 ;
  'INTEGER' D2;
  'REAL' D1;
  'ARRAY' P[1:N];
  CHOLDET1 (N,A,P,D1,D2,FAIL);
  CHOLSOL1 (N,B,A,P,B  );
'END' OF PROCEDURE EQSOLV ;

'PROCEDURE' INTERCHANGE(K,M,IN,N);
'VALUE' N; 'INTEGER' N;'ARRAY' K,M; 'INTEGER' 'ARRAY' IN;
'BEGIN' 'INTEGER' I,J,Q,P; 'REAL'R,S;
'FOR' I:=1 'STEP' 1 'UNTIL' N 'DO' IN[I]:=I;
Q:=N;
'FOR' I:=1 'STEP' 1 'UNTIL' N 'DO'
'IF' K[I,I] =0.0 'THEN'
'BEGIN'
AGAIN:'IF' K[Q,Q]=0.0 'THEN'
'BEGIN' Q:=Q-1;
'IF' Q 'LE' I 'THEN' 'GOTO' OUT; 'GOTO' AGAIN;
'END';
'FOR' J:=1 'STEP' 1 'UNTIL' N 'DO'
'BEGIN' R:=K[I,J]; S:=M[I,J];K[I,J]:=K[Q,J];M[I,J]:=M[Q,J];
K[Q,J]:=R; M[Q,J]:=S;
'END';
'FOR' J:=1 'STEP' 1 'UNTIL' N 'DO'
'BEGIN'
                              R:=K[J,I]; S:=M[J,I];K[J,I]:=K[J,Q];
M[J,I]:=M[J,Q]; K[J,Q]:=R; M[J,Q]:=S;
'END';
P:=IN[I];IN[I]:=IN[Q];IN[Q]:=P;
'END';
OUT:
'END' PRO INTERCHANGE;
'PROCEDURE'  IBEAM(Z,G,IJ,T,W );
'ARRAY' IJ;  'INTEGER' 'ARRAY' T; 'INTEGER' Z,G,W;

'BEGIN' 'INTEGER' I,S;
WRITETEXT('(' '('1C')'ELEMTYPE%%%%BEAM%PROPERTIES
'('1C')' ')');
'FOR' I:=1 'STEP' 1 'UNTIL' Z  'DO'
'BEGIN' PRINT(I,5,0) ;SPACE(5);
```

```
'FOR' S:=1,2,3,4  'DO'
'BEGIN'  IJ[I,S]:=READ; PRINT( IJ[I,S],0,5);
'END'; NEWLINE(1);
'END';
WRITETEXT('('''('2C')'BEAMZELEMENT '('SS')' GEOMETRYX TYPE '('1C')''')');
'FOR' I:=1 'STEP' 1 'UNTIL' 6 'DO'
'BEGIN'
            SPACE (5);
W:=READ; PRINT(W,3,0);

SPACE(10);
T[W]:=READ; NEWLINE(1);
'END';
'END' PROC INBEAM ;
'PROCEDURE' MATMULT4(T,V,K,C,B);
'ARRAY' K,C,B; 'INTEGER' T,V;
'BEGIN' 'COMMENT'  [B]T*[C]*[B]  4*4 MATRIX;
'INTEGER' I,J,R,S,N,G;
N:=(T-1)*4;  G:=(V-1)*4;
'FOR'R:=1 'STEP' 1 'UNTIL' 4 'DO' 'FOR' S:=1'STEP' 1 'UNTIL' 4 'DO'
'FOR'I:=1 'STEP' 1 'UNTIL' 2 'DO' 'FOR' J:=1'STEP' 1 'UNTIL' 2 'DO'
K[N+R,G+S]:=K[N+R,G+S]+B[I,R]*C[(T-1)*2+I,(V-1)*2+J]*B[J,S] ;
'END' PROC MATMULT4;
'PROCEDURE' BEAM(R,U,X,Y,E,EM,T,K,MA,B,BD,IJ,BUCK,PL,PID);
'ARRAY' X,Y,K,B,E,IJ,MA;
'INTEGER' 'ARRAY' EM,U,T,PID;
'INTEGER' BD,R,BUCK,PL;
'BEGIN' 'ARRAY' A[1:2,1:4],D[1:4,1:4];'INTEGER' I,J,W,V;
      'REAL' S,C,L,BE ;
C:=X[U[R,2]]-X[U[R,1]]; S:=Y[U[R,2]]-Y[U[R,1]]; L:=SQRT(C↑2+S↑2);
      C:=C/L ; S:=S/L;  A[1,1]:=1.0; A[1,2]:=A[1,3]:=A[2,1]:=0.0;
      A[2,2]:=C ;  A[2,3]:=S ;
A[1,4]:=A[2,4]:=0.0; C:=L;S:=1/L;
BE:=L/(6*E[EM[R],1]*IJ[T[R],1]);
L:=IJ[T[R],4]/L;
BE:=BE*IJ[T[R],4]↑2;
'FOR' I:=1,2,3,4 'DO' 'FOR' J:=1,2,3,4 'DO' D[I,J]:=0.0;
D[1,2]:=D[3,4]:=D[2,1]:=D[4,3]:=L;
D[1,4]:=D[2,3]:=D[4,1]:=D[3,2]:=-D[1,2];
D[2,2]:=D[4,4]:=2*BE;  D[2,4]:=D[4,2]:= BE ;
'FOR' W:=1,2 'DO' 'FOR'V:=1 'STEP' 1 'UNTIL' 2 'DO'
MATMULT4(W,V,B,D,A);
ASSEMBLY(U,K,R,R,BD,PID,6);
'FOR' I:=1 'STEP' 1  'UNTIL' 6 'DO'
'FOR' J:=1 'STEP' 1 'UNTIL' 6 'DO' BI[I,J]:=0.0;
'FOR' I:=1,2,3,4 'DO' 'FOR' J:=1,2,3,4 'DO' D[I,J]:=0.0;
'IF' BUCK=100 'THEN'
'BEGIN' C:=(C+IJ[T[R],2]*IJ[T[R],3])/6;
D[1,1]:=D[3,3]:=2*C;
D[1,3]:=D[3,1]:=C;
'END' 'ELSE'
'BEGIN' S:=IJ[T[R],5]*S; D[1,1]:=D[3,3]:=S;D[1,3]:=D[3,1]:=-S;
'END';
'FOR' W:=1,2 'DO' 'FOR' V:=1,2 'DO' MATMULT4(U,V,B,D,A);
ASSEMBLY(U,MA,E,R,BD,PID,6);
'END' PROC BEAM;

'PROCEDURE' MATERIAL(N,M,NM,E,EM,C,TT,PL);
'ARRAY' E,C ;
'INTEGER' 'ARRAY' EM;
```

```
'INTEGER' M,NM,TT,N,PL;
'BEGIN'
'INTEGER' I,J;
WRITETEXT('('NUMBER%OF%DIFF.%MATERIALS')');
PRINT(NM,4,0);NEWLINE(1);
'IF' PL=0 'THEN'
'BEGIN'
'IF' M=1 'THEN'
WRITETEXT('('ISOTROPIC%MATERIAL '('1C')''')') 'ELSE'
WRITETEXT('('ORTHOTROPIC % MATERIAL  '('1C')' ')');
'IF' M=1 'THEN' 'GOTO ' LG1 'ELSE' 'GOTO' LG2;
LG1; WRITETEXT('('MAT.TYPE '('10S')' YOUNGS% MOD,'('13S')'

     POISONS % RATIO '('1C')''')');
'FOR' I:=1  'STEP' 1 'UNTIL' NM 'DO'
'BEGIN'
PRINT(I,4,0);SPACE(10);
E[I,1]:=READ; PRINT(E[I,1],0,4);SPACE(10);
E[I,2]:=READ; PRINT(E[I,2],0,4);NEWLINE(1);
C[I,1]:=1/E[I,1];
          C[I,2]:=C[I,3]:=-E[I,2]; C[I,4]:=2*(1+E[I,2]);
'END'; 'GOTO' LG3;
LG2; WRITETEXT('('MAT.TYPE'('20S')'EX'('20S')'EY'('20S')'E1'('20S')'
   GXY'('1C')' ')');
'FOR' I:=1 'STEP' 1 'UNTIL' NM 'DO'
'BEGIN' PRINT(I,4,0); SPACE(10);
'FOR' J:=1,2,3,4 'DO'
'BEGIN' E[I,J]:=READ ;SPACE(10); PRINT(E[I,J],0,4);
'END'; NEWLINE(1);
'IF' TT 'NE' 1 'AND' M=2 'THEN'
'BEGIN'
C[I,1]:=1/E[I,1] ; C[I,2]:=1/E[I,2]; C[I,3]:=-1/E[I,3];
C[I,4]:=1/E[I,4];
'END';
'IF' TT=1 'AND'M=2 'THEN'
'BEGIN' C[I,1]:=E[I,1];C[I,2]:=E[I,2];C[I,3]:=-E[I,3];
C[I,4]:=E[I,4];
'END';
'END';
'END' 'ELSE'
'BEGIN' WRITETEXT('('PLASTIC%BUCKLING'('1C')'
YOUNGS%MOD,%%STRESS0.7F  '('1C')' ')');
'FOR' I:=1 'STEP' 1 'UNTIL' NM 'DO'
'BEGIN' E[I,1]:=READ;PRINT(E[I,1],0,6);
E[I,2]:=READ;PRINT(E[I,2],0,6);
NEWLINE(1);
'END';
'END';
LG3; WRITETEXT('('ELEMENT'('10S')'MAT.TYPE '('1C')''')');
'FOR' I:=1  'STEP' 1  'UNTIL'  N 'DO'
'BEGIN' PRINT(I,4,0); SPACE(10);
EM[I]:=READ; PRINT(EM[I],4,0); NEWLINE(1);
'END' ;
'END' PROC  MATERIAL ;
'PROCEDURE' COMPLIANCE(R,TT,MT,EM,CC,C,T);
'VALUE' TT,MT,R;
'INTEGER''ARRAY' EM;
'ARRAY'  CC,C;

'INTEGER' R,TT,MT;
'REAL' T;
```

```
'BEGIN' 'REAL' S   ; 'INTEGER' I,J;
'IF' MT=1 'THEN'
  'BEGIN' C[1,1]:=C[2,2]:=1; C[1,2]:=C[2,1]:=CC[EM[R],2];
          C[3,3]:=CC[EM[R],4];
  'END' 'ELSE'
  'BEGIN' C[1,1]:=CC[EM[R],1]; C[1,2]:=C[2,1]:=CC[EM[R],3];
      C[2,2]:=CC[EM[R],2]; C[3,3]:=CC[EM[R],4];
  'END';
 C[1,3]:=C[2,3]:=C[3,1]:=C[3,2]:=0.0;
  'IF' TT=1  'AND'  MT=1  'THEN'
 'BEGIN'  S:=12*CC[EM[R],1]/(T↑3);
  'FOR' I:=1,2,3 'DO' 'FOR' J:=1,2,3 'DO' C[I,J]:=S*C[I,J];'GOTO' FIM;
 'END';
  'IF' TT'NE' 1 'AND' MT=1  'THEN'

  'BEGIN'  S:=12*CC[EM[R],1];
      'FOR' I:=1,2,3 'DO' 'FOR' J:=1,2,3'DO' C[I,J]:=S*C[I,J];'GOTO'FIM;
   'END';
   'IF' TT 'NE' 1  'AND'  MT 'NE' 1 'THEN'
   'BEGIN' 'FOR' I:=1,2,3 'DO' 'FOR' J:=1,2,3 'DO' C[I,J]:=12*C[I,J] ;
         'GOTO'  FIM;
   'END';

'IF' TT=1 'AND' MT=2 'THEN'
  'FOR'  I:=1,2,3  'DO' 'FOR' J:=1,2,3  'DO' C[I,J]:=C[I,J] ;
FIM;
'END' PROC COMPLIANCE ;
'PROCEDURE' MATMULT3(W,S,F,B);
'ARRAY' F,B;
'INTEGER'W,S;
'BEGIN''ARRAY' M[1:3]; 'INTEGER' I,J;
      'FOR' I:=2,1,0 'DO'
  'BEGIN'
      M[3-I]:=F[4*W-1];  F[4*W-1]:=0.0;
  'END';
  'FOR' I:=2,1,0  'DO' 'FOR' J:=1,2,3 'DO'
   F[4*W-I]:=F[4*W-I]+B[S,3-I,J]*M[J];
'END' PROC MATMULT3;
'PROCEDURE' MATMULT(T,V,K,B);
'VALUE' T,V;
'ARRAY' K,B;
'INTEGER' T,V;
'BEGIN' 'COMMENT' [R]T*[C]*[B];
'INTEGER' I,J,R,S,N,G;
N:=(T-1)*4;  G:=(V-1)*4;
'BEGIN' 'ARRAY' C[N+1:N+4,G+1:G+4];
'FOR' I:=N+1 'STEP' 1 'UNTIL' N+4 'DO'
'FOR' J:=G+1 'STEP'1 'UNTIL' G+4 'DO'
'BEGIN' C[I,J]:=K[I,J];  K[I,J]:=0.0;
'END';
'FOR' R:=1 'STEP' 1 'UNTIL' 4 'DO'
'FOR' S:=1 'STEP' 1 'UNTIL' 4 'DO'
'FOR' I:=1 'STEP' 1 'UNTIL' 4 'DO'
'FOR' J:=1 'STEP' 1 'UNTIL' 4 'DO'
K[N+R,G+S]:=K[N+R,G+S]+B[I,R]*C[N+I,G+J]*B[J,S];
'END';
'END' PROC MATMULT;
'PROCEDURE' MATMULT1(T,V,K,B);
   'VALUE' T,V;

'ARRAY' K,B;
```

```
'INTEGER' T,V;
'BEGIN'
'COMMENT' [R]T*LC];
'INTEGER' N,G,I,J,R;
N:=(T-1)*4;  G:=(V-1)*4;
'BEGIN' 'ARRAY' C[N+1:N+4,G+1:G+4];
'FOR' I:=N+1 'STEP' 1 'UNTIL' N+4 'DO'
'FOR' J:=G+1 'STEP'1 'UNTIL' G+4 'DO'
'BEGIN'  C[I,J]:=K[I,J];  K[I,J]:=0;0;
'END';
'FOR' I:=1 'STEP' 1 'UNTIL' 4 'DO'
'FOR' J:=1 'STEP' 1 'UNTIL' 4 'DO'
'FOR' R:=1,2,3,4 'DO'
K[N+I,G+J]:=K[N+I,G+J]+B[R,I]*C[R+N,J+G];
'END';
'END' PROC MATMULT1;

'PROCEDURE' MATMULT2(T,V,K,B);
'VALUE' T,V;
'ARRAY' K,B;
'INTEGER' T,V;
'BEGIN'
'COMMENT' [C]*[B];
'INTEGER' N,G,I,J,R;
N:=(T-1)*4;  G:=(V-1)*4;
'BEGIN' 'ARRAY' C[N+1:N+4,G+1:G+4];
'FOR' I:=N+1 'STEP' 1 'UNTIL' N+4 'DO'
'FOR' J:=G+1 'STEP'1 'UNTIL' G+4 'DO'
'BEGIN'  C[I,J]:=K[I,J];  K[I,J]:=0.0;
'END';
'FOR' I:=1 'STEP' 1 'UNTIL' 4 'DO'
'FOR' J:=1 'STEP' 1 'UNTIL' 4 'DO'
'FOR' R:=1,2,3,4 'DO'
K[N+I,G+J]:=K[N+I,G+J]+C[N+I,G+R]*B[R,J];
'END';
'END' PROC MATMULT2;
'PROCEDURE' TRANSF(W,K,B);
'INTEGER' W;
'REAL' 'ARRAY' K,B;
'BEGIN' 'INTEGER' T,V;
'IF' W=1 'THEN'
'BEGIN' 'FOR' V:=1,2,3,4 'DO''IF' V=1 'THEN' MATMULT(1,V,K,B)
'ELSE' MATMULT1(1,V,K,B);
'END';
'IF' W=2 'THEN'
'BEGIN' 'FOR' V:=1,2,3,4 'DO' 'IF'V=1 'THEN'MATMULT2(1,2,K,B)
'ELSE' 'IF'V=2 'THEN'MATMULT(2,2,K,B) 'ELSE'MATMULT1(2,V,K,B);
'END';
'IF' W=3 'THEN'
'BEGIN' 'FOR' T:=1,2 'DO' MATMULT2(T,3,K,B);MATMULT(3,3,K,B);
MATMULT1(3,4,K,B);
'END';
'IF' W=4 'THEN'
'BEGIN' MATMULT(4,4,K,B);
'FOR' T:=1,2,3 'DO' MATMULT2(T,4,K,B);
'END';
'END' PRO TRANSF;
'PROCEDURE' AUX(L1,L2,B,D,SFM,SF,X,Y,U,N,Z,JO);
'VALUE' L1,L2,Z,JO;
'INTEGER' Z,JO;
```

```
'REAL' L1,L2,U;
'INTEGER' 'ARRAY' N;
'ARRAY' X,Y,B,SF,SFM,D;
'BEGIN'
'ARRAY' P[1:2,1:4],JL1:2,1:2],C[1:12,1:2];
'INTEGER' I,V,W,S;
'REAL' CHANGE,DN1,DN2,DN3,DN4,DN5,DN6;
'COMMENT' EVALUATES THE JACOBIAN J ITS DETERMINNANT U,
THE ARRAY B AND SHAPE  FUNCTIONS AT THE INTEGRATING POINT;
DN1:=0.25*(1-L2);
DN2:=0.25*(1+L2);
DN3:=0.25*(1-L1);
DN4:=0.25*(1+L1);
DN5:=1-L2;  DN6:=1+L2;
SF[1]:=DN3*DN5;SF[2]:=DN4*DN5;SF[3]:=DN4*DN6;SF[4]:=DN3*DN6;
J[1,1]:=-DN1*X[N[Z,1]]+DN1*X[N[Z,2]]+DN2*X[N[Z,3]]-DN2*X[N[Z,4]];
J[1,2]:=-DN1*Y[N[Z,1]]+DN1*Y[N[Z,2]]+DN2*Y[N[Z, 3]]-DN2*Y[N[Z,4]];
J[2,1]:=-DN3*X[N[Z,1]]-DN4*X[N[Z,2]]+DN4*X[N[Z,3]]+DN3*X[N[Z,4]];

J[2,2]:=-DN3*Y[N[Z,1]]-DN4*Y[N[Z,2]]+DN4*Y[N[Z,3]]+DN3*Y[N[Z,4]];
'COMMENT' U REPLACES DET J;
U:=JL1,1]*J[2,2]-J[1,2]*J[2,1];
CHANGE:=J[1,1];
J[1,1]:=J[2,2]/U;
J[1,2]:=-J[1,2]/U;
J[2,1]:=-J[2,1]/U;  J[2,2]:=CHANGE/U;
'FOR' I:=1,2 'DO'
'BEGIN'
P[I,1]:=-DN1*J[I,1]-DN3*J[I,2];
P[I,2]:=DN1*J[I,1]-DN4*JL1,2];
P[I,3]:=DN2*J[I,1]+DN4*J[I,2];
P[I,4]:=-DN2*J[I,1]+DN3*J[I,2];
'END';
'IF' JO 'NE' 2 'THEN'
'BEGIN'
'FOR' I:=1 'STEP' 1 'UNTIL' 12 'DO'
'FOR' V:=1,2 'DO' C[I,V]:=0.0;
'FOR' I:=1 'STEP' 1 'UNTIL' 4 'DO'
'BEGIN'
C[3*I-2,1]:=C[3*I,2]:=P[1,I];
C[3*I-1,2]:=C[3*I,1]:=P[2,I];
'END';
'IF' JO=3 'THEN'
'BEGIN'  'FOR' I:=1 'STEP' 1 'UNTIL' 12 'DO'
'FOR' V:=1,2 'DO' B[I,V]:=C[I,V];
      'GOTO' TAG;
        'END';
'COMMENT' [C]*[P] TO OBTAIN CONTRIBUTION KEMW;
'FOR' I:=1 'STEP' 1 'UNTIL' 12 'DO'
'FOR' W:=1 'STEP' 1 'UNTIL' 4 'DO'
'BEGIN'
B[I,W]:=0.0;
'FOR' V:=1,2 'DO'
B[I,W]:=B[I,W]+C[I,V]*P[V,W];
'END';
'COMMENT' COEF OF THE MULT OF SHAPE FUNCTIONS TO EVA, KEM CONT.;
'FOR' I:=1,2,3,4 'DO'
'FOR' S:=I 'STEP' 1 'UNTIL' 4 'DO'
        SFM[I,S]:=SF[I]*SF[S];
'END';
```

```
'IF' JO=2 'THEN'

'BEGIN'
'FOR' I:=1,2 'DO' 'FOR' V:=1,2,3,4 'DO'  B[I,V]:=P[I,V];
'END';
'FOR' I:=1,2 'DO' 'FOR' V:=1,2,3,4 'DO'D[I,V]:=P[I,V];
TAG:'END' OF AUX;
'PROCEDURE' KEFORM(K,B,S,C);
'ARRAY' K,B,S,C;
'BEGIN'
'INTEGER' I,J,V;
'FOR' I:=1,2,3  'DO' 'FOR' J:=1,2,3 'DO'
'BEGIN'

K[1+I,J+1 ]:=K[1+I,J+1 J+S[1,1]*C[I,J];
K[1+I,J+5 ]:=K[1+I,J+5 J+S[1,2]*C[I,J];
K[1+I,J+9 ]:=K[1+I,J+9 J+S[1,3]*C[I,J];
K[1+I,J+13]:=K[1+I,J+13]+S[1,4]*C[I,J];
K[5+I,J+5]:=K[5+I,J+5]+S[2,2]*C[I,J];
K[5+I,J+9]:=K[5+I,J+9]+S[2,3]*C[I,J];
K[5+I,J+13]:=K[5+I,J+13]+S[2,4]*C[I,J];

K[9+I,J+9 ]:=K[9+I,J+9 ]+S[3,3]*C[I,J];
K[9+I,J+13]:=K[9+I,J+13]+S[3,4]*C[I,J];
K[13+I,J+13]:=K[13+I,J+13]+S[4,4]*C[I,J];
'END';
'FOR' I:=1,2,3,4 'DO' 'FOR' V:=1,2,3,4 'DO'
'FOR' J:=1,2,3 'DO'
'BEGIN'
K[4*(I-1)+1+J,4*(V-1)+1]:=K[4*(I-1)+1+J,4*(V-1)+1]+
B[3*(I-1)+J,V];
K[4*(V-1)+1,4*(I-1)+1+J]:=K[4*(V-1)+1,4*(I-1)+1+J]+
B[3*(I-1)+J,V];
'END';
'FOR' I:=1 'STEP' 1 'UNTIL' 16 'DO'
'FOR' J:=I 'STEP' 1 'UNTIL' 16 'DO' K[J,I]:=K[I,J];
'END' PROC KEFORM;
'PROCEDURE' ASSEMBLY(Q,K,A,R,B,P,DF);
'INTEGER' R,B,DF;
'INTEGER' 'ARRAY' Q,P;
'ARRAY' K,A;
'BEGIN' 'INTEGER' 'ARRAY' U[1:16];
'INTEGER' S,V,J,W;'IF' DF=8 'THEN' W:=2 'ELSE' W:=4;
'FOR' S:=1 'STEP' 1 'UNTIL' W 'DO' 'FOR' V:=3,2,1,0 'DO'
U[4*S-V]:=P[Q[R,S]*4-V];
'FOR' S:=1 'STEP' 1 'UNTIL' DF 'DO'
'FOR' J:=S 'STEP' 1 'UNTIL' DF 'DO'
'IF' U[S] 'NE' 0 'AND' U[J] 'NE' 0 'THEN'
'BEGIN' 'IF' U[S] 'LE' U[J] 'THEN'
'BEGIN'
B:=U[J];
K[U[J],U[S]-U[J]+B ]:=K[U[J],U[S]-U[J]+B]+A[S,J]  ;
'END'
'ELSE'
'BEGIN' B:=U[S];
K[U[S],U[J]-U[S]+B]:=K[U[S],U[J]-U[S]+B]+A[S,J];
'END';
'END';
'END' PROC ASSEMBLY;
'PROCEDURE' SIDES(CODE,X,Y,AA,D,R,SINB,COSB,A1);
'INTEGER' 'ARRAY' CODE;
```

```
'ARRAY' X,Y,AA,D,SINB,COSB,A1;
'INTEGER' R;

'BEGIN'
  'ARRAY' XX,YY[1:4];
'INTEGER' I;
          XX[1]:=X[CODE[R,1]]-X[CODE[R,2]];
          XX[2]:=X[CODE[R,2]]-X[CODE[R,3]];
XX[3]:=X[CODE[R,3]]-X[CODE[R,4]];
XX[4]:=X[CODE[R,4]]-X[CODE[R,1]];
          YY[1]:=Y[CODE[R,1]]-Y[CODE[R,2]];
          YY[2]:=Y[CODE[R,2]]-Y[CODE[R,3]];
YY[3]:=Y[CODE[R,3]]-Y[CODE[R,4]];
YY[4]:=Y[CODE[R,4]]-Y[CODE[R,1]];
      'FOR' I:=1 'STEP' 1 'UNTIL' 4 'DO'
      'BEGIN'
           A1[I]:=SQRT(XX[I]↑2+YY[I]↑2);
            SINB[I]:=XX[I]/A1[I];
            COSB[I]:=-YY[I]/A1[I];
A1[I]:=0.5*A1[I];
            AA[I,1]:=COSB[I]↑2 ;
            AA[I,2]:=SINB[I]↑2 ;
            AA[I,3]:=2*SINB[I]*COSB[I] ;

            D[I,1]:=-0.5*AA[I,3] ;
            D[I,2]:=-D[I,1] ;
            D[I,3]:=AA[I,1]-AA[I,2] ;
'END';
'END' PROC SIDES;

'PROCEDURE' MNSWSDS(WW,A,KE,D,X,Y,N,Z,C,SI,L);
'INTEGER' Z;
'ARRAY' WW,A,KE,D,X,Y,C,SI,L;
'INTEGER' 'ARRAY' N;
'BEGIN' 'ARRAY' B[1:12,1:1],P[1:2,1:4],SF[1:4],
SFM[1:4,1:4],PP[1:2,1:4];
'INTEGER' I,J,S,V,W;
'REAL' U;
'FOR' I:=1,2,3,4 'DO' 'FOR' W:=1,2   'DO'
'BEGIN'
AUX(A[W,2*I-1],A[W,2*I],P,PP,SFM,SF,X,Y,U,N,Z,   2);
'FOR'J:=1,2,3,4 'DO'
'BEGIN' P[2,J]:=P[2,J]*C[I];   P[1,J]:=-P[1,J]*SI[I];
SFM[1,J]:=L[I]*(P[1,J]+P[2,J]);
'END';
'FOR' V:=1,2,3,4 'DO' 'FOR' J:=1,2,3 'DO'
B[3*(V-1)+J,1]:=SF[V]*D[I,J];
'FOR' S:=1 'STEP' 1 'UNTIL' 12 'DO'
'FOR' J:=1,2,3,4 'DO'
KE[S,J]:=KE[S,J]-WW[W,I]*P[S,1]*SFM[1,J];
'END';
'END' PROC MNSWSDS;
'BEGIN'
'ARRAY'          WW[1:2,1:4],ZN[1:2,1:8],SF[1:4],SFM[1:4,1:4],
     H[1:9,1:3];
          'INTEGER' N,M,V,S,Q,R,J,I,W,G,BD,GC,DF,LL,NSETS,U,Z,EI,
MTYPE,THTYPE,TYLOAD,NE,NB     ,NUQ,NII ,
ET1, NUDL,GA,BUCK,
GG,MMAT,IFAIL,VV,NW,PL ,ZZ;
'REAL' W1,W2,W3,T,UQ,F1,MD,TO,TA;
```

```
NSETS:=READ;
'FOR' I:=1,2 'DO'
'BEGIN'
'FOR' J:=2,7 'DO'

ZN[1,J]:=-1;
'FOR' J:=3,6 'DO' ZN[I,J]:=1;
'END';
'FOR' I:=1,2,3,4 'DO' H[I,1]:=1.0;
W1:=0.57735026919;
H[1,2]:=H[1,3]:=H[2,3]:=H[3,2]:=W1;
H[2,2]:=H[3,3]:=H[4,2]:=H[4,3]:=-W1;
ZN[1,1]:=ZN[1,4]:=ZN[1,5]:=ZN[1,8]:=-W1;
ZN[2,1]:=ZN[2,4]:=ZN[2,5]:=ZN[2,8]:=W1;
'FOR' I:=1,2 'DO' 'FOR' J:=1,2,3,4 'DO'  WW[I,J]:=1.0;
          'FOR' LL:=1 'STEP' 1 'UNTIL' NSETS 'DO'
    'BEGIN'
BUCK:=READ;
PL:=READ;
NW:=READ;
MTYPE:=READ; THTYPE:=READ; TYLOAD:=READ;
NMAT:=READ;
NB:=READ;'IF' NB 'NE' 0  'THEN'
NII:=READ;
              N:=READ ;
             GG:=READ ;

ET:=READ;
GF:=READ;
             WRITETEXT('('NO.% OF % ELEMENTS')') ;
             PRINT(N,3,0) ;
             NEWLINE(2) ;
             WRITETEXT('('NO.% OF% DEGREES % OF% FREEDOM')') ;
     G:=4*GG;M:=G;G:=G-GC;
               PRINT( G,3,0);
'IF' NB=0 'THEN' NII:=1;
             NEWLINE(2) ;
'IF' ET=0 'THEN' ET1:=1 'ELSE' ET1:=ET;
'IF'  MTYPE=1 'THEN' NE:=2 'ELSE' NE:=4 ;
      'BEGIN'
'ARRAY' B[1:ET1,1:3,1:3],F[1:G],E[1:NMAT,1:NE],ESP[1:GG ],UDL[1:1],
SINB,COSB[1:4],ANG[1:ET1],
      CC[1:NMAT,1:4],IJ[1:NII,1:4], IAMB[1:NW],EVL[1:NW,1:NW];
'INTEGER' 'ARRAY' CODE[1:N,1:4],VNS,VNN,VNT[1:ET1],EMAT[1:N],
EUDLL[1:1],FIJ[1:N], IN[1:G],PL,PID[1:M];
'COMMENT' IF PLASTIC%BUCKLING UQ=SHAPE PARAMETER
ELSE UQ=0;
'IF' BUCK 'NE' 101 'THEN'
MP:=READ;
UQ:=READ;
WRITETEXT('(' '('1C')' NODE/ELEM%%%%THICKNESS'('1C')' ')');
'IF' THTYPE=1  'THEN'
'BEGIN' T:=READ;SPACE(12);PRINT(T,0,5);
NEWLINE(4);
'END' 'ELSE'
'BEGIN' 'IF' THTYPE=12 'THEN' J:=N 'ELSE' J:=GG;
'FOR' I:=1 'STEP' 1 'UNTIL' J 'DO'
'BEGIN'
ESP[I]:=READ;
PRINT(I,4,0); SPACE(5)  ; PRINT(ESP[I],0,5); NEWLINE(1);
'END';
```

```
'END';
MATERIAL(N,MTYPE,NMAT,E,EMAT,CC,THTYPE,PL);
'COMMENT' READ IN BEAM 2NDMOMENT OF AREA,AREA,DENSITY OR
TRIAL BUCKLING FORCE,LENGTH ELEMENT;

'IF' NB 'NE' 0 'THEN'
INBEAM(NII,NB,IJ,EIJ,W );
              WRITETEXT ('('ELEMENT '('10S')' CODE ')') ;
              'FOR' I:=1 'STEP' 1 'UNTIL' N 'DO'
       'BEGIN'
              NEWLINE(2);
              PRINT(I,4,0) ;
              'FOR' S:=1 'STEP' 1 'UNTIL' 4 'DO'
       'BEGIN'
              CODE[I,S]:=READ ;
              PRINT(CODE[I,S],4,0) ;
         'END';
         'END';
WRITETEXT('(' '('1C')'NODE%TRANSF%%ANGLE%DEG.
'('1C')' ')');
'FOR' S:=1 'STEP' 1 'UNTIL' ET 'DO'
'BEGIN'
VNN[S]:=READ;PRINT(VNN[S],4,0);
SPACE(4);
ANG[S]:=READ;PRINT(ANG[S],3,5);
NEWLINE(1);
ANG[S]:=3.141592654*ANG[S]/180;

'END';
              'COMMENT' TO CALCULATE HALFBANDWIDTH ;
       'BEGIN'
'ARRAY' D,AA[1:4,1:3],A1[1:4],
B2[1:12,1:4],
       K[1:6,1:6],KE[1:16,1:16],          B1[1:12,1:4],A[1:4,1:4],
MM[1:4,1:4],MA[1:6,1:6],
QXY[1:1,1:2],SG[1:2,1:2],KG[1:4,1:4],ST[1:GG,1:3],POL[1:2,1:4],
     FE[1:16],X,Y[1:GG],                C[1:3,1:3];
'REAL' AREA,S1,DETJ;
NEWLINE(1);
WRITETEXT('('NODE '('16S')' X&COO'('8S')'Y&COO '('1C')' ')');
'FOR'I:=1 'STEP' 1 'UNTIL' GG 'DO'
'BEGIN'
NEWLINE(1);
PRINT(I,4,0);
SPACE(2);
X[I]:=READ;
PRINT(X[I],0,4);
Y[I]:=READ;
SPACE(2);
PRINT(Y[I],0,4);
NEWLINE(2);
'END';
ZZ:=0;
ITER; ZZ:=ZZ+1;
              'FOR' I:=1 'STEP' 1 'UNTIL' G 'DO'
       'BEGIN'
              F[I ]:=0;
         'FOR' S:=1 'STEP' 1 'UNTIL' 6 'DO'
'BEGIN'
 MA[I,S]:=0.0;
```

```
                K[I,S ]:=0 ;
            'END';
    'END';
        NEWLINE(1);
    'IF' ZZ=1 'THEN'
    'BEGIN'

     'FOR' I:=1 'STEP' 1 'UNTIL' M 'DO'
    'BEGIN' PI[I]:=1; PID[I]:=0;
    'END';
    WRITETEXT('('' '('10')'BOUNDARY%CONDITIONS
    '('10')' ')');
    'FOR' I:=1 'STEP' 1 'UNTIL' GC 'DO'
    BOUNDARY(VV,W,TA,PI);
     'COMMENT' TO READ IN INITIAL STRESSES;
    'IF' BUCK 'NE' 100 'THEN'
    'BEGIN'
    WRITETEXT('('''('10')'NODE'('6S')'SIGX'('16S')'SIGY'('16S')'
            SIGXY')');
    'FOR' I:=1 'STEP' 1 'UNTIL' GG 'DO'
    'BEGIN' NEWLINE(1);
    PRINT(I,3,0);
    'FOR' J:=1,2,3 'DO'
    'BEGIN'
    ST[I,J]:=READ;SPACE(3);
    PRINT(ST[I,J],0,7);
    'END';
    'END';
    'END';
     S:=1;

    'FOR' I:=1 'STEP' 1 'UNTIL' GG 'DO'
    'BEGIN' 'FOR' J:=1,2,3,4 'DO'
    'BEGIN' DF:=(I-1)*4+J;
    'IF' PI[DF]=1 'THEN'
    'BEGIN' PID[DF]:=S;S:=S+1;
    'END';
    'END';
    'END';
    'END';
          'FOR' R:=1  'STEP' 1 'UNTIL' N 'DO'
        'BEGIN'
    'FOR' I:=1 'STEP' 1 'UNTIL' 16 'DO'
    'FOR' J:=1 'STEP' 1 'UNTIL' 16 'DO'  KE[I,J]:=0.0;
    'FOR'I:=1 'STEP' 1 'UNTIL' 16 'DO' FE[I]:=0.0;
    'FOR'I:=1 'STEP' 1 'UNTIL' 12 'DO'
    'FOR' J:=1,2,3,4 'DO' BZ[I,J]:=0.0;
    'FOR'I:=1,2,3,4 'DO' 'FOR' J:=I 'STEP' 1  'UNTIL' 4 'DO'
    'BEGIN'  MM[I,J]:=0.0;
    A[I,J]:=0.0;
    'END';
    'FOR' I:=1,2,3,4 'DO' 'FOR'J:=1,2,3,4 'DO' KO[I,J]:=0.0;
    'IF' CODE[R,3] 'NE' 0  'THEN'
    'BEGIN'
    'IF' PL=0 'THEN'
    COMPLIANCE(R,THTYPE,MTYPE,EMAT,CC,C,T) 'ELSE'
            COMPLBUCK(C,ST,SO,E,UO,EMAT,CODE,R,FAIL);
    'IF' PL 'NE' 0 'AND' THTYPE=1 'THEN'
    TO:=1/(T**3);
    'FOR' U:=1 'STEP' 1 'UNTIL' 4 'DO'
```

```
'BEGIN'
AUX(H[U,2],H[U,3],N1,PO,SEM,SF,X,Y,DETJ,CODE,R,1);
DETJ:=H[U,1]*DETJ;
'IF' PL=0 'THEN'
'FOR' I:=1,2 'DO' 'FOR' J:=1,2 'DO' SO[I,J]:=0.0;
'FOR' I:=1 'STEP' 1 'UNTIL' 12 'DO' 'FOR' J:=1,2,3,4 'DO'
B2[I,J]:=B2[I,J]+B1[I,J]*DETJ;
'IF' THTYPE=1 'THEN'

'BEGIN'
'FOR' I:=1,2,3,4 'DO' 'FOR' J:=I 'STEP' 1 'UNTIL' 4 'DO'
'BEGIN'
'IF' PL 'NE' 0 'THEN'
A[I,J]:=A[I,J]+SEM[I,J]*DETJ*TO 'ELSE'
A[I,J]:=A[I,J]+SEM[I,J]*DETJ;
'END';
'END' 'ELSE'
'BEGIN'

'IF' THTYPE=12 'THEN'
T:=ESP[R] 'ELSE'
'BEGIN'
T:=(SF[1]*ESP[CODE[R,1]]+SF[2]*ESP[CODE[R,2]]+SF[3]*ESP[CODE[R,3]]
+SF[4]*ESP[CODE[R,4]]);
'END';
TO:=1/(T↑3);
  'FOR' I:=1,2,3,4 'DO' 'FOR' J:=I 'STEP' 1 'UNTIL' 4 'DO'
'BEGIN'
AREA:=SEM[I,J]*DETJ;
'IF' BUCK 'NE'101 'THEN'
MM[I,J]:=MM[I,J]+AREA*T;
A[I,J]:=A[I,J]+AREA*TO;
'END';

'END';
'IF' BUCK 'NE' 100 'THEN'
'BEGIN'
 'IF' PL=0 'THEN'
'BEGIN'
'FOR' I:=1,2,3,4 'DO'
'BEGIN'
SO[1,1]:=SO[1,1]+SF[I]*ST[CODE[R,I],1];
SO[1,2]:=SO[1,2]+SF[I]*ST[CODE[R,I],3];
SO[2,2]:=SO[2,2]+SF[I]*ST[CODE[R,I],2];
'END'; SO[2,1]:=SO[1,2];
'END';
'COMMENT' POT*SO*PO  GEOMETRICAL MATRIX;
'FOR' V:=1,2,3,4 'DO' 'FOR'S:=1,2,3,4 'DO'
'FOR'I:=1,2 'DO' 'FOR' J:=1,2 'DO'
KO[V,S]:= KO[V,S]+PO[I,V]*SO[I,J]*PO[J,S]*DETJ*T;
'END';
'END';
'IF' THTYPE=1 'AND' BUCK 'NE' 101 'THEN'
'FOR' I:=1,2,3,4 'DO' 'FOR' J:=I 'STEP' 1 'UNTIL' 4 'DO'
MM[I,J]:=A[I,J]*T;
STDES(CODE,X,Y,AA,D,R,SINB,COSB,A1);
MNSUSDS(WW,ZN,B2,D,X,Y,CODE,R,COSB,SINB,A1);
KEFORM(KE,B2,A,C);
     NEWLINE(1);
'FOR'S:=1 'STEP' 1 'UNTIL' ET 'DO'
```

```
'BEGIN' 'FOR' W:=1,2,3,4 'DO'
 'BEGIN' 'IF' CODE[R,W]=VNN[S] 'THEN'
'GOTO' L8 'ELSE' 'GOTO' L9;
L8:
'BEGIN' A[2,2]:=A[3,3]:=SIN(ANG[S])↑2;
A[2,3]:=A[3,2]:=COS(ANG[S])↑2;
A[4,3]:=COS(ANG[S])*SIN(ANG[S]);
A[4,2]:=-A[4,3];A[2,4]:=-2*A[4,3];
A[3,4]:=2*A[4,3];A[4,4]:=A[2,3]-A[2,2];
A[1,1]:=1.0;

'FOR' I:=2,3,4 'DO' A[1,I]:=A[I,1]:=0.0;
TRANSF(W,KE,A);
'FOR' I:=1,2,3 'DO' 'FOR' J:=1,2,3 'DO'
B[S,I,J]:=A[1+I,1+J];
'GOTO' L10;
'END';
L9:
'END';
L10:
'END';
'FOR' I:=1 'STEP' 1 'UNTIL'16 'DO'
'FOR' J:=I 'STEP' 1 'UNTIL' 16 'DO' KE[J,I]:=KE[I,J];
ASSEMBLY(CODE,K,KE,R,BD,PID,16);

'IF' BUCK =100 'THEN'
MASS(MM,PID,KE,MA,CODE,R,MD,BUCK);
'IF' BUCK=101 'THEN'
MASS(KO,PID,KE,MA,CODE,R,MD,BUCK);
'END' 'ELSE'
BEAM(R,CODE,X,Y,E,EMAT,EIJ,K,MA,KE,BD,IJ,BUCK,PL,PID);
'END' LOOP EL. MATRIX;
'FOR' I:=1 'STEP' 1 'UNTIL' G 'DO'
'FOR' J:=I 'STEP' 1 'UNTIL' G 'DO'
'BEGIN' K[I,J]:=K[J,I];MA[I,J]:=MA[J,I];
'END';


NEWLINE(1);
W:=G-NW;
INTERCHANGE(K,MA,IN,G);

NEWLINE(1);
EQSOLV(W,NW,K,K,FAIL);
'FOR' I:=1 'STEP' 1 'UNTIL' NW 'DO'
'FOR' J:=1 'STEP' 1 'UNTIL' NW 'DO'
'FOR' S:=1 'STEP' 1 'UNTIL' W 'DO'
K[W+I,W+J]:=K[W+I,W+J]+K[W+I,S]*K[S,W+J];
'FOR' I:=1 'STEP' 1 'UNTIL' NW 'DO'
'FOR' J:=I 'STEP' 1 'UNTIL' NW 'DO'
'BEGIN' K[I,J]:=K[J,I]:=K[W+I,W+J];
MA[I,J]:=MA[J,I]:=MA[W+I,W+J];
'END';
NEWLINE(2);
IFAIL:=0;
'IF' BUCK 'NE' 101 'THEN'
FOZABA(K,MA,NW,LAMB,EV,IFAIL);
'IF' BUCK=101 'THEN'
FOZABA(MA,K,NW,LAMB,EV,IFAIL);
'IF' PL 'NE' 0 'THEN'
```

```
'BEGIN' AREA:=1/LAMB[NW];
NEWLINE(3);PRINT(AREA,0,7);  NEWLINE(5);
'IF' ABS(1-AREA) >0.0025   'AND'ZZ 'LE' 10  'THEN'
'BEGIN'
'FOR' I:=1 'STEP' 1 'UNTIL' GG 'DO'
'FOR' J:=1,2,3 'DO'
ST[I,J]:=ST[I,J]*(1.0-AREA)*ST[I,J]/(ZZ*2);
'GOTO'  ITER;
'END';
NEWLINE(1);
WRITETEXT('('NO. %%ITERATIONS=')');
PRINT(ZZ,2,0);

WRITETEXT('('  '('1C')'  NODAL%%PLASTIC%%BUCKLING
%%STRESSES '('1C')'')');
WRITETEXT('('('('1C')'    NODE'('6S')'SIGX'('16S')'
SIGY'('16S')'  SIGXY')');
'FOR' I:=1 'STEP' 1 'UNTIL' GG 'DO'
'BEGIN' NEWLINE(1); PRINT(I,3,0);
'FOR' J:=1,2,3 'DO'
'BEGIN' SPACE(3);  PRINT(ST[I,J],0,7);
'END';
'END';
'END';
NEWLINE(2);
 'IF' BUCK 'NE' 101 'THEN'
'BEGIN' WRITETEXT('('NATURAL%FREQUENCY '('1C')'')');
'FOR' I:=1 'STEP' 1 'UNTIL' NW 'DO'
'BEGIN' LAMB[I]:=SQRT(LAMB[I]);PRINT(LAMB[I],0,6);
'END';
'FOR' I:=1 'STEP' 1 'UNTIL' NW 'DO'
'BEGIN' WRITETEXT('('('('1C')' MODE%SHAPE=')');PRINT(I,2,0);
WRITETEXT('('  '('1C')'POSITION')');
'FOR' J:=1 'STEP' 1 'UNTIL' NW 'DO'
'BEGIN' NEWLINE(1); PRINT(IN[G-NW*J],3,0);
PRINT(EV[J,I],0,6);
'END';
'END';
NEWLINE(1);

'END' 'ELSE'
'BEGIN' WRITETEXT('('BUCKLING%FACTOR=')');
LAMB[NW]:=1/LAMB[NW];PRINT(LAMB[NW],0,6);
NEWLINE(2);
S:=0;
'FOR' I:=NW 'STEP' -1 'UNTIL' 1 'DO'
'BEGIN' S:=S+1;
WRITETEXT('('('('1C')'MODE%SHAPE')');PRINT(S,2,0);
WRITETEXT('('('('1C')' POSITION')');
'FOR' J:=1 'STEP' 1 'UNTIL' NW 'DO'
'BEGIN' NEWLINE(1);PRINT(IN[G-NW*J],5,0);PRINT(EV[J,I],0,6);
'END';
'END';
'END';
    'END';
      'END';
NEWLINE(2);
   'END';
FAIL:
       'END';
          'END' OF PROGRAM;
```

APPENDIX 6

THE MOIRE TECHNIQUE

A.6.1) The Moire Apparatus.

The Moire Apparatus (Fig.A.6.1) basically consists of a steel structure with a curved screen, a camera, and provision for fixing and loading the slab. The screen surface, in the form of a circular cylinder segment is covered with line paper. The lines are equally spaced at a distance d apart and they are parallel to the axis of the cylinder.

The screen can be rotated so that the lines can be set at any chosen angle from the vertical and can also be adjusted in the horizontal and vertical direction. A camera, which is mounted behind the screen, views, through a circular hole in the screen, a model of the plate which acts as a first surface mirror, in front of the screen. The model is fixed to the structure by means of G clamps. The application of loads is achieved through levers attached to the structure behind the model. For the photographic process the screen is evenly illuminated by photo-flood lamps conveniently positioned on the frame.

A.6.2) Fundamentals of the Moire Method.

In this method the polished model of the slab acts as a first surface mirror, reflecting the images of the lines on to the photographic plate (Fig.A.6.2). When a picture is taken of the unflexed model, the photograph will record the undistorted image of the lines as reflected by the model. When the model is loaded, a distorted image of the lines is obtained, and a superposition of two images by a double exposure of the photographic plate results in the formation of Moire fringes. The screen has a particular shape determined by Ligtenberg [73] so that the fringes are contours of

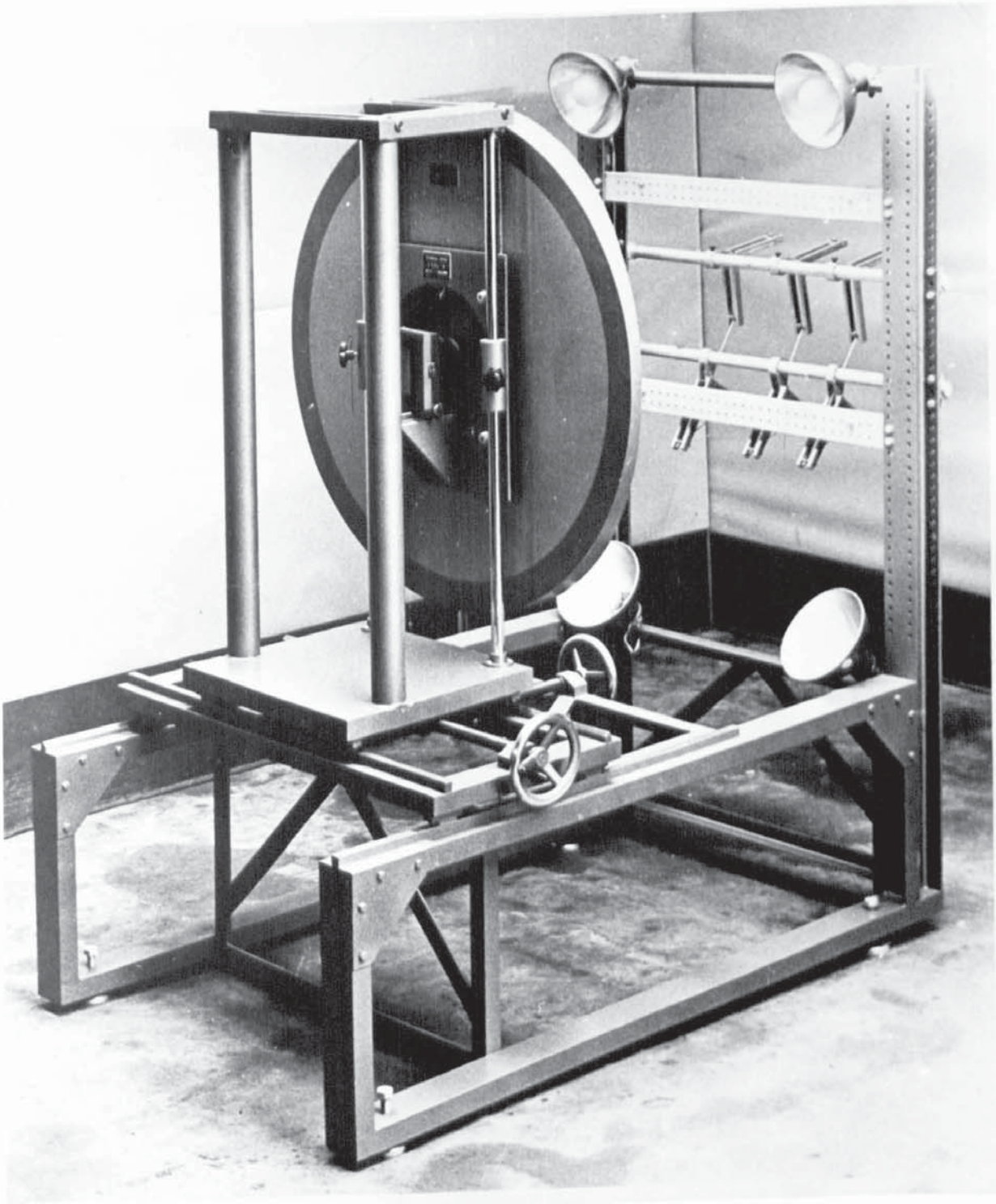

Fig.(A.6.1) The Moire Apparatus.

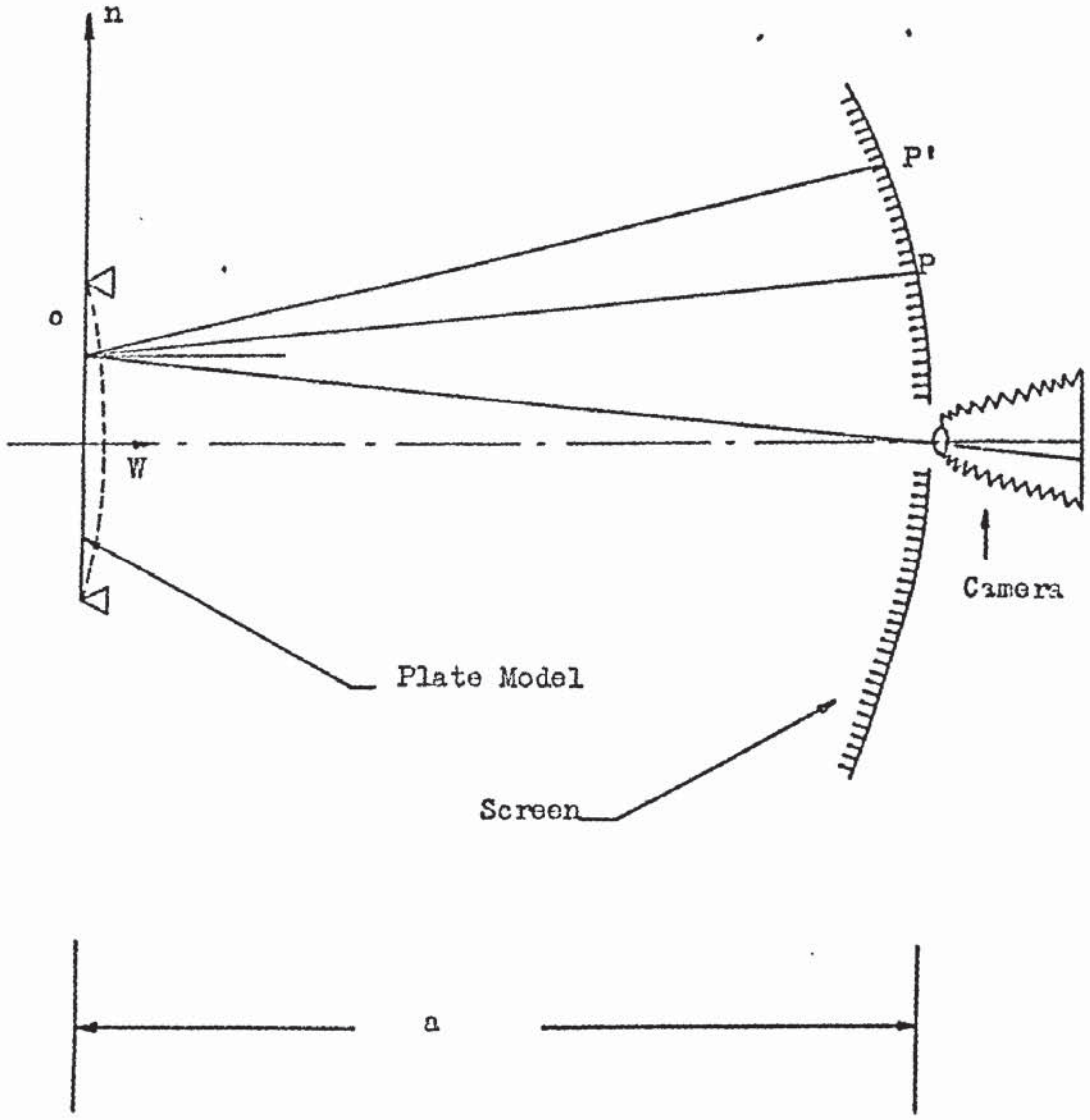

Fig.(A.6.2) Schematic Arrangement of Moire Apparatus.

constant slope.

It is seen from Fig.(A.6.2) that, with an unloaded model, an image of a point P will be obtained in the camera. When the model is loaded the image of P' will coincide with that of P.

Ligtenberg showed that Moire fringes will be obtained whenever

$$PP' = N\,d\,,$$

where N is an integer, and is called the "fringe order".

For the thin plate bending theory to hold, the model deflections must be small so that:

$$PP' = a \angle POP',$$

where a is the distance from model to screen.

Therefore:

$$\psi = N \frac{d}{2a} \qquad (A.6.1)$$

where ψ is the slope of the model at the point O.

The fringes give the slope in the direction normal to the ruled lines on the screen so that the measurements of slopes in any required direction merely involves the rotation of the screen about the optic axis relative to the model. From the fringe photographs a graph of fringe order N versus position on the model may be obtained. This process will be shown for a specific case later. Fringe patterns obtained whilst the lines are in a direction normal to the x-axis of the plate model give the slope $\partial N/\partial x$ and those obtained whilst the lines are in a direction normal to the y-axis of the model give the slope $\partial N/\partial y$. The deflection, W, is obtained by graphical integration, and the second derivatives, and hence bending and twisting moments are obtained by graphical differentiation. Methods for graphical integration and differentiation are given in Appendix 7.

The slope curve may be drawn without actually assigning

a zero slope axis, and differentiation of the slope curve does not require that the line of zero slope be known although the correct sign must be established. The curvature curve may then be assigned a zero curvature axis to which other values of the curvature are related. It is unlikely that neither the slope nor the curvatures is known at some point on the plate.

A.6.3) Technical Details.

Ligtenberg [73] showed that a radius of 3.5a for the circular cylinder, of which the screen is a segment, gives results with acceptable accuracy. The lines on the screen were found to give the clearest fringe patterns when the ruling was chosen as d/2 white and d/2 black where d is the distance between the centre lines. Also, d should be chosen to be between 0.004a and 0.002a. As a material for the models, almost any reflecting material may be used. Black perspex was found to be suutable.

A.6.4) Experimental Details.

As a guide, the practical experiences of Richards [84] and Elson [85] in using the Moire Apparatus were followed. The models were made of 5 mm thick black perspex. The screen was illuminated by four 500 watt photo-flood lamps. A bellows-type camera with a 1:4.5/13.5 cm lens was used to take the negatives using Ko dalith Ortho (sheet) Film, Type 3. A diaphragm setting of f16 and exposure time of 45 seconds for each exposure was found to give good sharp fringe photographs. The relevant screen dimensions were a = 86 cm (based on R = 3.5a) and $d/_{2a}$ = 0.00125.

A.6.5) Details of the Clamping Arrangements for the Test Cases.

The clamped edge conditions are simulated by sandwiching

the edges of the perspex model between a pair of steel frames bolted rigidly together by several bolts (Fig.A.6.3).

A.6.6) Experimental Procedure.

The procedure explained here was executed for each test case in turn.

The perspex model was bolted to its frame and fixed to the Moire Apparatus. The screen was adjusted to the required distance from the model, i.e. 86 cm. The screen rotated about the optic axis relative to the model such that the ruled lines were parallel to the x-direction of the plate. The photo-flood lamps were arranged so that the illumination over the surface of the screen was of uniform intensity. The camera was adjusted such that the image of the ruled lines on the screen were in focus on the ground glass plate mounted in the camera. The sheet film was then placed in the camera, the diaphragm was set to f16 and the film was exposed for 45 seconds. The model was then subjected to the required loading configuation and the same sheet film was exposed again for the same length of time. The screen was then rotated through 90 degrees so thatthe lines were parallel to the y-direction and the procedure was repeated with a new film. To save on loading and unloading time, the procedure for the second orientation of the screen was carried out by photographing the loaded plate first, then removing the load and exposing the new film for the zero-load state. The films after being suitably developed and fixed display contours of the slopes $\partial N/\partial x$ and $\partial N/\partial y$.

The application of concentrated forces can be carried out directly. That of distributed loads require the use of 3" thick foam rubber and $\frac{1}{2}$" thick plank of wood as shown in Fig.(A.6.4).

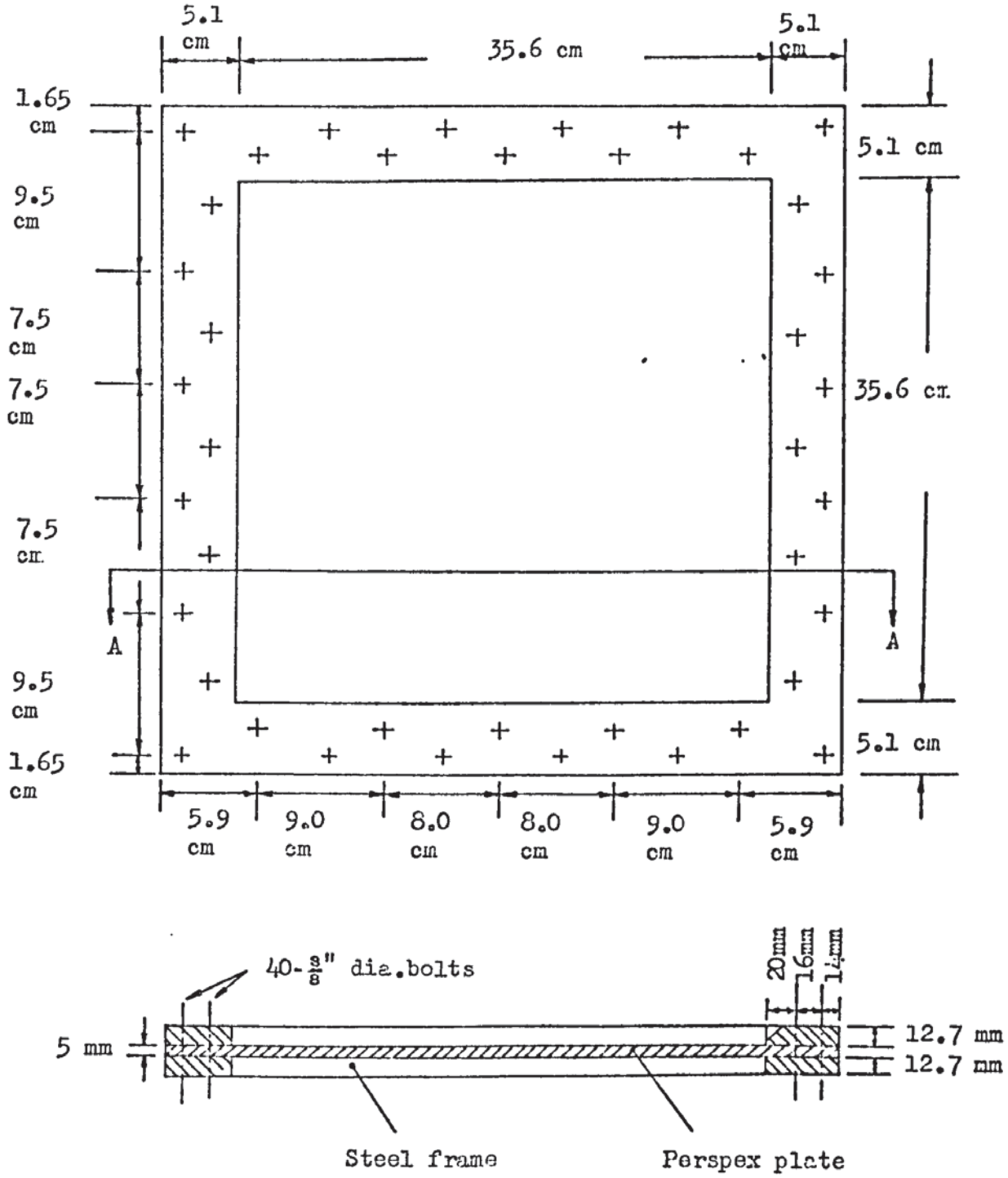

Section A-A

Fig.(A.6.3)
Details of clamping.

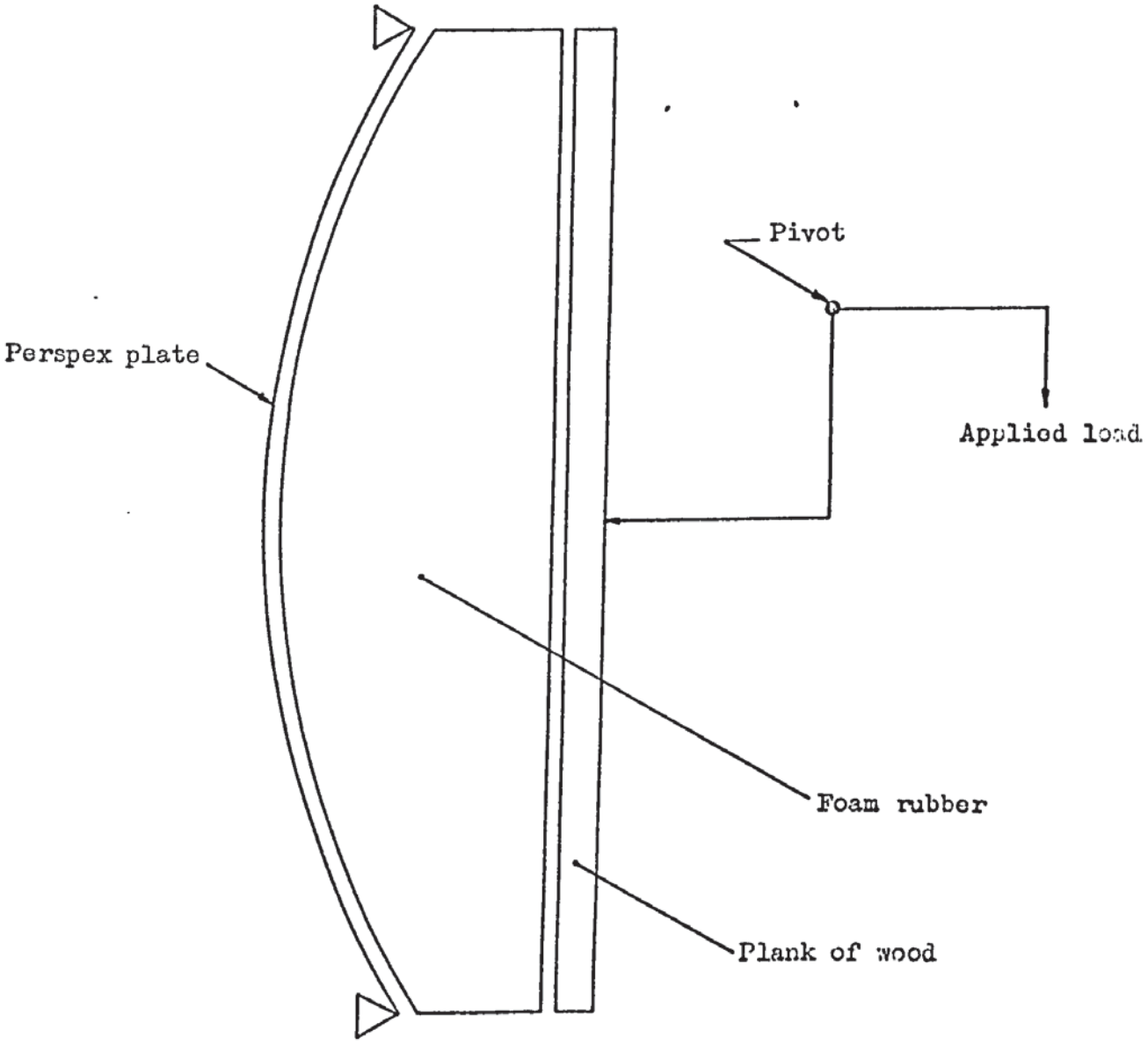

Fig.(A.6.4) Arrangement for the simulation of a uniform load in the Moire Apparatus.

A.6.7) Analysis of the Moire Fringes.

The variation of the slope across a section XX of the plate may be obtained from the fringe photographs which represent contours of slopes as shown in Fig.(A.6.5).

The points necessary to draw the slope curve are obtained by fixing a point P on one of the drawn normal lines and fixing other points on other normal lines in increments of d/2a (=0.00125 in our case). The direction of the increments relative to the first point is established on physical grounds. If a point of zero slope is known we assign a zero slope axis ox. If a fringe crosses the line XX in more than one point, then the values of the slope should be the same at such points.

Carrying out the analysis for two photographs of slopes in direction normal to one another, the bending and twisting moments may be obtained by appropriate graphical differentiation and the deflection is obtained by integrating the slope curve, details of the graphical methods may be found in Appendix 7.

The results of the model can be converted for those of the prototype as shown in reference [73]. Since, here, the experiment is aimed at comparing the results of the computer program with those of the tests, the perspex model is taken as being also the prototype.

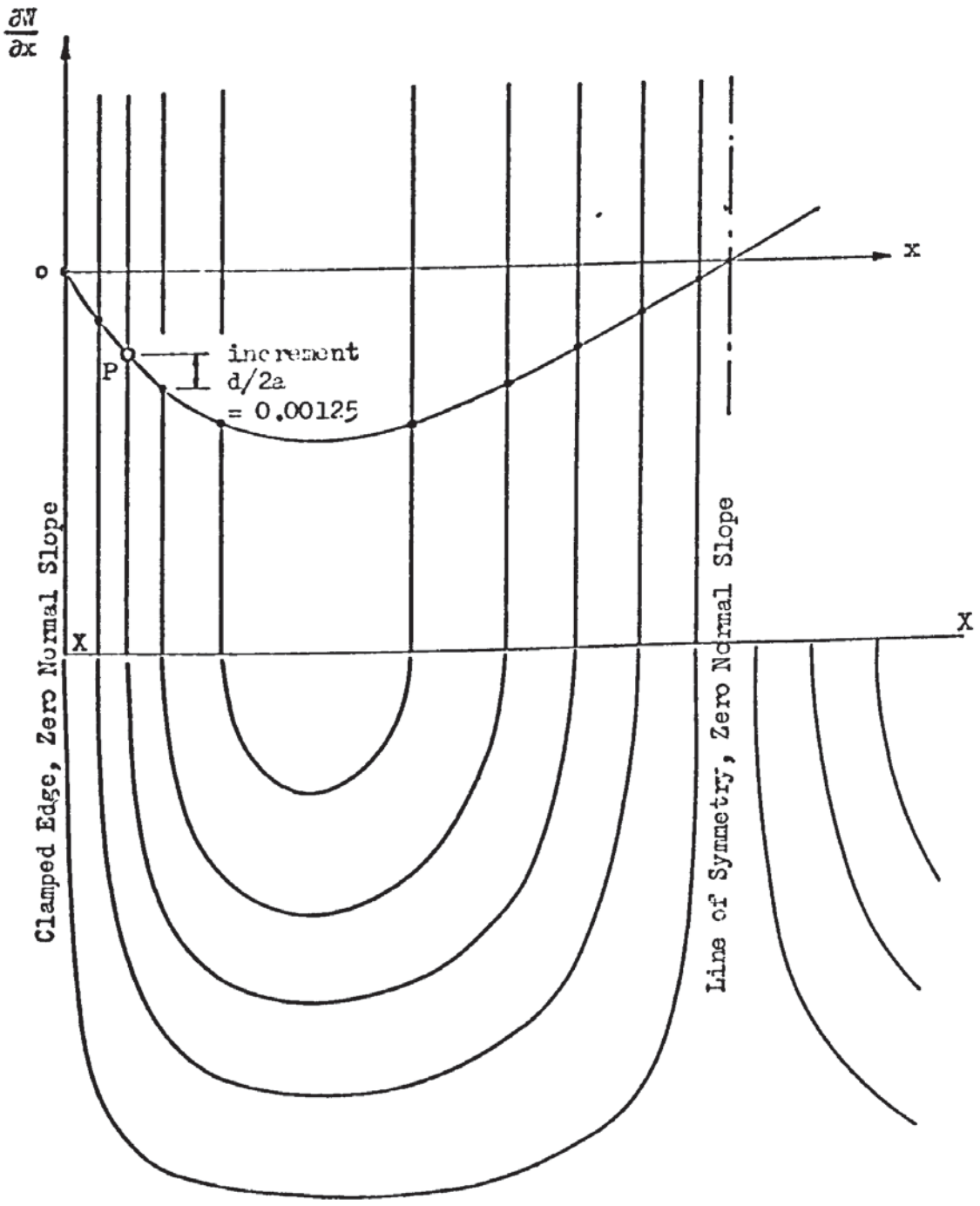

Fig.(A.6.5) Method of plotting the slope curve from the Moire Fringes.

APPENDIX 7

GRAPHICAL DIFFERENTIATION AND INTEGRATION

A.7.1) Differentiation Method.

A curve is plotted of fringe order N versus distance s along the model and the angle of inclination e_s at selected points on the curve is measured with the help of an optical differentiator. The tangent of the angle is then obtained from tables, so that

$$\tan \theta_s = \frac{\partial \bar{N}}{\partial \bar{s}}$$

where $\bar{N}$ and $\bar{s}$ are lengths measured in cm, along the vertical and horizontal scales respectively. If the vertical and horizontal scales are n fringes/cm and m cm on model/cm respectively then

$$N = n\bar{N} \quad ; \quad s = m\bar{s}.$$

From equation (A.6.1), the slopes are given by:

$$\phi_s = N \frac{d}{2a}$$

$$\text{Now} \quad \frac{\partial \phi_s}{\partial s} = \frac{\partial^2 W}{\partial s^2} = \frac{n}{m} \frac{d}{2a} \frac{\partial \bar{N}}{\partial \bar{s}}.$$

Therefore:

$$\frac{\partial^2 W}{\partial s^2} = \frac{n}{m} \frac{d}{2a} \tan \theta_s$$

where $\frac{\partial^2 W}{\partial s^2}$ is the curvature component in the direction s on the model.

A.7.2) Integration Method.

The requirement is to integrate the slope curve I (Fig.A.7.1), which is divided into segments and the mid-ordinates such as P are projected on the $\bar{N}$ axis at Q. A pole X is conveniently chosen at a distance ℓ cm from O and a line XQ is drawn. Taking a

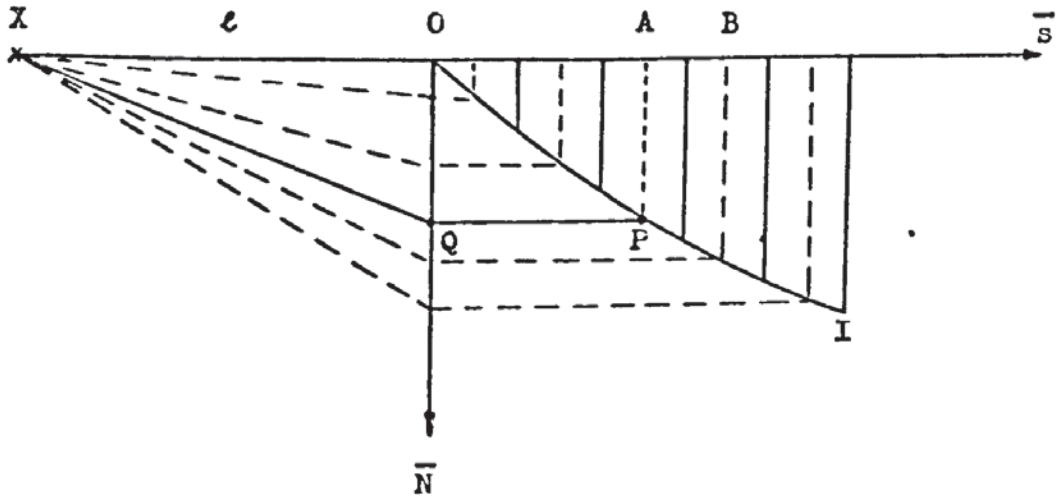

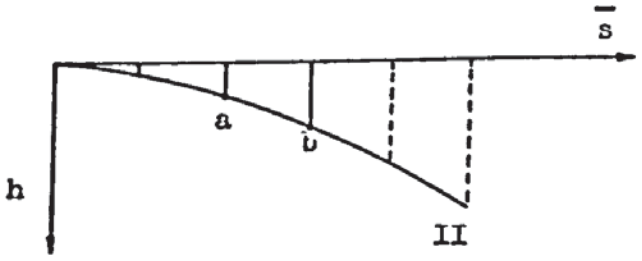

Fig.(A.7.1) Illustration of method of integration.

parallel line to XQ, the line ab is drawn on curve II. Then:

$$\Delta h = \frac{\Delta A}{\ell} \text{ cm}.$$

Thus, in moving from A to B, the increment of ordinate of curve II gives the increment of area under curve I. If this procedure is repeated for all segments, the integral curve is obtained, and

$$h = \frac{\int dA}{\ell} .$$

With the same scales as for differentiation:

$$h = \frac{2a}{d} \int \frac{1}{mn\ell} \psi_s \, ds = \frac{2a}{d} \cdot \frac{W}{mn\ell} .$$

Hence

$$W = m \, n \, \ell \, \frac{d}{2a} \, h$$

where W is the deflection of the model.

REFERENCES.

1) Washizu K., "Variational Methods in Elasticity and Plasticity", Pergamon Press, Oxford, 1968.

2) Pian H.H., Pin Tong, "Basis of the Finite Element Method for Solid Continua", Int.J.Numerical Methods in Engineering, VOL.1, pp.3-28, 1969.

3) Reissner E., "On a Variational Theorem in Elasticity", J.Math. and Physics, 29, pp.90-95, 1950.

4) Herrmann L.R., "A Bending Analysis for Plates", Proceedings of the Conference on Matrix Methods in Structural Mechanics, A.F.F.D.L. TR80, 1965, Wright-Patterson Air Force Base, Ohio.

5) Cook R.D., "Finite-Element Bending Analysis for Plates", Journal of the Eng.Mechanics Division VOL.94, No.EM3, June 1968, pp.895-898.

6) Brown J.,Dhatt G., "Mixed Quadrilateral Elements for Bending", AIAA Journal, VOL.10, Oct.1972.

7) Timoshenko S.P.,Goodier J.N., "The Theory of Elasticity", McGraw-Hill, 3rd.Ed. 1970.

8) Fung Y.C., "Foundations of Solid Mechanics", Prentice-Hall, 1965.

9) Forray M.J., "Variational Calculus in Science and Engineering", McGraw-Hill, 1968.

10) Timoshenko S.P., "Theory of Plates and Shells", McGraw-Hill Kogakusha, 2nd Ed., 1959.

11) Reissner E., "The Effect of Transverse Shear Deformation", Journal of Applied Mechanics, pp.69-77, June 1945.

12) Reissner E., "On Bending of Elastic Plates", Quarterly of Applied Mathematics, 5, pp.55-68, 1947.

13) Brebbia C., Tottenham H., "Finite Element Techniques in Structural Mechanics", Southampton University Press, 1971.

14) Panc V., "Theory of Elastic Plates", Noordhoff International Publishing, Leyden, 1975.

15) Meirovitch L., "Analytical Methods in Vibrations", MacMillan Co., N.York, 1967.

16) Dym C.L., Shames I.H., "Solid Mechanics: Variational Approach", McGraw-Hill, 1973.

17) Timoshenko S.P.,Gere J.M.,"Theory of Elastic Stability", McGraw-Hill Book Company, 2nd Ed., 1961.

18) Bulson P.S., "The Stability of Flat Plates", Chatto and Windus, London, 1970.

19) Brush D.O., "Buckling of Bars, Plates and Shells", McGraw-Hill Book Company, 1975.

20) Szilard R., "Theory and Analysis of Plates", Prentice-Hall,Inc, N.Jersey, 1974.

21) Salerno V.L., Goldberg M.A., "Effect of Shear Deformations on the Bending of Rectangular Plates", Journal of Applied Mechanics, Transactions of ASME, pp.54-58, March 1960.

22) Leissa W.A., "Vibrations of Plates", Nasa SP-160, National Aeronautics and Space Administration, Washington, 1969.

23) Salvatori M.G.,Baron M.L., "Numerical Methods in Engineering", Prentice-Hall Inc., 1961.

24) Kantorovich L.V., "Approximate Methods of High Analysis", Interscience Pub., 1964.

25) Turner M.J., Clough R.W., Martin H.C., and Topp L.C.,"Stiffness and Deflection Analysis of Complex Structures", J.Aeronaut. Sci., VOL.23, No.9, 1956.

26) Clough R.W., "Finite Element Method in Plane Stress Analysis", Proc. of 2nd ASCE Conference on Electronic Computation, Pittsburgh, Pa., September 8 and 9, 1960.

27) Zienkiewicz O.C., "The Finite Element Method in Engineering Science", McGraw-Hill, London, 1971.

28) Huebner K.H., "The Finite Element Method for Engineers", John Wiley and Sons, 1975.

29) Cook R.D., "Concepts and Applications of Finite Element Analysis", John Wiley and Son, 1974.

30) Desai C.S., Abel J.F., "Introduction to the Finite Element Method", Van Nostrand Reinhold Co., 1972.

31) Herrmann L.R., "Finite Element Bending Analysis for Plates", Journal of the Eng.Mechanics Div. A.S.C.E. VOL.93, No.EM5, Oct. 1967.

32) Ergatoudis I., Irons B.M., Zienkiewizc O.C., "Curved isoparametric Quadrilateral elements for Finite Element Analysis", Int.J.Solids Structures, VOL.4, pp.31-42, Pergamon Press,1968.

33) Melosh R.J., "A Stiffness Matrix for the Analysis of Thin Plates in Bending", Journal of Aeronat. Science, VOL.28, No.4,1961.

34) Adini A., and Clough R., "Analysis of Plate Bending by the Finite Element Method", Report to the National Science Foundation, Grant G7337, 1961.

35) Papenfuss S.W., "Lateral Plate Deflection by Stiffness Matrix Method with Application to a Marquee", M.Sc. Thesis, Dept. of Civil Eng., University of Washington, Seattle, Wash.,1959.

36) Besseling J.F., "The Complete Analogy Between the Matrix Equations and the Continuous Field Equations of Structural Analysis", International Symposium on Analogue and Digital Techniques Applied to Aeronautics, Liege, Belgium, 1963.

37) Melosh R.J., "Basis for the Derivation of Matrices for the Direct Stiffness Matrix", AIAAJ., VOL.1, 1963.

38) Fraeijs de Veubeke B., "Upper and Lower Bounds in Matrix Structural Analysis", AGARD-ograph 72, B.F.Veubeke (ed.), Pergamon Press, New York, 1964.

39) Jones R.E., "A Generalization of the Direct-Stiffness Method of Structural Analysis", AIAA J., VOL.2, 1964.

40) Gallangher R.H., "Analysis of Plate and Shell Structures", Proc. of Conf. on Application of Finite Element Method in Civil Eng., Vanderbilt University, Nashville pp.155-206, 1969.

41) Finlayson B., and Scriven L., "The Method of Weighted Residuals - A Review", Applied Mechanics Review, VOL.18, pp.735. 1966.

42) Szabo B., and Lee G., "Stiffness Methods for Plates by Galerkin's Method", Proc.ASCE, Journal of Eng.Mech.Div., VOL.95, No.EM3, June, 1969.

43) Morley L.S.D., "A Triangular Equilibrium Element with Linearly Varying Bending Moments for Plate Bending Problems", Journal of the Royal Aero.Soc., VOL.79, pp.715, 1967.

44) Morley L.S.D., "Triangular Equilibrium Element in the Solution of Plate Bending Problems", Aeronautical Quarterly, pp.149-169, May,1968.

45) Anderheggen E., "Finite Element Plate Bending Equilibrium Analysis", Proc.ASCE, Journal of the Eng.Mech.Div., VOL.95, No.4, Aug, 1969.

46) Pian T.H.H., "Derivation of Element Stiffness Matrices by Assumed Stress Distribution", AIAA Journal, 2, pp.1333-1336, 1964.

47) Wolf J.P., "Generalized Hybrid Stress Finite-Element Models", AIAA Journal, VOL.11, No.3, March, 1973.

48) Cook R.D., "Two Hybrid Elements For Analysis of Thick,Thin and Sandwich Plates", Int.Journal For Numerical Methods in Engineering, VOL.5, pp.277-288, 1972.

49) Cook R.D., "Finite Element Bending Analysis for Plates", Journal of the Eng.Mechanics Div. ASCE, EM3, pp.895-898, June 1968.

50) Cook R.D., "Eigenvalue Problems with Mixed Plate Element"., A.I.A.A. Journal VOL.7 No.5, pp.982-983, May 1969.

51) Visser W., "A Refined Mixed-Type Plate Bending Element", AIAA Journal, pp.1801-1803, Sept.1969.

52) Tahiani C., "Analyse des Voiles Minces dans les Domains Lineaire et Geometriquement Non-Lineaire par la Method des Elements Finis Mixtes", These de Doctorat, Departement de Genie Civil, Universite Laval, Aout 1971.

53) Chatterjee A., Setlur A.V., "A Mixed Finite Element Formulation for Plate Problems", International Journal For Numerical Methods in Engineering, VOL.4, pp.67-84, 1972.

54) Kikuchi F., Ando Y., "Rectangular Finite Element for Plate Bending Analysis Based on Hellinger-Reissner's Variational Principle", Journal of Nuclear Science and Technology, 9[1], pp.28-35, January 1972.

55) Brown J, Dhatt G.S., "Comportment des Elements Mixtes Pour L'Analyse des Plaques en Flexion", Rapport Technique, Faculte des Sciences Department de Genie Civil Universite Laval, Janier 1972.

56) Lekhnitskii S.G., "Anisotropic Plates", Gordon and Breach Science Publishers, 2nd Edition,1968.

57) Johns D.J., "Thermal Stress Analysis", Pergamon, 1965.

58) Froberg C.E., "Introduction to Numerical Analysis", 2nd Edition Addison-Wesley Publishers Comp., 1970.

59) Handelman G.H and Prager W., "Plastic Buckling of Rectangular Plate under Edge Thrust", Rept. 946, 1949, NACA.

60) Pearson C.E., "Bifurcation Criterion and Plastic Buckling of Plates and Columns", Journal of the Aerospace Sciences, VOL.17, No.7, July 1950, pp.417-424.

61) Ilyushin A.A., "The Elasto-Plastic Stability of Plates, TM1188, Dec. 1947, NACA.

62) Stowell E.Z., "A Unified Theory of Plastic Buckling of Columns and Plates", TR898, 1948 NACA.

63) Pride R.A., and Heimerl G.J.,"Plastic Buckling of Simply Supported Compressed Plates", TN1817, April 1949, NACA.

64) Gerald G. and Becker H., "Handbook of Structural Stability, Part I-Buckling of Flat Plates", TN3781, July 1957, NACA.

65) Pifko A. and Isakson G., "A Finite-Element Method for the Plastic Buckling Analysis of Plates", AIAA Journal VOL.7, No.10, pp.1950-1957, Oct. 1969.

66) Ramberg W. and Osgood W.R., "Description of Stress-Strain Curves by Three Parameters", TN902, 1943, NACA.

67) Nottingham Algorithms Group, ICL 1900 System, N.A.G. Library Manual-F02AEA, Document No.377, 1st May, 1972.

68) Thurnau D.H., "Collected Algorithms from CACM, Algorithm 195-P1.

69) Wilkinson J.H., Martin R.S, Peters G., "Symmetric Decomposition of a Positive Definite Matrix", Numerische Mathematik 7, pp.362-383, 1965.

70) Moody W.T., "Moments and Reactions for Rectangular Plates", Engineering Monograph No.27, U.S.Depart. of the Interior, Bureau of Reclamation, Denver, 1963.

71) Morley L.S.D., "Bending of Clamped Rectilinear Plates", Quart. Journal and Applied Maths, VOL.XVII, Pt.3, 1964.

72) Harden C.T. and Rushton K.R., "Numerical Analysis of Variable Thickness Plates", Journal Strain Analysis, 1, No.3, pp.231-238, 1966.

73) Ligtenberg F.K., "The Moire Method - A New Experimental Method for the Determination of Moments in Small Slab Models", Proc.Soc.Expt.Stress Analysis, 12, 2, pp.83-98, 1955.

74) Hussain K.M., "Examination of a Semi-Analytic Finite Element Method for Plate Bending Problems", Ph.D. Thesis, Department of Mechanical Engineering, University of Aston in Birmingham, Aug. 1975.

75) Barton M.V., "Vibration of Rectangular and Skew Plates", Journal Appl.Mech., 18, 2, 1951.

76) Plass H.J., Gaines J.H, Newton C.D., "Application of Reissner's Variational Principle to Cantilever Plate Deflection and Vibration Problems", Journal of American Society of Mechanical Engineers, March 1962.

77) Dawe D.J., "A Finite Element Approach to Plate Vibration Problems", Journal of Mech.Engineering Science, VOL.7, No.1, pp.28-32,1965.

78) Ripperper E.A., Dally J.W., "Experimental Values of Natural Frequencies for Skew and Rectangular Cantilever Plates", Report No.DRL231, CF-1354, Defense Research Lab., University of Texas, Austin, 1949.

79) Kapur K.K., Hartz B.J., "Stability of Plates Using the Finite Element Method", Journal of the Eng.Mechanics Division VOL.92, No.EM2, pp.177-195, April 1966.

80) Wittrick V.H., "Correlation Between Some Stability Problems for Orthotropic and Isotropic Plates Under Bi-Axial and Uni-Axial Direct Stress", Aeronautical Quarterly, London, England, VOL.4, Part 1, pp.83-92, Aug.1952.

81) Martin R.S., Wilkinson J.H., "Reduction of the Symmetric Eigen problem $Ax=\lambda Bx$ and Related Problems to Standard Form", Numerische Mathematik, Band 11, pp.99-110, 1968.

82) Martin R.S., Reinsch C, Wilkinson J.H., "Householder's Tridiagonalization of a Symmetric Matrix", Numerische Mathematik, Band 11, pp.293-306, 1968.

83) Bowdler H., Martin R.S., Wilkinson J.H., "The QL and QR Algorithms for Symmetric Matrices", Numerische Mathematik, Band 11, pp. 293-306, 1968.

84) Richards T.H., "Analogy Between the Slow Motion of a Viscous Fluid and the Extension and Flexure of Plates: A Geometric Demonstration by Means of Moire Fringes", British Journal of App.Physics, 2, pp.244-254, June 1960.

85) Elson M.G.J., "Use of the Slab Slice Analogy for the Study of Thermal Stress Problems", M.Sc.Thesis, Dept.of Mechanical Engineering, College of Advanced Technology, Birmingham,1965.